29TH INTERNATIONAL TOWING TANK CONFERENCE

1st VIRTUAL CONFERENCE

Proceedings - Volume I

CENTRALE NANTES

DGA Hydrodynamics
FRANCE

29TH INTERNATIONAL TOWING TANK CONFERENCE

Editor
Dr. Didier FRECHOU

Preface

Dear all, Members of ITTC, observers and sponsors,

As co-chairmen of the ITTC 29Th, we, Didier Fréchou from DGA Hydrodynamics and Pierre Ferrant from Centrale Nantes, are very pleased and honoured to welcome everyone to 29th International Towing Tank Conference organized by Centrale Nantes & DGA Hydrodynamics from France.

From the early days, France has been always supporting the idea of an international community of experts willing to share their knowledge on hydrodynamics procedures and methods.

The last time France organized the ITTC conference was back in 1960, and before that in 1935. You may notice that every time France organizes the ITTC, the number of attendees is increasing a lot. But as you know, correlation does not necessarily means causal relationship.

This dynamism in the field of hydrodynamics is well alive because France has a long tradition of shipbuilding and is still very active thanks to the Navy Shipyard Naval Group and to the Cruise liners Shipyard Chantiers de l'Atlantique. The innovation in that field is also driven by the French investments in maritime renewable energy especially on the Atlantic coast, where projects of offshore wind energy and current turbine are now underway.

As you know the ITTC conference was due to be held in September 2020 at Nantes in France. Due to the worldwide public health crisis (Corona Virus deease), we initially decided to postpone until spring 2021. Unfortunately, the circumstances have prevailed longer than anticipated and we have to cancel all the bookings we have made.

That is why the organizing committee, Centrale Nantes and DGA Hydrodynamics, with the support of the Executive Committee

suggested that the ITTC conference be held virtually for the first time. The bright side of this crisis is that the first ITTC Virtual Conference is born !

Of course, this has required radical changes to the conference format. As you noticed, the conference is programmed in short sessions to facilitate the worldwide attendance. Although we get rid of the jet lag, we understand that it might be a bit late for Asian attendees and a little early for American attendees. We hope that your biological clock will not be too much disturbed.

Within this format, this means that the time set aside for conference sessions is reduced to 3 hours per day from today to Friday. Within this daily timeframe, only 30 minutes will be allocated to each committee.

The web conference platform was provided by SeatoSky whose team is assisting us on the web conference management. The virtual meeting platform is user friendly. Anytime we need help, just click on the help button in the top right corner of your screen.

Ahead of the live sessions, all committee presentations were pre-recorded in full length, as for a standard conference, and have been available on the platform over the last two weeks. They are still available under the "May 1" tab and these videos will be available for two more weeks after the conference.

I would like to sincerely thank all the committee chairs who have been trained to get their master's degree of professional YouTuber and they all successfully passed.

Another issue we had to face was that it was not possible to open the floor, I should say the screen, for questions from more than 200 participants. That is the reason why we asked the participants to post questions in advance after viewing of the pre-recorded presentation or during the live session.

In order to do that, please select the button "Submit questions for the presenter" to post your question, so that the moderator will refer the question to the committee chair.

I must admit that it took us some times to figure out what would be the best ratio between the time reserved for the presentation and the time reserved for the discussion. Each live presentation was first planned to last about 10min in order to give more time for discussion. Then because there were not many posted questions, we asked lately the presenters to go for 20min presentation and 10min is left for Questions / Answers. Anyway my message to the presenters would be do as you feel in between this two timeframes. .

Now, let us just give you a brief overview of the program. The session will take place from 10 am to 1 pm Universal Time Coordinate. The local time is directly accessible on the platform when you connect.

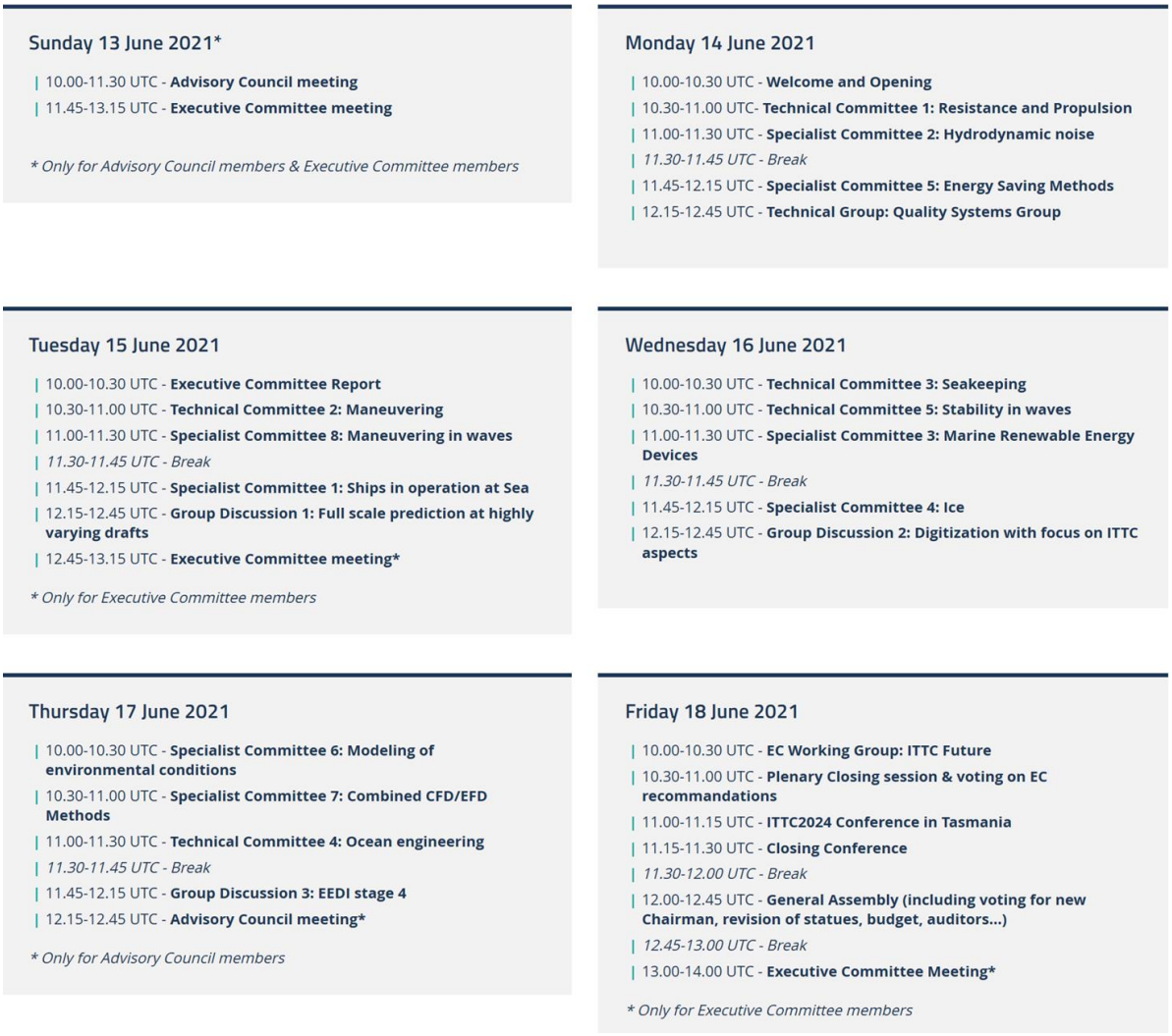

29th ITTC conference Program

From today up to Thursday, the conference is fully dedicated to presentations of the Technical Committees, the Specialist Committee. Technical committees are dedicated to all the classical technical topics of our fields. Specialist committees are more focused on recent technical problems that needs to be addressed. In addition to these technical presentations, there are also 3 groups of discussion which will give us new insights on three major topics.

After the short summary of the committee work presented by the chairman of the committee, the moderator will ask the questions that have been pre-posted during the pre-view or that will be posted during the live session.

Friday is dedicated to ITTC Future report, EC report and to the General Assembly.

All sessions will begin on time, but if you want to follow a discussion that will go beyond the 30 minutes, it is possible although you are going to miss the start of the following live session.

I wish to take the opportunity to thank all the committees members who worked hard in the last four years. It is always important to recall that this work is often done in addition to the daily duty.

Yet the results are there, and the quality of the work done can be easily found either in committee reports and presentations, as well as in released procedures. This shows that ITTC is a very efficient organization which remains strong and, most important, that ITTC is able to adapt to new challenges introduced by Computer Science and Machine learning algorithms.

All the conference materials are available for download at the ITTC website, where the presentations and reports of the committees as well as the procedures and guidelines are stored. This web site is the permanent website of the ITTC.

We would also like to thank the organizing committee and specially the persons backstage.

First of all the team from Centrale Nantes Professor Pierre Ferrant, the co-chairman of the conference, Sandrine Jamet, the conference web master and the manager of the web conference who did a great job, and Blandine Mariot the Finance and administration head.

Secondly the team of SeatoSky who will help us all along the conference week behind the screen for the web platform management: Brittany Minskip, Helena Yang and Ian Holliday

Finally we would like to thank the Director of DGA Hydrodynamics Laurent Le Saint and the Director of Centrale Nantes Jean-Baptiste Avrillier.

I did not wish to end this welcome without addressing few words on the spirit of the ITTC although it is not going to be words.

As a matter of fact, in France, we like to say that “a picture is worth a thousand words”.

So I will leave you to think about this first picture, which best describes the ITTC spirit in the early days of hydrodynamics.

The spirit of ITTC in the early days

Today the hydrodynamics tools have tremendously changed but the spirit is still alive !

That is the reason why, since a while, ITTC community is supporting the idea to build bridges between Computational Fluid Dynamics and Experimental Fluid Dynamics.

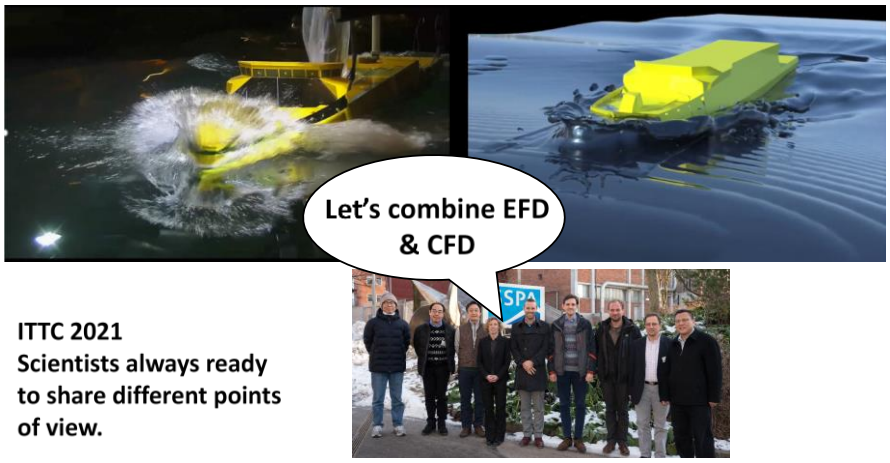

The spirit of ITTC in 2021

On behalf of the organizing committee, we declare the 29th ITTC Conference and the first ITTC web conference open and I hope you all enjoy this event.

FRANCE, Monday 14th June,

Dr. Didier **Fréchou**
Co-chairman of 29th ITTC Conference

Professor Pierre **Ferrant**
Co-chairman of the 29th ITTC Conference

Table of Content
Volume I

Table of Content
Volume II

The Executive Committee

Final Report and recommendations to the 29th ITTC

1. INTRODUCTION

The roles and responsibilities of the Executive Committee are defined in the ITTC Rules and include

- Implementing the decisions of the Full Conference
- Representing ITTC between Conferences
- Replacing members of technical committees and groups as necessary between Conferences
- Accepting new member organisations to the ITTC
- Managing the finances
- Approving the arrangements and associated costs and registration fees for the Conference
- Reporting on its activities to the Full Conference

In addition, the Executive Committee appoints members of the Advisory Council and reviews the members on a regular basis.

During the 29th ITTC, the Executive Committee has performed its duties in accordance with the above. The Executive Committee has worked together with the Advisory Council on the presentation of recommendations to be adopted by the 29th Full Conference.

2. OBITUARIES

2.1 Dr. Yusuke Tahara

Dr. Yusuke Tahara, a senior research engineer of National Maritime Research Institute (NMRI), sadly passed away on January 25th 2019 at the age of 56. Dr. Tahara earned his Bachelor of Engineering and Master of Engineering in 1985 and 1987, respectively, both from Yokohama National University. After one-year experience as a system engineer at Japan IBM, he started his postgraduate study in the University of Iowa, Iowa Institute of Hydraulic Research (currently IIHR-Hydroscience & Engineering-) in 1988. In 1992, he earned his Ph.D. degree with the dissertation title "Interactive Approach for Calculating Ship Boundary Layers and Wakes for Nonzero Froude Number". Dr. Tahara started his academic carrier as the post-doctoral scholar at IIHR for 2 years, and then returned back to Japan as the assistant professor at Osaka Prefecture University (OPU) in 1994. In 2009, he chose NMRI as the next base of his research career after 15 years of activities at OPU, lastly appointed as an associate professor.

Dr. Tahara was the professional in developing codes in computational ship hydrodynamics including potential and viscous flow solvers, grid generation, overset grid assembler and optimization. In the meantime, he put great importance on industrial application of his research works. He was also the yacht scientist. As the core representative of technical team of Nippon Challenge America's Cup during 1995 to 2000, the appendages for two challenger boats, "Asyura" (JPN44) and "Idaten" (JPN52), were designed and equipped owing to enormous efforts of Dr. Tahara and his team. As a research engineer, professor and yacht scientist, the achievement of Simulation Based Design throughout R+3D, including Research, Development, Demonstration and Dissemination, was his life work.

Dr. Tahara was nominated as the member of Resistance Committee in 25th and 26th ITTC. He accomplished many tasks including worldwide round robin tests in towing tanks for establishing benchmark data to identify the facility bias. As the conference operational director, several international workshops were able to be carried out with success, such as Osaka Colloquium, New S-Tech, and AMEC. His contributions to the field of naval architecture and ocean engineering were domestically and internationally awarded, including SNAME ABS Captain Joseph H. Linnard Prize in 2010 and JASNAOE Paper Award on 2012. Dr. Tahara supervised more than 30 students at OPU, and kept training young researchers after he moved to NMRI. "Face up. Find the way forward. No matter what. We can do it." We were always encouraged by Dr. Tahara's extremely positive attitude. Dr. Tahara will be missed by the worldwide ship hydrodynamics community.

2.2 Prof Seizo Motora

Professor Emeritus Seizo Motora passed away peacefully at the age of 98 on May 1st, 2020. He studied naval architecture at the Second School of Engineering, University of Tokyo. After graduation in 1944, he worked as a faculty member in the Department of Naval Architecture at University of Tokyo until 1982. After he retired University of Tokyo, he was the

president of Nagasaki Institute of Applied Science from 1982 to 1989.

He made a great contribution to developing the field of manoeuvrability of ships. He revealed the hydrodynamic characteristics of the added mass of the hull and presented a practical estimation method based on extensive experimental studies. In 1970, Seakeeping and Manoeuvring Basin with a length of 50 m, a width of 30 m, and a depth of 2.5 m was constructed under his leadership in the university and was engaged in education and research until 2010s. In addition to university education and research, he authored numerous academic papers and several textbooks, including Ship Dynamics and Dynamics of Ships and Offshore Structures. As a social activity, he was in charge of analysis of an accident in 1954 when the Seikan ferry Toyamaru sank due to the effect of a typhoon. He played a key role in research on ship safety standards and contributed significantly to the development of ship building industries. As an academic activity, he was President of the Society of Naval Architects of Japan from 1981 to 1983. He also established STAB Conference (The International Conference on Stability of Ships and Ocean Vehicles) and initiated PRADs Symposium (The International Symposium on Practical Design of Ships and Other Floating Structures). He participated in the Maritime Safety Committee and Marine Environment Protection Committee of the International Maritime Organization (IMO) as a Japanese representative more than 20 times and contributed to developing the limitation of the size of tanks in tankers and international standards regarding ship stability. For such outstanding achievements, he was awarded Compass International Award of Marine Technology Society, Stanley Gray Award of the Institute of Marine Engineering, Science and Technology and other awards.

He participated in ITTC many times. He was a member of Manoeuvrability Committee in the 10th and 11th from 1960 to 1966 and served as a chairman of the committee. He was a member of Japan Organizing Committee of the 11th in Tokyo in 1966 and the 18th in Kobe in 1987. He served as a member of Executive Committee in the 14th, 15th and 16th from 1972 to 1981. He joined the 25th Conference as a special guest in Fukuoka in 2008. Through joining, hosting and organizing conferences and related meetings, he had contributed greatly to the development of ITTC and to the development of the academic field of naval architecture since the early days.

In 1997, he received the Order of the Sacred Treasure, Gold and Silver Star in Japan. Here, we would like to express our deep homage to his achievements over the years, and to express our sincere condolences.

2.3 Prof. Baoshan Wu

Prof. Wu Baoshan, deputy director of China Ship Scientific Research Center (CSSRC), passed away at the age of 52 at 05:40 on February 10, 2020.

Born in Tianmen City, Hubei Province on Dec. 29, 1968, Prof. Wu Baoshan graduated from the Department of Engineering Mechanics of Xi'an Jiaotong University in 1993, and in the same year joined China Ship Scientific Research Center (CSSRC). He obtained a doctorate in

fluid mechanics from China Ship Research and Development Academy in 2012. He served as director of the CSSRC Hydrodynamic Research Department（2002-2018）, director of CSSRC Graduate Department, deputy director and technical director of CSSRC(2018-2020).

Since 2002, Prof Wu had been the Academic Committee Member of Ship Mechanics Committee, Chinese Society of Naval Architecture and Marine Engineers(CSNAME).

Since 2005, Prof. Wu had been a member of the 25th and 26th ITTC Uncertainty Analysis Committee, the 27th ITTC Resistance Committee, the 28th ITTC Executive Committee and the Advisory Committee and the 29th ITTC Advisory Committee. As secretary of the 28th ITTC Organizing Committee, he had exerted great efforts for the success of the 28th ITTC held in Wuxi, China.

Prof. Wu Baoshan was not only an outstanding scientist who had long been engaged in the research on the overall performance of ships, but also an excellent tutor who had instructed more than 10 students for master's and Ph. D degrees.

We extend deepest condolences to Prof. Wu's family and mourn the loss of an exceptionally gifted colleague.

Prof. He Chunrong
On behalf of
China Ship Science Research Center

2.4 Prof. Ichiro Tanaka

Ichiro Tanaka, Professor Emeritus of Osaka University, Japan passed away on 23rd June 2019 at the age of 87.

He was born on September 9, 1931 in Kobe City, Hyogo Prefecture Japan. He was a member of the 16th (1978-1981) and 17th (1981-1984) ITTC resistance committee. He was also a member of Japan executive committee for 18th Conference held in Kobe. He started Osaka Colloquium on Ship Viscous Flow on 1985 and was a Chairman of first and second Colloquium.

Prof. Tanaka started his scientific career on the viscous flow around ship stern as a student and a colleague of Professor Hideo Sasajima at Osaka University. He worked for Osaka University as an assistant professor (1952-1967), an associate professor (1967-1973) and a professor (1973-1995) and he retired on March 1995. He made a lot of achievement on simplified computation method of turbulent boundary layer around ship. He also made the prediction method of scale effect for the wake distribution in the stern region and the simple formula for estimating form factor of viscous resistance especially for viscous pressure resistance based on turbulent boundary layer theory. From those achievement, he got many awards such as JASNAOE Awards in 1976. He extended his research field to ship propulsion

and performance prediction and did a lot of excellent works.

Prof. Tanaka supervised more than 200 students at Osaka University and many graduates from his research group are working in the ship hydrodynamics community.

2.5 Prof. Bruce Johnson

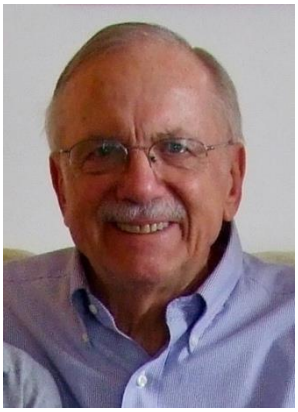

Prof. Bruce Johnson passed away on 4 June 2018, at the age of 85 years old. He had been a professor for 35 years, in the Naval Architecture and Ocean Engineering Department at the United States Naval Academy.

Prof. Johnson received a BSME in Mechanical Engineering from Iowa State University where he was a member of the Navy Reserve Officers Training Corps in 1955. He earned a MSME in 1962 and a PhD. in 1965, both degrees in Mechanical Engineering from Purdue University.

From 1955–1959, Prof. Johnson served In the US Navy, as an Engineering Repair Division Officer on the U.S.S. Kearsarge (CVA-33) and then as a Naval Officer Instructor at the US Naval Academy. While he was a graduate student at Purdue University from 1959–1964, he was also an instructor. He then joined the faculty of the US Naval Academy in the Department of Naval Architecture and Ocean Engineering, where he was an Associate Professor from 1964–1970, and a full Professor from 1970–1999. He became a Professor Emeritus upon his retirement in 2000.

At the Naval Academy, Prof. Johnson taught courses and did research. He was the Director of the Hydromechanics Laboratory in Isherwood Hall from 1967–1972, where he began development of the towing tanks for Rickover Hall. He then became a Project Manager in the Hydromechanics Laboratory in Rickover Hall from 1972–1975. He was the Naval Sea Systems Command Professor of Hydromechanics from 1975–1986; Director, Hydromechanics Laboratory in Rickover Hall, 1976–1987; and Program Director, Ocean Engineering, 1996–1999.

Prof. Johnson performed research in many fields including fluid mechanics, hydrodynamics, naval architecture, ocean-wave mechanics, time-series analysis, brain-wave analysis, and engineering-economic analysis. He was advisor or co-advisor for nineteen Trident Scholars, four of whom were awarded the Harry E. Ward Trident Scholar Prize. Two of them made flag rank, including one four-star admiral. He received an American Society for Engineering Education Excellence in Engineering Teaching Award in 1970, and he received the William H. Webb Medal from the Society of Naval Architects and Marine Engineers for outstanding contributions to education in Naval Architecture, Marine, or Ocean Engineering in 2017.

In addition to teaching and research, Prof. Johnson was the author or co-author of many papers. After he retired he focused his writing on the stability of fishing vessels and sailing ships. He also co-authored several textbooks including Introduction to Naval Architecture published by the U. S. Naval Institute with Prof. Thomas Gillmer. He was responsible for major revisions to the chapters on ship stability in the second edition of

Introduction to Naval Engineering by Blank, Bock, and Richardson. He was a coauthor of the 5th edition of Engineering Economic Analysis with Donald Newnan, for which he rewrote chapters on the use of spreadsheets in cash-flow analysis for the 6th and 7th editions. He was the first author of Hydrostatics and Stability of Ships and Offshore Floating Systems.

Prof. Johnson was active in the ITTC for 40 years. He was a member of the Presentation and Information Committee for the 15th and 16th ITTC's (1978–1981), a member of the Information Committee for the 17th ITTC (1984–1987). He was the chairman of the Symbols and Terminology Group for the 18th–22nd ITTC's (1987–1999). Finally, he was a member and then Corresponding member of the Quality Systems Group for the 26th–28th ITTC's from 2011 until his death in 2018.

Prof. Johnson was an avid sailor and spent many happy hours racing sailboats on the Chesapeake Bay. In addition, he loved the arts, including classical music, opera and ballet performances.

Arthur M. Reed

2.6 Dr. Kostadin Yossifov

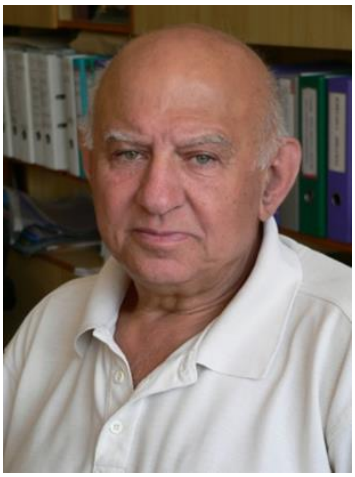

Bulgarian Ship Hydrodynamics Centre – Varna sadly announces, that on April 12 2021 Dr. Kostadin Yossifov (1943 – 2021), the former BSHC director, passed away.

Dr. Yossifov is one of the founders of the BSHC, who participated in the design, construction, commissioning and development of its scientific and experimental facilities. Specialist in the design of ship propellers, with significant personal contribution to the creation and development of the Cavitation Laboratory.

During his long scientific career he was Deputy Director R&D, long-term director of BSHC, having an indisputable contribution to the establishing its international recognition.

He has been a longtime member of several ITTC Technical Committees as well as a member of ITTC AC until 2013.

A tribute to his bright memory!

2.7 Jan Holtrop

Jan Holtrop was born in Amsterdam on May 5th, 1945. On June 6th, 2021, he passed away at the age of 76. His name was one of the great names in ship propulsion hydrodynamics, known to most naval architects around the world.

Colleagues and customers of MARIN alike all know Jan as a friendly, helpful, modest, and patient person with a bright mind. In addition to having a healthy sense of humor, he could at times have strong opinions and act decisively if he felt it was needed. A strong sense of responsibility towards the people around him and towards his work also characterized him. Jan was genuinely interested in people, as well in nature and the environment. In line with this, one of his primary professional interests was the improvement of the energy efficiency of ship propulsion.

Jan studied naval architecture at Delft University of Technology with a keen interest in the then emerging computer technology. He graduated in April 1970 and subsequently joined the Netherlands Ship Model Basin (NSMB) in Wageningen, The Netherlands (which became the Maritime Institute Netherlands (MARIN) in 1981). His first assignment was at the (then) new IT department, but after just a few years he was invited to join the crew that had to set up working procedures for the Depressurized Towing Tank (DTT), of which the construction started then in the nearby town of Ede. There he met and joined forces with Frits Mennen, with whom he would work together and became close friends since then.

In the DTT ship propulsion tests could only be done as “captive” tests. Since this technique was not yet used at MARIN in its traditional towing tanks until then, this required new ways of analyzing test results. A “3D”-method, including the use of e.g. form factors and wake scale effects was introduced. However, correlation allowances were lacking for that method. Jan Holtrop and Frits Mennen therefore started to re-analyze many full-scale ship trial results and related model test results to obtain correlation allowances. Having analyzed all these data, they started to use these also as the basis of a ship power prediction method, which is still known as the Holtrop-Mennen method and widely used around the world. Later, he introduced the powering analysis tools in the other towing tanks of MARIN as well.

Early 1990-ies Jan-started studying propeller design and related issues, and soon became a specialist in that field. He introduced specially designed blade section profiles of ship propellers and shaft brackets for reducing cavitation. He showed keen interest in energy saving ship concepts like the asymmetric stern ship and the application of energy saving devices like pre-swirl stators.

Also, through his participation in the work of the ITTC Powering Performance and Propulsion Committees Jan contributed greatly to the science of ship hydrodynamics. Jan was a member of the Powering Performance Committee of the 17th, 18th and 19th ITTC (1981 – 1990), the last three years being chairman. Later, he was member of the 22nd and 23rd ITTC Propulsion Committee (1997 – 2002). He was at the fore front of the development of new methods for extrapolation of model tests with methods for podded propulsors and the introduction of the Grigson friction line. He also laid the groundwork for the quasi-stationary method of ship model propulsion testing, a different approach from the usual stationary model propulsion tests.

Jan Holtrop will be missed by many people. First and foremost, by his family, but also by many colleagues, MARIN customers and scientists around the world. He was a very special and kind person and will surely be remembered especially as such.

Do Ligtelijn
Gert-Jan Zondervan
On behalf of MARIN

3. COMMITTEE MEMBERSHIP

Membership of the 29th Executive Committee has been the following:

ITTC Association Chairman: Fabio di Felice, CNR

Northern Europe representative: Kourosh Koushan, SINTEF Ocean

Central Europe representative: Janou Hennig, HSVA

Southern Europe representative: Fabio di Felice, CNR

Pacific Islands representative: Shotaro Uto, NMRI

East Asia representative: Suak Ho Van, KRISO, until 2018, Yonghwan Kim, SNU, from 2019 onwards

Americas representative: Antonio Fernandes, LabOceano.

Non-voting ex-officio members of the Executive Committee were:

Didier Fréchou, DGA Hydrodynamics, as Chairman of the 29th Conference

Gerhard Strasser, Vienna Model Basin, as Advisory Council Chairman,

Zhenping Weng, CSSRC, as past Chairman,

Aage Damsgaard, FORCE Technology, as ITTC Secretary.

4. COMMITTEE MEETINGS

The committee has held three physical meetings between 2017, 2018 and 2019 and, due to the pandemics situation, six virtual meetings in 2020 and 2021. Further virtual meetings are foreseen, and the final virtual meeting will be held during the 29th Full Conference.

The first meeting was held in Wuxi during the 28th Conference. The committee reviewed the comments made by the Conference to the Terms of Reference for the new technical committees and endorsed the revised version, which was subsequently issued to the technical committee chairpersons together with their appointment.

The committee elected Fabio di Felice as interim chairman of ITTC.A and authorised him to proceed with the registration of the association in Switzerland.

The committee appointed Kourosh Koushan as chairman of the Working Group on the Future of ITTC, the continuation of which had been endorsed by the Full Conference.

The committee confirmed the financial support to representation of ITTC at IMO meetings, and appointed Gerhard Strasser as the representative for EEDI/EEOI matters.

The committee appointed new members of the joint ISSC/ITTC committee and, finally, decided to seek additional members of the SC on Energy Saving Methods, which had just five members.

The second committee meeting was held in September 2018 in Gdansk, Poland, hosted by CTO.

The inaugural meeting of the ITTC Association, ITTC.A, was held on this occasion, and Fabio di Felice was elected chairman. He was authorised to proceed with the formalities in accordance with the statutes.

The Working Group on the Future of ITTC reported its progress and mentioned that a separate meeting would be arranged early 2019.

The committee endorsed that the speed-power sea trial procedure should be revised in cooperation between the AC Chairman and the SC on Ships Operating at Sea, and that the revised procedure should be published soonest possible.

Formal liaison with IEC was endorsed and action would be taken by the chairman.

The cooperation with ISSC was criticised, and it was discussed whether it should continue.

The AC Chairman reported on the IMO cooperation, specifically the ongoing activities in MEPC.

The secretary presented draft final accounts for the 28th ITTC secretariat. There had been some problems as the accountant in FORCE had left the company without informing the secretary. In the light of this, the secretary was given the mandate to look for an independent accounting firm to assist.

The 29th conference arrangements were discussed.

The Pacific Islands region proposed that the 30th conference should be held in Tasmania. Following the usual sequence of host regions, it should have been held in Central Europe, but the CE representative agreed to shift the sequence.

Antonio Fernandes was elected vice-chairman.

The secretary was authorised to make payments from the ITTC bank account up to 5000 USD. Larger payments should be co-signed by the chairman.

The committee decided that a general disclaimer shall be included in all ITTC procedures.

The third meeting was hosted by DGA Hydrodynamics in Val de Reuil, France, September 2019.

The committee, on the recommendation of the Advisory Council, decided to establish a working group to look at extrapolation procedures at varying draft. It would be chaired by SSPA, and members were appointed.

Membership of ITTC has been terminated for six organisations that had not paid the fee and had not responded to reminders.

Hiring an external accounting firm to handle the ITTC accounts appeared to be excessively costly, so the committee accepted that the accounting is done by the secretary and checked by two internal auditors.

The WG on the Future of ITTC had been considering a large number of suggestions for modernising ITTC. It was agreed to follow some of the recommendations and introduce new procedures. Others would need further discussion.

The fourth meeting was planned to be held in Tokyo March 2020, hosted by NMRI. However, the meeting was cancelled due to the worldwide health crisis, and all subsequent meetings were held online.

A total of six virtual meetings were held between 15th April 2020 and 25th May 2021.

The meetings held in April, October and November 2020 and January 2021 mainly concerned the practical aspects of the conference. In April, it was decided to postpone the conference to 2021 and the 30th conference to 2024, and the consequences of this were communicated to the member organisations and the technical committees. At the next meetings, it was decided to arrange a virtual conference, and the practical aspects of that were discussed.

Among others, it implied that all committee presentations would have to video recorded and that there would not be a printed version of the Proceedings. Reports, presentations and the usual appendixes would be available on the ITTC website.

The last two virtual meetings before the conference handled the "normal" committee activities that had been given less attention up to then. The review of AC membership was performed and some AC members consequently asked to confirm their commitment to AC work, TC member evaluations were reviewed, the Terms of Reference for new committees proposed by AC were reviewed, new Area Representatives identified, the budget and fee for the next period approved, and the accounts and fee payment status for the 29th period reviewed.

The WG on the Future of ITTC had proposed a number of revisions to the ITTC Rules and the ITTC.A Statutes, which were discussed and formulated. The proposed changes are presented later in this report and the revised documents are included in the Proceedings on the ITTC website.

The committee supported the recommendations of the Advisory Council with regard to Group Discussions at the conference.

New Area Representatives have been appointed as follows:

- East Asia: Chunrong He, CSSRC
- Southern Europe: Lanfranco Benedetti, CNR
- Northern Europe: Claus D. Simonsen, FORCE
- Pacific Islands: Toru Katayama, Osaka Prefecture University
- Americas: Martin Donnelly, NSWCCD

The representative for Central Europe will continue for the next period.

5. WORKING GROUP ON THE FUTURE OF ITTC

The Working Group on the Future of ITTC continued its activities during this period and produced a set of recommendations to the Executive Committee. The WG Presentation is included in these Proceedings as a separate report to which reference is made.

6. COMMITTEE ACTIVITIES

6.1 Revision of ITTC Rules

The committee decided to recommend to the 29th Full Conference to adopt a number of modifications to the ITTC Rules. The proposed modifications are:

- The membership of ITTC shall be open to organisations that carry out hydrodynamic work in support of the designers, builders and operators of ships and marine installations with numerical capabilities, only. AC membership shall be for towing tank organisations, only.
- East Asia shall be split into two areas and EC consequently increased to seven area representatives with voting right.
- There shall be one type of technical committees, only, and the requirements to them shall be the same.
- Membership of technical committees shall be based primarily on expertise, not on even geographical distribution.
- The ITTC and AC fees are merged into one account administered by EC.

The present version of the Rules is found as Procedure 1.0-01 in the 2017 version of the Quality Systems Manual, and the proposed

revised Rules are included as an appendix in the Proceedings on the ITTC website.

If these changes are accepted, a number of procedures need to be changed consequentially. This will be done during the next period.

6.2 Revision of ITTC.A Statutes

As a consequence of the proposed revision of the ITTC Rules, a number of revisions of the ITTC.A Statutes are required.

They concern:

- Revising the aim to include members that do not operate towing tanks or other physical test facilities
- Increasing the number of EC members

The proposed revised Statutes are included in Appendixes to the Proceedings on the ITTC website.

6.3 Appointment of ITTC.A Chairman

The Executive Committee has sent all members the call for candidacy for the position as Chairman of ITTC.A to be elected at the General Assembly. One candidate, only, submitted his application before the deadline 15th April 2021, Kourosh Koushan, SINTEF Ocean, Norway. The candidate will be the only one presented for election at the ITTC.A General Assembly, and the committee recommends the ITTC.A General Assembly to elect Kourosh Koushan as the new chairman.

6.4 Committees and Tasks of the 30th ITTC

Based on input from the technical committees, AC members, ITTC members and the Executive Committee Working Group on the Future of ITTC, the Advisory Council prepared the document proposing the structure and Terms of Reference of technical committees and groups of the 30th ITTC enclosed as an appendix to the Proceedings of the 29th Conference on the ITTC website.

6.5 Changes in ITTC Membership

The following new members of ITTC have been approved during this period (or late last period):

- National Iranian Marine Laboratory, Iran
- Gdansk University of Technology, Poland
- University of Sao Paolo, Brazil
- University College Cork, Ireland
- Daewoo Shipbuilding and Marine Engineering, Korea
- University of Galati, Romania
- Tallinn University of Technology, Estonia
- Changwon National University, Korea
- Laboratory for Waves and Currents, UFRJ, Brazil
- Coastal and Marine Engineering Research Institute, Israel

Membership was terminated for the following:

- Naval Science and Technological Institute, India
- Sharif University of Technology, Iran
- Universiti Teknologi Petronas, Malaysia
- BMT Seatech, UK
- Cranfield University, UK
- Orion Energy Centre, UK

Several members have changed their Designated Representatives. The member information as known by the secretariat on 1st May 2021 is included as an appendix to the Proceedings of the 29th Full Conference.

The total number of members is 103.

6.6 Changes in Advisory Council Membership

There has been no change of AC membership this period. AC has 39 members.

6.7 Changes in Technical Committee Membership

The Executive Committee has endorsed a number of changes of membership of the technical committees. An appendix to the Proceedings includes a list of all past and present members of the committees of the 29th ITTC.

6.8 Advisory Council Membership Review

During this period, approximately half of the Advisory Council members were reviewed using the evaluation form that was revised during the 27th ITTC. Some AC members had not demonstrated the desired commitment to AC activities and were asked to reconfirm their interest in staying on the AC. As a result of this, all AC members were accepted.

6.9 ITTC Website

The website is continuously updated with member information and provides links to ITTC Recommended Procedures and Guidelines, Symbols and Terminology, Dictionary, and the Sample QA Manual. The link to the ITTC wiki has not been functioning for some time as the server holding the wiki was not in operation.

The website furthermore holds the Proceedings of all ITTC Conferences and the Catalogue of Facilities. Under the News menu, you will find the ITTC News, and under Miscellaneous, other relevant information may be found. A new menu Benchmark Data has been implemented. This will, in time, link to the available benchmark data.

A password protected Member's area holds information for the Executive Committee and Advisory Council.

6.10 ISBN and ISSN Number on Publications

In 2020, the ITTC Association registered as publisher at the Swiss ISBN Agency. The association bought a quota of 1000 ISBN numbers for 861,60 CHF that can be assigned to digital and printed publications. After publication, a copy of the published document must be submitted to the Swiss National Library.

The request of the ISSN (International Standard Serial Number) assignment for the ITTC proceedings series is in progress.

6.11 IMO Activities

ADVISORY COUNCIL CHAIRMAN

The ITTC AC Chairman attended the following meetings, with travel and hotel costs paid by ITTC:

MEPC 72 (Marine Environment Protection Committee): 9 to 13 April, 2018

MEPC 73: 22 to 26 October, 2018

MEPC 74: 13 to 17 May, 2019

The following submissions have been made or co-sponsored by ITTC:

MEPC 72/INF.4, ITTC Recommended Guideline on Model Scale Cavitation Noise Measurements.

MEPC 72/INF.6, Updated ITTC Recommended Procedures and Guidelines concerning the determination and verification of EEDI.

MEPC 73/5/5, Draft amendments to 2014 guidelines on survey and certification of EEDI.

STABILITY IN WAVES COMMITTEE

The Stability in Waves Committee (SiW) had representatives to the Subcommittee Ship Design and Construction (SDC) of IMO as follows:

SDC 6: 4 to 8 February, 2019 (Akihiko Matsuda)

SDC 7: 3 to 7 February, 2020 (Akihiko Matsuda)

The SiW has been particularly involved in the discussions concerning the second generation intact stability requirements.

ITTC MEMBERS

Several members of ITTC participate via the member states to IMO.

6.12 ITTC Accounts

The final accounts of the 28th ITTC and the projected accounts for the 29th ITTC are shown below. All amounts are in USD. The accounts for the 28th ITTC were checked and approved by the internal auditors Marco Ferrando, University of Genova, and R. U. Franz von Bock und Polach, Technical University of Hamburg.

Account item	29th projected (4 years)	28th Final
ITTC fee	80,000	57,800
AC fee	150,000	72,200
Financial income	2,670	116
Total income	232,670	130,116
Secretariat hours	120,000	95,000
Secretariat expenses	6,000	10,915
IMO/ISO activities	18,000	11,688
Support to Conference	6,000	6,000
Financial costs	1,500	1,171
Website	2,000	6,748
ITTC Association	20,000	1,712
Total costs	173,500	133,234
Net Result	59,170	-3,117
Total equity capital	88,117	28,947

6.13 Budget for 30th ITTC

The proposed budget (in USD) for the 30th ITTC is shown below. The budget is based on the assumption that the ITTC membership fee is reduced from 250 USD to 225 USD annually and the additional fee for AC membership is reduced from 1,100 USD to 1,000 USD annually.

Account item	30th ITTC Budget
ITTC fee	69,525
AC fee	117,000
Financial income	0
Total income	186,525
Secretariat hours	90,000
Secretariat expenses	15,000
IMO/ISO activities	20,000
Support to Conference	6,000
Website	3,000
ITTC Association	15,000
Financial costs	2,000
Miscellaneous costs	10,000
Total costs	161,000
Net Result	25,525

7. RECOMMENDATIONS TO THE FULL CONFERENCE

The Executive Committee recommends the following to the Full Conference:

- Adopt the new and revised procedures and guidelines recommended by the technical committees and group as listed in the report of the Quality Systems Group
- Delete and remove the procedures and guidelines from the ITTC Recommended Procedures and Guidelines, as being obsolete as listed in the report of the Quality Systems Group
- Adopt the revised Register of ITTC Recommended Procedures and Guidelines as prepared by the Quality Systems Group
- Adopt the revised ITTC Rules as reflected in the revised procedure 1.0-01
- Adopt the committee structure and Terms of Reference for the 30th ITTC as presented in the appendix to the Proceedings of the 29th ITTC Conference
- Accept the proposed chairs and members of the technical committees and groups
- Accept that the Executive Committee continues the working group to consider the future of ITTC

The Advisory Council
Report to the 29th ITTC

1. MEMBERSHIP AND MEETINGS

The membership of the 29th Advisory Council consisted of 39 organisations. One new organisation, Akishima Laboratories (Mitzui Zosen), Japan, was admitted to the Advisory Council.

Prof. Gerhard Strasser was elected Chairman and Dr. Takuya Omori Vice Chairman. Mr. Aage Damsgaard was appointed Secretary. Dr. Omori resigned from JMUC in 2020, and Prof. Daisuke Kitazawa, University of Tokyo, was elected.

The Advisory Council held two physical meetings since the last Conference, in Gdansk, Poland, September 2018, and in Val de Reuil, France, September 2019. As a new initiative, the technical committee chairs were invited to attend the second AC meeting and, except for two, all attended. This was generally valuated as a good initiative and will be considered for the next period as well. The third meeting was planned for March, 2020, in Tokyo, Japan, but was cancelled due to the worldwide pandemics situation. Instead, a virtual meeting was held in March,2021, and another virtual meeting was held in May, 2021. Finally, a meeting will be held in connection with the virtual conference in June, 2021.

The roles and responsibilities of the Advisory Council as defined in the ITTC Rules are primarily to support the Executive Committee on all technical matters.

2. ACTIVITIES OF THE ADVISORY COUNCIL

2.1 Kick-off Meeting with Technical Committees

The kick-off meeting with technical committees implemented at the 26th Conference was repeated at subsequent conferences where also the chairman of the Quality Systems Group has participated and given his contribution to securing an efficient start-up of the committee activities. It is planned that these kick-off meetings shall be held also in the future, and that the QSG Chairman shall attend.

2.2 Review of the Work of the Technical Committees and Groups

The new format of progress reporting from the committees to the Advisory Council implemented during the last term has been used throughout the 29th ITTC. The new progress report template, among other changes, defines clearly which procedures and guidelines have to be reviewed by which committee.

The technical committees and group submitted more than 60 revised or new procedures for review by the Advisory Council and proposed a number of procedures to be deleted. With such a large number of documents, it is evident that keeping deadlines, as well as maintaining a high standard of the procedures is crucial. During this period, about 65% of all "final" procedures had to be returned to the committees for further corrections following the last AC review, and some even had to go back to the committees once more. Should the AC review procedures have been taken literally, all these procedures would have been postponed to the next period.

During the final review of procedures, it became evident that several procedures dealing with uncertainty analysis were using outdated references that should have been revised this term. In addition, some examples contained in the procedures were not consistent with other ITTC procedures. This was discovered too late to revise all the procedures (about 20 dealing with uncertainty analysis), so it will be defined as tasks for the next committees to revise all the faulty procedures and include consistent examples. The procedures in question will have a note of concern to this effect.

2.3 Advisory Council Working Groups

As in the recent periods, the work of the Advisory Council was organised in four working groups, each dealing specifically with the work of selected committees. This time the distribution of committees between the AC working groups was as shown in the table below

WG 1	WG 2	WG 3	WG 4
SC on Combined CFD/EFD Methods	Resistance and Propulsion	Manoeuvring	Ocean Engineering
SC Ice	SC Operation of Ships at Sea	Seakeeping	SC Environmental Modelling
SC Hydrodynamic Noise	SC Energy Saving Methods	Stability in Waves	SC Hydrodynamic Testing of Marine Renewable Energy Devices
		SC Manoeuvring in Waves	

The work of the Quality Systems Group was monitored by the AC Chairman.

The main responsibilities of the working groups are to review committee progress reports, review procedures and guidelines and define the Terms of Reference for the next committees. In order to use the time at the AC meetings efficiently, the working groups as far as possible perform their review before the meetings. This is of course possible, only, if the documents are submitted timely by the committees. The meetings are then used to consolidate the comments resulting from the review in discussions with the entire AC and preparing responses to the committees.

2.4 ITTC Recommended procedures

A total of about 80 procedures and guidelines was prepared by the committees and group, some new, some with major revisions and most with minor revisions. The report from the Quality Systems Group contains a detailed account of the work with procedures and guidelines.

In addition to the revisions of the contents of the procedures and guidelines, all had a new title page layout, including a general disclaimer.

The proposed new Register of ITTC Recommended Procedures and Guidelines has been published on the ITTC website.

2.5 Technical Committees for the 30th ITTC

Several proposals for new specialist committees were tabled for the Advisory Council, partly by the present committees and partly by AC members. After discussion in the AC, it was recommended to establish the following committees for the 29th ITTC.

General committees
Resistance & Propulsion
Manoeuvring
Seakeeping
Ocean Engineering
Stability in Waves
Full Scale Performance

Specialist committees
Ice
Ocean Energy Devices
Combined CFD/EFD Methods
Cavitation and Noise
Wind Powered Ships

Groups
Quality Systems Group

Despite the fact that some of the specialist committees had already been running for two periods, it was agreed that they should continue through the next period, albeit with a new title.

2.6 Cooperation with IMO

The Advisory Council, represented by its Chairman, has continued to actively be involved in activities concerning EEDI and GHG-emissions.

3. OFFICERS FOR THE 30TH ITTC ADVISORY COUNCIL

Prof. Gerhard Strasser was reappointed as Chairman for the 30th ITTC Advisory Council and Prof. Daisuke Kitazawa as Vice Chairman.

Resistance and Propulsion Committee
Final Report and Recommendations to the 29th ITTC

1. INTRODUCTION

1.1 Membership and meetings

The members of the Resistance and Propulsion Committee of the 29th ITTC were:

- Richard Pattenden (Chair)
  QinetiQ, United Kingdom
- Nikolaj Lemb Larsen (Secretary)
  FORCE, Denmark
- João L. D. Dantas
  IPT, Brazil
- Bryson Metcalf
  Naval Surface Warfare Center, Carderock Division, USA
- Wentao Wang
  China Ship Scientific Research Centre, China
- Yasuhiko Inukai
  Japan Marine United Corporation, Japan
- Tokihiro Katsui
  Kobe University, Japan
- Seok Cheon Go
  HHI, South Korea
- Haeseong Ahn
  KRISO, South Korea
- Patrick Queutey
  ECN, France
- Devrim Bulent Danisman
  Istanbul Technical University, Turkey
- Yigit Kemal Demirel
  University of Strathclyde, United Kingdom
- Aleksey Yakovlev
  Krylov State Research Centre, Russia

Four meetings were held during the term of the committee:

- QinetiQ, Gosport, United Kingdom, 16-18 January 2018.
- Japan Marine United Corporation, Yokohama, Japan, 23-24 October 2018.
- FORCE, Copenhagen, Denmark, 8-9 May 2019.
- KRISO, Daejeon, South Korea, 14-16 January 2020.

1.2 Tasks

The 28th ITTC recommended the following tasks for the 29th ITTC Resistance and Propulsion Committee:

1. Update the state-of-the-art for predicting the performance of different ship concepts emphasizing developments since the 2017 ITTC

Full Conference. The committee report should include sections on:

a. The potential impact of new technological developments on the ITTC, including, for example superhydrophobic materials, new types of propulsors (e.g. hybrid propulsors), azimuthing thrusters, cycloidal propellers, propulsors with flexible blades and rim drives.

b. New experimental techniques and extrapolation methods

c. New benchmark data

d. The practical applications of computational methods to performance predictions and scaling.

e. New developments of experimental and computational methods applicable to the prediction of cavitation.

f. The need for R&D for improving methods of model experiments, numerical modelling and full-scale measurements.

2. During the first year, review ITTC Recommended Procedures relevant to resistance, propulsion and performance prediction, including CFD procedures, and a. identify any requirements for changes in the light of current practice, and, if approved by the Advisory Council, update them, b. identify the need for new procedures and outline the purpose and contents of these.

3. Develop a new procedure for wave profile measurement and wave resistance analysis.

4. Develop a procedure for verification and validation of the detailed flow field data.

5. Cooperate and exchange information with the Specialist Committee on Energy Saving Methods on subjects of common interest.

6. Cooperate and exchange information with the Specialist Committee on Ships in Operation at Sea regarding consequences of EEDI, especially with respect to ITTC Recommended Procedures.

7. Investigate the need of change of standard hull and propeller roughness. Develop and propose new roughness correction methods for both hull and propeller.

8. Conduct the validation of the procedure 7.5-02-03-01.7, 1978 ITTC Performance Prediction Method for Unequally Loaded, Multiple Propeller Vessels.

9. Continue with the monitoring of existing full scale data for podded propulsion. If there is available data, refine the existing procedure.

10. Continue the benchmark campaign with regard to the examination of the possibilities of CFD methods regarding scaling of unconventional propeller open water data. Continue comparative CFD calculation project.

11. Continue with monitoring the use of and, if possible, develop guidelines for quasi-steady open water propeller and propulsion model tests.

12. Conduct a survey of cavitation erosion modelling and predicting methods and identify the need of change of ITTC procedures in this respect.

13. Identify the need of the elaboration of the procedure concerning the rim drives model testing and performance prediction. Elaborate the procedure when necessary.

14. Identify the influence of the new FD definition on power prediction.

15. Investigate the need of changing the standard criterion for Re in model tests of

propulsors as well as in the aspect of CFD validation.

16. Investigate the need of change of scaling methods with regard to propulsors (including pods).

17. Investigate and describe a propulsor performance in waves, and discuss the scale effects on its modelling.

2. STATE OF THE ART

2.1 Technological developments

Composite propellers are one of the technologies that are gathering attention for improving efficiency and reducing cavitation and noise. Many papers on composite propellers were presented at SMP'19.

Grasso et al. (2019) presented the measurement results for the deformation of composite propellers not only at model scale but also at ship scale, which contributed valuable knowledge on the full scale hydro-elastic behaviour to exploit the full potential of this technology. The Digital Image Correlation (DIC) technique was used for measuring the deformation. This technique is an image analysis method that tracks and correlates the grey value pattern in small square groups of pixels called subsets. The commercial software, Vic3D, was used for the DIC analysis to perform the camera system calibration, calculate the displacements and output the results for post-processing. To filter out the effect of the non-periodic higher frequency blade vibrations, a surface averaging procedure was developed. Model scale tests were conducted using two composite propellers operating in non-uniform flow in a cavitation tunnel, with a wake generator mounted inside the tunnel (Figure 1 and Figure 2). After confirming the accuracy of the measurement system at model scale, the full scale measurements were performed during a sea trial on the Royal Netherlands Navy Diving Support Vessel "Nautilus", equipped with a flexible composite propeller. The measurement system was composed of two cameras on the rudder and two sets of strobe lights synchronized with the propeller shaft and camera that are mounted on the rudder and on the hull (Figure 3). In spite of more challenging conditions, i.e. underwater visibility, cavitation and vibrations, compared to the model test, excellent measurement quality was achieved and the blade deformations were delivered with an accuracy comparable to the test at model scale (Figure 4).

Shiraishi et al. (2019) developed a different measurement technique for the deformation of a composite propeller. They used combination-line CCD cameras to measure the amount of deformation of a five bladed, highly skewed propeller made from a carbon filled nylon material (Figure 5). From the amount of deformation measured, the deformed 3D blade shape was estimated using an image-registration in which the deformation was assumed to be represented by a rotation matrix and a translation vector (Figure 6). This measurement technique was utilized by Suyama et al. (2019) who conducted an exhaustive study to predict the performance of a composite propeller. They compared calculations using Fluid-Structure Interaction (FSI) analysis, which combines Computational Fluid Dynamics (CFD) and Finite Element Analysis (FEA), with experiments on the performance in uniform flow and wake flow. The amount of deformation for the same highly skewed propeller as Shiraishi et al. was measured. The difference in the performance and the deformation between propellers made from two kinds of material, i.e. aluminium and carbon, could be well predicted and it was concluded that FSI analysis can be useful for a design of a composite propeller.

Figure 1: Camera setup in the cavitation tunnel (Grasso et al., 2019)

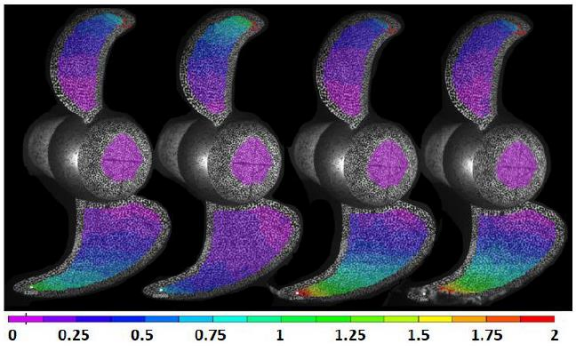

Figure 2: Example of variation in total blade deflection at the tip (Grasso et al., 2019)

Figure 3: Stereo camera setup installed on the port side of the diving support vessel "Nautilus" (Grasso et al., 2019)

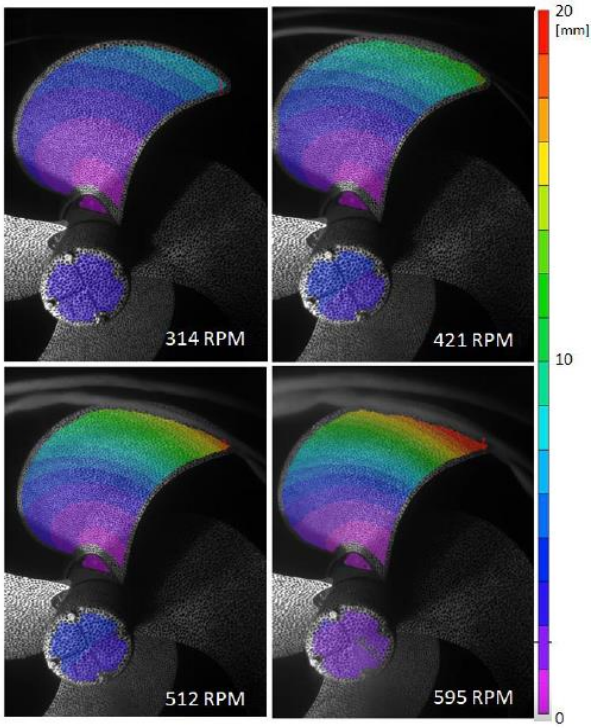

Figure 4: Propeller deflection with only one propeller engaged at increasing RPM (Grasso et al., 2019)

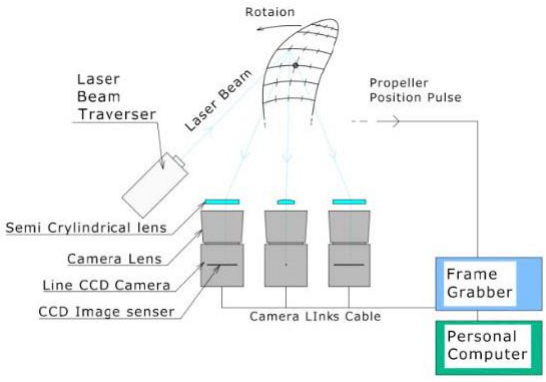

Figure 5: Schematic of measurement system using line CCD cameras (Shiraishi et al., 2019)

Aktas et al. (2019) presented numerical and experimental investigations on a new propeller noise mitigation method, PressurePores^{TM}. This technology implements pressure-relieving holes (PressurePores^{TM}) on marine propellers to

mitigate the cavitation induced noise for a more silent propeller. The results showed a significant reduction of cavitation noise (up to 17dB) with the pressure pores while losing only 2% of propeller efficiency.

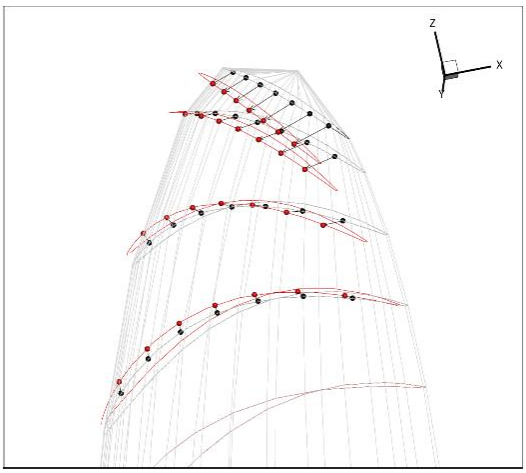

Figure 6: Estimated wing section positions of the model propeller from the deformation measured using line CCD cameras

Figure 7: PressurePores™ as applied on the Princess Royal propeller (Aktas et al., 2019)

Klinkenberg et al. (2017) carried out an experimental campaign to evaluate the performance of a rim-driven tunnel thruster model. The results presented focus on the noise measurements. They found disturbances in signals believed to be due to undesired electromagnetic current, inadequate grounding or engine control switches. Furthermore, for the complex set-up developed in-house, shown in Figure 8, they discussed the challenges and issues encountered during the experiments.

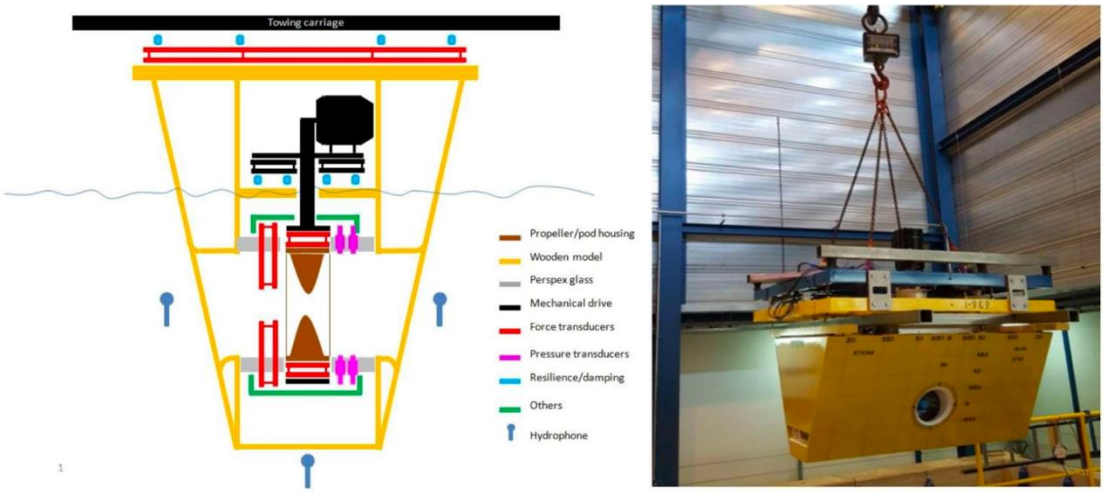

Figure 8: Experimental setup to measure performance of rim driven tunnel thruster (Klinkenberg et al., 2017)

2.2 Experimental techniques and extrapolation methods

Hiroi et al. (2019) conducted the full scale measurement for flows around a duct, fitted to a 63,000DWT bulk carrier, using PIV (Figure 9). Underwater noise and propeller induced pressure fluctuations were also measured in the project. Wake data on the two planes shown in Figure 9 were recorded in 2D2C (2-Dimensions, 2-Components) and transformed afterwards into 0D2C (0-Dimensions, 2-Components) data by spatial averaging. The measured data was compared with RANS simulation by Sakamoto et al. (2020). CFD showed good agreement as shown in Figure 10 and the authors claimed that the surface roughness will be one of the indispensable parameters to be considered for CFD simulations in full scale.

Inukai (2019) conducted the full scale measurement at the stern of a 14,000 TEU container ship using Multi-Layered Doppler Sonar (MLDS) which is an acoustic Doppler sonar capable of measuring relative water velocity at multiple arbitrary depths along an ultra-sonic beam. Although the largest obstacle against the measurements of flow fields at full scale is the complexity and high cost associated with the measurement system, an MLDS is less expensive and easier to install and handle compared with other methods such as LDV or PIV because it uses the same hardware as the commercially available Doppler Sonar. Velocities in six directions of the ultrasonic beam transmitted from the transducer can be measured. They showed that MLDS can measure velocities within a reasonable accuracy and offers good validation data for CFD calculations. Figure 11 shows the measurement area of the MLDS and a comparison of velocities in the ultrasonic beam direction between the measurement and the RANS simulation.

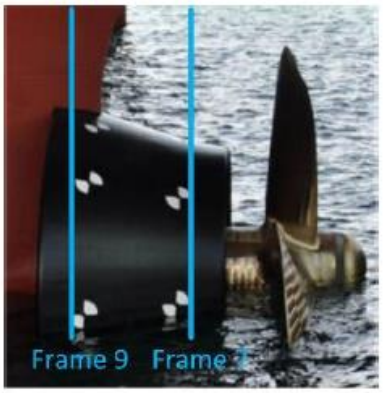

Figure 9: Photo of a duct around which flow was measured using PIV (Hiroi et al., 2019)

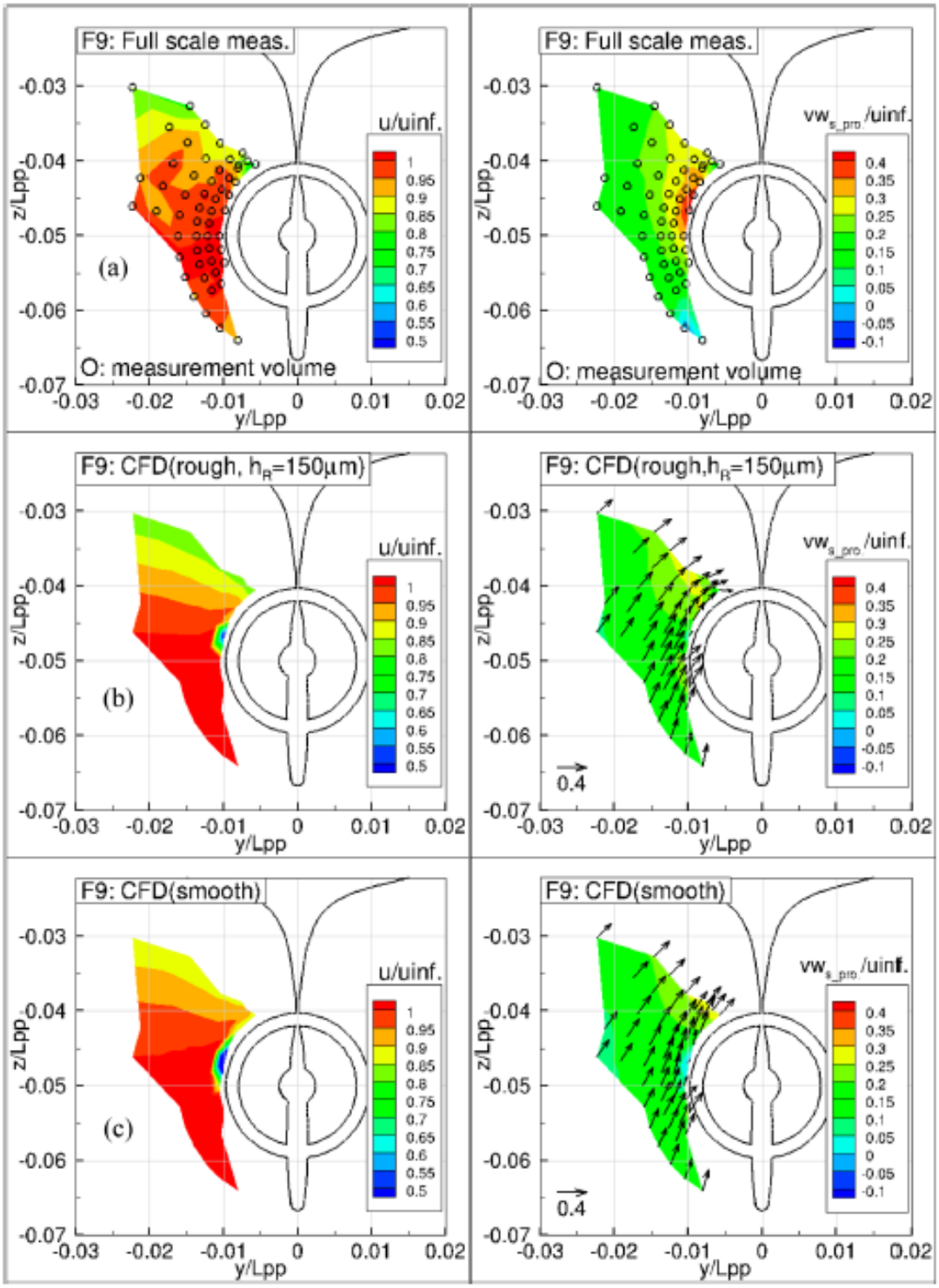

Figure 10: Experimental and computational results of total wake distribution; (a) PIV, (b) CFD with roughness, (c) CFD without roughness (Sakamoto et al., 2020)

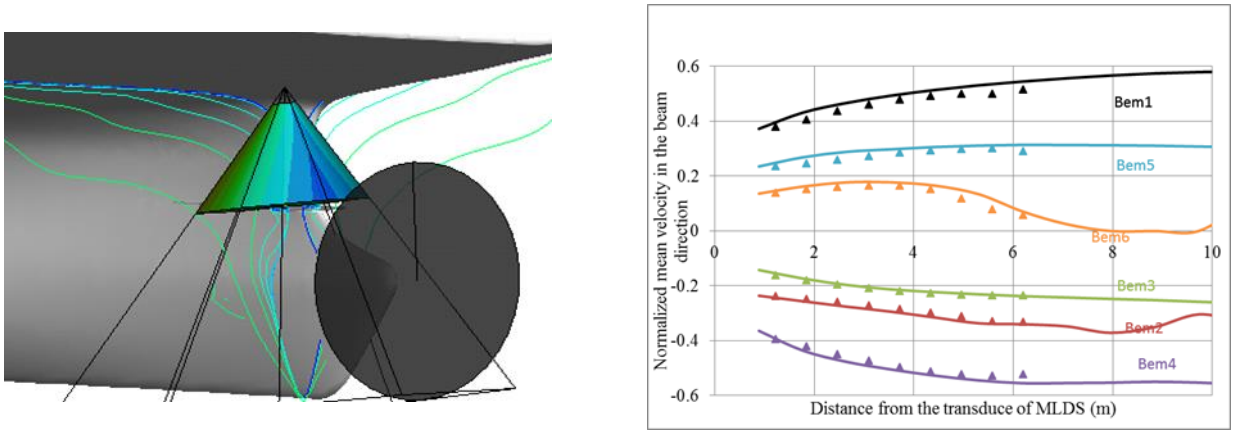

Figure 11: Measurement area by MLDS (left) and comparison of normalized mean velocity in the ultrasonic beam direction between CFD (lines) and measurement (marks) (right) (Inukai, 2019)

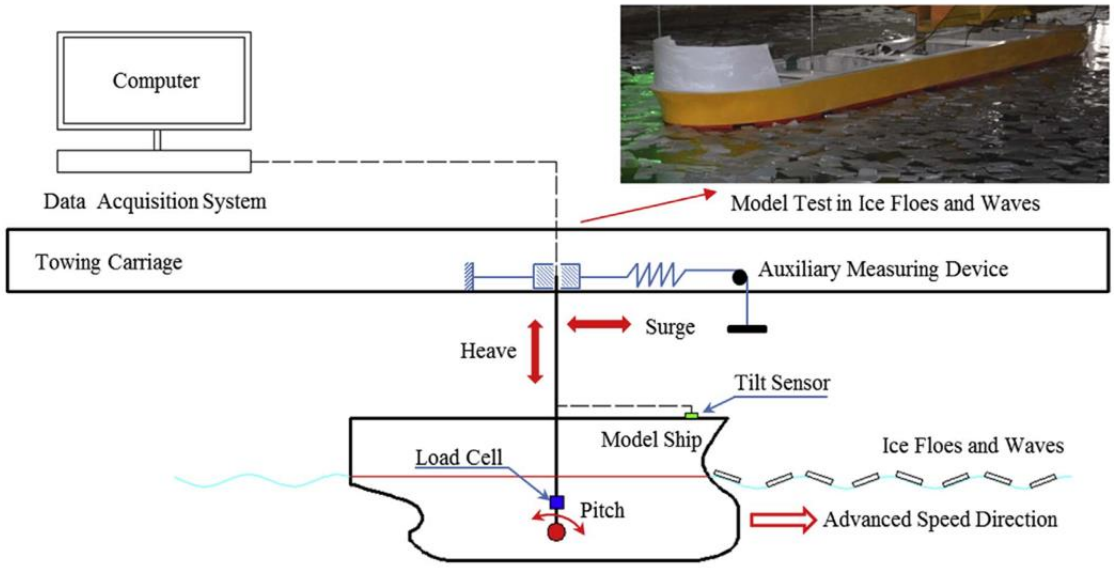

Figure 12: Experimental setup for test in MIZ (Luo et al., 2018)

Ravina and Guidomei (2018) developed an air-bubbling technique for resistance reduction. An original, customised, pneumatic distribution circuit was designed for the air-bubbling and it was applied to different types of flat plates and a hull model. From the towing tests of the plates and hull models, the effective shape of air bubbles is observed while measuring the local skin friction. The result showed that the advantage of air bubbling is more evident at high speed. Also, they concluded that using fewer holes with larger diameters compared favourably to using more holes with a smaller diameter.

Luo et al. (2018) carried out an experimental campaign to investigate the ship-wave-ice

interaction in marginal ice zones. Using paraffin as model ice, the ship model test was conducted at a towing tank equipped with a wave generator. The results showed that the motion of the ship model is more unstable in marginal ice zones than in ice floes (Figure 12).

Song et al. (2021a) conducted tank testing of a flat plate and a model ship in smooth and rough surface conditions to examine the validity of using Granville's similarity law scaling (1958; 1987) for predicting the roughness effect on the resistance of a 3D ship hull (Figure 13). Conducting the towing test of the flat plate, the roughness function of the given roughness was determined and used to predict the frictional resistance of the model ship in the rough condition. The total resistance of the model ship was predicted using conventional hypotheses of Froude and Hughes and compared with the experimental result of the rough model ship. The results showed a good agreement.

Demirel et al. (2017) conducted an extensive series of towing tests of flat plates covered with artificial barnacle patches to find the roughness functions of barnacles with varying sizes and coverages. Different sizes of real barnacles, categorised as small, medium and big regarding their size, were 3D scanned and printed into artificial barnacle patches. From the experimental results, they determined the roughness functions of barnacles with varying sizes and coverages (Figure 14).

Song et al. (2021b) investigated the effect of heterogeneous hull roughness on ship resistance. In addition to the homogeneous hull conditions (i.e. smooth and rough conditions), heterogeneous hull roughness conditions (i.e. bow-rough, ¼-aft-rough, ½-bow-rough and ½-aft-rough conditions) were realised by applying sand grit on the hull systematically and towing the Wigley hull model in forward and backward directions. The bow-rough conditions (i.e. ¼-bow-rough and ½-bow-rough) showed larger added resistance compared to the aft-rough conditions (¼-aft-rough and ½-aft-rough) with the same wetted surface area of the roughness region.

Guo et al. (2018) proposed an experimental technique using a stereoscopic underwater particle image velocimetry (SPIV) system to identify the flow characteristics in the wake of a ship model. Using the proposed methodology, the bilge vortex, propeller boss cap vortex, and hook speed contour structure were analysed (Figure 18).

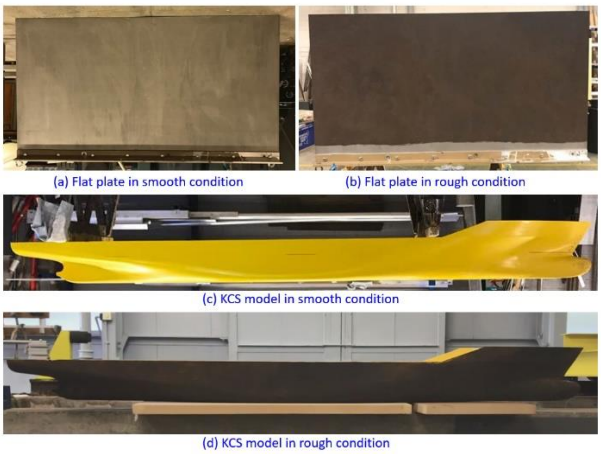

Figure 13: Flat plate and model ship in smooth and rough surface conditions (Song et al., 2021a)

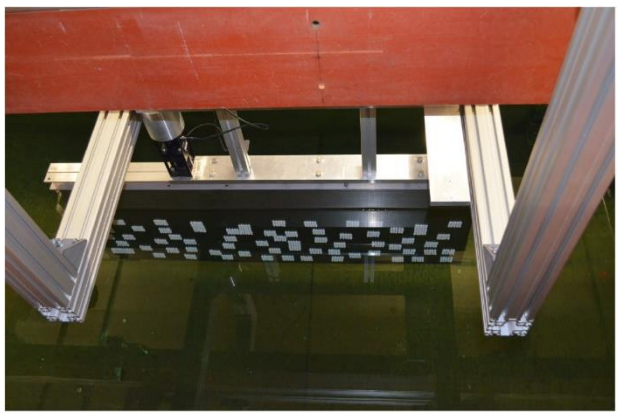

Figure 14: Flat plate with barnacle cluster roughness elements (Demirel et al., 2017)

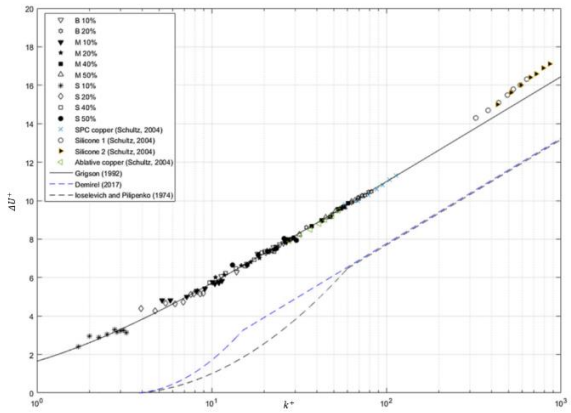

Figure 15: Roughness functions of different barnacle surfaces (Demirel et al., 2017)

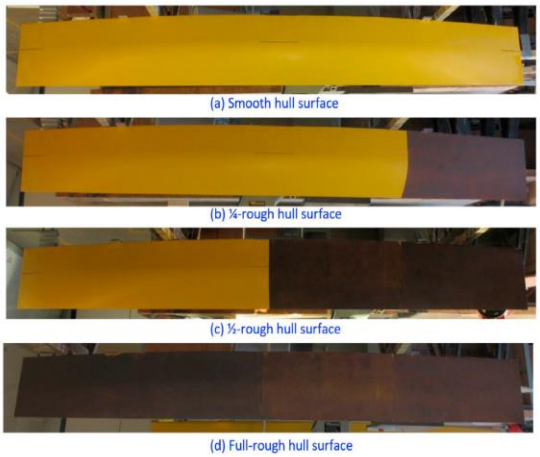

Figure 16: Wigley hull with different surface conditions (Song et al., 2021b)

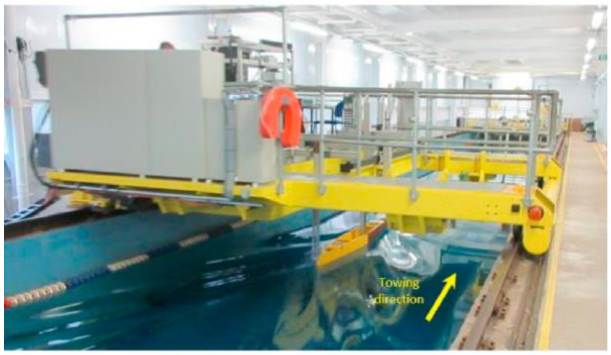

(a) ½-bow-rough condition

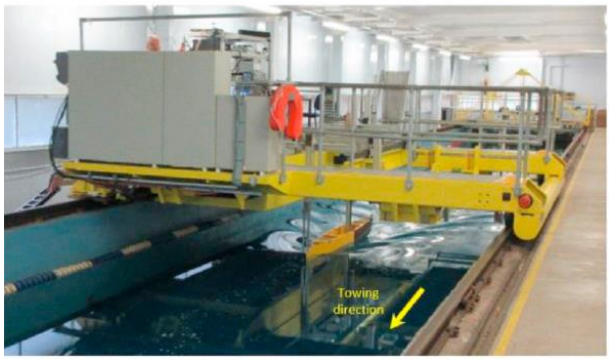

(b) ½-aft-rough condition

Figure 17: The towing carriage of the Kelvin Hydrodynamics Laboratory and the Wigley model; (a) ½-bow rough condition, (b) ¼-aft rough condition (Song et al., 2021b)

Dogrul et al. (2020) conducted CFD simulations of a containership (KCS) and a tanker (KVLCC2) at different scales to investigate the scale effects of the ship resistance components and form factors. The results showed that the scale effects of the ship resistance components significantly differ between the two hull types, and these differences lead to different compliances in the resistance extrapolations. They compared the total resistance predictions obtained from different extrapolation methods against the full-scale CFD simulation results. The result showed that the Froude's 2D extrapolation shows a better agreement for KCS than Hughes' 3D extrapolation. Contrarily, for KVLCC2, Hughes' 3D method showed a better agreement than the 2D method (Figure 19).

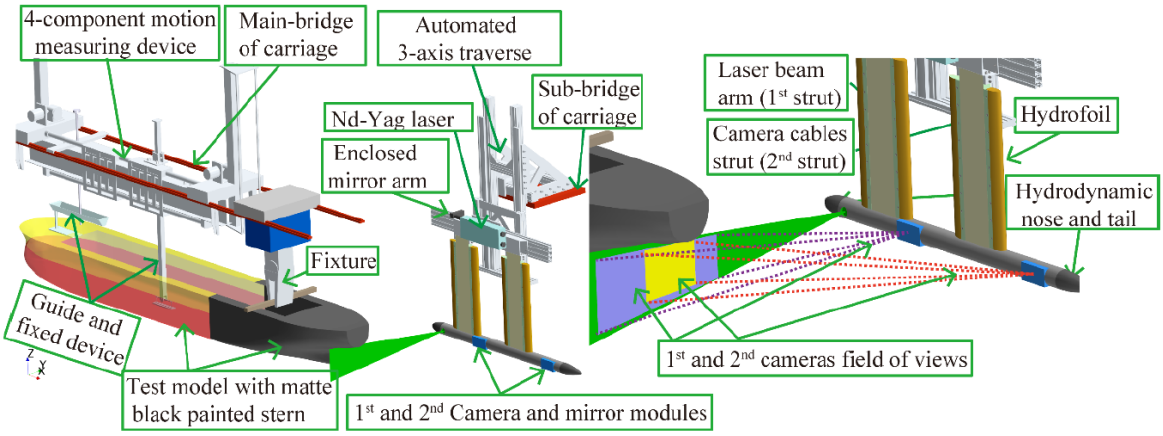

Figure 18: SPIV set up with a test model (Guo et al., 2017)

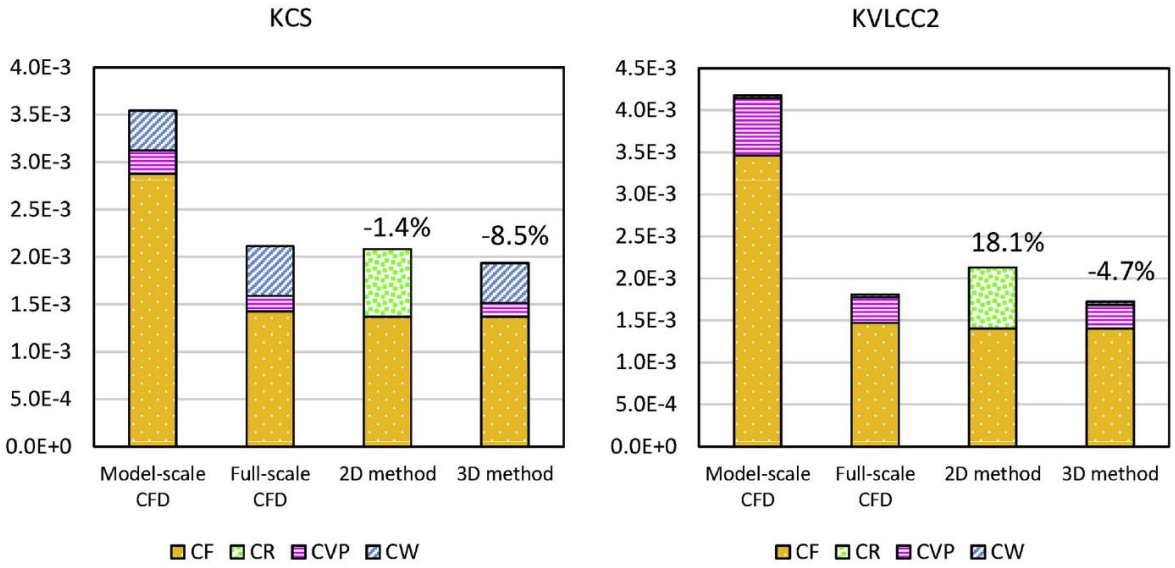

Figure 19: Resistance components from the CFD simulation and the different extrapolation methods for KCS (left) and KVLCC2 (right) (Dogrul et al., 2020)

Ravenna et al. (2019) presented a towing tank study to assess the effect of different configurations of biomimetic tubercles on a flat plate (Figure 20). They used 3-D printed tubercles inspired by humpback whales and the plate was towed at a speed range of 1.5 – 4.5 m/s. The results showed that when these tubercles, where positioned in rows upstream or downstream of the flat plate, the hydrodynamic resistance of the plate was reduced up to 1.3% compared to the bare flat plate.

Charruault et al. (2017) proposed an experimental technique to characterize the free-surface topology and air losses at the cavity closure. A Dot Tracking Algorithm (DTA) based on the Particle Tracking Velocimetry was implemented with a synthetic Schlieren method to measure strong curvature more accurately

than with a standard Digital Image Correlation method. It was shown that the capillary waves travelling on the cavity interface could be measured using the newly developed method (Figure 21 and Figure 22).

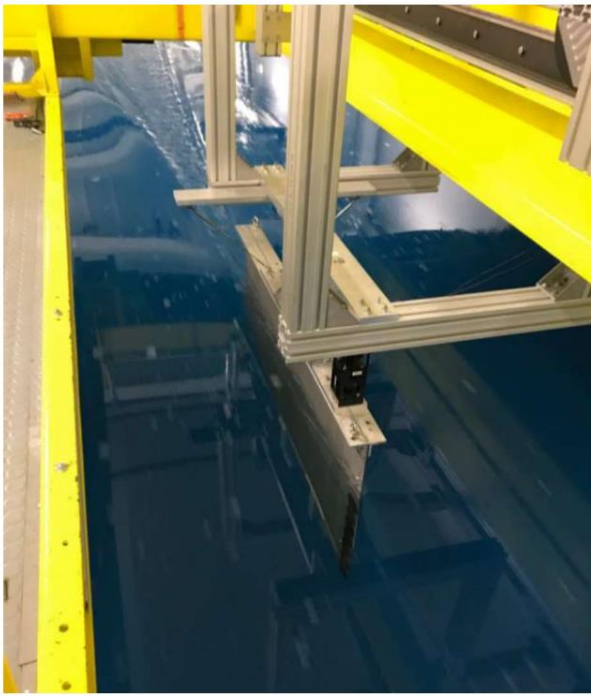

Figure 20: Flat plate towed at 4.5 m/s (Ravenna et al., 2019)

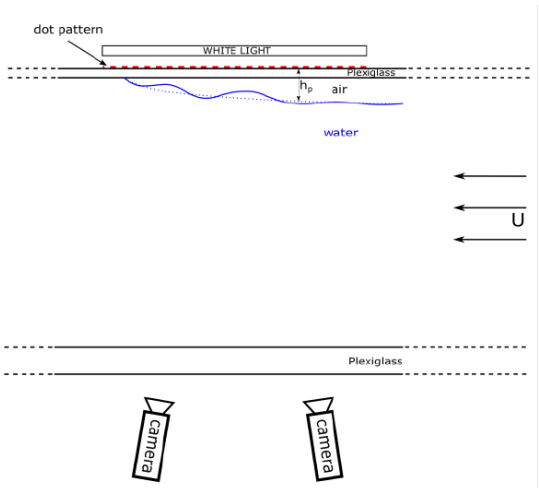

Figure 21: Two cameras in stereo configuration looking at the dot pattern through the bottom of the cavitation tunnel open test section (Charruault et al., 2017)

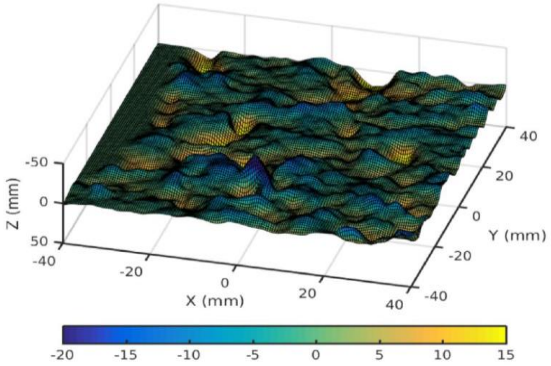

Figure 22: Free surface topology of the cavity closure (Charruault et al., 2017)

Delfos et al. (2017) conducted PIV measurements to investigate the flow characteristics over a smooth compliant coating in a cavitation tunnel at high Reynolds numbers (flow velocities of 1-6 m/s). They used high-speed Background Oriented Schlieren measurements to determine the instantaneous deformation of the compliant coating surface. At velocities of 1-4 m/s, the elastic surface formed large scale undulations that travel with a high velocity over the interface, but their amplitude was lower than the viscous sublayer such that they do not affect the skin friction. On the other hand, at higher speeds, slender trails were observed on top of the undulations and acted as artificial flow-induced roughness increasing the friction (Figure 23).

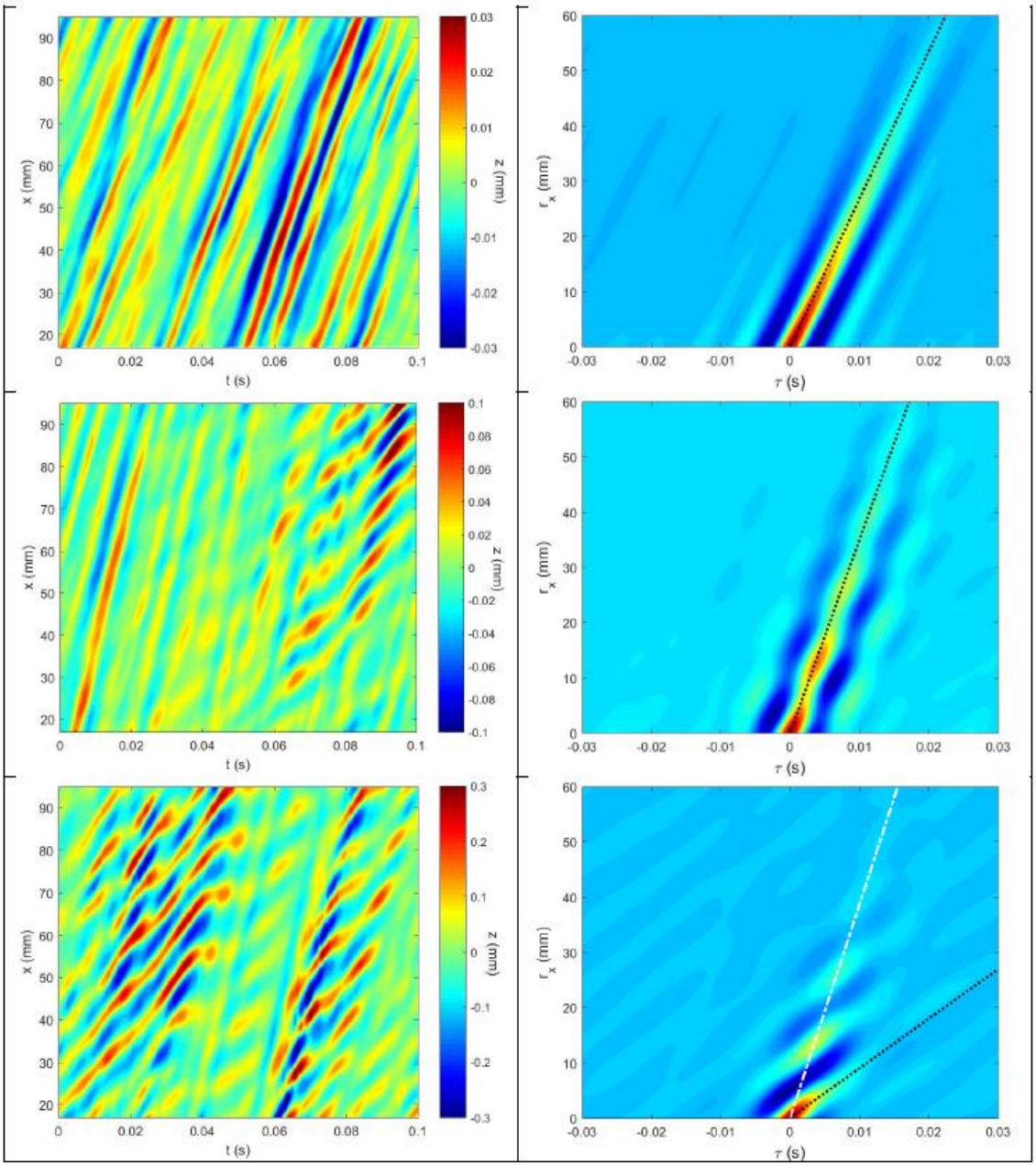

Figure 23: Measurements of surface deformation of compliant coatings by Delfos et al. (2017)

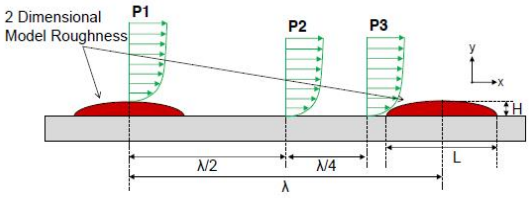

Fig. 7 – Parameters of 2 dimensional artificial roughness and measurement positions (Side view)

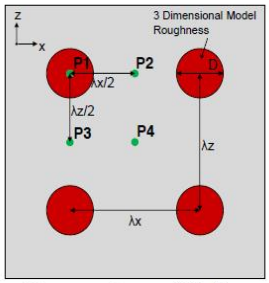

Fig. 8 – Parameters of 3 dimensional artificial roughness and measurement positions (Top view)

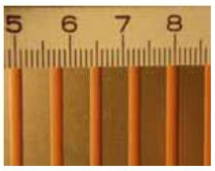

Fig. 9 – 2D-L

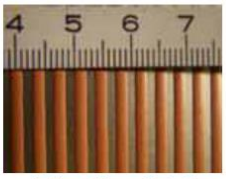

Fig. 10 – 2D-S

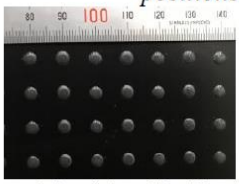

Fig. 11 – 3D-H

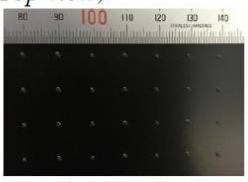

Fig. 12 – 3D-L

Figure 24: Measurements by Hiroi et al. (2017) of 2D and 3D artificial roughness

Hiroi et al. (2017) used two-dimensional (2D) and three-dimensional (3D) artificial roughness to investigate the relation between skin friction and the geometric roughness parameters such as roughness height, slope and wavelength. Using Laser Doppler Velocimetry (LDV) the turbulent boundary layers over the surfaces with artificial roughness were measured and a comprehensive review was made on the relationship between the roughness parameter and the turbulence statistics (Figure 24).

Guzel (2017) presented an experimental approach to observe the change in hydrodynamic friction due to hydrophobicity. A cylindrical Taylor-Couette flow setup consisting of an inner cylinder that rotates with an angular velocity within a stationary concentric larger outer cylinder has been constructed (Figure 25). The drag reduction due to hydrophobicity was observed over a range of Reynolds numbers in the measured torque on the inner cylinder.

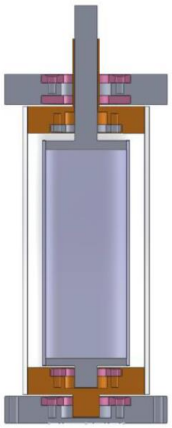

Figure 25: Sketch of the Taylor Couette setup of Guzel (2017)

Greidanus et al. (2017) performed force and PIV measurements of the interaction of smooth compliant coatings with turbulent boundary layer flow at high Reynolds numbers. They found that the skin friction, mean velocity profiles and turbulent statistics are different from the smooth flat plate only at free stream velocities (FSV) beyond the transition of 4.5 m/s (Figure 26).

Fabio et al. (2017) developed a methodology to investigate the interaction between air bubbles and turbulent flow. In order to obtain a simultaneous measurement of the water velocity field and of the bubbles size, shape and orientation, the Particle Image Velocimetry (PIV) has been used, combined with Laser-Induced Fluorescence (LIF). The image analysis allows a proper detection and separation of the two phases with a subsequent accurate analysis of the liquid phase (Figure 27).

Fabbri et al. (2017) developed an experimental technique using a marine biofilm flow-cell in which biofilms can either be cultured under flow or grown statically and then assessed under flow for drag and other properties. Using optical coherence tomography (OCT), the changes of physicomechanical properties of the marine biofilms during flow loading/unloading cycles were observed and compared to simultaneously collected frictional drag properties (Figure 28).

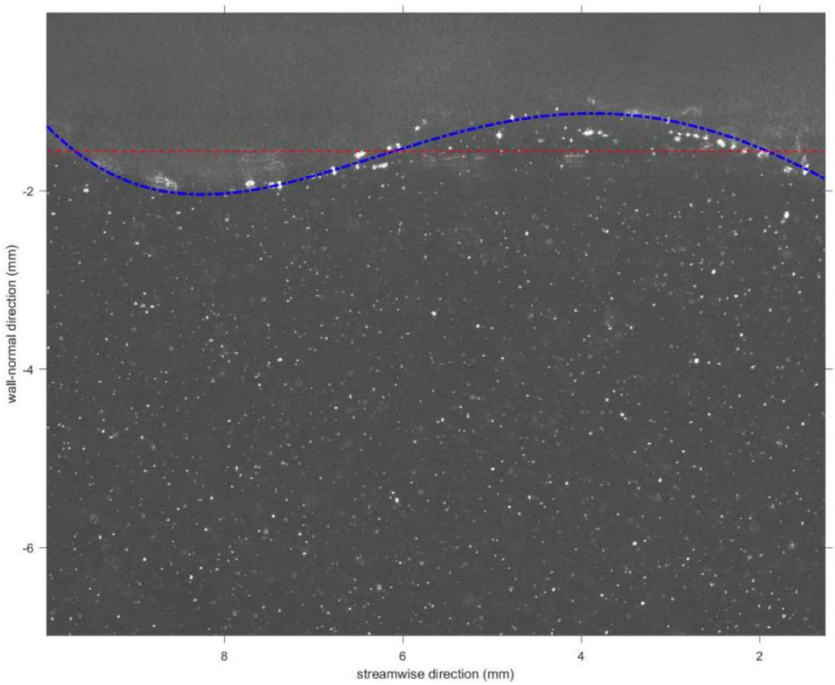

Figure 26: PIV images from measurements of interaction of smooth compliant coatings with turbulent boundary layer flow (Greidanus et al., 2017)

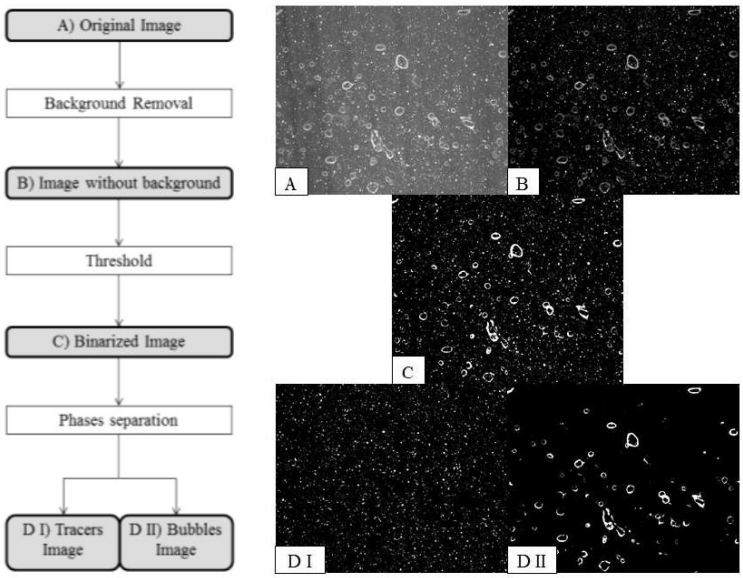

Figure 27: Measurement of interaction between air bubbles and turbulent flow using PIV and LIF (Fabio et al., 2017)

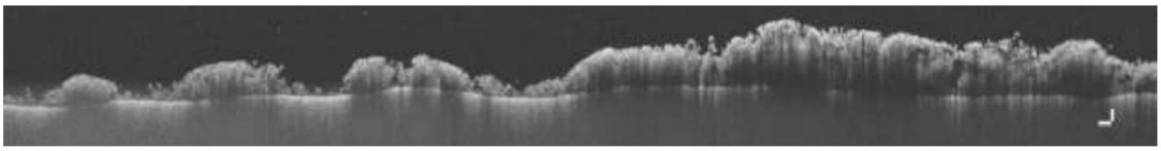

Figure 28: Cross-section of fouling biofilm on a coated panel fully immersed in the flow cell as imaged by optical coherence tomography (Fabbri et al., 2017)

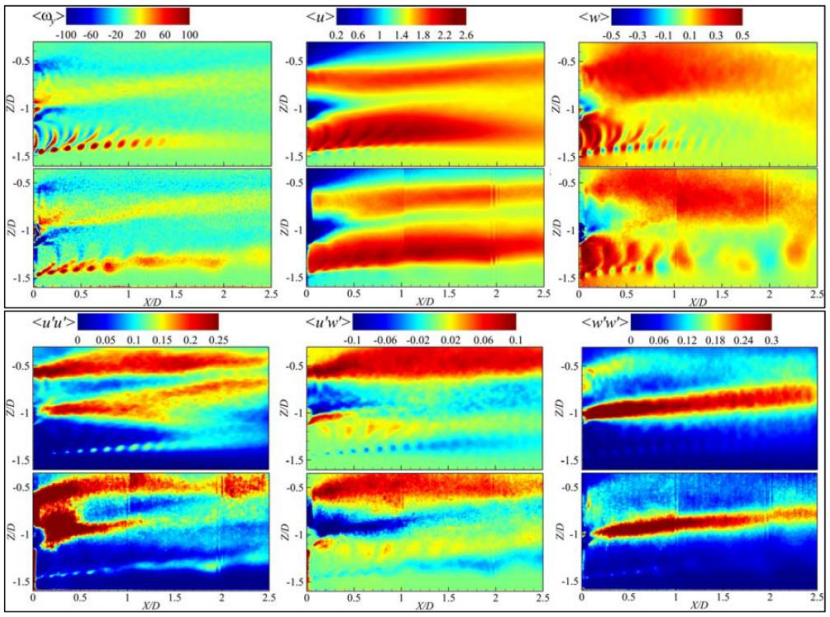

Figure 29: Phase averaged flow behind DARPA Suboff beneath free surface (Wang et al., 2019)

Wang et al. (2019) conducted experiments and CFD simulations of the DARPA Suboff submarine model fitted with the E1658 propeller with different immersion depths. The flow was measured in a phase-locked fashion using particle image velocimetry (PIV) in a cavitation channel, while CFD simulations were modelled with a single-phase level set approach to model the free. Both the experimental and numerical results showed strong interactions between the hull and free surface, producing higher local advance coefficients and blade loads near the free surface (Figure 29).

2.3 New benchmark data

The workshop, held in December 2015 in Tokyo, on CFD in hydrodynamics was the seventh in a series started in 1980 with the objective to assess up-to-date numerical methods of the current CFD codes for ship hydrodynamics (Hino et al., 2021). Three model scale ship hulls were selected with a total of 17 possible test cases specified by the organizers: (i) 5 cases for the KRISO Container Ship (KCS) already used in previous workshops; (ii) 9 cases for the Japan Bulk Carrier (JBC) equipped with a stern duct as an energy saving device (ESD); and (iii) 3 cases for the ONR Tumblehome model 5613 (ONRT) as a preliminary design of a modern surface combatant.

2.3.1 Available experiments

- JBC: towing tank tests at the Tokyo National Maritime Research Institute (NMRI) and Osaka University (OU) including resistance tests, self-propulsion tests and SPIV measurements of stern flow fields. Additional LDV/SPIV data in wind tunnel are available from the Technical University of Hamburg (TUHH).
- KCS: towing tank tests carried out at the Korea Research Institute of Ships and Ocean Engineering (KRISO), self-propulsion tests and also resistance tests at the NMRI. Data for pitch, heave and added resistance are also available from FORCE/DMI measurements.
- ONRT: this modern frigate model is appended with skeg and bilge keels; it also has rudders, shaft and propellers with shaft brackets. Free-running tests include course keeping, zigzag and turning circles in both calm water and regular waves performed at the IIHR Hydraulics Wave Basin Facility.

2.3.2 Participants and Methods

31 organizations have participated in the workshop with 12 submissions from in-house codes, 11 open-source codes and 13 commercial codes. The novelty here is the increase in the number of open-source codes compared with the previous Gothenburg Workshop where there were 14 in-house, 3 open-source and 16 commercial codes. The majority of methods use two-equation k-ω SST or k-ε turbulence models with no-slip wall boundary conditions. Wall-functions are also used, particularly by open-source or commercial codes. The technique of volume of fluid remains the most popular to take into account the free surface. The propellers are traditionally modelled though a body force approximation or represented directly as actual rotating propeller. Discretization is mostly based on finite volume for unstructured grids and pressure based equation to solve the incompressibility.

2.3.3 Results

The summary of the results is taken from the analysis and main conclusions of the various chapters dedicated to the different cases:

JBC: the mean signed comparison error for resistance (Measured-Computed)/Measured is around 1%, the same accuracy reported for the experimental data. The scattering of results is about 2% for towed cases and 4% for self-propulsion. In 2005 the standard deviation was 6% and reduced to 1% in 2010 similar to the 2015 deviations. The effect of the ESD is found to reduce the resistance by 1%, in agreement with the measurements. The accuracy of the methods through grid convergence is still difficult to reach as the order of accuracy is in many cases far from the theoretical order. Concerning the grid size, it is observed that 10M cells are needed to obtain a comparison error below 5% whereas the limit was 3M cells in 2010. It is reasonable to think that the increase in this limit is not so much the absolute need for more points as the increased use of automatic grid generators. To note the better accuracy when wall-functions are used as errors are twice higher with wall resolved.

Conclusions from the analysis of the self-propulsion and ESD performance predictions lead to an averaged absolute error of the model scale delivered power (DP) about 5% to 6%. The experimental value of the DP reduction rate due to the duct is 0.94 whereas the scatter of the predictions is between 0.88 and 1.0. It concludes that CFD estimation of ESD efficiency may not be sufficient for precise reduction of only few percent of this DP.

The major influence on the local flow analysis comes from the turbulence modelling. Non-linear anisotropic closure (EARSM) is now a good compromise although the vorticity is slightly under-predicted in some key stations. For the specific and simplest case of the naked hull no spectacular advantage was noticed with hybrid RANS/LES simulations compared to the best RANS models. However on the case with propeller and without ESD duct, only a hybrid model type was able to capture most of the fine flow details revealed by the phase-averaged measurements. The same comment holds for the ducted propeller about phase-averaged quantities where some URANS computations are in agreement with the measurements. Among the submissions, we would like to highlight the only contribution of wall-resolved LES computation of the double body model (4 billion cells) is in good agreement with measurements and particularly the level of turbulent kinetic energy in the core of the bilge vortex.

KCS: the mean comparison error for all 6 speeds is 0.43% and standard deviation 2.48% with higher error at low Froude simulations. The mean absolute error is 2% which remains in line with the 1.64% of the Gothenburg 2010 workshop. For the self-propulsion submissions the mean K_T and K_Q errors are 0.5% and 3.5% respectively, slightly better than the results of the previous workshop (-0.6% and -4.6%). In this case of captive (fixed rps) test, the body force approach gives slightly better parameters but, as expected, local flow predictions are improved when solving the actual propeller. There were 10 submissions for the assessment of CFD for added resistance of captive test in waves to lead to the overall result of an error of 13%. This error includes the result of the free-running ONRT tests for which the same level of error is observed on the speed loss.

ONRT: with this geometry the new interest in this workshop consisted in the study of free running in head, beam, following and oblique waves. Probably because of the high CPU cost for CFD, there were only 4 submissions, not all of them complete, to be analysed for comparisons with the motions and trajectories measured at IIHR. While high levels of experimental uncertainty are pointed out for some quantities, the numerical uncertainty remains high with a mean error still higher than 5%. Nevertheless, it was concluded that "*in view of the comparable CFD capability for ONRT free running vs. KCS captive conditions,*

the prognosis for CFD capacity is excellent". This first call for comparison on such a challenging case for the CFD will continue at the SIMMAN workshop to be held in 2021, during which this geometry will again be proposed as a validation test case.

2.4 Practical applications of computational methods to performance prediction and scaling

Ships intended for operation in shallow-water need to be tested in shallow model basin, but while blockage corrections for tank walls are well understood for deep water, there is no established procedure for applying a blockage correction for tank walls in a shallow-water test. Raven (2019) has proposed a method, based on the hypothesis that the overspeed induced by the tank walls is uniformly distributed across the tank's cross-section, which has been confirmed by computed flow fields. An algebraic equation is obtained for the overspeed induced by the tank walls, separately from that induced by shallow water. The change in volume flux that is required by this equation is obtained from a single potential flow calculation for each depth to be tested. The resulting overspeed is used to correct the resistance curve of the ship. The effects of the tank walls on dynamic sinkage was also studied and found to be substantial.

Computational techniques are increasingly being used to predict full-scale ship and propeller performance. As well as applying the traditional analysis techniques to these predictions, CFD solutions can be used to obtain richer information about the performance. An example of this is the application of energy loss analysis to a CFD prediction of the flow field around a propeller in behind condition as described by Schuiling and Terwisga (2018). In this study the authors propose a method by which the individual components of energy losses can be computed by calculating the integral energy equation on a control volume surrounding the propeller. This gives a breakdown of the losses into axial, rotational and viscous losses, enabling a more informed choice of design modifications, or energy saving device, based on the type and distribution of the losses. The method was demonstrated on a large diameter propeller, which showed a reduction in the axial losses. The use of an asymmetric stern to generate pre-swirl was shown to improve the rotational losses, but also to increase the axial losses.

2.5 Experimental and computational prediction of cavitation

RANS solvers have become a common tool for the prediction of sheet cavitation in the past decade. Recently, there has been a need for more accurate predictions of whole cavitation pattern, e.g. tip vortex cavitation (TVC), in response to various demands, including increasing attention to underwater noise radiated from the propeller, to protect marine mammals. To meet such demands, advanced methods such as LES and DES have been applied to describe more complicated phenomena.

Yilmaz et al. (2019) applied LES to analyse the tip vortex on the INSEAN E779a four bladed propeller with the Schnerr-Sauer cavitation model. To fully capture TVC, they developed a new mesh refinement method, called MARCS, composed of volumetric control method and adaptive mesh method. First, a spiral geometric mesh was generated by the volumetric control method in a region where the TVC may occur. The region was determined using an absolute pressure value specified as the threshold. The spiral mesh is then refined by the adaptive mesh method (Figure 30). Comparing the simulation results with the experiments, it was shown that

MARCS could reproduce the structure of TVC much better compared to a conventional mesh treatment (Figure 31).

Shin et al. (2018) used DES to predict TVC on a four bladed propeller with a rudder behind. They refined meshes around TVC using an adaptive mesh method based on the Q-criterion instead of the absolute pressure. They showed that the extent of TVC and the pressure fluctuation became closer to the experimental results by applying the adaptive mesh method. On the other hand, the high-order pressure pulses could not be simulated well because the TVC collapse at the rudder was not reproduced well, which required much finer meshes in the region where TVC interacted with the rudder. In order to accurately simulate TVC, the mesh generating strategy is most important and the adaptive mesh method is useful to effectively generate fine meshes around TVC.

The usage of LES and DES is shown in many papers in SMP'19. For example, Bhatt el al. (2019) calculated thrust break-down on a five bladed propeller using LES, and Kumar el al. (2019) and Paskin et al. (2019) evaluated tip vortices over a three dimensional hydrofoil with LES and DES respectively. All of them verified the accuracy of the calculations by comparisons with the model tests.

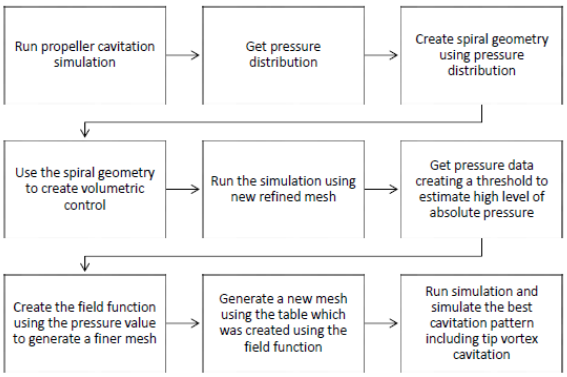

Figure 30: Flowchart summarizing new Mesh Adaption and Refinement approach for cavitation simulation (MARCS)

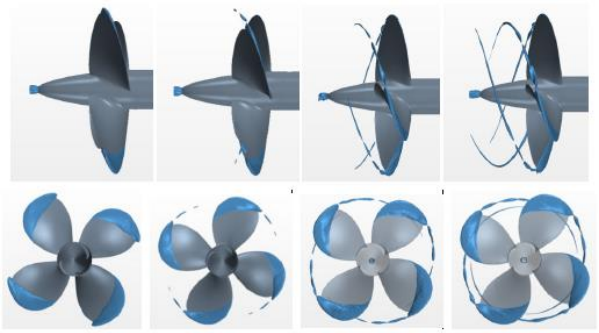

Figure 31: Improvement of tip vortex cavitation extension (From left to right; Result without mesh refinement, with tube refinement, with spiral geometry refinement and with mesh adaption refinement MARCS)

Zhang et al. (2019) presented a post processing technique against the obtained high speed images of a cavitating propeller. A phase congruency method was applied instead of the conventional brightness-gradient based method to detect the edges of cavitation structures, which enables the detailed illustration of the interface topology of the propeller cavitation. The weak tip vortex cavitation that is not apparent in the high speed images can be clearly detected (Figure 32). There are two methods of cavitation inception detection: the acoustic technique and optical or visual technique. It is known that those give different criteria for the inception, while this post processing technique might be used to explain the discrepancies between them.

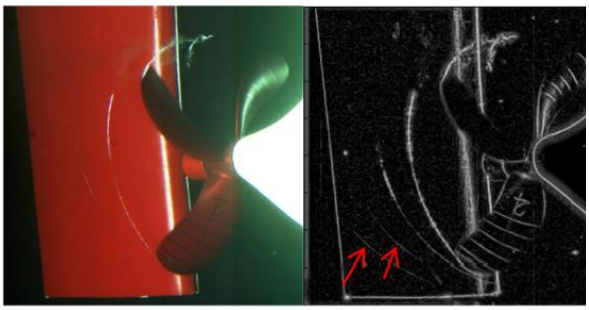

Figure 32: Cavitation topology obtained using the edge detection method (Zhang et al., 2019)

3. DEVELOPMENT OF PROCEDURE FOR WAVE PROFILE MEASUREMENT AND WAVE RESISTANCE ANALYSIS

The RPC committee was requested to develop a new procedure on wave profile measurement and wave resistance analysis. Generally, the purpose of observing, measuring or simulating the wave profile for a model ship at a given speed in a towing tank is to evaluate the ship hull form, and to reduce the wave resistance by modifying the ship hull form. Quantitative measurement techniques of wave height around the model ship free surface field include intrusive and non-intrusive techniques. Resistive and capacitive type wave gauges are widely used as intrusive methods. While non-intrusive techniques include optical sensors, acoustic sensors, radar, imaging methods, and combined laser-scanner and video hybrid systems. Although quantitative wave profile measurement is now mainly used for CFD validation, there is still a need to incorporate it in routine towing tank resistance tests to estimate the wave resistance in a more rapid way.

As a complementary procedure to resistance test in towing tank within ITTC recommended procedures, the main purpose of the new procedure is to provide guidance on the towing tank wave profile measurement and to analyze the wave pattern resistance. Since the single wave profile measurement is relatively rare in the commercial towing tank test, in order to incorporate the wave profile measurement with the routine resistance test, the widely used longitudinal wave cut method together with the Newman-Sharma Method for wave pattern resistance analysis is recommended for the procedure. An example of a wave pattern resistance calculation from wave profile measurement data is demonstrated in the appendix of the procedure. The recommended procedure is suggested to be numbered with 7.5-02-02-04, which is under the category of Resistance 7.5-02-02.

As for the further investigation on the model ship wave measurement, it is suggested for the next ITTC term to review the state-of-the-art of high Froude number surface ship wave breaking, which is multi-phase complex flow and is also difficult for both quantitative measurement and CFD simulation.

4. VERIFICATION AND VALIDATION OF DETAILED FLOW FIELD DATA

4.1 Introduction

This document does not pretend to provide an exhaustive answer to the question of Verification and Validation (V&V) of detailed flow field analysis in the area of ship hydrodynamics for resistance and propulsion. Instead, a review of recent published studies is presented for most advanced Computational Fluid Dynamics (CFD) results with comparison to advanced Experimental Fluid Dynamics (EFD) measurement, not only for global integrated quantities such as the forces or trajectories but also for local quantities of the flow field including turbulence.

First of all, a brief reminder of the V&V objective is given, then what is meant by the notion of local and global data in relation to existing procedures, and finally what is practiced in complex situations to address and to analyse detailed flow field data.

4.2 Code verification and validation

Verification concerns the code verification for correct coding of the model implementation. The solution verification is aimed at estimating the numerical error/uncertainty of a given solution whereas the validation process is concerned with numerical model meaning the modelling errors/uncertainties.

For the estimation of the numerical uncertainty, a set of geometrically similar grids is required, where grid properties remain the same and the refinement ratio be constant in the computational domain. The task of generating a series of embedded grids by coarsening a fine grid or refining a coarse grid is feasible with most of structured grid generators.

The CFD error related to the discretization error is the difference between the exact solution of the PDE and the exact (round-off-free) solution of the algebraic equations used. The possible sources of numerical error to consider for accurately control the precision of a physical model are:

- Round-off errors: its influence is commonly neglected.
- Iterative error (to solve the couplings/segregated equations and the non-linearities): its influence is often neglected assuming the condition of the residuals "low enough" for all the quantities.
- Discretization error (or solution error due to incomplete grid convergence): it is computed from a series of systematically refined grids from which the exact solution is extrapolated and the uncertainty can be evaluated from the computed error.

The ITTC procedure 7.5-03-01-01 "Uncertainty Analysis in CFD Verification and Validation Methodology and Procedures" provides details for estimating the uncertainty of a simulation. A brief but comprehensive note by Celik et al. (2008) is intended to provide guidelines for authors.

4.3 Global and averaged variables

The aforementioned ITTC procedure is commonly used to assess and to justify the results of the simulations, and quite often based on integrated (or global) quantities such as forces. This is the regular practice for simulation where a steady solution is expected. However the numerical uncertainty of unsteady flow simulations in industrial activity remains a non-trivial task, Eça et al (2019): this makes it necessary to control both iterative error and statistical error (induced by initial conditions) even before addressing discretization errors, i.e. grid/time refinement.

The procedure also gives indication for estimating errors for "Point Variables". This is a way to estimate error and uncertainty on local flow details over a distribution of grid points. Thus, an L2-norm can be used to compute the solution changes within the profile-averaged quantity. As an example the ITTC procedure 7.5-03-03-02 "Practical Guidelines for RANS Calculation of Nominal Wakes" highly recommends the computational results to be presented in accordance with the format proposed in the ITTC procedure 7.5-02-03-02 "Nominal Wake Measurement by a 5-Hole Pitot Tube". In this case the computed wake field on the propeller plane is interpolated along specific radius and circumferential angles. In this way, such a guidance is

followed by Bakica et al (2019) to assess ship-propulsion using CFD.

For further research as an alternative to produce manually geometrically similar series of meshes for convergence studies, which is not straightforward with unstructured grid generators, Wackers et al (2017) shown that the technique of adaptive grid refinement can produce converged local-flow solutions: the numerical accuracy of the computed wake flows is sufficient to assess modelling errors due to turbulence models on meshes with acceptable numbers of cells. The technique was validated in the propeller plane of the KVLCC2 bare hull for both the velocity and the turbulent kinetic energy fields. However, this approach for V&V on non-local and global quantities is still an ongoing research topic. The next section is intended to illustrate code verification, in comparison with detailed EFD in complex situations, where the verification process is almost unfeasible.

4.4 Detailed investigations of the flow field

The present challenge of CFD applied to ship hydrodynamics concerns ship powering, manoeuvring and sea-keeping. In this context CFD has reached a high level of fidelity to address such complex situations: the SIMMAN 2008 and 2014 Workshops only covered calm water manoeuvring situations, the Tokyo 2015 CFD Workshop included free running course keeping in waves as a test case for the first time, and the SIMMAN 2021 workshop will also focus on manoeuvring in waves.

Concerning CFD about these most advanced studies of free-running ships and moving propellers and rudder the desired exercise to conduct a grid convergence analysis has never been done in the literature. This is due to complexity and cost of computations, Carrica et al (2014, 2016), Wang et al (2018), Hashimoto et al (2019): coarsening a grid may be impossible and refining is prohibitively expensive. On the EFD side for currently available data about free-running ships, only the propeller revolution speed is known very accurately during calm water tests and the uncertainty is estimated on the motions and on the forces. Bottiglieri (2016) estimates the random error based on repeated tests and the uncertainty is found as a combination of systematic and random uncertainties representing the propagation of errors within the tracking system and the deviation between repeat trials. In Sanada et al. (2013, 2014) the statistical convergence error on measurements is derived from repeated test results to know how many runs should be performed to get the converged mean trajectories for PIV measurements: for the ONR Tumblehome model the statistical convergence errors are almost converged when the sample size is over twelve. For zigzag manoeuvres of the KCS container, Carrica et al (2016), the repeatability error that contributes to experimental uncertainties of thrust, torque, motions and propeller RPM at self-propulsion is calculated based on ten experiment runs.

Going back to simpler cases for thorough V&V analysis the Tokyo 2015 Workshop the result of the Japanese Bulk Carrier (JBC) case is that the resistance predictions using the finest grids are within 1% of the measured data both with and without the energy saving device. An exhaustive presentation of the JBC test data from NMRI is available in Hirata (2015).

On the other hand, the flow around this JBC hull appears to be difficult to predict accurately with statistical turbulence closures. Compared to measurements, all RANS simulations are able to predict a satisfactory agreement for the mean longitudinal component of the velocity in the core of the vortex whereas the level of turbulent kinetic

energy (TKE) is generally underestimated by at least a factor of four. During this workshop the apparent contradiction from a RANS point of view between high levels of TKE and vorticity was removed with hybrid RANS-LES modelling by Abbas et al (2015), Kornev et al (2011), and later by Visonneau et al (2016) using a similar LES closure. On the same case Nishikawa (2015) presented successful fully-resolved LES simulations but at the cost of 39 billion grid points during 2.4 million hours of CPU time.

This highlights how important it is to support research activities focused on detailed analysis either by experiments and high-fidelity simulations. As noted above on the JBC case, the development of more sophisticated turbulence models requires the analysis of TKE and vorticity budgets.

For such needs, Falchi et al (2014) published the results of measurements of a catamaran in steady drift conditions which is typical of naval vessel operating in off-design conditions. The paper introduces a detailed review in literature about the SPIV (Stereo-Particle Image Velocimetry) adopted to acquire the three velocity components in a plane (mean and fluctuating components). Therefore mean vorticity field as well as velocity and vorticity fluctuations are available in five transversal planes and their interaction with the free surface. Possible sources of uncertainty are considered to state that instantaneous velocity field error is about 3% of the mean velocity and 12% of the exact value on the second-order statistical moments. For CFD validation the EFD dataset is available for downloading under request.

On these EFD basis, the results of CFD assessment for these static drift conditions has been done by Broglia et al (2019). The originality of the study is that the validation is based on cross-comparisons between three different CFD codes with different grid strategies and various turbulence modelling, from the Spalart-Allmaras model to hybrid RANS-LES. Assessment of numerical predictions focuses on the onset and propagation of the vortical structures, axial velocity and vorticity, TKE distribution and interaction with the free surface and loads. At a general level the loads are correctly predicted within the numerical uncertainty and differences occur among the turbulence model adopted. Only RANS simulations have been compared to the EFD cases with drift angle and measurement planes. To shortly summarize the validation exercise, the predicted TKE from RANS in the core of the fore body keel vortex is underestimated by at least one order of magnitude than experiments.

Yoon et al (2014) presented the results of experiments for the DTMB model in straight ahead and static drift conditions using a tomographic particle image velocimetry (TPIV) system. This allows detailed description the flow volume structures in specific region of interest and, for example the second invariant Q can be computed from EFD. As reported in Bhushan et al (2019) it was then possible to assess CFD in these conditions about the overall vortex structures with comparison of 3D predicted structures to TPIV measurements. Here again, the originality of the study is that the validation process is based on different codes and it appears that if full Reynolds stress transport model could improve unsteady RANS prediction, only hybrid RANS-LES models of the study are able to explain the high level of TKE from the sonar dome powered by instabilities and therefore higher production from the resolved turbulence.

5. INTERACTION WITH SHIPS IN OPERATION AT SEA COMMITTEE

The specialist committee on Ships in Operation at Sea (SOS) found an inconsistency in the load variation test (LVT) in the current Recommended Procedure 7.5-02-03-01.4. Figures 4 and 5, which are used for a calculation of the load variation coefficient of the ship speed ξ_V, are derived from different data sets.

The Resistance and Propulsion Committee (RPC) and the SOS calculated load variation factors for the SSPA benchmark (Werner, 2018), according to the Procedure. The data has been analysed using the ITTC 1978 performance prediction method version 0, as published in 1999, in the same way as the SOS.

The load variation factors calculated are summarized in

Table 1. The load variation coefficient of the delivered power, ξ_P, and the coefficient of the shaft revolution speed, ξ_n, are identical between SSPA, the SOS and the RPC, while ξ_V is slightly different. A reason of the difference is supposed to be that the ξ_V is derived by an interpolation of an interpolation. However, ξ_V doesn't affect EEDI and thus this slight difference can be considered negligible. In conclusion, the load variation factors derived from the same data set are almost the same among all facilities. The RPC replaced Figure 4 and 5 in the current procedure with new ones derived from the same dataset and described the detail of the calculation as an appendix of Recommended Procedure 7.5-02-03-01.4

Table 1: Comparison of load variation factors between SSPA, the SOS and the RPC for the SSPA benchmark case

	SSPA	SOS	RPC
ξ_P	-0.19	-0.19	-0.19
ξ_n	0.25	0.25	0.25
ξ_V	0.33	0.34	0.32

Table 2: Difference of subscripts between ITTC and ISO

No.	Description	ISO	ITTC	New ITTC (proposal)
1	Full scale resistance without overload	R_{id}	R_0	
2	Added resistance coefficient	C_{TSadd}	C_{TAadd}	
3	Propulsive efficiency in ideal condition	η_{Did}	η_D	η_{D0}
4	Propulsive efficiency considering the load variation effect	η_{Dms}	η_{DM}	η_D
5	Delivered power in ideal condition	P_{Did}	P_{D0}	
6	Propeller shaft speed in ideal condition	n_{id}	n	

Differences in the names of coefficients between the RP 7.5-02-03-01.4 and the International Standard, ISO15016 (2015), was also investigated. Six different subscripts between ITTC and ISO were identified as shown in Table 2. The committee does not consider it to be a problem that ITTC and ISO have their own subscripts because they have a consistency within each document. However, η_{DM} of No.4 in ITTC is inadequate because the subscript "M" represents "Model scale" in the procedure but is not case for η_{DM}.

Thus, the committee replaced η_D of No.3 with η_{D0} of which subscript "0" means "in ideal condition" and η_{DM} of No.4 with η_D.

6. HULL AND PROPELLER ROUGHNESS

6.1 Introduction

The ship hull or propeller surface roughness due to coatings or biofouling have a significant influence on the ship performance. The effects of hull surface roughness due to the coatings are often taken into account in the total resistance

prediction as the roughness allowance ΔC_F which is defined by the Townsin formula with the following formulation.

$$\Delta C_F = 0.044\left[\left(\frac{k_S}{L_{WL}}\right)^{\frac{1}{3}} - 10 \cdot Re^{-\frac{1}{3}}\right] + 0.000125 \quad (1)$$

In this formulation, the standard value of hull surface roughness k_S is defined to be 150 μm in case that no measured data is available.

This roughness height may not be a correct representation for modern hull coatings and recent research pointed out that the effective roughness of the coated hull surfaces in real life is much lower than this. Each type of coating may follow a different roughness function model, which makes the use of a single roughness height parameter difficult.

6.2 Roughness effects on ship resistance and propulsion

The impacts of hull roughness on ship resistance have been noted since the experiments of Froude (1872, 1874). McEntee (1915) conducted towing tests to investigate the effect of biofouling on frictional drag. Flat plates were coated with anticorrosive paints and exposed in the Chesapeake Bay. After 12 months, the frictional resistance of the plates increased up to four times due to the barnacles on the surface. Hiraga (1934) reported the effect of biofouling on the resistance of a towed brass plate coated with Veneziani composition. The plate was towed after 24 days of immersion and showed a 20% increase in the total drag with grown slime and barnacles on the surface. Lewthwaite et al. (1985) carried out an experiment measuring the boundary layer velocity profiles on a 23m fleet tender. An 83% increase in the frictional resistance and a 15% reduction in ship speed were observed over the 2-year exposure. Haslbeck (1992) conducted a full-scale trial on a Knox class frigate which was coated with an ablative antifouling paint. The delivered power and ship speed were measured after 22 months moored in Pearl Harbour. With a slime film and little macrofouling on the hull, an 18% increase in the delivered power was observed. Schultz (2004) carried out towing tests using flat plates exposed to seawater and concluded that the most dominant effect on resistance was the height of the largest barnacles on the plates. Andrewartha et al. (2010) conducted an experimental study to investigate the effect of biofilm on skin friction using a recirculating water tunnel. The test plates were deployed in the open channels of a hydroelectric power station (Tarraleah Power Scheme, Tasmania, Australia) for varying durations for biofilm growth. They measured up to a 99% increase in the drag of the test plates due to the biofilms on the plates. Li et al. (2019) investigated the effect of marine biofilm on the surfaces coated with different sized cuprous oxide (Cu2O) particles. In order for the biofilms

Figure 33: Testing panels installed on the twin strut assembly (left) and the strut system deployed under the moon-pool plug (right) (Yeginbayeva and Atlar, 2018)

to develop under 'in-service' conditions, the test panels were installed on a detachable twin strut system. The strut system was deployed under the moon-pool plug of a catamaran research vessel, *Princess Royal*, and exposed in the sea for various periods (Figure 33). The frictional drag of the test panels was measured using a turbulent flow channel after every 6-week deployment period. The result showed an up to 83% increase in frictional drag due to the biofilm developed for 6 months.

There have also been investigations into the roughness effect on propeller performance. Bengough and Shepheard (1943) reasoned that the case of HMS Fowey which failed to reach its designed speed can be attributed to its fouled propeller. When subsequently docked, the propellers were found to be almost completely covered with calcareous tubeworms. The target speed could be finally achieved after cleaning the propeller. McEntee (1916) conducted experiments on artificially roughened model propellers to compare the efficiencies of similar propellers in different surface conditions. A model propeller was painted and stippled while the coating was wet to roughen the surface. The efficiency loss was about 20% due to the roughened surface. In another test, they used a propeller covered with ground cork, which resulted in an efficiency drop of 35%. Taylor (1943) insisted that even the ships operating with a propeller in moderately good condition can suffer a power loss in order of 10%. Townsin et al. (1981) recognised that propeller fouling can be as destructive as hull fouling but the remedy is much cheaper. Mosaad (1986) claimed that although the impact of propeller fouling may seem less severe than hull fouling, the losses per unit area are much greater. Mutton et al. (2005) compared the propeller open water performances in intact and damaged coating conditions and showed reduced propeller efficiency under the damaged scenarios. Korkut and Atlar (2012) conducted experiments to examine the roughness effect of foul release coatings on the propeller open water performances.

6.3 Roughness function

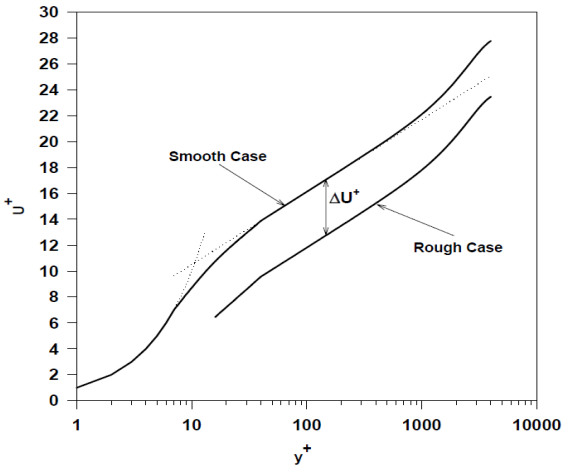

Figure 34: The roughness effect on velocity profile, adapted from Schultz and Swain (2000)

The roughness function, ΔU^+, represents the downward shift of the velocity profile due to the surface roughness in the turbulent boundary layer (Figure 34). Once the roughness function of a given surface is known, it can be utilised with the boundary layer similarity law analysis or Computational Fluid Dynamics (CFD) based methods to predict the added resistance due to the rough surface. The roughness functions can be determined from experiments either directly or indirectly. While the direct method requires the costly measurement of the boundary layer profiles, indirect methods are generally simpler and require less expensive equipment. Granville (1987) derived three indirect methods to estimate the roughness function of arbitrarily rough surfaces. However, the roughness functions are not universal and thus they have to be determined for individual roughness types.

Schultz (2004) has compared the frictional resistance of several coatings in the unfouled, fouled, and cleaned conditions by carrying out flat plate towing tests. The roughness function

for the unfouled coatings showed reasonable collapse to a Colebrook-type roughness function when the centreline average height k=0.17R_a was used as the roughness length scale. An excellent collapse of the roughness function for the barnacle fouled surfaces was obtained using a new roughness length scale based on the barnacle height and percent coverage.

Yeginbayeva and Atlar (2018) have investigated the hydrodynamic performance of typical coatings under in-service conditions of roughened ships' hull surfaces. They have presented comprehensive and systematic experimental data on the boundary layer and drag characteristics of antifouling coating systems with different finishes. The coating types investigated were linear-polishing polymers, foul-release and controlled-depletion polymers. The roughness functions were collected with a 2-D laser Doppler velocimetry (LDV) system in a large circulating water tunnel. The roughness length scale defined by the peak-to-trough height (k=0.14R_t) and combination of root mean square roughness and spatial distribution of height parameters presented a satisfactory correlation with ΔU^+ for coatings in the transitionally rough flow regimes. They have pointed out that further studies to explore the adequacy of the correlation for fully rough regimes is required.

Katsui et al. (2018) have shown roughness functions for various painted rough surface based on the experimental results using rotating cylinders. The obtained roughness function depends on the roughness Reynolds number, and it also depends on both the roughness wave height and wave length fraction to its height which are obtained FFT analysis for measured paint surface profiles.

Lee et al. (2015) investigated the performance of a new skin-friction reducing polymer named FDR-SPC (Frictional Drag Reduction Self-Polishing Copolymer). The drag-reducing functional radical such as PEGMA (Poly(ethylene) glycol methacrylate) has been utilized to participate in the synthesis process of the SPC. In the high-Reynolds number flow measurement with a flush-mounted balance and an LDV (Laser Doppler Velocimeter), the skin friction of the present FDR-SPC is found to be smaller than that of the smooth plate in the entire Reynolds number range, with the average drag reduction efficiency being 13.5% over the smooth plate.

Demirel et al. (2017) conducted an extensive series of towing test of flat plates covered with artificial barnacle patches to find the roughness functions of barnacles with varying sizes and coverages. Different sizes of real barnacles, categorised as small, medium and big regarding their size, were 3D scanned and printed into artificial barnacle patches. From the experimental results, they determined the roughness functions of barnacles with varying sizes and coverages. The roughness functions collapsed to the Colebrook-type roughness function of Grigson (1992).

6.4 Prediction methods for roughness effect

6.4.1 Similarity law analysis

The boundary layer similarity law scaling method, which was proposed by Granville (1958), has been widely used to predict the increased ship resistance due to hull roughness. The benefit of using this method is that once the roughness function, ΔU^+, of the surface is known, the skin friction with the same roughness can be extrapolated for flat plates with arbitrary lengths and speeds.

Schultz (2004) predicted the increases in the frictional resistance of a 150 m flat plate with different antifouling surfaces in unfouled, fouled and cleaned conditions, using the similarity law analysis. The increase in the

frictional resistance of the surfaces in fouled condition ranged from 50% for an SPC TBT coating to 217% for a silicone coating. Using the same method, Schultz (2007) predicted the power penalty of an *Oliver Hazard Perry class* frigate of 144 m with different coating and fouling conditions. The increase in the required shaft power at a constant speed (30 knots) due to the heavy calcareous fouling condition was 59%, while the speed loss at a fixed power was 10.7%. Schultz et al. (2011) also analysed the overall economic impact of hull fouling on a mid-sized naval surface ship based on the resistance predictions using the similarity law analysis. The results indicate that the primary cost associated with fouling is due to increased fuel consumption attributable to increased frictional drag and the cost related to hull cleaning and painting is much lower than the fuel costs.

Demirel et al. (2019) presented practical added resistance diagrams based on the similarity law analysis to be used for predicting the increases in the frictional resistance and effective powers of the ships due to the use of a range of coating and biofouling conditions (Figure 29). Roughness effects of a range of representative coating and fouling conditions on the frictional resistances of flat plates were predicted across a range of ship lengths and speeds. The added resistance diagrams were then used to predict the resistance and powering penalties of different ships including DTMB 5415, KCS, JBC and KVLCC2.

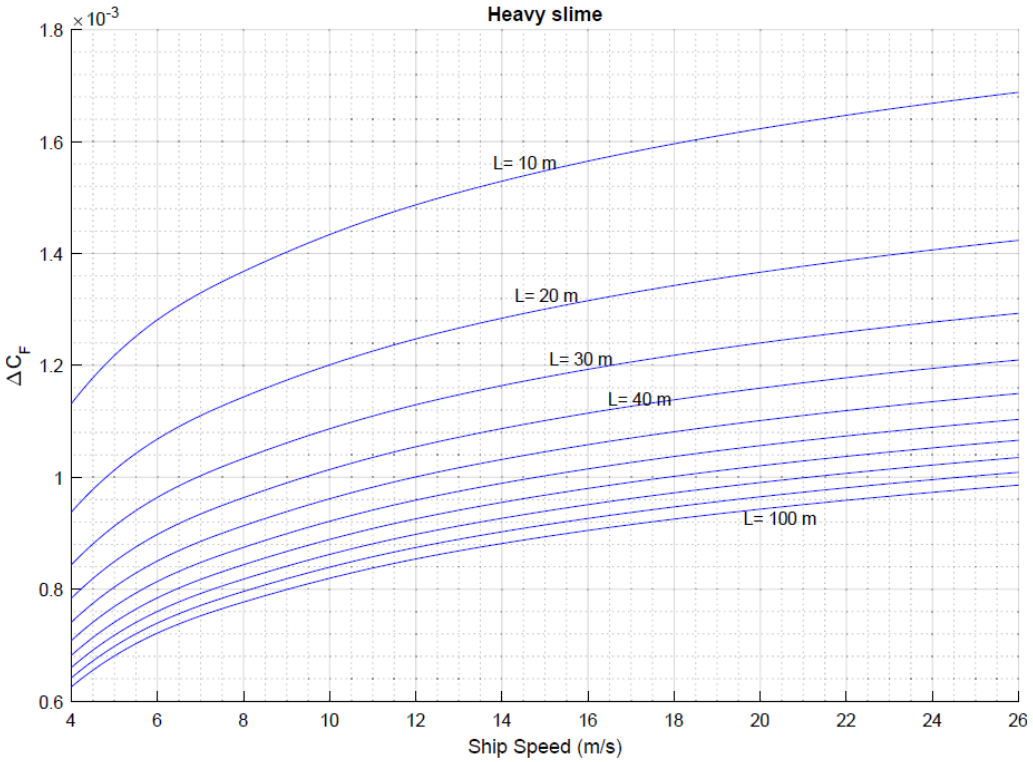

Figure 35: Added resistance diagram generated by Demirel et al. (2019)

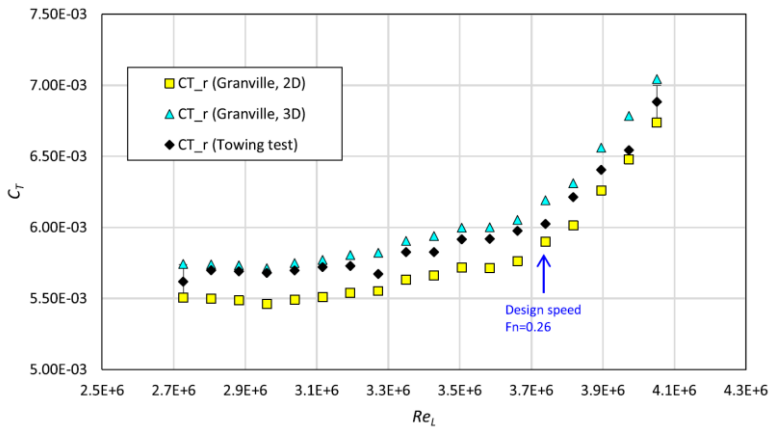

Figure 36: Total resistance predictions based on the similarity law analysis and the experimental data (Song et al., 2021a)

However, there have been questions regarding the validity of the similarity law analysis for predicting the total resistance of a 3D hull, because of its assumption of flat plate. In other words, this method only considers the roughness effect on the frictional resistance, while recent studies claim that the hull roughness affects the pressure-related resistance components as well as the frictional resistance (Farkas et al., 2018).

Recently, Song et al. (2021a) examined the validity of the similarity law scaling method for predicting the total resistance of a 3D hull. They conducted towing tests using a flat plate and a ship model in the smooth and sand-grit surface conditions. The roughness function of the sand-grit was determined from the flat plate test result using the overall method of Granville (1987). The frictional resistance of the ship model was predicted using the similarity law scaling with the obtained roughness function. The total resistance of the model ship was predicted using conventional hypotheses of Froude and Hughes (namely, 2D and 3D methods) and compared with the experimental result of the rough model ship. The total resistance predictions from the 3D method showed better agreement with the experimental result compared to the 2D method, suggesting that the resistance prediction can be more accurate when the roughness effect on the viscous pressure resistance is considered (Figure 36).

Monty et al. (2016) proposed a new prediction approach based on the boundary layer similarity law. The advantage of this approach is that the procedure can cope with varying roughness heights along the flat plate. Using the newly proposed method, they predicted the effect of tubeworm fouling on an FFG-7 Oliver Perry class frigate and a very large crude carrier, which showed 23% and 34% increases in total resistance respectively.

Katsui et al. (2018) have shown a method to evaluate the performance of the paints to reduce the added frictional resistance in full-scale ship Reynolds number. Simultaneous non-linear ordinary differential equations are developed to calculate the hydrodynamic frictional resistance of a flat plate based on the momentum equation and Coles' wall wake law which is the similarity law of the velocity distribution in the turbulent boundary layer. The effects of the roughness of the painted surface are taken into account by adding the roughness function to Coles' wall wake law. The calculated local frictional stress coefficients on the painted surfaces agreed well

with the measured ones. The total frictional resistance coefficients of a painted surface in the actual ship scale Reynolds number can be evaluated considering various kinds of paints and the effects of the paint surface profile.

Mieno et. al. (2021) investigated the similarity law of added friction due to painted rough surface based on rotating cylinder tests. They have shown a relation between the friction increase rate and roughness Reynolds number and pointed out that friction increase rate depends not only on roughness height but also on roughness wave length. The roughness parameters of a painted surface which are related with roughness height and wavelength are measured by portable 3D hull roughness analysis which is developed by Mieno et. al. (2020).

6.4.2 CFD approaches

Recently, Unsteady Reynolds Averaged Navier-Stokes (URANS) based CFD simulations have been widely used to predict the added resistance due to surface roughness. The mainstream is using modified wall-functions by employing the roughness function in the CFD model.

Song et al. (2020b) validated the modified wall-function approach for predicting the added resistance of a 3D hull, which had been only validated for flat plates with zero pressure gradient. The flat plate and the KRISO Container Ship (KCS) model of Song et al. (2021a) were modelled in CFD simulations in both smooth and rough surface conditions using the modified wall-function approach. The simulation result showed a good agreement and thus demonstrated the validity of the CFD approach for predicting the roughness effect on 3D hulls.

Demirel et al. (2017b) conducted CFD simulations to predict the effect of marine coatings and biofouling on ship resistance on the full-scale 3D KCS hull. Different coating and fouling surfaces were modelled using a modified wall-function approach. The roughness effects of such conditions on the resistance components and effective power of the full-scale 3D KCS model were then predicted. The increase in the effective power of the full-scale KCS hull was predicted to be 18.1% for a deteriorated coating or light slime whereas that due to heavy slime was predicted to be 38% at a ship speed of 24 knots.

Farkas et al. (2018, 2019) conducted CFD simulations to investigate the effect of biofilm on the resistance a full-scale KCS, using a modified-wall function with the implementation of the roughness functions of diatomaceous biofilm of Schultz et al. (2015). By comparing the 3D KCS simulations with and without the presence of free surface, they decomposed the ship resistance into individual components. The result showed that the total resistance and frictional resistance of KCS increase with the presence of biofilm, whereas the wave-making resistance showed decreases.

Seok and Park (2020) also used the modified wall-function approach to analyse the variation in resistance performance of three different containership models. The simulation results were compared with the predictions based on Townsin's formula (Townsin and Dey, 1990) and showed a satisfactory agreement.

Song et al. (2019) conducted full-scale KCS simulations with different barnacle fouling conditions using the modified wall-function approach. They employed the roughness functions of barnacles (Demirel et al., 2017a) into the wall-function of the CFD model and conducted towed plate simulations to validate the CFD model against the experimental data. The same approach was used to predict the effect of barnacles on the resistance of a full-scale KCS. The results showed significant

increases in the frictional resistance and effective power, up to 93% and 73% respectively, due to the barnacles on the hull. By decomposing the resistance components, they found different roughness effects on different resistance components. For example, the wave-making resistance showed decreases while the viscous pressure resistance increases with the presence of hull fouling. They also investigated the roughness effects on other hydrodynamic characteristics, such as the form factor, wake, velocity field and pressure field around the hull.

Owen et al. (2018) conducted CFD simulations to investigate the effect of biofouling on the open water performances of a model-scale propeller. The modified wall-function approach of Demirel at al. (2017b) was adopted to approximate the surface conditions of different coating and fouling surfaces. The effect proved to be drastic with the most severe fouling condition resulting in an 11.9% efficiency loss at J=0.6 ranging to an alarming 30.3% loss at J=1.2 compared to the smooth condition. The study acts as a proof of concept for the proposed CFD assessment method which can be used as a very practical approach to predicting the impact of realistic conditions on propeller characteristics and energy efficiency. Song et al. (2020c) conducted CFD simulations of a full-scale propeller (KP505) to investigate the effect of propeller fouling on the propeller open water performance, using the same modified wall-function approach as used by Song et al. (2019). They found increases in torque coefficient (10.2%) and decreases in thrust coefficient (-11.1%), which leads to a significant loss in the open water efficiency (19.3%).

Song et al. (2020d) conducted full-scale CFD simulations of self-propelled KCS with hull and/or propeller fouling using the same modified wall-function approach (Song et al., 2019). The roughness effects on the self-propulsion characteristics were investigated at the design speed of the KCS in various configurations of the hull and/or propeller fouling conditions. The result suggested that the required shaft power at the design speed of KCS increases by up to 82% due to the hull and propeller fouling. The roughness effects on the flow characteristics around the hull and propeller were investigated to be correlated with the findings on the roughness effect of the self-propulsion characteristics.

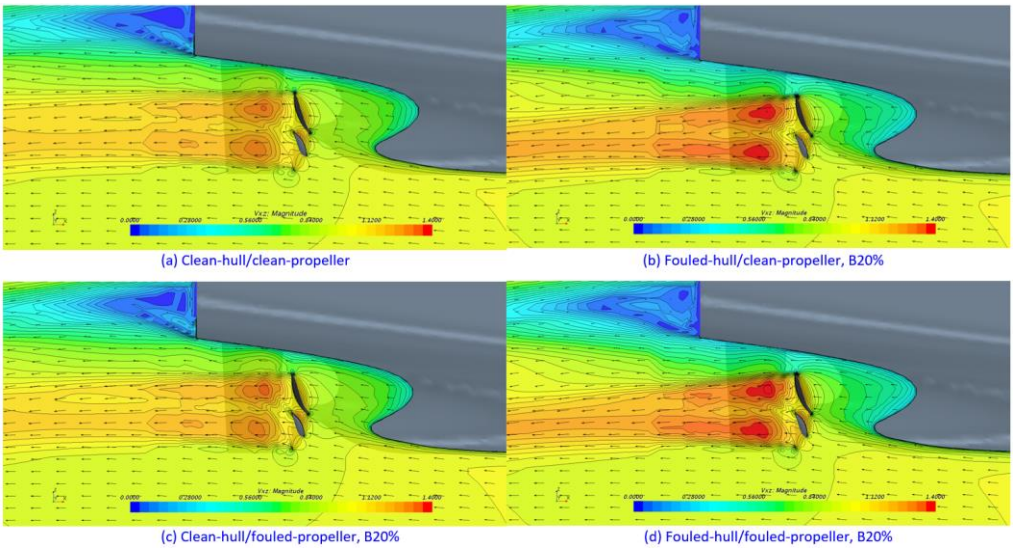

Figure 37: Velocity field around the hull and propeller, with different fouling scenarios (Song et al., 2019)

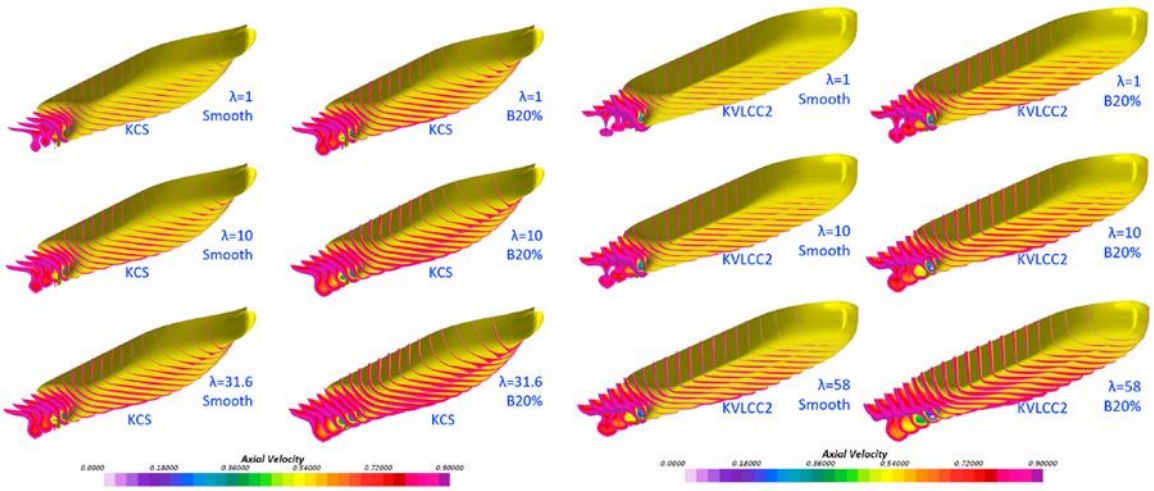

Figure 38: Boundary layer representations around the KCS and KVLCC2 hulls in different hull conditions and scales (Song et al., 2020e)

Song et al. (2020e) continued utilising the CFD method to investigate the effect of biofouling on the resistance of different ship types. A containership (KCS) and a tanker (KVLCC2) were modelled in CFD simulations with various scale factors (i.e. model, moderate and full scales) and speeds. The simulations were conducted with several fouling conditions using the modified wall-function approach. Significant differences in the roughness effects were observed on the resistance components varying with the hull types, lengths and speeds of the ships.

6.5 Conclusion

There is a need to adopt/develop new methods to predict the roughness effect of modern fouling-control coatings and marine

biofouling on ship hydrodynamic performance. The similarity law scaling and CFD can be regarded as the most promising potential methods to predict such effects. Both methods require the use of roughness functions of the surfaces in question. The similarity law scaling can be used to predict the effect of roughness on the frictional resistance of flat plates of ship lengths effectively with less computational cost whereas CFD methods can be adopted for accurate prediction of roughness effects on the resistance components, propeller performance characteristics, and hydrodynamics of full-scale 3D ships. While these prediction methods require the roughness functions, there exists no universal roughness function model and no single roughness length scale for all types of marine coatings and biofouling surfaces. Therefore, there is a need to generate a database of roughness functions of modern fouling-control coatings and surfaces representing heterogenous biofouling accumulated on ship hulls and propellers. For this reason, it is recommended that standardised methods for roughness function determination should be adopted by researchers. It would, therefore, be useful to investigate the need for a guideline or procedure for the measurement of roughness functions for different surface finishes or conditions so that this information can be used for predicting the roughness corrections for both hull and propeller.

7. UNEQUALLY LOADED MULTIPLE PROPELLER VESSELS

7.1 Introduction

The objective of this task was to validate the procedure 7.5.02-03-01.7 1978 Performance Prediction Method for Unequally Loaded, Multiple Propeller Vessels proposed from 28th ITTC. Contrary to the single screw vessel or twin screw vessel having identical propellers, each propeller's loading is normally different due to the position of propeller (and as a result, the inflow condition will be different) and the design of propeller for unequally loaded, multiple propeller vessels as shown in Figure 39.

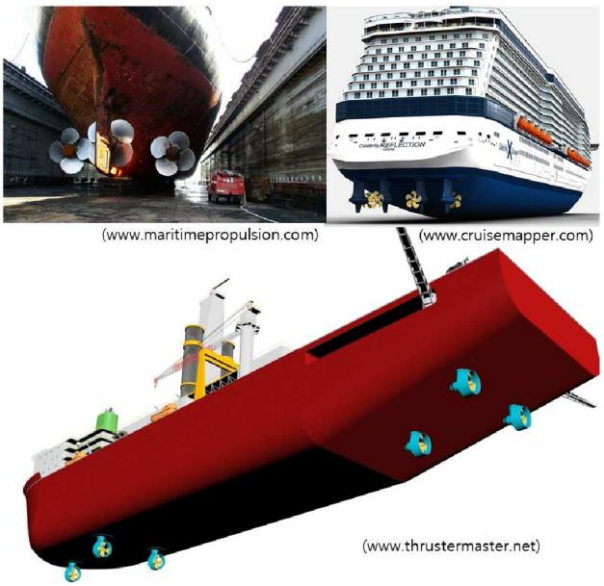

Figure 39: Unequally loaded, multiple propeller vessels

This feature lead to the requirement for the 28th ITTC to implement a new procedure, to consider the different interaction effect between propeller and hull by a new method for thrust deduction factor. By this new method for thrust deduction factor, each propeller's delivered power can be predicted.

To validate this procedure, sea trial data for unequally loaded, multiple propeller vessels is necessary, so that each measured power can be compared with model test prediction value. During the last 4 years, the committee tried to collect sea trial data in the public domain first, and then contacted shipping companies operating this kind of vessel, but unfortunately no sea trial data was available.

The committee has left this validation task as future work until such time as sea trial data

becomes available, and decided to make this procedure more comprehensive by adding more graphs, formulae, description and model test data to calculate the thrust deduction factor for unequally loaded, multiple propeller vessels. Through this, the committee expects this recommended procedure and guideline can give more practical guidance for performance evaluation of this kind of vessel.

7.2 Calculation procedure of thrust deduction factor

The unique characteristics of the model test procedure for unequally loaded, multiple propeller vessels is how to get the proper value of thrust deduction factor in the self-propulsion test, the question being how much (i.e. what portion of) resistance is burdened or distributed over each propeller. To answer this, we can devise a factor as shown in Figure 41.

To obtain this factor, some methods were proposed with the assumption that the resistance would be distributed by the ratio of thrust of the propeller or the ratio of power of the propeller (Seo et al, 2011) and the results were compared.

As another way of getting the factor, the 28th ITTC Propulsion Committee proposed the RPG 7.5-02-03-01.7 and suggested load variation tests to calculate the resistance fraction, load fraction and finally the thrust deduction factor of each propeller. The definition of each value is as below;

$$1 - t_i = \gamma_i \frac{R_{TM} - F_D}{T_i} \quad \text{(thrust deduction factor)}$$

$$\gamma_i = \frac{T_i(1-\tau_i)}{\sum_{j=1}^{3} T_j(1-\tau_j)} \quad \text{(load fraction)}$$

$$1 - \tau_i = -\left(\frac{\Delta F}{\Delta T}\right)_i \quad \text{(resistance fraction)}$$

here, $\triangle$F is the change of towing force and $\triangle$T is the change of thrust in the load variation test, R_{TM} is the resistance of the model at each speed, corrected for temperature differences between resistance and propulsion tests, and F_D is the tow force expected at each speed for the propelled ship self-propulsion point condition.

In this suggestion, the resistance fraction of the i-th propeller is calculated from the load variation test of that propeller (i.e., the revolutions of i-th propeller only is changed and the other propellers are keeping their revolutions around self-propulsion point). This situation is illustrated in Figure 42 and the slope of the relation (resistance fraction) can be calculated.

To calculate the thrust deduction factor of each propeller, the portion of resistance burdened by each propeller should be defined first and the resistance fraction accounts for artificial distribution of ship resistance by using the ratio of towing force decrease and the corresponding thrust increase of each propeller.

Again, a larger value of (1-resistance fraction) means the thrust force is well transferred to ship's resistance without any significant increase of resistance from the interaction effect between propeller and hull: less interaction effect to resistance means low thrust deduction factor.

The more important consideration is that the ratio of resistance fraction (not the absolute value) determines the thrust deduction factor of each propulsion system by definition. The result from a sample calculation is shown in Figure 40.

Item	1-τ$_i$	γ$_i$	t
	[-]	[-]	[-]
Center	1.0	68.7%	0.153
Side	1.0	15.7%	0.153
		31.3%	

Item	1-τ$_i$	γ$_i$	t
	[-]	[-]	[-]
Center	0.9	68.7%	0.153
Side	0.9	15.7%	0.153
		31.3%	

Item	1-τ$_i$	γ$_i$	t
	[-]	[-]	[-]
Center	0.92	67.1%	0.173
Side	0.99	16.5%	0.110
		32.9%	

Figure 40: Sample calculation

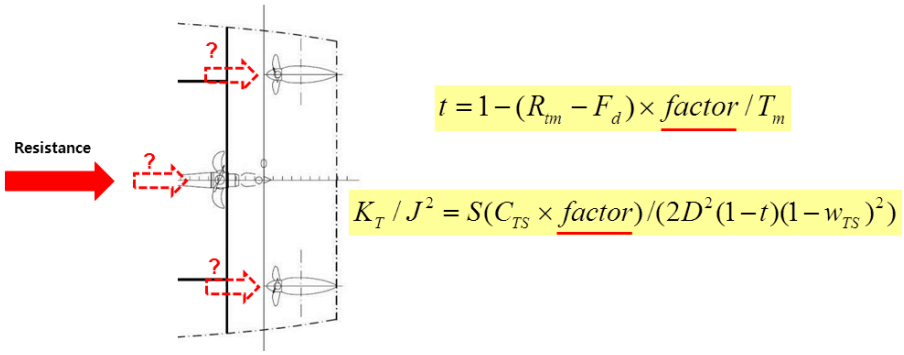

Figure 41: Resistance distribution to each propeller

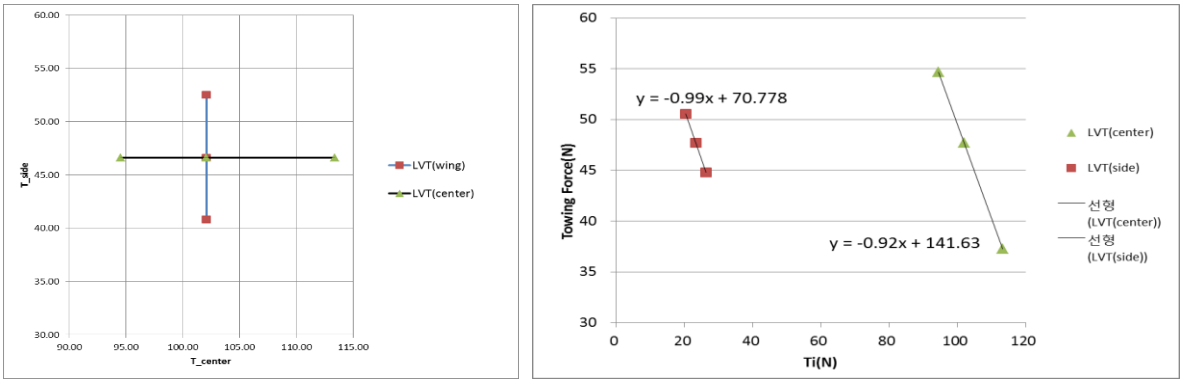

Figure 42: Load variation test to get resistance fraction and sample calculation result

7.3 Sample calculation result based on the proposed procedure

Sample calculations based on the method presented at SMP'11 and 28th ITTC were carried out and compared.

The distributed resistance can be calculated by the definition from SMP'11 and 28th ITTC as below:

$$R_i = \frac{T_i}{\sum_{j=1}^{3} T_j}(R_{TM} - F_D), \quad \text{SMP'11}$$

$$R_i = \frac{T_i(1-\tau_i)}{\sum_{j=1}^{3} T_j(1-\tau_j)}(R_{TM} - F_D), \quad \text{ITTC 28th}$$

By the definition of thrust deduction factor, if the resistance is distributed by the thrust ratio from SMP'11, the thrust deduction factor of each propeller has the same value and this does not account for the different loading of the propeller or the interaction effect. But if the resistance is distributed by the load fraction, the large value of (1-resistance fraction) accounts for large resistance distribution, low interaction effect and finally low thrust deduction factor. Sample calculation results are as Figure 43.

Even though the two methods showed different values of thrust deduction by the different distribution of resistance, the total sum of delivered power of each propeller was almost the same. This sample calculation is just one example and it is expected that more test cases will help to decide which method can give more accurate results compared to sea trial results.

The 29th ITTC Resistance and Propulsion Committee tried to get sea trial data of unequally loaded, multiple propeller vessels but could not obtain it and it is recommended that the next committee should continue trying to obtain this data to validate the procedure.

Rtmc	Fd
[N]	[N]
173.63	47.71

SMP'11

	Ti	Ri	Ti/T	t
Center	102.1	86.5	68.7%	0.153
Side	23.3	39.5	15.7%	0.153

ITTC 28th

	Ti	Ri	Ti/T	t
Center	102.1	84.4	67.1%	0.173
Side	23.3	41.5	16.5%	0.110

Resistance may be distributed by thrust ratio(from SMP'11)

	Ti/T	t	wts	KT/J2	JTS	etaH	EtaO	EtaD	EHP	DHP	DHP_total		
		-	-						[kW]	[kW]	[kW]		
Center	68.7%	0.153	0.185	0.349	0.785	1.039	0.671	0.691	6325	9159	14599	100.0%	62.7%
Side	15.7%	0.153	0.045	0.131	1.101	0.887	0.591	0.531	2888	5440			37.3%

Resistance may be distributed by "resistance fraction from ITTC 28th

Item	1-ti	yi	t	wts	KT/J2	JTS	etaH	EtaO	EtaD	EHP	DHP	DHP_total		
	[-]	[-]	[-]	-	-	-	-	-	-	[kW]	[kW]	[kW]		
Center	0.92	67.1%	0.173	0.191	0.355	0.782	1.023	0.669	0.678	6178	9106	14546	99.6%	62.6%
Side	0.99	16.5%	0.110	0.045	0.131	1.101	0.932	0.591	0.558	3035	5440			37.4%

Figure 43: Example calculation

8. FULL SCALE DATA FOR PODDED PROPULSION

Podded propulsion is typically installed on large cruise vessels and is also seen on large icebreakers.

Pods are characterized by having an electric engine mounted directly behind a pulling propeller inside an azimuth housing. This has the advantage that there is no gear (reduction or angle gear) and only a very short propeller shaft resulting in a quite effective propulsion seen from the mechanical point of view. The electric power is traditionally generated by diesel gensets and therefore some efficiency loss must be expected. However, for future vessels the electric power could possibly be generated in a more sustainable way e.g. fuel-cells, solar panels etc.

Pods are normally installed in twin or triple formations. For twin installations, both pods

will act as a steering device with 360 degree. azimuthing ability. For triple installations, the centre pod could be fixed in angle and therefore only used as propulsion and not steering.

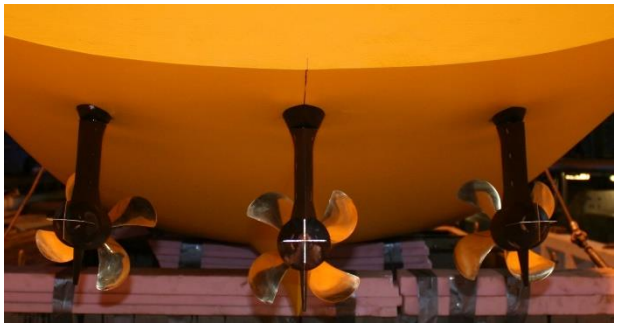

Figure 44. Model scale triple pod installation

The present committee have been in contact with ship owners within the cruise industry. They have the full scale data needed for verification/modification of the current procedure (7.5-02-03-01.3). However, for them it is not possible to share the data with ITTC due to commercial interests even though they would like to from a technical perspective. Seen from this perspective getting full scale data from icebreakers seems to be the way forward since there shouldn't be any commercial restrictions.

9. QUASI-STEADY PROPELLER AND PROPULSION TESTS

The quasi-steady (QS) method is a promising technique for significantly reducing the time required to conduct a propeller open water (POW) test and propulsion test. The QS method is suitable for meeting the growing demands for large series of model tests by ship owners and/or operators, such as trim/draught combination tests. MARIN has studied the method in the past and has shown a good correlation between the QS POW tests and the conventional ones, as shown in the committee report of 28th ITTC. The last committee stated that validation by organisations other than MARIN was a future issue.

During this term, HSVA presented the effectiveness of the QS resistance tests (Larssen, 2018). The QS tests required only a single run to cover the full speed range, saving 4.5 times the time of conventional tests. The towing speed was constantly accelerated until the maximum speed and decelerated until the minimum speed. The hysteresis was removed by averaging of the acceleration and the deceleration data. From two pictures taken during the acceleration and the deceleration, it was found that the deformation along the ship's hull matched well, which indicated a similar pressure distribution on the hull surface during both runs (Figure 45). They conducted both QS tests and conventional tests on the same day and confirmed the deviation of a root mean square value was within only 0.6%, which was comparable to the usual repeatability for conventional tests. Moreover, more than 18 different ships were tested in several different setups. Figure 46 shows the discrete probability density of the deviation between the QS method and conventional test. It shows that the expected value was only 0.07%.

The reliability of the QS method has been confirmed by MARIN and HSVA, and it looks ready to replace the conventional test. However, to develop the guidelines, the limits of applicability, e.g. how large wave making and/or dynamic trim and sinkage are allowed, should be clarified. Since the method has a great potential to replace the conventional test, it is recommended in the next term to conduct benchmark tests and validate the method by more model basins.

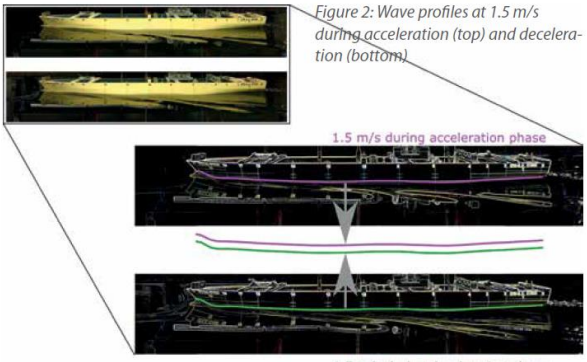

Figure 45: Wave profiles during acceleration (top) and deceleration (bottom)

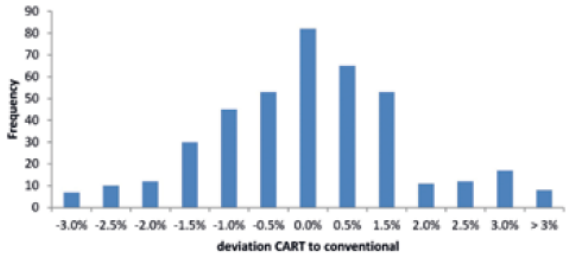

Figure 46: Distribution of discrete deviations of the QS propulsion tests to the conventional tests.

10. CAVITATION EROSION MODELLING AND PREDICTION

10.1 Introduction

Cavitation erosion has long been recognized as a problem in the shipping industry. It degrades propeller performance and imposes high maintenance costs. Thus, accurate prediction of erosion at the design stage is important.

Cavitation erosion on marine propellers and rudders attracted attention as a big issue with the emergence of a new generation of large and fast container ships, ferries and ROPAX vessels in the early 2000s.

Against such a background, the Specialist Committee on Cavitation Erosion on Propellers and Appendages on High Powered/High Speed Ships was organized in the 24th ITTC and developed the RP 7.5-02-03-03.5 “Cavitation Induced Erosion on Propellers, Rudders and Appendages Model Scale Experiments”. Then, the Specialist Committee on Cavitation for the 25th ITTC developed the RP 7.5-02-03-03.7 “Prediction of Cavitation Erosion Damage for Unconventional Rudders or Rudders Behind Highly-Loaded Propellers”. These were developed from experimental aspects because numerical prediction for cavitation was immature at that time.

Since then, cavitation simulation techniques have advanced greatly due to rapid evolutions in numerical modelling as well as in computational hardware. The state-of-art of the technology has been reported by the following ITTC committees, 26th ITTC (2011), 27th ITTC (2014), and 28th ITTC (2017).

Accordingly, numerical prediction of cavitation erosion is becoming feasible.

10.2 Erosion modelling

Cavitation erosion occurs when impulsive pressure from shock waves and/or microjets generated by bubble collapse exceeds some material threshold, such as its yield stress.

The detailed mechanism is still a subject to be solved, but many researchers have attempted to explain it more accurately. For example, Dular et al. (2019) recently developed a technique on simultaneous observation of one single cavitation bubble collapse and the damage it creates. The dynamics of the bubble created by Nd:YAG laser was observed with two high-speed cameras. They concluded that the most pronounced mechanism is the impact of the microjet when the cavitation bubble implodes near the wall. On the other hand, the influence of the micro-jet diminishes and the collapse of microscopic bubbles in the rebound

cloud is more important when the bubble collapses away from the wall.

Although the detail is not fully understood, various cavitation erosion models have been proposed to describe the physical mechanisms.

Fortes-Patella et al. (2004) proposed a model based on the energy balance illustrated in Figure 48. Potential power included in vapour clouds converts into acoustic power by the bubble collapse. The emitted pressure waves interact with the neighbouring solid surface, leading to material damage. Two transfer efficiencies η^{**} and η^{*} are used in the model. η^{**} is a hydrodynamic efficiency between the initial power P_{pot} and the flow aggressiveness power P_{pot}^{mat}, which is a function of the hydrodynamic characteristics (V_{ref}, σ) of the flow and the distance between the vapour structures and the solid surface. η^{*} is a collapse efficiency between P_{pot}^{mat} and pressure wave power P_{wave}^{mat}, which depends mainly on the local pressure and on the initial gas pressure P_{go} within the bubble. Then, the volume damage rate, V_d, was derived by the following formula.

$$V_d = \frac{P_{wave}^{mat}}{\beta \Delta S} \quad (1)$$

Where ΔS is an analysed sample surface and β is a mechanical characteristics of the material.

Dular et al. (2006) proposed a model based on the microjet formation illustrated in Figure 49. Pressure waves emitted from the bubble collapse make a single bubble near the wall oscillate and a microjet occur. The high-velocity liquid jet impact on the wall causes material damage. Through the experiment using hydrofoils, they found that the value of the standard deviation of the grey level in the image of cavitation relates to the time derivative of cavity volume for calculating the pressure wave power P_{wave}. The jet velocity is determined based on the theory developed by Plesset and Chapmann (1971) and the pit depth and the damaged surface area can be estimated using the jet velocity and material property.

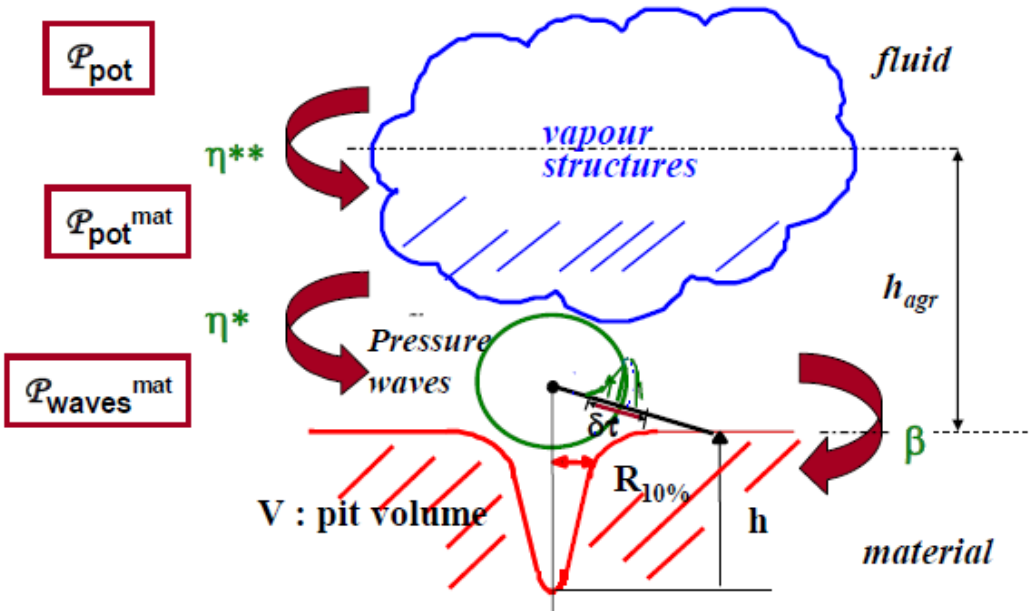

Figure 47: The physical scenario based on the energy balance, Fortes-Patella, et al. (2004)

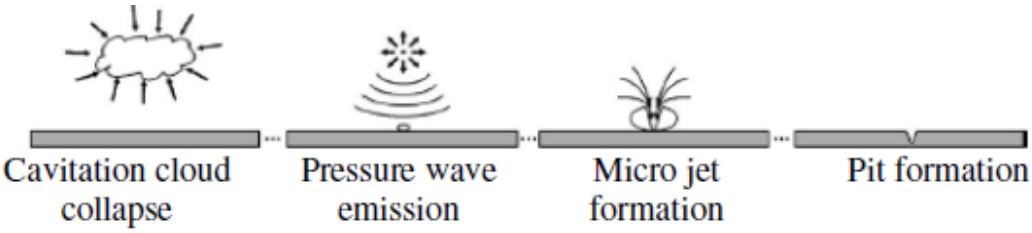

Figure 48: The physical scenario based on the microjet formation, Dular et al. (2006)

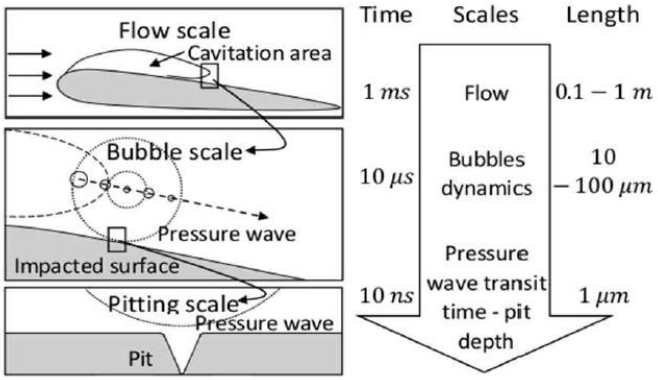

Figure 49: Illustration of time and length scales phenomena induced by cavitation erosion, Leclercq et al (2017)

Melissaris and Terwisga (2019) have recently reviewed the cavitation erosion models published during the last decade. In addition to the abovementioned models, they introduced the concept of the "collapse detector" by Mihatsch et al. (2011), while they addressed that the energy balance model by Fortes-Patella et al. (2004) is the most appropriate for erosion risk assessment using an incompressible pressure based URANS solver.

It is a common concept in all the above models that the process starts with a collapse of vapour structures.

10.3 Numerical approach for erosion prediction

To predict the erosion accurately, one must calculate the whole process from the bubble collapse to the impact of the pressure wave on the surface. However, it is difficult to simulate numerically because a wide range of scale in time and space should be treated in the calculation, as illustrated by Leclercq et al. (2017) in Figure 49. Besides, there are many parameters to be considered, such as water quality and gas content.

Schmidt et al. (2008) attempted to directly solve shock waves emitted from bubble collapse in the flow around the prismatic body and the sphere. However, such a direct simulation requires quite a fine mesh with a small time-step, below one microsecond. The practical implementation with complicated geometry such as a propeller is impractical at the moment.

Alternatively, as a practical solution for assessing erosion, many researchers have

proposed erosion indicators derived from the macroscopic flow solved using CFD calculation.

10.4 Erosion indicator

Most indicators relate to pressure p, cavity volume V, void fraction α and their time derivatives, which are terms for describing the potential power P_{pot} included in the vapor structure. P_{pot} can be calculated as a time derivative of potential energy E_{pot} suggested by Vogel and Lauterborn (1988) as follows:

$$E_{pot} = \Delta p \cdot V \tag{2}$$

$$P_{pot} = \Delta p \cdot \frac{dV}{dt} + \frac{dp}{dt} \cdot V \tag{3}$$

where $\Delta p = (p_d - p_v)$ is the difference between the ambient pressure driving cavity collapse, p_d, and the vapour pressure, p_v. By dividing $Ppot$ by a cell volume, V_{cell}, potential power density can be expressed with a void fraction α as follows:

$$\frac{P_{pot}}{V_{cell}} = \Delta p \cdot \frac{d\alpha}{dt} + \frac{dp}{dt} \cdot \alpha \tag{4}$$

Hasuike et al. (2009) applied the following four indicators suggested by Nohmi et al. (2008) to a four bladed propeller whose individual blades have different tip load.

$$index1 = \alpha \cdot max\left[\frac{\partial p}{\partial t}, 0\right]$$

$$index2 = \alpha \cdot max[p_d - p_v, 0]$$

$$index3 = max\left[-\frac{\partial \alpha}{\partial t}, 0\right] \tag{4}$$

$$index4 = max[p_d - p_v, 0] \cdot max\left[-\frac{\partial \alpha}{\partial t}, 0\right]$$

RANS with k-ε turbulence model was used for the cavitation simulation. Cavitation was modelled by Singhal's full cavitation model based on Rayleigh-Plesset equation. In this cavitation model, the pressure fluctuation due to turbulence and the effect of non-condensable gas are taken into account in the mass transfer process. Index 2 could give a reasonable prediction for the area where the paint was peeled in model tests and describe the difference of the damaged area among different blades. Although the absolute values of the indexes have no physical meaning, they showed the possibility to estimate erosion risk qualitatively.

Eskilsson and Bensow (2015) applied three indicators called Discrete Bubble Method (DBM), Gray Level Method (GLM) and Intensity Function Method (IFM) to the case of cavitation over a NACA0015 foil. GLM is an index related to $dV/dt \cdot \Delta p$ and IFM related to dp/dt. DBM is based on the development of advected microscopic bubbles. However, the cavitation pattern was not well simulated by LES with Sauer cavitation model, and none of the methods could predict the erosive behaviour successfully. The authors stressed the need for further work.

Usta et al. (2017) applied GLM and IFM to the case of the King's College-D (KCD)-193 model propeller with five blades. In addition, they proposed the Erosive Power Method (EPM), which focuses on both the derivative of the vapor fraction and the pressure. The cavitating flow was simulated by DES with SST k-omega turbulence model. Cavitation was modelled by Schnerr-Sauer(S-S) cavitation model with Reboud correction, which implements a simplified Rayleigh-Plesset equation neglecting the influence of bubble growth acceleration, viscous effects and surface tension effects. All three indicators showed reasonable prediction for the erosion area. Figure 50 shows an example of a comparison of erosion area from model test and EPM. The

colours going red and blue in Fig. 4 show the area of high erosion risk. The maximum and minimum scalar values of the erosive intensity are limited with a threshold to make a meaning prediction. Although the threshold was chosen as $1*10^{-7}$-$1*10^{7}$ in this case, how to determine it is unclear. The authors addressed the need for further work to determine the erosion intensity thresholds numerically.

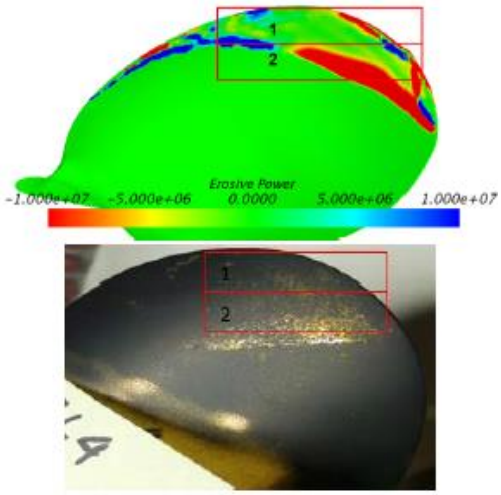

Figure 50: Comparison of erosion area from model test and EPM, Usta et al. (2017)

Melissaris et al. (2018) calculated the cavitating flow over the KCD-193 model propeller by RANS with SST *k*-omega turbulence model. The S-S cavitation model was applied. They investigated the difference of the contribution of the time derivative of pressure $\Delta\alpha \cdot dp/dt$ and the time derivative of void fraction $\Delta p \cdot d\alpha/dt$ to the cavitation aggressiveness. They found that the time derivative of the void fraction contributes more when using the time-averaged local pressure as the driving pressure *p*, while the time derivative of the pressure contributes more when using the instantaneous local pressure. $\Delta p \cdot d\alpha/dt$ using the time-averaged pressure as the driving pressure shows the best agreements with the paint test. The results shows an importance of a correct definition of the driving pressure for assessing the erosion intensity.

The European project "CaFE (Development and experimental validation of computational models for Cavitating Flows, surface Erosion damage and material loss)" was conducted from 2015 to 2018. Many papers have been published as fruits from the project. The following erosion indicators were developed within the project, Melissaris and Terwisga (2019).

$$\langle \dot{e}_s \rangle_{e_s} = \left(\frac{1}{e_s} \int_0^t \dot{e_s}^{n+1} dt \right)^{1/n} \quad (6)$$

$$\langle \dot{e}_s \rangle_f = \left(\frac{1}{T} \int_0^t \dot{e_s}^{n+1} dt \right)^{1/(n+1)} \quad (7)$$

where

$$e_s = \int_0^t \dot{e}_s dt = \int_0^t -\Delta p \cdot \frac{\partial \alpha}{\partial t} dt \quad (8)$$

These indicators relate to the time derivative of the void fraction which is the first term of Eq. (4). The indicator $\langle \dot{e}_s \rangle_{e_s}$ averages the local energy impact rate over the surface accumulated energy e_s, amplifying the local extreme events. The indicator $\langle \dot{e}_s \rangle_f$ is normalized by the total impact time T. The parameter n is used to emphasize the peak events.

These indicators were applied to the erosion risk assessment for the KCD-193 model propeller by Melissaris et al. (2019), the Delft twist 11 hydrofoil by Melissaris et al. (2019) and 2D NACA0015 hydrofoil by Schenke et al.

(2019). In general, the predicted high erosion risk area agreed well with the paint test. However, there were some cases that the erosion areas were overestimated or underestimated. The authors said that more insight is necessary, especially on the determination of pressure driving cavity collapse, p_d, for calculating Δp in Eq. (8).

10.5 Conclusion

To assess the cavitation erosion risk practically, various erosion indicators have been proposed, which can be derived from macroscopic features of the flow calculated using RANS, DES or LES. Most of them relate to pressure p, cavity volume V, void fraction α and their time derivatives. These indicators are helpful for propeller designers to predict potential erosion areas and locations.

However, it is unclear whether they always give reasonable predictions against various kinds of cavitation pattern. To evaluate the cavitation aggressiveness, some threshold for the indicator is required. Although they influence much on the erosion prediction, how to determine it is also unclear.

To develop the procedure on predicting cavitation erosion, it seems necessary to study further, such as the determination of pressure driving collapse, the influence of the distance between the bubble collapse and the surface, the influence of water quality and so on. Needless to say, the material response and the scale effect, which are not considered in most works, are to be studied as well.

Cavitation erosion modelling is a rapidly developing topic, and further developments should continue to be monitored, and updates to procedures should be considered in future.

11. RIM DRIVE TESTING

The committee was tasked to identify the need to develop a procedure for rim driven propulsor model testing and performance prediction. To understand the need for this and the extent of involvement of ITTC members in rim driven propulsor testing, a questionnaire was prepared and distributed to the ITTC members.

The questionnaire consisted of 39 questions ranging from general questions on the organisation's involvement with rim driven thrusters, to more specific questions on the procedures used to conduct model tests and performance prediction.

Out of 92 organisations to whom the questionnaire was sent, 13 completed responses were received. This immediately indicates that rim driven propulsors are currently of interest to a small group of organisations.

The first question asked whether the organisation was involved in activities related to rim driven thrusters. The responses to this are summarised in Figure 51. A total of 6 organisations are actively involved in these type of devices. A further question then asked what type of activities these organisations carried out on rim driven thrusters. The responses are summarised in Figure 52. Of the respondents, 5 are carrying out model tests, which may include model manufacture, while 3 are involved in design or theoretical studies.

Respondents were then asked whether a specific ITTC procedure should be developed for rim driven thruster testing and performance prediction. The response to this was largely positive, even from some who are not actively involved (Figure 53).

A few publications were identified by the respondents, notably Dang and Ligtelijn (2019),

Klinkenberg et al. (2017), Yakovlev et al. (2011) and Sokolov et al. (2012). These may be used to understand some of the key considerations in rim driven thruster testing.

Notably, no respondent was aware of any full scale test data for rim driven thrusters, which seems a significant loss. It is likely that the manufacturers would have such information, and it may be useful for a future committee to try to obtain examples of such data.

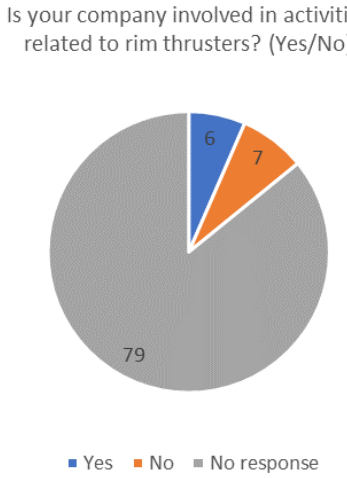

Figure 51: Rim drive responses (question 1)

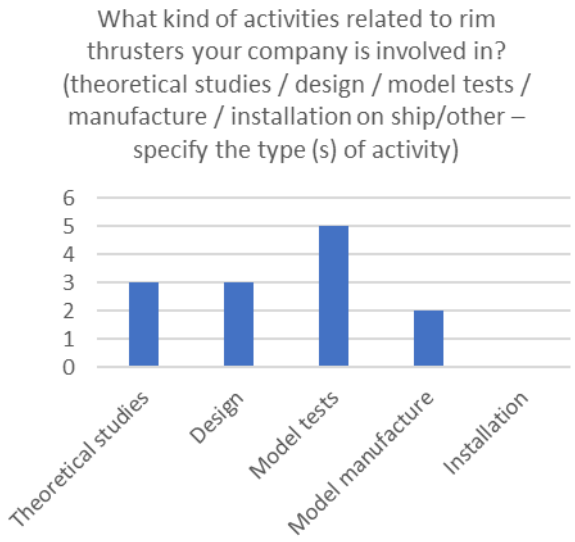

Figure 52: Rim drive responses (question 2)

Figure 53: Rim drive responses (question 4)

Model tests are carried out in either a towing tank or a cavitation tunnel, in common with standard propeller testing. Special mounting arrangements are required to support the nozzle, and in some cases a special drive is built to allow measurement of thrust and torque on the blades. If the thruster has a hub, the propeller can be mounted on a standard propeller dynamometer shaft, but this is not possible with hubless designs.

Measured parameters are in line with those expected for a propeller test, including thrust, torque, flow velocity and RPM, as well as the tank/tunnel environmental conditions and perhaps the electrical performance of the motor.

The key challenges that have been reported include isolating the thrust and torque of the thruster blades, scaling issues due to the flow in the gap, friction in the bearings and manufacturing and mounting issues associated with hubless designs.

Thrust is either measured on the whole unit, using load cells or a 6-component balance, or can be measured using a ring-shaped transducer. For a hub-type thruster, the thrust of the rotor

can be measured using a standard propeller dynamometer.

Torque can also be measured using the same methods, but can also be derived from the power consumption of the motor, with a correction for friction. The torque of the rim thruster is affected by friction in the gap between the inner and outer ring. This is not Froude scaled. Also the torque on the nozzle may not be negligible so should be measured.

Performance prediction of rim driven thrusters is typically based on model test results, with ITTC blade friction corrections to account for scale. This does not account for the scaling of the gap flow, and currently the only method for assessing the Reynolds number effects in this part of the flow is to use CFD. A number of the respondents mentioned that they use CFD to account for the scale effects.

In summary, there are a number of ITTC members carrying out model tests of rim driven thrusters, and no consistent approach is currently taken to measure the thrust and torque, or to scale the results to make full scale predictions. It is therefore recommended that the next Resistance and Propulsion Committee should work towards developing a new procedure to fill this gap.

12. INFLUENCE OF F_D ON POWER PREDICTION

12.1 Introduction

The objective of this task was to identify the influence of the new F_D definition on power prediction. As is well known, F_D is the skin friction correction in a propulsion test and represents an additional towing force to compensate the difference of resistance between model and ship scale (relatively higher resistance in model scale than ship scale). From this definition, the F_D value can be calculated considering the model scale speed, density of water, wetted surface area and non-dimensional coefficient of resistance in model and ship scale. In practice, some parts of the resistance at ship scale are not included and some parts are added to get a more reliable prediction.

The 28th ITTC general conference accepted to adopt the new F_D definition to enhance the accuracy of powering performance prediction by adding C_A in the formula. However, it did not provide an appropriate basis on whether it actually improves accuracy, so the committee was asked to evaluate the extent of the impact.

12.2 History of F_D definition change

Before looking at the impact of F_D change, the history of previous F_D changes was reviewed and summarized as below:

~ ITTC 24th (2005):

$$F_D = 1/2\rho_M V_M^2 S_M [C_{FM} - (C_{FS} + \Delta C_F)]$$

$$\Delta C_F = [105(\frac{k_S}{L_{WL}})^{1/3} - 0.64] \times 10^{-3}$$

ITTC 25th (2008) ~ 27th (2014):

$$F_D = 1/2\rho_M V_M^2 S_M [C_{FM} - (C_{FS} + \Delta C_F)]$$

$$\Delta C_F = 0.044[(\frac{k_S}{L_{WL}})^{1/3} - 10Re^{-1/3}] + 0.000125$$

ITTC 28th (2017):

$$F_D = 1/2\rho_M V_M^2 S_M [C_{FM} - (C_{FS} + \Delta C_F + C_A)]$$

$$\Delta C_F = 0.044[(\frac{k_S}{L_{WL}})^{1/3} - 10Re^{-1/3}] + 0.000125$$

$$C_A = (5.68 - 0.6logRe) \times 10^{-3}$$

From 2008, the existing (old) $\triangle C_F$ was divided into new $\triangle C_F$ and C_A (i.e., C_{TS} includes new $\triangle C_F$ and C_A, but still (new) $\triangle C_F$ was only included in F_D calculation). This separation had been proposed from 19th ITTC because the

existing $\triangle C_F$ has been criticized for not properly reflecting the roughness effect of the hull and was finally adopted by the 25th ITTC in 2008. However, the C_A value left room for continued use of the empirical formula previously used in each towing tank and the standard C_A value was chosen to be similar to those before they were separated.

In addition, it should be noted that despite these changes in the standard procedure, each towing tank adheres to the existing method, taking into account the continuity of their own analysis method.

12.3 How to identify the influence of F_D definition change

As described in last chapter, the history of F_D change was reviewed and the actual value of F_D in propulsion tests with normal size of model ships is as shown in Table 4.

Separation of the old $\triangle C_F$ into the new $\triangle C_F$ and the C_A had to be consistent and the actual value of F_D has a similar level comparing ITTC 28th and ~24th, but comparing 28th and 25th through 27th, there is a considerable difference. If we take the change from 27th to 28th, the typical value of change is as below (Table 3).

Table 3: Change in FD for different ship types

VLCC	-5.6%
Aframax	-10.7%
Suezmax	-9.1%
VLGC	-9.9%
174k LNGC	-3.2%
15.1k CC	2.6%

Table 4: Values of FD for different ship types

Ship Type	Value	ITTC 28th(2017)	ITTC 25th(2008)~27th(2014)	ITTC ~24th(2005)
VLCC (14.5kts)	F_D(N)	14.47	15.33	14.85
	$\triangle C_F$*1000	0.118	0.118	0.169
	C_A*1000	0.092		
Aframax (14.5kts)	Fd(N)	13.70	15.33	14.03
	$\triangle C_F$*1000	0.117	0.117	0.251
	C_A*1000	0.167		
Suezmax (15kts)	Fd(N)	19.46	21.41	19.93
	$\triangle C_F$*1000	0.122	0.122	0.224
	C_A*1000	0.135		
84k LPGC (17kts)	Fd(N)	12.64	14.03	12.72
	$\triangle C_F$*1000	0.137	0.137	0.279
	C_A*1000	0.151		
174k Twin LNGC (19.5kts)	Fd(N)	25.44	26.27	25.36
	$\triangle C_F$*1000	0.152	0.152	0.199
	C_A*1000	0.043		
15.1k CC (22kts)	Fd(N)	36.95	36.02	36.31
	$\triangle C_F$*1000	0.162	0.162	0.152
	C_A*1000	-0.033		

The objective of this study is to identify the impact of this change on the powering performance prediction and this can be achieved through evaluating the corresponding change of propulsion efficiency and propeller revolutions.

To calculate the change of propulsion efficiency and propeller revolutions, the propulsion test data was re-analysed with several values of F_D around the definition from ITTC 27th as shown in Figure 54. This shows the general trend of the change of propulsion efficiency and propeller revolutions along with the change of F_D value and finally can identify the influence of the new F_D definition.

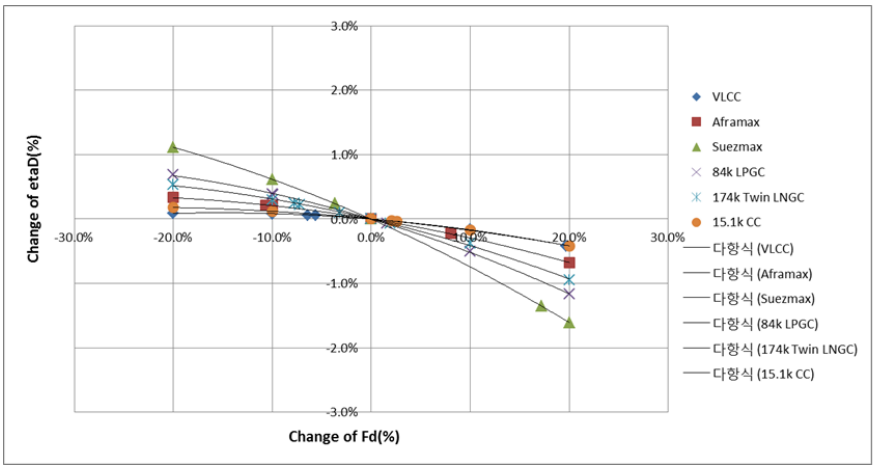

Ship Type	△Fd	△EtaD
VLCC	-5.6%	0.1%
Aframax	-10.7%	0.2%
Suezmax	-9.1%	0.6%
VLGC	-9.9%	0.4%
174k LNGC	-3.2%	0.1%
15.1k CC	2.6%	0.0%

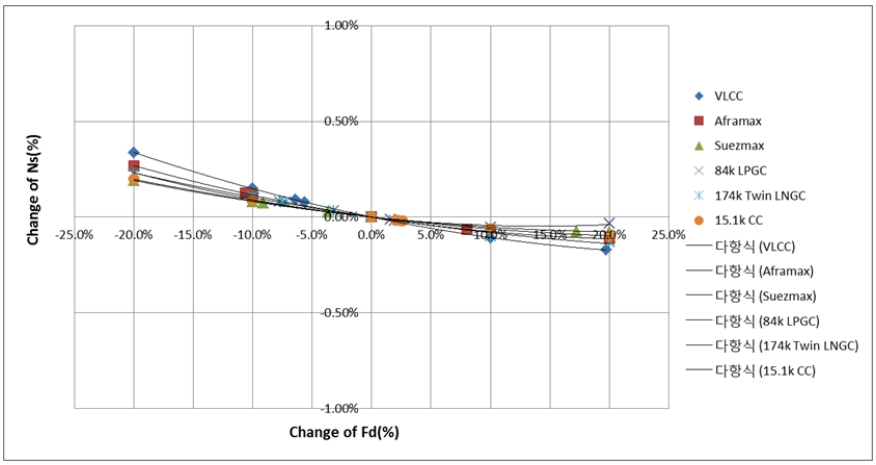

Ship Type	△Fd	△Ns
VLCC	-5.6%	0.08%
Aframax	-10.7%	0.12%
Suezmax	-9.1%	0.07%
VLGC	-9.9%	0.09%
174k LNGC	-3.2%	0.03%
15.1k CC	2.6%	-0.02%

Figure 54: Sample analysis of propulsion test with the different value of F_D

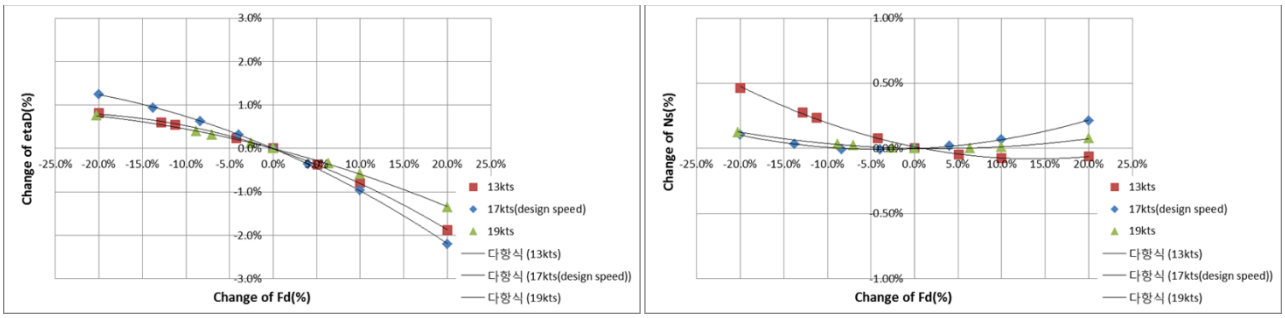

Figure 55: Effect of speed on the change of propulsion efficiency and revolution of propeller

The committee members were asked to re-analyse their own propulsion test data with the different value of F_D and finally 31 cases were collected. During this analysis, the design speed only was chosen and the effect of speed was investigated to be limited, as shown in Figure 55.

12.4 Result of sample calculation on the effect of the new F_D definition

The definition of F_D includes $\triangle C_F$ and C_A and these two parameters are dependent on the ship length and Reynolds number as in Figure 56. There is a wide variety of ship types and speed, so it is necessary to organize them into a single parameter to present the result. The Reynolds number was already included in the definition of friction resistance compensation, so it was used as an independent parameter.

The overall trend of F_D change is shown in Figure 56. First of all, the amount of F_D change itself is relatively small for large and high speed and vice versa. By this trend, the influence of large and high speed vessel on the power prediction is relatively limited. For small and slow vessels, the impact of the F_D definition change on power prediction is considerable and the propulsion efficiency change (EtaD) is about 1~2%. For the revolution of propeller, the impact of the F_D definition change is very limited at around 0.2%.

As a general conclusion, the new F_D definition appears to make a very small difference to the powering prediction compared to the previous definition. Many towing tanks still use the old definition, but should be aware of what the effect of this is on their prediction.

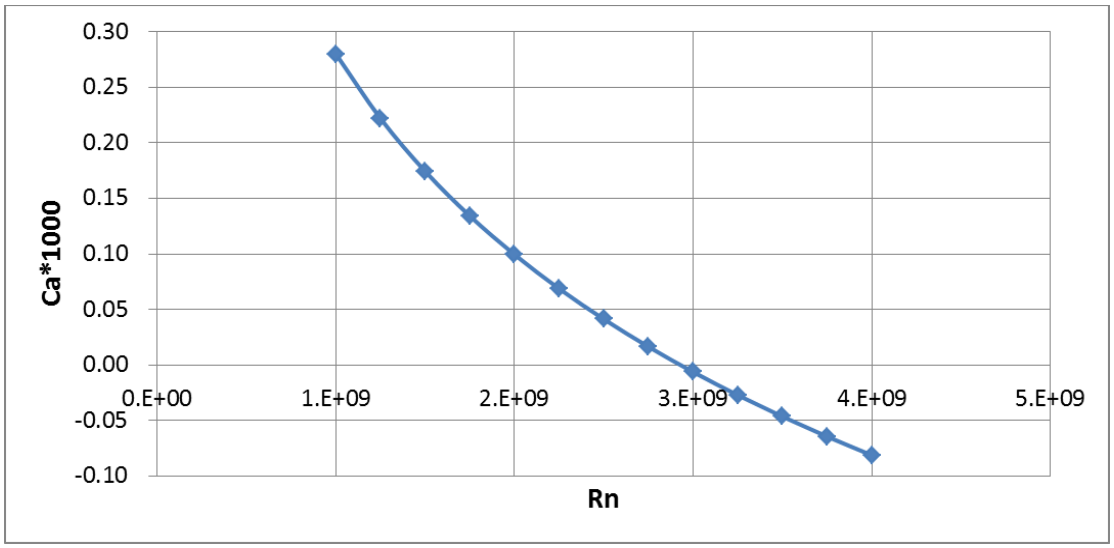

Figure 56: Dependency of Reynolds number on C_A

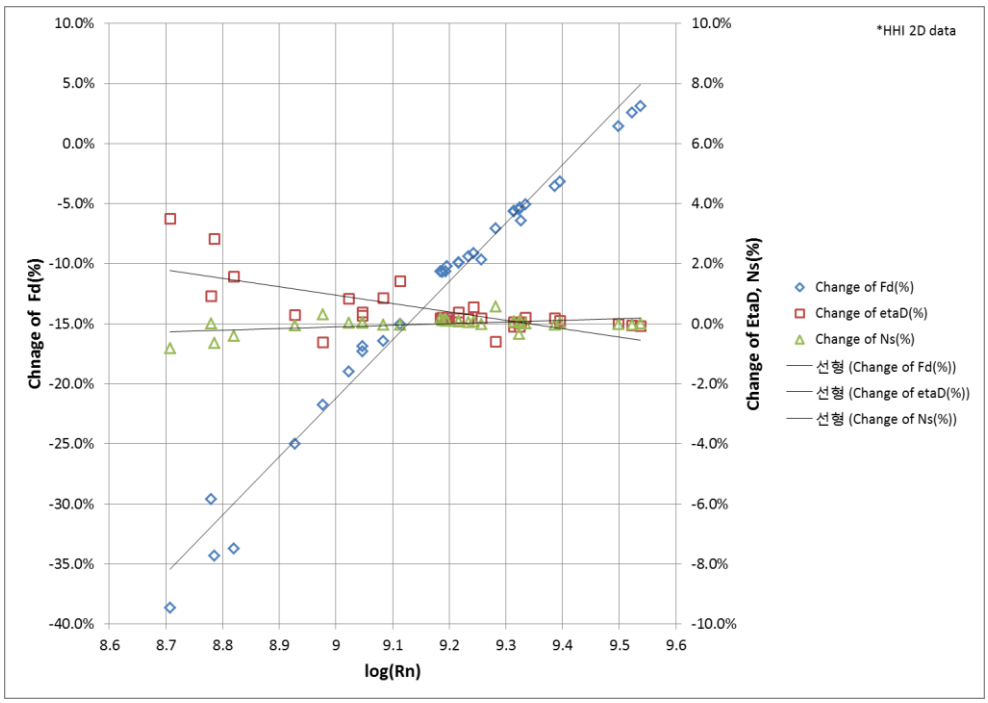

Figure 57: Overall trend of F_D definition change and the impact on the propulsion efficiency and revolution of propeller

13. REYNOLDS NUMBER EFFECTS ON PROPELLER TESTING

As described in the ITTC recommended procedures 7.5-02-03-01.4, "1978 ITTC Performance Prediction Method", and 7.5-02-03-02.1, "Open Water Test", the minimum Reynolds number, based on the representative chord length at r/R=0.75, must not be lower than 2×10^5. Some concerns about unstable open water test results and the applicability of corrections for low blade ratio propellers or

other unconventional propulsors when the Re is below a critical value have been raised. The 28th ITTC Propulsion Committee suggested that it might be necessary to increase the minimum Reynolds number to at least 3×10^5 to have enough margin to obtain reliable data. An additional literature review for the minimum Re has been conducted during the 29th ITTC term.

From Kim et al. (1985), the variation in K_T and K_Q with Reynolds number is inconsistent at $Re<5\times10^5$ for a propeller model KP088 (D=0.25m, P/D=1.635, Ae/A0=0.779) in the towing tank open water test. There is no difference in terms of the thrust and torque of the propeller due to three different wing section profiles (NACA 66, MAU and NSMB series). The measured values are stabilized when $Re\geq3\times10^5$.

Sheng et al (1979) investigated the scale effect by using five propeller models of the same MAU 4-60 profile (P/D=0.788) in towing tank open water tests at Reynolds numbers ranging from 1.2×10^5 to 8.1×10^5. The recommended critical Re was 3.0×10^5. If $Re < 2.5\times10^5$, the scale effect was still evident after ITTC 1978 scale effect correction.

Hasuike et al (2017) presented extensive oil flow visualization and numerical calculations of the scale effect of a series of propellers (27 in total) for a chemical tanker. The blade profiles were parametrically changed. Oil flow visualization of the propeller open water test (POT) and self-propulsion test (SPT), showed flow patterns in SPT condition at $Re=2.7\times10^5$ were similar (laminar and include laminar flow separation) to that in the POT condition at $Re=3\times10^5$ which was a typical Reynolds number in SPT condition, as shown in Figure 60.

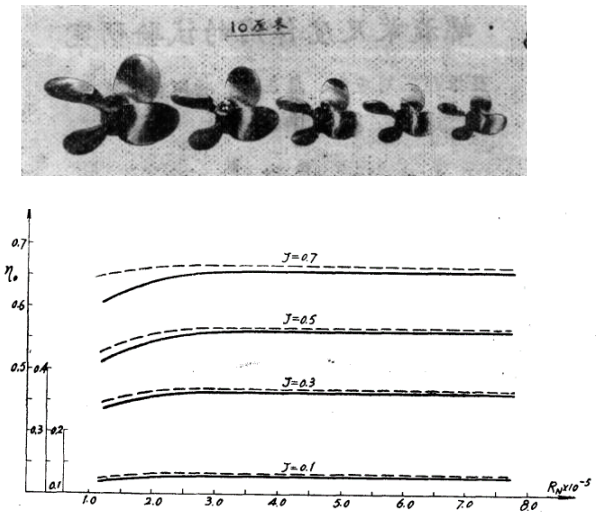

Figure 58: The open water efficiency variation against Re number from Sheng (1979). The dotted lines represented the efficiency after scale effects correction using ITTC1978 method and solid lines represented the model test results.

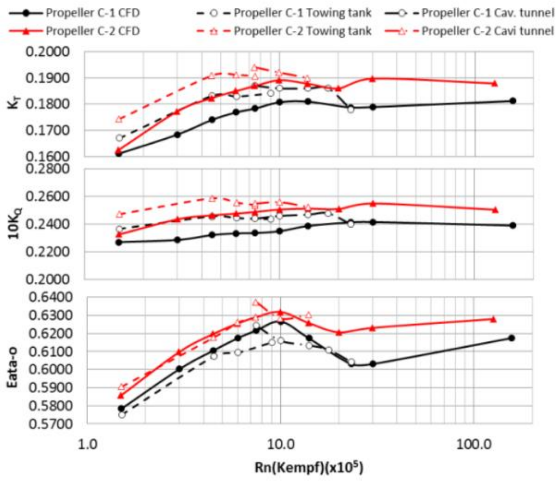

Figure 59: KT 10KQ and Eta0 Variation of Propeller C-1 (D=0.25m, Ae/A0=0.48) and Propeller C-2 (D=0.25m, Ae/A0=0.38) against Reynolds number from Hasuike et al (2017)

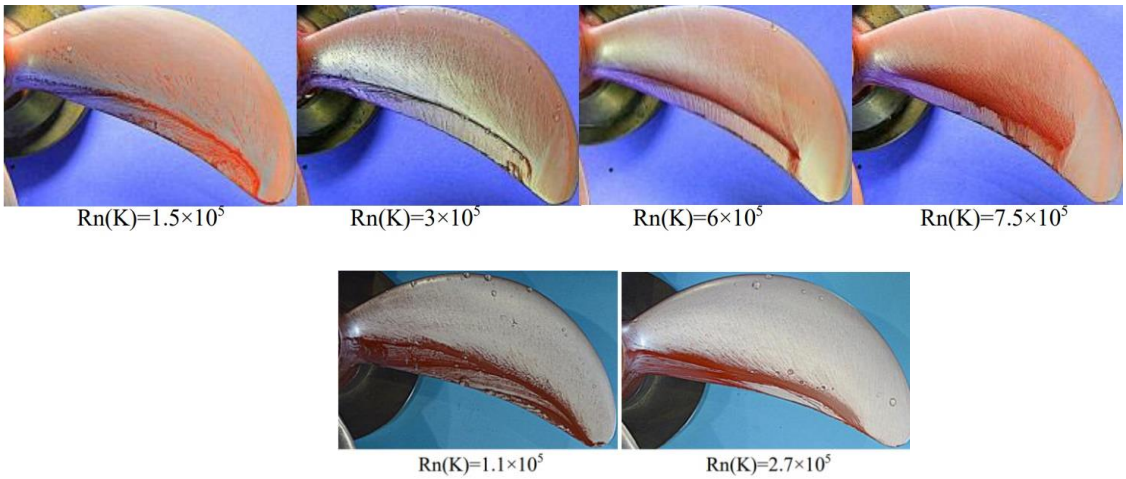

Figure 60: Oil flow visualization results for POT condition (above) and SPT condition (below) of Propeller C-2 (D=0.25m and Ae=0.38) from Hasuike et al (2017)

In the POT condition, K_T and K_Q increase in the range of Re=1.5×10^5 to 4.5×10^5 due to the flow separation extent decreasing gradually. K_T is almost flat and K_Q is decreasing in the range of Re=4.5×10^5 to 7.5×10^5. The range of laminar and turbulent flow is maintained and the thickness of the boundary layer was decreased. The flow characteristics of POT condition are thought to be mainly laminar in the range of Re=1.5×10^5 to 7.5×10^5.

The "2POT method" of ITTC recommended procedure 7.5-02-03-02.1, with the lower Reynolds number corresponding to propulsion factors evaluation and the higher Reynolds number as high as possible, was supported based on such investigation. However, similar laminar-turbulent transition flow, not the laminar flow for the propeller model surface flow at lower Reynolds number POT with corresponding SPT should be achieved by careful investigation. From Lücke et al (2017), the lower Reynolds number POT test should be 40% higher than during flow pattern for small blade area propeller.

Baltazar et al (2019) presented numerical predictions of an open water propeller (P0.7R /D=0.757 and Ae/A0=0.464) at different Reynolds numbers ranging from 10^4 to 10^7 using the RANS code, ReFRESCO V2.1, with two turbulence models, k-ω SST turbulence model and γ-(Re)̃θt transition model. These are shown in Figure 61 and can be compared to paint test results from Boorsma (2000) in Figure 62. The limiting streamlines at outer radii predicted using the k-ω SST turbulence model agreed well with the leading edge roughness (LER) propeller paint test. On the other hand the limiting streamlines predicted using the γ-(Re)̃θt transition model matched the smooth propeller paint test when inlet turbulence quantities were properly selected. From the numerical results at Re=1×10^5 and 5×10^5 and the K_T K_Q trend with Re between 10^4 to 10^7, it seems that 5×10^5 might be the minimum Re.

Yao (2019) presented the CFD investigation on the flow pattern of a PPTC propeller model (D=0.25m, P/D=1.635, Ae/A0=0.779) using commercial codes STAR-CCM+ with transition turbulent model, the Reynolds number ranged from 2.32×10^5 to 3.63×10^7. From Re 2.32×10^5

to 3.48×10^5, the flow pattern on the back side transited from laminar to turbulent in the outer radii closing to trailing edge, while the full scale flow pattern is fully turbulent both on back and face sides. The critical Re for such case is estimated to be around 3.48×10^5.

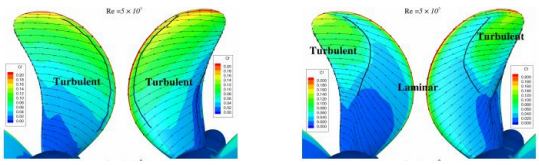

Figure 61: Flow pattern for POT at Re=5×105 using k-ω SST turbulence model (left) and γ-(Re)˜θt transition model (right) from Baltazar et al (2019).

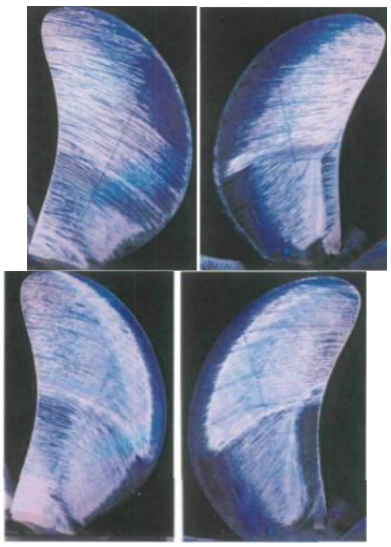

Figure 62: Propeller paint test for at Re=5×105 with (left) and without (right) leading edge roughness (LER) from Boorsma (2000)

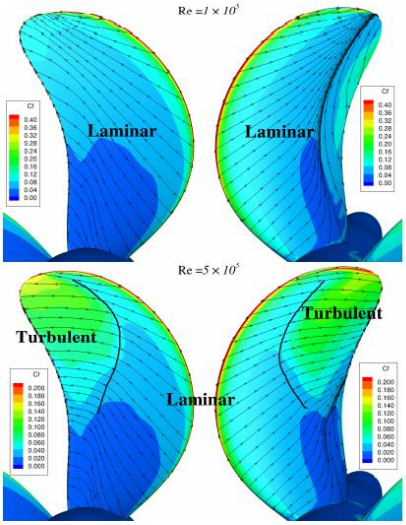

Figure 63: Flow pattern for POT at Re=1×105 (above) and Re=5×105 (below) using γ-(Re)˜θt transition model from Baltazar et al (2019).

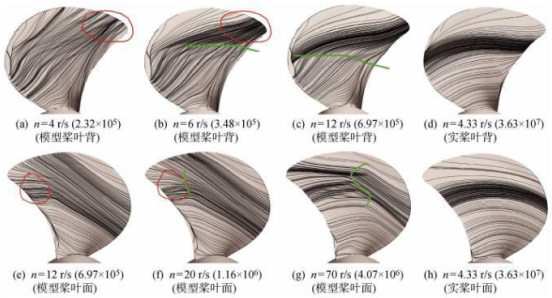

Figure 64: Different Re flow patterns on a PPTC propeller surface from Yao (2019)

Heinke et al (2019) investigated the Reynolds number influence on open water characteristics using four short chord length model propellers. For propeller A (D=0.239m, Ae/A0=0.418) and propeller B (D=0.239m, Ae/A0=0.444), the thrust coefficients are nearly constant, while the torque coefficient decreases linearly with rising Reynolds number if Re is above 5×10^5, as shown in Figure 65. The ITTC 1978 correction method is applicable for consistent full scale propeller open water characteristics when the Re is above 5×10^5.

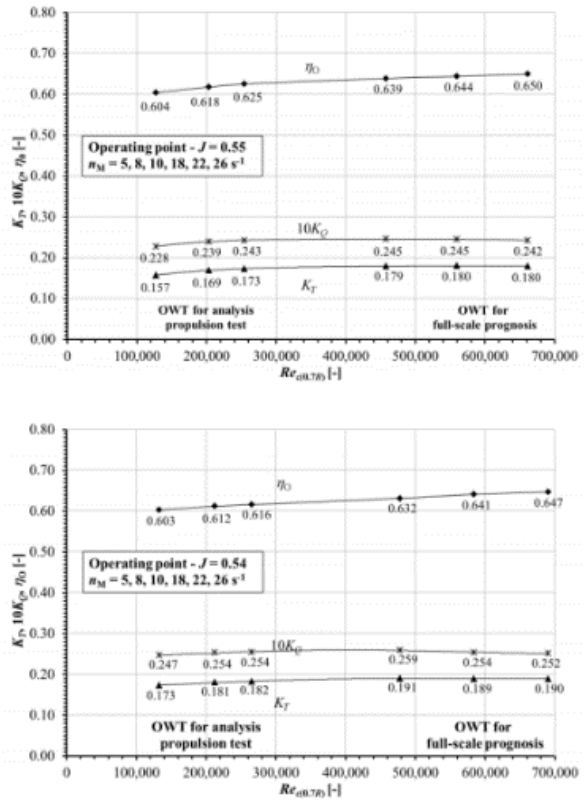

Figure 65: Variation of propeller coefficients of propeller A (left) and propeller B (right) with the Reynolds number from Heinke (2019)

From the above literature review, the minimum Reynolds number (2×10^5) in the present ITTC procedure is probably not sufficient for obtaining stable open water test data. This minimum Reynolds number generally ranges from 3×10^5 to 5×10^5 for different propeller types. This range might not be suitable for other propeller types, like CLT propellers or ducted propellers etc., which should be treated separately.

One specific minimum Reynolds number which is applicable for all propeller types may not be possible. Each model basin is recommended to analyse their specific propeller case and to choose the proper minimum Reynolds number, especially for propulsion factors evaluation purpose. Careful attention should be paid to propeller open water RPM selection to achieve the similar transition or turbulent flow, not fully laminar flow pattern on the propeller model surface, and also for the proper propeller dynamometer range to reach the sufficient measurement resolution. A series of Reynolds number variation open water tests or CFD simulations covering the self-propulsion Reynolds number range is recommended for investigating the Reynolds number dependency. The ITTC procedures 7.5-02-03-01.4, "1978 ITTC Performance Prediction Method", and 7.5-02-03-02.1, "Open water test", are recommended to be revised during the 30th ITTC term.

14. SCALING METHODS FOR PROPULSORS

Scaling of open water curves is an important topic since the effect will be directly visible in the speed and power curve.

Today, several empirical methods are used where the ITTC'78 (7.5-02-03-01.4) method is widely adopted by the ITTC members. This method is relatively simple and therefore easy to apply. Of other scaling methods the following can be mentioned: "Strip method", Streckwall et al. (2013) and "Stone", Helma (2015). Both are comprehensive to apply and would typically require a software solution. Additionally, for ITTC'78 scaling, only data for one representative chord will be needed where the "other" methods need data for several chords from the root to the tip.

In contrast to the empirical scaling methods, a future solution for scaling of open water curves could be simply to use CFD to predict open water curves at both model scale and full scale and to derive the scale effects from these. The 28th ITTC Propulsion committee presented a CFD open water benchmark study. There 13-14 ITTC members presented CFD open water curves of an unconventional 4-bladed FP propeller and a conventional 5-bladed CP propeller. The results showed some scatter in the

curves, especially at the higher J-values corresponding to the operating point in a self-propulsion condition. This could lead to the question of whether CFD is mature enough for detecting open water scale effects.

14.1 Case study

In the below, scale effects (ITTC'78, Strip method and CFD scaled) are investigated for six different propellers designed for the same medium size container vessel. There is an as-built propeller designed for full speed and five retrofit alternatives designed for slow steaming. Additionally, the five new propellers represent 15-years of development in propeller design. The as-built propeller must be designed pre-RANS CFD and the new ones with RANS CFD available.

Figure 66: Original (dark) and the five new (shiny) model propellers

The propellers have the following characteristics / features:

1) Original / lower middle. Six bladed with high area ratio. Typical design for a container vessel delivered before slow steaming.
2) Retrofit / lower right. Four bladed with special tip feature. Slightly larger in diameter relative to original.
3) Retrofit / upper left. Four bladed with special profile feature. Larger in diameter relative to original.
4) Retrofit / upper middle. Six bladed with slender blades and untraditional rake slope. Identical diameter to original.
5) Retrofit / lower left. Four bladed with some tip loading. Larger in diameter than original.
6) Retrofit / upper right. Four bladed with special tip feature. Larger in diameter relative to original.

The scale effect is investigated for the full open water curve. However, in the following only results for J=0.8 are presented. This is around the operating point in a self-propulsion condition.

Figure 67, Figure 68 and Figure 69 show the percentage change from model scale to full scale, for the three scaling methods.

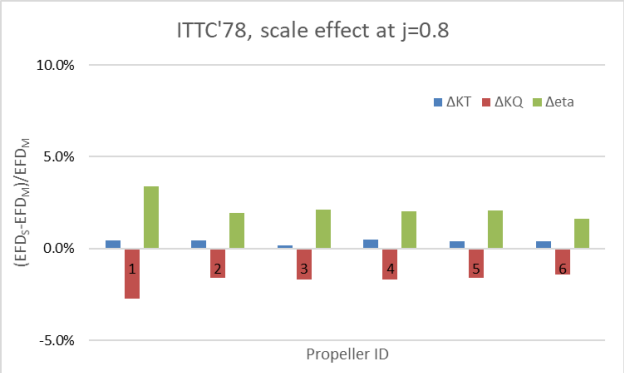

Figure 67: ITTC'78 scaling

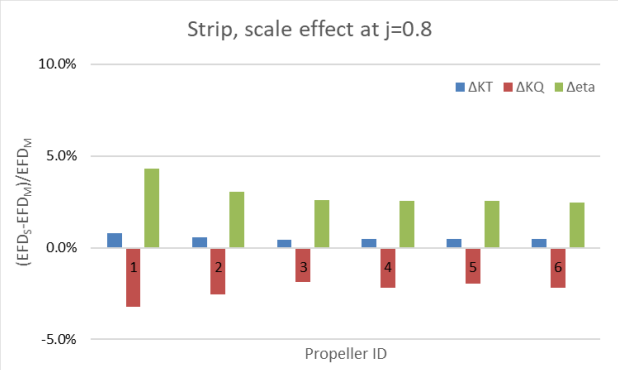

Figure 68: Strip method scaling

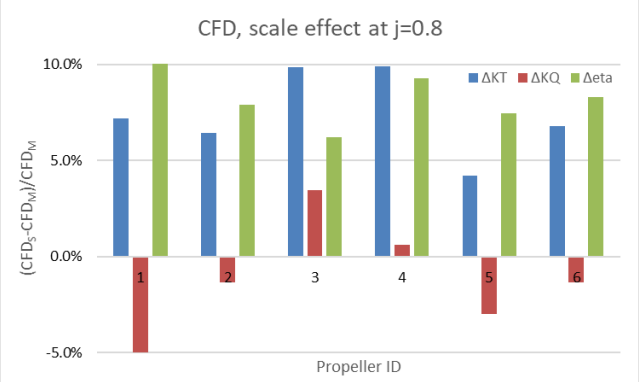

Figure 69: CFD scaling

From the figures it is clearly visible that the result of ITTC'78 and Strip method are in line. That said, the Strip method prescribes slightly larger scale effects for all six propellers. On average (of the six propellers) the scale effect is 0.1% larger for KT and 0.6% for KQ. This might not seem much, but it results in 0.7% (again in average of the six) more efficient propellers at this advance ratio (J=0.8).

The scale effects from CFD scaling is somewhat off in this example compared to the two empirical methods and without doubt it is the CFD scaling that is way too optimistic in this specific example. However, with some progress in CFD open water calculations the method should in theory work, and this could replace any empirical method. CFD open water will require a 3D CAD file of the actual propeller and this is not always available for commercial projects. Additionally, the workload with CFD open water compared to a well-known empirical method is somewhat larger.

15. PROPULSOR PERFORMANCE IN WAVES

15.1 Introduction

A literature study was undertaken to investigate and identify the influences of operating propellers in waves. The influences on the propeller inflow are broken down into two categories; wave dynamics, and induced flows from ship motions in waves.

Wave dynamics refers to a propeller operating in waves, without the influence of a ship, which causes non-uniformity in the propeller inflow as a function of the orbital wave velocities, assuming trochoidal wave theory. Induced flows from ship motions refer to the influences from a hull that is surging, pitching and heaving in waves.

Influences were identified as added resistance, temporal and spatial variations of inflow wakes, ventilation, and shaft speed variation affecting thrust, torque, efficiency, cavitation, and pressure pulses.

15.2 Wave dynamics

McCarthy (1961), illustrated that, for deeply-submerged propellers, fluctuations in the open water thrust and torque in waves is in good agreement with the calm-water uniform-flow performance curves for the propeller, when the mean orbital velocities of the waves are considered in the advance coefficient (Figure 70 and Figure 71).

For the low frequencies of encounter of a propeller in waves, unsteady effects may be neglected in calculating the instantaneous thrust

and torque of a propeller in a wave crest or trough.

The results shown indicate that the percentage changes in the propeller's thrust and torque increase with:

1. Increasing average speed coefficient (J_m)
2. Increasing wave height-propeller diameter ratio (a/D)
3. Decreasing propeller speed-wave celerity ratio (V/V_w)
4. Increasing wave height-wave length ratio (a/λ)

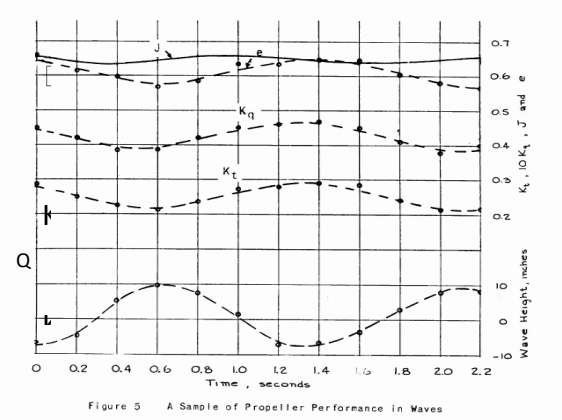

Figure 70: Propeller performance as a function of wave oscillation from McCarthy et al (1961)

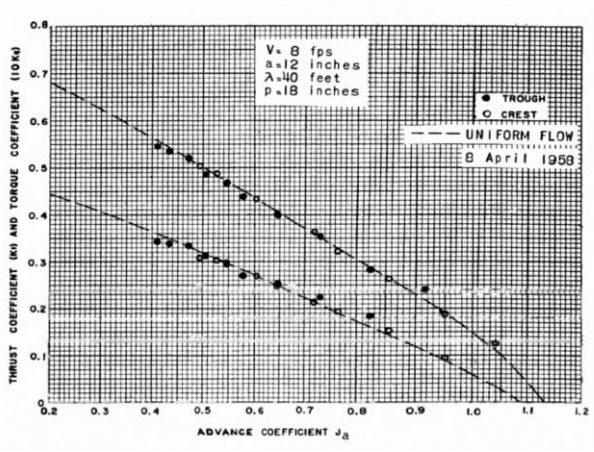

Figure 71: Calm water and wave agreement considering propeller inflow speed from McCarthy et al (1961)

Taskar et al (2016) showed that when K_T, K_Q and efficiency in the presence of waves is plotted against the corresponding advance coefficients, the data points follow the propeller open water curves. From this, we can conclude that the efficiency is primarily affected by the average change in wake fraction and not much by wake distribution (Figure 72).

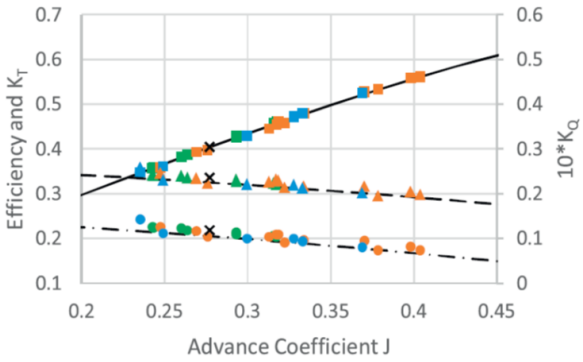

Figure 72: Calm water and wave agreement considering propeller inflow speed from Taskar et al (2016)

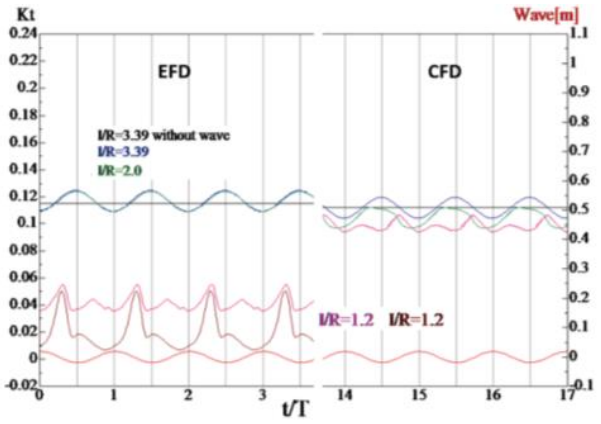

Figure 73: Correlation of K_T from waves and calm water and influence of ventilation for KVLCC2 propeller at J=0.5 from Tokgoz et al (2017)

Tokgoz et al (2017) investigated the depth of propeller immersion in waves and corroborated the results of McCarthy and Taskar for deeply submerged propellers. Due to wave orbital velocities, the minimum thrust is achieved when

the wave crest is at the propeller plane. Ventilation was shown to significantly affect the trend of thrust fluctuations where the maximum value of thrust occurs in the wave crest while the minimum values of thrust occur in the wave trough when ventilation occurs. This effect is stronger and more prevalent with the reduced expanded area ratio propeller since the suction pressures are greater at the blades. The influence of ventilation is strongly related to the depth of immersion.

Tokgoz et al (2017) illustrate by computations of KVLCC2 in waves without including the surge motion of the vessel that when surge is essentially zero (region B), the mean values of the EFD and CFD results are comparable. In region A where the ship surges forward the thrust is not comparable. Although the mean levels are different, the characteristics of ventilation on thrust is apparent in both regions (Figure 74 and Figure 75).

Taskar et al (2017) show that the mean wake fluctuations due to the wave orbital velocities are relatively constant and greater than that due to surge regardless of the wavelengths (Figure 76). The mean change in wake is more significant at low ship speeds. The propeller efficiency is dependent on the average wake changes rather than the changes in the wake distribution and is effected the most when the wavelength is close to the ship length.

Hsin, Ching-Yeh et al (2016) concluded that the unsteady flow effects due to the ship wake is more important than that due to the ship motions.

15.3 Ship motions

Taskar et al (2016) showed that cavitation and pressure pulses are directly related to wake distribution, and they depend less on average wake fluctuations. The relative stern motion was only shown to affect the range of Cp_{min} and not the angle of attack; since it only affects the cavitation number, while the wake change can affect both the variables. It was observed that wake change, due to wave orbital velocities and hull interactions, does not significantly affect the amount of cavitation hence cavitation margin should be considered only to handle increased load and relative stern motions.

Taskar et al (2016) additionally revealed that the blade root circulation in short waves was always greater than calm water and generally higher for all other wave conditions. The change in tip circulation, at top dead centre, when operating in waves was equal to or shown to be substantially lower than in calm water.

Taskar et al (2017) found that contrary to the expectation of less hull wake influence for a twin-screw ship, both the cavitation and pressure pulses increased remarkably due to the effect of waves, as did the cavitation volumes.

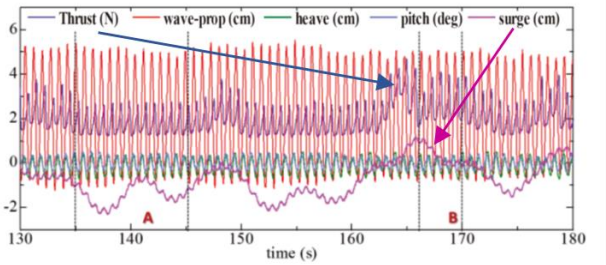

Figure 74: EFD time series of KVLCC2 in λ/L=0.6 illustrating wave height, thrust, and ship motions from Tokgoz (2017):

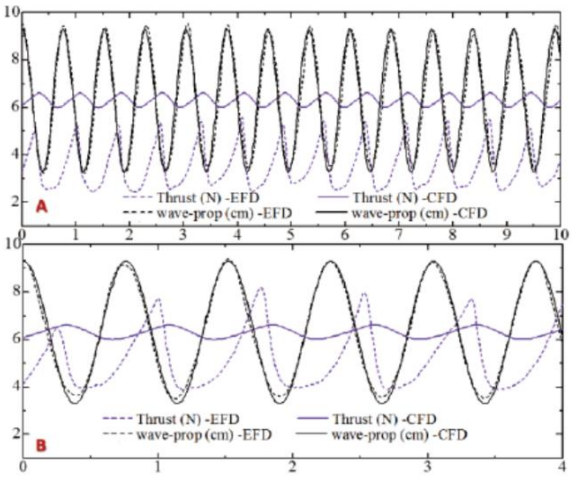

Figure 75: Surging influence on thrust in waves from Tokgoz (2017)

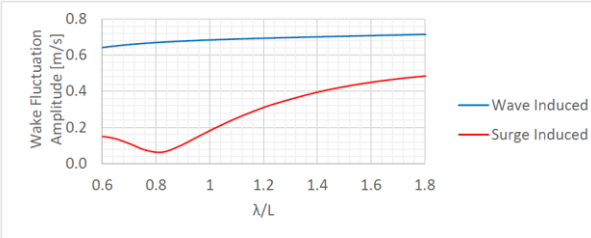

Figure 76: Comparison of the contribution of wave induced and surge induced fluctuation in the wake fluctuation

15.4 Conclusions

Propeller thrust, torque and efficiency are primarily affected by the average change in wake fraction. Propeller cavitation and pressure pulses are primarily affected by variation in the distribution of the wake.

Mean wake fluctuations due to the wave orbital velocities are relatively constant and greater than that due to surge regardless of the wavelengths.

If ventilation is present, the trend of thrust fluctuations significantly alter from deeply submerged conditions and there can be severe reductions in thrust followed by higher harmonics before recovering.

Hub vortex cavitation was found to be more likely to occur while operating in waves than tip vortex cavitation. The hull interaction with the wake changes due to waves resulted in lower levels of cavitation for a single screw in comparison to a twin screw.

It is recommended to perform scaling studies to decipher the level of model hull wake interactions with the wave field when conducting model scale measurements of propellers in waves.

The influence of ventilation on propeller performance is recommended for further evaluation during 30th ITTC term.

16. CONCLUSIONS AND RECOMMENDATIONS

16.1 Task 2

Adopt the updated procedures:

7.5-02-02-01
7.5-02-02-02
7.5-02-02-02.1
7.5-02-02-02.2
7.5-02-03-01.1
7.5-02-03-01.3
7.5-02-03-01.4
7.5-02-03-01.7
7.5-02-03-02.1
7.5-03-01-01
7.5-03-01-02
7.5-03-02-02
7.5-03-02-04

16.2 Task 3

A new procedure has been written on measurement of wave profiles and the

calculation of resistance from the wave profile data.

It is recommended that the conference adopt this new procedure. It is also recommended that the next committee should conduct some validation of this new procedure.

16.3 Task 4

A review of the literature on verification and validation of flow field data has been undertaken. However, while verification and validation, including uncertainty analysis, of CFD predictions are commonly performed for integral values such as resistance, it is much less common to find uncertainty studies on flow field quantities.

There are existing procedures on CFD V&V, which includes some description of uncertainty assessment for point data in the flow field. There are also procedures related to the uncertainty of flow measurement e.g. 7.5-01-03-*.

16.4 Task 5

Following interaction with the Specialist Committee on Energy Saving Methods, there is increasing interest in low friction coatings. It is recommended that characterisation of low friction coatings to be treated in a manner consistent with that of roughness effects. Guidelines for model tests of air lubrication, low friction coatings, wind assisted vessels may need to be developed as these technologies evolve.

16.5 Task 6

In collaboration with the Specialist Committee on Ships in Operation at Sea, an inconsistency in the load variation test procedure was identified and resolved.

16.6 Task 7

The ship hull or propeller surface roughness due to coatings or biofouling have a significant influence on the ship performance. The effects of hull surface roughness due to the coatings are often taken into account in the total resistance prediction as the roughness allowance ΔC_F which is defined by the Townsin formula. In this formulation, the standard value of hull surface roughness k_S is defined to be 150 μm in the case that no measured data is available. This roughness height may not be a correct representation for modern hull coatings and recent research pointed out that the effective roughness of the coated hull surfaces in real life is much lower than this. Each type of coating may follow a different roughness function model, which makes the use of a single roughness height parameter difficult.

There is a need to adopt or develop new methods to predict the roughness effect of modern fouling-control coatings and marine biofouling on ship hydrodynamic performance. Similarity law scaling and CFD can be regarded as the most promising potential methods to predict such effects. Both methods require the use of roughness functions of the surfaces in question. Similarity law scaling can be used to predict the effect of roughness on the frictional resistance of flat plates of ship lengths effectively, with less computational cost, whereas CFD methods can be adopted for accurate prediction of roughness effects on the resistance components, propeller performance characteristics, and hydrodynamics of full-scale 3D ships. While these prediction methods require the roughness functions, there exists no universal roughness function model and no single roughness length scale for all types of marine coatings and biofouling surfaces. Therefore, there is a need to generate a database of roughness functions of modern fouling-control coatings and surfaces representing heterogenous biofouling accumulated on ship

hulls and propellers. For this reason, it is recommended that standardised methods for roughness function determination should be adopted by researchers. It would, therefore, be useful to investigate the need for a guideline or procedure for the measurement of roughness functions for different surface finishes or conditions so that this information can be used for predicting the roughness corrections for both hull and propeller.

16.7 Task 8

The procedure 7.5-02-03-01.7, 1978 ITTC Performance Prediction Method for Unequally Loaded, Multiple Propeller Vessels, has been revised to make it more comprehensive by adding more explanations and graphs of model test data of a triple shaft vessel. The procedure is not limited to just triple shaft vessels but has been extended to multiple shaft propulsion ship with more general description. One aspect of the task was to validate the procedure using full-scale data, however, despite requests to operators, it was not possible to obtain any suitable data. It is recommended that the next committee should continue trying to obtain this data in order to validate the procedure.

16.8 Task 9

No full-scale data on podded propulsors was available to support this task. It is recommended that a future committee should continue to seek data to be used in the development of the procedures. The majority of podded propulsors are fitted to commercial vessels, which have proved difficult to obtain information from. An alternative approach might be to seek data from government (non-military) owned vessels such as icebreakers.

16.9 Task 10

The results of the benchmark study carried out by the previous committee were considered to be complete, and it was not felt to be worthwhile adding more data to the benchmark dataset. It would be more beneficial in future to perform a benchmark of the full scale and model scale predictions in order to support scaling using CFD.

16.10 Task 11

The reliability of quasi-steady propulsion testing has been confirmed by a limited number of organisations. While a guideline or procedure would clearly be useful, there remain some unknowns, which would need to be clarified before a guideline or procedure could be developed, such as the limitations of applicability of the method. More testing is required to understand these limits. It would therefore be useful for benchmark tests to be carried out to validate the method in more model basins.

16.11 Task 12

The topic of cavitation erosion is one which is receiving much attention, and modelling techniques are developing rapidly. Much of the work has been focussed on the development of cavitation erosion risk indicators based on CFD solutions, which can be used by propeller designers to predict potential erosion areas and locations. However, research is still needed to determine thresholds for these indicators that predict when erosion will occur. A combination of CFD and EFD will be needed to further understand the physical mechanisms and quantities that drive the erosion behaviour.

The ITTC should continue to monitor the progress in this field, and updates to procedures could be considered in future.

16.12 Task 13

A survey has been carried out to determine the level of activity on rim driven thrusters within the ITTC membership. At least six members are actively working with rim driven thrusters, and there is a consensus that a dedicated procedure should be developed for testing them. Specific issues relate to the measurement arrangements for thrust and torque, given the absence of a shaft, and to the scaling from model scale to full scale. This is often done using CFD. It is recommended that the next committee should continue working to develop a procedure, but it is clear that only a few institutions have experience of such testing.

16.13 Task 14

The new F_D definition appears to make a very small difference to the powering prediction compared to previous definitions. Some institutions still use alternative definitions, and should be aware of what the effect of this is on the predictions. Each institution should check their own method against the 28th ITTC definition to understand the impact.

16.14 Task 15

The minimum Reynolds number (2×10^5) in the present ITTC procedure is probably not sufficient for obtaining stable open water test data. This minimum Reynolds number generally ranges from 3×10^5 to 5×10^5 for different propeller types. This range might not be suitable for other propeller types, such as CLT propellers and ducted propellers, which should be treated separately, and it may not be possible to provide a single value that is universally applicable.

A series of Reynolds number variation open water tests or CFD simulations covering the self-propulsion Reynolds number range is recommended for investigating the Reynolds number dependency. The ITTC procedures 7.5-02-03-01.4 1978 ITTC Performance Prediction Method and 7.5-02-03-02.1 Open water test procedures are recommended to be revised during 30th ITTC term.

A benchmark study looking at the effects of Reynolds number on propeller performance measurements could be useful for a future committee to make a more informed assessment, and to propose changes to the procedures.

16.15 Task 16

Alternative methods of propeller scaling tend to be proprietary and not universally applicable, being extremely complicated to implement, so are unlikely to be a viable alternative to the current ITTC procedure. In the long-term CFD is likely to provide an alternative method of scaling unconventional propeller performance, however a limited case study has shown that CFD can over-predict the scale effects compared to other methods. A benchmark study on CFD open-water scaling could therefore be useful.

16.16 Task 17

It is recommended to perform scaling studies to decipher the level of model hull wake interactions with the wave field when conducting model scale measurements of propellers in waves. The influence of ventilation on propeller performance is recommended for further evaluation during 30th ITTC term.

16.17 Proposals for future tasks

1. A benchmark study looking at the effect of Re at model scale, and scaling methods for full scale prediction could be carried out. This could use the two propellers that were provided for the previous benchmark study run by the

28th ITTC. CFD calculations would be run at a range of Re at model scale and full scale, along with open-water model tests at a range of Re.
- Modern propeller designs with low blade area may suffer from laminar effects in self-propulsion test. A procedure to carry out two open water tests at different Reynolds number has been suggested.
- Survey how ITTC members tackle this issue, and which scaling method they use for low blade area propellers.
- Review literature on the subject
- Suggest modification to recommended procedures.

2. The procedures on CFD verification and validation should be reviewed and updated to ensure that they represent best practise for the types of calculations being required by other ITTC procedures.

3. The requirements for testing and numerical evaluation of high-speed marine vessels should be investigated and the need for updated procedures assessed.

4. The use of CFD to predict full-scale ship performance and the need for validation at full-scale should be investigated.

5. The measurement and prediction of breaking waves should be further investigated.

6. Developments in hull and propeller model manufacturing should continue to be monitored. These would include advances in additive manufacturing techniques and novel materials. The use of 3D scanning techniques to validate the model geometry should also be investigated with a view to updating the procedures.

7. Guidelines should be developed for model testing of low skin friction coatings and air lubrication systems, including scaling laws.

17. REFERENCES

Abbas, N., Kornev, N., 2015, "Computations of the Japan Bulk Carrier Using URANS and URANS/LES Methods Implemented into OpenFOAM Toolkit", Tokyo 2015 CFD Workshop.

Aktas, B., Yilmaz, N., Atlar, M., Sasaki, N. Fitzsimmons, P., Taylor, D., 2019, "Suppression of Tip Vortex Cavitation noise using PressurePoresTM technology: A numerical and experimental investigation", Paper presented at the Sixth International Symposium on Marine Propulsors, smp'19, Rome, Italy, May 2019.

Andrewartha, J., Perkins, K., Sargison, J., Osborn, J., Walker, G., Henderson, A., Hallegraeff, G., 2010, "Drag force and surface roughness measurements on freshwater biofouled surfaces", Biofouling, Vol. 26, pp 487-496.

Bakica, A., Gatin, I., Vukčević, V., Jasak, H., Vladimir, N., 2019, "Accurate assessment of ship-propulsion characteristics using CFD", Ocean Engineering, Vol. 175, pp 149-162, February 2019.

Baltazar J., Rijpkema D., Campos J., 2019, "Prediction of the Propeller Performance at Different Reynolds Number Regimes with RANS", Sixth International Symposium on Marine Propulsors, smp'19, Rome, Italy, May 2019.

Bengough, G.D., Shepheard, V.G., 1943, "The corrosion and fouling of ships", Paper presented at the Marine Corrosion Sub-committee of the Iron and Steel Institute and the British Iron and Steel Federation.

Bhatt, M., Mahesh, K., 2019, "Investigation of propeller cavitation using compressible large eddy simulations", 6th International

Symposium on Marine Propulsors smp'19, Rome, Italy, May 2019.

Bhushan, S., Yoon, H., Stern, F., Guilmineau, E., Visonneau, M., Toxopeus, S., Simonsen, C., Aram, S., Kim, S.E., Grigoropoulos, G., 2019, "Assessment of CFD for Surface Combatant 5415 at Straight Ahead and Static Drift β=20°", Journal of Fluids Engineering, Vol. 141, May 2019.

Boorsma, A., 2000, "Improving Full Scale Ship Powering Performance Predictions by Application of Propeller Leading Edge Roughness, Part 1: Effect of Leading Edge Roughness on Propeller Performance". Master's thesis, University of Technology Delft.

Bottiglieri, M.J., 2016, "Uncertainty assessment for free-running model cases at the IIHR wave basin", MSc thesis, University of Iowa.

Broglia, R., Zaghi, S., Campana, E.F., Dogan, T., Sadat-Hosseini, H., Stern, F., Queutey, P., Visonneau, M., Milanov, E., 2019, "Assessment of Computational Fluid Dynamics Capabilities for the Prediction of Three-Dimensional Separated Flows: The DELFT 372 Catamaran in Static Drift Conditions", Journal of Fluid Engineering, Vol. 141, Sept. 2019.

Carrica, P.M., Mofidi, A., 2014, "Simulations of zigzag maneuvers for a container ship with direct moving rudder and propeller", Computers and Fluids, Vol. 96, pp 191–203.

Carrica, P.M., Mofidi, A., Eloot, K., Delefortrie, G., 2016, "Direct simulation and experimental study of zigzag maneuver of KCS in shallow water", Ocean Engineering, Vol. 112, pp 117–133.

Celik, I.B., Ghia, U., Roache, P.J., Freitas, C.J., Coleman, H., Raad, P.E., 2008, "Procedure for Estimation and Reporting of Uncertainty Due to Discretization in CFD Applications", Journal of Fluid Engineering, Vol. 130, July 2008.

Charruault, F., Westerweel, J., Terwisga, T.v., Breugem, W.-P., 2017, "On the drag reduction induced by an air cavity and characterisation of its free surface", Paper presented at the 5th International Conference on Advanced Model Measurement Technology for the Maritime Industry (AMT'17), Glasgow, UK.

Dang, J., Ligtelijn, Th., 2019, "Development of Tunnel Thruster Series Propellers for Low Noise and Vibration", 6th International Symposium on Marine Propulsors smp'19.

Delfos, R., Greidanus, A., Charruault, F., & Westerweel, J., 2017, "Wave characteristics of a compliant coating under a turbulent flow", Paper presented at the 5th International Conference on Advanced Model Measurement Technology for the Maritime Industry (AMT'17), Glasgow, UK.

Demirel, Y.K., Song, S.S., Turan, O., Incecik, A., 2019, "Practical Added Resistance Diagrams to Predict Fouling Impact on Ship Resistance", Ocean Engineering, Vol. 186, 106112, 2019.

Demirel, Y.K., Turan, O. and Incecik, A., 2017, "Predicting the Effect of Biofouling on Ship Resistance Using CFD", Applied Ocean Research, Vol. 62, pp. 100-118.

Demirel, Y.K., Uzun, D., Zhang, Y., Fang, H.C., Day, A.H., Turan, O., 2017, "Effect of Barnacle Fouling on Ship Resistance and Powering", Biofouling, Vol. 33, No. 10, pp. 819-834.

Dogrul, A., Song, S., Demirel, Y.K., 2020, "Scale effect on ship resistance components and form factor". Ocean Engineering, Vol. 209, 107428.

Dular M., Stoffel B., Sirok B., 2006, "Development of a cavitation erosion model", WEAR, Vol. 261, pp 642-655.

Dular M., Pirc Z., Pozar T., Petkovsek R., 2019, "High speed observation of damage created by a collapse of a single cavitation bubble: Development of a cavitation erosion model", WEAR, Vol. 418-419, pp 13-26.

Eça, L., Vaz, G., Toxopeus, S.L., Hoekstra, M., 2019, "Numerical Errors in Unsteady Flow Simulations", Journal of Verification, Validation and Uncertainty Quantification, Vol. 4.

Eskilsson, C., Bensow, R., 2015, "Estimation of Cavitation Erosion Intensity Using CFD: Numerical Comparison of Three Different Methods", Fourth International Symposium on Marine Propulsors SMP'15, Austin, USA.

Fabbri, S., Dennington, S., Stoodley, P., Longyear, J., 2017, "A marine biofilm flow cell for in situ determination of drag, structure and viscoelastic properties". Paper presented at the 5th International Conference on Advanced Model Measurement Technology for the Maritime Industry (AMT'17), Glasgow, UK.

Fabio, D.N., Francisco, A.P., Giovanni, d.M., Fabio, D.F., Rudy, G., Francesco, G., Massimo, M., 2017, "Bubble size and velocity measurements in high void fraction bubbly flows using PIV-LIF technique". Paper presented at the 5th International Conference on Advanced Model Measurement Technology for the Maritime Industry (AMT'17), Glasgow, UK.

Falchi, M., Felli, M., Grizzi, S., Aloisio, G., Broglia, R., Stern, S., 2014, "SPIV measurements around the DELFT 372 catamaran in steady drift", Exp. Fluids, Vol. 55, No. 1844.

Farkas, A., Degiuli, N., Martić, I., 2018, "Towards the prediction of the effect of biofilm on the ship resistance using CFD", Ocean Engineering, Vol. 167, pp 169-186.

Farkas, A., Degiuli, N., Martić, I., 2019, "Impact of biofilm on the resistance characteristics and nominal wake", Proceedings of the Institution of Mechanical Engineers, Part M: Journal of Engineering for the Maritime Environment.

Fortes-Patella, R., Reboud, J.L. and Briancon-Marjollet, L., 2004, "A Phenomenological and Numerical Model for Scaling the Flow Aggressiveness in Cavitation Erosion", EROCAV Workshop, Val de Reuil, France.

Froude, W., 1872, "Experiments on the surface-friction experienced by a plane moving through water". In The collected papers of William Froude. British Association for the Advancement of Science: Institution of Naval Architects, 1955.

Froude, W., 1874, "Report to the Lords Commissioners of the Admiralty on Experiments for the Determination of the Frictional Resistance of Water on a Surface, Under Various Conditions".

Granville, P.S., 1958, "The frictional resistance and turbulent boundary layer of rough surfaces". Journal of Ship Research, Vol. 2, No. 3, pp 52-74.

Granville, P.S., 1987, "Three Indirect Methods for the Drag Characterization of Arbitrarily Rough Surfaces Flat Plate", Journal of Ship Research, Vol. 31, No. 1, pp 70-77.

Grasso, N., Hallmann, R., Schlocz, T., Zondervan, G., Maljaars, P., Schouten, R., 2019, "Measurements of the hydro-elastic behaviour of flexible composite propellers in non-uniform flow at model and full scale", 6th International Symposium on Marine Propulsors smp'19.

Greidanus, A., Delfos, R., Westerweel, J., 2017, "Fluid-structure interaction of compliant coatings under turbulent flow conditions: force and PIV analysis". Paper presented at the 5th International Conference on Advanced Model Measurement Technology for the Maritime Industry (AMT'17), Glasgow, UK.

Grigson, C.W.B., 1992, "Drag Losses of New Ships Caused by Hull Finish", Journal of Ship Research, Vol. 36, pp 182–196.

Guo, C.-Y., Wu, T.-C., Luo, W.-Z., Chang, X., Gong, J., She, W.-X., 2018, "Experimental study on the wake fields of a Panamax Bulker based on stereo particle image velocimetry", Ocean Engineering, Vol. 165, pp 91-106.

Güzel, B., 2017, "Experimental investigation of hydrophobic effects on drag reduction". Paper presented at the 5th International Conference on Advanced Model Measurement Technology for the Maritime Industry (AMT'17), Glasgow, UK.

Hashimoto, H., Yoneda, S., Omura, T., Umeda, N., Matsuda, A., Stern, F. and Tahara, Y., 2019, "CFD prediction of wave-induced forces on ships running in irregular stern quartering seas", Ocean Engineering, Vol. 188, 2019.

Haslbeck, E.G.B., 1992, "Microbial biofilm effects on drag-lab and field". Proceedings of the Ship Production Symposium.

Hasuike, N., Okazaki, M., Okazaki, A., Fujiyama, K., 2017, "Scale effects of marine propellers in POT and self-propulsion test conditions", Fifth International Symposium on Marine Propulsors smp'17, Espoo, Finland, June 2017.

Hasuike, N., Yamasaki, S., Ando, J., 2009, "Numerical Study on Cavitation Erosion Risk of Marine Propellers Operating in Wake Flow", Proceedings of the 7th International Symposium on Cavitation CAV2009, Michigan, USA.

Heinke, H., Hellwig-Rieck, K., Lübke, L., 2019, "Influence of the Reynolds Number on the Open Water Characteristics of Propellers with Short Chord Lengths", Sixth International Symposium on Marine Propulsors smp'19, Rome, Italy, May 2019.

Helma, S., 2015, "An Extrapolation Method Suitable for Scaling of Propellers of any Design", Fourth International Symposium on Marine Propulsors smp'15, Austin, Texas, USA.

Hino, T., Stern, F., Larsson, L., Visonneau, M., Hirata, N., Kim, J., 2021, "Numerical Ship Hydrodynamics: An assessment of the Tokyo 2015 Workshop", Springer.

Hiraga, Y., 1934, "Experimental investigations on the resistance of long planks and ships", Zosen Kiokai, Vol. 55, pp 159-199.

Hirata, N., 2015, "JBC test data in NMRI", Tokyo 2015 CFD Workshop.

Hiroi, T., Kawashima, H., Sawada, Y., Fujisawa, J., Mieno, H., 2017, "Experimental investigation of the effect of geometric roughness parameters on turbulent boundary layer by LDV measurements". Paper presented at the 5th International Conference on Advanced

Model Measurement Technology for the Maritime Industry (AMT'17), Glasgow, UK.

Hiroi, T., Winden, B., Kleinwachter, A., Ebert, E., Fujisawa, J., Kamiirisa, H., Damaschke, N., Kawakita, C., 2019, "Full-Scale On-board Measurements of Wake Velocity Profiles, Underwater Noise and Propeller Induced Pressure Fluctuations", The Japan Society of Naval Architecture and Ocean Engineers, Vol. 29, pp 193-198.

Inukai, Y., 2019, "Full Scale Measurement of The Flow Field at The Stern by Using Multi-Layered Doppler Sonar (MLDS)", 6th International Symposium on Marine Propulsors smp'19, Rome, Italy.

ISO, 2015, "Ships and marine technology – guidelines for the assessment of speed and power performance by analysis of speed trial data", ISO15016 second edition.

ITTC, 2017, "Propulsion Committee Final Report", 28th ITTC Full Conference Proceedings, Vol. 1, Wuxi, China.

Katsui, T., Tanaka, H., 2018, "The Evaluation Method of the Hydrodynamic Frictional Resistance for the Painted Rough Surface", Proceedings of the ASME 2018 37th International Conference on Ocean, Offshore and Arctic Engineering, OMAE2018-77693.

Kim, K., Lee, C., 1985, "Influence of Reynolds Number on Propeller Open Water Characteristics", Korea Institute of Machinery & Materials Report.

Klinkenberg, Y., Bosman, R., Dang, J., Ligtelijn, D., 2017, "Advanced measurements of rim-driven tunnel thrusters". Paper presented at the 5th International Conference on Advanced Model Measurement Technology for the Maritime Industry (AMT'17), Glasgow, UK.

Korkut, E., Atlar, M., 2012, "An experimental investigation of the effect of foul release coating application on performance, noise and cavitation characteristics of marine propellers". Ocean Engineering, Vol. 41, pp 1-12.

Kornev, N., Taranov, A., Shchukin, E. and Klein-sorge, L., 2011, "Development of hybrid URANS-LES methods for flow simulations in the ship stern area", Ocean Engineering, Vol. 38, Issue 16, pp. 1831–1838.

Kumar, P., Mahesh, K., 2019, "Large Eddy Simulation of flow over a confined elliptic hydrofoil", 6th International Symposium on Marine Propulsors smp'19.

Larssen J., Kluwe, F., 2018, "Seven in One Sweep – Constantly Accelerated Resistance Test (CART)", HSVA Newswave 2018, Issue 1.

Leclercq, C., Archer, A., Fortes-Patella, R., Cerru, F., 2017, "Numerical Cavitation Intensity on a Hydrofoil for 3D Homogeneous Unsteady Viscous Flows", Journal of Fluid Machinery and Systems, Vol. 10, No. 3, pp 254-263.

Lee, I.W., Park, H., Chun, H.H., 2015, "Drag Reduction Performance of FDR-SPC (Frictional Drag Reduction Self-Polishing Copolymer)", Proc. of International Symposium on Turbulence and Shear Flow Phenomena (TSFP-9), Vol. 5A-1.

Lewthwaite, J., Molland, A., Thomas, K., 1985, "An investigation into the variation of ship skin frictional resistance with fouling", Transactions of Royal Institution of Naval Architects, Vol. 127, pp 269-284.

Li, C., Atlar, M., Haroutunian, M., Norman, R., Anderson, C., 2019, "An investigation into the effects of marine biofilm on the roughness and drag characteristics of surfaces coated with different sized cuprous oxide (Cu2O) particles", Biofouling, pp 1-19.

Lücke T., Streckwall H., 2017, "Experience with Small Blade Area Propeller Performance", Fifth International Symposium on Marine Propulsors smp'17, Espoo, Finland.

Luo, W.-Z., Guo, C.-Y., Wu, T.-C., & Su, Y.-M., 2018, "Experimental research on resistance and motion attitude variation of ship–wave–ice interaction in marginal ice zones", Marine Structures, Vol. 58, pp 399-415.

McCarthy, J.H., Norley, W.H., Ober, G.L., 1961, "The performance of a fully submerged propeller in regular waves, David Taylor Model Basin, Report No. 1440.

McEntee, W., 1915, "Variation of frictional resistance of ships with condition of wetted surface", Trans. Soc. Nav. Arch. Mar. Eng., Vol. 24, pp 37-42.

McEntee, W., 1916, "Notes from Model Basin", Transactions of the Society of Naval Architects and Marine Engineers.

Melissaris T., Bulten N., van Terwisga T., 2018, "On Cavitation Aggressiveness and Cavitation Erosion on Marine Propellers using a URANS Method", Proceedings of the 10th International Symposium on Cavitation, Baltimore, USA.

Melissaris T., van Terwisga, T., 2019, "On the Applicability of Cavitation Erosion Risk Models with a URANS Solver", Journal of Fluids Engineering, Vol. 141.

Melissaris. T., Bulten, N., Oprea, I., 2019, "The necessity of accurate prediction of cavitation behaviour for fuel efficient propellers", Sixth International Symposium on Marine Propulsors SMP'19, Rome, Italy.

Mieno, H., Katsui, T., 2020, "Development of a portable 3D hull roughness analyser", Journal of Marine Science and Technology, Vol. 25, pp 498–509.

Mieno, H., Katsui, T., 2021, "Experimental investigation of added frictional resistance by paint rough surface using a rotating cylinder", Journal of Marine Science and Technology, Vol. 26, pp 1–15.

Mihatsch, M.S., Schmidt, S.J., Thalhamer, M., Adams, N., 2011, "Numerical Prediction of Erosive Collapse Events in Unsteady Compressible Cavitating Flows", Fourth International Conference on Computational Methods in Marine Engineering, Lisbon, Portugal.

Monty, J.P., Dogan, E., Hanson, R., Scardino, A.J., Ganapathisubramani, B., Hutchins, N., 2016, "An assessment of the ship drag penalty arising from light calcareous tubeworm fouling", Biofouling, Vol. 32, No. 4, pp 451-464.

Mosaad, M.A.A.-R., 1986, "Marine propeller roughness penalties", PhD thesis, Newcastle University, Newcastle Upon Tyne.

Mutton, R.J., Atlar, M., Anderson, C.D., 2005, "Drag Prevention Coatings for Marine Propellers". Paper presented at the 2nd International Symposium on Seawater Drag Reduction, Busan, Korea.

Nishikawa, T., 2015, "Application of Fully resolved Large Eddy Simulation to Self-Propulsion Test Condition of Double-Model KVLCC2", 14tth International Conference

on Computer and IT Applications in the Maritime Industries (COMPIT'15), pp.191-199.

Nishikawa, T., 2015, "Application of fully resolved large eddy simulation to Japan Bulk Carrier with an energy saving device", Tokyo 2015 CFD Workshop.

Nohmi, M., Iga, Y., Ikohagi, T., 2008, "Numerical Prediction Method of Cavitation Erosion", Proceedings of FEDSM2008, Jacksonville, USA.

Owen, D., Demirel, Y.K., Oguz, E., Tezdogan, T., Incecik, A., 2018, "Investigating the Effect of Biofouling on Propeller Characteristics Using CFD", Ocean Engineering, Vol. 159, pp. 505-516.

Paskin, L., Visonneau, M., Guilmineau, E., Wackers, J., 2019, "Computational Modeling of Turbulent Flows on the Tip Vortex of a Marine Propeller's Blade", 6th International Symposium on Marine Propulsors smp'19.

Plessett, M.S., Chapman, R.B., 1971, "Collapse of an initially spherical vapour cavity in the neighbourhood of a solid boundary", Journal of Fluid Mechanics, Vol. 47, pp 283-290.

Raven, H., 2019, "A method to correct shallow-water model tests for tank wall effects", Journal of Marine Science and Technology, Vol. 24, No. 2.

Ravenna, R., Marino, A., Song, S., Demirel, Y. K., Atlar, M., Turan, O., 2019, "Experimental Investigation on the Effect of Biomimetic Tubercles on the Hydrodynamics of a Flat Plate". Paper presented at the Sixth International Conference on Advanced Model Measurement Technology for The Maritime Industry (AMT'19), Rome, Italy.

Ravina, E., Guidomei, S., 2018, "Experimental Investigation on Resistance Reduction by Means of Air-Bubbling Technique".

Sakamoto, N., Kobayashi, H., Ohashi, K., Kawanami, Y., Winden, B., Kamiirisa, H., 2020, "An overset RaNS prediction and validation of full scale stern wake for 1,600 TEU container ship and 63,000 DWT bulk carrier with an energy saving device", Applied Ocean Research, Vol. 105.

Sanada, Y., Tanimoto, K., Takagi, K., Gui, L., Toda, Y., Stern, F., 2013, "Trajectories for ONR Tumblehome maneuvering in calm water and waves", Ocean Engineering, Vol. 72, pp 45–65.

Sanada, Y., Elshiekh, H., Toda, Y., Stern, F., 2014, "Effects of Waves on Course Keeping and Maneuvering for Surface Combatant ONR Tumblehome", The 30th Symposium on Naval Hydrodynamics, Hobart, Tasmania, Australia.

Schenke, S., Melissaris, T., van Terwisga, T., 2019, "On the Relation between the Potential Cavity Energy and the Acoustic Power Signature caused by Periodic Vapor Cavity Collapses", Sixth International Symposium on Marine Propulsors SMP'19, Rome, Italy.

Schmidt, S., Sezal, I., Schnerr, G., 2008, "Numerical Analysis of Shock Dynamics for Detection of Erosion Sensitive Areas in Complex 3-D Flows", Cavitation: Turbo-machinery & Medical Applications WIMRC FORUM 2008, Warwick University, UK.

Schuiling, B., Terwisga, T., 2018, "Energy loss analysis for a propeller operating behind a ship", 32nd Symposium on Naval Hydrodynamics, Hamburg, Germany.

Schultz, M.P., 2004, "Frictional Resistance of Antifouling Coating Systems", Journal of Fluids Engineering, Vol. 126, No. 6, pp 1039-1047.

Schultz, M.P., 2007, "Effects of coating roughness and biofouling on ship resistance and powering". Biofouling, Vol. 23, No. 5, pp 331-341.

Schultz, M.P., Bendick, J.A., Holm, E.R., Hertel, W.M., 2011, "Economic impact of biofouling on a naval surface ship". Biofouling, Vol. 27, No. 1, pp 87-98.

Seo, H., Go, S., Lee, S., Kwon, J., 2011, "A Study on the Powering Performance of Multi-axes Propulsion Ships with Wing Pods", SMP'11, Hamburg, Germany.

Seok, J., Park, J.-C., 2020, "Numerical simulation of resistance performance according to surface roughness in container ships". International Journal of Naval Architecture and Ocean Engineering, Vol. 12, pp 11-19.

Sheng, Z., et al, 1979, "Experimental study on propeller scale effects" (in Chinese), Journal of Shanghai Jiaotong University.

Shin, K., Andersen, P., 2018, "CFD Analysis of Propeller Tip Vortex Cavitation in Ship Wake Fields", 10th Symposium on Cavitation (CAV2018).

Shiraishi, K., Sawasda, Y., Arakawa, D., Kumura, K., 2019, "A Study on Deformation Measurements and Hydrodynamic Investigation of the Flexible Composite Marine Propeller", 6th International Symposium on Marine Propulsors smp'19.

Sokolov, M., Marinich N., 2012, "Experimental study on hydromechanic properties of hubless propeller in RIM-drive propulsion system", 10th International Conference on Hydrodynamics, St. Petersburg, Russia.

Song, S., Dai, S., Demirel, Y. K., Atlar, M., Day, S., Turan, O., 2021a, "Experimental and Theoretical Study of the Effect of Hull Roughness on Ship Resistance". Journal of Ship Research, Vol. 65, No. 1, pp 62-71.

Song, S., Demirel, Y.K., Atlar, M., 2019, "An investigation into the effect of biofouling on the ship hydrodynamic characteristics using CFD", Ocean Engineering, Vol. 175, pp 122-137.

Song, S., Demirel, Y.K., Atlar, M., 2020c, "Propeller Performance Penalty of Biofouling: Computational Fluid Dynamics Prediction". Journal of Offshore Mechanics and Arctic Engineering, Vol. 142, No. 6.

Song, S., Demirel, Y.K., Atlar, M., 2020d, "Penalty of hull and propeller fouling on ship self-propulsion performance", Applied Ocean Research, Vol. 94.

Song, S., Demirel, Y.K., Atlar, M., Dai, S., Day, S., Turan, O., 2020b, "Validation of the CFD approach for modelling roughness effect on ship resistance". Ocean Engineering, Vol. 200.

Song, S., Demirel, Y.K., De Marco Muscat-Fenech, C., Tezdogan, T., Atlar, M., 2020e, "Fouling effect on the resistance of different ship types", Ocean Engineering, Vol. 216.

Song, S., Ravenna, R., Dai, S., DeMarco Muscat-Fenech, C., Tani, G., Demirel, Y. K., Atlar, M., Day, S., Incecik, A., 2021b, "Experimental investigation on the effect of heterogeneous hull roughness on ship resistance", Ocean Engineering, Vol. 223.

Streckwall, H., Greitsch, L., Scharf, M., 2013, "An advanced Scaling Procedure for Marine Propellers", Third International Symposium on Marine Propulsors smp'13, Launceston, Australia.

Suyama, N., Fujita, S., Kumura, K., Shiraishi, K., Sawada, Y., Kawakita, C., 2019, "Study on Method to Predict Performance of Composite Propeller Using FSI Analysis", 6th International Symposium on Marine Propulsors smp'19.

Taskar, B., Yum, K.K., Steen, S., Pedersen, E., 2016, "The effect of waves on cavitation and pressure pulses", Applied Ocean Research, Vol. 60, pp 61-74.

Taskar, B., Steen, S., Eriksson, J., 2017, "Effect of waves on cavitation and pressure pulses of a tanker with twin podded propulsion", Applied Ocean Research, Vol. 65, pp 206-218.

Taylor, D.W., 1943, "The speed and power of ships: a manual of marine propulsion", Washington: U.S. G.P.O.

Tokgoz, E., Takasu, S., Wu, P-C., Toda, Y., 2017, "Computation and Experiment of Propeller Thrust Fluctuation in Waves for Propeller Open Water Condition", Journal of JASNAOE, Vol. 25, pp 55-62.

Townsin, R.L., Byrne, D., Svensen, T.E., Milne, A., 1981, "Estimating the technical and economic penalties of hull and propeller roughness", Trans SNAME, pp 295-318.

Usta, O., Aktas, B., Maasch, M., Turan, O., Atlar, M., Korkut, E., 2017, "A study on the numerical prediction of cavitation erosion for propellers", Fifth International Symposium on Marine Propulsors SMP'17, Espoo, Finland.

Visonneau, M., Deng, G., Guilmineau, E., Queutey, P., Wackers, J., 2016, "Local and Global Assessment of the Flow around the Japan Bulk Carrier with and without Energy Saving Devices at Model and Full Scale", Proceedings of the 31st ONR Symposium on Naval Hydrodynamics, Monterey, California, September 2016.

Vogel, A., Lauterborn, W., 1988, "Acoustic transient generation by laser-produced cavitation bubbles near solid boundaries", Journal of The Acoustical Society of America, Vol. 84, pp 719-731.

Wackers, J., Deng, G., Guilmineau, E., Leroyer, A., Queutey, P., Visonneau, M., Palmieri, M., Liverani, A., 2017, "Can adaptive grid refinement produce grid-independent solutions for incompressible flows?", Journal of Computational Physics, Vol. 344, pp 364-380.

Wang, J., Zou, L., Wan, D., 2018, "Numerical simulations of zigzag maneuver of free running ship in waves by RANS-Overset grid method", Ocean Engineering, Vol. 162, pp 55–79.

Wang, L., Martin, J. E., Carrica, P. M., Felli, M., Falch, M., 2019, "Experiments and CFD for DARPA Suboff Appended with Propeller E1658 Operating Near the Surface". Paper presented at the Sixth International Symposium on Marine Propulsors, smp'19, Rome, Italy.

Werner, S., 2018, "Derivation of load variation factors – an example case", SSPA-Report No: RE70178533-01-00-A, SSPA.

Yakovlev, A., Sokolov, M., Marinich, N., 2011, "Numerical design and experimental verification of a RIM-driven thruster", Second International Symposium on Marine Propulsors smp'11, Hamburg, Germany.

Yao, H., Zhang, H., 2019, "Improvement of scaling method recommended by ITTC at lower Reynolds Number Range" (in Chinese), Journal of Shanghai Jiaotong University, Vol. 53, No. 1.

Yeginbayeva, I.A., Atlar, M., 2018, "An Experimental Investigation into the Surface and Hydrodynamic Characteristics of Marine Coatings with Mimicked Hull Roughness Ranges", Biofouling, Vol. 34, No. 9, pp. 1001-1019.

Yilmaz, N., Atlar, M., Khorasanchi, M., 2019, "An improved Mesh Adaption and Refinement Approach to Cavitation Simulation (MARCS) of Propellers", Ocean Engineering, Vol. 171, pp 139-150.

Yoon, H., Gui, L., Bhushan, S., Stern, F., 2014, "Tomographic PIV Measurements for a Surface Combatant at Straight Ahead and Static Drift Conditions", 30th Symposium on Naval Hydrodynamics, Hobart, Tasmania, Australia.

Zhang, C., Lu, F., Lu, L., 2019, "High-speed visualization of cavitation evolution around a marine propeller", Journal of Visualization, Vol. 22, Issue 2, pp 273-281.

The Manoeuvring Committee
Final Report and Recommendations to the 29th ITTC

1. INTRODUCTION

1.1 Membership and Meetings

The 29th ITTC Manoeuvring Committee (MC) consisted of:

- Dr. Guillaume Delefortrie (Chair). Flanders Hydraulics Research (FHR), Belgium.
- Prof. Dr. Eduardo A. Tannuri (Secretary). Escola Politécnica da Universidade de São Paulo (USP), Brazil.
- Prof. Dr. Xide Cheng, Wuhan University of Technology, China.
- Prof. Dr. Sanghyun Kim. Inha University, South-Korea.
- Dr. Takashi Kishimoto. Akishima Laboratories Inc., Japan
- Dr. Zhi Leong, Australia Maritime College, Australia (since January 2019).
- Dr. Salvatore Mauro. INM, Italy (until October 2018).
- Ms. Janne Flensborg Otzen. FORCE Technology, Denmark.
- Dr. Zhiming Yuan. Universities of Glasgow and Strathclyde, UK.

Three meetings have been held as follows:

- INM, Rome, Italy, January 22–24, 2018;
- Akishima Laboratories Inc., Tokyo, Japan, November 6–8, 2018;
- Universities of Glasgow and Strathclyde, Glasgow, UK, June 5–7, 2019, prior to OMAE 2019.

The fourth meeting was planned in 2020, subsequently in Wuhan (China), Seoul (South-Korea) and Ostend (Belgium), but could never happen due to the Covid-19 threat. Instead, video calls were used to finalize the present report. These video calls took place on April 1–3, 2020 (4th virtual meeting) and on January 7–8, 2021 (5th virtual meeting).

1.2 Tasks and report structure

The following lists the tasks given to the 29th MC together with explanation on how the tasks have been executed.

1. Update the state-of-the-art for predicting the manoeuvring behaviour of ships, emphasizing developments since the 2017 ITTC Conference. The committee report should include sections on:
   a. the potential impact of new technological developments on the ITTC
   b. new experiment techniques and extrapolation methods
   c. the practical applications of computational methods to manoeuvring predictions and scaling, including CFD methods
   d. the need for R&D for improving methods of model experiments, numerical modelling and full-scale measurements
   e. the effects of free surface, roll, sinkage, heel and trim in numerical simulation of manoeuvring
   f. Include specifically, the prediction and testing of low speed manoeuvring to understand the impact of these types of manoeuvres in model testing.

The state of the art has been updated based on a comprehensive literature review spanning publications from 2017-2020. This is elaborated in section 3 of the present report, where the literature has been grouped in research in deep (unrestricted) or shallow (restricted) areas. A massive amount of literature on unmanned navigation and autopilots has been published, which is discussed in dedicated subsections.

2. During the first year, review ITTC Recommended Procedures relevant to manoeuvring, including CFD procedures, and
   a. identify any requirements for changes in the light of current practice and, if approved by the Advisory Council, update them,
   b. identify the need for new procedures and outline the purpose and contents of these.

No new procedures have been proposed, but the changes to the existing procedures are discussed in section 3.1.

3. Coordinate and exchange information with the Specialist Committee on Ice with regard to the possible updating of ITTC Recommended Procedure 7.5-02-04-02.3, Manoeuvring in Ice.

Some preliminary work has been performed by the MC, however, the Specialist Committee on Ice did not require further input. More details are provided in section 4.2.

4. Update 7.5-02-06-03 2014 Validation of Manoeuvring Simulation Models, including verification, sensitivity analysis, results from the SIMMAN conferences and step by step validation of manoeuvring models.

The procedure has been updated. Details are provided in section 4.3.

5. Investigate the missing elements in the Procedure on Uncertainty Analysis for Manoeuvring Prediction Based on Captive Model Tests, such as the accuracy of carriage kinematics and the data filtering (noise). Update 7.5-02-06-04 if necessary according to the requirements of the ISO GUM.

The procedure has been updated by providing information on the mentioned missing links, discussed in section 7.1. The ISO GUM update is recommended for the 30th term as part of an integrated example. See section 4.4 for more information.

6. Update 7.5-02-06-02 Captive model test procedure to provide a definitive, agreed, method for each of the testing approaches.

The procedure has been significantly updated. See section 4.4 for more details.

7. Assist with the organization of SIMMAN 2019. Use the output from this conference and others to develop a guideline for the setup, execution of benchmark tests and use of benchmark data for manoeuvring.

The MC has supported the SIMMAN organization (see section 5). As SIMMAN is postponed to the end of 2021 the output of this conference could not be used in the guideline. The guideline itself is discussed in 4.5.

8. Investigate the uncertainties associated with manoeuvring tests in shallow water including aspects such as structural strength of moveable bottoms, extent of gaps around the edges and the degree to which a fixed floor is level.

Section 6.2 is dedicated to the issues of the tests on shallow water. The MC has executed potential flow calculations to investigate the effects of gap extents.

9. Investigate the results from the previous ITTC questionnaire on captive model tests especially related to concerns over turbulence stimulation and full scale effects; update 7.5-02-06-02, if necessary, concerning this matter.

A new questionnaire has been setup and the results are discussed in section 6.3.

10. Liaise with Specialist Committees on Combined CFD/EFD Methods and Manoeuvring in Waves as required.

Contacts have been established with these committees. Specifically the Specialist Committee on Combined CFD/EFD reviewed our RANS procedures.

11. Develop guidelines for the model testing and sea trials of autonomous underwater vehicles (AUVs) (resistance, manoeuvring, propulsion and control, computational methods for the low Reynold's Number flow around AUVs).

The original TOR as mentioned here was very broad and has been limited by the AC afterwards to the study of AUVs and the creation of guidelines for model testing and sea trials focusing at manoeuvring. This is elaborated in section 4 and section 5.

2. STATE OF THE ART

2.1 Deep Unrestricted Water

1.1.1 EXPERIMENTAL METHODS.

General. Bonci et al. (2017) investigated the effects of heel and drift angle on the hydro-dynamic forces acting on a high-speed craft via captive model tests as shown in Figure 77 and numerical predictions using a 3-D potential flow method. The results between model tests and predictions were in a good agreement over a broad range of Fr, including semi-planing and planing conditions. The proposed prediction method is considered as a valuable and less-time

consuming alternative to EFD techniques and more complex approaches such as RANS tools.

Figure 77: Model test run in heeled condition (Bonci et al., 2017)

Yasukawa et al. (2019) proposed a pragmatic extension to 4-DOF of the standardized 3-DOF MMG model. The roll moment was modelled using the vertical application lever of the sway force (acting on hull and rudder). The roll damping coefficients were derived from roll decay tests. Roll dependencies were added to the surge, sway and yaw moment expressions as well, including in the expression for the propeller wake and straightening coefficient of the rudder. The practicality here is that different roll dependent terms are predicted using new empirical formula derived from experimental tests with 4 ship models. The simulation model was then validated against free running model tests executed with variations of GM.

Yeo et al. (2018) performed captive model tests with the KCS hull to investigate the effect of a heel angle as shown in Figure 78. A number of manoeuvring simulations were conducted to apply the hydrodynamic derivatives obtained from the model tests. The results showed the difference in turning and zigzag characteristics according to heel angle.

Figure 78: Captive model test in heeled condition (Yeo et al., 2018)

Yun et al. (2018) reported results of free running model tests of the KCS hull form with CG variations, i.e., trimmed condition, heeled condition and smaller GM condition. The test results can be used as benchmark data sets for future simulation research.

Reichel (2020) adequately pointed out the challenges of podded ships to comply with the IMO Standards for Ship Manoeuvrability when the pod angle was used instead of the rudder angle (comparative steering angle). Based on manned model tests executed with a marginally unstable ship equipped with two pods at the Ship Handling Research and Training Centre in Poland, he demonstrated that remarkably smaller steering angles can be acceptable to fulfil the IMO turning criteria for podded ships.

Innovations. Measurements applying new test devices have been reported. Ortolani and Dubbioso (2019) developed two novel transducer setups that allow to monitor the in-plane loads of a propeller and the loads in 6-DOF developed by a single blade respectively. CFD and PIV were used to compare the transducers' measurements in a selection of manoeuvring conditions. The authors highlighted that such setups were scarcely described in literature and they could potentially be valuable inputs to understand the phenomena affecting the performance of a propeller behind a ship hull

and their induced loads on ship structures and manoeuvrability.

A valuable report to explore the mechanism of flow separation was published by Lee and Jones (2018), who conducted multiple pressure measurements around a slender body with drift angles in a uniform flow. They thoroughly investigated the pressure field on the body surface and compared the locus of the flow separation with results of the flow visualization. Such research is of importance to update various estimation methods for the flow field and the hydrodynamic forces acting on a ship's hull, subject to large manoeuvring motion, which is characterized by highly non-linear effects (Figure 3).

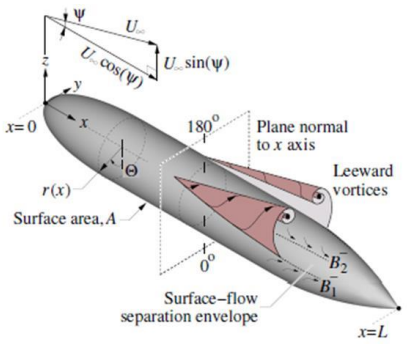

Figure 79: Flow separation on an inclined slender body in translation (Lee and Jones., 2018)

Iseki (2019) proposed a real-time identification procedure to estimate linear hydrodynamic derivatives based on on-board monitoring data regarding wind and ship's manoeuvres. Furthermore, by applying those results, the manoeuvrable range and limit in wind disturbance were shown (Figure 80). Although some derivatives of the estimation were unstable, the result of the proposed method shows the possibility to obtain feedback for ship design from on-board monitoring data.

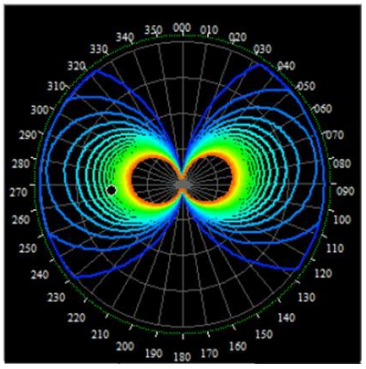

Figure 80: Manoeuvrable range in wind (Iseki, 2019)

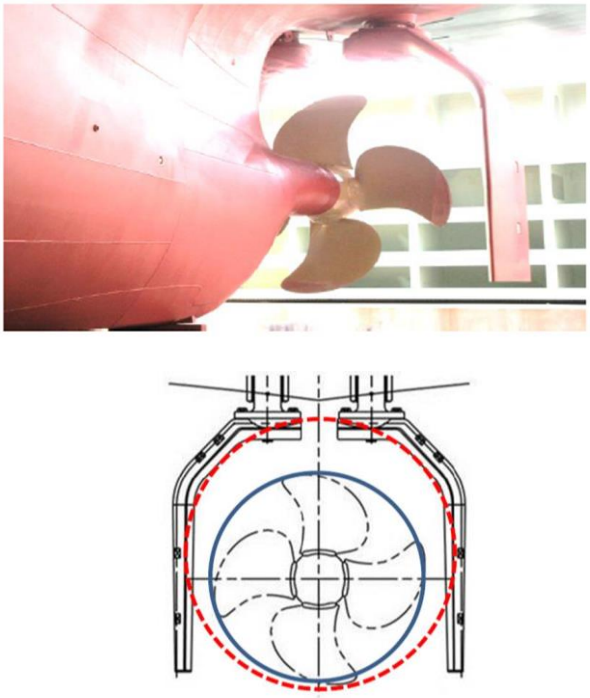

Figure 81: Gate Rudder (Sasaki et al., 2019)

Sasaki et al. (2019) investigated the performance of the world first Gate Rudder system installed on a container ship "Shigenobu". The Gate Rudder can be categorized as a new type of ducted propeller, i.e., open type ducted propeller as distinct from conventional ducted propeller (Figure 81). Comparing the full-scale data analyses with the sister ship "Sakura" equipped with a conventional rudder, they presented the

superior performance of the Gate Rudder in terms of fuel efficiency, course keeping performance, speed deduction in turning manoeuvres and steerability in harbour operation. Carchen et al. (2021) presented a numerical model, based on an extension of the MMG model to cope with the specific angle definitions of the gate rudder. The wake was studied with RANS under different drifting conditions. The merits of the paper are the innovative design of the rudder being studied with an appropriate combination of the present engineering tools, but further discussion is expected to validate the Gate Rudder performance.

1.1.2 NUMERICAL METHODS

Potential flow methods. Dashtimanesh et al. (2019) proposed a mathematical model based on 2D+T theory to simulate the steady turning manoeuvres and PMM tests. They calculated the hydrodynamic derivatives of a planing hull at different speeds as well as different yaw and sway amplitude. The hydrodynamic derivatives seemed hardly influenced by the amplitude of pure sway and yaw motion and the motions in the vertical plane (heave, roll and pitch) seemed to affect the horizontal motion derivatives. Carstensen (2019) coupled a lifting line approach with a panel method to quickly predict the rudder-propeller interaction.

Commercial RANS methods. Most of the studies on RANS simulations are performed using commercial CFD software, among which STAR-CCM+ is most frequently cited. Liu Y. et al. (2018) investigated the effect of a ship's attitude on its manoeuvrability index by using the CFD package STAR-CCM+. They concluded that considering the dynamic sinkage and trim could improve the hydrodynamic force predictions, especially in the pure sway tests. They also analysed the attitude impact on the hydrodynamic derivatives and found that the predicted inherent dynamic stability of the ship could also be improved when the dynamic sinkage and trim were considered. Xia L. et al. (2018) analysed the hull-spacing effects on the manoeuvrability of a SWATH by using STAR-CCM+. Their results showed a larger demi-hull spacing leaded to a better inherent dynamic stability. However, the effect of demi-hull spacing upon the initial turning ability and the course-changing ability is not pronounced. Jin et al. (2019) simulated the self-propelled turning circle and zigzag manoeuvres for the benchmark combatant DTMB 5415M by using the URANS solver STAR-CCM+. Two different propulsion techniques were applied to drive the free running vessel: the body force propeller model (BFM) and the discretised propeller model (DPM). In general, the comparison between experimental and numerical results agreed mostly within about 10% for the turning circle and zigzag manoeuvres. The BFM propulsion method seemed to under-predict the magnitude of the propeller induced wake passing the rudders compared to the DPM approach. Rameesha and Krishnankutty (2018) used STAR-CCM+ to investigate the influence of the Froude number on the manoeuvring characteristics of a container ship The turning parameters were found to increase as the Froude number changed from 0.14 to 0.29. Steady turning radius and tactical diameter increased by 22.69%, 21.93% respectively, and transfer and advance by 18.79%, 13.73%, respectively.

Other commercial CFD packages are also being used. Gatin et al. (2018) simulated the ship's full-scale turning circle manoeuvre by using a Finite Volume (FV) based CFD software called Naval Hydro Pack. Two different approaches for modelling the free surface are investigated: a single-phase flow model with a simplified linearized free-surface method, and a two-phase numerical model with Volume of Fluid (VOF) method for interface capturing.

The two-phase simulation showed a good agreement with the full-scale trial, which were performed in the Adriatic Sea by Brodardski Institut Zagreb, with errors mainly below 7%, while the linearized free surface model showed a reasonable agreement for a smaller rotation rate. At a higher rotation rate, the linearized free surface simulation exhibited larger differences up to 20%. However, it also exhibited more stable evolution of the circular trajectory and less computational efforts. Duman and Bal (2019) used a commercial unsteady RANS solver software based on FVM (Finite Volume Method) to predict the manoeuvring coefficients of a catamaran. It was concluded that the impact of the leeward-sided hull on Y_v and N_v was more dominant than the windward-sided hull. The commercial CFD software suite FINE/Marine was used by Van Hoydonck et al. (2018) to determine the open-water rudder characteristics. It was shown that for the CFD computations tested at full-scale, reliable coefficient graphs were obtained: the maximum lift coefficient in the astern flow condition was significantly lower than in the ahead condition and the lift curve slope in the ahead condition was steeper than that in the astern condition. The modelled full-scale drag values are also significantly lower than those obtained in the towing tank experiments. The same software was used by Visonneau et al. (2020) to analyse the flow around a surface combatant at various static drift and dynamic sway conditions. It was concluded that the Hybrid RANS/LES turbulence models based on Delayed Detached Eddy Simulation showed a better performance against the RANS model on capturing the flow around a ship under drift conditions. Similar conclusions are also supported by the results of Shevchuk and Sahab (2020) and Wang and Wan (2020).

Open source RANS methods. Apart from commercial software, open source RANS solvers provide good alternatives. The open source solver OpenFOAM has been used by Islam and Guedes Soares (2018) to predict the hydrodynamic derivatives. Wang J. et al. (2017) used their in-house CFD solver naoe-FOAM-SJTU to simulate the zigzag manoeuvre of a fully appended ONRT model in calm water and waves. A dynamic overset grid method was applied to handle the complex ship motions with consideration of the propeller and rudder. The same solver and overset grid technique are also used by Wang and Wan (2020) to simulate different types of stopping manoeuvres of a KVLCC1 model, including reversing propeller with/without turning rudder, inertia stopping, and the original turning circle manoeuvre. The reversing propeller case with port rudder could reduce the stopping distance, while the starboard rudder increased the stopping distance and the lateral deviation was smaller, as shown in Figure 82. They also investigated the shallow water effects on stopping manoeuvres.

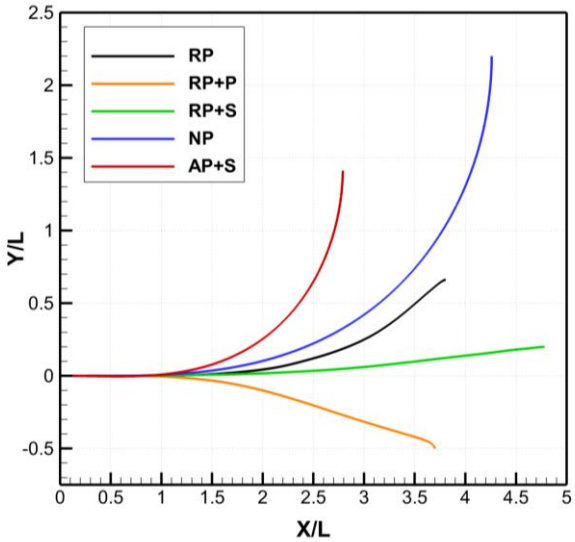

Figure 82: Comparisons of trajectories of different manoeuvres (Wang and Wan (2020)). RP: reversing propeller; RP+P: reversing propeller with port rudder; RP+S: reversing propeller with starboard rudder; NP: no rudder; AP+S: turning circle with actual rotating propeller and starboard rudder.

Ferrari et al. (2019) used the RANS solver ReFRESCO to investigate the effects of the center skeg installed with twin screw ships not only on the basic manoeuvrability such as

turning circle and zigzag manoeuvres but also on the performance at low speed, i.e., in harbour operation such as turning on the spot and crabbing manoeuvres. Based on their CFD analysis, which also included propeller streams in combination of forward & reverse rotation, they mentioned the (dis)advantages on the manoeuvrability caused by the presence of the skeg and its size. Vink et al. (2017) conducted a verification and validation study of CFD simulations of the flow around a tugboat. The CFD code used in their study is ReFRESCO. Both EFD and CFD had high computed uncertainties for the prediction of the hydrodynamic forces of the tug. The selection of turbulence models did not improve the comparison error.

Very few studies are based on in-house developed CFD code. Silva and Aram (2018) used an in-house CFD solver, NavyFOAM, to perform captive model simulations of an Office of Naval Research Tumblehome (ONRT) under various conditions.

Hybrid methods. Calcagni et al. (2017) proposed a generalised hybrid viscous/inviscid flow computational model to simulate the propeller-rudder interaction. The methodology combines a Boundary Element Method (BEM) to predict propeller perturbation under inviscid-flow assumptions and a Detached Eddy Simulation (DES) Navier-Stokes solver to describe the viscous, turbulent flow around the rudder with propeller effects recast as volume-force terms from the BEM solution. The authors compared the results of the hybrid method against those of the full DES, and a very good agreement was achieved. This hybrid method could be applied to various hydrodynamic problems, including propeller-rudder interaction and propeller action during manoeuvres. A similar approach was also used by Su and Kinnas (2018), Dubbioso et al. (2017a) and Muscari et al. (2017) and the flow chart of a typical hybrid method is shown in Figure 83.

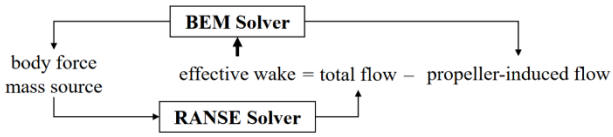

Figure 83: Flow chart of a typical hybrid BEM/RANS method (Su and Kinnas, 2018).

Dubbioso et al. (2017) and Muscari et al. (2017) used the hybrid approach to analyse the propeller bearing loads when a ship was in straight-ahead, steady turning (Dubbioso et al., 2017a) and transient manoeuvres (Muscari et al., 2017). Su and Kinnas (2018) applied the BEM/RANS scheme to analyse the hull-propeller-rudder interactions. The computational cost analysis showed the hybrid BEM/RANS scheme was around 6 times faster than a fully RANS simulation.

Mofidi et al. (2018) used a hybrid CFD/potential flow approach (CFD code REX and the propeller code PUF-1) to simulate the manoeuvring of a ship with consideration of propeller-rudder interaction. They analysed a 5/1 zigzag manoeuvre for the KCS container ship. It is shown that the hybrid approach provides an effective and economical way to perform direct manoeuvring simulation of surface ships at low to moderate propeller loading. However, it cannot resolve tip vortices and other flow structures generated by the propeller, which could potentially affect separation at the rudder for manoeuvres involving large angles of attack. A similar hybrid approach is also used by Ohashi et al. (2018). They developed a new structured URANS solver to estimate the free-running conditions of a

conventional type of ship. The propeller effects were accounted for according to the body forces derived from the propeller model, which was based on potential flow theory. This hybrid approach was applied to predict the turning circle and zigzag motions.

Sukas et al. (2019) used a system-based approach to predict the manoeuvring performance of a twin-propeller/twin-rudder ship. An URANS method was used to obtain the hydrodynamic derivatives, which were then implemented in a MMG model to simulate turning circle and zigzag manoeuvres. Sakamoto et al. (2019) used a similar CFD-MMG method.

2.2 Shallow, Restricted or Confined Water

In the 28th MC shallow, restricted and confined water have been defined. The same definition is confirmed here.

New facilities. New facilities have been reported by Delefortrie et al. (2019). In May 2019 a brand new laboratory has been opened in Ostend, Belgium. The official name of the new lab is Flanders Maritime Laboratory (FML), which hosts two state of the art model scale facilities for the maritime industry, namely a Coastal & Ocean Basin (COB) and a Towing Tank for Manoeuvres in Shallow Water (see Figure 84). Especially the latter is of importance for the MC. The design and build of the towing carriage for the new towing tank (useful dimensions: 140 m × 20 m × 1 m and design ship model length of 8 m) is planned for 2021-2022. The facility is expected to be operational by 2022 (free running model tests) and 2023 (captive model tests). More details are expected in the report of the 30th MC.

Figure 84. Top: view from the dock section of the new towing tank at FML (Delefortrie et al., 2019). Bottom: status January 2021. Due to COVID-19, the basin is being used as a training centre for the Belgian Olympic kayak team. (©Sporza.be).

Shallow water. Liu Y. et al. (2019b) used a RANS solver (STAR-CCM+) to simulate pure sway tests of a DTC in shallow water. A moving no-slip condition was used on the bottom as the boundary layer developed on the bottom may influence the flow in the gap. The predicted non-dimensional hydrodynamic forces and dynamic sinkage and trim were compared with benchmark test results and other numerical results with promising correspondence.

Lee and Hong (2017) did a RANS (STAR-CCM+) study to investigate the manoeuvring derivatives of a vessel in shallow water in order to analyse the course stability of different large vessel types cruising at low speeds.

RoyChoudhury et al. (2017) used a RANS solver (SHIPFLOW) to investigate the steady drift and yaw motions of the KVLCC2 in deep

and shallow water. An Explicit Algebraic Stress Model (EASM) turbulence model was applied for all the calculations. The results compared well with the experimental model test data.

A scaled inland container ship with twin propellers and quadruple rudders was selected by Kaidi et al. (2018) to investigate the interaction between hull, rudder and propeller in deep, shallow and very shallow water. The flow around the ship was modelled by a steady RANS (ANSYS Fluent) with a free surface. The frame motion technique was selected to simulate the rotation of the propellers. The CFD model validation concerned only the hull and the propeller because of the unavailability of experimental rudder data. The impact of the water depth was found to have the largest effect on the hull-rudder-propeller interaction. It was also shown that the advance coefficient of the operating propellers amplified the hydrodynamic forces exerted on the hull and rudders.

Delefortrie et al. (2018) executed captive model tests with an estuary vessel, equipped with two Z-drives. The program focussed on the effects of the interaction between the Z-drives, each one being independently steerable over a 360° azimuth range, on the manoeuvring forces and lead to the development of a 6-DOF manoeuvring model, which accounts for these interaction effects.

Gornicz et al. (2019) estimated the push-pull manoeuvre of a twin shaft ship under three different environmental conditions: unrestricted deep, shallow and close to quay. The RANS viscous flow solver ReFRESCO was used and the free surface effects were neglected. The propellers were modelled with a Smart Actuator Disc (SAD) able to customize the distributions of the body forces based on the propeller mode. The accuracy of the SAD decreased for large rudder angles and in very shallow water due to the increased complexity of the flow (Figure 85).

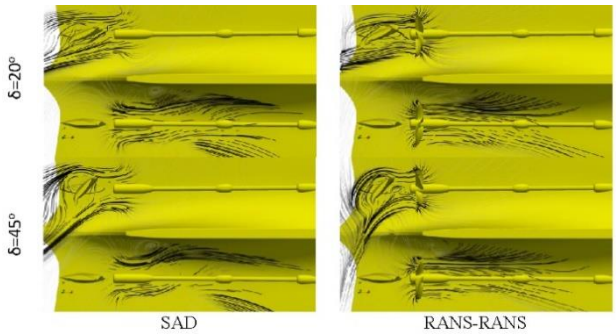

Figure 85. Streamlines in the horizontal plane through the shaft line for two different propeller modelling approaches. (Gornicz et al., 2019).

Squat. Hu et al. (2017) presented squat calculations in shallow water based in RANS (STAR-CCM+) simulations. To avoid negative under keel clearance and unphysical grounding in the start-up phase, an under-relaxation factor was included to slowly release the model in the vertical direction.

Terziev et al. (2018) investigated the sinkage, trim and resistance of a DTC model advancing in shallow water for varying channel cross-sections and ship speeds by using Star-CCM+. They confirmed the sinkage is important at low-speed range, whereas the trim is the leading factor at high-speed range.

In the investigation by Bechthold and Karstens (2020) RANS (STAR-CCM+) simulations were used to predict sinkage and trim of a ship in extreme shallow water with a water depth to draft ratio less than 1.2. The results were validated against the benchmark data of the DTC from the 5th MASHCON. A fair agreement was seen between experiments and numerical results for the towed setup without propeller.

Different authors, such as Ha & Gourlay (2018), Harkin et al. (2018) and Verwilligen et al. (2018) use full-scale measurements to validate or supplement model test tank measurements, especially to investigate the squat phenomenon. The presented methodology

could be included in an extended version of the full-scale manoeuvring trials to extract information from any full-scale manoeuvre and to account for the environmental effects.

Ship-bank interaction. Studies have been conducted to investigate the importance of free surface modelling in shallow and confined water. Razgallah et al. (2019) used RANS (ANSYS Fluent) with and without free surface for the computations of an inland vessel at various water depths and drift angles in the middle of a waterway with sloped sides applying VOF method or symmetry condition in the waterplane respectively (Figure 86).

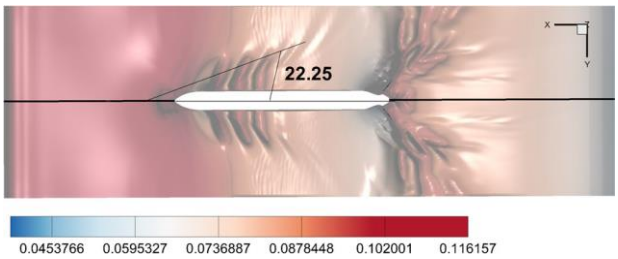

Figure 86. Model ship wave profile in confined water (h/T=1.2) at high speed. (Razgallah et al., 2019).

Van Hoydonck et al. (2019) used the RANS viscous flow solvers ISIS-CFD (Fine/Marine) and ReFRESCO with and without free surface deformation and with and without propellers for various computations at different water depth and distances to a vertical bank. The results were compared to potential flow predictions using RoPES (a 3D double-body potential flow solver) and model test data.

For both the above studies, it was found that the consideration of free surface deformation does not significantly influence the predicted forces and moments, except for very small under keel clearance values and/or distances to the bank. Furthermore, it was seen that for sailing close to a vertical bank in shallow water, the potential flow solver RoPES is not able to accurately predict the bank effects and viscous-flow methods should be adopted to obtain the correct trends of bank suction or repulsion.

Ship-lock interaction. A 3D boundary element method based on the Rankine Green function with free surface conditions was used by Yuan (2019) to predict ship hydrodynamics in different confined waterways. Predictions of the ship-ship, ship-bank and ship-bottom interactions showed reasonable correlation with the benchmark data sets of the MASHCON conferences except for the sign of the yaw moment for the ship-bottom and ship-bank interaction, indicating a so called Kutta condition should be imposed on the trailing edge of the wake region. For the ship-lock problem the method was able to predict the resistance and lateral forces but fails to predict the yaw moment due to flow separation at the lock entrance and the ship stern.

Veldman et al. (2018) presented a simple but accurate calculation method based on a calibrated Schijf's method to estimate vessel speed in a minimum capacity lock. The method is calibrated and verified against full-scale measurements with a prototype ship from five locks and one lift.

Ship-ship interaction. A number of studies using inviscid flow solutions have been reported. Yuan et al. (2018) proposed a superposition method to handle the unsteady free-surface boundary condition containing two or more speed terms and validated its feasibility in predicting the hydrodynamic behaviour in ship encountering. The methodology used in their study was a three-dimensional boundary-element method (BEM) based on a Rankine-type (infinite-space) source function. The results showed the free-surface effects need to be taken into account for Fr > 0.2. Ren et al. (2020) used a double body 3D potential flow code to compute hydrodynamic interaction forces. The

code included a mesh cutting scheme to include the varying sinkage and trim during interaction.

RANS simulations have also been used to investigate ship-ship interactions. Wnęk et al. (2018) used a RANS solver (STAR-CCM+) to study the flow between a tug and a tanker at various relative distances in shallow water. The simulations were carried out with and without free surface and validated against model test data to study the influence of viscosity and wave making. The model accounting for viscosity and free surface effects resulted the most accurate.

Sano and Yasukawa (2019) performed captive model tests with 1/110 scale models of both KVLCC2 and Aframax tanker to assess the ship to ship interaction forces during steady lightering. A comprehensive captive manoeuvring test program was carried out with both ships rigidly connected to each other. The results lead to a dedicated MMG model for this two ship test system, which was validated by free running tests: course keeping with PD control and small +/-10° turns.

Moored ships. Van Zwijnsvoorde et al. (2018) also applied the RoPES package to simulate the behaviour of a moored vessel in a passing ship event. The passing ship force calculated by RoPES served as input to an in-house time domain package. The results of the simulations were validated against full-scale measurements recorded using AIS information logged in the port of Antwerp. The simulations showed good agreement with the full-scale measurements except for a single case, where the linear model for elasticity of the mooring line was seen insufficient to predict the motions accurately due to highly elastic lines and low pretension force.

Li, L. et al. (2018) used a hybrid method founded on the combination of 3-D Rankine source method and impulse response theory to estimate the transient response of a moored ship exposed to sea waves and wash waves produced by nearby passing ships. Nam and Park (2018) developed a time-domain numerical method based on a finite element method to investigate the passing ship problem with a moored barge alongside a quay. Separation & gap distance and water depth were identified as critical parameters for the passing ship forces. To handle the moving boundary problem, both Li, L. et al. (2018) and Nam and Park (2018) implemented a re-meshing algorithm using a local body-fixed mesh to overlap the global background mesh, thereby replacing the re-mesh process by simple connection operations.

Tug operations. Aydın et al. (2018) used RANS (ANSYS Fluent) to estimate the towline forces of tractor type escort tugs in a bare hull configuration. The simulations were carried out with and without free surface effects and heel angles. Up to the stall angle, the inclusion of the effects only slightly affected the results. However, after the stall, the inclusion of the free surface effect increased the obtained lift significantly compared to the lift in the simulations without the effect.

Barrera and Tannuri (2018) developed an offline interpolation method to obtain the actuation model of a vector tug during pull operations in real time. The formulation significantly increases the realism of manoeuvres when vector tugs are used including the actual position of actuation by exploiting the output of an advanced algorithm not able to run in real time.

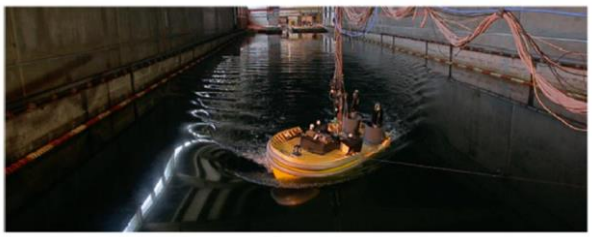

Figure 87: Free escort model test (Figari et al., 2020)

Figari et al. (2020) conducted a comprehensive model tests campaign using a model scale tugboat. They also showed CFD results compared against the tank test results with practical precision. Their results imply a substantial possibility of the CFD application as a method of predicting hydrodynamic forces and moment in low speed manoeuvres. Related to the model test campaign summarized in Figari et al. (2020), Piaggio et al. (2020) gives an overview of the full CFD study carried out in parallel to the EFD campaign including a detailed study on the skeg effects and with references to their studies on identifying hydrodynamic forces acting on the tug and their examination and validation of EFD and CFD-arising manoeuvring models used for a real-time simulator (Figure 87).

Simulation studies. Lataire et al. (2018) presented methodologies used to evaluate manoeuvres in shallow or confined water based upon five different simulation techniques. The first four are fast time simulations, each with a different level of detail and control and the last is real time simulations, where the human factor is included as well.

Iribarren et al. (2018) described a methodology to analyze the effects of passing ships in a new terminal. Based on fast-time simulation of the ship speed and distance to the moored vessels, the program RoPES was used to obtain the interaction forces in shallow water considering bathymetry and lateral restrictions.

Ruggeri et al. (2018) presented an automatic draft computation system called ReDRAFT, which integrates the environmental conditions collected in real time (or a forecast) to the hydrodynamic model of the port and the customized dynamic ship model in order to define the safe under keel clearance for the manoeuvre.

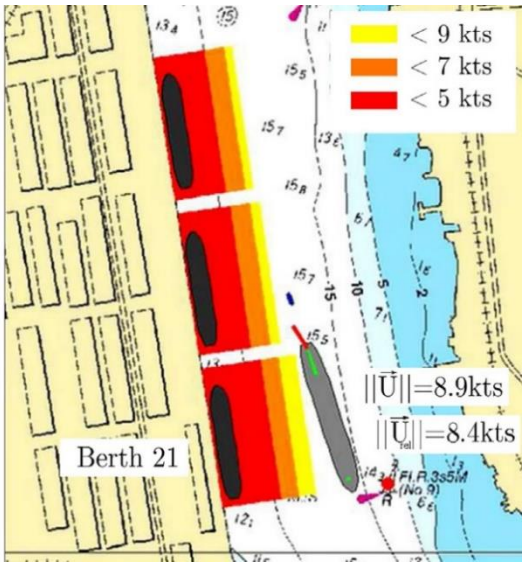

Figure 88. Operational limits for three passing distances printed in nautical chart of Port of Santos. (Watai et al. (2018)).

An analysis methodology for the passing ship problem in port combining a 3D time domain Rankine panel method with a dynamic simulator for moored ships and a real time simulator is presented by Watai et al. (2018) Emphasis is given to the proposed approach of including important contributions from the real time manoeuvring simulations in the analysis process. In many circumstances it is not possible to follow the desired path or speed as it depends on the pilot's ability to handle the ship rudder and engine (Figure 88).

2.3 Unmanned Surface Vehicles (USVs)

Preliminary remark. A vast amount of literature has been published on this topic and the closely related topic of Autopilot (see 3.4), however, articles have a fluctuating quality and mostly lack experimental validation. Here only the most significant contributions are covered. The topic of unmanned navigation should be a main point of attention for the next MC. Observe that the control of AUV is discussed in the

dedicated section 6.2 and that this remark applies there as well.

Path Planning and Path Optimization are a fundamental research topic in USV navigation. Kim H. et al. (2017) proposed a path optimization method using a genetic algorithm and a new fitness function considering environmental loads, obstacle avoidance, and minimization of travel time. An optimized path is determined using evolutionary processes and repeating fitness evaluations of each chromosome over all generations using the fitness function. The simulation results show that the proposed path optimization method is effective to determine the optimal path for several conditions of environmental loads and obstacles (Figure 89).

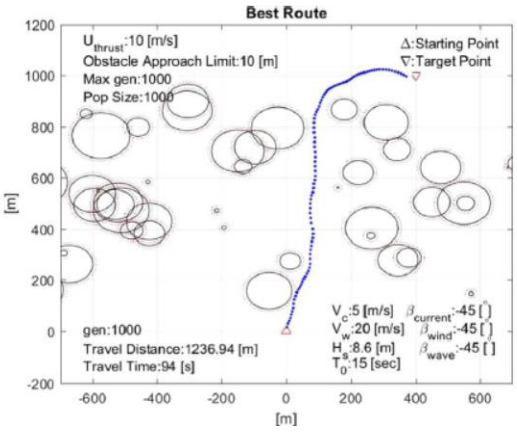

Figure 89. Optimized path by genetic algorithm (adapted from Kim H. et al. (2017)).

Chen C. et al. (2019) proposed a path planning and manipulating approach based on Q-learning, which can drive a cargo ship by itself without requiring any input from human experiences. Q-learning is introduced to learn the action–reward model and the learning outcome is used to manipulate the ship's motion. By comparing the proposed approach with the existing methods, it is shown that this approach is more effective and closer to human manoeuvring. Wang Y. et al. (2018) proposed a path searching-based algorithm called the local normal distribution-based trajectory (LNDT) based on the COLREGs (Convention on the international regulations for preventing collisions at sea). The simulation results show that the proposed algorithm can plan paths to avoid static and dynamic obstacles safely. Wang N. et al. (2019b) also proposed a multilayer path planner (MPP) with global path-planning layer, collision avoidance layer and routine correction layer for an USV under complex marine environments including both coastal and surface constraints.

Xie L. et al. (2019) developed a trajectory planning based on a global multi-direction A* algorithm for working ships within offshore wind farms. The artificial potential field (APF) approach is modified to create a penalty function for perceiving a potential risk ahead in the trajectory. The simulation results indicate that the developed approach is a useful for ships navigating within wind farms. Niu et al. (2020) proposed a spatially-temporally energy efficient path planning algorithm by integrating the Voronoi diagram, Visibility graph, Dijkstra's algorithm and GA algorithm. To evaluate the performance, the Voronoi-GA energy efficient algorithm and Voronoi- Visibility energy efficient path re-planning algorithm are also implemented. The numerical simulation results indicate that the proposed algorithm has shown clear advantages in generating the most energy efficient path. Singh et al. (2018) proposed a constrained A* approach for optimal path planning of USVs in a confined maritime environment containing dynamic obstacles and ocean currents. Xu J. et al. (2019) studied an autonomous route planning algorithm based on the modified RRT (rapidly-exploring random tree) approach for ship through a canal estuary area with the strong currents.

Path Following and Trajectory Tracking are essential performance criteria for USV

manoeuvring and navigation. Liu Y. et al. (2017) developed a novel guidance and control (NGC) system for a USV with environmental influences such as surface current and winds. The system is developed by integrating multiple functional modules, a robust autopilot module and an intelligent path planning. Hinostroza et al. (2018) investigated a motion planning, guidance and control system for an autonomous surface vessel in a practical maritime environment. The motion planning algorithm is developed by using the angle-guidance fast marching square method and the guidance system is developed by using the line-of-sight trajectory tracking algorithm. Huang H. et al. (2019) proposed a trajectory tracking controller for an USV with multiple uncertainties and input constraints. A trajectory tracking guidance law based on yaw angle and surge is proposed, and inner and outer disturbances is observed by reduced order extended state observers in the controller. Zhao et al. (2020) proposed a broken lines path following algorithm which USV can follow a series of broken lines by path following controller in an uncertain environment. The numerical simulations and water experiments verify the effectiveness of the proposed path following algorithm.

Peng et al. (2017) reviewed the design and implementation of the USV, including its hull design and structure of the control system. A trajectory tracking test and autonomous collision avoidance test were carried out to validate the controller of USV. Eriksen and Breivik (2018) proposed a Model-based speed and course controller for high-speed ASVs operating in the displacement, semi-displacement and planing regions. Through full-scale experiments, the proposed controller has been shown the improvement of the control performance for time-varying references. Liao et al. (2019) discussed berthing-oriented trajectory planning and trajectory tracking control, considering the dynamic changes of USV in berthing tasks and also divided the planning and control modes into two phases: the remote phase and the terminal phase. An improved artificial potential field method is proposed to complete autonomous berthing trajectory planning and an improved adaptive fuzzy PID control method is used to track the expected trajectory of USV. The simulation and field experiments show that the proposed method is more effective to plan the trajectory and has a better tracking performance than the traditional PID method (Figure 90).

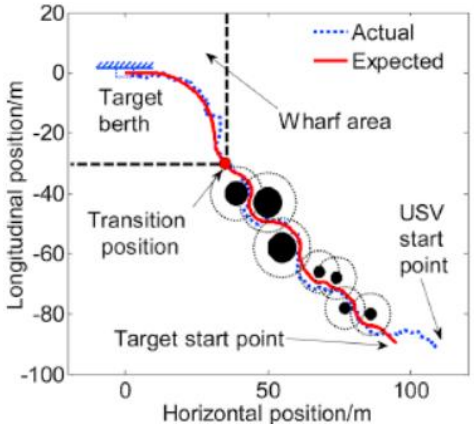

Figure 90. Berthing-oriented tracking control (adapted from Liao et al. (2019)).

Wen et al. (2020) proposed an adaptive path following controller for the USV. The path following controller uses the intelligent adaptive control method and vector field (VF) guidance law and the characteristic model-based heading angle. The comparisons with experimental results indicate the developed path following controller can simultaneously ensure accuracy in the expected range and defend negative effects induced by environmental disturbances.

Collision Avoidance is the most important ability required for USV to realize safe navigation. Song et al. (2018) proposed a two-level dynamic obstacle avoidance algorithm. In the first level (non-emergency situation), the primary task of the USV is to move to the next path target point while avoiding any obstacles by using the velocity obstacle algorithm. In the

second level (emergency situation), the primary task of the USV is to move away from the obstacle immediately by using an improved artificial potential method. Li S. et al. (2019) also proposed a distributed coordination strategy which is composed of two phases for assisting ships in making decisions on the most efficient anti-collision operations when multiple ships encounter. Zhou et al. (2020) proposed an USV motion-planning method based on topological position relationships (TPR) to find the shortest search time and the shortest path for collision avoidance. Through numerical simulations and field tests, the effectiveness of the proposed method is verified.

Shen et al. (2019) proposed a novel approach based on deep reinforcement learning (DRL) for automatic collision avoidance of multiple ships particularly in restricted waters. A training method and algorithms for collision avoidance of ships, incorporating ship manoeuvrability, human experience and navigation rules, are studied in detail. Xie S. et al. (2019) proposed a model predictive control (MPC) based on an improved Q-learning beetle swarm antenna search (I-Q-BSAS) algorithm and neural networks for real-time collision avoidance with full consideration of ship manoeuvrability, collision risks and COLREGs. Zhao & Roh (2019) proposed an efficient method to overcome multi-ship collision avoidance problems based on the Deep Reinforcement Learning (DRL) algorithm. The proposed method directly maps the states of encountered ships to an own ship's steering commands in terms of rudder angle using the Deep Neural Network (DNN) which is trained over multiple ships in rich encountering situations using the policy-gradient based DRL algorithm and COLREGs. The simulation results indicate that multiple ships can avoid collisions with each other while following their own predefined paths simultaneously (Figure 91).

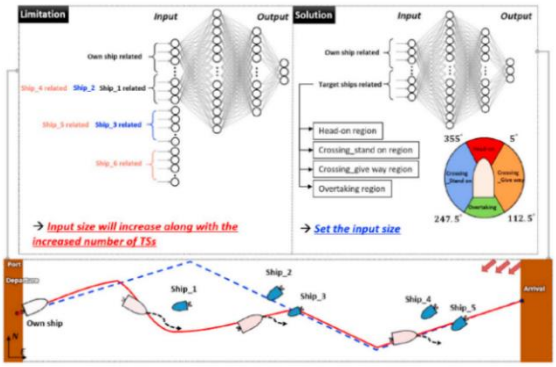

Figure 91. DNN learning-based collision avoidance method (adapted from Zhao & Roh (2019)).

Woo and Kim (2020) proposed a deep reinforcement learning (DRL)-based collision avoidance method for an USV. For the composition of the DRL network for collision avoidance, a neural network architecture and semi-Markov decision process model are used. The resulting DRL network is trained based on repeated collision avoidance simulations in various encounter circumstances. Simulations and experiments are conducted to validate the proposed method's effectiveness.

Huang Y. et al. (2019) proposed a collision avoidance system using a generalized velocity obstacle (GVO) algorithm. The system is composed of three main modules: Global planner, Local planner (searches a collision-free velocity to avoid collision) and Controller (calculates the required control force to follow the desired velocity). The simulation results show that the proposed collision avoidance system can work properly in various maritime environments. Wang X. et al. (2017) proposed a ship collision avoidance dynamic support system in close-quarters situation, which combines a mathematical manoeuvring model, a ship manoeuvring control mechanism and a ship collision avoidance parameter calculation model. The simulation results show that the proposed dynamic support system is an effective and practicable system for collision avoidance, particularly in close-quarters situation.

Zhang G. et al. (2018a) developed a novel DVS (Dynamic Virtual Ship)-based obstacles avoidance guidance with a priority selecting strategy and a robust adaptive path-following control for underactuated ships. The simulation results showed that the developed scheme is effective to improve the path following and the obstacle avoidance without information on the system model or external disturbances. Shi et al. (2019) proposed an intelligent collision avoidance and a recovery path planning system which combine an initial path generation module, a path optimization module and an autonomous recovery module for a waterjet-propelled USV. The simulation results proved that the proposed system is effective to avoid collision accidents for multiple obstacles and to plan a safe recovery path in the cluttered marine environment. An automatic collision avoidance system to calculate the risks and economic preferences of all vessels within a certain range and to select the optimal manoeuvring way is developed by Nakamura & Okada (2019). The comparison between the manoeuvring results by the developed system and by pilots, using a full mission type simulator, showed that the system was effective for realizing strategic collision avoidance and for preventing human errors. Wang T. et al. (2020) proposed an autonomous decision-making support algorithm for multi-ship collision avoidance based on the inference of objective's intention. Every ship makes decisions from its own perspective and only considers keeping itself safe during the decision-making process. In order to verify the flexibility of the algorithm, different scenarios are considered in simulations, including the non-compliance of ships with COLREGs. Lee M. et al. (2020) developed a collision avoidance and route-finding algorithm for multi-ship encounter situations based on artificial potential fields, complying with the COLREGs and local navigation regulations. The method was tested in a simulated environment with various traffic scenarios. The potential field model is consonant with the concept of ship handling and appears to be well suited for the automatic collision avoidance algorithm for multi-ship encounter situations.

Formation control of multi-USVs is getting more important due to the expansion of the application area of USVs. Gu et al. (2019) studied a distributed containment manoeuvring controller for a fleet of under-actuated USVs. The vehicle fleet was converged to a convex combination of multiple virtual leaders regardless of the model uncertainties and ocean disturbances. The simulation results show that the multiple virtual leaders could move along multiple parameterized paths with a formation. Hinostroza et al. (2019) proposed a full navigation system for cooperative operation of a USVs fleet in a complex marine environment including static (environment) and dynamic obstacles. In the proposed system, a formation shape is determined using strategy of team formation and a cooperative algorithm is deployed using a fast-marching method depending on the desired mission of the USVs. Tan et al. (2020) also proposed a path planning algorithm based on the fast-marching square (FMS) method for an USV swarm. In the proposed algorithm, the FMS method-based path planning algorithm is used to generate a path and the COLREGs rule is considered to avoid collision.

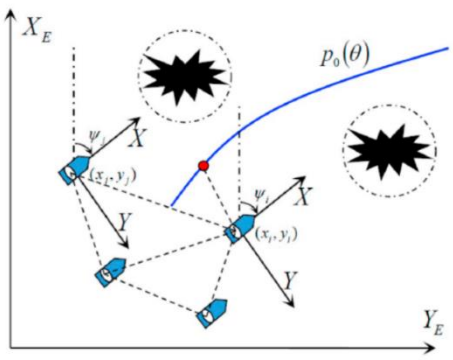

Figure 92. Path-guided time-varying formation control with collision avoidance (Peng et al. (2019)).

Peng et al. (2019) proposed a path-guided time-varying formation controller for a swarm of under-actuated autonomous surface vehicles. The proposed controller is based on a consensus approach, a path-following design, artificial potential functions, and an auxiliary variable approach. The advantage of the proposed controller is to have robustness against model uncertainties, ocean disturbances and unknown input gains, and the capability of collision avoidance and connectivity preservation. Simulation results show that the proposed controller has a good formation control performance and capability of obstacle avoidance for under-actuated USVs (Figure 92).

Liang et al. (2020) studied a coordinated tracking strategy with swarm center identification, self-organized aggregation, collision avoidance and distributed controller design for multiple USVs in complex marine environments including both unknown dynamics and external disturbances. Simulation studies are also performed to demonstrate the validity of the proposed coordinated tracking strategy.

Estimation and Simulator. Liu L. et al. (2019) studied a nonlinear extended state observer to estimate the state and disturbance of unmanned surface vehicles. Simulation results of state recovery and uncertainty estimation are provided to validate the effectiveness of the proposed state observer. Gu et al. (2020) studied a state estimation problem of a robotic unmanned surface vehicle with the measurements of GPS and IMU. Two nonlinear observers are used to estimate the position and velocity information. Kim S.Y. et al. (2018) developed an USV base station simulator for the purpose of training USV operators and to improve the user interface. The applicability of the USV base station simulator was confirmed by pilot tests.

2.4 Autopilot applications

Restricted Waters and Berthing. Autopilots are normally applied in non-restricted navigation areas, with the propeller at a constant rotation/pitch and the vessel subjected to slowly varying disturbances. However, the application of autopilots in restricted areas are being considered nowadays. Wang J. et al. (2019a) proposed a path following controller based on robust H_∞ theory to keep the vessel close to the centre line of the restricted channel, subjected to wind disturbance. Liu H. et al. (2018a) did a more comprehensive work, with a combination of Model Predictive Controller (MPC) and a Linear Quadratic Regulator (LQR) to design a course following autopilot considering bank and shallow water effects. They also demonstrated the advantages of adopting the speed variation as a second control input.

Automatic/autonomous berthing is an active research topic, with the popularization of machine learning techniques. A comprehensive review of automatic ship berthing is presented by Ahmed et al. (2020). Zhang Q. et al. (2017) proposed a PID-based nonlinear feedback algorithm for course keeping even when the propeller is stopping or reversing, in order to regulate the speed for berthing. The tests with a MMG ship model demonstrated that the controller could provide acceptable results during berthing (reduced speed). Maki et al. (2020) solved the off-line automatic berthing problem using an optimal control minimum-time technique. The collision risk with the berth was taken into account. The covariance matrix is adapted using an evolution strategy (CMA-ES). Simulation results demonstrated the performance of the proposed berthing control.

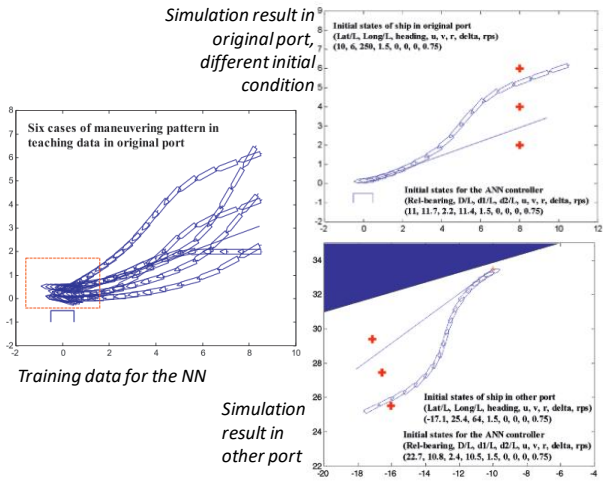

Figure 93. Automatic Berthing tests (adapted from Im and Nguyen, 2018).

Im and Nguyen (2018) noticed that the existing NN have limited capacity of generalization. The controllers can only berth a ship in the same port of the teaching data. By using the headup coordinate system, which includes the relative bearing and distance from the ship to the berth, a novel NN controller is proposed to automatically control the ship into the berth in different ports without retraining the NN structure. The results are satisfactory as illustrated in the Figure 93, but still did not take into account the environmental conditions.

Offshore Operations and Special Vessels. Modified versions of a conventional autopilot were applied to offshore cargo/fuel transfer operations. Liu Y. et al. (2019a) developed a MPC based target-follow autopilot to the underway replenishment operation. The numerical simulation considered the ship-to-ship interaction forces and the results proved the efficiency of the proposed controller. Moreno et al. (2019) proposed a sliding-mode based autopilot, with the objective of controlling the distance from a tanker underway and to transfer the oil cargo. It is an alternative to the ship-to-ship underway operation, in which both tankers navigate at low speed and are connected side-by-side, with high risks associated to the relative motion between the vessels and failure of the mooring lines. The operation was tested in fast-time and real-time simulations, including evasive manoeuvres in case of propeller drive-off. The hose system for this operation still needs to be developed and offers engineering challenges due to the large distance between the manifolds.

The application of autopilots has been extended to special vessels, such as hovercraft and sailboats. Wang Y. et al. (2019) presented a nonlinear adaptive path following controller for an amphibious hovercraft, that typically has a shallow draft and a lack of lateral force characteristics, resulting in a large sideslip angle. Therefore, the controller has to accurately estimate and compensate such sideslip angle. The authors proposed a bounded gain forgetting estimator, with an adaptive update law. The good performance of the controller was demonstrated by numerical simulations. Concerning sailboat autopilots, the surge motion is mainly controlled by the sail while the yaw motion by the rudder. Based on this strategy, Deng et al. (2019) proposed a controller with 2 objectives: to obtain the sail angle to maximize ship speed and to control rudder angle to keep the vessel in the desired course. The novelty of the paper is to apply such controller to a retrofitted bulk carrier.

Machine Learning Autopilots. Non-Supervised Machine Learning based controllers are getting more popular due to the increase on computational capacity, with the advantages of a self-learning process, non-necessity of training data and previous knowledge of the mathematical model. Martinsen (2018a) and Amendola et al. (2019) proposed a framework, based on deep reinforcement learning, to solve the straight-path following problem for under-actuated marine vessels under the influence of

unknown disturbances. The policy search algorithm has no prior knowledge of the system it is assigned to control. A deep neural network is used as function approximator. Different reward functions are proposed, trying to minimize the distance of the vessel to the required path. The first paper also proposed a reward function to prevent noisy rudder behaviour. The simulation results demonstrated good performance. Martinsen (2018b) extended the previous results and implemented a frame-work based on deep reinforcement learning for curved path following of marine vessels in the presence of ocean currents. The algorithm was tasked to find suitable steering policies without having any prior info about either the vessel or its environment. The author tested the controller with three different vessels to demonstrate the practicality of the approach and its ability to generalize, using transfer learning technique, with success. Similar results were obtained by Amendola et al. (2020) in a real port access channel. Woo et al. (2019) went a step further. They developed a path controller based on deep reinforcement learning using deep deterministic policy gradient (DDPG) algorithm. The control policy is obtained from a self-training stage using a numerical simulator, and was then tested in a model scale experiment, but still without external disturbances. The results are quite satisfactory, as shown in Figure 94. Four control policies (A, B, C, D) are extracted from different stages of the training, being the policy D (with the best track performance) the one with most adequate number of episodes.

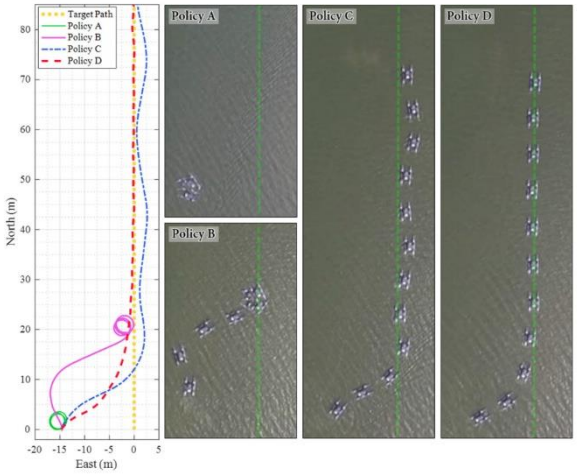

Figure 94. Trajectory data from path-following experiment (Woo et al., 2019).

Nonlinear Controllers. Zhang X. et al. (2019) proposed a concise robust integrator back-stepping control in which the user can define a steering restriction, to avoid rapid variation of rudder control. The controller design procedure is simple with only two tuning parameters. Adaptive control theory (combined with other techniques) has been applied to improve the performance of autopilots and path controllers. For example, Wang N. et al. (2019b) combined a fuzzy observer with robust adaptive control. Esfahani et al. (2019) developed a trajectory control based on higher order sliding mode theory (Super-Twisting), improved by a method for the optimal tuning of gains.

General Topics / Improvements in existing Autopilots. Zhang J. et al. (2017) proposed a MPC based path following controller that takes into account the roll motion in the optimization process. They improved the work of previous researchers, by integrating a Kalman Filter to estimate the full state of the vessel and the disturbances. This makes the proposed MPC feasible to be implemented in real applications. Gupta et al. (2018) improved the trajectory control algorithm named Target Path Iteration (that is similar to a Model Predictive Control - MPC), integrating to a genetic optimization to

define the best parameters in real time. The proposed control algorithm was implemented on straight line and curved trajectories and the results show that the method used is accurate and robust. Chen C. et al. (2020) executed towing tank tests in shallow water with 4 different autopilot controllers (PID, adaptive PID, IMC and fuzzy). They concluded that the adaptive PID is the one that performed better, followed by the fuzzy. The advantage of the fuzzy controller is the simplicity, since it is a model-free control strategy. Only the controller coefficients need to be tuned. It does not depend on the identification of ship model parameters.

In order to improve the position control accuracy, Wang L. et al. (2018) applied a Beetle Antennae Search (BAS) self-optimizing PID control algorithm, that automatically optimizes the ship motion control parameters using a biomimetic algorithm. They demonstrated by means of numerical simulations that the BAS self-optimizing PID algorithm can optimize the system control parameters, with higher efficiency and accuracy than manual adjustment of control parameters.

Lee and Chang (2018) tested an improved version of the traditional LOS guidance method, with different approaches to determine the reference heading angle based on the cross-track and the heading errors (Figure 95). The numerical simulations revealed that the alternative methods have, smaller deviation, better rudder response and heading error under environmental disturbances. Wang Y. et al. (2020) designed an intelligent autopilot based on Extended Kalman Filter (EKF) trained Radial Basis Function Neural Network (RBFNN) control algorithm. Model scale tests indicated that the proposed autopilot is robust and can deal with random environmental disturbances and complex reference trajectory. The controller is compared to a conventional PD controller showing better performance regarding course keeping and trajectory tracking.

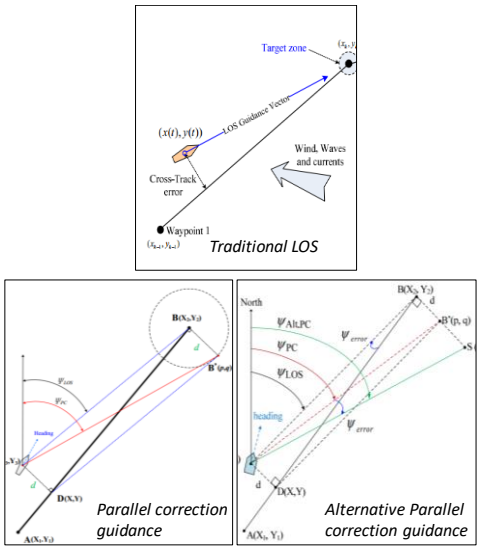

Figure 95. New Guidance Concepts (Lee and Chang, 2018).

3. PROCEDURES

3.1 Overview

The MC reviewed the procedures and guidelines under its responsibility and made updates as follows.

The MC updated the following four procedures:

- 7.5-02-04-02 Manoeuvring Tests in Ice. (see section 4.2)
- 7.5-02-06-03 Validation of Manoeuvring Simulation Models. (see section 4.3)
- 7.5-02-06-04 Uncertainty Analysis for Manoeuvring Predictions Based on Captive Manoeuvring Tests. (see section 4.4.)
- 7.5-02-06-02 Captive Model Test Procedure. (see section 4.4)

The MC made minor updates to the following procedures:

- 7.5-02-06-01 Free Running Model Tests. Minor updates were carried out to make sure that the procedure keeps track with the captive model test procedure.

- 7.5-04-02-01 Full Scale Manoeuvring Trials. Missing references were included, and minor English corrections were carried out.
- 7.5-03-04-02 Validation and Verification of RANS Solutions in the Prediction of Manoeuvring Capabilities. Missing references were included, and minor English corrections were carried out.
- 7.5-03-04-01 Guideline on Use of RANS Tools for Manoeuvring Prediction. A correction of a few references was carried out.
- 7.5-02-06-05 Uncertainty Analysis for Free Running Model Tests. Minor English corrections were carried out.
- 7.5-02-01-06 Determination of Type A Uncertainty Estimate of a Mean Value from a Single Time Series Measurement. Different corrections were proposed to the QSG to solve the differences with the original paper.

The MC also developed three new guidelines, with the following topics:

- 7.5-04-02-02 UV Full Scale Manoeuvring Trials (see Section 4.6)
- 7.5-02-06-06 Benchmark Data for Validation of Manoeuvring Predictions (see Section 4.5)
- 7.5-02-06-07 Captive Model Test for Underwater Vehicle (see Section 4.4)

In November 2020 a review was performed of two guidelines proposed by the Specialist Committee Manoeuvring in Waves. The suggestion was made to include the wave relevant information next term in the procedures 7.5-02-06-01 and 7.5-02-06-02, rather than creating new guidelines.

3.2 Manoeuvring in Ice

Manoeuvring Tests in Ice (7.5-02-04-02.3). During the 2nd meeting in Tokyo, the MC members discussed the possible updating of 7.5-02-04-02.3. These recommendations have been sent to the Specialist Committee on Ice to review. The MC recommended the following updating:

- include the captive manoeuvring tests in ice;
- include the zigzag test in the free-running manoeuvring tests in ice;
- include an example from a “breaking out of channel test”;
- include captains turn/modified captains turn in the free-running manoeuvring tests in ice;
- consider the other important manoeuvres in the free-running manoeuvring tests in ice;
- update the parameters from all tests;
- identify uncertain parameters and consider repeatability of the tests;
- include all references.

The Specialist Committee on Ice reviewed the recommended procedure for manoeuvring tests in ice and finalized the revision, which was sent to the MC committee to review after the 5th MC meeting (online, January 2021). More information can be found in the report of the Specialist Committee on Ice.

3.3 Validation of Manoeuvring **Simulation Models**

This procedure mainly addresses the necessary steps and documentation for the development of a simulation model. The updated procedure distinguishes the purpose of the manoeuvring simulation model. The step-by-step validation of manoeuvring simulation models using benchmark data, model test data, full-scale data and pilot expertise was recommended.

In section 3, the purpose of the model was distinguished into 5 levels, based on the required complexity of the model:

- ship manoeuvrability in deep water;
- ship manoeuvrability in shallow water;
- ship manoeuvrability in restricted water;

- ship manoeuvrability using a 4-DOF or a 6-DOF model;
- application of simulator design for training of crews.

In particular, the purpose of application of simulator design for training of crews was added to emphasize the assessment of new ports and crew training. The necessity of measuring and documenting the environmental conditions was added in the use of full-scale trials for the purpose of identifying forces.

In section 4, the step-by-step validation procedure of manoeuvring simulation models was proposed:

- Step 1: direct evaluation of the mathematical model and comparison with benchmark and/or model scale data;
- Step 2: fast-time simulations and comparison with benchmark, model and/or full-scale data;
- Step 3: real-time simulations commanded by local pilots and qualitative evaluation based on his/her expertise.

In particular, the effectiveness of the assessment of free running trajectories using benchmark data such as SIMMAN 2008 and SIMMAN 2014 was described. The questionnaire results of the validation procedure of simulation models (see section 7.3) was also described briefly to emphasize that each institute chooses more than one validation method.

3.4 Captive Model Tests

Captive model test procedure (7.5-02-06-02). The 2017 version of this procedure was marked as a concern by the AC because of too many options that were presented to carry out captive model tests. It is indeed a fact that many options or reasons exist to carry out such tests, however, the main goal is believed to be to check IMO standard manoeuvres. For that reason, the procedure was corrected to focus on such manoeuvres. This also meant that some sections, such as executions of simulations, which present the goal of the procedure were moved forward. From the results of the 2015 questionnaire, only the main points were maintained, and reference is made to the Appendix of the 28th MC for more background information. Effects of water depth and blockage on the results are now highlighted by giving these a dedicated chapter in the procedure.

Uncertainty Analysis for manoeuvring predictions based on captive manoeuvring tests. (7.5-02-06-04). The procedure has been extended with the effect of the uncertainty of the carriage kinematics, for which a new example has been added to an Appendix G. No newer material was found with respect to carriage kinematics than the publications of Vantorre (1988, 1989, 1992). The contents of these publications were added to the procedure expressed with the ISO GUM guidelines and applied to the KCS.

The effect of the uncertainties induced by noise and data reduction, or signal processing in general, are now also included (see section 6.1). The procedure is now built up with different examples in different appendices written by different MC's. It is recommended to have a single integrated example, based on a well-known ship such as the KCS, which was the subject ship in the latest Appendices.

3.5 Guideline on Benchmark Data

The aim of the guideline "Benchmark Data for Validation of Manoeuvring Predictions" is to highlight the processes relevant for bench-marking within the field of manoeuvring, to provide a list of the present benchmark database

available and to serve as an aid in selection of benchmark cases for validation.

The first part of the guideline describes the procedure of benchmarking; summarizes the steps of data collection, uncertainty assessment, analysis and sharing; and highlights additional requirements to be considered and possible pitfalls. In the second part of the guideline the present manoeuvring benchmark database is presented. An overview of the available benchmark hull forms covering tankers, container vessels, surface combatant hull forms, bulk carriers and underwater vehicles (UV) is given along with a summary of available restricted water cases and a complete table listing all available data, including references to these.

The database is intended to be updated continuously (following the cycle of ITTC), based on recommendations from the steering committees of the manoeuvring workshops, who will also be responsible for QA and availability of the data.

3.6 Guidelines for Underwater Vehicles

Investigations into the manoeuvring hydrodynamics of Underwater Vehicles are becoming more common and more complex. To date, there are not yet standardised test guidelines for such vehicles. The MC has developed two new guidelines that are specific to Underwater Vehicles, with the following topics:

Captive Model Test for Underwater Vehicle (7.5-02-06-07). The guideline is specifically intended for underwater vehicles, such as Autonomous Underwater Vehicle (AUV), Remotely Operated Vehicles (ROV) or submarine models, which all share similar hydrodynamic characteristics. The aim of this guideline is to provide an outline of captive model tests for underwater vehicles to determine the values of the manoeuvring coefficients for a simulation model of the underwater vehicle. The guideline is based on literature and especially the book of Submarine Hydrodynamics by Renilson (2018). It includes an overview of test facilities, test manoeuvres and the respective coefficients obtained for underwater vehicles and recommendations concerning model tolerance and blockage effects. Recommendations on benchmark data and uncertainty analysis are provided at the end.

UV Full Scale Manoeuvring Trials (7.5-04-02-02). The guideline provides an outline of full-scale trials to determine the manoeuvring characteristics of an Underwater Vehicle. The present version focuses on the behaviour of an AUV as a reaction to rudder, elevator, and other control device actions. The guideline includes a total of 12 manoeuvring tests with descriptions of the manoeuvres, measured variables, and AUV handling characteristics checked for each test. It also includes an overview of the instrumentation and AUV system components that are commonly involved. Recommendations on uncertainty analysis are provided at the end.

Acknowledgements. The following scientists kindly reviewed the Guidelines for Underwater Vehicles in 2019:

- Professor Ettore A. Barros, University of São Paulo (7.5-04-02-02)
- Dr. Toshifumi Fujiwara, National Maritime Research Institute, Offshore Advanced Technology Dept. (7.5-04-02-02 and 7.5-02-06-07)
- Dr. Hisashi Koyama, Mitsui E&S Shipbuilding CO., Ltd. Naval ship &

Defence system design Dept. (7.5-04-02-02 and 7.5-02-06-07)
- Professor Ye Li, Harbin Engineering University (7.5-02-06-07)
- Professor Zuyuan Liu, Wuhan University of Technology (7.5-02-06-07)
- Professor Hua Zhang, China Ship Scientific Research Center (7.5-02-06-07)

4. BENCHMARK DATA

4.1 SIMMAN 2021

In continuation of the Workshop on Verification and Validation of Ship Manoeuvring Simulation Methods in 2008 (SIMMAN 2008) and SIMMAN 2014 (Quadvlieg et al., 2014), the new workshop SIMMAN 2021 was scheduled for April 2020, but has been postponed to the end of 2021. The objective of the workshop is the assessment of current simulation methods for ship manoeuvring to aid code development, establish best practices and guide industry.

For the new workshop, some of the deep and shallow water cases have been replaced with new measurements, in particular the free running model tests in shallow water, to enable better comparisons.

Further, a few changes have been made to the test cases of SIMMAN 2021 compared to 2008 and 2014:

- The 5415M has been replaced with the ONR Tumblehome (ONRT) model 5613. Like the 5415M, the ONRT is an established surface combatant hull form test case used in workshops with twin screw arrangement with struts and rudders.
- The captive and free running test cases are reduced to maximize the number of submissions for more robust statistical analysis.
- KCS and ONRT turning circles in a regular wave are included a new tests cases, extending the test matrix to include manoeuvres in waves, since this is also of importance in assessment of manoeuvring prediction capability.

4.2 Datasets

To be able to predict manoeuvring behaviour, reliable predictions or simulation methods are required. Therefore, it is important to make a dedicated verification and validation effort related to the simulation methods and hereby asses the accuracy of the methods.

At present the benchmark database covers the following hull forms and test cases:

- Tankers (KVLCC2 in both deep and shallow water)
- Container Vessels (KCS in deep and shallow water and in waves, DTC in shallow water and in waves, HTC in deep water)
- Surface Combatants (5415M in deep water, ONRT in deep water and in waves)
- Bulk Carriers (JBC in deep water)
- Underwater Vehicles (DARPA Suboff in deep water)
- Manoeuvring in restricted water (Bank effects, Locks and ship-ship interaction)

The full list including references to all data is found in the new guideline 7.5-02-06-06. This lists shows that the focus is on the seagoing

vessel types and none of them, except the HTC, a 153.7 m container ship built by Bremer Vulkan in 1986, exists in full-scale. It would be a reinforcement of the present benchmark database to include model scale vessels with a documented full-scale variant. This would open opportunities to investigate scale effects and increase the quality of manoeuvring predictions.

In general, benchmark studies are essential, also for inland vessels. According to Quadvlieg et al. (2019) inland waterway transport plays an important role in the transport of cargo in Western Europe and the manoeuvrability of the vessels dictates amongst others the capacity of the waterways. The knowledge on manoeuvring models for inland ships and pushed/towed convoys can be deepened, considering inland benchmark ships/datasets. This will stimulate the development and validation of manoeuvring simulations in waterways. Mucha et al. (2019) support the statement of Quadvlieg et al. (2019) of the need for inland vessels in the benchmark dataset. Both papers suggest typical inland vessels and are willing to share their data to give an impulse to the research.

Besides the need for inland vessels, benchmark datasets for (autonomous) under water vehicles are also on the wish list for new datasets. At present only data for the DARPA Suboff, a submarine hull form, is available.

5. UNDERWATER VEHICLES

5.1 Manoeuvring Hydrodynamics

Overview. The focus is put on research that have been carried out on the hydrodynamics and manoeuvring of underwater vehicles. As expected, a lot of attention is devoted to the methods adopted within the research in the pursue of accurate evaluation or prediction of the vehicle hydrodynamic characteristics; be it experimental, numerical or empirical.

The purpose of the research on the manoeuvring hydrodynamics of underwater vehicles can be commonly categorised into the following:

- to identify and understand the hydrodynamic manoeuvring performance of an underwater vehicle and/or its components (Dubbioso et al. 2017b, Go and Ahn 2019, Kim H. et al. 2018, Maki et al., 2018, Pan et al. 2019);
- to identify and understand the effects of the interaction between an underwater vehicle and its environment (Crossland 2017, Amiri et al. 2020);
- to identify and understand the underlying flow phenomena that affects the performance attributes of the underwater vehicle and/or its components (Ellis et al. 2018, Patterson et al. 2018), or
- a combination of the above (Harwood et al. 2018).

Numerical Methods. A review of the methods adopted in the research above shows a clear transition from experimental methods to numerical methods in recent years with CFD RANS being the dominant approach. The aim of such studies tends to focus on evaluating the manoeuvring hydrodynamics of underwater vehicles in conditions that are beyond the spatial and instrumentation limits of conventional experimental testing facilities, or when there are multiple design or operation options.

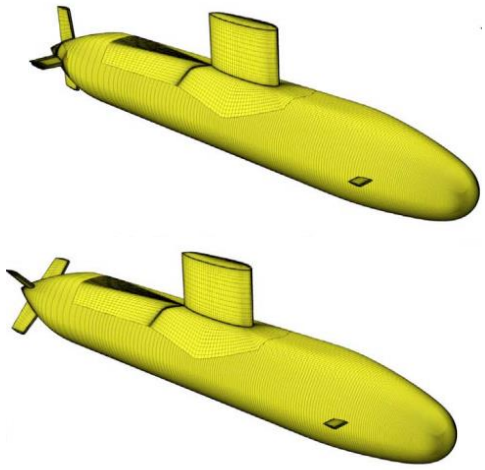

(b) X rudder configuration

Figure 96. CFD models of the CNR-INSEAN 2475 (Dubbioso et al. 2017b)

Dubbioso et al. (2017b) analysed the turning ability of the CNR-INSEAN 2475 free running submarine model with different rudder configurations, i.e. cruciform (default) and X (see Figure 96). The study was carried out using a 3-DOF RANS model with active control planes and an actuator disc to represent the propeller. Partial validation was carried out for the cruciform configuration against published experimental data from QinetiQ. The study showed that the turning abilities of the X rudder configuration are superior to the cruciform configuration for the CNR-INSEAN 2475. The findings were also supported by breakdown of the forces on the hull and individual rudders.

Amiri et al. (2020) investigated the free surface effect on the manoeuvrability of an axisymmetric underwater vehicle in the horizontal plane traveling close to the free surface using CFD (Figure 97). Captive tests involving straight-ahead resistance, drift and circular motion tests were performed to predict the coefficients over various submergence depths. The obtained coefficients were then used in a coefficient-based manoeuvring model to evaluate the free surface effect on the vehicle undergoing turning circle and zigzag manoeuvres at the respective submergence depths. Observations regarding the forces and moments on the vehicle and its stability at different submergence depths are also shown.

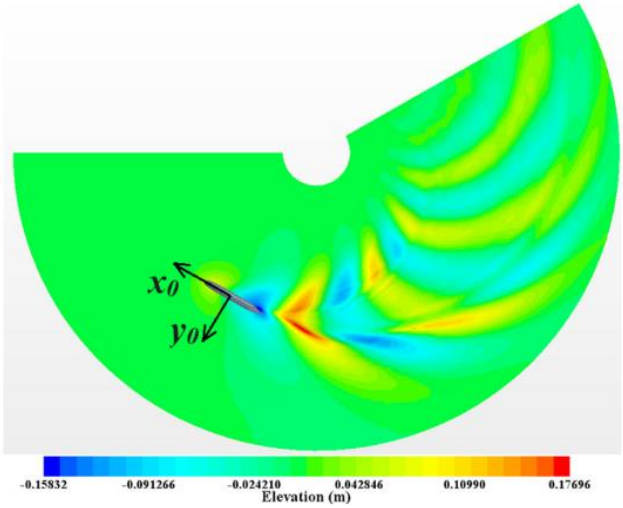

Figure 97. Free surface elevation of the rotating arm test on the axisymmetric underwater vehicle (Amiri et al. 2020)

Go and Ahn (2019) presented a new methodology to determine hydrodynamic derivatives of a tow-fish underwater vehicle using CFD. The linear and non-linear hydrodynamic derivatives of the vehicle were determined using RANS and the added mass coefficients were obtained analytically using strip theory. The effectiveness and applicability of the methodology were demonstrated via coefficient-based 6-DOF manoeuvring simulations using the CFD-determined derivatives for three different scenarios (*L*-, *U*-, and *S*-turn manoeuvres) at various towing speeds (see Figure 98). Verification was carried out by comparing the forces and moments produced by the 6-DOF manoeuvring model and the CFD results which was shown to be in good agreement. Go and Ahn noted that validation of the methodology via experimental tests is currently in progress and soon to be reported in a subsequent paper. The highlight of the paper is the demonstration of a comprehensive new

methodology to determine and assess the applicability of the hydrodynamic derivatives of an underwater vehicle.

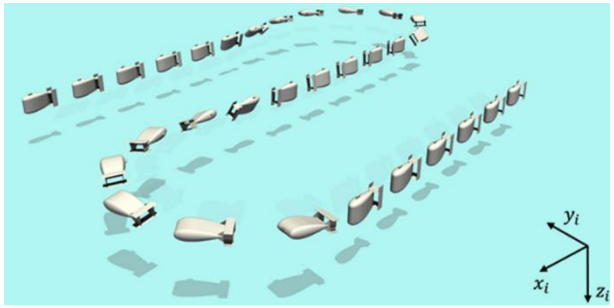

Figure 98. S-turn manouvres of the tow-fish vehicle (Go & Ahn 2019)

Kim H. et al. (2018) developed a 6-DOF free running CFD simulation model of the BB2 submarine model with active control planes and assessed its fidelity for straight line and turning manoeuvres. The depth keeping of the model was controlled via an autopilot. The propeller was explicitly modelled for the straight-line manoeuvre. For the turning manoeuvre, the propeller was replaced with an actuator disk to reduce computational requirements. The simulation results were found to be in good agreement with published free running test data from MARIN. The comparison included time histories of the vehicle trajectories and the deflections of the control planes (Figure 99).

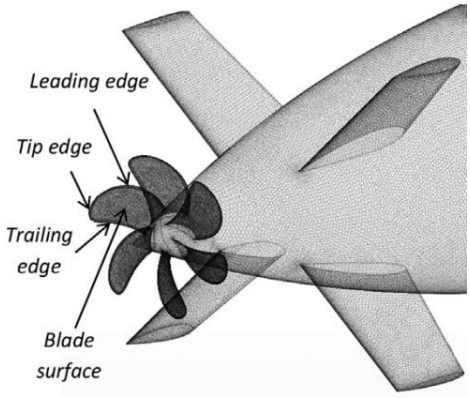

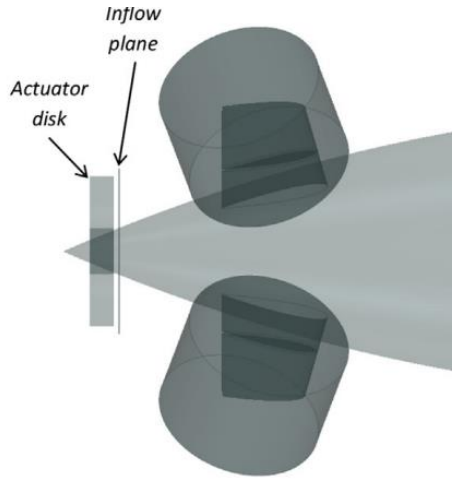

Figure 99. Overview of the propeller arrangement for the CFD free running model: with propeller (top), with actuator disk (bottom) (Kim H. et al., 2018).

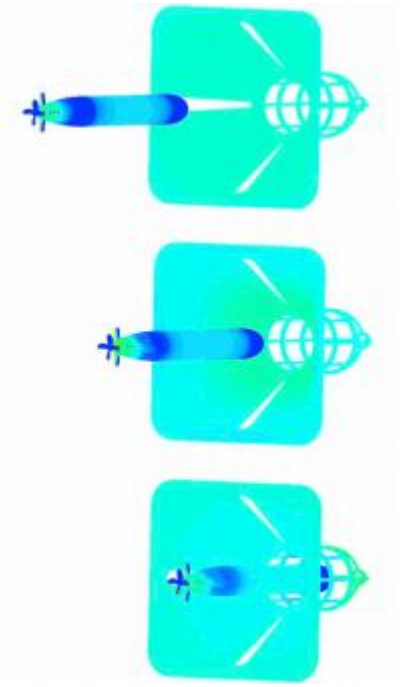

Figure 100. Overview of the SARV AUV approach the dock (Wu et al., 2019)

Wu et al. (2019) carried out a CFD-based study to analyse two straight line docking approaches (i.e. constant RPM docking and brake docking) with a dock for their SARV AUV. They used a coupled RANS and equations of motion model to simulate the

straight-line manoeuvring dynamics of the AUV. The coupled model was validated against field tests data and then extended to simulate the two straight line docking approaches with the dock. The results were then analysed to identify the pros and cons of the approaches.

Pan et al. (2019) investigated the flow field around a modified SUBOFF submarine model with rudder flaps during straight ahead motion and steady diving conditions using RANS (Figure 25). The two conditions were simulated with and without its propeller. The CFD model was validated using the original SUBOFF submarine model (no rudder flaps) against published experimental data by the David Taylor Research Center (DTRC). The results showed the harmonic characteristic of the nominal wake at the propeller plane and the unsteady propeller force for the different flap deflections and manoeuvring conditions investigated. Visualisation of the wake profile was also provided to support the findings.

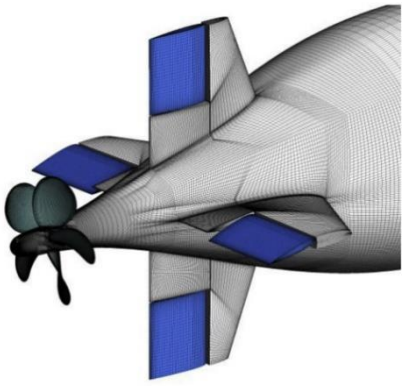

Figure 101. Surface mesh of the modified SUBOFF with rudder flaps (Pan et al., 2019)

Petterson et al. (2018) carried out a detailed LES-based study of the vorticity and wake flow structures generated by a full-scale, fully appended generic conventional submarine at 0°, +10° and -10° yaw with a speed of 4.6 knots and propeller turning at 23 rpm. Detailed visualisation of the flow structures were provided and discussed with additional insight into the influent of the propeller on the flow structures over the three yaw angles (Figure 102). The study also examined the time-history and frequency spectra of forces induced on the hull, fin and components of the propeller. The work was carried out using mesh models of up to 344 million elements and approximately 2 million CPU hours. The work highlights the intensive computational requirements, but also, the progress of CFD and the fidelity of result that is achievable for such studies.

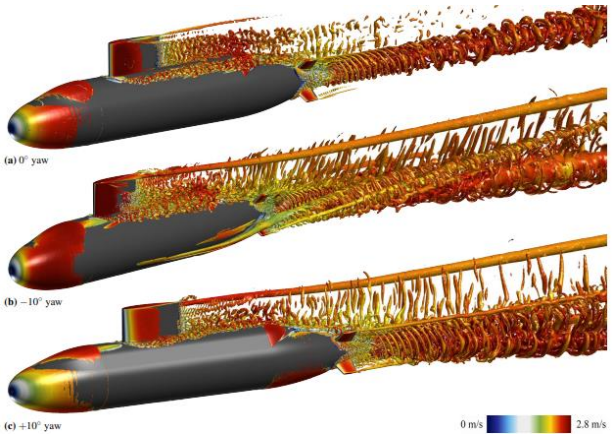

Figure 102. Visualisation of the vorticity and wake flow around the full-scale BB2 submarine at different yaw angles (Patterson et al., 2018)

With many of the CFD-dominant research, they still involve a degree of experimental work or data at model scale or limited conditions for the purpose of validating the numerical models. However, in cases where confidence in the measured physics is difficult to establish, both CFD and experimental methods are employed with equal emphasis to co-validate the two methods and co-supplement the findings. A good example of this approach is the study by Harwood et al. (2018) on the drag and wave-making of a blunt submersible over a range of forward speeds. The study was conducted in a towing tank and replicated numerically using CFD with reasonable agreement between the two methods. The comparison included hydrodynamic loads and the free surface elevation (Figure 103).

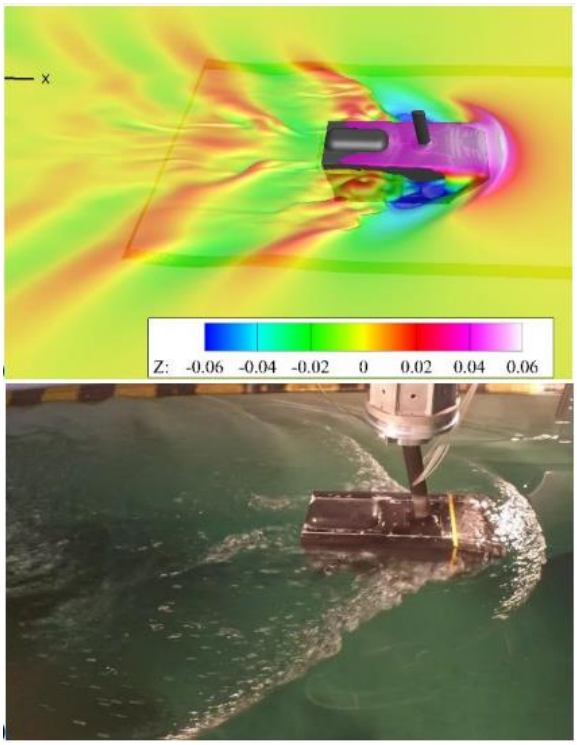

Figure 103. Free-surface deflection generated by the blunt submersible: CFD (top), experiments (bottom) (Harwood et al., 2018)

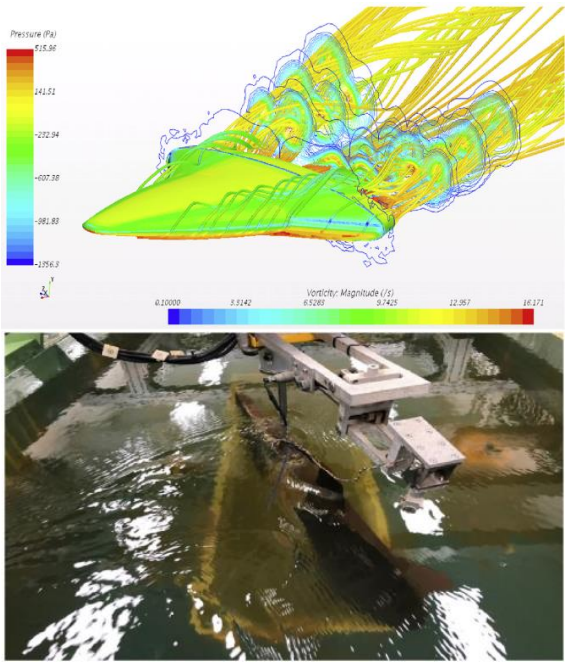

Figure 104. Pressure and vorticity contours 8n drift conditions(top), static drift model test at CWC (bottom) (Lee S. et al. 2020)

Lee S. et al. (2020) estimated the hydrodynamic manoeuvring derivatives for the heave-pitch coupling motion of a ray-type underwater glider (RUG) using RANS-based CFD method (Figure 104). Validation studies were performed using the resistance and the oblique motion of a manta-type UUV and compared to model test results. After validating the method, resistance, static drift, and dynamic PMM calculations for the RUG were performed to obtain the hydrodynamic manoeuvring derivatives. The CFD method can be utilized to obtain the hydrodynamic manoeuvring derivatives, which can be used in manoeuvring simulations of underwater gliders in the initial design stages. However, further studies on the optimization of the turbulence model and the grid refinement are required, and more model tests should be performed for underwater vehicles such as the RUG to confirm the CFD method.

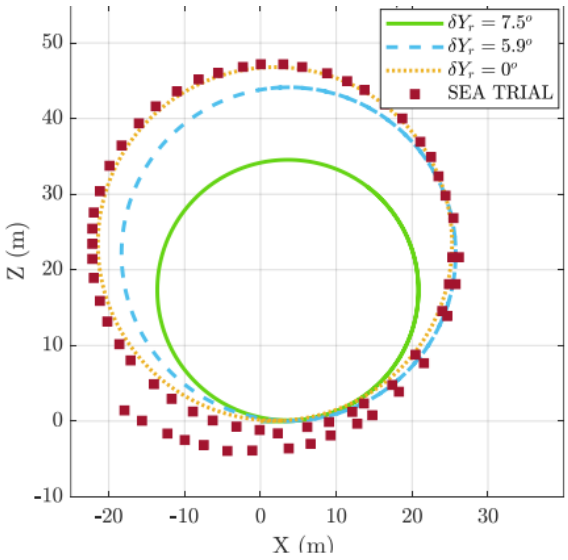

Figure 105. Simulated trajectories of a turning circle manoeuvre for the cycloidal propeller-augmented UUV (Desai et al. 2020)

Desai et al. (2020) studied the manoeuvring characteristics of a UUV driven by a screw propeller and control fins only, and compared it

to that of the UUV augmented with retractable cycloidal propellers. The cases considered are a turning circle manoeuvre, a low-speed 180° turn and a low-speed heave manoeuvre. A 6-DOF motion prediction model that accounts for the non-linear and coupled loads on an underwater vehicle was developed and validated using MATLAB code. Simulation results showed that compared to conventional propulsion systems, cycloidal propellers could potentially enable more swift, compact and decoupled manoeuvres in unmanned marine vehicles (Figure 105).

Experimental Methods. It is important to note that critical bodies of research with experiments as the primary method still prevail, in particular, for the following purposes:

- tests involving strong transient physics dependency in the manoeuvre or environment;
- evaluation of physical and hydrodynamic changes at a microlevel that affect the performance of a body of a much larger spatial scale;
- benchmarking of experimental facility for UV tests, and
- evaluation of propriety technology

Figure 106. Submarine model in-situ for the under waves experiment (Crossland, 2017)

Crossland (2017) carried out captive model tests in the Qinetiq Towing Tank at Haslar, UK to investigate the hydrodynamics characteristics of a submarine manoeuvring under head seas (Figure 106). A mathematical model was developed to describe observed hydrodynamics in the tests which enabled the implementation of an appropriate depth controller in response to the wave loads, providing guidance on hydrodynamic and hydrostatic control mechanisms. The paper also highlighted that a fully captive experimental arrangement suppresses the second order forces on a submarine under waves and the improvements observed with arrangement that restrained the model in the horizontal plane and surge but allowed it to freely move in the vertical direction whilst being lightly restrained using a suitable spring system.

Ellis et al. (2018) investigated the influence of root gap and boundary layer thickness on the performance of a rudder that is representative of those used on submarines (Figure 107). The work was carried out at the Australian Maritime College Cavitation Research Laboratory. The results showed that increased roots gaps increased stall angle, increase drag and reduced lift at low angles of incidence. The thickened boundary layer was observed to increase stall angle and maximum lift and significantly reduce the stall hysteresis.

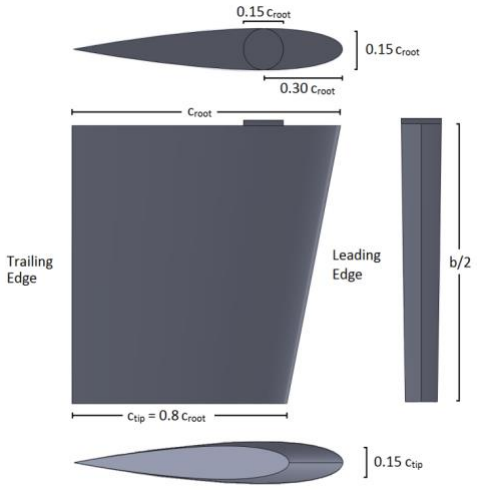

Figure 107. Overview of the submarine rudder (Ellis et al., 2018)

Lin Y.H. et al. (2018a) carried out PMM tests on the SUBOFF submarine model at the towing tank of the National Cheng-Kung University. The results were benchmarked the manoeuvring derivatives with good agreement against experimental data published by the DRTC with the observable discrepancies discussed. The adopted test arrangement was bespeaking with the model mounted to a single cylinder strut whereas a twin strut arrangement was used in the DTRC experiments (Figure 32).

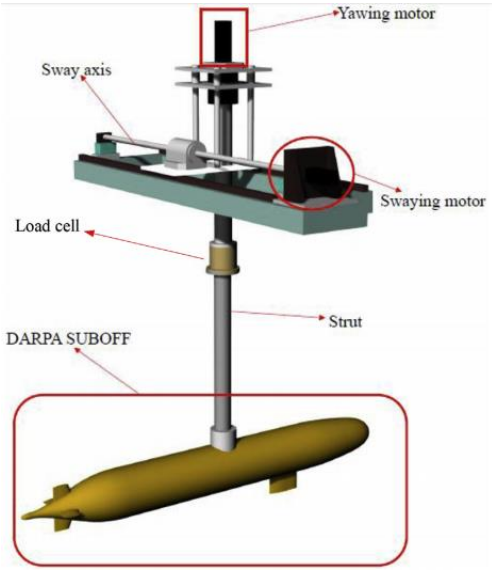

Figure 108. Arrangement of the PPM test for the single strut mounted SUBOFF (Lin Y.H. et al. 2018a)

Maki et al. (2018) carried out both captive model and free running model tests to evaluate a novel thrust vectoring system (TVS) for underwater vehicles in the towing tank of the Naval Systems Research System (NSRC) Cat Tokyo, Japan (Figure 33). The VTS was integrated into NSRS's free running model. The tests identified the hydrodynamics coefficients of the system which then used develop a mathematical model of the TVS dynamics. Optimal control theory was applied to the mathematical model, and manoeuvres were simulated to understand the performance of the TVS.

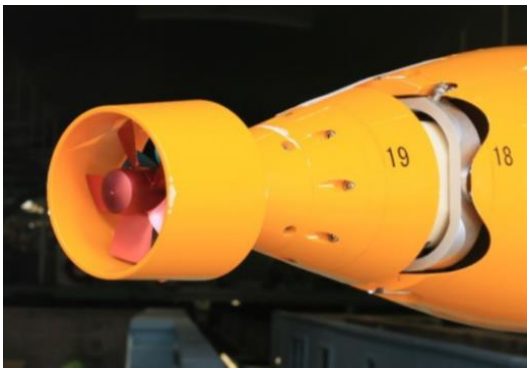

Figure 109. VTS integrated with the NSRC free running model (Maki et al., 2018)

Park et al. (2020) performed captive model tests with and without propulsors using the VPMM equipment to investigate the propulsor effects on AUV manoeuvrability (Figure 110). A mathematical manoeuvring model using a polynomial model was established, and static drift, control fin deflection, pure heave and pure pitch tests using VPMM equipment were performed to obtain manoeuvring coefficients. In static drift tests, the yaw moment with respect to the drift angle was remarkably reduced by the propulsor operation under large drift angle conditions. In the control fin tests, the results were analysed by focusing on the flow acceleration induced by the propulsor and increased lift on the control fins. The dynamic tests, i.e., the pure heave and pitch tests, showed that the propulsor affected the added mass and second moment of inertia.

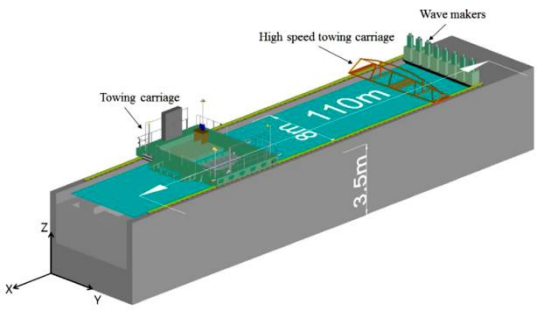

Figure 110. A drawing of the Seoul National University towing tank (Park et al., 2020)

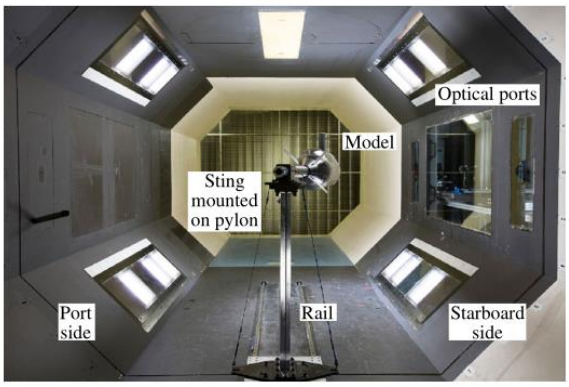

Figure 111. Test section of wind tunnel (Lee S.-K. et al., 2020)

Lee S.-K. et al. (2020) carried out the generic submarine BB2 model tests at 10° yaw in the DST wind tunnel (Figure 111). The most significant flow feature is on the model upper hull. Surface-streakline patterns obtained from China-clay allowed the visualisation of flow separation on the model BB2 cruciform appendage. Ensemble-averaged measurements of the wake, by high-resolution (planar 3-component) stereoscopic particle image velocimetry (SPIV), allowed the tracking of vortices downstream of the cruciform. The tests provided a benchmark to allow future comparisons with numerical simulations and other experiments on the BB2 (or a variant of this model geometry).

5.2 Control

In the case of Underwater Vehicles (UV), a control system for controlling the UV's motion is indispensable in order to achieve the operation purpose of an UV. The control system is the key technology and the main indicator for measuring the advanced level of an UV.

Path Following. Path following control aims at regulating a vehicle to converge to and follow a desired path, without any temporal specifications. Yu C. et al. (2017) proposed a simplified and nonlinear single-input fuzzy controller to follow the guidance speeds and angles for an autonomous underwater vehicle with unknown environmental disturbances. An improved 3D line-of-sight guidance law is derived to transform 3D path following position errors into controlled guidance speeds (Figure 36).

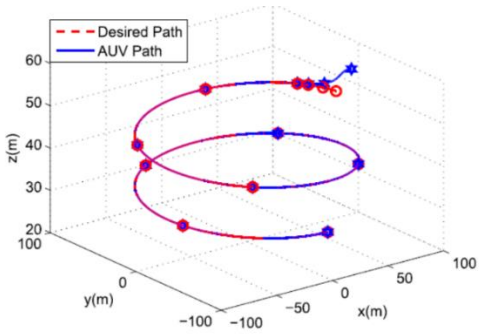

Figure 112. 3D helix path following (adapted from Yu C. et al., 2017).

Sans-Muntadas et al. (2019) proposed a path planning and guidance control law for under-actuated autonomous underwater vehicles with limited field-of-view, in particular vehicles that cannot control their sway motion and can only move forward. In this research, a path planning method which calculates a series of waypoints that generate a path that ensures the visibility is proposed. A guidance and control system that enables an underactuated vehicle to follow the proposed path preserving the vision of the landmark is also proposed. Abdurahman et al. (2019) studied an application and stability result of a modified line-of-sight guidance law for 3-D path-following of an unmanned underactuated underwater vehicle subject to environmental disturbances. The PF problem is solved using a revised relative system model with an improved FLOW frame and a complete model of ocean disturbances. The vertical course control and speed allocation are also used. Zhang G. et al. (2018b) proposed an adaptive second order sliding mode controller to eliminate the chattering motion through a sliding surface during the path following control considering

nonlinearities and external disturbances. An adaptive tuning law was applied to estimate the upper bound of external disturbances.

Qi et al. (2020) investigated the coordination control of multiple Underactuated Underwater Vehicles (UUVs) moving in 3D space. The coordinated path following control task was decomposed into two sub tasks, path following control and coordination control. In the path following subsystem, the control law was designed based on Lyapunov theory and back-stepping techniques. In the coordinated control subsystem, by adjusting the speed of the UUV, the coordination error tended to zero. The effectiveness of the controller was visualized by simulation experiments.

Sun et al. (2020) proposed a DDPG algorithm based on optimized sample pools and average motion critic network (OSAM-DDPG) to realize the path following control of an AUV. The random interference force model was added in the training process to simulate the dynamic underwater environment to train a DDPG-based control system with anti-interference ability. The conventional DDPG algorithm was improved by optimizing the sampling mode and the motion evaluation. Compared with other control algorithms, using the improved reinforcement learning algorithm as the controller of the AUV does not require an accurate mathematical model for the AUV, and has the advantages of anti-interference, good stability and high robustness (Figure 113).

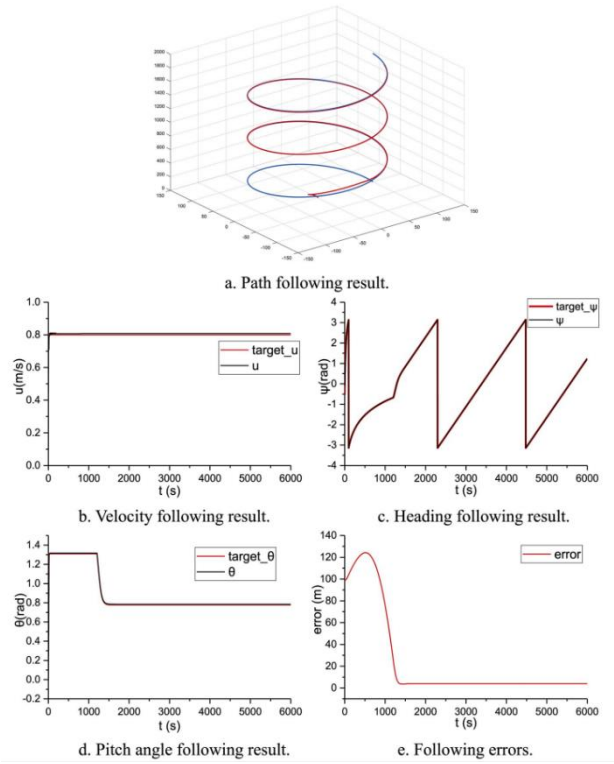

Figure 113. Simulation results of the AUV's 3D curve path following (adapted from Sun et al., 2020).

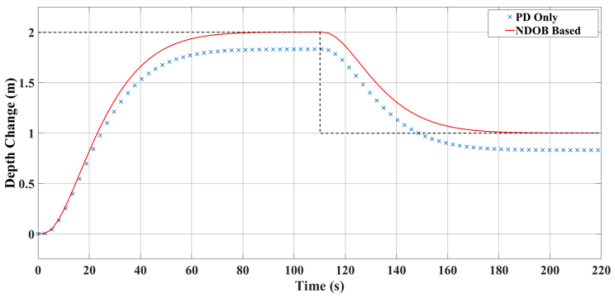

Figure 114. Depth responses of different control schemes (adapted from Bi and Feng, 2019).

Bi and Feng (2019) proposed a composite hovering control scheme to improve the disturbance rejection performance of under-water vehicles via variable ballast systems (VBSs). Simulation results showed that the NDOB based composite hovering control system exhibits more desirable performance in disturbance rejection than a conventional PD control system.

Trajectory Tracking is the most studied subject in UV control. Trajectory tracking requires a vehicle to track a time-parameterized reference trajectory, which means the vehicle needs to reach the specified position at the specified time. Al Makdah et al. (2019) developed trajectory tracking controller based on a 6-DOF nonlinear kinematic and dynamic model for a Hybrid Autonomous Underwater Vehicle. In the developed controller, a time-varying linear quadratic regulator is designed and applied to the nonlinear model of AUV to track the trajectory ensuring minimal tracking error and energy consumption in the thrust mode and gliding mode. Yan J. et al. (2019) studied a tracking control problem for a remotely operated vehicle (ROV) in the presence of time delay and actuator saturation constraints. A model-free PD controller is designed to enforce the position tracking and the domain of attraction (DOA) is estimated and optimized by using linear matrix inequalities (LMIs) to guarantee the tracking stability.

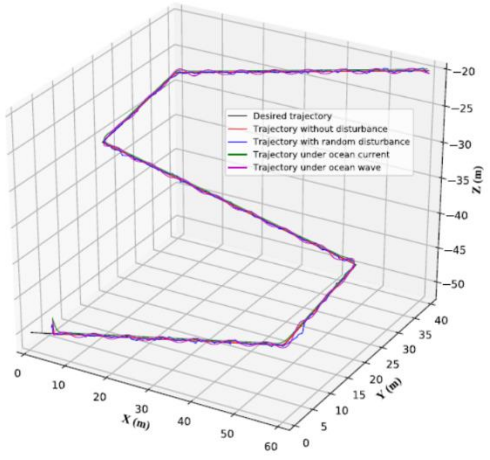

Figure 115. 3-D trajectory tracking for raster scan task under different disturbances. (adapted from Zhang et al. (2019)).

Zhang Y. et al. (2019) studied a novel three-dimension (3-D) underwater trajectory tracking method for an autonomous underwater vehicle using model predictive control (MPC). In the research, the trajectory tracking control is proposed as an optimization problem and then transformed into a standard convex quadratic programming (QP) problem. The optimal control inputs be recalculated at each sampling instant, which can improve the robustness of the tracking control under model uncertainties and time-varying disturbances. The simulation results are given to show the feasibility and robustness of the MPC-based underwater trajectory tracking algorithm (Figure 115).

Kumar & Rani (2020) proposed an efficient hybrid trajectory tracking control scheme for an AUV in the presence of structured and unstructured uncertainties. In the proposed scheme, the model-dependent control scheme is combined with the model-free control scheme to cope with the uncertainties. An adaptive compensator is also added to the part of the controller to compensate for the unknown external disturbances and the reconstruction error of the neural network.

Shojaei & Dolatshahi (2017) studied a line-of-sight target tracking control of AUVs with model uncertainties and environmental disturbances. Dynamic surface control, neural networks and adaptive control techniques are utilized to develop a target tracking controller and to compensate model uncertainties and environmental disturbances. Dai & Yu (2018) proposed an indirect adaptive control scheme to solve the trajectory tracking problem of the underwater vehicle and manipulator system (UVMS) in the presence of dynamic uncertainties and time-varying external disturbances. They proposed an indirect adaptive control scheme which consists of three parts: an extended Kalman filter (EKF) estimation compensative system, a model-based computed torque controller (CTC), a H_∞ robust compensative tracking controller. Simulation results show that the proposed control scheme can provide a better tracking performance than

traditional methods. Wadi et al. (2019) proposed a novel adaptive Nussbaum-function-based controller to solve the trajectory tracking problem for an underactuated AUV. In the proposed controller, high- and low-level controllers are synthesized to guide the vehicle to its set trajectory, and a novel adaptation law tunes the gains of kinematic and dynamic controllers so that the AUV can safely track the desired trajectory. Xu R. et al. (2019) studied the trajectory tracking problem of an underwater vehicle based on control moment gyros (CMGs) in the three-dimensional (3D) space. In the proposed controller, the tracking errors are converged to zero and the error dynamics are stabilized by introducing virtual control laws. Anti-windup compensators are taken in order to deal with the problem of input saturation and then back-stepping methods are exploited to construct the dynamic controller. Finally, the constrained steering law is utilized to achieve the actual control input for the CMG system. Zhou et al. (2018) proposed a method of integrating bio-inspired models and the back-stepping technique to carry out 3D trajectory tracking control for an underactuated AUV with constant external disturbances. A bio-inspired model which is based on the biological neuron system is adopted to express surge velocity error and angular velocity error and is used to design dynamic velocity regulation controller for a three-dimensional trajectory tracking. Wang J. et al. (2019b) presented a nonlinear robust control scheme based on the command filtered backstepping method for the three-dimensional trajectory tracking control problem of an AUV. The effectiveness and good robustness of the proposed tracking controller were illustrated by comparative simulations.

Elmokadem et al. (2017) developed a terminal sliding mode control scheme to solve the trajectory tracking problem of AUVs in the horizontal plane. The obtained simulation results indicated that the proposed control schemes work well for the trajectory tracking of AUVs moving in the horizontal plane and has a robustness against bounded disturbances. Yan Z. et al. (2019a) studied an adaptive sliding mode controller for the trajectory tracking control of underactuated AUVs in 5-DOF (exclusion of roll), where the vehicle dynamics are unknown and also subject to environmental disturbances. In the research, the dual closed-loop control is designed to achieve the trajectory tracking and a novel direct adaptive neural network controller, combined with a conditional integrator, is designed to provide the robustness and adaptation for underactuated AUVs. Yu H. et al. (2019) studied a spatial trajectory-tracking control for underactuated unmanned underwater vehicles (UUVs) in the presence of model parameter perturbation and unknown ocean currents. In the research, the spatial trajectory-tracking guidance, based on the dynamic virtual vehicle method, is proposed to compute the desired motion states of an UUV for trajectory tracking. The globally finite-time control strategy based on the PID sliding mode control is also proposed to globally stabilize all tracking errors in the finite time. Karkoub et al. (2017) designed a hierarchical robust nonlinear (HRN) controller for the trajectory tracking of an AUV with disturbances and system uncertainties. In the proposed controller, the virtual reference input is designed based on a kinematic model using the backstepping control technique and then a sliding-mode controller is designed to achieve control of the planned virtual reference input. Gao et al. (2017) proposed a hybrid visual servo (HVS) controller for the tracking control of underwater vehicles with various motion sensors. A dynamic inversion-based sliding mode adaptive neural network control (DI-SMANNC) method is developed to track the HVS reference trajectory and a single hidden-layer (SHL) feedforward neural network is used to compensate for dynamic uncertainties.

Ferreira et al. (2018) presented multivariable control strategies, based on a backstepping methodology and a Control Lyapunov Function (CLF) for the trajectory tracking problem of a Hybrid ROV. The proposed control responded appropriately to the trajectories selected as reference and presents robustness for unmodelled external disturbances. Chen J.W. et al. (2018) proposed a path tracking method based on a line-of-sight method and designed a fuzzy controller based on the fuzzy control algorithm for underwater robots. Results show that the path control method, based on the fuzzy controller optimized by the genetic algorithm, ensures that the vehicle sails along the expected path. Guerrero et al. (2019) presented an adaptive high order sliding mode controller for trajectory tracking of underwater vehicles. The robustness of the controller in depth and yaw dynamics was demonstrated through real-time experiments. An et al. (2020) proposed a modified proximate time-optimal control (PTOC) based on a reduced order extended state observer (RESO) and a controller scaling method. First, a simple and practical modified ADRC is proposed for heading control with input nonlinearities. Then, a parameter self-tuning strategy is proposed for the feedback controller with the control gain changed by the controller scaling method. Finally, the modified PTOC, based on RESO and with an updating strategy for the limit of linear region, was proposed to improve the control performance.

Xia Y. et al. (2020) addressed the trajectory tracking problem of a X-rudder AUV in vertical plane subjects to velocity sensor failure and uncertainties. An optimal robust trajectory tracking controller was developed based on linear velocity observers, a LOS based back-stepping kinematics controller, a robust disturbance rejection dynamics controller, and a multi-objective optimal rudder allocator.

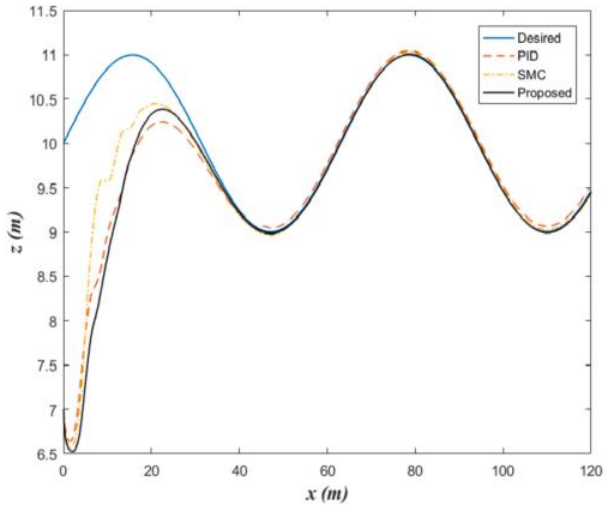

Figure 116. Trajectory tracking comparison (adapted from Xia Y. et al. 2020).

Collision avoidance is usually the research content of path planning, which is mainly to improve the safety of the UV and to reduce both energy consumption and navigation time. Lin Y.H. et al. (2018b) integrated a PSO (Particle Swarm Optimization) − based dynamic routing algorithm, a self-tuning fuzzy controller, a stereo-vision detection technique and a 6-DOF mathematical model into the inspection system of an AUV. The result verified that the MOPSO-based dynamic routing algorithm in the system of the AUV is not only able to estimate the feasible routes intelligently, but also to identify features of underwater structures for the purpose of positioning. Albarakati et al. (2019) developed a 3D trajectory planning framework that can account for multiple static obstacles and the ocean state, as provided by an Ocean General Circulation Model (OGCM) simulation or forecast. The efficiency of the model was demonstrated by the optimal time trajectory planning of an AUV operating in the Red Sea and Gulf of Aden. Zhuang et al. (2019) presented a two-stage cooperative path planner for multiple AUVs operating in a dynamic environment. A novel, Legendre pseudo spectral method based, cooperative path planner was proposed that works offline and online. The simulation results show that the proposed path

planner is capable to react quickly to a dynamic ocean environment, and to avoid the collisions successfully and efficiently.

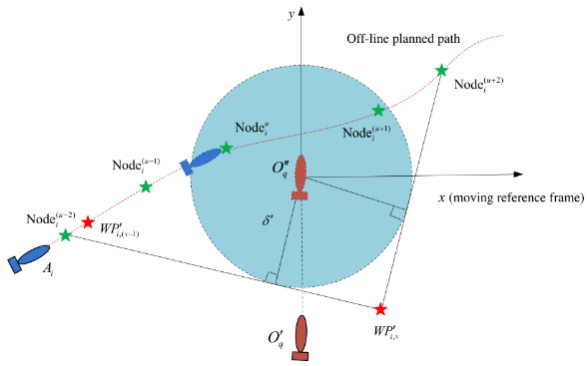

Figure 117. Template for the collision resolution. (adapted from Zhuang et al., 2019)

Li Y. et al. (2017) presented an AUV optimal path planning method for seabed terrain matching navigation, namely to avoid some of these areas and to solve the problem of existing methods of terrain matching having low precision in areas with small eigenvalues. This method builds a field map and value map that represent obstacle and matching performance, respectively, and a planning algorithm, which includes a dynamic matching algorithm, a cost function, a search length and a min length, a second-goal point and a dynamic path planning algorithm, based on a star algorithm. The simulation results show the proposed method is feasible.

Li J.H. et al. (2019) presented the autonomous swimming technology developed for an AUV operating in the environment of an underwater jacket structure. To prevent the position divergence of the inertial navigation system constructed for the primary navigation solution for the vehicle, a sonar image processing based underwater localization method was developed. According to an Occupancy Grid Map (OGM) based path planning algorithm, an obstacle collision-free reference path was derived. Wang D. et al. (2020) investigated an obstacle avoidance strategy for a wave glider in a marine environment. Aiming at dynamic obstacle avoidance for the wave glider, a collision prediction model (CPM) and an improved artificial potential field (IAPF) based fusion algorithm (CPM-IAPF) was developed. The simulation results show that the wave glider can accomplish the obstacle avoidance task with the proposed algorithm when facing different dynamic obstacles in marine environments.

Formation Control and Docking Control. The formation control is a fundamental problem of multiple-UV cooperation and is getting more important due to the expansion of the role of USV. Fabiani et al. (2018) proposed a general framework to manage a team of AUVs, while keeping the communication constraints, during mission execution. In the proposed framework, a virtual spring-damper coupling is utilized to define the distributed interaction forces between neighbouring vehicles. The passivity theory is applied to ensure stable convergence of the network vehicles to an equilibrium point and to provide robustness in presence of communication fading and delays. Moreover, the potential Bilateral Symmetric Interaction (BSI) game theory is adopted to maintain desired communication performance and fulfil each agent task.

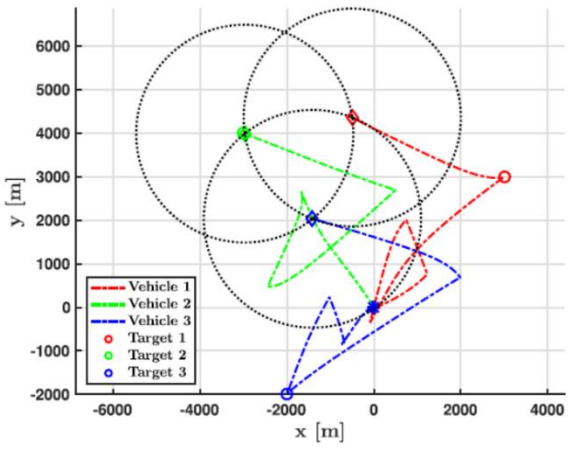

Figure 118. Cooperative exploration task of a AUVs team. (adapted from Fabiani et al., 2018)

Li J. et al. (2019) developed a robust control scheme for time-varying formation of multiple underactuated AUVs with disturbances under input saturation. In the developed control scheme, firstly, the reference trajectory of the follower is defined using a body-fixed coordinate transformation based on the leader position and predetermined time-varying formation. The robust time-varying formation control law is designed so that the trajectory of the follower can track the reference trajectory while securing the formation of AUVs. The disturbance observer is also constructed to estimate unknown time-varying disturbances in the control system. Jia et al. (2019) proposed a novel distributed cooperative search strategy based on the initial target information for multiple underwater robots to reduce the average time of searching target and improve the search target probability. Yan Z. et al. (2019b) proposed coordinated control protocols with or without time delay for the coordination control problem of multiple AUVs under switching communication topologies based on discrete information. The coordination control protocols are designed for the cases of no time delay and time delay, and sufficient conditions for the consensus algorithm are analysed and given based on the matrix theory. Wang J. et al. (2020) investigated a neural adaptive formation control of leader-following AUVs with model uncertainties and external disturbances in 3D space. A filter-backstepping technique has been effectively utilized to design a formation tracking controller. Simulation results for a group of AUVs are provided to demonstrate the tracking performance of the designed formation controller. Chen Y. et al. (2020) introduced a control strategy for multiple AUVs to improve the cooperative operation ability in formation control, to cluster search operations and to minimize the likelihood of collisions and interference with teammates and obstacles in complex working conditions. The simulation results show that the proposed formation control and path planning strategies are suitable for complex, unknown underwater environments.

The docking control for autonomous docking is a basic, required ability for an AUV to reduce the need for frequent launch and recovery operations at the surface. Sans-Muntadas et al. (2019) proposed the use of a convolutional neural network (CNN) to guide and control an autonomous underwater vehicle into the entrance of a docking station by using mapping camera input. The CNN is trained to estimate the error between the actual vehicle heading and the desired vehicle heading that guides the vehicle into the docking station. After the training period, the camera input and the CNN are used to control the vehicle towards the docking station, achieving autonomous docking. Experimental tests show that the approach allows the vehicle to reliably perform a docking manoeuvre using only a camera as sensor.

Lin et al. (2019) developed a non-contact docking system for AUVs. The system includes both acoustic and optical navigation, underwater wireless communication, non-contact power transfer, and monitoring and controlling of the docking system. The reliability of the developed docking system was verified by sea trials at depths 50 m and 105 m. Trslic et al. (2020) studied an autonomous docking system of a ROV to both static and dynamic docking stations using visual based pose estimation techniques. The full system including the ROV automated navigational control was tested using a static docking station in the North Atlantic Ocean and the results were within the tolerances to allow multiple successful dockings.

6. CHALLENGES WITH RESPECT TO EXPERIMENTAL RESEARCH

6.1 Signal processing

Deformation of the measured signals during model tests or during full-scale tests may be induced by signal processing techniques, due to characteristics of e.g. filters, AD-conversion (time step, resolution). The 29th MC has studied this issue with the aim of improving the test quality for manoeuvring purposes. This section gives more information on these uncertainties.

AD-conversion. During model testing the measurements are still dominantly performed in an analogue way. The conversion from such an analogue signal to a digital signal is governed by a resolution or least significant bit (LSB), which is given by (with range typically the measured voltage):

$$\text{LSB} = \frac{\text{Range}}{2^{\text{bit}}}$$

For instance, the measurement range could be 20 volt. As the quantization is now mostly 16 bits or more, the AD-conversion only induces a negligible uncertainty. Care should be taken for converters which have a quantization below 16 bits.

The LSB uncertainty is mostly expressed as ± 0.5LSB.

Filtering. An analogue filter can be used to smooth a measured signal. There are a few reasons to do this:

- To have a better graphical representation of the signal, but at the same time this does not always improve the measurement accuracy;
- To remove high frequency noise (so-called blue noise, to be investigated in the frequency domain), which may deteriorate the signal to noise ratio of the low frequency manoeuvring components due to the "aliasing" effects;
- To condense oversampled signals, e.g. when applying a 1 kHz sampling rate.

Analogue low pass filters (or online filters) should be applied to smoothen the measured signal when unwanted harmful noise exists, but care is needed when applying this technique:

- The transfer function characteristics have to be known. In particular, the cut off frequency and the transition band are of importance, see Figure 119.
- Care should be taken that the governing manoeuvring (or PMM) frequency is on the low pass side of the transition band (no filtering of relevant frequency range).
- The filter is never perfectly real time and a time delay is therefore introduced.
- Even in the passing band, signal variations may occur due to gain differences which depend on the filter design, see Figure 119.
- Additional noise can be induced by the filter.
- Actual noise can be hidden by the filter and should be accounted for during the uncertainty propagation.

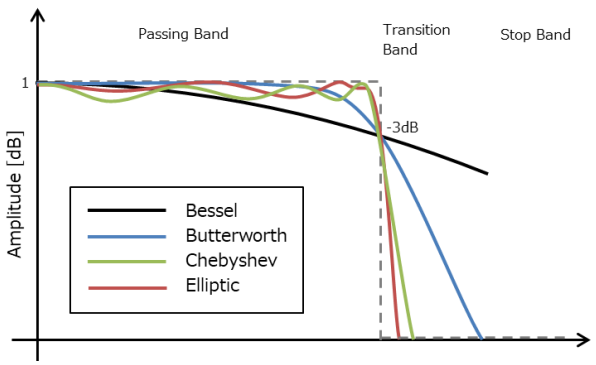

Figure 119. Amplitude response of an ideal filter and actual filters

For these reasons, applying a software filter (or offline filter) in post processing should be considered.

Mansuy et al. (2017) compared different filtering techniques applied to shallow water tests with the DTC. Although the aim was oriented towards the seakeeping tests, the outcome seems useful for harmonic PMM tests.

Time step. A sufficiently small time step (or a sufficiently large sampling rate) is required to capture all manoeuvring effects. In practice sampling rates between 10 Hz and 1000 Hz have been reported with 50 Hz and 100 Hz as most frequently used values. The sampling rate has to be at least twice the filter rate.

Propagation of noise uncertainty. Figure 120 shows a typical time trace of force measured by a dynamometer during captive model tests. During a PMM test, the force will also follow a harmonic trace, which is mostly analysed with Fourier harmonics up to the 3rd order (see the appendix of the 28th MC report). The question is then how this noise affects the different Fourier components. A dedicated study has been carried out by the 29th MC, which has been published by Delefortrie & Kishimoto (2019). In this report a summary is given.

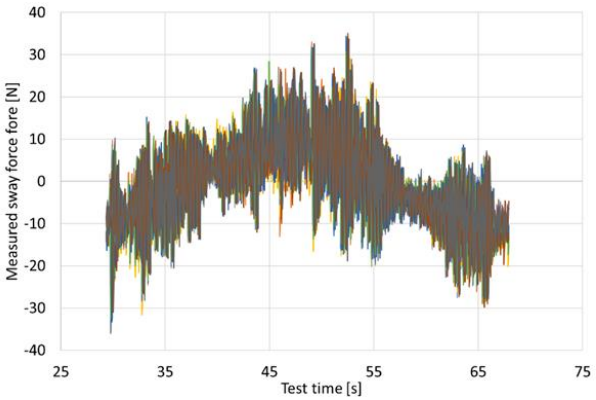

Figure 120. Measured sway force at the fore dynamometer during a captive harmonic yaw test with the KCS at 20% ukc, first cycle of 9 repetition tests (Delefortrie & Kishimoto, 2019).

This work extends the research carried out by Brouwer et al. (2019) for steady straight-line tests and is currently adopted by the ITTC as 7.5-02-01-06. Taking account of the assumption that the Fourier components represent the true signal, the difference between the time trace and true signal is attributable to noise.

Monte Carlo simulations have been performed based on a true signal supplemented with realistic Gaussian noise levels. Such synthetic signals were each subjected to a Fourier analysis and the resulting distribution of the harmonics was investigated, leading to the observation that the uncertainty in the higher harmonics is always $\sqrt{2}$ times the uncertainty of the mean value or 0th harmonic.

The uncertainty of the latter is dependent on the noise level. The application of analogue filters, however, lowers the noise level, and thus affects the outcome of the uncertainty analysis, without changing the physics behind it. For captive model tests, it seems more useful to apply filtering in post processing, however, if this is not feasible, it is recommended to multiply the obtained uncertainty with the frequency cut off ratio.

System identification techniques heavily rely on signal processing and are thus affected by the previously described uncertainties. Revestido Herrero et al. (2018) investigated an estimation efficiency when determining experimental coefficients on a 6-DOF non-linear manoeuvring model for underwater vehicles, and proposed a procedure that solves problems such as reduction in autocorrelation, elimination of heteroscedasticity and reduction of multicollinearity. They also assessed the effectiveness of the procedure by Monte Carlo studies. The methodology is considered to be applicable to other type of test data. Furthermore, Xu H. & Soares (2019) proposed another method, optimal truncated LS-SVM (Least Squared - Support Vector Machine) which has a low computational cost by reducing the dimensionality of the kernel matrix. This

method is a robust method for estimating coefficients, diminishing the uncertainty of the measured signal from captive model tests.

Another possible SI technique is the use of wavelets. An example of such approach is given by Todorova & Parvanova (2019), who apply the technique to a synthetic decaying signal to find the corresponding inertia and damping terms.

More complex applications can be found in the field of deep learning algorithms (Woo et al., 2018), which introduce artificial intelligence to increase the automation level of ships. In the present case the deep learning mechanism can couple e.g. yaw rates at times t and $t-1$ (referred to as LSTM or Long Short-Term Memory) rather than perceiving them as independent data as in a common feed forward neural network. In the SI process, a Savitsky-Golay filter (polynomial fitting) is used to differentiate the positions towards velocity. A simplified linear manoeuvring model of USV was identified by using the free running test data and the proposed model identification method. Simulation results show that the proposed dynamic model identification significantly outperforms conventional simplified manoeuvring models and the effectiveness of the proposed method is validated by comparing simulation results and free running test data.

Another way to cope with nonlinearities is the use of the so-called LWL or locally weighted learning, which approximates the nonlinear function by segmented linear functions. An example of this application is given by Bai W. et al. (2018).

Wang Z.H. and Zou (2018) assessed the degree of collinearity in ship manoeuvring identification modelling. A variance Inflation Factor (VIF) was applied to quantify and analyse the collinearity with different model structures and training samples. The results showed the hybrid approach was capable to predict the trajectory of ships in typical manoeuvring tests. Their results showed that quantifying collinearity was meaningful before modelling by the identification algorithm. It can be applied to evaluate the rationality of selected model structure and training sample, and it can also be combined with model selection and optimization design algorithms, which is a good way to help deal with parameter drift issues and build accurate mathematical models. This approach has been enhanced by Wang Z. et al. (2020a). They proposed a nonparametric identification method based on ν (‘nu’)-support vector regression, which can establish robust models of ship manoeuvring motion without prior model structure. This method avoids high dimensionality when solving matrices and provides powerful modeling capabilities with high computation efficiency. In addition, the principle of structural risk minimization allows a balance between approximation accuracy and model complexity, which minimizes overfitting.

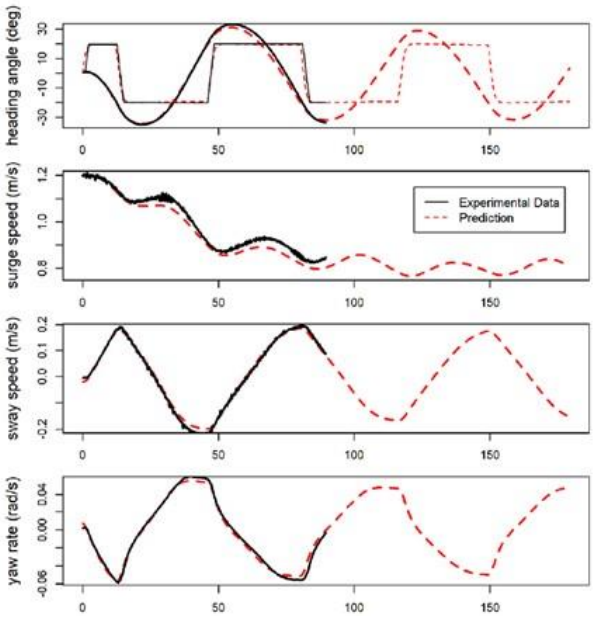

Figure 121. Comparison of predicted manoeuvre with experiment (Wang Z. et al., 2020a).

Wang Z. et al. (2020b) also proposed an optimal design scheme of excitation signal (i.e. steering) to determine the training data that can provide the maximum dynamic information which can improve the stability and accuracy of the identification of ship manoeuvring models. They demonstrated that the optimized training data had significant effects on improving the performance of the identified model.

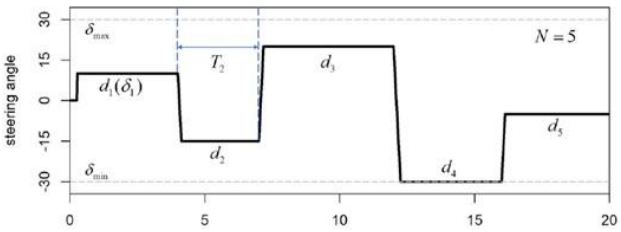

Figure 122. Excitation signal in time domain (Wang Z. et al., 2020b).

Sensitivity studies are a useful method to analyse the uncertainties not only induced by noise or filtering, but also due to other causes. Gavrilin and Steen (2018) performed a sensitivity analysis on the coefficients of the MMG model. They revealed that steering and interaction coefficients significantly affect the results of simulation. Through identification of those coefficients from full-scale trials, they found that different combinations of the coefficients results in similar time-series, and clarified the presence of correlation between the coefficients and showed its difficulties to solve the scale effect problem.

Giles et al. (2018) conducted a frequency domain based analysis of a submarine manoeuvring model, and investigated the effects on the sensitivity and the stability of the coefficients used in the model. They clarified that a more simplified manoeuvring model was obtained by reducing insensitive coefficients and excluding insignificant modes of motion.

Sensitivity studies are considered to be applicable not only for uncertainty analyses but also for initial conceptual design for various vehicles. Jeon et al. (2018) performed sensitivity analyses for a torpedo shape under-water vehicle taking into account the geometric parameters for the bare hull and the rudder. Through those analyses, they specified sensitive geometric parameters which significantly affect the dynamic characteristics and suggested a procedure to determine the configuration of the vehicle which satisfies required performance.

6.2 Shallow water testing

Recently, several towing tanks are equipped with a false bottom to enable model tests in shallow water conditions. For large size towing tanks, primarily aiming at model tests in deep water, the size of the false bottoms is generally limited and the towing tank is only partially covered: the length and the breadth of the false bottom are smaller than the length and the breadth of the towing tank. In this section, the uncertainties with respect to the false bottom are discussed based on recent published literature.

Li M. et al. (2019) investigated the error caused by such imperfection of the false bottom on the realization of the shallow water conditions. They applied the boundary element method (BEM) based on the potential theory, and quantified the false bottom effect on the wave making coefficient C_W as function of the depth to draft ratio (H/D), the false bottom breadth to tank breadth ratio (Bd/Bt) and Froude number (Fr). The y_{infl} formula seems appropriate to determine the necessary width of the false bottom.

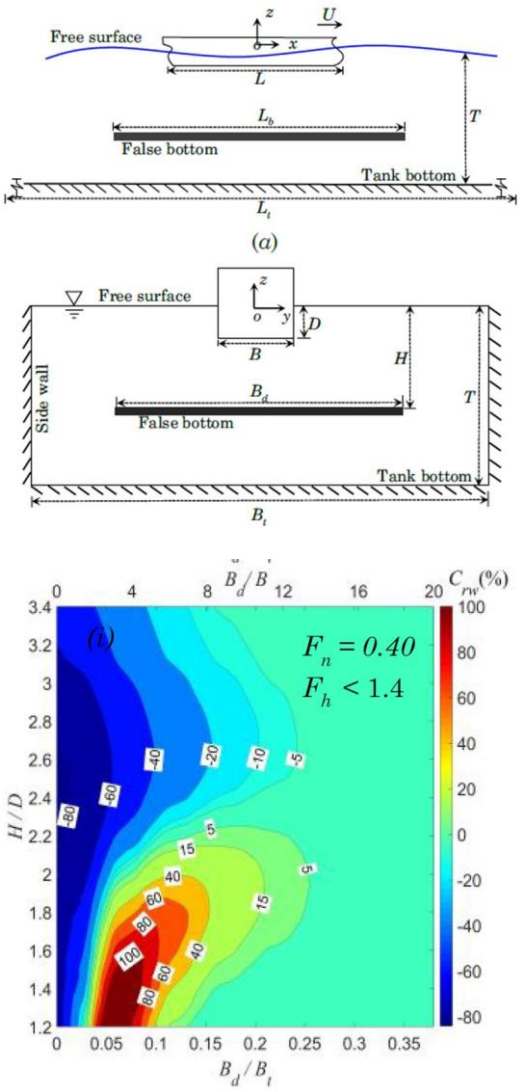

Figure 123: Sketch of tank equipped with false bottom and error coefficient Crw as function of H/D and Bd /Bt (Li M. et al., 2019)

Liu H. et al. (2018b) used the false bottom facility of the circulating water channel of Shanghai Jiaotong University to perform ship-bank interaction tests with KVLCC2 at scale 1/128.8. No details are provided on the setup of this false bottom. The novel content is rather the application of uncertainty propagation methods to assess the uncertainty on the ship bank interaction forces based on the well-known Norrbin formulae. It seems that the uncertainty from the water depth has the major contribution in the total uncertainty, which confirms the importance of a well-designed false bottom.

6.3 Turbulence stimulation and scale effects

Questionnaire. In order to gain more insight in the issues concerning turbulence stimulation and scale effects, a new questionnaire has been sent out in March 2018 to the 32 institutes who participated in the 2015 questionnaire (see 28th MC) and who carry out manoeuvring tests. By the closure of the questionnaire in October 2018, 19 institutes responded or almost 60%.

The questionnaire had four main parts:

- measures taken to deal with scale effects prior or while executing tests;
- measures taken to deal with scale effects after executing tests;
- means of validating the test results;
- applications of turbulence stimulation.

Each part consisted of a number of statements with five possible agreements (not at all or 0% or -2, not really or 25% or -1, not applicable or 50% or 0, likely or 75% or +1 and certainly or 100% or +2). The average percentage of the answers gives then a resulting agreement percentage for a given statement. The integer values are used as short hand abscissa notations in the following histograms.

Scale effects. 77% is concerned with scale effects in the results of captive model tests. The 27th ITTC MC proposed an estimation scheme to deal with scale effects, which is known by 69%, but only (partially) used by 52%. Observe, that the questions were mainly organized according to that estimation scheme. In general scale effects are counteracted by selecting the ship model as large as possible (82% agree), but as visualised on Figure 124 the tank size is a first order limiting factor, followed by the carriage

possibilities and the available stock propeller's size.

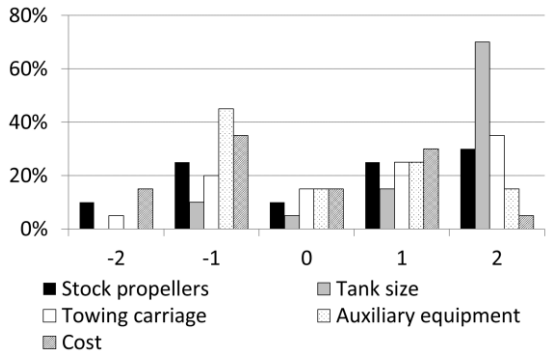

Figure 124. Factors limiting the maximal ship model size.

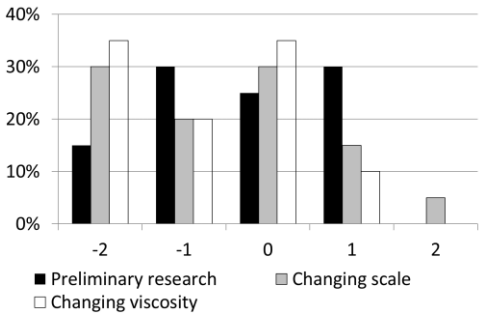

Figure 125. Preliminary numerical research.

Due to these limitations, turbulence stimulation is frequently applied (86%). A second mean to deal with scale effects is changing the propeller rate (58%). A limited number of institutes use auxiliary thrusters, but this seems more applicable for free running tests. A last alternative concerns preliminary numerical research (42%), which is not so common as the turbulence stimulation, see Figure 125. If preliminary numerical research is performed it is not necessarily aimed at scale effects. Only 4 institutes mentioned that they perform preliminary research at a different scale and 2 institutes investigate the effect of the Reynolds number.

The treatment of the test results for scale effects is mostly performed in longitudinal direction only, with the ITTC 1978 performance method being the first choice (74% agreement) and an equal share of more complex or simpler methods (Figure 126).

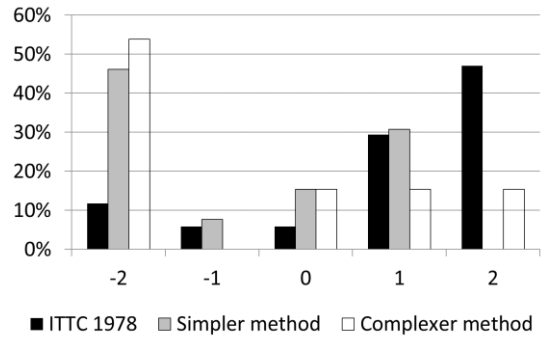

Figure 126. Means to correct for scale effects in longitudinal direction.

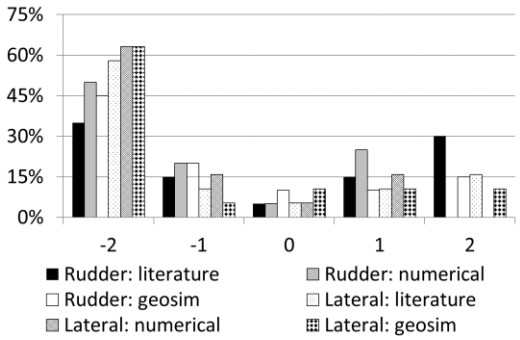

Figure 127. Means to correct for scale effects for manoeuvring forces.

In case of manoeuvring lateral forces and rudder forces play an important role, however, corrections for these components are less frequent (Figure 127). If corrections are used it is mostly for the rudder forces and the institutes rely on information available in literature.

The opinion of the MC is that scale effects will become more important with increasing drift angle (increasing viscous force) and with decreasing water depth. In the latter case, the return flow will play a dominant role and hence influence the frictional resistance. However, this

opinion is not generally accepted based on the responses to the questionnaire.

Validation of test results. Given the uncertainty connected with captive model tests, the institutes were asked how they validated their results. These results can either be validated directly, for instance by comparing them with free CFD trajectories or with other ships, or indirectly by deriving a mathematical model based on the results and check the agreement of simulated manoeuvres with the information on wheelhouse posters or by expert judgement, comparison with free running trajectories or even real time simulation runs. Figure 128 gives an overview of the responses to each method. The comparison with other (benchmark) ships is by far the preferred validation method (78%), followed by free running tests (63%) or expert judgement (62%). As can be seen on the graph, CFD is mostly validated by EFD and not the other way round and real-time simulations are not a frequent choice for most institutes. Either they do not have a real-time simulator and if they had one, the process is too complex to be used as a validation tool.

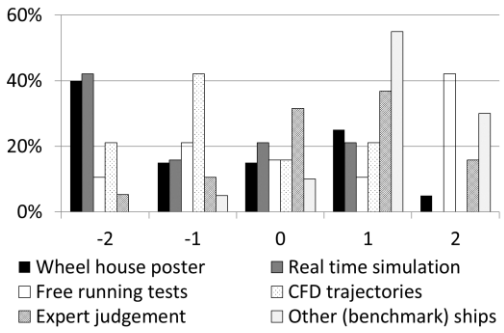

Figure 128. Ways to validate the results of captive manoeuvring tests.

Based on the validations, the results are tuned in 52% of the cases. This is mostly achieved by changing the rudder dependent coefficients as shown in Figure 129. As an alternative the rudder area itself of the simulated ship is changed in order to achieve the desired behaviour. As can be seen in Figure 130 tuning is mostly needed in shallow water conditions.

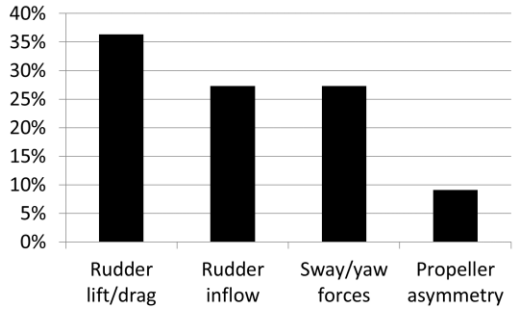

Figure 129. Components of the mathematical model that are tuned if necessary.

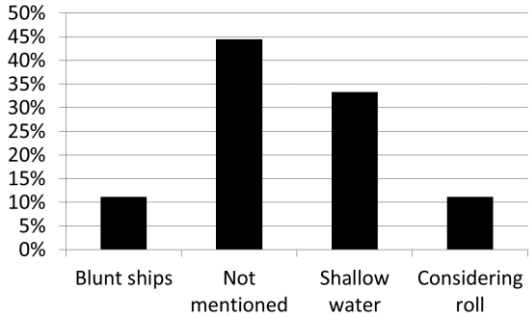

Figure 130. Conditions when tuning is mostly needed.

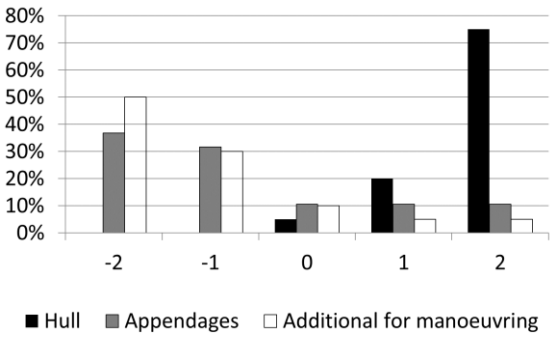

Figure 131. Use of turbulence stimulation.

Turbulence stimulation. Figure 131 shows that turbulence stimulation is almost only applied on the ship's hull and mainly based on the prescription for resistance tests. On the hull

79% uses studs and 21% uses sand strips and 92% does it according to the ITTC, while on the appendages the sand strips are the most popular choice (75%). The occasional additions for manoeuvring are mostly classified, although the bilge keels have been mentioned by some.

Literature review. No new references were found with respect to turbulence stimulation for manoeuvring purposes. A limited number of authors described scale effects in the field of manoeuvring. Araki (2018) performed research on scale effects for the manoeuvring behaviour of the KVLCC2. Geosim (scale 1/1 and 1/110) captive simulations with deflected rudder were carried out with the RANS solver of NMRI. The lift generation is less effective on model scale, unless the model scale self-propulsion point is used instead the ship self-propulsion point, which seems to confirm previous literature (see the report of the 27th MC).

In order to solve the scale effect problem, Suzuki et al. (2017), Ueno et al. (2017) and Suzuki et al. (2019) have been carrying ongoing investigations on free running model tests with auxiliary thrusters. They attempt predictions of full-scale ship performance in wind and wave disturbances taking into account the operational limit of main engine as well.

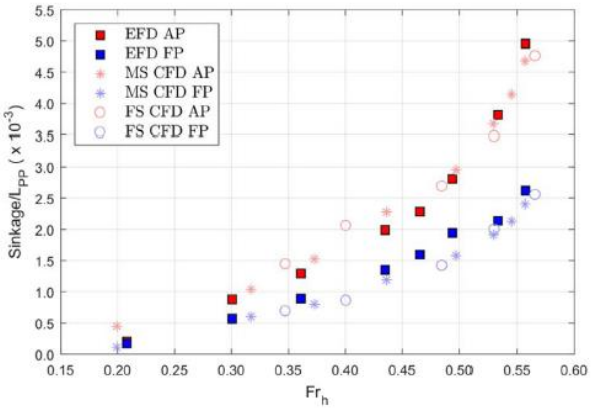

Figure 132 Comparison of model-scale and full-scale CFD AP and FP sinkage against that of the benchmark EFD at h/T = 1.23 (Kok et al., 2020)

Scale effects on squat in shallow water were investigated by Shevchuk et al. (2019). Squat computations were performed using an in house CFD package and focussing of geosim conditions of (post) Panamax container vessels. The scale effects become more dominant with decreasing water depth and lead to an under-prediction of up to 15% of the full-scale squat. This phenomenon can be counteracted by changing the hull's roughness; however, no general guideline could be derived. A similar research was conducted by Zhang H. et al. (2018) who studied scale effects with an in-house RANS code on a bare hull DTMB 5415. They only considered a deep water condition, but contrary to Shevchuk et al. (2019) the obtained heave and pitch motion were smaller on full-scale. The most recent research was performed by Kok et al. (2020), who studied scale effects of squat in confined environments with the DTC hull. Star-CCM+ RANS computations were used with a full-scale ship and a 1/40 model scale variant, including the propeller effect on squat. The latter was implemented with a body force model. The study revealed that the differences due to scale effects are smaller than 6%.

Based on the different conclusions the MC recommends that more extensive CFD research (covering various hull forms and a broad range of speeds and water depths) are needed to investigate this effect.

7. CONCLUSIONS

7.1 State of the Art

Deep Unrestricted Water. Recent research results focus on the topics of manoeuvring performance, unmanned surface vehicles and autopilot applications. Particularly for the latter too many articles have been published.

Manoeuvring performance studies are carried out using a variety of methods such as experimental methods, empirical methods, potential flow methods, RANS methods, and hybrid methods. Among these methods RANS simulation using commercial CFD software has become the most popular.

For unmanned surface vehicles (USV) or MASS (Maritime Autonomous Surface Ships), articles can be grouped according to a focus on path planning, trajectory tracking, collision avoidance, or formation control. In particular, many studies have been conducted on collision avoidance, which considers COLREGs and moving obstacles also artificial intelligent methods such as DRL (Deep Reinforcement Learning) or DNN (Deep Neural Network).

More advanced autopilot applications are being studied such as autopilots for berthing in restricted areas or for offshore operations. In particular, with the rapid development of machine learning techniques, studies on the application of machine learning based controllers and on the improvement of the existing autopilots by applying model predictive control, adaptive PID, neural network, etc., have been actively conducted.

Shallow, Restricted or Confined Water. As for deep water applications a raise in numerical research is noted. In most of these studies the free-surface effects, considering low-speed cases, are neglected. Another interesting trend is that there are more shallow water studies focusing on hull-rudder-propeller interaction, which benefit from flow visualization capabilities of CFD techniques.

For ship-bank interaction free surface effects are mostly considered. This should certainly be the case for very small under keel clearances and/or distances to the bank. RANS solvers outperform potential flow methods in the ship-bank problem.

Ship-lock and ship-ship interactions continue to be challenging problems in ship hydrodynamics. Although the RANS method has been successfully applied to predict the interaction forces, the potential flow method is still the most popular way to investigate the ship-ship interaction problem. The free surface effects in the ship-ship problem were quantified in some studies based on potential flow methods. There are still many research gaps in ship-lock interaction problem, e.g. the wave phenomenon in front of the ship. Further research is required to provide an accurate prediction of the hydrodynamics of a vessel when entering a lock.

Research trends. It is clear that USV is the research trend of the coming years. In general, the number of articles with respect to manoeuvring is booming, which has to be attributed to a vast number of papers dealing with numerical methods, which are cheaper to apply, compared to experimental research.

The downside of these numerical articles is that very few present experimental validation material to proof the applicability of the presented statements.

7.2 Procedures and Guidelines

The MC reviewed the procedures and guidelines under its responsibility. Major updates and improvements were made to:

- Validation of Manoeuvring Simulation Models (7.5-02-06-03)
- Uncertainty Analysis for Manoeuvring Predictions based on Captive Manoeuvring Tests (7.5-02-06-04)
- Captive Model Test Procedure (7.5-02-06-02).

The MC developed three new guidelines:

- UV Full Scale Manoeuvring Trials (7.5-04-02-02) provides an outline of underwater vehicle full-scale trials to determine their manoeuvring characteristics.
- Benchmark Data for Validation of Manoeuvring Predictions (7.5-02-06-06) highlights the processes relevant for benchmarking and provides a list of the present benchmark database available.
- Captive Model Test for Underwater Vehicles (7.5-02-06-07) outlines captive model tests for underwater vehicles to determine the hydrodynamic coefficients for a manoeuvring simulation model.

7.3 Benchmark Data

The third SIMMAN workshop has been postponed to late 2021. The workshop introduces new benchmark data, in particular in shallow water and in waves, to enable better comparisons and to extend the assessment of manoeuvring prediction capability.

All presently available benchmark datasets, including references, have been collected in the new guideline 7.5-02-06-06. The overview of the benchmark data shows that the main part of the available data concerns seagoing vessel types, which do not exist in full-scale. The database should be reinforced so that, in the future, datasets for full-scale variants of vessels, inland vessels and underwater vehicles are created/considered and added as well.

7.4 Underwater Vehicles

Manoeuvring hydrodynamics. A lot of attention has been devoted to methods adopted to evaluate or predict the UV characteristics. In recent years an increasing transition from experimental methods to numerical methods is observed, in particular for conditions that are beyond the spatial and instrumentation limits of conventional experimental testing facilities, or when there are multiple design or operation options. In certain research, such as strong transient or microlevel physics dependency and establishing benchmark data, experimental methods as the primary method prevail. Also noted is the combination of numerical and experimental methods to evaluate complex variables, having low measurement confidence in either methods when carried out individually.

Manoeuvring control. Increasing research in control systems, for the purpose of path following, trajectory tracking, collision avoidance, formation control and docking, is noted. Control systems are indispensable to achieving the operation purpose of underwater vehicles. The advancements in control system research provide a key indicator for measuring the state of UV manoeuvring and technologies.

7.5 Challenges with Experimental Research

Signal processing. The propagation of noise and the effect of filters has been investigated. Noise as such is mostly neglected, which is acceptable for sufficiently long measurements and a uniformly distributed noise in terms of frequency. The procedure 7.5-02-01-06 can also be used for manoeuvring tests, provided that the uncertainty of the mean propagates with a factor $\sqrt{2}$ in the higher order harmonics. A minimum necessary filtering is advised when performing measurements.

Shallow water testing. The MC conducted a literature search concerning the effects on the measurements induced by imperfections of a false bottom, including side-wall interaction. The uncertainty from the water depth has the major contribution in the total uncertainty,

which confirms the importance of a well-designed false bottom.

Turbulence stimulation and scale effects. A questionnaire has been distributed to ITTC members. Almost 8/10 are concerned with scale effects for manoeuvring. These tend to be more important with increasing drift and decreasing water depth. The latter is also confirmed by literature, although not much was published lately in this field. Means to counteract scale effects include extra turbulence stimulation, but details on this seem classified. Tuning of manoeuvring coefficients is common, especially in shallow water conditions.

8. RECOMMENDATIONS

Study the potential impact of Unmanned Surface Vehicles (or Autonomous Navigation) to the Manoeuvring Committee:

- the state of the art of autopilots, with proven applicability in a tank environment or at full-scale;
- the state of the art of artificial intelligence.

Support SIMMAN with the post processing and analysis of the results of SIMMAN 2021.

Continue the work with (autonomous) underwater vehicles towards completion of the guidelines:

- draft a guideline on the validation of UV models for manoeuvring purposes;
- extend the AUV full-scale trials guideline to consider submarines and ROV as well.

Support the creation of benchmark data, specifically for:

- (autonomous) under water vehicles;
- inland navigation, including pushed or towed convoys;
- model scale vessels with a documented full-scale variant.

Expand the full-scale manoeuvring trials procedure to account for the measurement of any kind of full-scale manoeuvre as a supplement to (virtual) tank tests.

Maintain the attention on scale effects and the effect of tank blockage on the interpretation of results, by stimulating geosim research.

Continue the update of the captive model test procedure, with specific attention to the treatment of amplitudes, frequencies and inertial coefficients as recommended by SIMMAN.

Update the captive model uncertainty procedure, to have a single integrated example, based on the SIMMAN results (2021), instead of different appendices.

Investigate the effect of novel manoeuvring devices and clean fuel technologies on the manoeuvrability.

The Manoeuvring Committee recommends to the Full Conference to adopt the updates to the procedures and the newly created guidelines.

9. REFERENCES

Abdurahman, B., Savvaris, A. and Tsourdos, A., 2019, "Switching LOS Guidance with Speed Allocation and Vertical Course Control for Path-Following of Unmanned Underwater Vehicles under Ocean Current Disturbances", Ocean Engineering, Vol. 182, pp. 412–426.

Ahmed, Y. A., Hannan, M. A. and Siang, K. H., 2020, "Artificial Neural Network Controller for Automatic Ship Berthing: Challenges and Opportunities", Marine Systems and Ocean Technology, Vol. 15, No.4, pp. 217–242.

Al Makdah, A. A. R., Daher, N., Asmar, D. and Shammas, E., 2019, "Three-Dimensional Trajectory Tracking of a Hybrid Autonomous Underwater Vehicle in the Presence of Underwater Current", Ocean Engineering, Vol. 185, pp. 115–132.

Albarakati, S., Lima, R. M., Giraldi, L., Hoteit, I. and Knio, O., 2019, "Optimal 3D Trajectory Planning for AUVs Using Ocean General Circulation Models", Ocean Engineering, Vol. 188, pp. 1–15.

Amendola, J., Tannuri, E. A., Cozman, F. G. and Reali Costa, A. H., 2019, "Port Channel Navigation Subjected to Environmental Conditions Using Reinforcement Learning", OMAE2019, Glasgow, Scotland, UK, pp. 1–10.

Amendola, J., Miura, L. S., Costa, A. H. R., Cozman, F. G. and Tannuri, E. A., 2020, "Navigation in Restricted Channels under Environmental Conditions: Fast-Time Simulation by Asynchronous Deep Reinforcement Learning", IEEE Access, Vol. 8, pp. 149199–149213.

Amiri, M. M., Esperança, P. T., Vitola, M. A. and Sphaier, S. H., 2020, "An Initial Evaluation of the Free Surface Effect on the Maneuverability of Underwater Vehicles", Ocean Engineering, Vol. 196, pp. 1–22.

An, L., Li, Y., Cao, J., Jiang, Y., He, J. and Wu, H., 2020, "Proximate Time Optimal for the Heading Control of Underactuated Autonomous Underwater Vehicle with Input Non-linearities", Applied Ocean Research, Vol. 95, July 2019.

Araki, M., 2018, "Scale Effects on Ship Maneuverability Using RANS", OMAE2018, Madrid, Spain, pp. 1–7.

Aydın, Ç., Ünal, U. O., Karabulut, U. C. and Sarıöz, K., 2018, "Practical Computational Procedures for Predicting Steering and Braking Forces of Escort Tugs", Ocean Engineering, Vol. 166, pp. 159–171.

Bai, W., Ren, J., Zhang, X. and Sun, X., 2018, "Locally Weighted Learning Identification Modeling for Ship Maneuvering Motion with Reduced Computational Complexity", MARSIM 2018, Halifax, Canada.

Barrera, R. D. and Tannuri, E. A., 2018, "Offline Vector Tugs Actuation Model (an Efficiency Analysis of Towage Forces During Pull Operations)", MARSIM 2018, Halifax, Canada, pp. 1–14.

Bechthold, J. and Kastens, M., 2020, "Robustness and Quality of Squat Predictions in Extreme Shallow Water Conditions Based on RANS-Calculations", Ocean Engineering, Vol. 197, pp. 1–12.

Bi, A. and Feng, Z., 2019, "Composite Hovering Control of Underwater Vehicles via Variable Ballast Systems", Journal of Marine Science

and Technology, Vol. 25, No.3, pp. 659–666.

Bonci, M., Jong, P., Van Walree, F., Renilson, M., Keuning, L. and Huijsmans, R., 2017, "Experimental and Numerical Investigation on the Heel and Drift Induced Hydrodynamic Loads of a High Speed Craft", FAST 2017, Nantes, France, pp. 209–218.

Brouwer, J., Tukker, J., Klinkenberg, Y. and van Rijsbergen, M., 2019, "Random Uncertainty of Statistical Moments in Testing: Mean", Ocean Engineering, Vol. 182, pp. 563–576.

Calcagni, D., Salvatore, F., Dubbioso, G. and Muscari, R., 2017, "A Generalised Unsteady Hybrid DES/BEM Methodology Applied to Propeller-Rudder Flow Simulation", MARINE 2017, pp. 377–392.

Carchen, A., Turkmen, S., Piaggio, B., Shi, W., Sasaki, N. and Atlar, M., 2021, "Investigation of the Manoeuvrability Characteristics of a Gate Rudder System Using Numerical, Experimental, and Full-Scale Techniques", Applied Ocean Research, Vol. 106, 102419 .

Carstensen, B., 2019, "Calculation of Rudder Forces in the Design Process Using a Panel Method with a Lifting Line Approach for Wake Alignment", PRADS 2019, Yokohama, Japan, pp. 1–14.

Chen, C., Chen, X. Q., Ma, F., Zeng, X. J. and Wang, J., 2019, "A Knowledge-Free Path Planning Approach for Smart Ships Based on Reinforcement Learning", Ocean Engineering, Vol. 189, pp. 1–9.

Chen, C., Delefortrie, G. and Lataire, E., 2020, "Experimental Investigation of Practical Autopilots for Maritime Autonomous Surface Ships in Shallow Water", Ocean Engineering, Vol. 218, pp. 1–21.

Chen, J., Zou, Z.-J., Chen, X., Xia, L. and Zou, L., 2017, "CFD-Based Simulation of the Flow around a Ship in Turning Motion at Low Speed", Journal of Marine Science and Technology, Vol. 22, No.4, pp. 784–796.

Chen, J. W., Zhu, H., Zhang, L. and Sun, Y., 2018, "Research on Fuzzy Control of Path Tracking for Underwater Vehicle Based on Genetic Algorithm Optimization", Ocean Engineering, Vol. 156, pp. 217–223.

Chen, Y. L., Ma, X. W., Bai, G. Q., Sha, Y. and Liu, J., 2020, "Multi-Autonomous Underwater Vehicle Formation Control and Cluster Search Using a Fusion Control Strategy at Complex Underwater Environment", Ocean Engineering, Vol. 216, pp. 1–13.

Crossland, P., 2017, "Slow Speed Depth Control of a Submarine under Waves", PACIFIC 2017, Sydney, Australia.

Dai, Y. and Yu, S., 2018, "Design of an Indirect Adaptive Controller for the Trajectory Tracking of UVMS", Ocean Engineering, Vol. 151, pp. 234–245.

Dashtimanesh, A., Enshaei, H. and Tavakoli, S., 2019, "Oblique-Asymmetric 2D1T Model to Compute Hydrodynamic Forces and Moments in Coupled Sway, Roll, and Yaw Motions of Planing Hulls", Journal of Ship Research, Vol. 63, No.3, pp. 1–15.

Delefortrie, G., Tello Ruiz, M. and Vantorre, M., 2018, "Manoeuvring Model of an Estu-ary Container Vessel with Two Interacting Z-Drives", Journal of Marine Science and Technology, Vol. 23, No.4, pp. 739–753.

Delefortrie, G., Geerts, S., Lataire, E., Troch, P. and Monbaliu, J., 2019, "Coastal and Ocean Basin and Towing Tank for Manoeuvres in Shallow Water at Flanders Maritime Laboratory", AMT 19, Rome, Italy.

Delefortrie, G. and Kishimoto, T., 2019, "The Uncertainty Induced by Noise and Filtering on the Results of Captive PMM Tests", AMT 19, Rome, Italy.

Deng, Y., Zhang, X., Im, N., Zhang, G. and Zhang, Q., 2019, "Event-Triggered Robust Fuzzy Path Following Control for Underactuated Ships with Input Saturation", Ocean Engineering, Vol. 186, pp. 1–10.

Desai, M., Gokhale, R., Halder, A., Benedict, M. and Lu, Y., 2020, "Augmenting Maneuverability of UUVs with Cycloidal Propellers", 33rd ONR Symposium, Osaka, Japan, pp. 18–23.

Dubbioso, G., Muscari, R., Ortolani, F. and Di Mascio, A., 2017a, "Analysis of Propeller Bearing Loads by CFD. Part I: Straight Ahead and Steady Turning Maneuvers", Ocean Engineering, Vol. 130, pp. 241–259.

Dubbioso, G., Broglia, R. and Zaghi, S., 2017b, "CFD Analysis of Turning Abilities of a Submarine Model", Ocean Engineering, Vol. 129, pp. 459–479.

Duman, S. and Bal, S., 2019, "Prediction of Maneuvering Coefficients of Delft Catamaran 372 Hull Form", IMAM 2019, Varna, Bulgaria, pp. 167–174.

Ellis, C. L., Clarke, D. B., Butler, D. and Brandner, P., 2018, "Investigation of a Canonical All-Movable Control Surface in Thickened Boundary Layers", AFMC 2018, Adelaide, Australia, pp. 1–4.

Elmokadem, T., Zribi, M. and Youcef-Toumi, K., 2017, "Terminal Sliding Mode Control for the Trajectory Tracking of Under-actuated Autonomous Underwater Vehicles", Ocean Engineering, Vol. 129, pp. 613–625.

Eriksen, B. O. H. and Breivik, M., 2018, "A Model-Based Speed and Course Controller for High-Speed ASVs", CAMS 2018, Opatija, Croatia, pp. 317–322.

Esfahani, H. N., Szlapczynski, R. and Ghaemi, H., 2019, "High Performance Super-Twisting Sliding Mode Control for a Maritime Autonomous Surface Ship (MASS) Using ADP-Based Adaptive Gains and Time Delay Estimation", Ocean Engineering, Vol. 191, pp. 1–19.

Fabiani, F., Fenucci, D. and Caiti, A., 2018, "A Distributed Passivity Approach to AUV Teams Control in Cooperating Potential Games", Ocean Engineering, Vol. 157, pp. 152–163.

Ferrari, V., Gornicz, T., Kisjes, A. and Quadvlieg, F., 2019, "Influence of Skeg on Ship Manoeuvrability at High and Low Speeds", PRADS 2019, Yokohama, Japan, pp. 1–20.

Ferreira, C. Z., Cardoso, R., Meza, M. E. M. and Ávila, J. P. J., 2018, "Controlling Tracking Trajectory of a Robotic Vehicle for Inspection of Underwater Structures", Ocean Engineering, Vol. 149, pp. 373–382.

Figari, M., Martinelli, L., Piaggio, B., Enoizi, L., Viviani, M. and Villa, D., 2020, "An All-Round Design-to-Simulation Approach of a New Z-Drive Escort Tug Class", Journal of Offshore Mechanics and Arctic Engineering, Vol. 142, No.3, pp. 1–12.

Gao, J., An, X., Proctor, A. and Bradley, C., 2017, "Sliding Mode Adaptive Neural Network Control for Hybrid Visual Servoing of Underwater Vehicles", Ocean Engineering, Vol. 142, pp. 666–675.

Gatin, I., Vukcevic, V., Jasak, H. and Lalovic, I., 2018, "Manoeuvring Simulations Using the Overset Grid Technology in Foam-Extend", 32nd ONR symposium, Hamburg, Germany.

Gavrilin, S. and Steen, S., 2018, "Global Sensitivity Analysis and Repeated Identification of a Modular Maneuvering Model of a Passenger Ferry", Applied Ocean Research, Vol. 74, pp. 1–10.

Giles, S. and Valentinis, F., 2018, "A Frequency Domain - Based Sensitivity Study of a Submarine Manoeuvring Model", Journal of Ship Research, Vol. 62, No.4, pp. 183–199.

Go, G. and Ahn, H. T., 2019, "Hydrodynamic Derivative Determination Based on CFD and Motion Simulation for a Tow-Fish", Applied Ocean Research, Vol. 82, pp. 191–209.

Gornicz, T. M., Ferrari, V. and Toxopeus, S. L., 2019, "Estimating Berthing Performance of Twin Shaft Ship by Means of CFD", PRADS 2019 , Yokohama, Japan, pp. 1–20.

Gu, N., Wang, D., Peng, Z. and Liu, L., 2019, "Distributed Containment Maneuvering of Uncertain Under-Actuated Unmanned Surface Vehicles Guided by Multiple Virtual Leaders with a Formation", Ocean Engineering, Vol. 187, pp. 1–10.

Gu, N., Peng, Z., Wang, D., Liu, L. and Jiang, Y., 2020, "Nonlinear Observer Design for a Robotic Unmanned Surface Vehicle with Experiment Results", Applied Ocean Research, Vol. 95, pp. 1–7.

Gupta, D. K., Vasudev, K. L. and Bhatta-charyya, S. K., 2018, "Genetic Algorithm Optimization Based Nonlinear Ship Maneuvering Control", Applied Ocean Research, Vol. 74, pp. 142–153.

Guerrero, J., Torres, J., Creuze, V. and Chemori, A., 2019, "Trajectory Tracking for Autonomous Underwater Vehicle: An Adaptive Approach", Ocean Engineering, Vol. 172, pp. 511–522.

Ha, J. H. and Gourlay, T., 2018, "Validation of Container Ship Squat Modeling Using Full-Scale Trials at the Port of Fremantle", Journal of Waterway, Port, Coastal, and Ocean Engineering, Vol. 144, No.1, pp. 1–18.

Harkin, A., Harkin, J., Suhr, J., Tree, M., Hibberd, W. and Mortensen, S., 2018, "Validation of a 3D Underkeel Clearance Model with Full Scale Measurements", PIANC World Congress , Panama City, pp. 1–20.

Harwood, C., Martin, J. E., Di Napoli, I., Arnold, A. and Carrica, P., 2018, "Experimental and Numerical Investigation into the Drag and Wave-Making of a Blunt Submersible", 32nd ONR symposium, Hamburg, Germany, pp. 1–17.

Hinostroza, M. A., Guedes Soares, C. and Xu, H., 2018, "Motion Planning, Guidance and Control System for Autonomous Surface Vessel", OMAE2018, Madrid, Spain, pp. 1–10.

Hinostroza, M. A., Xu, H. and Guedes Soares, C., 2019, "Cooperative Operation of Autonomous Surface Vehicles for Maintaining Formation in Complex Marine Environment", Ocean Engineering, Vol. 183, pp. 132–154.

Hu, F., Qin, J., Zhou, L. and Chen, K., 2017, "Numerical Study on Squat of KVLCC2 in Infinite and Shallow Water", ISOPE 2017, San Francisco, USA, pp. 563–569.

Huang, H., Gong, M., Zhuang, Y., Sharma, S. and Xu, D., 2019, "A New Guidance Law for Trajectory Tracking of an Underactuated Unmanned Surface Vehicle with Parameter Perturbations", Ocean Engineering, Vol. 175, pp. 217–222.

Huang, Y., Chen, L. and van Gelder, P. H. A. J. M., 2019, "Generalized Velocity Obstacle Algorithm for Preventing Ship Collisions at Sea", Ocean Engineering, Vol. 173, pp. 142–156.

Im, N. K. and Nguyen, V. S., 2018, "Artificial Neural Network Controller for Automatic Ship Berthing Using Head-up Coordinate System", International Journal of Naval Architecture and Ocean Engineering, Vol. 10, No.3, pp. 235–249.

Iribarren, J. R., Trejo, I., Cal, C. and Pecharroman, L., 2018, "Methodology to Analyze the Moored Ship Behaviour Due to Passing Ships Effects", PIANC-World Congress, Panama City, pp. 1–11.

Iseki, T., 2019, "Real-Time Estimation of the Ship Manoeuvrable Range in Wind", Ocean Engineering, Vol. 190, pp. 1–6.

Islam, H. and Guedes Soares, C., 2018, "Estimation of Hydrodynamic Derivatives of a Container Ship Using PMM Simulation in OpenFOAM", Ocean Engineering, Vol. 164, pp. 414–425.

Jeon, M., Yoon, H. K., Hwang, J. and Cho, H. J., 2018, "Analysis of the Dynamic Characteristics for the Change of Design Parameters of an Underwater Vehicle Using Sensitivity Analysis", International Journal of Naval Architecture and Ocean Engineering, Vol. 10, No.4, pp. 508–519.

Jia, Q., Xu, H., Feng, X., Gu, H. and Gao, L., 2019, "Research on Cooperative Area Search of Multiple Underwater Robots Based on the Prediction of Initial Target Information", Ocean Engineering, Vol. 172, pp. 660–670.

Jin, Y., Duffy, J., Chai, S. and Magee, A. R., 2019, "DTMB 5415M Dynamic Manoeuvres with URANS Computation Using Body-Force and Discretised Propeller Models", Ocean Engineering, Vol. 182, pp. 305–317.

Kaidi, S., Smaoui, H. and Sergent, P., 2018, "CFD Investigation of Mutual Interaction between Hull, Propellers, and Rudders for an Inland Container Ship in Deep, Very Deep, Shallow, and Very Shallow Waters", Journal of Waterway, Port, Coastal and Ocean Engineering, Vol. 144, No.6.

Karkoub, M., Wu, H. M. and Hwang, C. L., 2017, "Nonlinear Trajectory-Tracking Control of an Autonomous Underwater Vehicle", Ocean Engineering, Vol. 145, pp. 188–198.

Kim, H., Kim, S. H., Jeon, M., Kim, J. H., Song, S. and Paik, K. J., 2017, "A Study on Path Optimization Method of an Unmanned Surface Vehicle under Environmental Loads Using Genetic Algorithm", Ocean Engineering, Vol. 142, pp. 616–624.

Kim, H., Ranmuthugala, D., Leong, Z. Q. and Chin, C., 2018, "Six-DOF Simulations of an Underwater Vehicle Undergoing Straight Line and Steady Turning Manoeuvres", Ocean Engineering, Vol. 150, pp. 102–112.

Kim, S. Y., Park, S. K., Son, N. sun, Gong, I.-Y., Park, J.-H., Kim, M.-H. and Lee, C., 2018, "Development of USV Base Station Simulator and Usability Test of USV Base Station", MARSIM 2018, Halifax, Canada, pp. 1–10.

Kok, Z., Duffy, J., Chai, S., Jin, Y. and Javanmardi, M., 2020, "Numerical Investigation of Scale Effect in Self-Propelled Container Ship Squat", Applied Ocean Research, Vol. 99, pp. 1–11.

Kumar, N. and Rani, M., 2020, "An Efficient Hybrid Approach for Trajectory Tracking Control of Autonomous Underwater Vehicles", Applied Ocean Research, Vol. 95, January.

Lataire, E., Vantorre, M., Candries, M., Eloot, K.,…, Mansuy, M., 2018, "Systematic Techniques for Fairway Evaluation Based on Ship Manoeuvring Simulations", PIANC-World Congress, Panama City, pp. 1–13.

Lee, M. C., Nieh, C. Y., Kuo, H. C. and Huang, J. C., 2020, "A Collision Avoidance Method for Multi-Ship Encounter Situations", Journal of Marine Science and Technology, Vol. 25, No.3, pp. 925–942.

Lee, S. K. and Jones, M. B., 2018, "Surface Pressure of Inclined Slender-Body Flows", AFMC 2018, Adelaide, Australia, pp. 1–4.

Lee, S. and Hong, C., 2017, "Study on the Course Stability of Very Large Vessels in Shallow Water Using CFD", Ocean Engineering, Vol. 145, pp. 395–405.

Lee, S. Der and Chang, B. W., 2018, "Design and Experiment of the New Type Parallel Correction Guidance Autopilot System", MARSIM 2018, Halifax, Canada, pp. 1–11.

Lee, S., Choi, H. S., Kim, J. Y. and Paik, K. J., 2020, "A Numerical Study on Hydro-dynamic Maneuvering Derivatives for Heave-Pitch Coupling Motion of a Ray-Type Underwater Glider", International Journal of Naval Architecture and Ocean Engineering, Vol. 12, pp. 892–901.

Lee, S.-K., Manovski, P. and Kumar, C., 2020, "Wake of a Cruciform Appendage on a Generic Submarine at 10° Yaw", Journal of Marine Science and Technology, Vol. 25, No.3, pp. 787–799.

Li, J., Du, J. and Chang, W. J., 2019, "Robust Time-Varying Formation Control for Underactuated Autonomous Underwater Vehicles with Disturbances under Input Saturation", Ocean Engineering, Vol. 179, pp. 180–188.

Li, J. H., Park, D. and Ki, G., 2019, "Autonomous Swimming Technology for an AUV Operating in the Underwater Jacket Structure Environment", International Journal of Naval Architecture and Ocean Engineering, Vol. 11, No.2, pp. 679–687.

Li, L., Yuan, Z.-M. and Gao, Y., 2018, "Wash Wave Effects on Ships Moored in Ports", Applied Ocean Research, Vol. 77, pp. 89–105.

Li, M., Yuan, Z. and Delefortrie, G., 2019, "Investigation of the False Bottom Effects on Ship Model Tests", AMT 19, Rome, Italy, pp. 1–16.

Li, S., Liu, J. and Negenborn, R. R., 2019, "Distributed Coordination for Collision Avoidance of Multiple Ships Considering Ship Maneuverability", Ocean Engineering, Vol. 181, pp. 212–226.

Li, Y., Ma, T., Chen, P., Jiang, Y., Wang, R. and Zhang, Q., 2017, "Autonomous Underwater Vehicle Optimal Path Planning Method for Seabed Terrain Matching Navigation", Ocean Engineering, Vol. 133, pp. 107–115.

Liang, X., Qu, X., Hou, Y., Li, Y. and Zhang, R., 2020, "Distributed Coordinated Tracking Control of Multiple Unmanned Surface Vehicles under Complex Marine Environments", Ocean Engineering, Vol. 205, pp. 1–9.

Liao, Y., Jia, Z., Zhang, W., Jia, Q. and Li, Y., 2019, "Layered Berthing Method and Experiment of Unmanned Surface Vehicle Based on Multiple Constraints Analysis", Applied Ocean Research, Vol. 86, pp. 47–60.

Lin, R., Li, D., Zhang, T. and Lin, M., 2019, "A Non-Contact Docking System for Charging and Recovering Autonomous Underwater Vehicle", Journal of Marine Science and Technology, Vol. 24, No.3, pp. 902–916.

Lin, Y. H., Tseng, S. H. and Chen, Y. H., 2018a, "The Experimental Study on Maneuvering Derivatives of a Submerged Body SUBOFF by Implementing the Planar Motion Mechanism Tests", Ocean Engineering, Vol. 170, pp. 120–135.

Lin, Y. H., Huang, L. C., Chen, S. Y. and Yu, C. M., 2018b, "The Optimal Route Planning for Inspection Task of Autonomous Underwater Vehicle Composed of MOPSO-Based Dynamic Routing Algorithm in Currents", Applied Ocean Research, Vol. 75, pp. 178–192.

Liu, H., Ma, N. and Gu, X. C., 2018a, "Ship Course Following and Course Keeping in Restricted Waters Based on Model Predictive Control", TransNav, Vol. 12, No.2, pp. 305–312.

Liu, H., Ma, N. and Gu, X., 2018b, "Uncertainty Analysis of Ship-Bank Interaction Tests Using Planar Motion Mechanism in a Circulating Water Channel", 13th International Conference on Hydrodynamics, Incheon, Korea, pp. 311–320.

Liu, L., Wang, D. and Peng, Z., 2019, "State Recovery and Disturbance Estimation of Unmanned Surface Vehicles Based on Nonlinear Extended State Observers", Ocean Engineering, Vol. 171, pp. 625–632.

Liu, Y., Bucknall, R. and Zhang, X., 2017, "The Fast Marching Method Based Intelligent Navigation of an Unmanned Surface Vehicle", Ocean Engineering, Vol. 142, pp. 363–376.

Liu, Y., Zou, Z., Zou, L. and Li, B., 2018, "URANS Simulation of Dynamic Captive Model Tests Considering the Effect of Ship Attitude Change", 13th International Conference on Hydrodynamics, Incheon, Korea, pp. 291–300.

Liu, Y., Zeng, Z., Zou, Z., Fan, S. and Feng, P., 2019a, "Adaptive Path Tracking of the Underway Replenishment in Consideration of the Hydrodynamic Interactions between Two Ships", 11th International Workshop on Ship and Marine Hydrodynamics, Hamburg, Germany, pp. 1–10.

Liu, Y., Zou, Z., Zou, L. and Fan, S., 2019b, "CFD-Based Numerical Simulation of Pure Sway Tests in Shallow Water Towing Tank", Ocean Engineering, Vol. 189, pp. 1–21.

Maki, A., Tsutsumoto, T. and Miyauchi, Y., 2018, "Fundamental Research on the Maneuverability of the Underwater Vehicle Having Thrust Vectoring System", Journal of Marine Science and Technology, Vol. 23, No.3, pp. 495–506.

Maki, A., Sakamoto, N., Akimoto, Y., Nishikawa, H. and Umeda, N., 2020, "Application of Optimal Control Theory Based on the Evolution Strategy (CMA-ES) to Automatic Berthing", Journal of Marine Science and Technology, Vol. 25, No.1, pp. 221–233.

Mansuy, M., Tello Ruiz, M., Delefortrie, G. and Vantorre, M., 2017, "Post Processing Techniques Study for Seakeeping Tests in Shallow Water", AMT 17, Glasgow, UK, pp. 460–473.

Martinsen, A. B. and Lekkas, A. M., 2018a, "Straight-Path Following for Underactuated Marine Vessels Using Deep Reinforcement Learning", CAMS 2018, Opatija, Croatia, Vol 51, pp. 329–334.

Martinsen, A. B. and Lekkas, A. M., 2018b, "Curved Path Following with Deep Reinforcement Learning: Results from Three Vessel Models", OCEANS 2018, Charleston, USA, pp. 1–8.

Mofidi, A., Martin, J. E. and Carrica, P. M., 2018, "Propeller/Rudder Interaction with Direct and Coupled CFD/Potential Flow Propeller Approaches, and Application to a Zigzag Manoeuvre", Ship Technology Research, Vol. 65, No.1, pp. 10–31.

Moreno, F. M., Amendola, J., Tannuri, E. A. and Ferreira, M. D., 2019, "Development of a Control Strategy for Underway Tandem-like Oil Transfer Operation between a Conventional and a DP Tanker", OMAE2019, Glasgow, Scotland, UK, pp. 1–10.

Mucha, P., Dettmann, T., Ferrari, V. and el Moctar, O., 2019, "Experimental Investigation of Free-Running Ship Manoeuvers under Extreme Shallow Water Conditions", Applied Ocean Research, Vol. 83, pp. 155–162.

Muscari, R., Dubbioso, G., Ortolani, F. and Di Mascio, A., 2017, "Analysis of Propeller Bearing Loads by CFD. Part II: Transient Maneuvers", Ocean Engineering, Vol. 146, pp. 217–233.

Nakamura, S. and Okada, N., 2019, "Development of Automatic Collision Avoidance System and Quantitative Evaluation of the Manoeuvring Results", TransNav, Vol. 13, No.1, pp. 133–141.

Nam, B. W. and Park, J. Y., 2018, "Numerical Simulation for a Passing Ship and a Moored Barge alongside Quay", International Journal of Naval Architecture and Ocean Engineering, Vol. 10, No.5, pp. 566–582.

Niu, H., Ji, Z., Savvaris, A. and Tsourdos, A., 2020, "Energy Efficient Path Planning for Unmanned Surface Vehicle in Spatially-Temporally Variant Environment", Ocean Engineering, Vol. 196, pp. 1–14.

Ohashi, K., Kobayashi, H. and Hino, T., 2018, "Numerical Simulation of the Free-Running of a Ship Using the Propeller Model and Dynamic Overset Grid Method", Ship Technology Research, Vol. 65, No.3, pp. 153–162.

Ortolani, F. and Dubbioso, G., 2019, "In-Plane and Single Blade Loads Measurement Setups for Propeller Performance Assessment during Free Running and Captive Model Tests", AMT 19 , Rome, Italy.

Pan, Y., Zhang, H.-X. and Zhou, Q., 2019, "Numerical Simulation of Unsteady Propeller Force for a Submarine in Straight Ahead Sailing and Steady Diving Maneuver",

International Journal of Naval Architecture and Ocean Engineering, Vol. 11, No.2, pp. 899–913.

Park, J., Rhee, S. H., Yoon, H. K., Lee, S. and Seo, J., 2020, "Effects of a Propulsor on the Maneuverability of an Autonomous Under-water Vehicle in Vertical Planar Motion Mechanism Tests", Applied Ocean Research, Vol. 103, pp. 1–10.

Peng, Y., Yang, Y., Cui, J., Li, X., …, Luo, J., 2017, "Development of the USV 'JingHai-I' and Sea Trials in the Southern Yellow Sea", Ocean Engineering, Vol. 131, pp. 186–196.

Peng, Z., Gu, N., Zhang, Y., Liu, Y., …, Liu, L., 2019, "Path-Guided Time-Varying Formation Control with Collision Avoidance and Connectivity Preservation of under-actuated Autonomous Surface Vehicles Subject to Unknown Input Gains", Ocean Engineering, Vol. 191, pp. 1–10.

Petterson, K., Fureby, C., Liefvendahl, M., Norrison, D. and Sidebottom, W., 2018, "LES of a Full-Scale Self-Propelled Conventional Submarine at ± 10° Yaw", 32nd ONR Symposium, Hamburg, Germany, pp. 1–19.

Piaggio, B., Villa, D., Viviani, M. and Figari, M., 2020, "Numerical Analysis of Escort Tug Manoeuvrability Characteristics – Part II: The Skeg Effect", Applied Ocean Research, Vol. 100, pp. 1–24.

Qi, X., Xiang, P. and Cai, Z., 2020, "Spatial Target Path Following and Coordinated Control of Multiple UUVs", International Journal of Naval Architecture and Ocean Engineering, Vol. 12, pp. 832–842.

Quadvlieg, F., Stern, F., Simonsen, C. D. and Otzen, J. F., 2014, "Workshop on Verification and Validation of Ship Manoeuvering Simulation Methods (SIMMAN 2014)", Workshop Proceedings, pp. 1–563.

Quadvlieg, F., Willemsen, C., Boer, W. de and Oud, G., 2019, "Manoeuvring Simulation Models For Inland Ships", MASHCON 2019, Ostend, Belgium, pp. 19–23.

Rameesha, T. V. and Krishnankutty, P., 2018, "Numerical Investigation on the Influence of Froude Number on the Maneuvering Characteristics of a Container Ship", International Shipbuilding Progress, Netherlands, Vol 65, pp. 149–185.

Razgallah, I., Kaidi, S., Smaoui, H. and Sergent, P., 2019, "The Impact of Free Surface Modelling on Hydrodynamic Forces for Ship Navigating in Inland Waterways: Water Depth, Drift Angle, and Ship Speed Effect", Journal of Marine Science and Technology, Vol. 24, No.2, pp. 620–641.

Reichel, M., 2020, "Application of the IMO Standard Manoeuvres Procedure for Pod-Driven Ships", Journal of Marine Science and Technology, Vol. 25, No.1, pp. 249–257.

Ren, H., Xu, C., Zhou, X., Sutulo, S. and Guedes Soares, C., 2020, "A Numerical Method for Calculation of Ship–Ship Hydrodynamics Interaction in Shallow Water Accounting for Sinkage and Trim", Journal of Offshore Mechanics and Arctic Engineering, Vol. 142, No.5, pp. 1–9.

Revestido Herrero, E., Velasco, F. J. and Riola Rodríguez, J. M., 2018, "Improving Parameter Estimation Efficiency of a Non Linear Manoeuvring Model of an Underwater Vehicle Based on Model Basin

Data", Applied Ocean Research, Vol. 76, pp. 125–138.

RoyChoudhury, S., Dash, A. K., Nagarajan, V. and Sha, O. P., 2017, "CFD Simulations of Steady Drift and Yaw Motions in Deep and Shallow Water", Ocean Engineering, Vol. 142, pp. 161–184.

Ruggeri, F., Watai, R., Rosetti, G., Tannuri, E. and Nishimoto, K., 2018, "The Development of Redraft® System in Brazilian Ports for Safe Underkeel Clearance Computation", PIANC-World Congress, Panama City, pp. 1–20.

Sakamoto, N., Ohashi, K., Araki, M., Kume, K.,…, Kobayashi, H., 2019, "Identification of KVLCC2 Manoeuvring Parameters for a Modular-Type Mathematical Model by RaNS Method with an Overset Approach", Ocean Engineering, Vol. 188, pp. 1–16.

Sano, M. and Yasukawa, H., 2019, "Maneuverability of a Combined Two-Ship Unit Engaged in Underway Transfer", Ocean Engineering, Vol. 173, pp. 774–793.

Sans-Muntadas, A., Kelasidi, E., Pettersen, K. Y. and Brekke, E., 2019, "Learning an AUV Docking Maneuver with a Convolutional Neural Network", IFAC Journal of Systems and Control, Vol. 8, pp. 1-7.

Sans-Muntadas, A., Kelasidi, E., Pettersen, K. Y. and Brekke, E., 2019, "Path Planning and Guidance for Underactuated Vehicles with Limited Field-of-View", Ocean Engineering, Vol. 174, pp. 84–95.

Sasaki, N., Kuribayashi, S., Fukazawa, M. and Atlar, M., 2019, "Gate Rudder® Performance", AMT 19, Rome, Italy, pp. 9–15.

Shen, H., Hashimoto, H., Matsuda, A., Taniguchi, Y., …, Guo, C., 2019, "Automatic Collision Avoidance of Multiple Ships Based on Deep Q-Learning", Applied Ocean Research, Vol. 86, pp. 268–288.

Shevchuk, I., Bottner, C.-U. and Kornev, N., 2019, "Numerical Investigation of Scale Effects on Squat in Shallow Water", MASHCON 2019, Ostend, Belgium, pp. 390–402.

Shevchuk, I. and Sahab, A., 2020, "Experimental and Numerical Studies of the Flow around the JBC Hull Form at Straight Ahead Condition and 8° Drift Angle", 33rd ONR Symposium, Osaka, Japan, pp. 1–25.

Shi, B., Su, Y., Wang, C., Wan, L. and Luo, Y., 2019, "Study on Intelligent Collision Avoidance and Recovery Path Planning System for the Waterjet-Propelled Unmanned Sur-face Vehicle", Ocean Engineering, Vol. 182, pp. 489–498.

Shojaei, K. and Dolatshahi, M., 2017, "Line-of-Sight Target Tracking Control of Under-actuated Autonomous Underwater Vehicles", Ocean Engineering, Vol. 133, pp. 244–252.

Shuai, Y., Li, G., Cheng, X., Skulstad, R., …, Zhang, H., 2019, "An Efficient Neural-Network Based Approach to Automatic Ship Docking", Ocean Engineering, Vol. 191, pp. 1–9.

Silva, K. M. and Aram, S., 2018, "Generation of Hydrodynamic Derivatives for ONR Top-side Series Using Computational Fluid Dynamics", STAB 2018 , Kobe, Japan, pp. 16–21.

Singh, Y., Sharma, S., Sutton, R., Hatton, D. and Khan, A., 2018, "A Constrained A* Approach towards Optimal Path Planning

for an Unmanned Surface Vehicle in a Maritime Environment Containing Dynamic Obstacles and Ocean Currents", Ocean Engineering, Vol. 169, pp. 187–201.

Song, A. L., Su, B. Y., Dong, C. Z., Shen, D. W., …, Mao, F. P., 2018, "A Two-Level Dynamic Obstacle Avoidance Algorithm for Unmanned Surface Vehicles", Ocean Engineering, Vol. 170, pp. 351–360.

Su, Y. and Kinnas, S. A., 2018, "A Time-Accurate BEM/RANS Interactive Method for Predicting Propeller Performance Considering Unsteady Hull/Propeller/ Rudder Interaction", 32nd ONR Symposium, Hamburg, Germany, pp. 5–10.

Sukas, O. F., Kinaci, O. K. and Bal, S., 2019, "System-Based Prediction of Maneuvering Performance of Twin-Propeller and Twin-Rudder Ship Using a Modular Mathematical Model", Applied Ocean Research, Vol. 84, pp. 145–162.

Sun, Y., Ran, X., Zhang, G., Wang, X. and Xu, H., 2020, "AUV Path Following Controlled by Modified Deep Deterministic Policy Gradient", Ocean Engineering, Vol. 210, pp. 1–14.

Suzuki, R., Tsukada, Y. and Ueno, M., 2019, "Estimation of Full-Scale Ship Manoeuvring Motions from Free-Running Model Test with Consideration of the Operational Limit of an Engine", Ocean Engineering, Vol. 172, pp. 697–711.

Suzuki, R., Tsukada, Y. and Ueno, M., 2017, "Experimental Estimation of Manoeuvrability of a Full-Scale Ship in Wind and Waves Using Free-Running Model", AMT 17, Glasgow, UK, pp. 484–497.

Tan, G., Zou, J., Zhuang, J., Wan, L., …, Sun, Z., 2020, "Fast Marching Square Method Based Intelligent Navigation of the Unmanned Surface Vehicle Swarm in Restricted Waters", Applied Ocean Research, Vol. 95, pp. 1–15.

Terziev, M., Tezdogan, T., Oguz, E., Gourlay, T., …, Incecik, A., 2018, "Numerical investigation of the behaviour and performance of ships advancing through restricted shallow waters", Journal of Fluids and Structures, Vol. 76, January 2018, pp. 185-215.

Todorova, M. G. and Parvanova, R., 2019, "Application of Wavelet Functions for Identification of Ship Models", IMAM 2019, Varna, Bulgaria, pp. 182–186.

Trslic, P., Rossi, M., Robinson, L., O'Donnel, C. W., … Toal, D., 2020, "Vision Based Autonomous Docking for Work Class ROVs", Ocean Engineering, Vol. 196, pp. 1–16.

Ueno, M., Suzuki, R. and Tsukada, Y., 2017, "Rudder Effectiveness and Speed Correction in Practice at Tank Test", Ocean Engineering, Vol. 145, pp. 124–137.

Van Hoydonck, W., Delefortrie, G., De Maerschalck, B. and Vantorre, M., 2018, "Open-Water Rudder Tests Using CFD", 32nd ONR Symposium, Hamburg, Germany, pp. 1–14.

Van Hoydonck, W., Toxopeus, S., Eloot, K., Bhawsinka, K., …, Visonneau, M., 2019, "Bank Effects for KVLCC2", Journal of Marine Science and Technology, Vol. 24, No.1, pp. 174–199.

Van Zwijnsvoorde, T., Vantorre, M. and Ides, S., 2018, "Container Ships Moored at the Port

of Antwerp: Modelling Response to Passing Vessels", PIANC-World Congress, pp. 1–18.

Vantorre, M., 1988, "On the Influence of the Accuracy of Planar Motion Mechanisms on Results of Captive Manoeuvring Tests", Scientific and Methodological Seminar on Ship Hydrodynamics, Vol 1, pp. 28.1–8.

Vantorre, M., 1989, "Accuracy Considerations and Optimization of Parameter Choice of Captive Manoeuvring Tests with Ship Models (in Dutch)" DSc Thesis, Ghent University, Ghent, Belgium.

Vantorre, M., 1992, "Accuracy and Optimization of Captive Ship Model Tests", 5th International Symposium on Practical Design of Ships and Mobile Units, Newcastle upon Tyne, UK, pp. 190–203.

Veldman, J. J., Bousmar, D., Kortlever, W. and Dam, M. A. C., 2018, "Simple but Accurate Calculation Method for Vessel Speed in a Minimum Capacity Lock", PIANC-World Congress , Panama City, pp. 1–20.

Verwilligen, J., Mansuy, M., Vantorre, M. and Eloot, K., 2018, "Squat Formula for Cape-Size Bulk Carriers Based on Towing Tank Results and Full-Scale Measurements", MARSIM 2018, Halifax, Canada, pp. 1–17.

Vink, B., Schot, J., Vaz, G. and Toxopeus, S., 2017, "A Verification and Validation Study of CFD Simulations for the Flow Around a Tug", NuTTS 2017, Wageningen, The Netherlands, pp. 216–221.

Visonneau, M., Guilmineau, E. and Rubino, G., 2018, "Computational Analysis of the Flow around a Surface Combatant at 10° Static Drift and Dynamic Sway Conditions", 32nd ONR Symposium, Hamburg, Germany, pp. 5–10.

Visonneau, M., Guilmineau, E., Rubino, G. and Nantes, C. C., 2020, "Local Flow around a Surface Combatant at Various Static Drift Conditions : The Role Played by Turbulence Closures", 33rd ONR Symposium, Osaka, Japan, pp. 1–23.

Wang, D., Wang, P., Zhang, X., Guo, X., …, Tian, X., 2020, "An Obstacle Avoidance Strategy for the Wave Glider Based on the Improved Artificial Potential Field and Collision Prediction Model", Ocean Engineering, Vol. 206, pp. 1–12.

Wang, J., Wan, D. and Yu, X., 2017, "Standard Zigzag Maneuver Simulations in Calm Water and Waves with Direct Propeller and Rudder", ISOPE 2017, San Francisco, EUA, pp. 1042–1048.

Wang, J., Zou, Z. and Wang, T., 2019a, "Path Following of a Surface Ship Sailing in Restricted Waters under Wind Effect Using Robust H∞Guaranteed Cost Control", International Journal of Naval Architecture and Ocean Engineering, Vol. 11, No.1, pp. 606–623.

Wang, J., Wang, C., Wei, Y. and Zhang, C., 2019b, "Command Filter Based Adaptive Neural Trajectory Tracking Control of an Underactuated Underwater Vehicle in Three-Dimensional Space", Ocean Engineering, Vol. 180, pp. 175–186.

Wang, J., Wang, C., Wei, Y. and Zhang, C., 2020, "Filter-Backstepping Based Neural Adaptive Formation Control of Leader-Following Multiple AUVs in Three Dimensional Space", Ocean Engineering, Vol. 201, pp. 1–11.

Wang, J. and Wan, D., 2020, "CFD Study of Ship Stopping Maneuver by Overset Grid

Technique", Ocean Engineering, Vol. 197, pp. 1–12.

Wang, L., Wu, Q., Li, S. and Liu, J., 2018, "Ship Course Control Based on BAS Self-Optimizing PID Algorithm", MARSIM 2018, Halifax, Canada, pp. 1–8.

Wang, N., Jin, X. and Er, M. J., 2019a, "A Multilayer Path Planner for a USV under Complex Marine Environments", Ocean Engineering, Vol. 184, pp. 1–10.

Wang, N., Sun, Z., Yin, J., Zou, Z. and Su, S. F., 2019b, "Fuzzy Unknown Observer-Based Robust Adaptive Path Following Control of Underactuated Surface Vehicles Subject to Multiple Unknowns", Ocean Engineering, Vol. 176, pp. 57–64.

Wang, T., Wu, Q., Zhang, J., Wu, B. and Wang, Y., 2020, "Autonomous Decision-Making Scheme for Multi-Ship Collision Avoidance with Iterative Observation and Inference", Ocean Engineering, Vol. 197, pp. 1–22.

Wang, X., Liu, Z. and Cai, Y., 2017, "The Ship Maneuverability Based Collision Avoidance Dynamic Support System in Close-Quarters Situation", Ocean Engineering, Vol. 146, pp. 486–497.

Wang, Y., Yu, X., Liang, X. and Li, B., 2018, "A COLREGs-Based Obstacle Avoidance Approach for Unmanned Surface Vehicles", Ocean Engineering, Vol. 169, pp. 110–124.

Wang, Y., Tong, H. and Fu, M., 2019, "Line-of-Sight Guidance Law for Path Following of Amphibious Hovercrafts with Big and Time-Varying Sideslip Compensation", Ocean Engineering, Vol. 172, pp. 531–540.

Wang, Y., Chai, S. and Nguyen, H. D., 2020, "Experimental and Numerical Study of Autopilot Using Extended Kalman Filter Trained Neural Networks for Surface Vessels", International Journal of Naval Architecture and Ocean Engineering, Vol. 12, pp. 314–324.

Wang, Z., Xu, H., Xia, L., Zou, Z. and Soares, C. G., 2020a, "Kernel-Based Support Vector Regression for Nonparametric Modeling of Ship Maneuvering Motion", Ocean Engineering, Vol. 216, pp. 1–12.

Wang, Z., Guedes Soares, C. and Zou, Z., 2020b, "Optimal Design of Excitation Signal for Identification of Nonlinear Ship Manoeuvring Model", Ocean Engineering, Vol. 196, pp. 1–10.

Wang, Z. H. and Zou, Z. J., 2018, "Quantifying Multicollinearity in Ship Manoeuvring Modeling by Variance Inflation Factor", OMAE2018, Madrid, Spain, pp. 1–10.

Watai, R. A., Ruggeri, F., Tannuri, E. A., Santos, N. F., …, dos Santos, J. M. G., 2018, "An Analysis Methodology for the Passing Ship Problem Considering Real-Time Simulations and Moored Ship Dynamics: Application to the Port of Santos, in Brazil", Applied Ocean Research, Vol. 80, pp. 148–165.

Wen, Y., Tao, W., Zhu, M., Zhou, J. and Xiao, C., 2020, "Characteristic Model-Based Path Following Controller Design for the Unmanned Surface Vessel", Applied Ocean Research, Vol. 101, pp. 1–12.

Wnęk, A. D., Sutulo, S. and Guedes Soares, C., 2018, "CFD Analysis of Ship-to-Ship Hydrodynamic Interaction", Journal of Marine Science and Application, Vol. 17, No.1, pp. 21–37.

Woo, J., Park, J., Yu, C. and Kim, N., 2018, "Dynamic Model Identification of Unmanned Surface Vehicles Using Deep Learning Network", Applied Ocean Research, Vol. 78, pp. 123–133.

Woo, J., Yu, C. and Kim, N., 2019, "Deep Reinforcement Learning-Based Controller for Path Following of an Unmanned Surface Vehicle", Ocean Engineering, Vol. 183, pp. 155–166.

Woo, J. and Kim, N., 2020, "Collision Avoidance for an Unmanned Surface Vehicle Using Deep Reinforcement Learning", Ocean Engineering, Vol. 199, pp. 1–16.

Wu, L., Li, Y., Liu, K., Wang, S., …, Feng, X., 2019, "A Physics-Based Simulation for AUV Underwater Docking Using the MH DG Method and a Discretized Propeller", Ocean Engineering, Vol. 187, pp. 1–12.

Xia, L., Zou, Z., Liu, Y. and Zou, L., 2018, "CFD-Based Analysis of Hull-Spacing Effects on Manoeuvrability of SWATH", ISOPE 2018, Sapporo, Japan, pp. 766–773.

Xia, Y., Xu, K., Wang, W., Xu, G., …, Li, Y., 2020, "Optimal Robust Trajectory Tracking Control of a X-Rudder AUV with Velocity Sensor Failures and Uncertainties", Ocean Engineering, Vol. 198, pp. 1–16.

Xie, L., Xue, S., Zhang, J., Zhang, M., …, Haugen, S., 2019, "A Path Planning Approach Based on Multi-Direction A* Algorithm for Ships Navigating within Wind Farm Waters", Ocean Engineering, Vol. 184, pp. 311–322.

Xie, S., Garofano, V., Chu, X. and Negenborn, R., 2019, "Model Predictive Ship Collision Avoidance Based on Q-Learning Beetle Swarm Antenna Search and Neural Networks", Ocean Engineering, Vol. 193, pp. 1–24.

Xu, H. and Soares, C. G., 2019, "Hydrodynamic Coefficient Estimation for Ship Manoeuvring in Shallow Water Using an Optimal Truncated LS-SVM", Ocean Engineering, Vol. 191, pp. 1–13.

Xu, J., Hou, C., Yang, R. and Wang, G., 2019, "Autonomous Route Planning for Ships in Complex Waterways", PRADS 2019, Yokohama, Japan, pp. 1–15.

Xu, R., Tang, G., Han, L. and Xie, D., 2019, "Trajectory Tracking Control for a CMG-Based Underwater Vehicle with Input Saturation in 3D Space", Ocean Engineering, Vol. 173, pp. 587–598.

Yan, J., Gao, J., Yang, X., Luo, X. and Guan, X., 2019, "Tracking Control of a Remotely Operated Underwater Vehicle with Time Delay and Actuator Saturation", Ocean Engineering, Vol. 184, pp. 299–310.

Yan, Z., Wang, M. and Xu, J., 2019a, "Robust Adaptive Sliding Mode Control of Underactuated Autonomous Underwater Vehicles with Uncertain Dynamics", Ocean Engineering, Vol. 173, pp. 802–809.

Yan, Z., Yang, Z., Yue, L., Wang, L., …, Zhou, J., 2019b, "Discrete-Time Coordinated Control of Leader-Following Multiple AUVs under Switching Topologies and Communication Delays", Ocean Engineering, Vol. 172, pp. 361–372.

Yasukawa, H., Sakuno, R. and Yoshimura, Y., 2019, "Practical Maneuvering Simulation Method of Ships Considering the Roll-Coupling Effect", Journal of Marine Science

and Technology, Vol. 24, No.4, pp. 1280–1296.

Yeo, D. J., Yun, K. and Kim, Y.-G., 2018, "A Study on the Effect of Heel Angle on Manoeuvring Characteristics of KCS", MARSIM 2018, Halifax, Canada, pp. 1–10.

Yu, C., Xiang, X., Lapierre, L. and Zhang, Q., 2017, "Nonlinear Guidance and Fuzzy Control for Three-Dimensional Path Following of an Underactuated Autonomous Underwater Vehicle", Ocean Engineering, Vol. 146, pp. 457–467.

Yu, H., Guo, C. and Yan, Z., 2019, "Globally Finite-Time Stable Three-Dimensional Trajectory-Tracking Control of Underactuated UUVs", Ocean Engineering, Vol. 189, pp. 1–16.

Yuan, Z.-M., 2019, "Ship Hydrodynamics in Confined Waterways", Journal of Ship Research, Vol. 63, No.1, pp. 16–29.

Yuan, Z.-M., Li, L. and Yeung, R. W., 2019, "Free-Surface Effects on Interaction of Multiple Ships Moving at Different Speeds", Journal of Ship Research, Vol. 63, No.4, pp. 251–267.

Yun, K., Yeo, D. J. and Kim, D. J., 2018, "An Experimental Study on the Turning Characteristics of KCS with CG Variations", MARSIM 2018, Halifax, Canada, pp. 1–9.

Zhang, C., Liu, X., Wang, J. and Wan, D., 2020, "Numerical and Experimental Study of Dynamic Pmm Tests of the Onrt Hull", ISOPE 2020, Shanghai, China, pp. 2020–2026.

Zhang, G., Deng, Y., Zhang, W. and Huang, C., 2018a, "Novel DVS Guidance and Path-Following Control for Underactuated Ships in Presence of Multiple Static and Moving Obstacles", Ocean Engineering, Vol. 170, pp. 100–110.

Zhang, G., Huang, H., Qin, H., Wan, L.,…, Su, Y., 2018b, "A Novel Adaptive Second Order Sliding Mode Path Following Control for a Portable AUV", Ocean Engineering, Vol. 151, pp. 82–92.

Zhang, H., Zhang, H., Chen, X., Liu, H. and Wang, X., 2018, "Scale Effect Studies on Hydrodynamic Performance for DTMB 5415 Using CFD", OMAE2018, Madrid, Spain.

Zhang, J., Sun, T. and Liu, Z., 2017, "Robust Model Predictive Control for Path-Following of Underactuated Surface Vessels with Roll Constraints", Ocean Engineering, Vol. 143, pp. 125–132.

Zhang, Q., Zhang, X. and Im, N., 2017, "Ship Nonlinear-Feedback Course Keeping Algorithm Based on MMG Model Driven by Bipolar Sigmoid Function for Berthing", International Journal of Naval Architecture and Ocean Engineering, Vol. 9, No.1, pp. 525–536.

Zhang, X., Han, X., Guan, W. and Zhang, G., 2019, "Improvement of Integrator Back-stepping Control for Ships with Concise Robust Control and Nonlinear Decoration", Ocean Engineering, Vol. 189, pp. 1–7.

Zhang, Y., Liu, X., Luo, M. and Yang, C., 2019, "MPC-Based 3-D Trajectory Tracking for an Autonomous Underwater Vehicle with Constraints in Complex Ocean Environments", Ocean Engineering, Vol. 189, pp. 1–10.

Zhao, L. and Roh, M. I., 2019, "COLREGs-Compliant Multi-Ship Collision Avoidance

via Deep Reinforcement Learning", Ocean Engineering, Vol. 191, pp. 1–15.

Zhao, Y., Qi, X., Incecik, A., Ma, Y. and Li, Z., 2020, "Broken Lines Path Following Algorithm for a Water-Jet Propulsion USV with Disturbance Uncertainties", Ocean Engineering, Vol. 201, pp. 1–9.

Zhou, J., Ye, D., Zhao, J. and He, D., 2018, "Three-Dimensional Trajectory Tracking for Underactuated AUVs with Bio-Inspired Velocity Regulation", International Journal of Naval Architecture and Ocean Engineering, Vol. 10, No.3, pp. 282–293.

Zhou, C., Gu, S., Wen, Y., Du, Z., …, Zhu, M., 2020, "Motion Planning for an Unmanned Surface Vehicle Based on Topological Position Maps", Ocean Engineering, Vol. 198, pp. 1–19.

Zhuang, Y., Huang, H., Sharma, S., Xu, D. and Zhang, Q., 2019, "Cooperative Path Planning of Multiple Autonomous Underwater Vehicles Operating in Dynamic Ocean Environment", ISA Transactions, Vol. 94, pp. 174–186.

The Ocean Engineering Committee
Final Report and Recommendations to the 29th ITTC

1. GENERAL

1.1 Membership and Meetings

The Committee appointed by the 28th ITTC consisted of the following members:

- • Prof. Claudio Alexis Rodríguez Castillo (Chairman), Laboratory of Ocean Technology (LabOceano), Federal University of Rio de Janeiro, Brazil;
- • Prof. Longfei Xiao, Shanghai Jiao Tong University, China;
- • Dr. Viacheslav Magarovskii, Krylov State Research Center, Russia;
- • Dr. Rae Hyoung Yuck, Samsung Heavy Industries Co. Ltd, Korea;
- • Dr. Halvor Lie, SINTEF Ocean, Norway;
- • Prof. Qing Xiao, University of Strathclyde, United Kingdom;
- • Prof. Ayhan Mentes, Istanbul Technical University, Turkey;
- • Prof. Yasunori Nihei, Osaka Prefecture University, Japan.

Two in-person committee meetings were held:

- • University of Strathclyde, Glasgow, United Kingdom, January 24-26, 2018;
- • Samsung Heavy Industries, Daejeon, Korea, September 12-14, 2018.

1.2 Tasks based on the Recommendations of the 28th ITTC

The Ocean Engineering Committee is responsible for the issues in relation with moored and dynamically positioned ships and floating structures. For the 29th ITTC, the modelling and simulation of waves, wind and current is the primary responsibility of the Specialist Committee on Modelling of Environmental Conditions, with the cooperation of the Ocean Engineering, the Seakeeping, and the Stability in Waves Committees.

The following terms of reference were determined by the 28th ITTC:

(1) Update the state-of-the-art for predicting the behaviour of bottom founded or stationary

floating structures, including moored and dynamically positioned ships, emphasizing developments since the 2017 ITTC Conference. The committee report should include sections on:

a. the potential impact of new technological developments on the ITTC;

b. new experimental techniques and extrapolation methods;

c. new benchmark data;

d. the practical applications of computational methods to prediction and scaling;

e. the need for R&D for improving methods of model experiments, numerical modelling, and full-scale measurements.

(2) Review ITTC Recommended Procedures relevant to ocean engineering, including CFD procedures, and

a. identify any requirements for changes in the light of current practice, and, if approved by the Advisory Council, update them;

b. identify the need for new procedures and outline the purpose and contents of these.

(3) Review the state-of-the-art in offshore aquaculture systems (deeper water, further from shore, not in sheltered waters), including harsher conditions, larger volumes and scaling of whole structure vs scaling forces acting on nets.

(4) Review the state-of-the-art in model tests of cable/pipe dynamics close to the sea surface (substantial wave and current forces) (e.g. electric cables, hoses offloading). Rationale:

a. Different from mooring lines: closer to surface (subject to wave forces) and flexible;

b. Different from risers: S-shape risers usually at very deep water, no need to consider wave forces;

c. Need to know more on the external forces for fatigue damage assessment / design;

d. Investigate dynamic interactions between 2 floating platforms and connecting flow lines.

(5) Review the state-of-the-art in hybrid testing - software-in-the-loop tests for modelling wind forces. Rationale:

a. Dominant frequencies are higher than those in hybrid mooring tests (wind change faster, quicker dynamics to be represented);

b. Reference cases/tests to verify system – cases available are too different to be compared;

c. Liaise with the SC on Hydrodynamic Testing of Marine Renewable Energy Devices for effects on wind turbine testing.

(6) Extend experimental wave run-up benchmark tests (four squared vertical cylinders) to measure wave run-ups and global forces on cylinders and to investigate scale effect.

(7) Carry out CFD benchmark study on two-body interactions, focusing on the investigation of viscous effects on the gap surface elevation using the benchmark experimental results produced by the 28th ITTC OE committee.

(8) Review the state-of-the-art for large diameter flexible risers used for deep water mining.

(9) Re-write Model Construction Procedure with focus on model construction issues (materials, tolerances, production methods, quality control, acceptance testing, etc.).

2. STATE-OF-THE-ART REVIEWS IN OFFSHORE STRUCTURES

2.1 Bottom Founded Structures

Bottom founded structures are widely used as production or oil recovering platform in shallow waters but have been also applied as offshore wind turbine supporting structures in the recent years.

Although the current trend in oil and gas industry is to explore and extraction in deeper waters which require more floating platforms, there is a high demand for life extension of existing fixed steel platforms in different regions, such as Gulf of Mexico, North Sea, Malaysian and Australian waters, that are now reaching, or have exceed, their design life. Dehghani and Aslani (2019) have reviewed and discussed the various loads on these structures. Fatigue loading exerted by wave and wind actions is one of the main loading experienced by these platforms. Fatigue and vessel impact are reported to be responsible for almost half of the damages to steel offshore platforms. Corrosion having the highest rate in splash zone accelerates the initiation and growth of fatigue cracks that usually occur at the weld toe at the intersection of the chord and brace members. Horn and Leira (2019) have presented a methodology for evaluating the fatigue reliability of a bottom-fixed offshore wind turbine with stochastic availability. Fatigue damage was calculated in the foundation of an offshore bottom-fixed monopile-mounted large wind turbine. A detailed metocean model was used to evaluate the long-term fatigue damage distribution in both operational and idling conditions. It is shown that a deterministic availability model may yield pessimistic fatigue life estimates compared to a stochastic model.

Luo-Theilen and Rung (2019) have presented hydrodynamic simulations of complex offshore installation procedures using mechanical couplings. To overcome the challenge of large relative motions, implicitly coupled overset-grids were applied. Special seaway boundary conditions combining viscous solutions in the near-field and inviscid solutions in the far-field were used to avoid undesirable reflections from the boundaries and allowed for the use of relatively compact domain sizes. With the help of the mechanical joints, three-phase (air-water-soil) flow simulations including structure-seabed interactions have been modelled realistically. The algorithm was successfully validated and applied to the installation process of a gravity foundation and a jack-up rig.

With the growing number of offshore wind installations, particular attention should be paid to the safe operation of assets. These assets are subject to extreme environmental conditions and high dynamic stresses caused by wind, waves, and currents. They are also largely exposed to hazards associated with collision with either commercial ships or infield support vessels. Moulas et al. (2017) have developed a numerical nonlinear finite element analysis (NLFEA) approach to evaluate the damage to wind turbine foundations when stricken by an offshore support vessel. Various accident scenarios were identified and the resulting damage to wind turbine foundations were analysed. Based on the results, an insight on how the next generation of wind turbine foundations can be designed in a more “collision-friendly” way has been provided. Chong (2017) have analysed the long-term offshore foundation that undergoes numerous mechanical cycles. A semi-empirical numerical

scheme was used to simulate two offshore foundations subjected to repetitive loads (i.e., monopile and shallow foundation). Numerical results show that the most pronounced displacements occur during early cycles (N < 100), yet their incremental rate approaches toward an asymptotic value.

More recently, T. Yu et al. (2019) have developed a physical model for the scour induced by waves and current around a composite bucket foundation. Foundation models with scales of 1:40 and 1:60 were placed in a flume, and the scour process was monitored. The experimental results showed that the combined wave–current condition induced a greater scour range than the wave-only or current-only condition, but it did not necessarily induce a greater equilibrium scour depth than the current-only condition. The effects of dimensionless parameters such as the Keulegan–Carpenter number, ratio of velocities and Froude number on the maximum equilibrium scour depth were considered.

Wu et al. (2019) have reviewed the present state of knowledge concerning geotechnical and structural issues affecting foundation types under consideration for the support structures of offshore wind turbines, and provided recommendations for future research and development. Cheng et al. (2019) presented an experimental and numerical study of the combined bearing capacity of a recent hybrid foundation concept that merges a skirted footing with a deeper caisson (Figure 133). A significant increase in capacity was observed in all directions compared to a circular skirted mat of the same size due to the inclusion of the caisson.

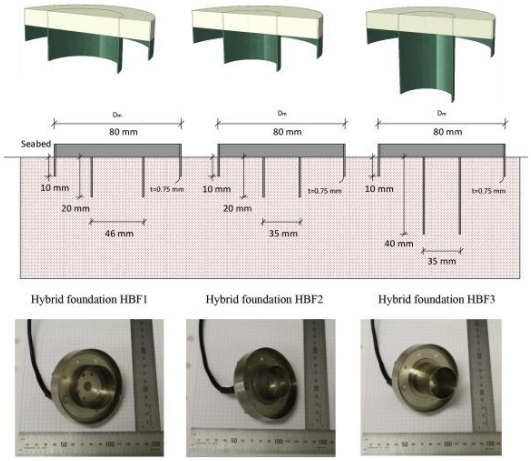

Figure 133: Hybrid foundation geometries (Cheng et al., 2019)

A structural optimization design method for jacket platform structure has been developed based on topology optimization theory (Tian et al., 2019). The method is applicable at an early design stage, which can determine the initial structure and force transmission path to maximize the structural stiffness. A set of constraints based on multi-criteria design assessment was applied according to standard requirements, which include stress, deformation, vibration, and design variable constraints (Figure 134). Results showed that the optimized structure had a 13.7% reduction in the global mass, 46.31% reduction in the maximum equivalent stress, and large ultimate carrying capacity ability under environmental loads.

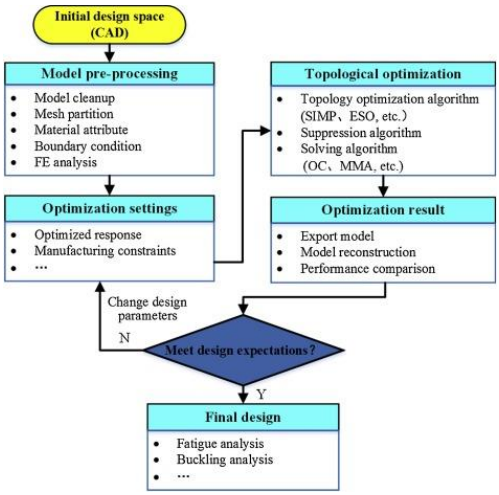

Figure 134: Flowchart of topology optimization solution (Tian et al., 2019)

Offshore wind turbines (OWTs) have played an important role in the field of renewable energy. The main issues in design of OWTs in regions of recent development have been aero- and hydro-dynamic loads; however, earthquake is a design concern in seismic areas such as East Asia and Western United states. Kaynia (2019) reviewed the state of practice in seismic design of offshore wind turbines. It was demonstrated that wind turbines are vulnerable to vertical earthquake excitation due to their rather high natural frequencies in vertical direction; however, inclusion of the radiation damping could contribute considerably to reduce the earthquake loads. Moreover, it was demonstrated how soil nonlinearity could lead to settlement and permanent tilting of offshore wind turbines on caisson foundations or tripods. Ju and Huang (2019) have provided an analysis framework for OWT support structures subjected to seismic, wind, and wave loads using the finite element method with soil-structure interaction, and a conservative soil liquefaction analysis. The NREL 5-MW jacket-type OWT under IEC 61400-3 was analysed. The results indicate that seismic loads combined with wind and wave loads during power production often control the design, especially near the rated wind speed. For PGA over 0.52 g, almost all the members are controlled by the seismic loads, and the increase in the steel design weight can be over 40%. First-mode tuned mass dampers for jacket-type support structure with deep piles are efficient to reduce the vibration coupled from wind, wave, and seismic loads even with 20-m soil liquefaction. Z. X. Li et al. (2019) experimentally investigated the earthquake-induced added mass and inertial coefficient in the Morison equation through a dynamic test system with a water tank and actuator on four cylindrical steel tubes

Karimirad and Bachynski (2017) performed sensitivity analyses to investigate the importance of limited actuation of aerodynamic and generator loads for the responses of a 5 MW bottom-fixed turbine. Normal operational, parked and fault conditions have been considered. The aerodynamic yaw moment was only important for the yaw/torsional responses, but the sensitivity was quite high (up to 80% changes in the dynamic responses). In severe conditions with a parked turbine, aerodynamic damping had a significant effect on the responses. Removing the aerodynamic pitch moment induced errors up to 20% for some important load actions, i.e., pile and tower fore-aft bending moments.

Ghassempour et al. (2019) dealt with vibration mitigation via tuned mass damper in bottom-fixed, horizontal-axis offshore wind turbines. Focusing on a baseline 5-MW turbine mounted on a monopile, equipped with an omnidirectional tuned mass damper inside the nacelle, the study explored a wide range of potential tuning frequencies, mass, and damping ratios, in both operational and parked rotor conditions. Due to inherent non-linearity of rotor dynamics, their results demonstrated that a conventional design of the tuned mass damper based on the natural frequencies of the support structure modes may not be suitable for offshore wind turbines.

O'Leary et al. (2019) investigated the application of lightweight fibre reinforced

composite materials in the construction of offshore wind turbine support structures. A composite tower design suitable for the NREL 5 MW reference wind turbine was presented. The design was based on the most automated and low-cost composite manufacturing methods (pultrusion and filament winding). The mass of the tower was minimized using gradient based optimization approach. The cost of a composite tower was calculated and levelized cost of energy (LCOE) projections were discussed in comparison with the existing steel tower cost. The study determined that while the composite tower is technically feasible and has a lower mass than a comparable steel tower, uncertainty remains in how it compares economically in terms of LCOE.

2.2 Stationary Floating Structures

Stationary floating structures addressed in this section include FPSOs, semisubmersibles, TLPs, spars, FLNGs, and their riser/mooring and dynamic positioning systems. Unless specified, this section is focused on platforms for oil and gas industry, while some platforms for the offshore wind energy industry are given in Section 2.2.5.

2.2.1 FPSO Vessels

In number of units, FPSOs platforms continue to be leading type of floating offshore structures for oil and gas production. Among the different concerns associated to this type of platforms, green water and wave impacts have been the issues that have attracted more attention in the recent years. Several works reporting experimental as well as numerical investigations have been found. In the latter, CFD simulations have been the main numerical tool adopted. For instance, green water on FPSOs subjected to beam and quartering irregular seas have been investigated through experimental model tests (Figure 135) and CFD simulations (Figure 136) in Silva et al. (2017a, 2017b). The model tests were performed for a 1:70 ship-type FPSO, with measurements of water elevations and loads during green water events. Many green water events have been monitored and critical regions for extreme elevation and loads have been identified along the deck edge. For the CFD simulations, extreme green water events at beam and quartering waves were selected and the whole wave vessel interaction was simulated, including the water on deck propagation. The applied methodology allowed access to high spatial resolution free surface position, water velocities and load distribution, aspects usually not available from experiments.

Figure 135: Evolution of a beam sea extreme green water event during model tests (Silva et al., 2017a)

Numerical prediction of green water was also carried out on a spread mooring FPSO (Wang et al., 2017). The numerical approach was based on 3D panel method and accounts for linear and nonlinear effects caused by bilge keel, mooring lines, and risers. The calculation is conducted in frequency domain with an iterative approach. Analysis of the results indicated a good agreement with model experiments and that the relative wave elevation at sides of the FPSO in oblique waves was strongly affected by bilge keel, mooring, and risers.

Hu et al. (2017) described numerical and experimentally the physical processes involved in offshore wave-breaking impacts on a truncated wall (representing the vertical section of a FPSO). Four types of wave impact were identified in the tests, and are referred to as slightly-breaking, flip-through, large air pocket and broken wave impacts (Figure 137).

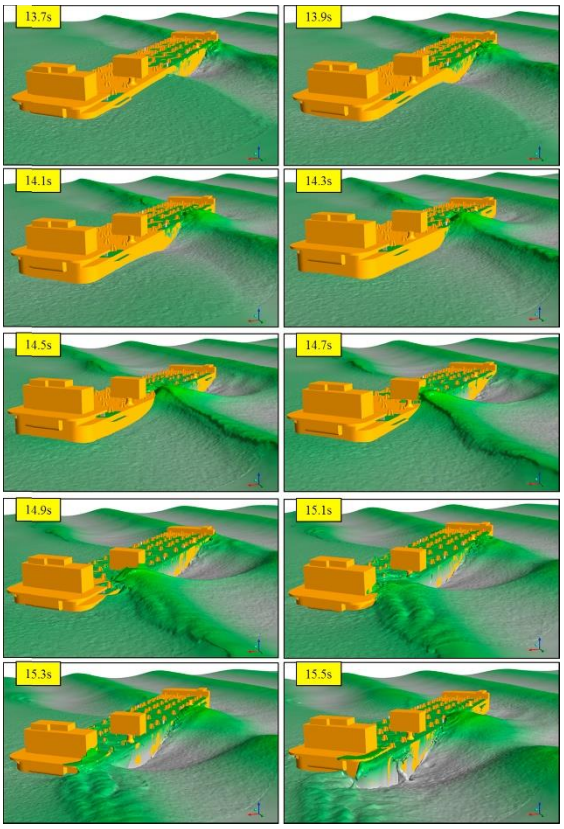

Figure 136: 3D simulation of a quartering sea green water event (Silva et al., 2017b)

Numerical prediction of green water was also carried out on a spread-moored FPSO (Wang et al., 2017). The numerical approach was based on 3D panel method and accounted for linear and nonlinear effects caused by bilge keel, mooring lines, and risers. The calculation is conducted in frequency domain with an iterative approach. Analysis of the results indicated a good agreement with model experiments and that the relative wave elevation at sides of the FPSO in oblique waves was strongly affected by bilge keel, mooring, and risers.

Hu et al. (2017) described numerical and experimentally the physical processes involved in offshore wave-breaking impacts on a truncated wall (representing the vertical section of a FPSO). Four types of wave impact were identified in the tests, and are referred to as slightly-breaking, flip-through, large air pocket and broken wave impacts (Figure 137).

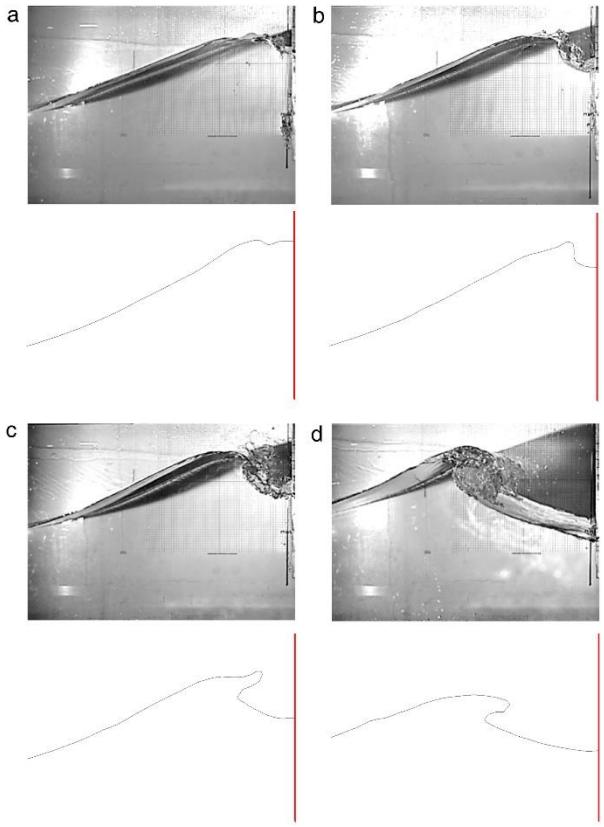

Figure 137: Wave profiles: numerical wave profiles (upper) and wave profiles (lower) (a) slightly-breaking (b) flip-through (c) large air pocket (d) broken wave (Z. Z. Hu et al., 2017)

Rosetti et al. (2019) performed an experimental analysis on green water events in a wave flume with a fixed model representing the middle-body of an FPSO hull, emulating the incidence of beam waves on such structure. Water elevations and impact loads on a deck structure were measured and water velocities were calculated with the purpose of correlating this information. Despite the variability in the peak impact forces observed from cycle to cycle, good agreement between mean values and deviation obtained in CFD and experiments evidenced that, in a statistical sense, numerical model captured the essence of the phenomena. Wang et al. (2019) have studied the effects of the asymmetric riser and bilge keel

arrangements on the motion response and relative wave elevation of a FPSO. A coupling effect between roll and heave has been identified, due to nondiagonal inertia terms associated to the asymmetric riser system.

Yan et al. (2019) have investigated, experimentally and numerically, plunging wave impacts on a box-shape structure focusing on three typical scenarios with distinct features, i.e. the wave impact occurs after, upon and before wave breaking. The wave elevations at typical positions, the wave impact pressures on the front and bottom of the platform, and the wave profiles of the transient wave impact process have been measured.

Hu et al. (2020) have experimentally and numerically studied the interaction between (nonbreaking) extreme waves, generated by focusing NewWave group, and a simplified FPSO. Both the two-phase incompressible CFD solver, OpenFOAM, and the fully nonlinear potential theory (FNPT) based solver, QALE-FEM, have been applied. The wave run-up and pressure on the FPSO surface, the wave load on and the response of the moored FPSO were examined. Viscous/turbulent effects were insignificant for the wave generation and propagation. Cases with a fixed FPSO were considered for quantifying the main sources of the error on the wave runup and the wave loading. The results revealed that a better reproduction of the incident wave by the self-correction wavemaker generally secures a higher overall accuracy on predicting the wave runup and the wave loading in a non-breaking extreme sea. Viscous effect played an important role in extreme motion response of an FPSO subjected to a focusing wave group, especially in cases with higher significant wave height. It is concluded that the QALE-FEM can accurately model the wave with high computational efficiency but may fail to achieve a reliable result when significant wave run-up or structure motions (especially the rotational motions) occur. In contrast, the two-phase OpenFOAM has capacity of modelling violent wave impact and aeration, can well capture the viscous/turbulence effect, but shows limitation on large-scale wave propagation due to its extensively high computational cost. To take advantages from each and minimize their disadvantages, one may develop a hybrid model combining the QALE-FEM and the OpenFOAM, as suggested by Li et al. (2018).

Ha et al. (2021) have conducted an experimental investigation of the characteristics of the slamming impact loads on the bow of a ship-type FPSO under breaking and irregular wave conditions for three heading angles: 180°, 165°, and 150°, with the largest slamming impact loads observed for 150°. The slamming impact loads can be categorized as loads with one peak and two peaks. For a heading of 180°, more slamming impact loads with two peaks were detected, while those with one peak are more frequent for a heading of 150°. In loads with two peaks, the second peak is smaller due to the damping effect of the first slam. Depending on the heading angle, sway, roll, and pitch motions appear as the more important factors for the slamming impact loads.

Issues associated to side-by-side configurations of FPSOs or box-shaped structures have also attracted a growing concern. For instance, Li (2020) studied the hydrodynamic interaction of side-by-side vessels based on the gap resonant modes theoretically derived by Molin et al. (2002). The hydrodynamic associated wave elevations, coefficients, and wave forces were analysed for a real hull shaped FPSO and a ship under parallel and nonparallel configurations for different wave headings. The numerical simulations of vessel motions, RAOs by white noise test and relative motion under irregular waves were validated by measurement in model tests. The shielding effect was also evaluated numerically and experimentally by exchanging vessels on lee-side and weather-side. Results indicate that the first mode which is superior

under beam sea may become less significant under oblique and head seas. Higher resonant mode shifts to lower frequency in the nonparallel configuration. The shielding effect only suppresses the motion caused by the gap resonance, the natural frequency resonance like roll remains without change. A numerical investigation of viscous effects on the gap resonance between side-by-side boxes have shown that flow separation accounts for most of the energy loss during the process of gap resonance (Feng et al., 2017).

Jiang et al. (2020) have also numerically investigated the hydrodynamic behaviour of box-systems with and without narrow gaps, by employing a numerical wave flume. Their results indicate that the wave resonance in the narrow gap increases the horizontal and vertical wave forces on each box around resonant frequency. The fluid resonance in the narrow gap can also significantly affect the total vertical wave forces on two-box systems; while the influence on total horizontal wave forces is not remarkable.

A two-dimensional numerical wave tank based on OpenFOAM was used to investigate the effect of heave motion on the gap resonance formed between two boxes under the action of regular waves (Gao et al., 2021). Two series of numerical experiments were conducted to compare the effects of upstream box motion on gap resonance. In the first series, the two boxes are fixed in the wave flume. In the second series, Box A heaves freely under incident wave actions, while Box B remains fixed. The heave motion of the upstream box leads to a lower wave height amplification inside the gap and a higher fluid resonant frequency (close to the natural frequency of the heave free decay).

Other issues associated to the behaviour of FPSOs in the presence the waves, wind and/or currents are reported in the following works:

Zangeneh et al. (2017) reported model tests of a turret-moored FPSO at 1:120 scale conducted with regular waves under two wind speeds (12 and 25 m/s full scale). Free-decay tests were also conducted to investigate the contribution of the wind damping to the total damping. Measured results show that in the presence of wind, the damping values are higher than those estimated due to hydrodynamics only. This wind induced damping on FPSOs, can result in smaller heading angles and play a large role in the station-keeping dynamics of moored-tankers.

Fonseca and Stansberg (2017) presented a method to estimate realistic surge and sway wave drift force coefficients for the Exwave FPSO. Model test data is used to identify the difference frequency wave exciting force coefficients based on a second order signal analysis technique. The process also identifies the linearized low frequency damping. Comparisons with empirical mean-wave drift coefficients showed that potential flow predictions underestimate the wave drift forces, especially at the lower frequency range where severe sea states have most of the energy.

Sanchez-Mondragon et al. (2017) have investigated the piston mode effects in moonpool on the motion behaviour in a turret-moored FPSO under regular waves. Two series of experimental test have been conducted in two different configurations: one using a turret that prevents water inflow, and the other using a turret that allows water inflow between the moonpool and the internal cylinder.

Kang et al. (2017) investigated the model test method of the FPSO and offloading system by using the development mode of “FPSO + CALM + TANKER” working in a 1700-m depth of offshore West Africa (Figure 138a). An equivalent design based on static and dynamic similarity criteria for oil offloading line (OOL) was discussed, and a type of creative method for the equivalent design of OOL in a model test

was proposed. It was observed that the calculated results of the truncated system (Figure 138b) are basically consistent with those of the prototype system, and the design of the model test scheme is demonstrated to be robust and reliable.

Sanchez-Mondragon et al. (2018) have also reported large slow yaw rotations under regular and irregular wave conditions. An analytical method was developed to predict the maximum yaw angle reached under the slow yaw varying oscillations and identify critical regular wave periods that provoke those large rotations. Based on time domain simulations, it was also concluded that large yaw motions are reached faster when the turret is near the centre of gravity.

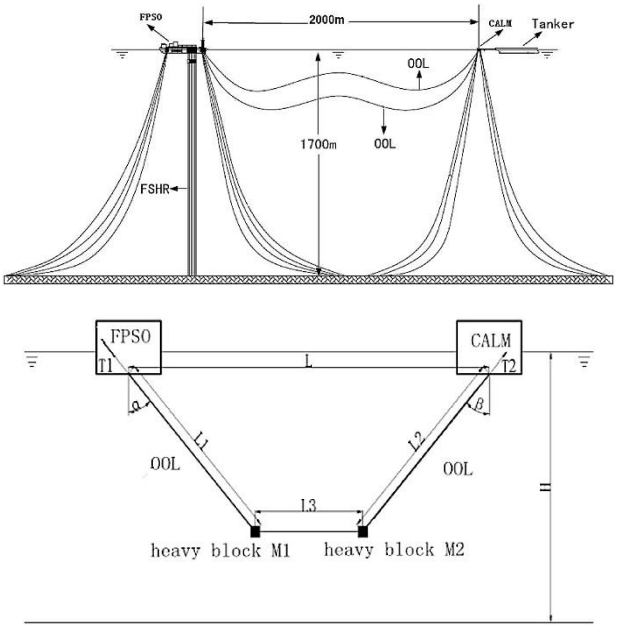

Figure 138: a) Full-depth system b) Truncated system (Kang et al., 2017)

Zanganeh and Thiagarajan (2018) have numerical and experimentally studied the mean heading of a turret-moored FPSO in bi-directional seas (swell and wind-seas). Experiments at 1:120 scale for two storm conditions, offshore Brazil, and West of Africa, show that the heading angle is self-limiting to a range of ±20° with respect to head sea direction. However, numerical simulations predict twice the heading angle observed in experiments – if the hydrodynamic interaction between the normal and the cross-wave spectrums is not considered. A cross-wave correction based on Pinkster's second order (bound) wave formula has been proposed to account for the interaction. The new numerical results demonstrated that the contribution of the bound wave will be sufficiently large to diminish the magnitude of the sway induced drift force and shift the heading of the vessel away from the wind-sea.

Chen et al. (2019) have used the Response based analysis (RBA) to establish the design metocean conditions (DMCs) of a generic weather-vaning FPSO off the North West Shelf (NWS) of Australia for determining green-water severity. Full-scale measurements from an operating FPSO collected in various environmental combinations, including wind dominant conditions, non-collinear wave and swell sea states and multi-stable heading cases has been used to validate a vessel heading prediction tool. Locations at the bow, amidships and the stern of the vessel have been found to be susceptible to green water risks and the vessel was often exposed to oblique waves during tropical cyclones. For a given location in the FPSO, the shapes of the wave time histories which give rise to extreme relative wave-vessel motions in a set of design metocean conditions were similar, indicating that a 'design wave', derived within the framework of linear wave theory, may be a useful approach to tackle highly nonlinear and complex green water overtopping problems.

Lyu et al. (2019) have developed a multi-body dynamic mathematical modelling with seven independent degrees of freedom (DOFs) for the Soft Yoke Mooring System (SYMS), a single point mooring system for shallow water (Figure 139). It is composed of a mooring framework, mooring legs, yoke, and single point, and is located at the FPSO through 13 hinge joints, such as universal joints and thrust

bearings. The mathematical formula of multibody dynamics of the SYMS considered tribological behaviours in the hinges. Based on field measurement data, the complete internal forces of single bodies and nodes under real sea states were calculated. The effects of six DOFs of FPSO on the horizontal and vertical mooring forces were analysed. Results indicate that, when six DOFs motions of FPSO are accounted, both number and amplitude of the cyclic loading are higher than those of the static analysis. The alternating loads influence the service life of hinge joints.

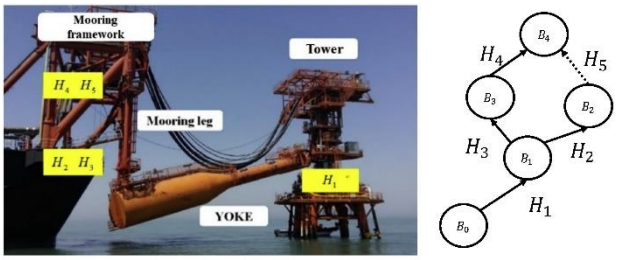

(a) The Soft Yoke Mooring system (b) Topology

Figure 139: Topological graph of the SYMS (Lyu et al., 2019)

Reynolds scale effects and shielding effects on current loads of offshore vessels in side-by-side configuration have been addressed by Koop (2020). Based on CFD calculations, those loads could be obtained with acceptable accuracy for most headings. The results for the current coefficients at full-scale Reynolds number are found to be lower than at model-scale Reynolds number, which implies that results from model tests are conservative for the current loads. However, current load coefficients may be used to estimate hydrodynamic damping and a lower coefficient implies lower damping.

Towing- and course-stability of a FPSO towed by a tug-boat was experimentally investigated by Park et al. (2021) using the conventional experimental method (CEM) in which the lateral motions of the tug-boat are neglected (Figure 140) and, a new experimental method (NEM) in which the lateral motions of the tug-boat are modelled as a sinusoidal motion using a forced oscillation device changing frequency and amplitude (Figure 141). Higher lateral speed of tug-boat compared to the towed FPSO or relatively large tension on the towline may cause poor course stability. The towed point had strong influence on the towing stability under the CEM.

Roll damping prediction for FPSO hulls have also attracted the attention of several authors during this ITTC term and several works have addressed this problem numerically, experimentally and/or a combination of both approaches (Asgari et al., 2020; Avalos and Wanderley, 2018; Fernandes et al., 2018; Ji et al., 2019; Kim et al., 2020; Rodríguez et al., 2020).

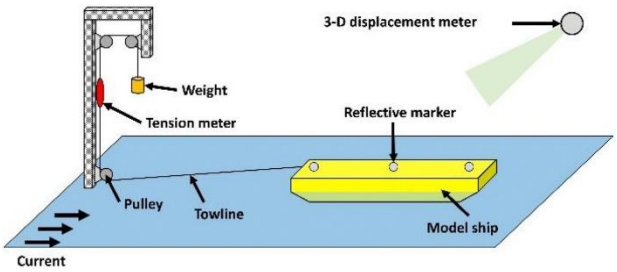

Figure 140: Layout of conventional experimental method (CEM) - (Park et al., 2021)

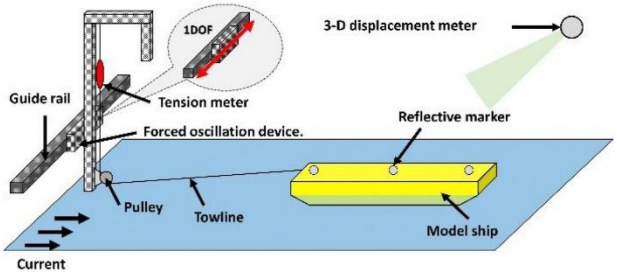

Figure 141: Layout of new experimental method (NEM) - (Park et al., 2021)

2.2.2 Semi-submersibles

Semi-submersibles have attracted much more attention in the recent years due to their suitability in reducing wave-induced motions of the floating system. However, there are various challenges related to vortex induced motions (VIM). Size of columns, corner shape and

helical strakes help in the mitigation of dynamic responses in waves, but their effects need to be further investigated in terms of VIM performance. Hydrodynamic loads evaluation continues to be another big challenge.

X. Hu et al. (2017) carried out numerical studies on vortex-induced motions of a deep draft semi-submersible with four columns based on improved delayed detached eddy simulation (IDDES) model. The transverse motions for 22.5° current incidence are larger than those for 0° and 45° current incidences in the study. The mean drag force coefficients for these simulated current incidence angles tend to grow as the transverse motion amplitudes increase. In addition, parametric studies have also been performed to examine the effects of the column corner radius on VIM.

Tan et al. (2017) presented a vortex-induced motion performance of a dry tree Heave and VIM Suppressed (HVS) semi-submersible designed to possess low VIM and low heave responses (Figure 142). VIM performance was estimated using model testing and Computational Fluid Dynamics (CFD) analysis. From model tests, VIM suppression was observed in the HVS semisubmersible due to the presence of the column steps. CFD simulations of the model tests showed results comparable to the measured data. Additional CFD analysis was performed to account for the external damping effect of the mooring lines and risers on the VIM performance of the HVS semisubmersible.

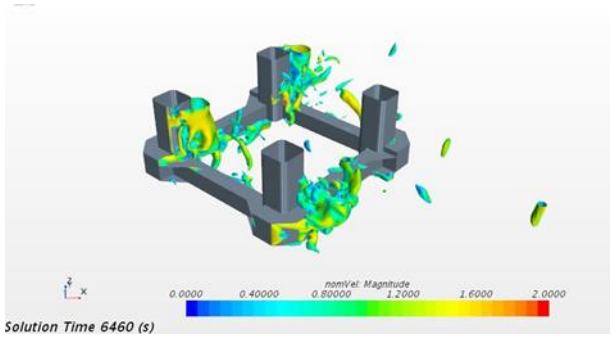

Figure 142: VIM Performance of HVS Semi-submersible (Tan et al., 2017)

Liao et al. (2017) presented numerical analysis of wave impact loads on semi-submersible platform which can result in structural damage. In the method, the FDM (Finite Difference Method) is applied for solving flow field, and the THINC/SW (Tangent of Hyperbola for INterface Capturing with Slope Weighting) model, which is kind of VOF (Volume-of-Fluid) model, is adopted to capture the free surface.

Yu et al. (2017) attempted to assess the ultimate strength of a new large-sized semi-submersible platform with lateral brace structures and square cross-section columns using a three-dimensional nonlinear finite element model under different loading conditions. Results showed that the time dependent dynamic explicit method was reliable and feasible for the calculation of ultimate strength of such complicated structure. For the target platform, the bracings and upper hull structure were the main bearing component and were critical for the ultimate strength of the whole structure. High stress occurred in connection areas and special attention shall be paid for.

M. Liu et al. (2017a) conducted a numerical study using CFD method on vortex-induced motions of semi-submersibles (SS) with various types of columns (Figure 143). Four semi-submersibles with different column designs: a SS model with four rounded square columns (SRC-SS), a SS model with four circular columns (CC-SS), a SS model with two tandem rounded square columns and two tandem circular columns (SRCT-CCT-SS), and a SS model with two staggered rounded square columns and two staggered circular columns (SRCS-CCS-SS) were considered with the current headings ranged from 0° to 180°. The most significant transverse motions of the CC-SS model occur at the 0° current heading with the largest nominal transverse amplitudes around 74% of the column diameter. On the other hand, the maximum amplitudes in the

transverse direction of the SRC-SS model, approximately 63% of the column width, are observed at the 45° current heading. It is suggested that the VIM responses could be mitigated when the semi-submersible consists of combined circular-section and square-section columns.

Cahay et al. (2017) presented ice load calculation on semi-submersible platform using Ice-MAS which uses a multi-agent technology and can simulate ice loadings on complex geometry by user input file like semi-submersible floaters with pontoon and columns. The study was focused on the results obtained for different geometries subject to ice sheet loading through different incidence angles. The issues related to the anchoring of the platform were addressed in a simplified way.

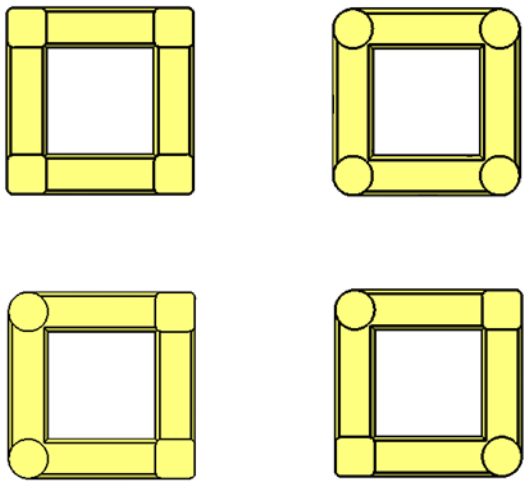

Figure 143: Different column designs for VIM study (M. Liu et al., 2017a)

Liang et al. (2017) presented an experimental study and numerical simulation with the aim to investigate the VIM effects on the overall hydrodynamics of the structure and study the fluid physics associated with VIM of a deep-draft semi-submersible (DDS), respectively. Good correlation has been demonstrated among the vortex shedding patterns, the fluctuating forces on the structure, and the VIM trajectory. Besides, the differences of the mooring line settings between the experiments and numerical simulations may affect the forces on the structures.

M. Liu et al. (2017b) presented an experimental study and three-dimensional simulations to analyse the pontoon effect on the VIM of two semi-submersible and a four-column structure. The results show that the presence of pontoons delays the onset of VIM to a higher reduced velocity in the cases of the four-pontoon DDS. Additionally, the four-column structure with no pontoons shows the most significant transverse response and yaw motions owing to the largest fluctuating lift forces induced by the well-established wake.

M. Liu et al. (2017c) conducted numerical simulations by the detached eddy simulation method validated by experimental data and then were used for parametric analysis of the VIM performance of various semi-submersibles with different column rounded ratios (*Rc/L*) and pontoon rounded ratios (*Rp/Lp*). The results show that the effect of pontoon shape on the transverse response is negligible for semi-submersibles with sharp square columns, while for semi-submersibles with rounded square columns or circular columns, the sharp rectangular pontoons greatly mitigate the VIM response.

Pessoa et al. (2018) presented an experimental and numerical study of the free surface elevation over the pontoons of a semi-submersible platform in waves. It was shown that the maximum free surface elevation over the pontoons in front of upwave columns can be severely overestimated if calculated with the current state of the art numerical models, which are based on linear diffraction-radiation theory. The observed discrepancy in this case can be explained primarily by a very high linear predicted amplification induced by the shallow pontoon, with resulting high local steepness leading to local breaking and dissipation. Such

pontoon effects should be addressed in semi-submersible platform air-gap analysis.

Batalla Toro et al. (2018) summarized the challenges of integrated decommissioning of a pentagon shaped production semisubmersible in the UK. The decommissioning process of the Buchan Alpha in the UK after more than 40 years since being built and more than 35 years of successful operation was explained. Significant challenges for the decommissioning team included the requirement to preserve the operational status of the subsea infrastructure for potential future field redevelopment and the diver disconnection of the subsea wells.

The float-over operation is less time-consuming and has larger lifting capacity, especially for large and medium sized offshore platforms. The float-over installation process of a deep-water semisubmersible platform topside was analysed by Gang et al. (2018). The calculation results show that the float movement condition meets float-over installation requirements of topside. The analysis can provide a reference for the project of the float-over installation in the future.

Larsen et al. (2018) presented results from small-scale model testing of three semi submersibles together with an overview of damping contributions of low frequency motions. The main parameters of the semis such as displacement, number of columns and diameter of columns were intentionally varied to assess the effects on total wave drift forces and corresponding damping. For accurate prediction of low frequency motions of moored semi submersibles in extreme sea states, a damping level in the range 40–70% of critical damping should be applied for surge and sway when the empirical correction formulas for wave drift forces are applied.

Yang et al. (2018) presented numerical predictions of low frequency horizontal motions of a semi-submersible in combined high waves and current condition. Low frequency surge responses calculated by the simulation model are compared with model tests for waves only and for combined collinear and noncollinear wave and current conditions.

He et al. (2018) presented a set of VIM CFD simulations for a semi-submersible with and without helical strakes (Figure 144). The Vortex Induced Motion (VIM) of semi-submersible with and without helical strakes was compared against each other for different reduced velocities (Ur). The flow characteristics of the semi-submersible platform is studied based on the characteristics of vortex shedding. For different current incident angles, time histories, trajectories, and vorticity of the semi-submersible at different reduced velocities were reported.

Zhu et al. (2018) investigated the fatigue damage of stiffened plates in splash zone for a semi-submersible. A global analysis model of the Gjøa semi-submersible, is built and the local response for the side structure was investigated. The contribution of fatigue damage due to global and local load effects are compared and presented.

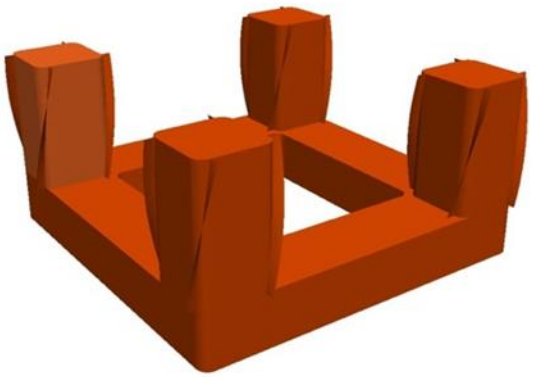

Figure 144: Semi-submersible with helical strakes (He et al., 2018)

Zhu (2018) designed a four column semi-submersible with low heave motions based on genetic algorithm. The geometry of a ring-pontoon four-column semi-submersible was

generated by parametric modelling. The heave transfer functions at the centre of gravity were calculated using WADAM. Genetic algorithm was used to find the most favourable heave responses. The parameters that influence the heave motions have been discussed.

Zhao and Wan (2018) presented a parametric study of geometrical variations on the vortex-induced motions (VIM) of a deep-draft semi-submersibles (DDS) - Figure 145. Paired-Column semi-submersible (PC-Semi) design involved paired-column gaps and column cross-section and these parameters could be tuned to mitigate dynamic response to waves and currents. A geometry model scaled at 1:54 from MARIN was selected as the baseline model for parametric study and CFD code validations. VIM characteristics of paired-column, gaps and other geometrical variations were numerically investigated. The ability of a CFD method in optimizing geometric design parameters for the mitigation of VIM response for a deep-draft semi-submersible was demonstrated.

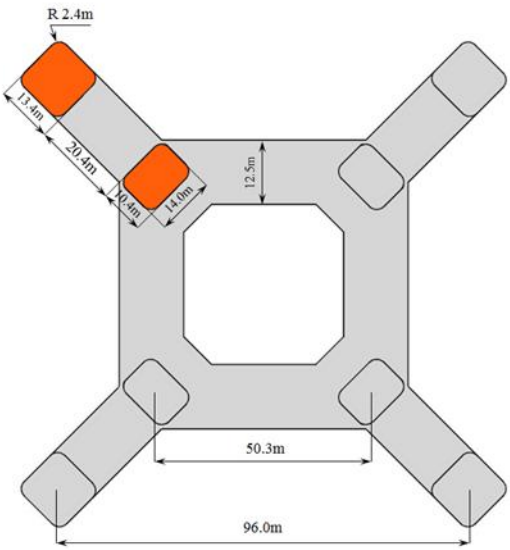

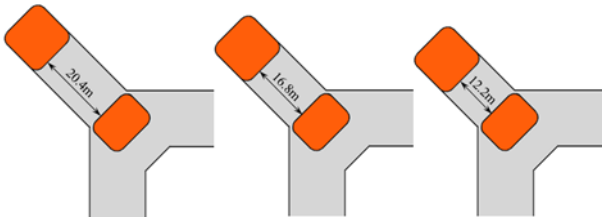

Figure 145: Geometrical Variations to mitigate VIM for PC-Semi (Zhao and Wan, 2018)

D.-J. Li et al. (2018) discussed the structural configuration selection and optimization design of 7th generation semi-submersible drilling unit (CSDU) based on the profound investigation on the load-resistance characteristics of the overall structures and considering the stress distribution variation of the deck box with the integration of different lower hull configurations. The study also investigated the effects of different types of upper and lower hull joints on the structural strength and fatigue in way of the main connection regions and provides the major connection optimization design.

Liang and Tao (2018) concentrated on the hydrodynamics around a deep-draft semi-submersible (DDS) to investigate the corner shape effects. Three models based on a typical DDS design with different corner shapes were numerically investigated under 45° incidence. It is demonstrated that, as the corner shape design changed, the hydrodynamic characteristics alter drastically. The flow patterns examined revealed some insights of the fluid physics due to the changing of different corner shape designs.

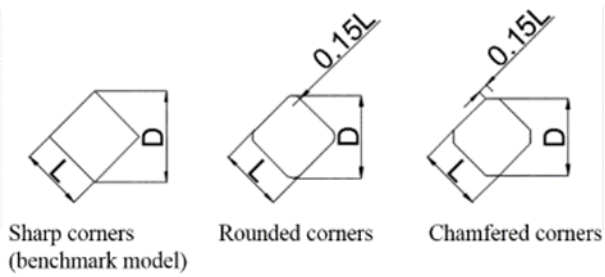

Figure 146: Corner shape effects for DDS (Liang and Tao, 2018)

Kim et al. (2019) conducted experimental and numerical study of horizontal wave impact loads for a semi-submersible drilling unit (Figure 147). A semi-submersible drilling unit model was tested to estimate horizontal wave impact loads on vertical side of deckbox following the procedure recommended by DNVGL OTG-14. The model test data showed that there is clear difference in the relationships between upwell and horizontal wave impact pressure between near column/pontoon and around centreline. The CFD simulation results clearly showed that the flows in front of column are strongly accelerated in vertical direction by blocking effect of column and pontoon, eventually producing strong run-up jets.

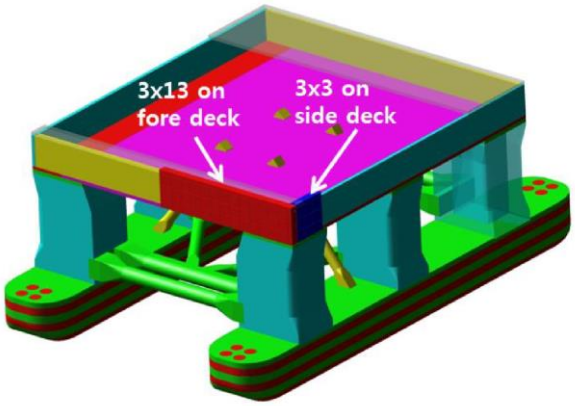

Figure 147: Semi-submersible drilling unit with force sensors to measure wave slamming loads (Kim et al., 2019)

Seo et al. (2019) also conducted experimental evaluation of wave impact loads on a semi-submersible structure according to trim angle. To evaluate wave impact loads on the semi-submersible structure, a series of experiments were conducted in a 2D wave flume. In the experimental test, a half-model semi-submersible was used, and 11 uniaxial force sensors were installed on deck side, column side, and deck bottom. To generate horizontal and bottom wave impact on the test model, focusing wave was applied. The model was fixed without any motion during each test, while the trim angle of the model was changed to examine the effect of trim angle on wave impact load. Through this, the characteristics of the wave impact force at each position were investigated.

Gonçalves et al. (2020) conducted an experimental study of the effect of the pontoon dimensions on flow-induced motions (FIM) of a semi-submersible platform with four square columns (Figure 148). FIM is an essential topic on multi-column platforms due to the effect on the mooring line fatigue life. Vortex-Induced Motions (VIM) or galloping behaviour can be observed for an array of four columns with square sections. The presence of pontoons showed to be important for changing the flow around the array and promoting different amplitude behaviours of the motions in the transverse direction.

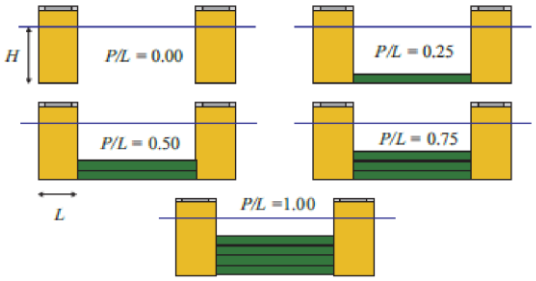

Figure 148: Five different pontoon ratios tested by Gonçalves et al. (2020)

Although some model-scale experiments have been conducted, there are still limited experimental studies especially pertaining to VIM and hydrodynamic loading estimation for semi-submersible floaters. Most of the studies are limited to CFD evaluations for a general description of the phenomenon. Therefore, it is recommended to conduct state of the art benchmark experiments to validate the use of different column designs and use of helical strakes in columns for VIM study.

2.2.3 TLPs

During the review period, TLPs behaviour has been investigated numerical and experimentally with special focus on responses under extreme wave conditions. For instance, Abdussamie et al. (2017) provided detailed experimental information on the global behaviour of a TLP due to wave-in-deck events in abnormal waves. The wave events that produced the maximum and minimum tendon tension generally did not correspond to the largest wave crest or the largest wave steepness; this indicates that selection of the design wave event or wave train, in the same sea state, may require special attention (Figure 149). Lim and Kim (2019) investigated the statistical behaviour of the airgap of a TLP based on potential flow theory up to second order to model wave elevation around the platform and eigen-value method to estimate the extreme airgap. The effect of short-crestedness and the platform set-down were investigated. Yu et al. (2019) investigated numerically a series of tendon one-time failure and progressive failure for a whole TLP with top-tension risers under an extreme cyclone. Different directions of environment load that include extreme wind, wave and current and tendon failure positions were considered.

Also of interest is the dynamic interaction of TLPs with other bodies, such as moored vessels, auxiliary platforms, etc. Choi et al. (2018) have conducted experimental and numerical analyses to investigate the coupled behaviour of a TLP combined with a tender semi-submersible platform with focus on the multi-modal behaviours. Free decay tests showed that the TLP and semi-submersible system had complex coupled behaviours with multiple natural mode frequency components. Dong et al. (2019) have systematically investigated the TLP - Tender Assisted Drilling coupled system under 0°, 45° and 90° headings by numerical and experimental analyses (Figure 150). The focus was on the global motion performance of the multi-body system, relative motion between gangway connection points, characteristics of dynamic gangway responses with predictions for extreme values and the definition of extreme sea conditions. Experiments with a 1:40 scale including decay tests, static offset tests, white noise wave tests, and irregular wave tests has been performed to validate the numerical model and addressed the difficulty of modelling of tendons, risers of TLP, hawsers and mooring lines.

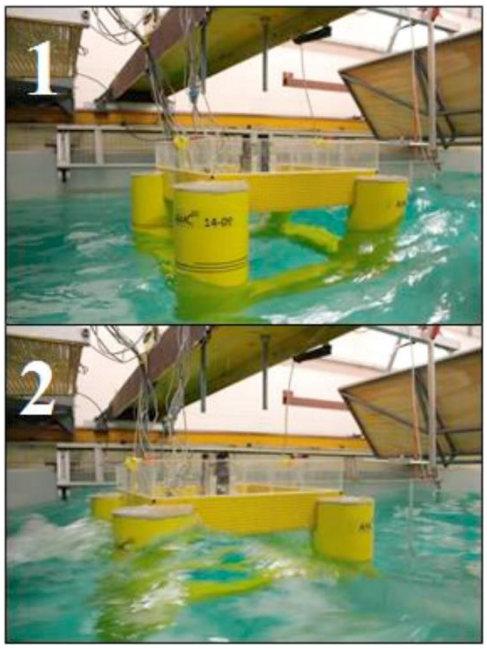

Figure 149: Wave impact at the TLP model: (1) water entry; (2) water exit (wave propagating from right to left) - Abdussamie et al. (2017)

Concerning TLPs design, Zhang et al. (2018) have proposed Innovative TLP Optimization Program (ITOP) to solve the multi-objective optimization problem for a TLP. Hull draft, column spacing, column diameter, pontoon height, and pontoon width are selected as design variables. The objective functions include the maximum dynamic tendon tension and the total weight of the platform, with three constraints being the maximum heave motion, the maximum surge motion, and the minimum airgap.

Figure 150: Experiment of TLP-TAD coupled system (Dong et al., 2019)

2.2.4 Spar platforms

Recently, spar platform has become one of the most attractive deep-water development concepts thanks to its superior stability and powerful operability in deep water offshore regions. Benefits of the deep drafted first-generation classic spar, such as excellent stability and hydrodynamic performances that allow dry tree drilling and production, large capacity of the mid hull section for oil storage, cost efficiency for construction and save in-service operations, are combined to provide a competitive solution from moderate deep water of 300 m to ultra-deep water of 3000 m. COOEC (China Offshore Oil Engineering Company) has made a great breakthrough to the new Spar Drilling Production Storage Offloading Platform (SDPSO) and therefore has successfully mastered the water-oil replacement technology (Figure 151). The integrated innovation technology creates a new model of integrating the drilling, production, storage, and exporting, and will lead the "second" deep-water technology revolution if applied successfully in engineering. The oil-water replacement technology is a core and key technology for SDPSO underwater wet storage (W. Liu et al., 2017).

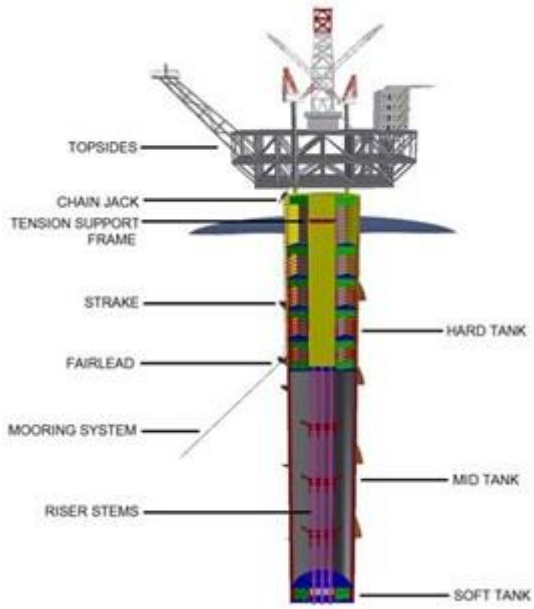

Figure 151: SDPSO Model (W. Liu et al., 2017)

Research has been carried out to address the global motions of spar platforms in waves, currents, and wind. Soeb et al. (2017) investigated the response of a fully coupled spar platform under a regular ocean environment. Considering the coupling effect of the platform and its mooring system, the responses of the spar platform were extracted and evaluated in time histories along with Response Amplitude Operator (RAO). The behaviours of coupled spar platforms were investigated under real sea environments for increasing water depth to ultra-deep together with the load variability employing sea current for surge, heave, pitch, and mooring tension responses. They modelled the integrated spar hull and mooring line in finite element code ABAQUS/AQUA. Motions showed consistency in the behaviour of spar platform responses. Surge response indicated the static offset of the platform due to the static current force under wave plus current and the current force compressed oscillations and reduced heave and pitch magnitude. For larger water depth, the platform responses were reduced significantly due to the increased damping of the mooring line.

Jin et al. (2018) focused on the influence of small-scale cylinders on the motion response under wave action to estimate the response more accurately. A mooring truss spar platform was used with a second-order wave-body interaction numerical model in the time domain based on the Laplace equation. This numerical model simulated the large amplitude slow drift motion of the truss spar platform under bi-chromatic waves. The results showed that small-scale cylinders influence damping. At the same time, the existence of small-scale cylinders increased the added mass of the platform, thus the nature frequency was changed and moved to lower frequency, which led to large amplitude slow drift motion of the structure.

VIV and VIM are phenomena that affect several offshore compliant structures such as spars. Harsh environmental conditions can induce VIV and VIM and cause the failure of these structures. In the recent years, several investigations have addressed those problems and ways to mitigated them. Sun et al. (2018) employed the discrete vortex method (DVM) based on the stream function equation and vorticity formulation to study large vortex-induced motions (VIM). Sway and surge displayed similar periodic vibration. As the reduced velocity increased, surge displacement got larger and changed from irregular-amplitude to stable-amplitude motions with a well-defined period. As the Reynolds number (Re) increased, initially, the sway displacement was in direct proportion to the Re, but then its amplitude ratio (amplitude/diameter) exceeded 1.0, and after, decreased to less than 1.0, evidencing the "lock-in" phenomenon. The VIM trajectory was not clear and regular at low reduced velocities. With the increase of Re, the trajectory exhibited an obvious shape of "8" that gradually become more regular, i.e., periodic, and repeatable. Kumar et al. (2018) focused on the experimental investigations of an elastically mounted circular cylinder shrouded with a net substructure called Ventilated Net (VN) to suppress VIV. The VN was an omnidirectional, economical, customizable net substructure comprising flexible hollow tubes in a systematic arrangement. This device could be retrofitted to the offshore structures/risers to attenuate VIV. Various configurations have been tested to address the reduction of VIV and drag forces acting on the oscillating cylinder shrouded with VN. VIV amplitudes have been measured at high Re regime, ranging from $(0.22–2.50) \times 10^5$. The effect of spaces between the flexible hollow tubes and shrouding radii of VN around the cylinder was also addressed. It was observed that a cylinder with VN of dense mesh at a radial spacing of twice the diameter of the bare cylinder, suppresses VIV by 98% and drag force by 40%, at Re of 1.2×10^5.

Samadi and Ghodsi Hassanabad (2017) analysed the catenary mooring of a non-classical spar truss platform in the Caspian Sea. The hydrodynamic analysis including the mooring system was based on the three-dimensional diffraction method. The effect of removing mooring lines was also investigated. Under that condition, roll and pitch motions were not significantly affected and kept their stability but sudden changes in surge motions were observed.

W. Li et al. (2018) investigated the nonlinear coupling internal resonance of heave, roll, and pitch motions of a spar platform when their frequencies are in the ratio of 2:1:1 under wave and vortex exciting loads. Three degree-of-freedom (DOF) nonlinear coupled equations were established by considering a time-varying wet surface with a first-order wave force in heave and pitch and a vortex-induced force in the roll motions equation. The first-order steady-state response was solved using the multi-scale method. Multiple solutions of the motion equations using an analytic method and a numerical simulation were discussed. The jump phenomenon and regions of multiple solutions depending on the values of damping and detuning parameter were detected.

O'Connell et al. (2018) developed a Computational Fluid Dynamics (CFD) model for a free heaving Oscillating Water Column (OWC) spar buoy with non-linear Power Take-Off (PTO). A comprehensive system comprising of the 3D numerical wave tank, 1-DOF set-up, and non-linear PTO allowed the development of a heave-only OWC spar buoy model with a non-linear PTO. Experiments completed by the UCC MaREI centre in LIR-NOTF ocean wave basin under the FP7 MARINET project were detailed and used to validate the comprehensive model. A range of regular waves was applied, and responses of heave and chamber pressures were compared to experimental data.

Yang and Xu (2018) analysed the parametric instability of a spar platform in irregular waves. A Hill equation was derived in this work, which can be used to analyse the parametric resonance under multi-frequency excitations. The derived the Hill equation for predicting the instability of a spar included non-harmonic excitation and random phases. The stability charts for multi-frequency excitation in irregular waves were given and compared with that for single-frequency excitation in regular waves. Three-dimensional stability charts with various damping coefficients for irregular waves were also investigated. The results showed that the stability properties in irregular waves have notable differences compared with those in the case of regular waves.

Banik et al. (2019) investigated the effect of the directionality of waves on the responses of a spar-type floating offshore platform restrained by four catenary mooring cables. The numerical model and simulation were validated based on experimental results (natural periods, RAOs, and response statistics).

Montasir et al. (2019) presented the effect of mooring diameters, fairlead slopes, and pretensions on the dynamic responses of a truss spar platform in intact and damaged line conditions. The spar was modelled as a rigid body with three degrees-of-freedom. The implicit Newmark Beta technique was used to analyse its motions in time-domain. The mooring restoring force-excursion relationship was evaluated using a quasi-static approach. To eliminate the conventional trial and error approach in the mooring system design, a numerical tool was settled and described.

Wang and Zhou (2020) carried out numerical simulations and experiments about the scale effect of internal solitary wave loads on spar platforms. The scale effect on the viscous pressure-difference force is important while the scale effect on the wave pressure-difference force is not clear for the horizontal force. Morison equation with the same set of inertia and drag coefficients is not applicable to estimate the internal solitary wave loads for both the prototype and experimental model. Those coefficients should be modified to account for the scale effect. It is possible to get dimensionless vertical forces measured in model scale and use directly on the prototype based on Froude similitude. However, for the dimensionless horizontal force, the measured values in the laboratory will overestimate the corresponding values on the prototype if the Froude extrapolation laws are directly applied.

Subbulakshmi and Sundaravadivelu (2021) investigated the heave and pitch responses of spar platforms with single and double damping plates under regular waves. Damping plates are generally used to decrease the response of the floating platform by increasing the added mass and damping. Regular wave experiments were conducted on a 1:50 scale spar hull with damping plates. Heave and pitch response amplitude operators (RAOs) were numerically predicted using ANSYS-AQWA and compared with model test results. Parameters of scaling ratios such as damping plate diameter to spar diameter ratio, damping plate position to spar draft ratio and spacing between the double damping plates to spar draft ratio were

considered for the analysis. Heave and pitch RAOs reduced with an increase in scaling ratio. Diameter ratios of 1.2–1.4, position to spar draft ratio of 0.16, and spacing to spar draft ratio of 0.16 were suggested for reducing the heave response. Similarly, diameter ratios of 1.2–1.4, position to spar draft ratio of 0.12 and spacing to spar draft ratio of 0.2 were recommended for pitch response reduction.

2.2.5 Floating LNG Production Storage and Offloading Vessels

The concept of Floating Liquefied Natural Gas (FLNG) has been developed over the past few decades with the increasing demands in LNG. Although the FLNG hull is usually designed to be a typical ship type which is similar to an FPSO, it owns great volume of displacement and large LNG tanks. In addition, FLNG has higher centre of gravity due to the low density of LNG and larger waterline area. Therefore, hydrodynamic characteristics of the FLNG are different from those of the FPSO.

Z.-Q. Hu et al. (2017) performed experimental analysis and numerical modelling with aims to address the inner-tank sloshing effect on motion responses of a FLNG system (Figure 152). The results show that LNG-tank sloshing has a noticeable impact on the roll motion response of the FLNG and a moderate tank filling level is less helpful in reducing the roll motion response.

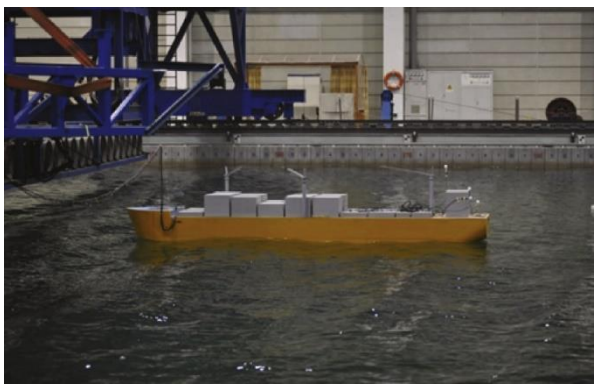

Figure 152: FLNG vessel model test setup in the basin (Z.-Q. Hu et al., 2017)

Zhao et al. (2017) presented an experimental investigation on dynamic responses of the connection system in the FLNG system during side-by-side offloading operations. Three typical irregular wave cases are used in the model test. Relationships between relative vessel motion and the load born by the connection system are obtained, and features of dynamic connection system responses are summarized. The results show that hawsers and fenders at different locations are sensitive to different motion patterns; loads on connection systems have distinct dynamic properties, and snap loading crucial to the safety of offloading processes can be induced. Moreover, FLNG is subjected to large low-frequency responses in side-by-side configurations due to hydrodynamic interactions and sloshing effects.

Y. Jin et al. (2018) presented numerical investigations of hydrodynamic interactions of a conceptual FLNG-LNG offloading system in regular head sea waves by using an unsteady Reynolds-Averaged Navier-Stokes solver. The gap wave responses and wave loads on the FLNG and LNG vessels were studied for different wave frequencies and varying lateral separations. The gap wave resonance appears when the incident wave frequency approaches the natural frequency of the gap fluid, resulting in significant variation of wave loads in the directions of sway, heave, pitch, and yaw.

Vieira et al. (2018) set up an experimental arrangement (Figure 153) to investigate the influence of the liquid inside the tanks in the wave behaviour of FLNG. The study comprised the vessel evaluation both in isolated and in side-by-side configurations. The latter considered the vessel operating close to an LNG carrier, emulating an offloading operation. The study shows that the analysis of coupled systems considering all the above effects is very important for the correct definition of the

dynamics of the vessels. Not considering one of these effects may underestimate the vessels motions and consequently underestimate the efforts regarding mooring lines, fenders, and the necessary power to carry out the operations with tugboats.

Zhao et al. (2018) developed a numerical code based on potential flow to investigate the coupling interaction between 6 degrees of freedom vessel motions and internal nonlinear sloshing. The impulsive response function (IRF) method and the boundary element method (BEM) is adopted to resolve vessel motions and internal liquid sloshing, respectively. The results show that significant coupling effects can be induced in beam sea conditions between sway and roll motions and internal sloshing; heave motion is slightly affected by internal sloshing. Besides, coupling effects will increase rapidly when the natural sloshing frequency is close to the main response frequency region of the ship.

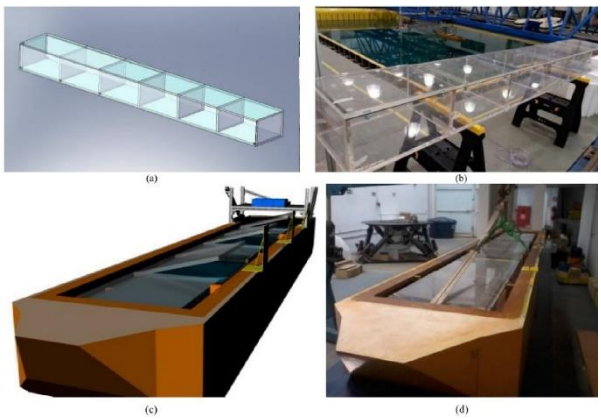

Figure 153 FLNG scaled model. Legend: (a) FLNG tanks (CAD), (b) FLNG acrylic tanks, (c) FLNG complete model (CAD), (d) FLNG complete model (Vieira et al., 2018)

Jin et al. (2019) investigated the hydrodynamics of a FLNG-LNG offloading system in a side-by-side configuration by using potential flow solver ANSYS AQWA. Time domain analyses are carried out for the FLNG-LNG system coupled with hawser, fender, and mooring systems under the combination of wind, current and waves. And the effects of varying hawser pretension and stiffness on the hydrodynamic performance are investigated.

Kawahashi et al. (2019) performed model experiments in an ocean model basin and discussed the coupling influence of FLNG motions with internal liquid sloshing. To verify the liquid cargo effect, the FLNG model was tested under two conditions: a liquid cargo condition and a fixed solid-cargo condition. The results show that the effect of internal liquid is significant for sway and roll motion (Figure 154).

Meng et al. (2021) developed a two-dimensional computational fluid dynamics (CFD) model for the structural packed column which is applied in FLNG in offshore platforms. The results show that the sloshing angle has significant effects on the liquid volume fraction in the central region of the column.

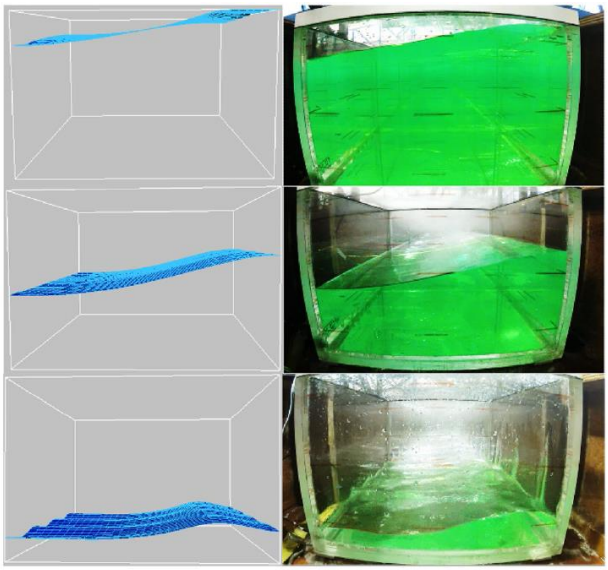

Figure 154 Free surface deformations in resonant period for different filling conditions: top: 90%, middle: 50%, bottom: 15% (Kawahashi et al., 2019)

2.2.6 Floating Offshore Wind Turbines (FOWT)

The application of floating stationary platforms as basis for wind turbines continues to attract the attention of the ocean engineering community. Semisubmersibles and TLPs have concentrated the major interest.

Some of the concepts related to semisubmersibles are:

Murai and Takahashi (2017) reported a study on the influence of arrangement of an array of semi-submersible type FOWTs (Figure 155). The study focused on hydrodynamic response of a wind farm and the investigation of how the arrangement of the array impacts on the hydrodynamic response including the motion of the nacelle. The change of the expected efficiency of the generator by change of the array arrangement in each sea area around Japan was discussed as an example scenario.

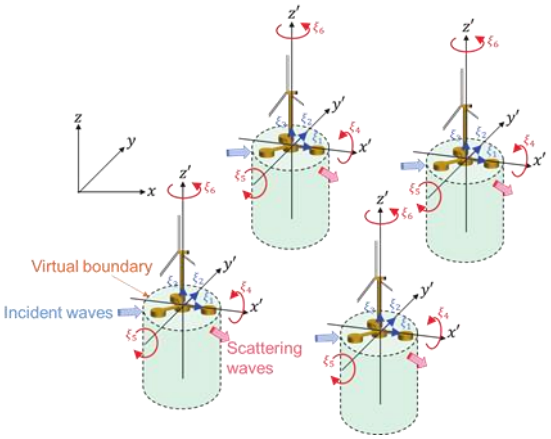

Figure 155: Hydrodynamic response of array of semi-submersibles (Murai and Takahashi, 2017)

Karimirad et al. (2017) compared real-time hybrid model testing (ReaTHM®) and numerical simulations of a braceless semi-submersible wind turbine. The experimental data was from a 1:30 scaled model of a semi-submersible wind turbine. Coupled aero-hydro-servo-elastic simulations were performed in MARINTEK's SIMA software. Low-frequency hydrodynamic excitation and damping are seen to be important, but these loads include a combination of viscous and potential forces. For the braceless semi-submersible concept, the second order potential flow forces have limited effects on the responses.

Krishnan and Seeninaidu (2017) investigated the hydrodynamic analysis of three column semi-submersible with vertical axis wind turbine (VAWT) in parked condition under regular and random waves. Free decay experiments were conducted for using scale model (1:75) in a laboratory wave basin and numerical simulations of hydrodynamic motion response of the floater were carried out using potential flow theory based on commercial software (ANSYS AQWA). The damping values obtained from experiments were used in numerical simulations to obtain motion response and Response Amplitude Operator (RAO).

Hegseth et al. (2018) presented the comparisons and validations of hydrodynamic load models for a semi-submersible floating wind turbine. A simplified method to include distributed, large volume hydrodynamics in the global analysis was considered. Furthermore, frequency-dependent loads from potential theory were applied on a finite element (FE) model of the hull in a strip-wise manner. The method is compared to a conventional load model for a braceless 5 MW semi-submersible FWT and validated against experimental results from model tests with focus on internal loads and rigid body motions in the main wave-frequency range. In combined wave-wind conditions, the measured bending moments are significantly increased because of the wind-induced mean angle of the platform.

Robertson et al. (2018) attempted to assess the sources of experimental uncertainty in an offshore wind validation campaign focused on better understanding the nonlinear hydrodynamic response behaviour of a floating semisubmersible. The test specimen and conditions were simplified compared to other floating wind test campaigns to reduce potential

sources of uncertainties and better focus on the hydrodynamic load attributes.

Kvittem et al. (2018) carried out a study focusing on the process of calibrating a numerical model to the experimental results of a 1:36 scale model of the public version of the 10 MW OO-Star Wind Floater semi-submersible offshore wind turbine. The hull was considered as rigid, while bar elements were used to model the mooring system and tower in a coupled finite element approach. First-order frequency-dependent added mass, potential damping, and excitation forces/moments were evaluated across a range of frequencies using a panel method. Distributed viscous forces on the hull and mooring lines were added to the numerical model according to Morison's equation. Potential difference-frequency excitation forces were also included by applying Newman's approximation.

Thys et al. (2018) presented the real-time hybrid model (ReaTHM®) tests that were performed on a 10-MW semi-submersible floating wind turbine in the Ocean Basin at SINTEF Ocean in March 2018. The physical model was subjected to physical waves, while the rotor and tower loads were simulated in real-time and applied on the model by use of a cable-driven parallel robot. Recent advances in the ReaTHM test method allowed for extended testing possibilities and load application up to the 3p frequency and the first tower bending frequency.

The study by Zhao et al. (2020) proposed a method for the structural control of an ultra-large semi-submersible floating offshore wind turbine. A 10 MW wind turbine braceless semi-submersible with an ideal tuned mass damper (TMD) installed in the nacelle of the FOWT was proposed to dynamically compensate the vibrations and reduce the structural loads. A fully coupled time-domain simulation of the FOWT with active TMD subjected to a set of environmental conditions was conducted using FAST, and the effect of the TMD on the load reduction of the FOWT was analysed.

Concerning TLPs equipped with FOWT, the following works may be of interest:

Oguz et al. (2018) describe an experimental and numerical investigation of the Iberdrola TLP wind turbine concept, TLPWIND, in realistic wind and wave conditions. The TLP was coupled to the NREL 5 MW reference turbine and was designed to operate in a water depth of 70 m. The test campaign included free oscillation tests, tests in regular and irregular waves and simulated wind conditions. A software-in-the-loop approach was adopted to account for the time-varying aerodynamic forces produced by the turbine during the physical experiments. The effect of wind was found to have a significant contribution to the overall response of the platform whilst variation in wave conditions was found to have a relatively small effect on the platform response.

Kiamini et al. (2018) proposed the stabilization control of a 5 MW tension leg platform used as FOWT. The TLP was structurally controlled based on fuzzy controller and its structural behaviour was evaluated in the presence of uncertainty, time delays and disturbances.

Figure 156: Extreme irregular wave test (Oguz et al., 2018)

Ren et al. (2018) presented a new concept by combining a 5 MW monopile type wind turbine and a heave-type wave energy converter, referred as the 'MWWC' (Monopile-WT-WEC-Combination) system (Figure 157). Hydrodynamic responses of the MWWC system under typical operational seas cases have been investigated by using both time-domain numerical simulations and scale model tests (1:50). For the numerical model, hydrodynamic loads of the monopile and the WEC are calculated by the AQWA code. For the scale test model, two air-dampers simulated the absorption effect of the wave energy (through the PTO damping force) without air compressibility effect.

Uzunoglu and Guedes Soares (2019) presented a systematic approach to the hydrodynamic design of a tension leg platform to host the NREL 5 MW turbine. Model development, hydrostatics, mooring setup, and estimation of motion dynamics in frequency domain were discussed. The time domain model built in FAST was used to compare simulations and the frequency domain calculations.

Manikandan and Saha (2019) proposed a novel controller technique and its application in tension leg platform(TLP) supported OWT to harvest optimized power. The TLP is mooring line stabilized and has a 5 MW NREL wind turbine on top of it. The results showed that the proposed nonlinear quadratic regulator can control the power, generator torque and rotor speed effectively without additional increase in platform motions vis-á-vis existing conventional baseline controller.

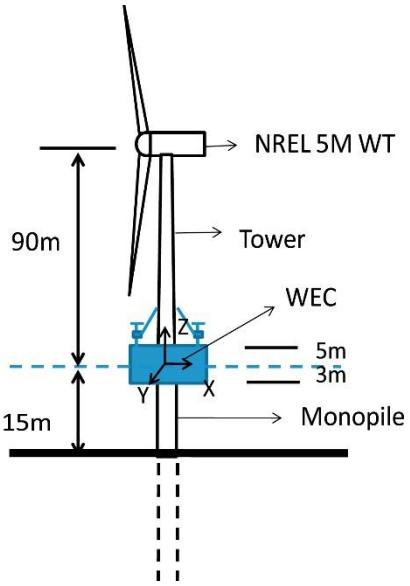

Figure 157: Sketch map of the MWWC concept system (Ren et al., 2018)

Chow et al. (2019) performed a validation study to test out the coupled 6-DoF rigid body motion solver, using the experimental results obtained for the floating wind turbine setup on a tensioned leg platform (Laugesen and Hansen, 2015). A modified restrain system was implemented to model the tendons with custom force-displacement functions and that also apply zero force when the ropes are slack.

2.3 Dynamically Positioned Floating Structures

In the recent years, advanced software-based protection systems to run DP with redundant power systems that are closer connected (closed bus-ties) are being introduced to produce more flexible designs to carry out efficient and environmentally friendly operations. Another trend is increased use of software to integrate more functions into larger software-dependent systems to ensure that DP vessels and operations comply with acceptable safety standards. Some of the most relevant recent works are described as follows:

Sayed et al. (2017) performed comparisons between numerical simulations based on an ice

dynamics model and an ice basin test of the dynamic positioning (DP) of a vessel in managed ice. The test case consisted of a vessel moving through a field of ice floes and brash ice (Figure 158). The set-up was intended to represent station keeping of a thruster-controlled vessel under the action of moving ice. Simulations were done to examine the effects of the ice basin set-up. The ice cover was driven using a uniform upstream velocity, while the vessel aimed to maintain position. The resulting thrust forces and offsets were close to those obtained with the set-up used in the ice basin test.

Figure 158: View of the ice basin and the model DP vessel (Sayed et al., 2017)

The positioning performances of the vessels with thruster failure modes was investigated by Xu et al. (2017) using time domain simulations. A novel synthesized positioning performance criterion was proposed to quantify the positioning performance including the aspects of positioning accuracy and power consumption. The synthesized criterion concerns how well the vessel is positioned rather than how large the environmental conditions the vessel can counteract. A semi-submersible employed with eight azimuth thrusters was adopted and six different thruster failure modes were considered. If the thruster system is well designed, thruster failure may not affect the thrust system in supplying sufficient thrust force with two or less than two thrusters' failure for the semi-submersible.

Detlefsen et al. (2017) presented a static and a time domain method to assess the position-keeping capability of mono hull vessels. For the static analysis method, the equilibrium between mean environmental loads and available actuator forces is determined. In case of the dynamic assessment, the motions of the fully actuated ship in all degrees of freedom are simulated in time domain and evaluated by criteria regarding the position and heading of the ship. The developed time domain simulation method benefits from the computational efficiency of linear strip methods in frequency domain, whereas important nonlinear force contributions were directly handled in time domain. The simulation results have been compared with model tests that were performed by Potsdam Model Basin and included measurements of fixed and free models in regular and irregular waves as well as dynamic capability test with a fully actuated model of an offshore supply vessel.

Skjong and Pedersen (2017) studied a co-simulation case study of a marine offshore surface vessel in Dynamic Positioning (DP) operation, where the DP-controller is placed on an Arduino micro-controller. This enabled the use of suited modelling software for different types of dynamical systems, as well as hardware, such as micro-controllers for Hardware-In-the-Loop testing in Figure 159. Such an integrated and open simulation method facilitated the development of new products as well as shortening the iterative process in design phases. As for co-simulation standard, the Functional Mock-up Interface (FMI) for co-simulation was used, and a communication Functional Mock-up Unit (FMU) that communicated with hardware and handled the signal flow between the hardware and the co-simulation was developed. The total co-simulation model consisted of a vessel model, including e.g. propulsors and environmental forces such as irregular wave forces and current forces, a nonlinear passive observer to filter out high frequent wave generated vessel motions, a serial

communication model, a reference model, in addition to a DP-control law uploaded to the micro-controller. The simulation results showed that even though the micro-controller is set to communicate with a lower frequency than the rest of the co-simulation sub-models, the total co-simulation is stable and produced good results.

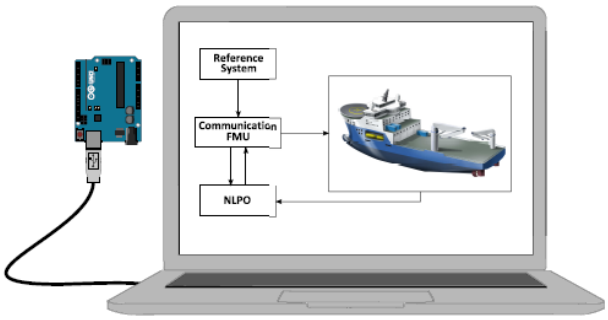

Figure 159: Co-Simulation of offshore marine vessel in DP operation using a hardware microcontroller as DP controller (Skjong and Pedersen, 2017)

Koop et al. (2017) presented the thruster-hull interaction effects for a drillship with 6 azimuth thrusters. The approaches investigated were the so-called Frozen Rotor approach, where the propeller rotation is modelled, the Actuator Disk approach with prescribed body forces and the unsteady Sliding Interface approach where the motion of the propeller was simulated in time. From the open-water calculations it was concluded that, using a Frozen Rotor approach, the propeller and nozzle thrust from the CFD correspond well with the experiments especially at bollard pull conditions. The thruster-hull interaction of one active thruster under the drillship was investigated using the three approaches. A comparison with experimental results was presented for the thruster-hull interaction coefficients. Using the Actuator Disk approach, a good agreement with the experiments was obtained. The results using the Actuator Disk and Sliding Interface were very similar to each other, but the computational costs for the Sliding Interface method were, at least, a factor of 20 higher. The results using the Frozen Rotor deviated due to an unphysical wake behind the thruster.

Zhang et al. (2017) studied the flow interaction between a dynamic positioning (DP) thruster and a floating structure (semi-submersible) hull. The Spalart-Allmaras RANS model has been evaluated to simulate a single thruster rotating in open water, with OpenFOAM. The actual thruster geometry was meshed with structured grid, and the gap between the blade tip and nozzle was carefully treated. The Moving Reference Frame (MRF) method was used for steady state simulation, and the arbitrary mesh interface (AMI) method was applied to simulate the rotating blade for transient dynamic mesh simulation. Experimental data from a JIP project conducted at MARIN with a single straight thruster at different RPMs, advance coefficients and inflow angles were used to validate the numerical simulations. It was concluded that the OpenFOAM was capable to handle such complicated investigation with both MRF method and dynamic mesh method.

Bjørnø et al. (2017) studied a thruster-assisted position mooring (TAPM) system with different control functions for station keeping and motion damping for a moored offshore vessel assisted by thrusters. The thrusters were used to provide damping and some restoring to the vessel motion to compensate if a line breakage occurs. The mooring system absorbed the main loads to keep the vessel in place. The complete modelling, parameter identification, and control design for a 1:90 scaled TAPM model vessel was reported. The experiments focus on the set-point chasing algorithm, where the position setpoint slowly moved to the equilibrium position while the environmental loads were balanced by the mooring forces. This approach avoided conflicts between the mooring system and the control actions. If the environmental loads were too large so that the set-point exceeded a user-defined safety radius, the set-point was set to this radius and thruster

forces grew to support the mooring system in counteracting the environmental loads to avoid line breakage. The experiments using Statoil's Cat I Arctic Drillship with six thrusters and mooring line (Figure 160) showed that the vessel and set point chasing control algorithm behaved as expected, minimizing thruster usage, and maximizing utilization of mooring system.

Figure 160: The model test for thruster-assisted position mooring (Bjørnø et al., 2017)

Cozijn et al. (2017) investigated the wave orbital motions that may cause variations in the inflow conditions of thrusters, that, in turn, result in variations in thrust and torque. Physical scale model tests were carried out to investigate these thruster-wave interaction effects, with an azimuth thruster running at constant RPMs. The observed effects included changes in the mean thrust, torque values, and associated wave frequencies. The test conditions were systematically varied to investigate the effects of the incoming waves, the presence of the hull and the vessel motions. First, measurements were carried out on an azimuth thruster in open water conditions. Thrust and torque in regular waves were compared with bollard pull conditions. Second, measurements were carried out on the azimuth thruster under the hull of a vessel, which was rigidly connected to the basin carriage. Third, measurements were carried out on the same azimuth thruster under the hull of the vessel in a soft-mooring system. In open water conditions the wave orbital motions caused a reduction of mean unit thrust and the observed effect was strongest in short waves. In the presence of the hull the thruster-wave interaction effects were much less pronounced. Furthermore, the thrust variations were larger in long waves. A reduction of the mean unit thrust was observed, as well as wave frequency thrust variations. The effects were stronger than in the captive tests, suggesting that both the wave orbital motions and the vessel motions played a role. The overall mean thruster interaction losses were derived from a series of tests in regular waves and still water, with and without active thrusters. Depending on the wave period, thruster-wave interaction effects of 5-10% were found as shown in Figure 161.

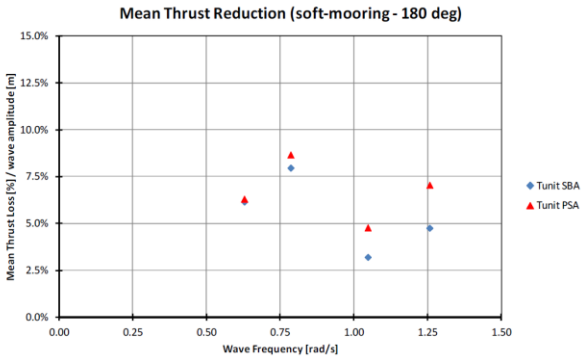

Figure 161: Mean thrust reduction due to thruster-wave interaction (Cozijn et al., 2017)

Pivano et al. (2017) presented the use of comprehensive dynamic operability analyses performed by time-domain simulations for understanding the vessel performance and limitations, providing reliable input to operational risk assessment and planning. The Dynamic Capability "DynCap" concept based on time-domain simulations (Level 3 in the new DNV GL standard) was introduced to overcome the traditional quasi-static approach. Full-scale validation of the DynCap concept was provided by comparing measurements from sea trials (with the platform supply vessel "Island Condor") with corresponding simulations using the DynCap methodology. DP footprint including standard deviations and max excursions for different vessel headings showed that the DynCap analysis was within the expected uncertainties in sea state measurements and the limited duration of the full-scale time series. A full DynCap wind envelope and power envelope for Island Condor was presented (Figure 162), including the

relevant full-scale data points. The results showed that DynCap simulations are comparable to full-scale measurements.

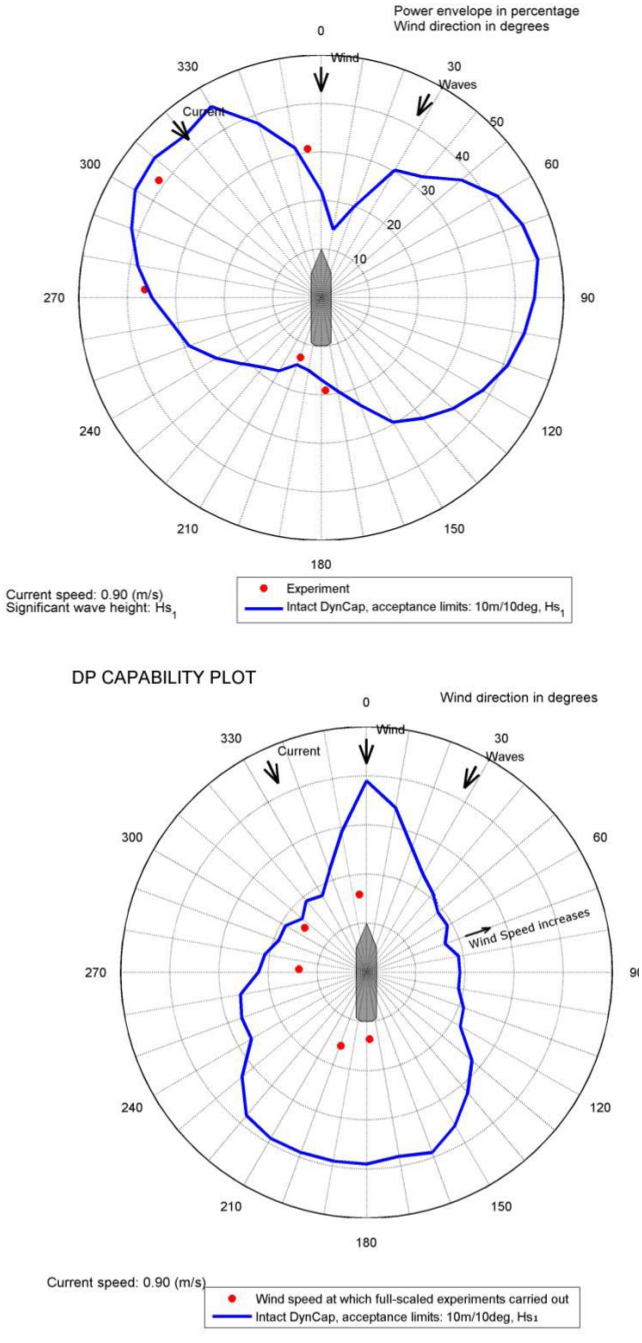

Figure 162: DynCap wind and power envelope comparison between experiments and simulations

Chen (2017) presented an overall framework for DP safety management in offshore marine operations. Three steps were considered: 1) identification of position loss scenarios, 2) risk analysis in terms of position loss frequency and consequences, and risk evaluation, 3) mitigation of risk via measures to eliminate the risk, or to reduce the likelihood of position loss, as well as to mitigate the consequences in marine operations given DP vessel position losses. Case studies from DP shuttle tankers and DP mobile offshore drilling units were presented to illustrate the key principles of each step. The challenges associated with this approach were: frequency of position loss, reliability of DP operators, and risk acceptance criteria for DP operations.

Huang et al. (2017) studied the utilization of a hold back vessel to support a drilling rig during the DP operation. Firstly, an analytical study of a simplified model of two vessels connected by a cable with two degrees of freedom (one for each vessel, i.e., the force applied by the cable was unidirectional) was considered. Using control theory, the limiting stiffness of the cable was determined by analysing the poles of the system. Considering a catenary model for the connecting cable, the maximum force that could be transmitted between the vessels without the system becoming unstable, was determined. The influence of the Kalman Filter in the stability of the system was also studied. It was shown that the hold-back vessel could be maintained in DP mode only when in stand-by, with the minimum cable traction required to avoid interference with the thrusters. When a higher force was applied, it was unsafe to operate with the hold-back vessel in DP mode, considering typical sizes of the vessels and the forces that should be transmitted. In summary, connecting two vessels reduced the stability margins of the system, requiring full attention of the operators since the DP was not designed to consider this external force. However, it may be a contingency solution to avoid drilling interruption and disconnection.

Li et al. (2018) investigated the approach of using supervised learning algorithms to estimate

thruster-thruster/current interactions between adjacent azimuth thrusters in tandem, based on scattered model test data. The model tests for thruster-thruster/current interaction study were conducted in a towing tank. As depicted in Figure 163, two ducted thrusters were mounted in tandem for thruster-thruster interaction and the inflow velocity ranged from 0.15 to 1.00 m/s for thruster-current interaction. The Gaussian radial basis function (RBF) network and feedforward neural network were applied to approximate the thrust efficiency function with respect to both thruster azimuth and current inflow velocity. The training results demonstrated that RBF network was not an appropriate model, mainly because of the insufficiency of the training sample. On the contrary, feedforward neural network performed much better in approximating the thrust efficiency function of the aft thruster, revealing its capability for handling complex function approximation problems even when the training set is not a big one.

Xu et al. (2018) presented the nonlinear time-domain mating simulations. The major findings were successfully applied in the design of the installation devices and in the selection of the dominant design parameters. The float-over vessel was equipped with 7 thrusters: two forward azimuth thrusters, one forward tunnel thruster, two aft tunnel thrusters and two aft main propellers. The vessel used DP mode in training and pre-entry stage but use manual mode in entry stage. So, a conventional method was used to simulate the float-over, entry, mating and exit stages. The float-over process was simulated in AQWA software, including hydrodynamic analysis, simulation of fenders & LMU mechanics.

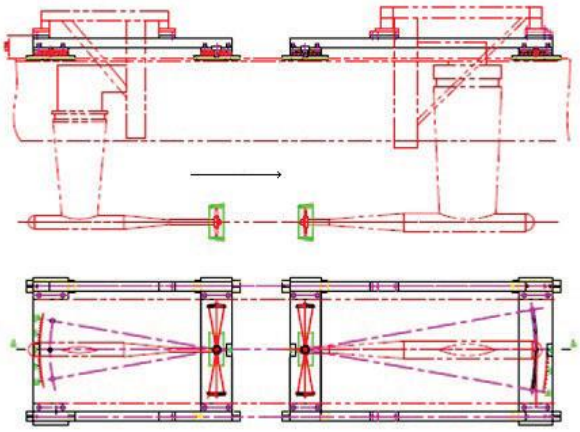

Figure 163: Test set-up for thruster-thruster/current interaction (Li et al., 2018)

X. Jin et al. (2018) presented a description of the DP float-over technology that was successfully applied in the float-over installation of the HZ25-8 DPP integrated topsides in South China Sea. A series of dynamic positioning (DP) model tests were conducted to assess the various float-over installation stages. Hydrostatic decay tests to calibrate the models, DP capacity tests at pre-defined survival conditions, docking tests and undocking tests at auto DP mode to ensure the feasibility at pre-defined operation conditions, and mating tests without DP operations were performed. A virtual simulation program was also developed to simulate the float-over installation of the 13000 Te integrated topsides with a dynamic positioning (DP2) semisubmersible vessel at a water depth of 100 m under a virtual reality environment of South China Sea.

Kerkeni et al. (2018) reported that standard DP systems may fail to perform in ice conditions and emphasized specific principles and position keeping philosophies that should be applied in ice covered waters. The tests were performed as a part of the station keeping trials performed in March 2017 in drifting ice in the Bay of Bothnia (Figure 164). Control algorithms limitations of Standard DP Systems were presented, showing the necessity of new control principles. The

importance of crew training was also demonstrated along with the approaches to keep position in ice. The limitations of a standard open water DP system to handle severe ice conditions were assessed at full scale. Station-keeping in manual control was successfully performed by the application of Dynamic Ice Loading Dodging (DIL-Dodging) manoeuvre. It combines the use of thrusters wake and heading changes to dodge ice floes and clear ice accumulation on the sides. The importance of the skilled operator was clearly observed.

Figure 164: Full scale DP test in ice (Kerkeni et al., 2018)

Harmsen et al. (2018) presented the instabilities caused by heavy lifting operation with the DP vessel connected to another fixed or floating objects through hoist wires. These DP-instabilities are caused by the inability of the DP system to handle the relatively stiff external spring of the hoist wire correctly. When two vessels are lifting a single object together (e.g., QUAD lift), existing solutions to prevent this DP-instability are insufficient, as the nature of such lift requires a synchronous move on DP. Heerema Marine Contractors presented the DP-stability challenges to Kongsberg Maritime, and a joint effort resulted in an implementation of a modified Kalman filter in the Kongsberg Maritime DP system. Also, a dedicated engineering analysis to predict risk of DP-instabilities for specific lift configurations has been developed. The modified DP-system was tested in large number of simulations (both desktop and a full mission simulator) to test the ability of the updated DP-system to deal with a wide range of specific heavy lift conditions. The system is tested during a dedicated DP-trial program onboard Thialf. As the results of all these tests were very successful, the new High Kalman filter was made available onboard Thialf as a permanent option next to the original functionalities. Offshore tests with High Kalman setting demonstrated the difference in DP stability for the oscillation periods of interest. These tests also showed that this Kalman setting provides good positioning ability for noisy reference systems. The High Kalman option leads to more thruster RPM and azimuth fluctuations. To prevent higher wear and tear of the thrusters, it should only be used when needed for a limited period of time.

Gundersen et al. (2018) studied a hawser-less tandem offloading operation between a FPSO and a DP shuttle. The structural limits of the flexible loading hose allowed for larger operational sectors and heading flexibility which enable the shuttle tanker to point away from the FPSO and hence reduce the probability of collision. An analysis model with two representative vessels for offloading operations in the North Sea was developed to investigate the new concept. The model included a compiled version of the DP system core algorithm, extracted from the real time system of both vessels. The new offloading strategy, with heading offset away from the FPSO was implemented in an updated control algorithm for the shuttle tanker. The complete tandem offloading system (Figure 165) has been simulated in time domain with measured wind, waves and current from a Hindcast database. Heading and relative motion between the FPSO and the shuttle tanker was statistically evaluated to determine the time in which the shuttle tanker is directed towards the FPSO. The proposed strategy reduced that time to a minimum, and prevented the risk of collision between the vessels, in case of a drive-off incident.

Fernandez et al. (2018) proposed a new concept of Dynamic Positioning Reliability Index (DP-RI) and a state-of-the art advisory decision-making tool. This tool was developed

based on information from various sources including Offshore Reliability Data (OREDA), International Marine Contractors Association (IMCA) Accident database, DP vendor equipment failure databases, DP System supplier's manuals, previous system level FMEA and HIL testing results, site specific risk analysis documents, project design specification and operator's operational experiences. The DP system was classified into various sub-systems using big data analysis and a correlation method. Each of the sub-systems has been given a weighting factor and a Reliability Index (RI) was calculated based on the DP class type, configuration, and mode of operation. DP-RI addressed the gaps found in the traditional reliability assessment methods of a DP system.

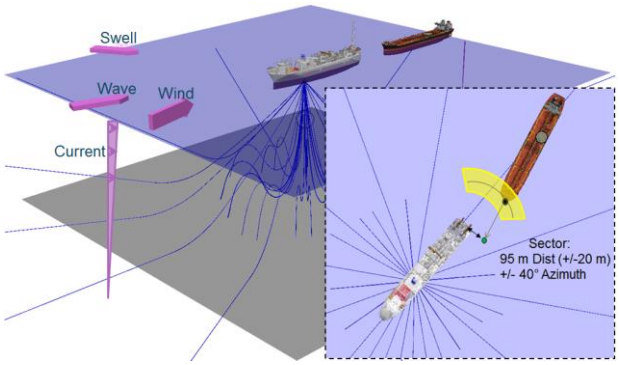

Figure 165: Time domain simulation model for FPSO and DP shuttle and tanker yellow restriction zone (Gundersen et al., 2018)

Lee et al. (2019) studied a heading control strategy to reduce the ice load acting on the arctic production platforms equipped with DP Assisted Mooring System. A heading control strategy considering real time tension under Artic conditions was proposed for safe and fuel-efficient operation. The strategy calculated the target heading using a ratio of the most loaded line and second loaded line. The target heading was an estimated direction of ice drift. From the simulations, the advanced performance in station-keeping of heading compared with no heading control was validated with 4 different conditions of ice drift direction.

An et al. (2019) applied the exogenous Kalman filter (XKF) algorithm to DP station-keeping numerical simulations. The algorithm was a two-stage cascade of NLO (Nonlinear Observer) and linearized KF, which used the first-stage NLO estimated states as exogenous inputs for the second-stage linearized KF. XKF approach had both the stability property inherited from NLO and the optimality from the linearized KF. To verify the applied XKF approach, a high fidelity 6 degree-of-freedom station-keeping vessel simulator was also developed. At the normal DP station-keeping scenario (Figure 166), the vessel stayed around the desired equilibrium point with the DP control action and showed similar errors in motions and velocities between NLO and XKF. The advantage of XKF comparing to the NLO is the error covariance calculations that can be monitored by DP operators.

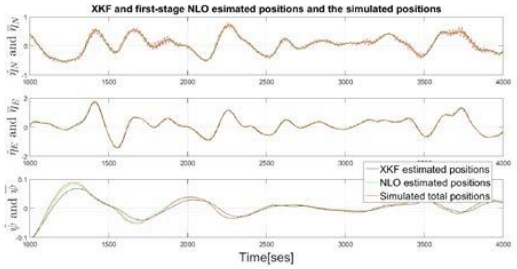

Figure 166: XKF Estimated vessel positions at normal DP station keeping simulation (An et al., 2019)

Moreno et al. (2019) developed a control system for an innovative configuration for oil transfer between a DP shuttle and a conventional tanker, using a modified tandem configuration. A control system design applied to the DP vessel inside the offloading site was investigated. This control applies two individual sliding mode controllers for rudder and thruster control, with coefficients obtained from numerical simulations, associated with a line-of-sight strategy for course and speed over ground controllers. Control performance and operation safety were evaluated through a set of real-time simulations of the transfer operation, where performance was evaluated through

measurement of the Bow Loading System point position in both straight-line navigation and in a 10 km radius curve. Real-time simulations showed that a lateral and longitudinal distance of, both, 50 m was enough to provide a safe escape route in case of a control drive-off failure.

Yenduri et al. (2019) presented a novel DP system for a flotel operating aside a FPSO. The system included an adaptive controller combined with an optimized thruster allocation law and a sea state detector. An optimized allocation algorithm for lower fuel consumption, wear, and tear of the thruster equipment and to ensure the resultant command in the respective direction of the azimuth thrusters was designed. The simulation results showed that the flotel exhibits nearly same mean offset as the FPSO (Figure 167).

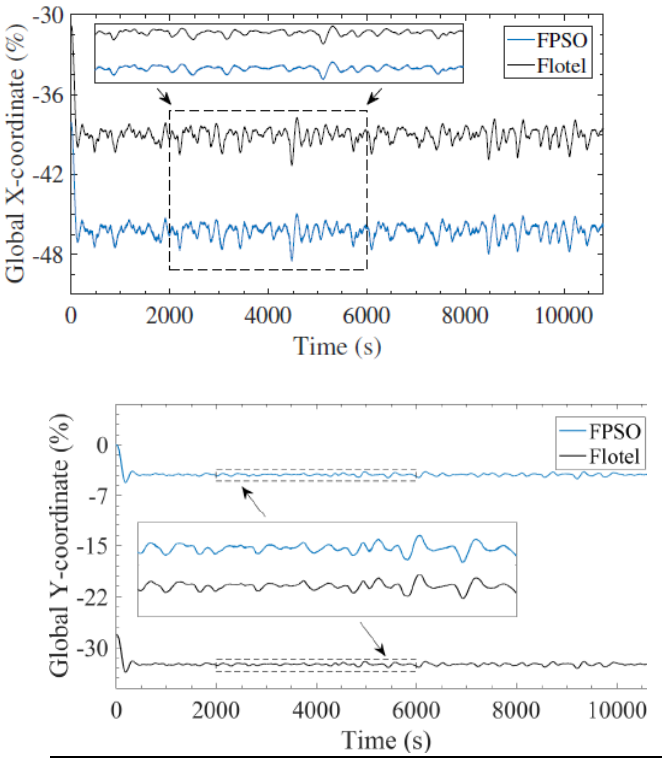

Figure 167: Demonstration of offset between flotel and FPSO by using DP system with adaptive neural network controller (Yenduri et al., 2019)

Fernandez et al. (2019) presented the Analytic Hierarchy Process (AHP) methodology for weight assignment among the DP subsystems. The developed DP-RI (Reliability Index) tool showed that the AHP technique was effective (Figure 168). Further, it eliminated the inherent uncertainty and level of inconsistency in the decision making during critical operations. The systematic assignment of weightings was attained through clear definition of criteria, objectives and data collection from experts and comparing against the results obtained through a machine learning algorithm with actual data from DP vessels.

A. M. Wang et al. (2019) presented a comprehensive description of an innovative training program and its successful simulation application, including virtual reality (VR) simulations of offshore field, numerical and visual modelling of met-ocean environment and DP2 float-over vessel, and performance of key personnel when executing float-over operations. The simulation scenarios are tested under normal/anticipated environmental conditions and extreme environmental conditions, as well as several stressful conditions, such as thruster failure, adverse internal wave current, power blackout, etc. Two mathematic models of the float-over vessel, DP2 X-Class semisubmersible vessel HYSY278, were developed for the DP simulations. The simulation runs encompassed all the scenarios of various float-over operations, including a series of positioning trials, moving to standoff position, approaching to pre-installed jacket, docking into jacket slot, undocking operation, etc.

Figure 168: DP RI tool - Online (real-time / dynamic) reliability analysis (Fernandez et al., 2019)

Song et al. (2019) developed high performance DP thruster for extreme environmental conditions such as the ice DP model test for the Arctic condition. In the performance analysis, three duct shapes were used: 19A-mod, 19A and 37 (Figure 169). CFD simulations and model tests proved that the thrust produced by the duct was not significant, but by the propellers was remarkably different.

Duct shape	19A-mod	19A	37
				
Length	0.045m	0.045m	0.045m
Diameter(Outer/Inner)	0.1197m/0.1080m	0.1197m/0.1080m	0.1173m/0.1080m
Propeller	Stock	Stock	Stock

Figure 169: Study on duct shape to develop high performance DP thruster (Song et al., 2019)

Lee and Lee (2019) proposed an adaptive PD based on the Deep Deterministic Policy Gradient (DDPG) – which is one of Reinforcement Learning (RL) algorithms, to overcome the restriction of conventional PD controller – which is inefficient in time-varying environments. The DDPG was developed by Google Deepmind and is trained with sequences of prior experience from interaction with environments. The fully trained model at the end of the epoch showed good position keeping performance (Figure 170).

Kato et al. (2020) described the development of a side thruster system that can maintain the heading direction of autonomous surface vehicles (ASVs) for mud collection. The side thruster system is implemented in an ASV and conducted the operation tests at a port in Soma city, Fukushima. The test results confirmed no kinking of the wire during mud collection operation. Therefore, the side thruster system maintained the heading of the ASV and prevented kinking of the wire under relatively gentle wave and wind conditions.

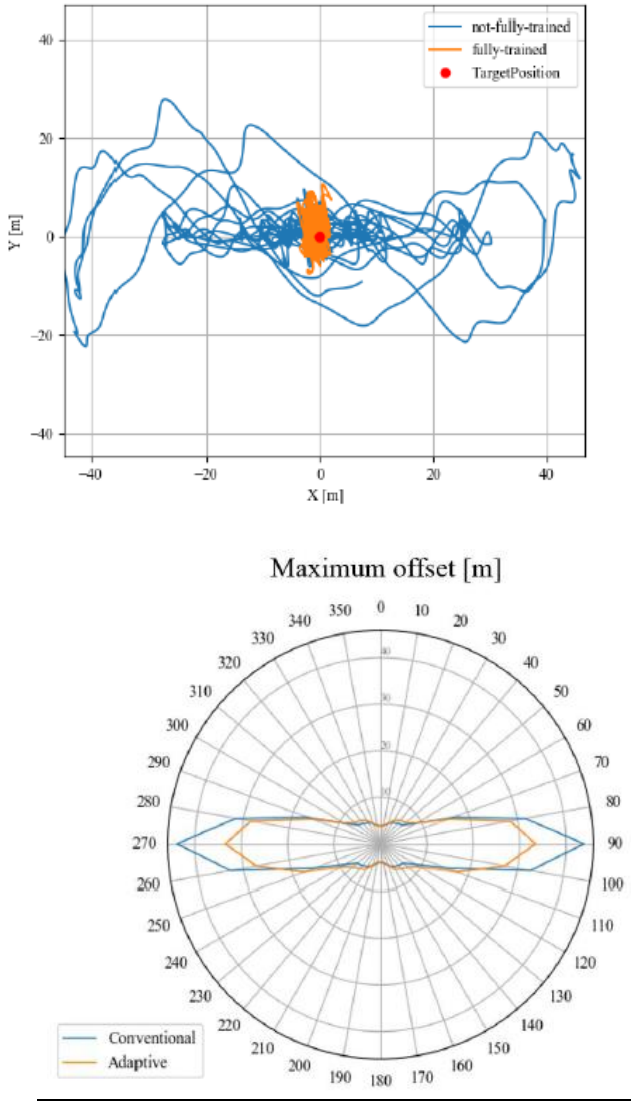

Figure 170: Enhancement of DP performance by using the adaptive PD control based on DDPG

L. Zhao et al. (2020) proposed a novel saturation protocol to refine the thrust allocation algorithm and improve the response speed to drastic changes in control force, under extreme wave conditions, i.e., when the DP system is in saturated state. When the thrust allocation modified strategy executes the saturation protocol, the limit of maximum thrust should be slackly set. The secondary thrust allocation makes the thrust of other unsaturated thrusters grow faster and improves the response speed of the propulsion system to the drastically changing control force (Figure 172).

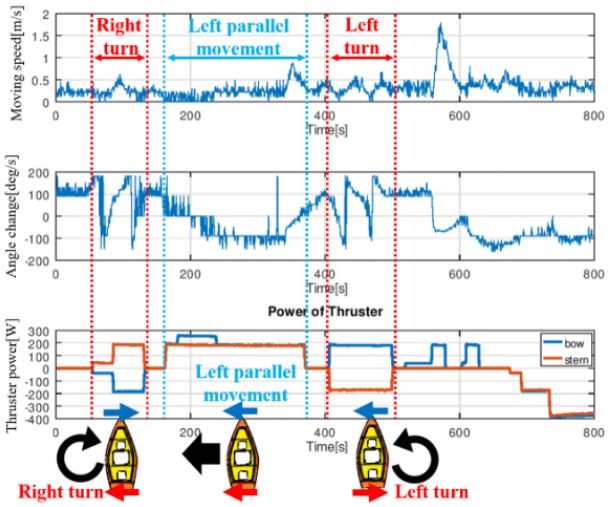

Figure 171: Test results of side thruster installed in ASV (Kato et al., 2020)

Lyu and Ding (2020) studied hydrodynamic characteristics such as thrust deduction of a submerged waterjet propelled vessel. Through a computational fluid dynamics method, the open water performance of the waterjet and the flow field around the hull were calculated. The results showed that when the advanced coefficient was in the range of 1.0 to 1.6, the open water efficiency of the submerged waterjet was more than 60%. Therefore, the waterjet showed potential to adapt to the multi-working conditions of transport vessels on inland rivers.

Fernandez et al. (2020) proposed a framework using Long Short Term Memory (LSTM) for prediction of reliability of DP sub-systems for computation of DP Reliability Index (DP-RI). The proposed framework included a mathematical computation approach and a data driven approach to predict the reliability at a sub-system level for evaluation of model performance and accuracy. The framework results demonstrated excellent performance under a wide range of data availability and guaranteed lower computational burden for real-time non-linear optimization. Numerical simulations were set-up using a state-of-the-art advisory decision-making tool with mock-up and real-world data to give insights into the

model performance and validate it against the existing risk assessment methodologies.

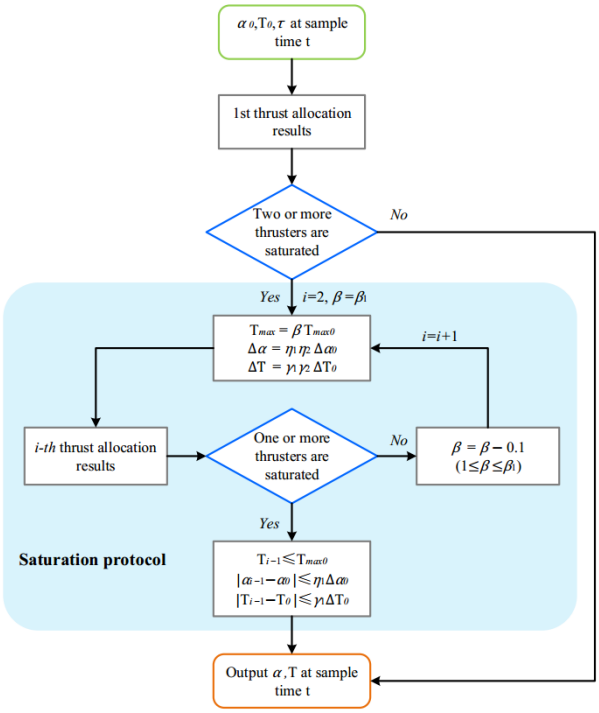

Figure 172: Flow chart of modified thrust allocation strategy in extreme operating condition (L. Zhao et al., 2020)

Tang et al. (2020) proposed an optimized thrust allocation algorithm based on Radial Basis Function (RBF) neural network and Sequential Quadratic Programming (SQP) algorithm, named RBF-SQP for the purpose of improving the traditional Forbidden Zone (FZ) method. The thrust coefficient was introduced to express the thrust loss in the mathematical model to remove forbidden zones. The training dataset of the RBF neural network was obtained from model tests of thrust-thrust interaction (Figure 173). Numerical simulations for the DP of a semi-submersible platform were conducted under typical operating conditions. The simulation results demonstrated that the demanded forces can be correctly distributed among available thrusters. Compared with the traditional methods, the proposed thrust allocation algorithm achieved a lower power consumption.

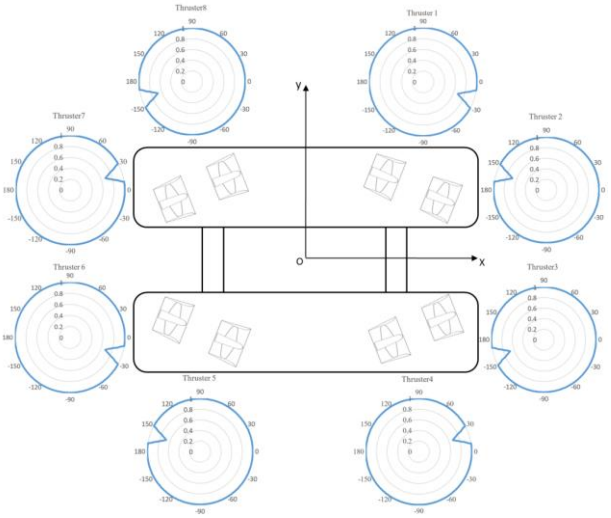

Figure 173: Thrust-thrust interaction as thrust coefficient of semi-submersible (Tang et al., 2020)

Rindarøy et al. (2020) presented SINTEF Ocean's vessel simulator, VeSim, and its results in a numerical DP3 study of a windfarm support vessel operating in DP mode near a platform. These results were validated against model-scale test results, also performed by SINTEF Ocean in its Ocean Basin Laboratory. In these tests, VeSim used SINTEF Ocean's in-house DP algorithm to control the model-scale vessel in a real- time hybrid testing environment. The proposed approach emphasised VeSim's use in both a hardware-in-the-loop and software-in-the-loop testing environment. Figure 174 displays maximum and minimum yaw angles from both simulations and model tests.

Fu et al. (2020) proposed a new concept to remove large and heavy structures with a single lift, utilizing three semi-submerged vessels. It requires high positioning accuracy especially under environmental disturbances to ensure the safety of transportation. To ensure efficiency and safety, a DP system was developed and model tests were performed for such twin-lift operation (Figure 175). The test results showed that twin vessels can achieve station keeping and low-speed manoeuvring capabilities, with PID controller and optimization-based thrust allocation.

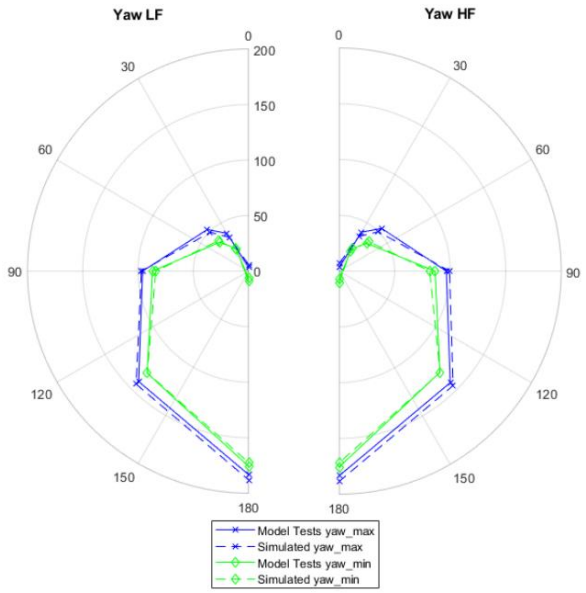

Figure 174: Comparison of maximum and minimum yaw angle for simulator and model tests (Rindarøy et al., 2020)

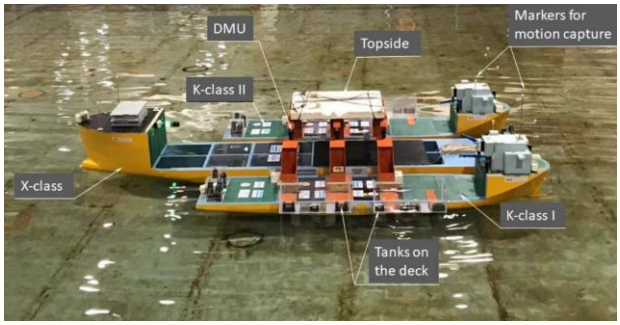

Figure 175: Sketch of wave tank test for twin-lift decommissioning operation (Fu et al., 2020)

Sauder and Tahchiev (2020) presented an active positioning system aimed at replacing the classical passive soft horizontal mooring system used in seakeeping tests of floating structures. An active positioning system was able to apply low frequency (LF) linear restoring and damping loads in surge, sway, and yaw, without directly affecting wave frequency (WF) motions, and motions in the vertical plane. Furthermore, this system enabled changes of heading, stiffness, damping, and decay tests, to be performed with high efficiency. These features enabled new possibilities in model identification. For the active system, six lines were used (Figure 176). Since the tension at the fairlead was feedback-controlled, the hydrodynamic loads on this limited portion of the line were compensated by the tension controller. Tie-back tests were performed and demonstrated that the active system can replicate results obtained with a passive mooring system.

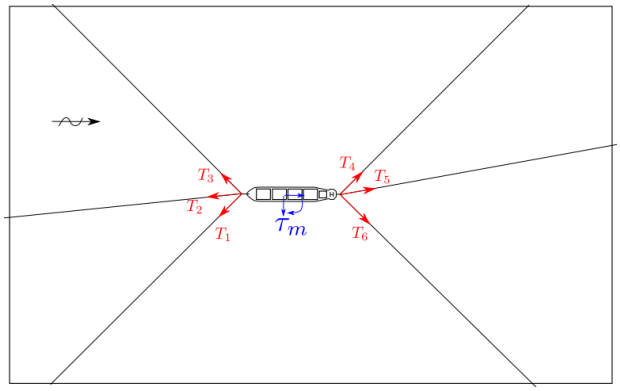

Figure 176: Sketch of active positioning system for seakeeping model test (Sauder and Tahchiev, 2020)

2.4 New technological developments

The hybrid foundation proposed by Cheng et al. (2019) is a novel and interesting development for bottom-founded OWTs, however further studies and validation at full-scale are still necessary. The topology optimization design method for jackets and other fixed structures proposed by Tian et al. (2019) is another development that deserves further studies and validation. W. Liu et al. (2017) have described the new concept of a Spar Drilling Production Storage Offloading Platform (SDPSO) for ultra-deep waters. Ren et al. (2018) have presented a new concept, the 'MWWC' (Monopile-WT-WEC- Combination) system that combines a 5 MW monopile type wind turbine and a heave-type wave energy converter. Fu et al. (2020) have proposed a new concept to remove large and heavy structures with a single lift, utilizing three semi-submerged DP vessels.

2.5 New experimental techniques and extrapolation methods

A creative method for the equivalent design of an oil offloading line for model tests was proposed by Kang et al. (2017). Park et al. (2021) have proposed a new experimental method for the assessment of towing- and course-stability of a FPSO towed by a tug-boat.

2.6 Practical applications of computational methods for prediction and scaling

Lyu et al. (2019) have developed a novel multi-body dynamic mathematical modelling for the Soft Yoke Mooring System (SYMS) of FPSOs. Koop (2020) have used CFD simulations to address Reynolds scale effects and shielding effects on current loads of offshore vessels in side-by-side configuration. Wang and Zhou (2020) carried out numerical simulations and experiments about the scale effect of internal solitary wave loads on spar platforms.

2.7 Need for R&D for model experiments, numerical modelling and full-scale measurements

Model tests and additional numerical simulations are necessary to investigate collision scenarios, loads on structures and foundations and performance of repaired/upgraded and life-extended structures for bottom-founded structures. Recent studies have also shown a concern with semisubmersibles and DP operations under ice conditions. Although, in the present ITTC period, some model tests results and field measurements have been reported on that topic, further investigation and validations are still required.

3. REVIEW OF THE EXISTING PROCEDURES

The Committee reviewed and updated the following procedures and guidelines:

- 7.5-02-07-03.1 Floating Offshore Platform Experiments;
- 7.5-02-07-03.2 Analysis Procedure for Model Tests in Regular Waves;
- 7.5-02-07-03.4 Active Hybrid Model Tests of Floating Offshore Structures with Mooring Lines;
- 7.5-02-07-03.5 Passive Hybrid Model Tests of Floating Offshore Structures with Mooring Lines;
- 7.5-02-07-03.6 Dynamic Positioning System Model Test Experiments;
- 7.5-02-07-03.10 Guideline for VIV Testing;
- 7.5-02-07-03.11 Model Tests of Multibodies in Close Proximity;
- 7.5-02-07-03.13 Guideline for VIM Testing;
- 7.5-02-07-03.14 Analysis Procedure of Model Tests in Irregular Waves;

The objective of the review was to update the procedures/guidelines according to the current practices, and to provide references to understand and implement the techniques.

4. STATE-OF-THE-ART REVIEW IN OFFSHORE AQUACULTURE SYSTEMS

Offshore aquaculture may be defined as the rearing of marine organisms in ocean waters beyond significant coastal influence, primarily in federal waters of exclusive economic zones.

According to C. M. Wang et al. (2019), for a fish farming site to be considered offshore, the following characteristics should be met:

(i) unsheltered waters, defined by the sea space outside a straight line joining two major capes/promontories or within 25 nautical miles from the shoreline for economic feasibility;

(ii) water depth greater than 3 times the cage height and at least 15 m between the cage bottom and the seabed for better dispersion of fish wastes and

(iii) current speed ranging from 0.5 m/s to 1 m/s.

In the recent years, fish farming worldwide is moving offshore due to lack of available nearshore production sites (where conflicts with shipping, fishing, tourism, conservation, and recreation are frequent), much larger sea space availability and better water quality (essential to produce healthy fishes). However, going offshore poses many challenges due to the high energy environment, inaccessibility of power supply and supporting services (C. M. Wang et al., 2019).

Recent reviews concerning offshore aquaculture systems and their classification can be found in Chu et al. (2020) and Xu and Qin (2020). There is a variety of designs that include open and semi-closed systems, floating and submersible options, as well as fixed. In the following various types of offshore aquaculture systems are presented with examples of relevant structures.

4.1 Open net cage system

4.1.1 Floating flexible cages

Flexible collar cages were first invented in the 1970s and are now widely used in Japan, Western Europe, North America, South America, New Zealand, Australia. High-density polyethylene (HDPE) is commonly used for the material in modern industrial fish farming. The main structural elements of these cages are the floatable pipes, which can be assembled in various ways to produce the floating collar. The pipes are held together by a series of brackets with stanchions and distributed throughout the entire boundaries to suspend the fish net. This type of structures is flexible and typically follow the shape of waves as indicated in Figure 177. The material tolerates relatively large elongation without major fatigue. The structures are also relatively cheap and have been a popular solution in confined environment. In harsh environment conditions, the floating flexible cages have problems with deformation of the net due strong waves and currents, stanchions that may cause twisting and turning problems. However, some plastic circular cages have been given an offshore designation and have survived storms with significant wave height Hs of 4.5 m (Turner, 2000). Examples of flexible circular cages are the Aqualine concept with PE pipes with circumference from 20 m to 100 m and PolarCirkel concept with HDPE pipes circumference of 60 m to 240 m (Figure 177).

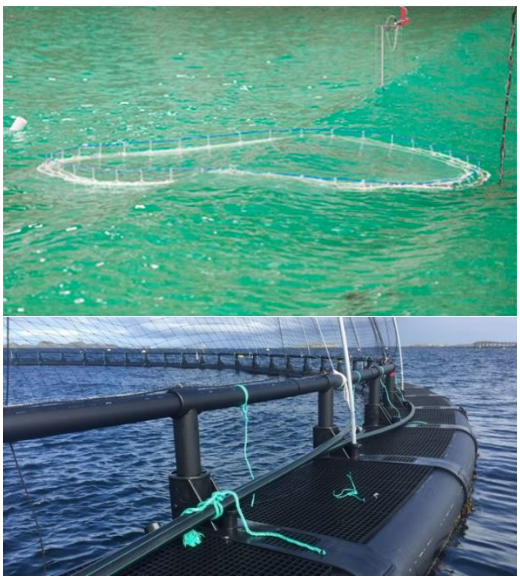

Figure 177: Floating flexible cages: (a) Model test in ocean waves (Picture courtesy of SINTEF Ocean) and (b) PolarCirkel HDPE Circular cage

https://www.akvagroup.com/merdbasert-oppdrett/r%C3%B8r-og-r%C3%B8rsystem

4.1.2 Floating rigid cages

Floating rigid cages with robust frame structures (for strength, stiffness, stability, and buoyancy) are designed to withstand large wave actions. They are generally large structures, constructed from steel or concrete, and incorporate a variety of management-related features. Their susceptibility to structural failure in extreme conditions and the requirement for heavier mooring systems due to their large masses are the main disadvantages.

Examples of floating rigid cages are: Pisbarca (Figure 178), Seacon (Figure 179) and Havfarm (Figure 180).

The Pisbarca was built by a Spanish company. It is a hexagonal steel structure with 7 cages, with a total volume of 10000 m^3 and a production capacity of 200 tons of fish per annum (Scott and Muir, 2000).

Figure 178: Pisbarca (https://www.pinterest.co.uk/pin/577728077003954 21/?lp=true)

Seacon, built also in Spain in 1987, consists of a hexagonal submerged pontoon construction and a deck construction in light-weight aggregate concrete. It has separated steel tube columns and pretensioned diagonal and vertical struts between top and bottom columns (Bjerke, 1990).

Figure 179: SEACON (https://www.lightcem.co.uk/fish-farm-c1gnk)

Havfarm has 385 m in length and 59.5 m wide and a capacity to contain 10000 tons of salmon (over 2 million fish). Havfarm was constructed as a steel-frame for 6 cages measuring 50 m × 50 m on the surface, with open nets at 60 m depth. The facilities were designed to withstand 10 m of significant wave height. It was installed in Hadsel, northern part of Norway, in June 2020.

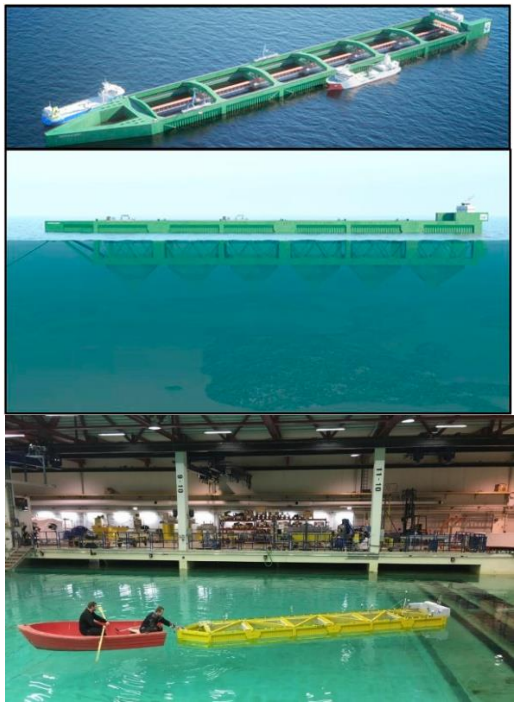

Figure 180: Havfarm. (a) concept (https://www.nskshipdesign.com/designs/aquaculture/fishfarm-2/fish-farm/) (b) Model tests (Picture courtesy of SINTEF Ocean).

4.1.3 Semi-submersible flexible cages

Semi-submersible cages can be characterized by their capability to be submerged from surface waters during a storm to avoid the higher energy regimes. Depending on mechanical types, semi-submersible cages may be divided into two structural classes: flexible and rigid. Tension Leg Cage (TLC) is the one of the representative types of semi-submersible flexible cage. In the TLC-submersible design, a buoyancy plastic-supporting frame is held in place by vertical mooring ropes attached to concrete blocks on the seabed and to sub-surface buoys. In storms or strong currents, the cage responds naturally, i.e., the net is being pulled under the water, thus escaping the worst wave action (Beveridge, 2008; Scott and Muir, 2000). Mooring strength is critical and the heavy block anchors used are difficult to install. Cage volume reduction due to submergence of cage for a long period of time may affect fish's welfare (Beveridge, 2008).

Tension leg mooring system will behave more like a fixed structure and wave forces can be directly countered by the tendon stiffness forces, thereby, a large volume with high mass cage may not be suitable due to vulnerability of mooring lines (DNV, 2010). An example is the Refa tension leg cage design concept (Figure 181). The cage is available in a variety of sizes up to 12000 m^3. The maximum harvest biomass is about 300 ton based on 25 kg/ m^3 of stock density. The cages have been deployed in Italy, Spain, Portugal, and Brazil.

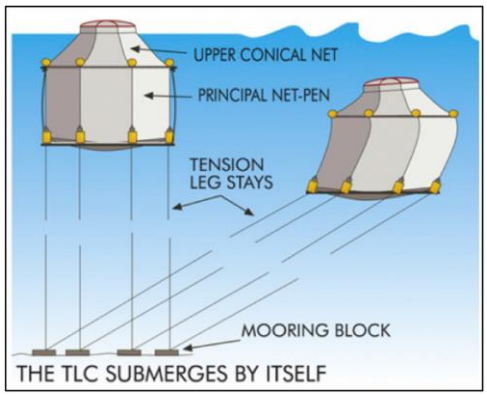

Figure 181: Refa tension leg cage concept design (http://refamed.com/gabbie_mare/tlc_system.html)

4.1.4 Semi-submersible rigid cages

Semi-submersible rigid cages are designed with rigid framework elements restricting movement or volume change in response to external wave and current forces. Normally having steel frame structures, the cages have adjustable ballast tanks to raise or lower the system. With a more rigid structure, it allows to have service facilities such as self-contained feeder systems (Scott and Muir, 2000). They are large and complex steel structures that require rigorous engineering analyses, design, and high-quality control in construction to ensure safety in offshore operation.

Examples of semi-submersible rigid cages are Ocean Farm 1, Shenlan 1, Shenlan 2, Viewpoint Seafarm, Spider Cage, SSFF150 Pen, and Keppel offshore rig fish farm.

Ocean Farm 1 was developed in Norway and built in China. Ocean Farm 1 is a result of robust technology and principles used in submersible offshore units. With diameter of 110 m and volume of 250000 m^3, the cage can accommodate 1.5 million salmons. It is intended for offshore installation in water at 100 to 300 m in depth with 25-year lifespan. It has more than 20000 sensors and over 100 monitors and control units.

Figure 182: Ocean Farm 1: (a) model tests (Picture courtesy of SINTEF Ocean); (b) https://www.fishfarmingexpert.com/article/world-s-first-offshore-fish-farm-arrives-in-norway/

Shenlan 1 and Shenlan 2 were developed for salmon farming about 130 nautical miles off the shore of Rizhao in east China's Shandong province. Shenlan 1 has already been deployed at the site, has a diameter of 60 m, a height of 35 m, and is able to culture 300000 salmons (Figure 183a). Shenlan 2 has 60 m diameter and a height of 80 m and can accommodate about 1 million salmons (Figure 183b).

Nova Sea AS, a Norwegian company, designed two innovative concepts: Viewpoint Seafarm (Figure 184) and Spider Cage (Figure 185) for offshore fish farm solutions based on semisubmersible technology. Viewpoint Seafarm comprises a hub, which supports four floating net cages interconnected through a dedicated hinge system. Each floater has a projected area of 50 m × 35 m. Model scale tests have been conducted with 11 m significant wave height and the system showed stable motion response (Hill, 2018). The Spider Cage has a dedicated barrier, with a diameter of 100 m having an outer steel ring with another ring inside with heave compensation. It is designed to shield the actual fish cage from heavy sea conditions and sea lice. The design has been tested up to sea states of 11 m with and without current, where general motions, accelerations, loads and sloshing have been assessed.

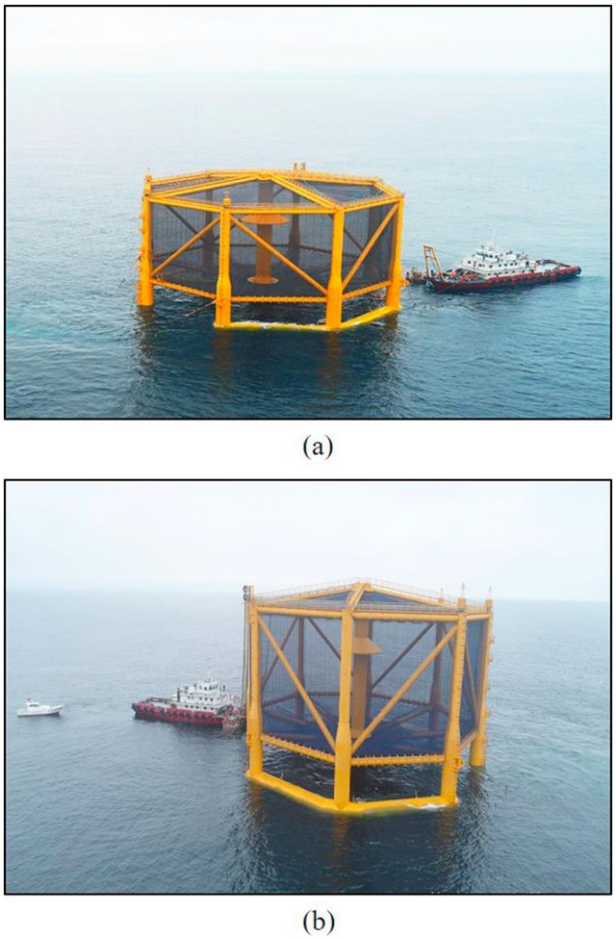

(a)

(b)

Figure 183: (a) Shenlan 1 (http://www.ccccisc.com/en/haiyanggongchengxianggua n/70.html), (b) Shenlan 2 (http://www.ccccisc.com/en/haiyanggongchengxianggua n/72.html)

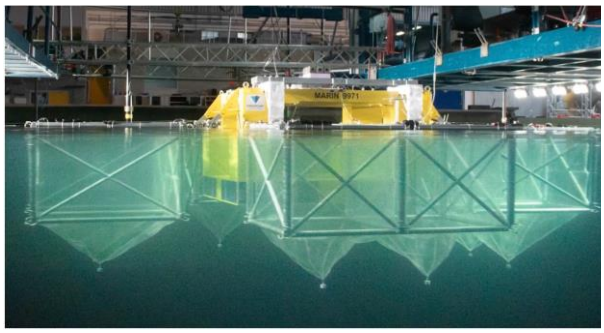

Figure 184: Viewpoint seafarm (https://www.youtube.com/embed/WWiU0dm-iKQ?autoplay=1&modestbranding=1&rel=0&showinfo=0&vd=hd1080)

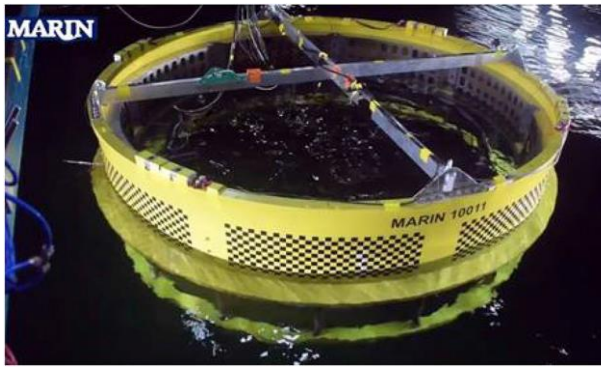

Figure 185: Spider cage (https://www.youtube.com/embed/gpPfUwD0te0?autoplay=1&modestbranding=1&rel=0&showinfo=0&vd=hd1080)

4.1.5 Submerged cages

Normal operating condition of submerged cages would be at a suitable water depth below from the hazardous upper water column. The systems could be raised temporarily to the surface for necessary maintenance requirements and for fish harvesting. Various designs have been proposed and some pilot scale or commercial systems have been built.

Submerged cages have the best features to avoid surface debris and effects of storms (Scott and Muir, 2000). The latter supports the fact that their structural strength does not need to be as great as surface structures. Examples of submerged rigid cage designs are Sadco (see Fig. 10), AquaPod (see Fig. 11a) and NSENGI sinking fish cages (see Fig. 11b).

Sadco is a Russian design that has been evolving since the early 1980s (Bugrov, 2006). A ballasted upper steel hexagonal superstructure carries the net kept in shape by a lower sinker tube. The cage volumes are available up to 2000 m^3.

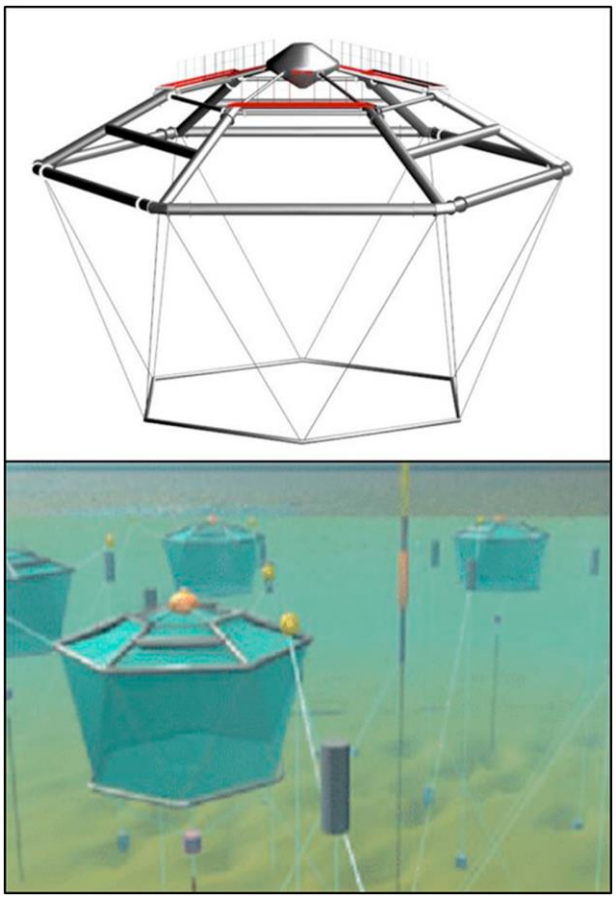

Figure 186: Sadco submerged rigid cage (http://www.sadco-shelf.com/)

AquaPod was developed by Ocean Farm Technologies in the United States. It has a two-point anchor for mooring and some operational advances such as net cleaning and removal of mortalities. NSENGI (Nippon Steel & Sumikin Engineering Co., Ltd) had carried out offshore verification testing of large-scale sinking cages at a salmon farm which is 3 km from shoreline of Sakaiminato, Tottori Prefecture, Japan. Each

cage has a volume of 50000 m^3 with wave of 7 m height and current speed of 2 knots. The cages are serviced by a jack-up platform that houses the equipment and feedstock storage facility for automated feeding of the fish.

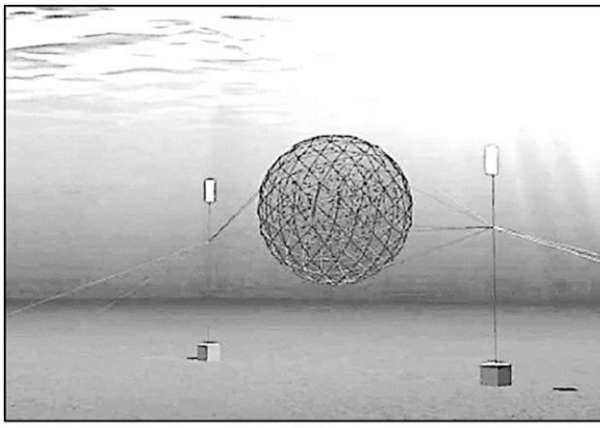

(a)

(b)

Figure 187: (a) Submerged AquaPod cage from Ocean Farm Technologies (Tidwell, 2012), (b) NSENGI sinking fish cage (https://www.eng.nipponsteel.com/english/news/2016/20161003.html)

4.2 Closed containment tank system

Floating closed containment tanks for offshore fish farming are very recent developments prompted by the need to protect the fish from sea lice and other parasites. Floating closed containment tanks contain water that is constantly refreshed by a flow through system which also helps to provide proper temperature, sufficient oxygen, and waste removal.

By having control over water replacement, the water can be constantly disinfected to remove pathogenic organisms. External environmental events like algae bloom are no longer a problem (Chadwick et al., 2010). Organic wastes can be removed by biofiltration system before discharging the water back to the sea. The threat of predators (such as sharks and seals) is eliminated. It also can achieve a higher production rate when compared to the open cage system (Tidwell, 2012). This is due to the greater control and inputs into these systems and the fact that their physical parameters can be optimized for maximum productivity. On the other hand, the main disadvantage of floating closed containment tanks is that they may lead to effects associated to the behaviour of the contained water, to both structure and fish.

An example of floating closed containment type is the fish farm egg (Figure 188), developed by “Hauge Aqua” using a fully enclosed egg-shaped structure. The water flow enables the system to draw inlet water segregated from where outlet water is released. Water enters using two main pumps that suck water from 20 m below the water surface. The water quality and volume can be controlled, ensuring steady oxygen levels. It is estimated to cost about NOK 600 million (about USD 60 million).

Figure 188: Closed fish farm concept "fish farm egg" (http://sysla.no/fisk/skalbruke-600-mill-pa-lukkedeoppdrettsegg/)

Neptun was developed by Aquafarm Equipment (Figure 189a). The tank has an internal diameter of 40 m, a depth of 22 m and the gross volume is 21000 m^3. Figure 189b shows an underwater view of the tank with inlet and outlet holes for water circulation. The tank is made from Glass Fibre Reinforced Polymers (GFRP) elements and reinforced with steel in areas that bear the most stress. The design also includes a pump system to extract large volumes of water from a depth of 25 m or more. As the concept of the containment tank is to collect the waste from the fish and uneaten fish feed from the sloped bottom, there is a flexible pipeline that connects the low point to the waste separator.

Figure 189: Neptun closed containment fish tank (a) As installed, (b) Overview of the structure http://aquafarm.no

Dr. Techn. Olav Olsen, Norway based marine technology consulting company, proposed a closed containment tank for offshore farming, built in concrete material (Figure 190). The cylindrical concrete tank has 14.8 m of inner diameter, 16.5 m of outer diameter and 6 m height. Its bottom has a sloping bottom for easy collection of organic waste (Chu et al., 2020).

Figure 190: Concrete containment fish tank (Picture courtesy of Tor Ole Olsen).

AME2 Pte Ltd., Singapore based company, has developed a closed containment flow through floating fish farm called Eco-Ark (Figure 191a). It has several containment tanks with flow through water supply system. It has a roof equipped with solar panels to supply electricity for the fish farm. The Eco-Ark allows augmentation and integration by forming a fleet connected to a lift dock facility that enables to cultivate and process massive amount of fish on site (Figure 191b). The Eco-Ark was constructed in Batam Island, Indonesia, and was deployed in Singapore waters in August 2019.

The Norwegian salmon farmer, Marine harvest, developed a closed containment tank design named marine donut (Figure 192). The marine donut can accommodate 200000 fish in each unit. In 2019, Norway's directorate of fisheries granted permission for 1100 tonnes of biomass to be used to test the design.

(a)

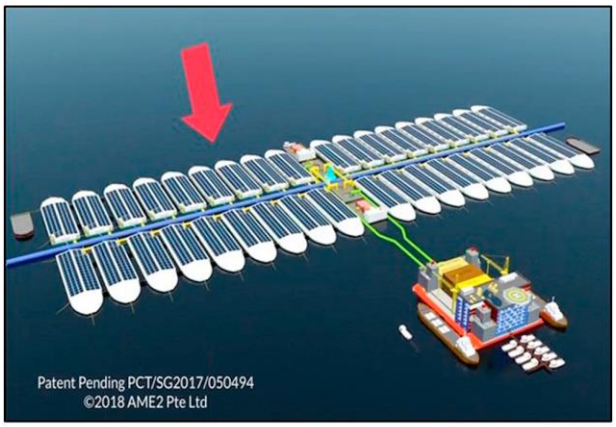

(b)

Figure 191: (a) Eco-Ark closed containment system, (b) Eco-Ark fleet connected to lift-dock (Picture courtesy of Mr. Ban Tat Leow, the inventor of Eco-Ark).

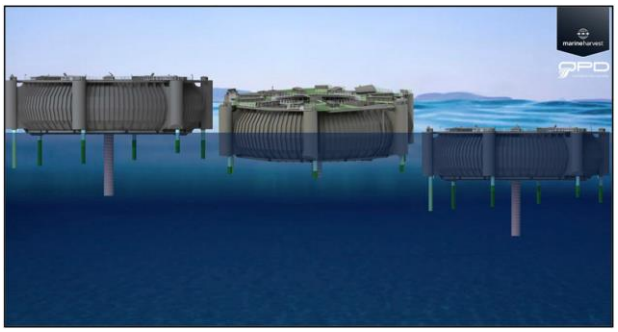

Figure 192: Marine donut – Close containment concept design of marine harvest (http://marin.bergen-chamber.no/en/teknologi/Growth-through-innovation/)

4.3 Recent challenges & developments

The preliminary study of the vessel-shaped offshore fish farm concept (that gave origin to

Havfarm - Figure 180a) for open sea applications was reported in the work of (Li et al., 2017). The structure included the vessel-shaped hull, a mooring system, and fish cages. The shape of the hull minimizes the wave loads coming from the bow, and the single-point mooring system is connected to the turret at the vessel bow. Such a system allows the whole fish farm to rotate freely about the turret, reduces the environmental loads on the structure, and increases the spread area of fish wastes. A basic geometry of the vessel hull was considered, and the hydrodynamic properties were obtained from frequency domain analysis. The preliminary mooring system was designed to avoid possible interactions with the fish cages. Time domain simulations coupling the hull with the mooring system were also performed. Fish cages were simplified by considering a rigid model. The global responses of the system and the mooring line loads were assessed in various waves and current conditions and the effects due to the misalignment of waves and current directions on the responses were also studied. Further studies on this system has been conducted and reported in (L. Li et al., 2019a, 2019b, 2018a, 2018b). For instance, L. Li et al. (2018a) conducted a numerical study to investigate the vessel's responses using flexible and rigid net models under steady current conditions; L. Li et al. (2019a) proposed an integrated optimization methodology for the design of mooring systems. The methodology integrates the design of experiments, screening analysis, time-domain simulations, and a meta-model-based optimization procedure; L. Li et al.(2019b) proposed an integrated method for the numerical prediction of the heading misalignment between the vessel-shaped fish farm and the currents under combined waves and currents. The probability distribution of the misalignment angle was calculated using the Kriging metamodel for a reference site and based on the prediction, the requirement for the dynamic positioning system to improve the flow condition in the fish cages was discussed.

Kristiansen et al. (2017) addressed the description of exposure from waves and currents in coastal regions for design of marine fish farms. Dedicated field measurements at two exposed aquaculture sites from February to December 2016 were presented. Results from statistical analyses of the measurement data demonstrated that common practice for characterization of exposure in design of fish farms has several deficiencies that should be improved to reduce uncertainties in design. Later, Kristiansen et al. (2018) investigated the seakeeping behaviour of a rigid type of floating closed fish cages, with focus on the effects of sloshing on the coupled motions and mooring loads. Scaled model tests of closed cages in waves revealed that the influence of sloshing on the rigid body motion is significant. Therefore, coupled motions with sloshing are important to consider in the design of this type of fish farming floating system.

Turner et al. (2017) have developed a net wake shielding and self-shielding model to accurately estimate the hydrodynamic loading on fin-fish aquaculture installation. The effect of containment net hydrodynamic wake shielding is important to avoid overly conservative estimation of loads on fish farm installations. The reduction in fluid velocity through a net can be significant in many cases, leading to decreased loading and changes in motion on downstream nets and mooring components. In as subsequent work, Turner et al. (2018) presented a comparative study of taut and catenary mooring systems for the fin-fish aquaculture installation. The results showed that a reduced footprint taut mooring configuration with integrated elastomeric mooring components can substitute a typical chain catenary mooring with no significant increase in peak mooring line loads at extreme sea states and significant reduction in peak loading at moderate and calm sea states.

Kitazawa et al. (2017) have performed water tank and field tests on the performance of a

submergible fish cage for farming silver salmon. A submergible cage using flexible tubes was proposed to farm silver salmon in deeper and cooler waters to overcome the limitation of cultivation during August. The cage was submerged and floated up by ejecting air from and injecting air into the flexible tubes, respectively. Water tank test using the 1/3.64 scaled model and field tests have been performed to assess the behaviour of the cage during floating up and submersion.

Lader et al. (2017) conducted a classification study of aquaculture locations in Norway with respect to wind wave exposure. The method was called fetch analysis and used long term wind data connected with the fetch length to estimate wind wave conditions. The method was divided into four steps: 1) Fetch analysis, 2) Wind data, 3) Estimating wave parameters Hs and Tp and 4) Wave statistics. Significant wave height Hs with return period 1 year and 50 years were estimated for each site. Hs 50 year is often used for design, and the analysis showed that for 38% of the sites Hs 50 year exceeds 1 meter, for 17% of the sites Hs 50 year exceeds 1.5 meter, while 1.4% of the sites have Hs 50 year larger than 2.5 meter. The most exposed site has a Hs 50 year of 2.9 meter. Thus, large differences in Hs 50 year in the various coastal regions of Norway exist.

Gansel et al. (2017) investigated the effects of different amount and sizes of fouling organisms (blue mussel and kelp) in Norwegian aquaculture on the drag on net panels. Drag forces on several clean and fouled nets were measured in a flume tank at a flow speed of 0.1 m/s. Drag on fouled nets largely depended on the distribution of fouling rather than on the wet weight. Knowledge about the effect of a given type of fouling on the drag on nets allows the use of drag as a proxy to find transfer functions between fouled and clean net solidity.

Føre et al. (2018) experimentally investigated traditional netting materials subjected to disinfecting chemicals during fish farming and treatment of net cages. A series of tests were performed to study the effect of various concentrations of disinfecting chemicals on the tensile strength of Raschel knitted Nylon netting materials. Simulated spill of diluted hydrogen peroxide to the jump fence during de-lousing did not affect the strength of the applied new and used knotless nylon netting samples. Hydrogen peroxide reacted with biofouling forming gas bubbles, but this did not result in reduced netting strength. The performed tests did not indicate any effect on netting strength from a simulated single, traditional bath disinfection as performed at service stations applying the disinfectant Aqua Des containing peracetic acid. However, increasing the Aqua Des concentration from 1 to 10 % resulted in a strength reduction of 3–6 %. Simulated spill of concentrated Aqua Des on the jump fence of a net with copper coating residuals resulted in a severe reduction in strength of 45 %.

Fredriksen et al. (2018) carried out simulations on response characteristics of a fish farm system when subjected to combined irregular waves and current conditions. The studied fish farm system had a large horizontal extension with variable environmental conditions across the entire structure and the drag loads on the fish nets are thought to be the governing environmental force. The results showed that, in most cases, using the maximum expected wave height in an irregular sea state as criteria for selecting an equivalent regular wave give realistic design values.

Zhou et al. (2018) experimentally examined the feasibility of the net-hauling system for set net fishery using water tank tests. A flexible hose net is proposed to harvest fish in the box chamber net of set net fishery (Figure 193). The flexible hose net is installed on the water bottom below the box chamber net. Compressed air is injected from one edge of the hose net to haul the box chamber net gradually, resulting in cornering fish in the other edge. The variation in

the formation of the hose net and the time for sinking and floating were examined, changing the parameters such as air pressure and buoyancy balance. The hose net sank automatically if the weight attached to the hose net was 39% of the total buoyancy of the hose net with full of air. To reduce the sinking time, the initial inner pressure of the hose net must be the atmospheric pressure before the beginning of the sinking operation. Motion analysis of flexible hoses revealed that the inside structure of the hoses may have to be improved to secure the air flow in any condition.

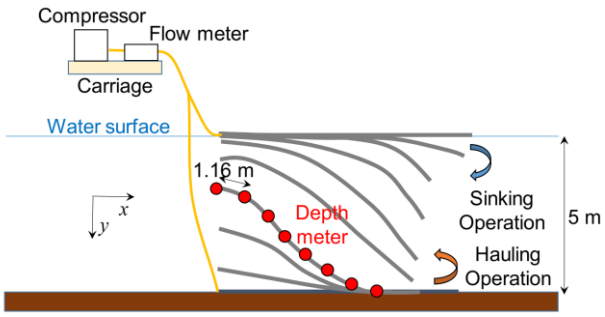

Figure 193: Two-dimensional schematic representation of the sinking and hauling experiments of the hose net (Zhou et al., 2018)

Yu et al. (2018) experimentally tested a controllable depth cage (CDC) with its mooring system (Figure 194). CDC consists of a cage, floats, and anchors, which are connected by ropes in this order. The vertical position of the cage is controllable by adjusting the buoyancy of floats. The effects of waves on the motions of the CDC were tested in smaller (1/100 scale model) and larger water tanks (1/25 scale model). The range of motion and the tension on the mooring ropes of CDC increased with increasing wave height. Close to the water surface, when the wavelength was around two times the size of the CDC, the tension of the mooring ropes increased. Under the same wave condition, the displacement and the inclination of the cage, and the tension of the mooring ropes decreased by about half when the cage was installed at 0.7 m below the water surface.

Figure 194: Controllable depth cage model test when the cage was at water surface (left) and at the submerged depth (right) (Yu et al., 2018)

Weiss et al. (2018) presented a new tool to identify potential zones for offshore aquaculture. A global case study for greater amberjack was reported highlighting unexploited offshore zones in South and North America, Oceania, and Africa. The tool aims to identify optimal conditions for the growth of fish species and for cage resistance, a methodology developed in the framework of the TEN-SHORES project. The first step was based on the Delphi method and consists of the selection of variables according to their relevance to fish species and to the cage location. The selected variables were acquired from reanalysis models and remote sensing data (time series of 20–30 years). In the second step, an evaluation system was developed to estimate the percentage of time (on a 0-1 scale) that the selected variables remain in optimum conditions, for the fish and the cage, in the whole data series (grid of 0.25°). Suitability maps were generated according to the conditions for the fish species growth and to house a generic cage.

Zhao et al. (2019) carried out a series of physical model experiments to investigate the hydrodynamic responses in regular waves of a semi-submersible offshore fish farm, whose structural configuration refers to Ocean Farm 1 (Figure 195). Mooring line tension and motion response of the fish farm at three draughts were analysed. The consideration of net resulted in approximately 42% reduction in mooring line tension and approximately 51% reduction in surge motion. However, the heave and pitch of the fish farm increased slightly with the existence of net.

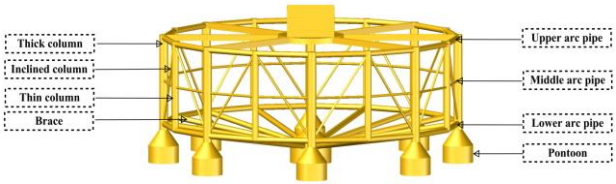

Figure 195: Primary frame of the fish farm (Zhao et al., 2019)

Xu and Qin (2020) examined the fluid-structure interactions between fluid, aquaculture cages and fish. A comparison between the traditional methods used to assess the interactions between environmental loads and aquaculture cages was presented. This comparison included analytical studies, numerical implementations, field tests, and laboratory experiments. Reviews on topics such as mooring and grid systems, drag coefficients of the net panel, hydrodynamic behaviours of cage components, velocity reduction of cage array, and volume reduction caused by cage deformation are also provided. Conclusive data shows that the Morison equation-based empirical formulae underestimated the drag force on the net, while the screen-based empirical formulae overestimated the drag force. The most reliable methods to use are validated physical models and numerical implementations.

Qin et al. (2020) investigated the effects of extreme wave conditions by leveraging a physical model approach on aquaculture structures. Physical model tests have been conducted with the purpose of investigating the nonlinear vertical accelerations and mooring loads of a scaled aquaculture cage (Figure 196). For the floating collar model, regular waves with wave steepness of 1/60, 1/30 and 1/15 were tested. For the floating cage model, the same regular waves combined with current 0.1 m/s and 0.2 m/s were examined. It was assumed that the wavelength was much larger than the size of the floating collar and that the wave frequency was much lower than the natural period of heave. For the floating collar model without netting, under wave-only conditions, the first- and second-harmonic components of the vertical acceleration are proportional to the wave amplitude and square of the wave amplitude, respectively. For the floating cage model under combined waves and current conditions, the first-harmonic component is more likely proportional to the wave amplitude, while the second-harmonic component shows erratic behaviour.

Huang et al. (2020) have developed a semi-submersible offshore fish farm with steel truss structure and single-point mooring system. The mooring forces and motion responses including heave, pitch, and roll for the fish farm exposed to waves and currents have been analysed through a series of laboratory experiments for the offshore fish farm with the scale of 1:30 (Figure 197). Their results indicate that the dynamic response of the fish farm in combined conditions of wave-current is lower than that of the pure waves, since the current velocity is helpful to decrease the impact of the pulse owing to the high stiffness of the anchor chain of the farm that is exposed to water loads. Increasing the drought of the fish farm can lead to both the mooring force and roll becoming larger, besides reducing the heave. However, the tentative variation for the pitch is not obvious. The current velocity inside the fish farm is significantly lower than the outside of the fish farm. The resulting total reduction falls within 32.25%–63.00%.

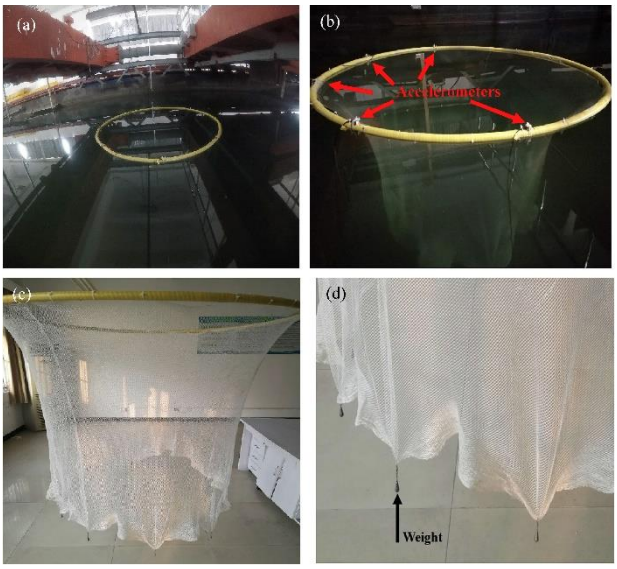

Figure 196: The physical model of the aquaculture cage: (a) model of the floating collar without netting from the top view; (b) installation of accelerometers along the floating collar model with netting; (c) floating cage model in the air and (d) details of the netting and weights (Qin et al., 2020)

Martin et al. (2020) derived a Lagrangian approach for the coupled numerical simulation of fixed net structures and fluid flow. The model was based on solving the Reynolds-averaged Navier-Stokes equations in a Eulerian fluid domain. The equations included disturbances to account for the presence of the net. Forces on the net were calculated using a screen force model and were distributed on Lagrangian points to represent the geometry of the net. Different solidities, inflow velocities and angles of attack were considered. The comparison of loads on and velocity reductions behind the net with available measurements indicates superior performance of the proposed model over existing approaches for a wide range of applications. The numerical model is extensively validated against existing experiments for fixed net panels, multiple panels and cages with varying geometries and solidities in current and regular waves.

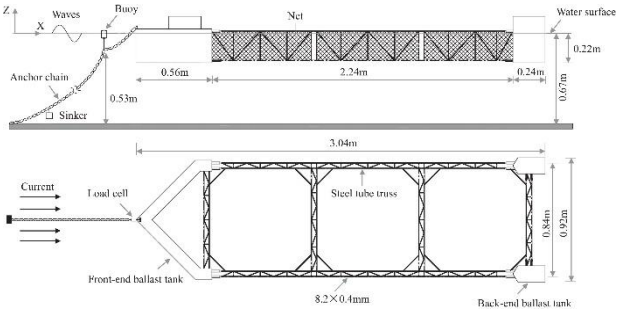

Figure 197: Physical model configuration of the offshore farm (Huang et al., 2020)

A concept of a floating wind-solar-aquaculture (WSA) system, combining multiple megawatt (MW) vertical-axis wind turbines (VAWTs) and solar arrays with a floating steel fish-farming cage, was presented in Zheng et al. (2020). An aerodynamic source code based on the double multi-streamtube theory is developed. It can be exported into the commercial software Orcaflex to achieve fully coupled analysis of the WSA system. Using the developed tool, turbine aerodynamic performance, tower base bending moments, global WSA motions, and tension of mooring lines were investigated. The results affirm that WSA is technically safe and feasible. It is a promising concept to deploy in intermediate and deep waters.

The study presented by Wang et al. (2020) aims to develop a fixed horizontal cylindrical fish cage which can rotate around the central axis. In this way, the biofouling on the main structure could be easy to be cleaned. For offshore engineering structures, the strong earthquake is one of the main loads leading to structural failure. Especially, some offshore fish farms may be located on the edge of the continental plate where strong seismic activity often occur. Therefore, it is necessary to study the dynamic characteristics of the fish cage under earthquake load. A finite element model of the fixed horizontal cylindrical fish cage was established to calculate the dynamic characteristics based on the ABAQUS software (Figure 198). The natural frequency and

vibration mode of the fish cage are obtained by modal analysis.

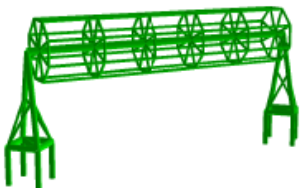

Figure 198: The finite element model of the fixed horizontal cylindrical fish cage structure (Wang et al., 2020)

5. STATE-OF-THE-ART REVIEW IN MODEL TESTS OF CABLE/PIPE DYNAMICS CLOSE TO THE SEA SURFACE

With the development of deep-sea oil production technology, a composite deep sea oil production system has emerged, namely the combination of spar & FPSO or other platform forms of compound oil production. The biggest advantage of this composite system is that as many facilities other than the production unit on the spar or semi oil production platform can be transferred and installed on the FPSO to reduce costs. This type of operation plan needs to connect the two platforms with FTL (Fluid Transfer Lines), as seen in Figure 199. Compared to the seabed pipelines, the suspended FTLs are well known to be an attractive alternative solution. The main advantages of the suspended FTL compared to the subsea pipeline are (a) improved flow assurance due to higher sea-water temperature leading to reduced risk of blockage by formation of wax and hydrates; (b) avoidance of seabed constraints, such as ground instability, irregular sea-bed profile, and subsea hardware congestion.

However, the free-hanging flow lines with single or multiple wave configuration or with bonded hose are much longer than the distance between the DTU and FPSO to have less local curvature. The long transfer line requires higher discharge pressure to withstand the pressure drop due to the friction loss along the long pipe inner wall. In the case the distance is too large (i.e., larger than 1000 m), the flow line motion may also significantly influence the FPSO and DTU motions in extreme environments, which results in the increase of the motion and load of the flow line itself.

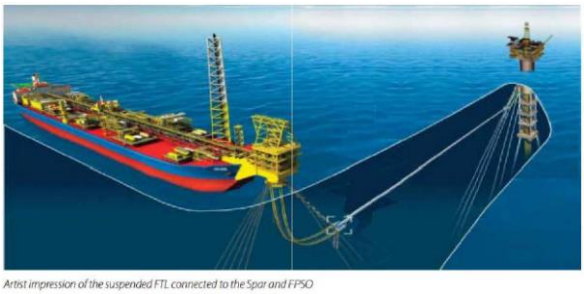

Figure 199: Suspended FTL connected to a spar and a FPSO

In summary, the disadvantages of the conventional suspended flow-transfer pipelines are limitation in the sizes of the FTLs, strength and fatigue problems, flow-assurance concerns due to the long line length with possible temperature drop, and the high cost of materials and installation.

5.1 Fluid Transfer Lines (FTL)

The FTL is one of the core equipment of the composite deep-sea oil production system, which is affected by ocean currents and waves near the water surface and produces complex hydrodynamic responses such as vortex-induced vibration (VIV). When the vortex frequency is close to the natural frequency of the FTL, resonance locking will occur, leading to fatigue damage. For offshore risers with similar structure and offshore pipelines with large slender ratio, the VIV responses of these flexible structures have sustained a lot of theoretical and experimental research. Carmo et al. (2013), Wu et al. (2012) and Chen et al. (2013) presented studies on VIV of long slender cylinders and circular cylinders. All of these can be used as the

basis for the research of VIV problem for special FTL structures.

Chang and Isherwood (2003) considered the effect of the platform heave motions on the VIV of steel catenary risers and steel offloading lines. The uniqueness of the FTL used in the composite production system lies in that both ends of the FTL are connected to the floating platform, which is bound to be coupled by the multi-degree of freedom movement of the platform, resulting in complex unsteady motion and oscillating inlet flow, which also significantly affects the hydrodynamic response of the FTL.

As part of the design process of deep-water marine risers to minimize top tensioning requirements, mitigate flow-induced vibrations, and to increase the expected fatigue life of these slender structural members, Fang et al. (2014) have employed external buoyancy modules and strakes in an experimental study. A horizontal cylinder with a length to diameter ratio of 263 was fitted with a variety of strake and buoyancy element configurations and towed at uniform speeds ranging from 0.4 to 2.0 m/s. Fibre optic strain gages were used to measure both in-line and crossflow strain response. The resulting time series information was processed to resolve the modal strain information that included frequency, mode shape, and critical damping ratio information. The test data for the 100% coverage by helical stakes demonstrated the effectiveness of that suppression device over the range of current velocities investigated.

Gao et al. (2016) investigated the VIM's influence for the spar-FPSO to mooring line tension by using API simple summation method. The results show that VIM phenomenon leads to a more complex mooring tension distribution, higher offset motion and more serious mooring line fatigue problem.

Yang and Kim (2018) used a fully coupled multi-body-mooring-riser time domain analysis program to model the pipeline bundle with finite elements as one line member with the equivalent diameter and structural properties. The axial friction forces as well as the transverse drags on the pipeline bundle are considered because their accumulated effects along the very long FTL can be significant. The coupled relative motions of the spar and FPSO can significantly affect the dynamics and tensions of the FTL. The dynamics of the FTL can also affect the relative motions of the two platforms two. The complex coupled system is also significantly affected by the headings of environmental loadings.

Cheng et al. (2018) performed a comprehensive test on straked riser buoyancy modules in a wave basin. The objective of the model test is to obtain hydrodynamic coefficients for the straked pipe and to better understand the global dynamic behaviour of pipe with distributed buoyancy modules due to vessel induced motion and vortex-induced-vibration (VIV). The response of the riser under floater motions including VIV were measured. The model test setup included a fully instrumented pipe, a planar motion mechanism (PMM) which simulates the vessel motion as shown in Figure 200. The riser was instrumented with Fibre Bragg Grating (FBG) strain gauges along the pipe length and circumference. Both in-plane and out-of-plane signals were recorded. The drag and inertia coefficients for the straked pipe are calculated using the modal reconstruction method. The response for different pipe and buoyancy modules were also discussed.

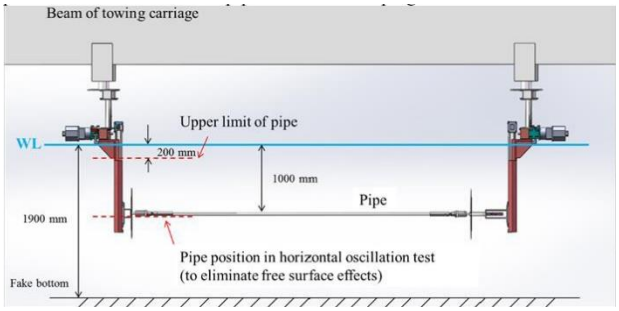

Figure 200: Sketch of horizontal oscillation test for the pipe with buoyancy modules (Cheng et al., 2018)

L. Zhao et al. (2018) studied the VIV response characteristics of flexible catenary riser model with the slenderness ratio of 578 by means of scale physical model experiments. In the experiment shown in Figure 201, the riser model was installed on a towing carriage, which might move horizontally above a wave basin with constant speed to simulate the working condition of the riser model under uniform current. The tension sensor was used to measure the time-history variation of the top tension. The acceleration sensor was used to measure the accelerations of the riser model in crossflow (CF) and in-line (IL) directions. The top tension, vibration spectrum, amplitude and vibration locus of the riser were analysed in accordance with the flexible riser model experiment, and the VIV law of the model experiment working condition was analysed. The hydrodynamic software Orcaflex was used to verify the finite element analysis (FEA) of the experiment. The experimental results showed that the physical model experimental results well matched those of Orcaflex numerical model. The physical model experimental results reflected the vibration law of flexible risers under actual working conditions. Through the analysis of the tension of the riser, it was evident that the top tension of the riser increases with the increase of the flow velocity due to the flexibility and the catenary shapes of the flexible catenary risers, and the faster the flow velocity increases, the faster the growth rate is. According to the displacement and spectrum analysis, the dominant frequency of the riser in IL direction was twice that in CF direction.

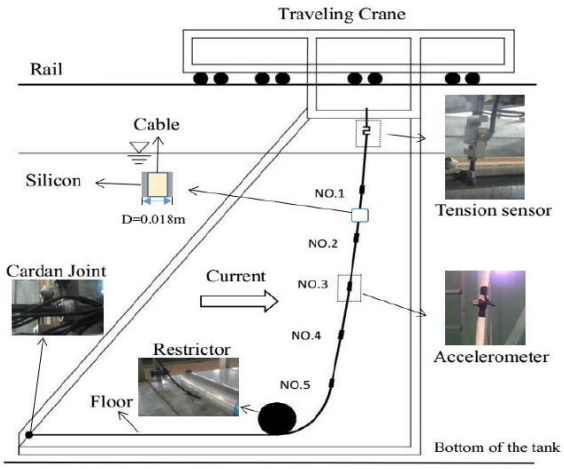

Figure 201: Experiment setup for VIV measurement of flexible catenary riser (L. Zhao et al., 2018)

Ren et al. (2019b) investigated the hydrodynamic forces on stationary partially submerged cylinder through towing test with Reynolds number ranging from 5×10^4 to 9×10^5. Three test groups of partially submerged cylinders with submerged depths of 0.25 D, 0.50 D, and 0.75 D and one validation group of fully submerged cylinders were conducted. The test results showed a considerable difference in the hydrodynamic coefficients for the partially submerged cylinders versus the fully submerged cylinders. A significant mean downward lift force is first observed for the partially submerged cylinders in a steady flow. The maximum of the mean lift coefficients can reach 1.5. Two distinct features are observed due to the effects of overtopping: random distributions in the mean drag coefficients and a clear quadratic relationship between the mean lift coefficients and the Froude number appear in the non-overtopping region. However, the novel phenomenon of a good linear relationship with the Froude number for the mean hydrodynamic coefficients was clearly shown in the overtopping region. In addition, fluctuating hydrodynamic coefficients were proposed and investigated.

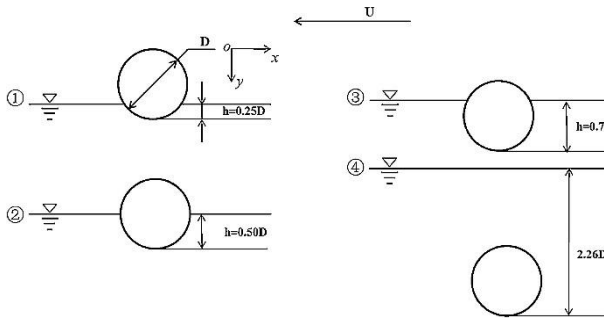

Figure 202: Sketch of the experimental cases (Ren et al., 2019b)

In another experimental study, Ren et al. (2019a) have investigated the oscillatory flow around a flexible pipe fitted with helical strakes for Keulegan-Carpenter (KC) number varying from 21 to 165 and maximum reduced velocities ranging from 4 to 12. The effects of the helical strakes on the VIV response, Strouhal number, suppression efficiency and fatigue damage were assessed. The results showed that the suppression efficiency and fatigue damage reduction ratio are not as ideal in oscillatory flow as those in steady flow. Moreover, under a lower reduced velocity ($V_R = 4$), the helical strakes significantly increased the VIV dominant frequency and the Strouhal number reached 0.439. Under a higher reduced velocity, two distinct branches in the variation of the St number against the KC number were observed.

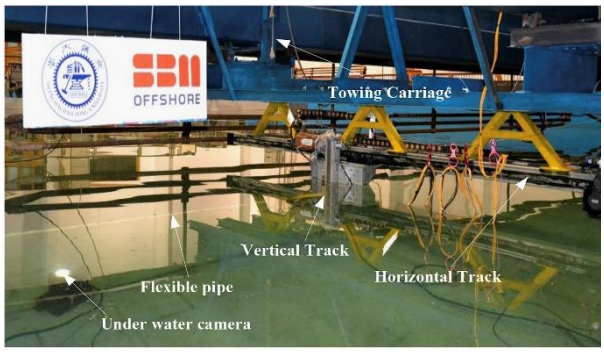

Figure 203: Overview of the whole experimental setup (Ren et al., 2019a)

Tumen Ozdil and Akilli (2019) compared the flow characteristics around horizontal single and tandem cylinders at different immersion elevations in shallow water. Particle Image Velocimetry (PIV) was used to evaluate the time-averaged and instantaneous velocity vector area in the wake zone at Reynolds number; $Re_D = 5000$ based on the diameter (D) of cylinder. The gap (L) between the tandem cylinders was enhanced from 0 until 90 mm through 15 mm enhancements to observe effect of the gap on flow characteristics. Five hundred instantaneous images were used to obtain the mean velocity vector field, the streamline topology, and the Reynolds stress correlation. For instance, Figure 204 presents the results for the gap configuration L/D =1 and different immersion distances. The investigation showed that the wake zone happens between tandem cylinders at the starting of L/D=1 location. Furthermore, when the space between tandem cylinders deepens, the dimension of the wake zone rises.

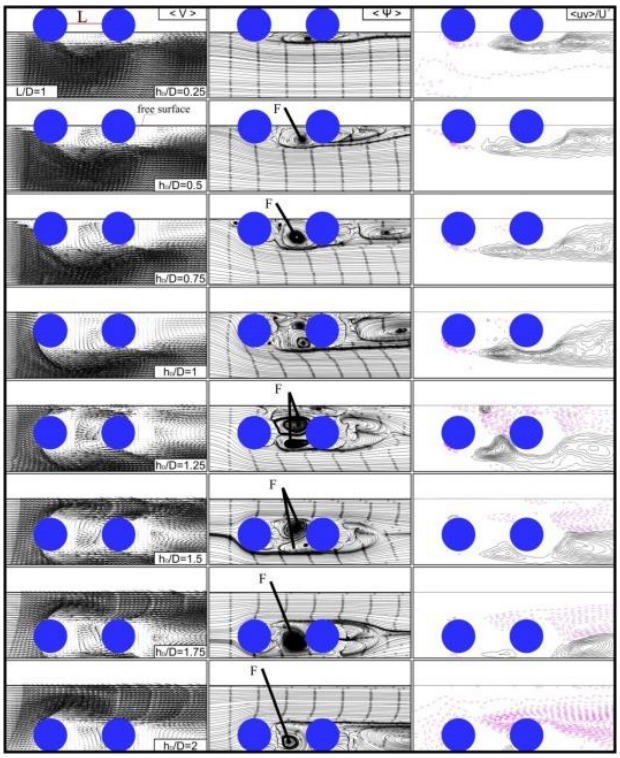

Figure 204: Flow structure around tandem horizontal cylinders for L/D = 1 situation.

Gao et al. (2020) presented some recommendations for the prediction of

hydrodynamic damping in WIR (Water Intake Riser) design based on experiments. In this study, the hydrodynamic damping of a smooth WIR oscillating in still water or in steady currents is measured with a series of experiments at KC < 5 and the Reynolds number (Re) in the range of 103 ~ 105. The effect of in-line or cross steady currents on the in-line hydrodynamic damping is investigated and the performance of the relative velocity Morison model for predicting the hydrodynamic damping at low KC is examined. Experiments are also conducted for a WIR with helical strakes in in-line or cross currents. The model test setup, as illustrated in Figure 205, includes a hexapod that generates the forced oscillation, a mass-spring system that simulates the dynamic behaviour for the WIR and a smooth/straked rigid WIR model. The mass-spring system consists of a trolley with four rollers, a rigid support beam along which the trolley can move and two springs that connect the trolley with both ends of the support beam. For the smooth WIR, the measured drag coefficients agree reasonably well with the published data and the theoretical Stokes-Wang's solution when it is applicable. The hydrodynamic damping is found to increase with the velocity of the in-line steady current, and the relative velocity with a constant drag coefficient is still applicable in the low KC flow regime when the in-line steady current is considered. For the WIR with helical strakes, a good correlation between the drag coefficient and the velocity ratio r is found, based on which the empirical formulae for drag coefficients are proposed.

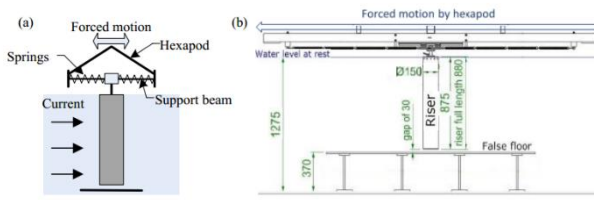

Figure 205: Experiment setup for drag coefficient (Gao et al., 2020)

5.2 Other types of pipes/cables

Besides the applications related to fluid transfer pipes/lines for the oil and gas industry, the dynamics of cables close to the sea surface is also of concern for other types of applications such as power cables for wave energy converters, cable net barriers, and towing cables. However, in the literature review only few numerical studies have been found. For instance, Yang et al. (2017) and (S.-H. Yang et al. (2018) numerically investigated a wave energy converter (WEC) system consisting of a buoy, a mooring system, and a power cable connected to a hub. The study assessed the characteristics of the entire system regarding the energy performance and fatigue life of the mooring lines and power cable. In the former study, the effects of marine biofouling and its growth on the system's components was considered. Hydrodynamic and structural response simulations were conducted in a coupled response analysis using the DNV-GL software SESAM. Energy performance analyses and stress-based rain flow counting fatigue calculations were performed separately using an in-house code. In the latter study, the WEC system formed an array, with several WECs located around a central hub to which they were each connected by a short, free-hanging power cable. The study is analysed the dynamic characteristics and estimate the fatigue life of the power cable which is not yet in use or available on the commercial market. A novel approach was adopted considering that the power cable's length was restricted by several factors (e.g., the clearances between the service vessel and seabed and the cable), and the cable was subjected to motion and loading from the WEC and to environmental loads from waves and currents (i.e., dynamic cable). The results of the numerical simulations were discussed regarding the responses of the power cables, including dynamic motion, curvature, cross-sectional forces, and accumulated fatigue damage. The effects of environmental conditions on the long-term mechanical life

spans of the power cables are also investigated. Important cable design parameters that resulted in a long power cable (fatigue) service life are identified, and the cable service life was predicted.

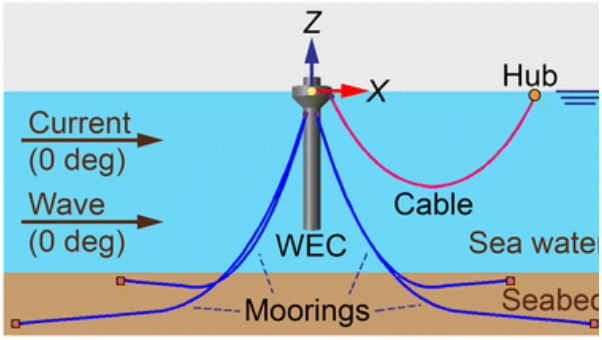

Figure 206: WEC system, including the WEC and its moorings, the hub and the cable (S.-H. Yang et al., 2018)

Da Silva Gomes and Pinheiro Gomes (2021) have proposed a new formalism for the dynamic modelling of a cable towing system, in which both the tugboat and the towed vessel were subject to forces from waves on the sea surface. The continuous flexibility of the cable was approximated by a discrete equivalent, formed by rigid links connected by fictitious elastic joints that allow elevation movements, since the dynamics are restricted to the vertical plane. The Euler-Lagrange formalism was used to determine the dynamic models considering two, three and four links. Vertical forces obtained from proportional and derivative control were applied to the tugboat and the towed vessel, thus simulating the wave motion of the sea surface. Simultaneously, a motor thrust is applied to the tugboat. An algorithmic procedure was also proposed to determine the dynamic tension in the cable.

Finally, motivated by the design of a protective anti-shark cable net enclosure located in heavy surf on La Réunion, France, Niewiarowski et al. (2018) presented a modelling technique for underwater cable structures subject to breaking wave action. In the presented work, the Morison equation was coupled with a high-resolution breaking wave simulation obtained by solving the full air-water Navier-Stokes equations, creating a time-domain analysis approach suitable for studying underwater cable structures subject to breaking waves. The hydrodynamic model was validated using the software package ProteusDS, and the presented model was used to characterize the mechanical response of a moored cable net.

6. STATE-OF-THE-ART REVIEW IN HYBRID TESTING – SOFTWARE-IN-THE-LOOP TESTS FOR MODELLING WIND FORCES

The Software-in-the-Loop (SIL) approach in the floating wind turbine model testing is to include a realistic force to represent the aerodynamic thrust in combination with wind and wave scaled tests. It is based on the use of a ducted fan substituting the wind turbine scaled rotor. The fan thrust is controlled by the fan rotational speed set by the controller, which again depends on a computer real time simulation of the full-scale rotor in the wind field. The real time simulation considers the platform motions measured in real time in the wave tank test. Therefore, the aerodynamic damping is modelled by the fan force (Müller et al., 2014). In those tests, a brushless motor was integrated with the ducted fan. The motor power electronics was regulated by an Electronic Speed Controller (ESC) card that was powered by an industrial AC/DC power supply. The rotational speed of the motor was controlled by a Pulse Width Modulation (PWM) signal that was generated with a LabVIEW control software, using servo libraries for Arduino. The demanded force for the fan was provided by the full-scale simulation of the rotor's aerodynamic thrust. Figure 207 shows the layout of the system hardware. The selection of the power of the fan system is based on the range of required thrust during the test. This depends on the nominal power of the wind turbine and the scale factor. In addition, the thermal stability of the

fan system must be considered, in order to run at the required power during the requested time of the test and avoid using a cooling down phase (Azcona et al., 2014).

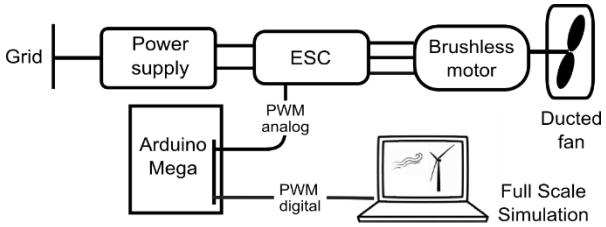

Figure 207: Fan control system layout (Azcona et al., 2014)

A typical SIL system can be found from the research of Azcona et al. (2014) and displayed in Figure 208. The left side describes the simulation part of the system, which works in full scale, and the right side represents the wave tank scaled test.

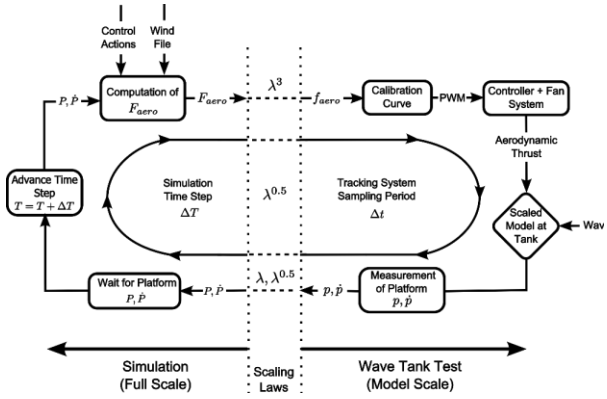

Figure 208: Software-in-the-Loop method diagram (Azcona et al., 2014)

The SIL approach required a communication protocol between the simulation and the tank hardware. Azcona et al. (2014) have used the LabVIEW software to acquire the data from the wave tank motion capture system at ECN (Qualisys) and to communicate with the wind turbine simulation software during the test execution. A TCP/IP network protocol was selected for the communication between LabVIEW and Qualisys and between LabVIEW and the simulation code.

SIL approach could overcome the limit of applying the actuating the forces through direct physical simulation such as lack of ability to simulate part of the physical environment (e.g. lack of wind generation in a test tank), issues of the size of the facility (e.g. simulation of spread moorings), or issues of the similarity between model and full-scale prototype.

6.1 Impact of the SIL approach

The SIL approach can provide a realistic aerodynamic thrust on the scaled model. As the computation of the force takes into consideration the motion of the platform, the effect of the aerodynamic damping is included. In addition, the control actions, the different types of wind (turbulent, constant, gusts) and the operating condition (idling, power production, etc.) are considered for the calculation of the thrust. Conditions where the waves and wind are misaligned are sometimes not easy to be reproduced in wave tanks with wind generation systems. With this method, it can be easily achieved by changing the fan orientation at the tower top. Furthermore, the SIL system allows performing test cases including wind at wave basins where the wind generation system is not available. In addition, the simplicity of the method makes it cost effective and flexible because the material is not specific for a certain wind turbine model and it could be used in different tests for different models (Müller et al., 2014). Some more key benefits are listed below (Day et al., 2017):

- the tests could take place without the need for deployment of a wind generation system;
- there is no requirement to construct a scale-model (or distorted-scale-model) rotor and drive;
- the scale of the tests is dictated only by the hydrodynamics of the floater, which in this case allows a test at relatively large scale;

- the test procedure can replicate the forces generated by turbulent or steady wind in a variety of directions relative to the wave heading;
- the impact of the turbine control system and blade elasticity may be modelled in the tests;
- correct simulation of the aerodynamic drag load on the tower and parked turbine in extreme conditions is possible;
- Some special cases, such as emergency stop tests can be simulated with correct full-scale behaviour.

Effects that are not scaled correctly with this procedure are the aerodynamic torque and the gyroscopic momentum. Alternatively, the use of a rotating scaled mass to represent the rotor inertia can be used to match the gyroscopic effects. Active research on the response of different fan units depending on the size of the wind turbine, scale factor, etc. is being conducted with the aim to explore the limits of the methodology.

6.2 SIL applications

In recent years, many research papers have been published by using the SIL approaches in different research area. SIL was used in wind tunnel testing to model behaviour of a floating wind turbine by mounting a Reynolds-scaled working turbine model on a hexapod (Bayati et al., 2014) and utilizing the hexapod to simulate the impact of the platform motions on the turbine performance.

A 6-Degrees-of-Freedom PKM-Hexaglide robot for simulating the dynamics of Floating Offshore Wind Turbines in wind tunnel scale tests is used in their experiments, as shown in Figure 209. They validate the sophisticated aero-hydro-elastic simulation tools as well as control strategies through the scale test experiments and to provide a complementary approach with respect to water basin scale tests, with a greater attention to the influence of the floating motion on the aerodynamics.

In addition, they define the requirements due to extreme sea-state and the related dynamics of three different platform concepts combined with the 5-MW reference floating turbine. A rigid multibody model is developed for assessing the dynamics of the robot due specific motion-tasks and for sizing the actuation system. The scaled motions of a 5-MW spar buoy floating turbine were analysed as reference case to verify the reliability of the robot to reproduce the dynamics of nominal operating conditions, in terms of slider displacements, forces and power within the design ranges.

Figure 209: 6-DoF Robotic platform “HexaFloat” for wind tunnel tests (Bayati et al., 2014)

In ship model testing, Tsukada et al. (2013) used a ducted fan as an auxiliary thruster mounted on a free-running ship model in order to correct for Reynolds scaling effects on the ship resistance in manoeuvring tests.

Azcona et al. (2014) implemented and performed a first validation of the SIL approach coupling in real time of rotor simulation that controls the fan with the measured motions of a 6 MW semisubmersible scaled floating wind turbine. The scaled model of the turbine is shown in Figure 210 and the fan system is shown in Figure 211. The described methodology was applied during a test

campaign of a floating semisubmersible platform performed during 2013 at the Ecole Centrale de Nantes (ECN) wave tank in France. The purpose of the test campaign was the verification of the platform design and the assessment of the performance of the SiL system. The experimental results have been compared with computations, in general, with good correspondence. The platform pitch displacements under different constant wind loading compare well between tests and computations, showing the correct static performance of the ducted fan system. The free decay test in pitch under a constant wind of 12.7 m/s illustrates the capability of the fan to capture the coupling of the aerodynamic thrust with the rotor's relative displacements within the wind field. Nevertheless, when the turbulent wind is included to the irregular wave cases, these differences disappear, and the experimental results match very well the computations. In particular, the effect of wind over the pitch motion is very accurately captured, which is important to calculate the correct rotor loads.

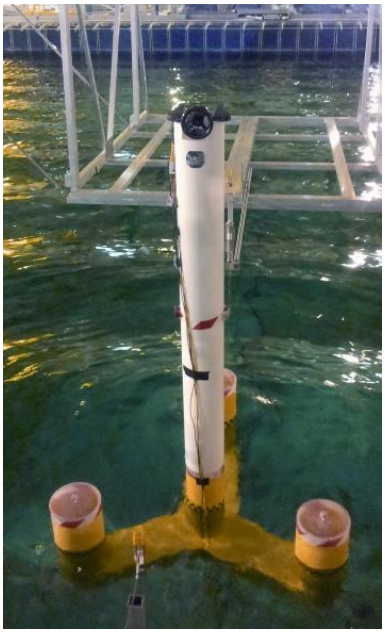

Figure 210: Scaled Model in the Wave Tank (Azcona et al., 2014)

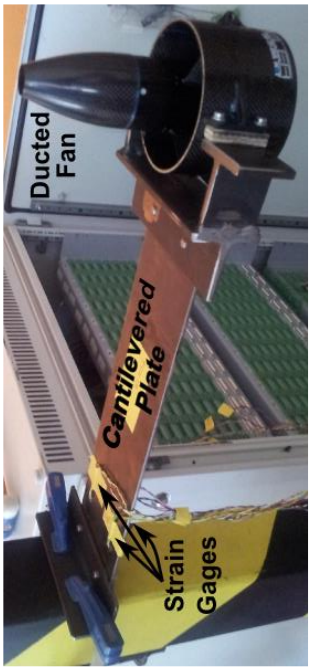

Figure 211: Fan Set Up for Calibration (Azcona et al., 2014)

Zamora-Rodriguez et al. (2014) generated the unsteady aerodynamic thrust force in a hydrodynamic test of a floating wind turbine using a speed-controlled fan. The Iberdrola TLPWT platform consists of a central cylindrical column with four square section pontoons (perpendicularly symmetrically distributed) attached at its bottom, each with two tendons as shown in Figure 212, aimed at supporting a 5 MW generator, positioned at a height of 89 m from MSL.

To consider the wind effect, a speed-controlled fan is positioned at the top of the tower. The fan produces thrust action only in the x direction. The fan thrust depends on the relative wind speed, which in turn, is mainly function of surge and sway velocities. Motion information is transferred in real time from OPTITRACK system to the fan control to adjust the thrust accordingly. Regular waves, operational, survival, failure and transport experiments have been conducted. They find that all motion RAOs are very small, except surge, consistently with the type of platform

(TLP). A maximum motion RAO of 5 in surge in a period range between 20-25s is found. That value decays quadratic for lower periods leading to operational sea states RAOs that is lower than one. Maximum accelerations values in nacelle are below 3 m/s^2 and tensions below 40% of MBL in survival conditions.

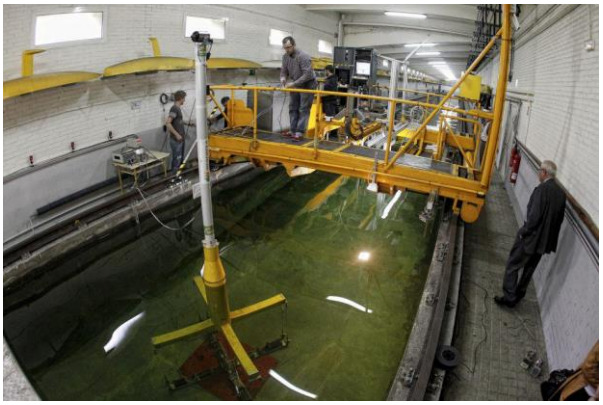

Figure 212: Floating wind turbine case study (Zamora-Rodriguez et al., 2014)

In the research work of Sauder et al. (2016) and Bachynski et al. (2016), all aerodynamic load components for the structure are identified and applied on the physical model, which is significantly different from other previous studies, where only the aerodynamic thrust force was applied on the physical model. The study is carried out at Real-Time Hybrid Model Testing with 5-MW-CSC design for a range of testing including turbine shutdown. The numerical substructure contains only the turbine while the floater and rigid tower are modelled physically.

Wave and current environment are modelled physically in the Ocean Basin, while the wind environment is modelled numerically. A detailed examination of the motions, mooring line forces, and tower and column bending moments in severe waves, aligned wind and waves, misaligned wind, and waves, wind-wave-current, and in several wind turbine fault conditions are thoroughly investigated. It is concluded that for the platform tested, the interaction between the aerodynamic and hydrodynamic loads was primarily at low frequencies.

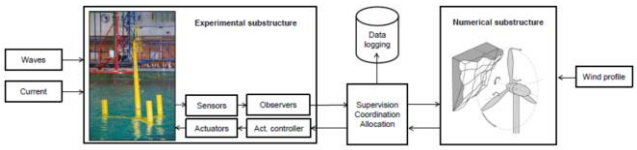

Figure 213: Sub-structuring strategy for the work of Sauder et al. (2016) and Bachynski et al. (2016)

The software in the loop approach was used by Day et al. (2017) and Oguz et al. (2018) to control a ducted fan to simulate the aerodynamic thrust load on a TLP floating wind turbine in the Kelvin Hydrodynamics Laboratory at the University of Strathclyde, as shown in Figure 214. The floater consists of a TLP designed for 70 m water depth with four pontoons in a cross arrangement each fitted with two tendons. The floater is designed to utilize the benchmark NREL 5 MW turbine. A ducted fan unit intended for use on a model aircraft was fitted at the correct vertical location for the drive train. This could develop up to 50 N of thrust. This was mounted on a load cell and extensively bench-tested to determine the relationship between steady speed and thrust. The SIL control system for the fan was developed by CENER. The 6-DOF rigid-body motions of the platform are computed from the measurements by the Qualisys motion capture system and output in real time to the control PC. The control PC runs a highly modified version of the well-known FAST aero-hydro-servo-elastic code, as shown in Figure 215, in which the standard hydrodynamic calculations to find instantaneous platform position, attitude and velocities are replaced by the values obtained from the tank measurements. The code then calculates the aerodynamic thrust expected with the instantaneous platform location and dynamics in the wind field (either steady or turbulent) and outputs the thrust demand to the fan controller. This in turn controls the fan to rotate at the speed associated with the target value of thrust.

Results for free oscillation tests and regular wave responses for the TLP turbine show that the implementation of the SIL approach gives greater quadratic damping and can affect the RAO in surge by as much as 20% compared to the case with no wind, and more than 10% compared to the case with a predefined thrust.

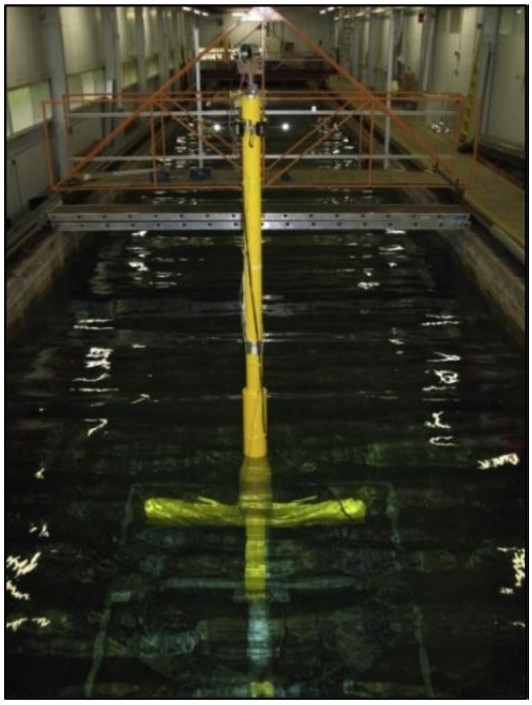

Figure 214: View of the model in KHL tank looking towards wave maker (Oguz et al., 2018)

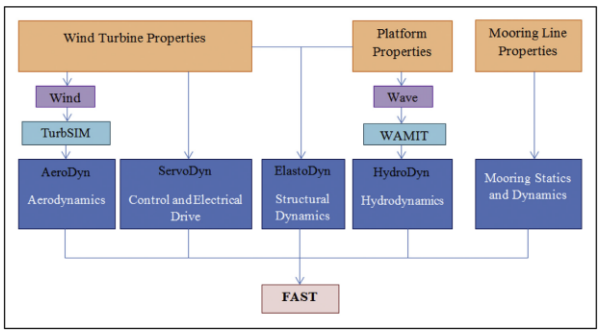

Figure 215: Fast structure (Oguz et al., 2018)

Vittori et al. (2018) at National Renewable Energy Center in Spain (CENER) has developed a hybrid testing method (SiP) to replace the rotor by a ducted fan at the model tower top. Like other SiL methods, the introduction of fan brought in a variable force representing the total wind thrust by the rotor. This load is obtained from an aerodynamic simulation that is performed in synchrony with the test and it is fed in real time with the displacements of the platform provided by the acquisition system. With the use of such method, the displacements of the turbine and the relative wind speed on the rotor is considered.

A test campaign is taken at the Ecole Centrale de Nantes wave tank of the OC4 semisubmersible 5 MW wind turbine, with a scale factor of 1/45. The experimental results are compared with NREL FAST. Simple cases as only steady wind and free decays with constant wind showed a good agreement with computations, demonstrating that the SiL method can successfully introduce the rotor scaled thrust and the effect of the aerodynamic damping on the global dynamics. Cases with turbulent wind and irregular waves showed better agreement with the simulations when mooring line dynamics and second order effects were included in the numerical models.

Thys et al. (2018) presents Real-Time Hybrid Model (ReaTHM) tests that are performed on a 10-MW semisubmersible floating wind turbine in the Ocean Basin at SINTEF Ocean in March 2018, see Figure 216 and Figure 217 for experimental setup and control loop. For the tests in the ocean basin, the FOWT system is divided into two substructures. The physical substructure contains the Froude-scaled floating substructure, tower, and mooring system subject to physical waves and current. The wind turbine tower and rotor were modelled in a modified version of NREAL FAST and used to compute the aerodynamic loads on the tower, and the rotor loads, except for inertia and gravity, which were modelled physically. The simulation model takes the real-time floater motions as input and computes the rotor and tower loads, which were then applied on the model by use of a cable-driven parallel robot.

Different from the campaign reported in Sauder et al. (2016) and Bachynski et al. (2016), there are several improvements of the ReaTHM in the aspect of modelling capabilities. These included the testing of design load cases with varying wind direction; inclusion of loads on the turbine tower to allowing for the tests with the wind turbine in parked condition and increase the bandwidth to model the 3p frequency and the first tower bending frequency. Test results show that the wind turbulence played an important role for the surge and pitch responses at low frequency. The surge and pitch response in the wave frequency zone is seen to be nearly unaffected by the wind. The pitch period varies depending on the wind conditions and the low frequency loads at base of tower are dominated by the gravity loads due to the pitch motions.

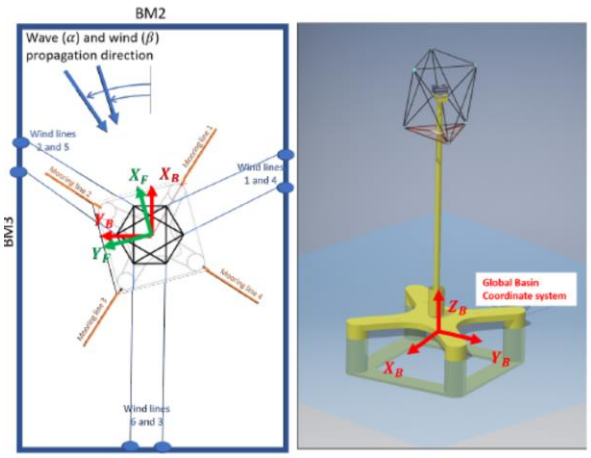

Figure 216: Experimental setup (Thys et al., 2018)

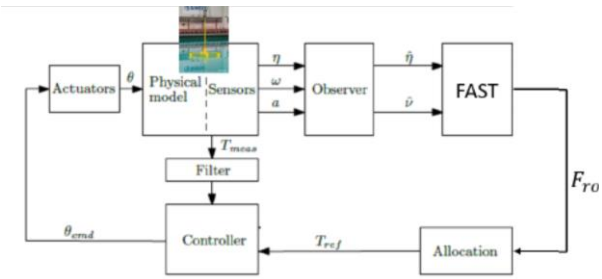

Figure 217: Control loop for REATHM tests (Thys et al., 2018)

A subsequent work led by Thys et al. (2019) for hybrid model tests performed in the EU H2020 LIFES50+ was published. LIFES50+ has two main test campaigns, where hybrid wind tunnel and ocean basin model tests with a FOWT were performed. Politecnico di Milano (POLIMI) developed a method for model tests in a wind tunnel and SINTEF Ocean developed a method for tests in an ocean basin. The setup of the hybrid model tests in the wind tunnel and ocean basin are shown in Figure 218 and Figure 219, respectively. In the wind tunnel, a physical wind turbine was connected to a 6-DOF parallel kinematic robot controlled by real-time simulations of the floater subject to hydrodynamic loads. In the ocean basin, a physical model of the FOWT, without the rotor geometry, was placed in the basin and coupled to a force actuator controlled by the simulated aerodynamic loads.

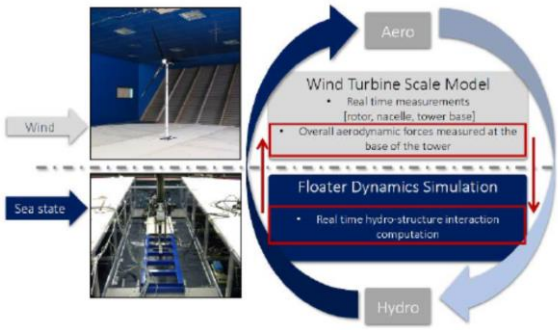

Figure 218: Setup of the hybrid model tests in the wind tunnel at POLIMI (Thys et al., 2019)

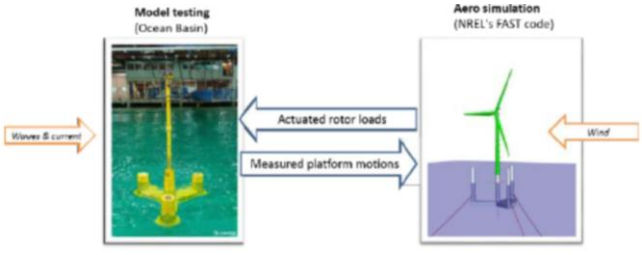

Figure 219: Setup of the hybrid model tests in the Ocean Basin at SINTEF OCEAN (Thys et al., 2019)

Comparison between wind tunnel and ocean basin results are made in terms of floater and mooring, rotor, and the characteristics of the

complete system (mooring, floater, wind turbine subject to wind and waves). The wind tunnel test results indicated that the linear response to small to moderate wave excitation is accurately modelled, but calibration of the numerical model is needed for accurate modelling of the low frequency response. The comparison between wind tunnel and ocean basin tests on irregular waves and wind results show that both testing techniques were giving comparable statistical values.

In the recent work of Pires et al. (2020), the hybrid testing method developed by National Renewable Energy Center in Spain (CENER) for floating wind turbine scaled tests combining wind and waves (SIL) has been upgraded in order to introduce not only the wind turbine rotor thrust, but also the out-of-plane rotor moments (aerodynamic and gyroscopic). To achieve this goal, the former ducted fan has been substituted by a multi-propellers actuator system. The new system has been completely developed, calibrated, and used on a test campaign carried out at MARIN's Concept Basin. It was installed on a 1/50 scaled model of the DeepCwind 5-MW semisubmersible turbine built by MARIN within the EU MARINET2/Call No. 3 under ACTFLOW project framework. The control strategy of the floating turbine was developed by POLIMI and TU-DELFT and integrated into the SIL numerical model. The experiment has proved a good behaviour of the enhanced SiL method. It has revealed that the relative importance of gyroscopic moments is low in comparison with the aerodynamic rotor moments in the considered cases. The results also show how rotor moments are particularly important in FOWT dynamics in cases with large rotor load imbalances such as situations where one blade fails to pitch.

Matoug et al. (2020) reports the testing result for the WindQuest 10-MW turbine in comparison to the reference DTU 10-MW horizontal axis turbine (HAWT) developed for the Lifes50+ project. Figure 220 shows a schematic diagram representing the WindQuest and the DTU scale models. The Nautilus-semi-submersible floater is used with both turbines. The seakeeping of the two FOWT is studied experimentally at the Ifremer waves & wind tank, Brest, France (Figure 221 and Figure 222).

In the SiL loop, the hydrodynamics are scaled in the wave tank, the aerodynamics is simulated using an actuator. The thrust is computed and applied in real-time. The measurements from the motion capture system are streamed in real-time to account for platform motions. Thrust set points are computed with tabulated aerodynamic parameters extracted from simulations. The resulting set point is computed in real-time, thus allowing for a feedback loop in between the aerodynamics and the hydrodynamics (plotted in Figure 223).

Test and post-processing results indicate the advantage of using a SiL for wind-driven cases. The SiL follows the FAST simulation trend by filtering the natural frequency and maximizing the power in the wave spectrum. Though the SiL configuration shows higher levels of energy around 0.5 – 0.7 Hz bandwidth when compared to OpenFAST.

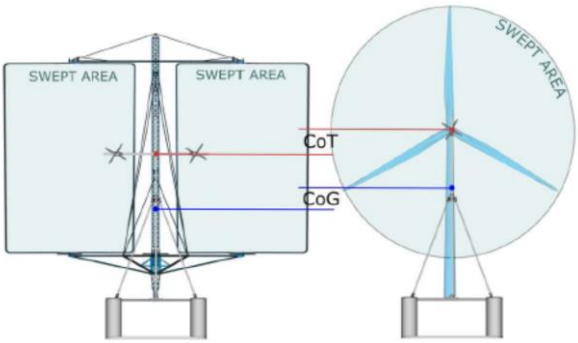

Figure 220: Comparison of the WindQuest (left) scale model with the DTU (right) (Matoug et al., 2020)

Figure 221: Scale model during wave tank tests (Matoug et al., 2020)

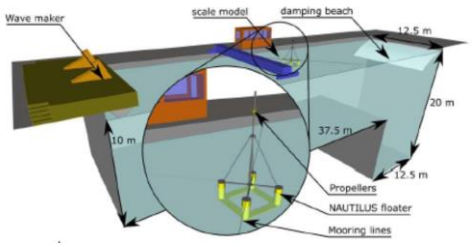

Figure 222: Representation of the Ifremer waves & wind tank with the scale model positioned for tests (Matoug et al., 2020)

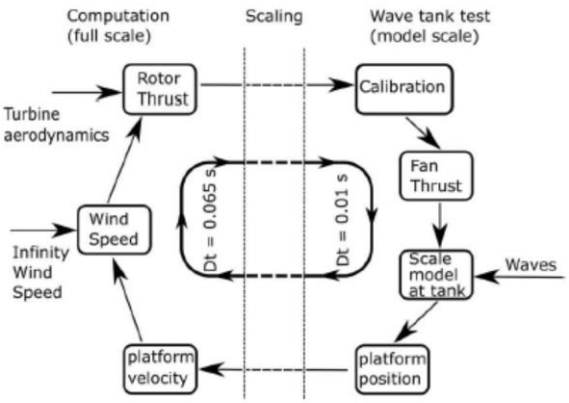

Figure 223: SiL retroaction loop: scaled part (right) and computations (left) - (Matoug et al., 2020)

7. EXPERIMENTAL BENCHMARK ON WAVE RUN-UP ON CYLINDERS

The Committee conducted benchmark studies of wave run-up heights on the fixed four-squared-cylinder system under regular and irregular waves and provided a set of benchmark results for analysing the influences of wave parameters and validating related numerical simulations. It extends the benchmark studies of wave run-ups on single and four truncated cylinders conducted in 2013.

The benchmark tests of wave run-ups on the fixed four-squared-cylinder system were carried out by State Key Laboratory of Ocean Engineering (SKLOE) at Shanghai Jiao Tong University. The benchmark test and data are summarized in the following sections.

7.1 Description of benchmark test

One configuration of fixed four-square-cylinder system is considered, as illustrated in Figure 224, in which the half column breadth a=8 m and the column spacing b=34 m, respectively.

The fillet radius, the height, and the constant draft of all columns are 3 m, 40 m, and 20 m, respectively. The model scale is selected as 1:50.

The locations of wave probes and four cylinders as well as wave headings are shown in Figure 224. The coordinates of wave probes are given in Table 5. Figure 2 shows the test setup of the model in the basin.

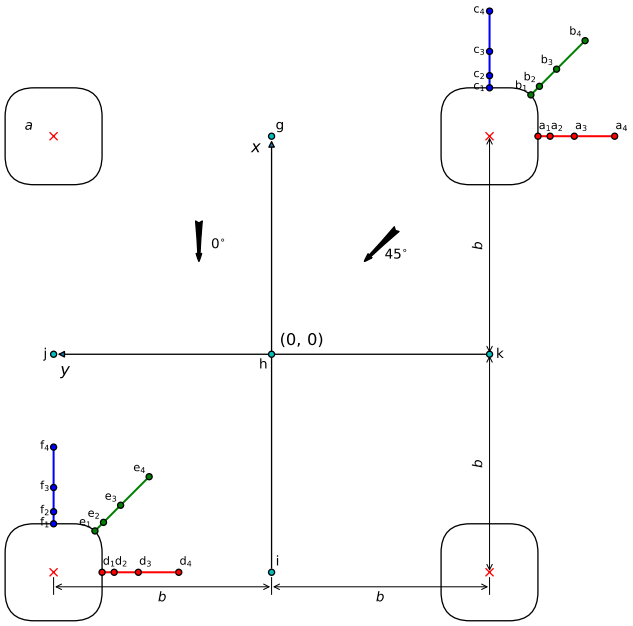

Figure 224: The fixed four-squared-cylinder system

Table 5: Locations of wave probes (in prototype)

	x (m)	y (m)
a_1	34.0	-42.0
a_2	34.0	-43.5
a_3	34.0	-46.5
a_4	34.0	-51.5
b_1	41.12	-41.12
b_2	42.18	-42.18
b_3	44.30	-44.30
b_4	47.84	-47.84
c_1	42.0	-34.0
c_2	43.5	-34.0
c_3	46.5	-34.0
c_4	51.5	-34.0
d_1	-34.0	26.0
d_2	-34.0	24.5
d_3	-34.0	21.5
d_4	-34.0	16.5
e_1	-26.88	26.88
e_2	-25.82	25.82
e_3	-23.70	23.70
e_4	-20.16	20.16
f_1	-26.0	34.0
f_2	-24.5	34.0
f_3	-21.5	34.0
f_4	-16.5	34.0
g	34.0	0
h	0	0
i	-34.0	0
j	0	34.0
k	0	-34.0

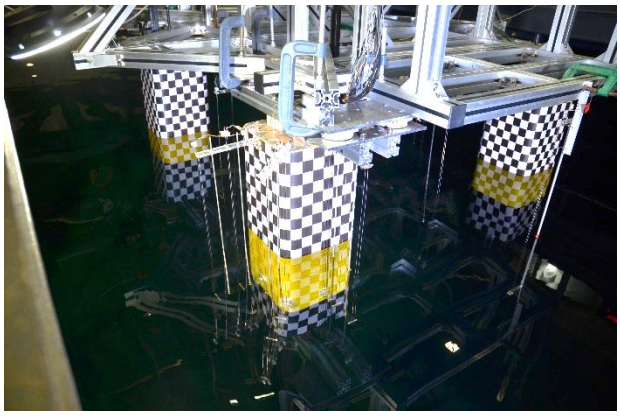

Figure 225: Test setup of the fixed four-squared-cylinder systems

Four (04) wave periods and three (03) wave steepness of regular waves were considered, as shown in Table 6. In addition,

Table 7 presents parameters of the irregular waves.

Table 6: Parameters of regular waves

Full scale					
Wave No.	H/λ	kA	T (s)	ka	A (m)
1	1/30	0.105	7	0.657	1.275
2		0.105	9	0.398	2.107
3		0.105	12	0.224	3.746
4		0.105	15	0.143	5.853
5	1/16	0.196	7	0.657	2.390
6		0.196	9	0.398	3.951
7		0.196	12	0.224	7.024
8		0.196	15	0.143	10.975
9	0.07	0.220	7	0.657	2.677
10		0.220	9	0.398	4.425
11		0.220	12	0.224	7.867
12		0.220	15	0.143	12.292

Table 7: Parameters of irregular waves

Wave No.	Hs (m)	Tp (s)	γ	Realization
13	12.0	12.0	5	Seed 1
14	12.0	12.0	5	Seed 2
15	12.0	12.0	5	Seed 3

In the benchmark studies, the max values of following measured items were compared at various wave periods and wave steepness in terms of H/λ (H is wave elevation and λ is wavelength) and kA (k is wave number and A is wave amplitude):

1) Horizontal force, F_x, F_y

2) Vertical force, F_z,

3) Wave elevations at 29 locations.

The sampling rate is 100 Hz. The wave calibrations were performed prior to placing the model in the basin. The effective duration of each regular wave test was approximately 1 minute in model scale, and that of each irregular wave test was no less than 3 hours in full scale after the wave profile reaches steady state.

7.2 Wave run-ups around the fixed four squared cylinders

7.2.1 Regular waves, 0º wave direction

Figure 226 and Figure 227 show the max values of wave run-ups at 6 locations (a_1, b_1, c_1, d_1, e_1, f_1) for fixed four-squared-cylinder system at various wave steepness (H/L=1/30, 1/16 and 0.07) and periods (T=0.99 s, 1.27 s, 1.69 s and 2.12 s) along the centre plane in terms of wave probes location (x/D). The max values are normalized by incident wave amplitude (A).

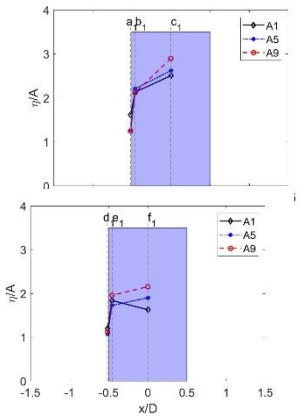

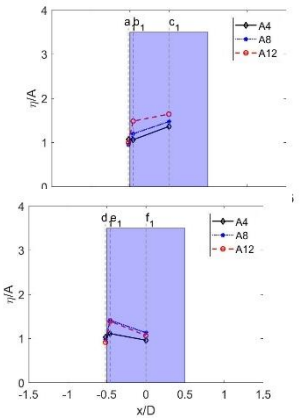

Figure 226: Max values of wave run-up heights at various wave steepness (heading 0º)

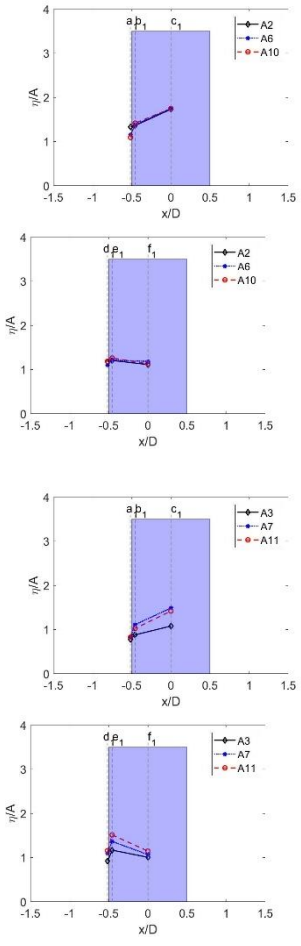

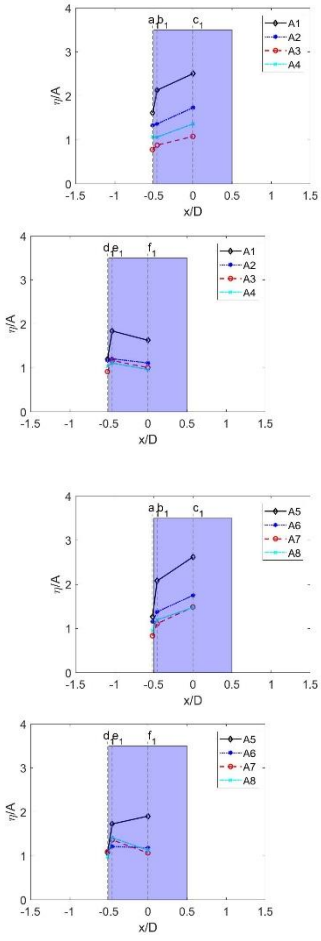

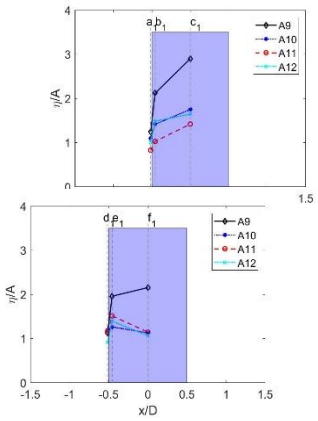

Figure 227: Max values of wave run-up heights at various wave periods (heading 0º)

7.2.2 Regular waves, 45º wave direction

Figure 228 and Figure 229 show the max values of wave run-ups at 6 locations (a_1, b_1, c_1, d_1, e_1, f_1) for fixed four-squared-cylinder system at various wave steepness (*H/L*=1/30, 1/16 and 0.07) and periods (*T*=0.99 s, 1.27 s, 1.69 s and 2.12 s).

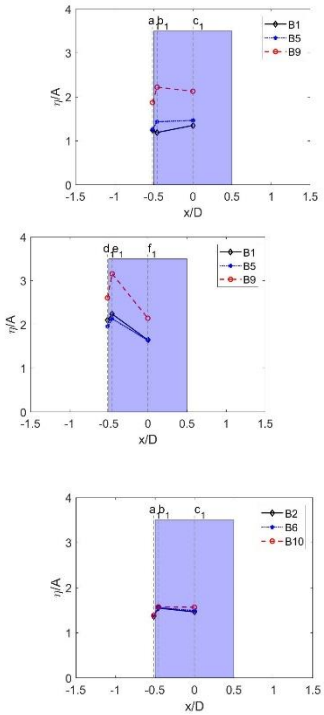

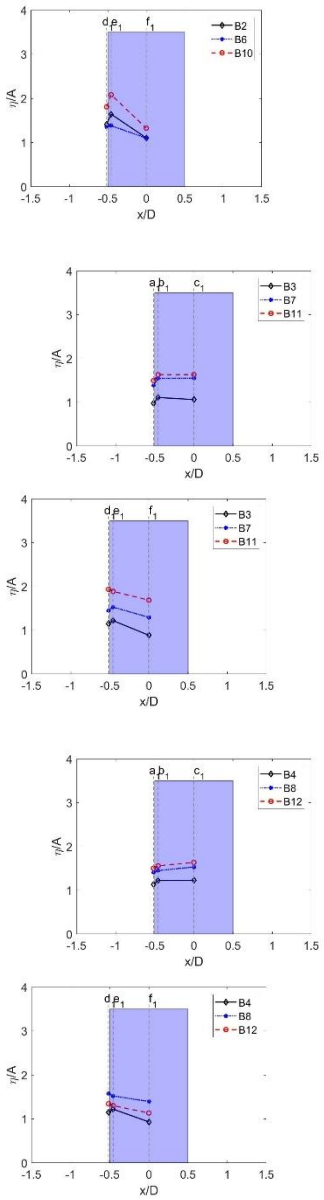

Figure 228: Max values of wave run-up heights at various wave steepness (heading 45º)

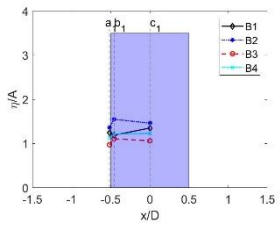

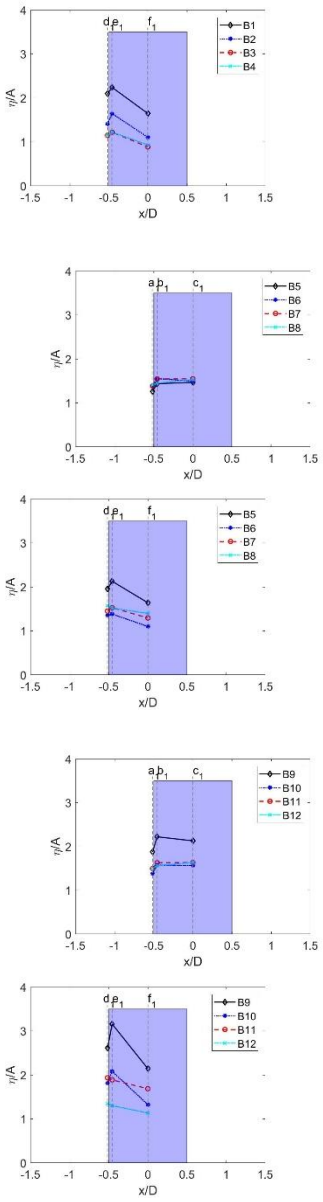

Figure 229: Max values of wave run-up heights at various wave periods (heading 45°)

Figure 230 shows the max values of wave run-ups at 24 locations (a_1-a_4, b_1-b_4, c_1-c_4, d_1-d_4, e_1-e_4, f_1-f_4) for fixed four-squared-cylinder system of each case with 0° wave direction. In the figure, D_1 means the distance from wave probe to the column surface, and D means the half column breadth. Figure 231 shows the max values for each case with 45° wave direction.

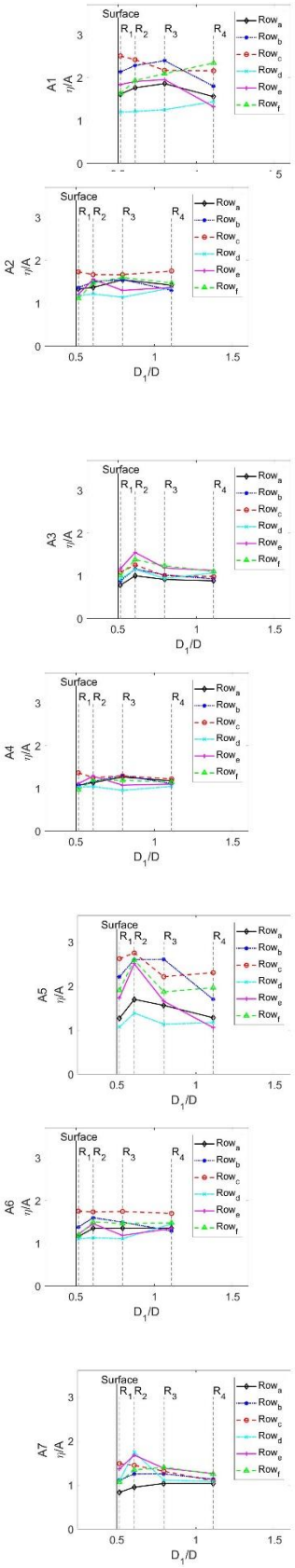

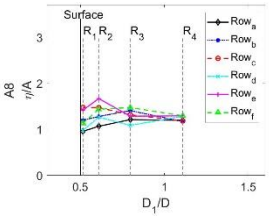

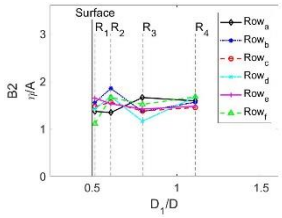

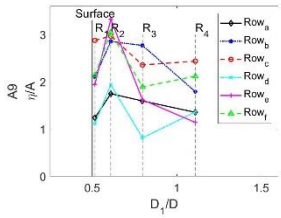

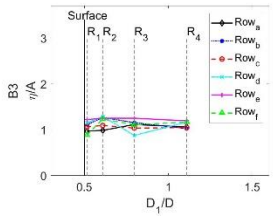

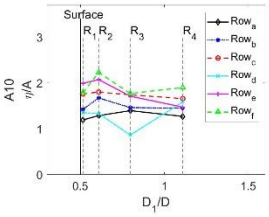

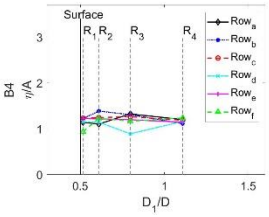

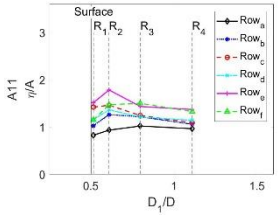

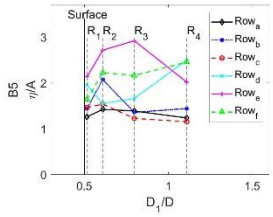

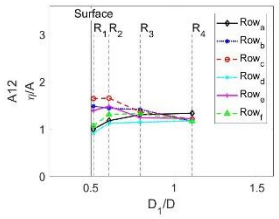

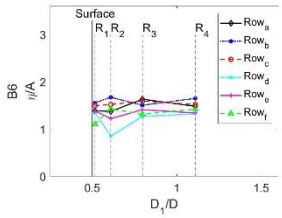

Figure 230: Max values of wave run-ups around the front and rear columns (heading 0°)

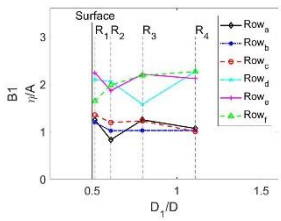

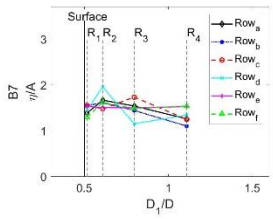

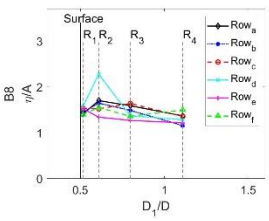

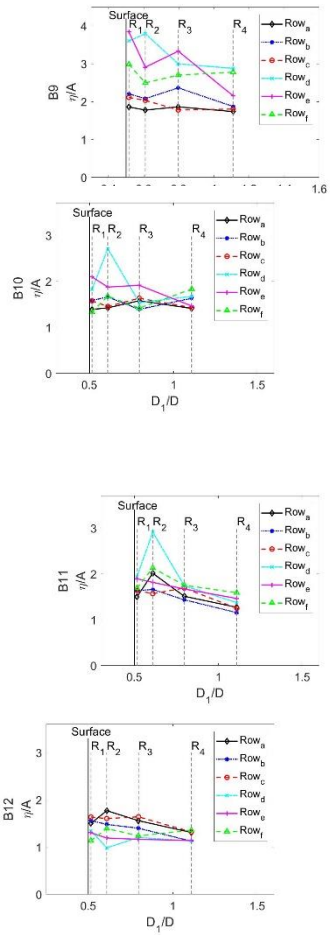

Figure 231: Max values of wave run-ups around the front and rear columns (heading 45°)

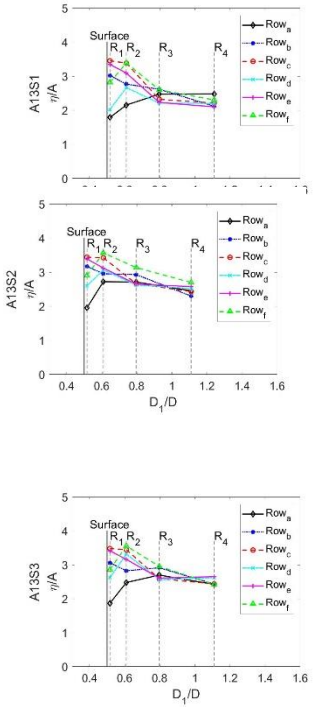

Figure 232: Max values of wave run-ups around the front and rear columns in irregular waves (heading 0°)

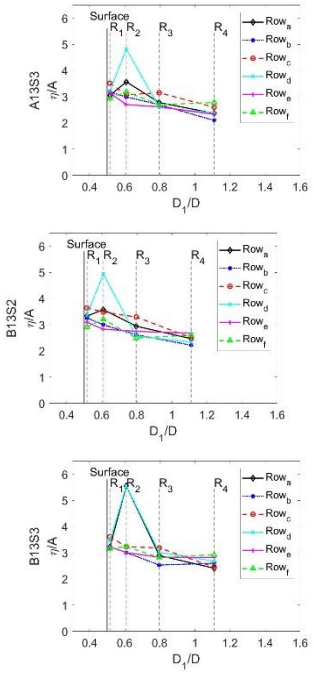

Figure 233: Max values of wave run-ups around the front and rear columns in irregular waves (heading 45°)

7.2.3 Irregular waves

Figure 232 and Figure 233 show the max values of wave run-ups at 24 locations (a1-a4, b1-b4, c1-c4, d1-d4, e1-e4, f1-f4) for fixed four-squared-cylinder system of each case with 0º and 45º wave directions, respectively.

7.3 Effects of wave period and steepness on wave forces

The max and mean values of wave forces of the front and rear columns at various wave steepness and periods were shown in Figures Figure 234-Figure 237 (0° wave direction) and Figure 238-Figure 241 (45° wave direction).

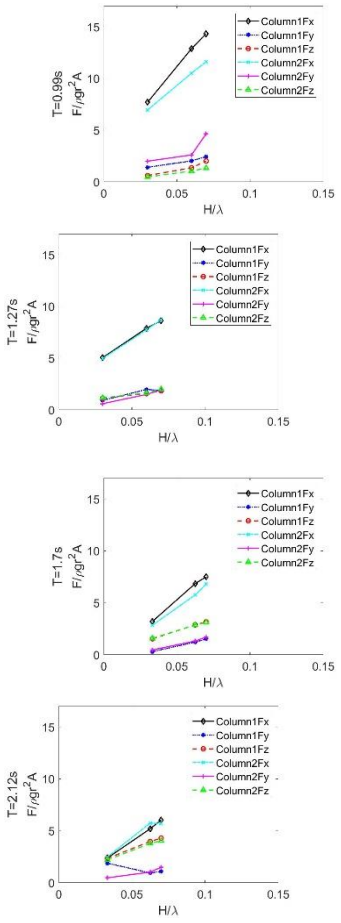

Figure 234: Max values of wave forces on the front and rear columns at various wave steepness (heading 0°)

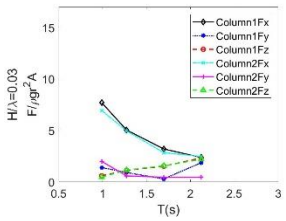

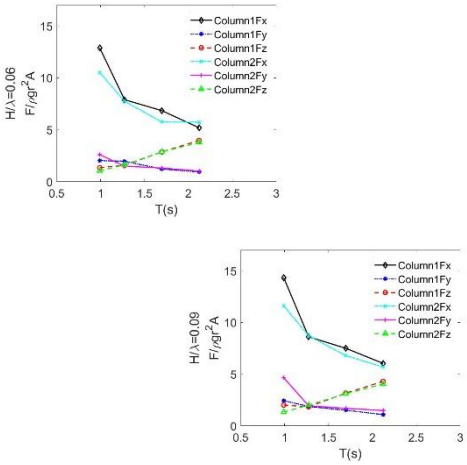

Figure 235: Max values of wave forces on the front and rear columns at various wave periods (heading 0º)

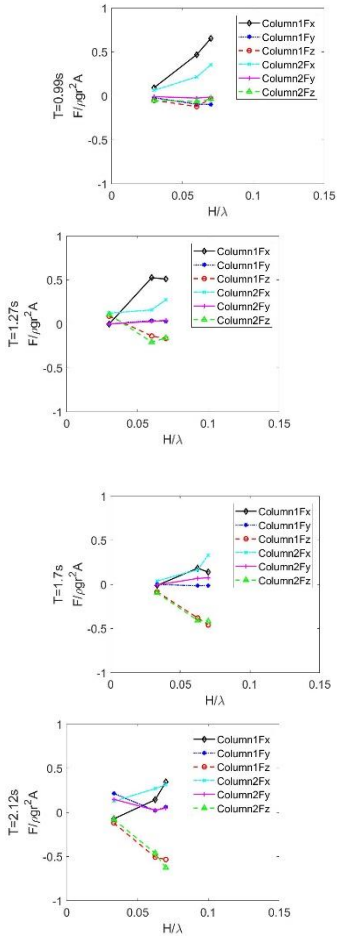

Figure 236: Mean values of wave forces on the front and rear columns at various wave steepness (heading 0º)

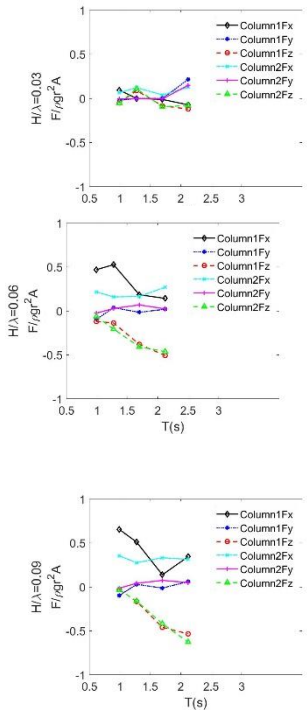

Figure 237: Mean values of wave forces on the front and rear columns at various wave periods (heading 0º)

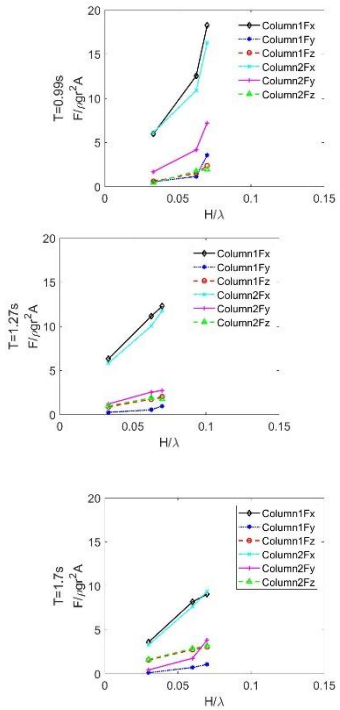

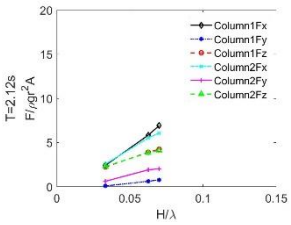

Figure 238: Max values of wave forces on the front and rear columns at various wave steepness (heading 45º)

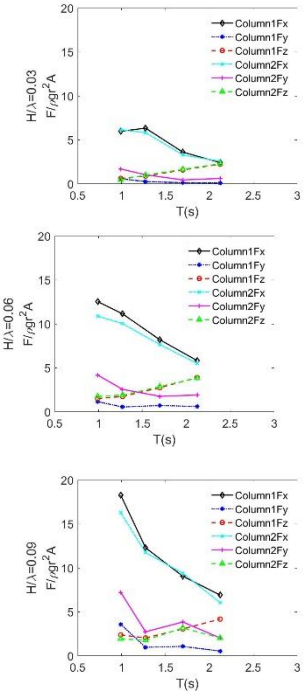

Figure 239: Max values of wave forces on the front and rear columns at various wave periods (heading 45º)

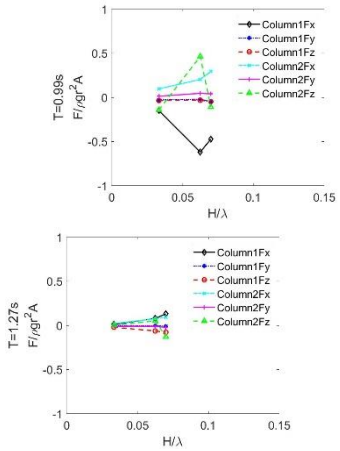

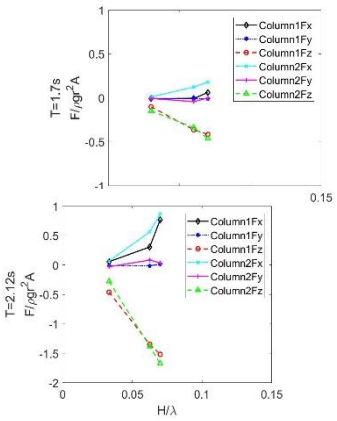

Figure 240: Mean values of wave forces on the front and rear columns at various wave steepness (heading 45º)

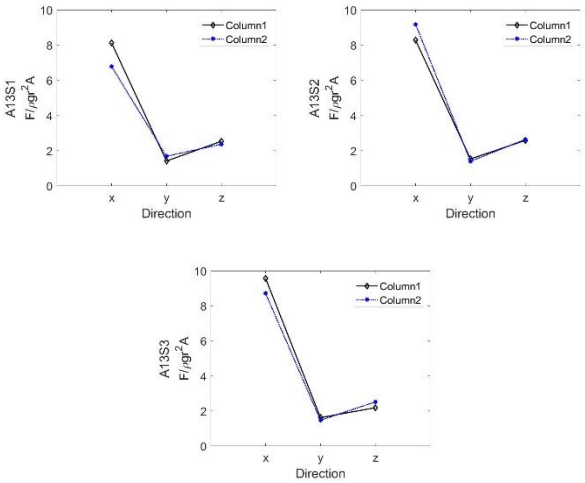

Figure 242: Max values of wave forces on the front and rear columns in irregular waves (heading 0º)

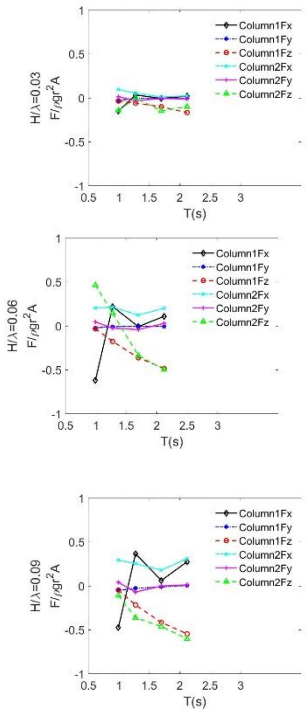

Figure 241: Mean values of wave forces on the front and rear columns at various wave periods (heading 45º)

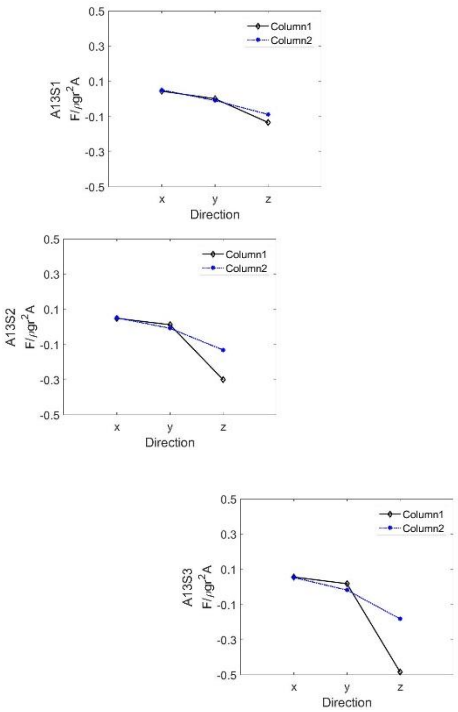

Figure 243: Mean values of wave forces on the front and rear columns in irregular waves (heading 0º)

7.4 Wave forces in irregular waves

Figure 242-Figure 245 show the maxima and mean values of wave forces on the front and rear columns in irregular waves with 0º and 45º wave directions for three random seeds.

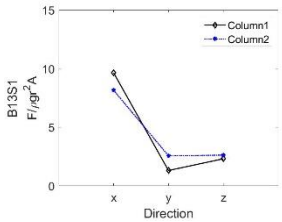

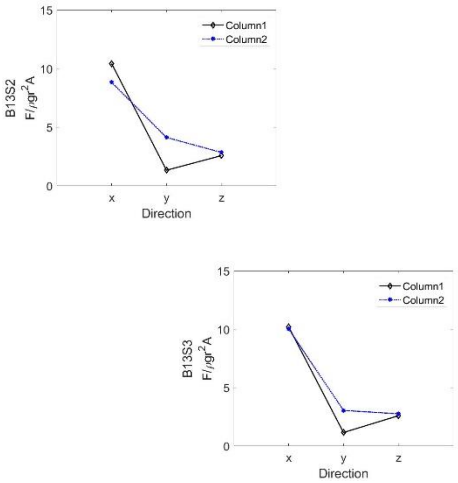

Figure 244: Max values of wave forces on the front and rear columns in irregular waves (heading 45º)

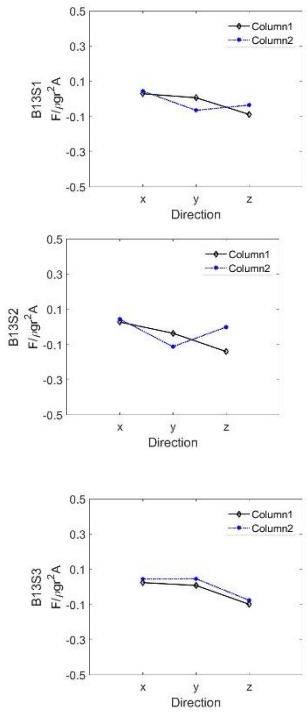

Figure 245: Mean values of wave forces on the front and rear columns in irregular waves (heading 45º)

8. CFD BENCHMARK ON TWO-BODY INTERACTIONS

8.1 Objective

The primary objective of this CFD program is to carry out benchmark studies on multiple-body interactions in regular waves, model test of two identical floaters in close proximity. The motions of two bodies, wave elevations in the gap and drift forces will be calculated and compared with the experimental data which were measured at the tests performed as a part of the test campaign of 27th and 28th ITTC Ocean Engineering Committee (OEC). The organizations participated in the benchmark studies can use the various CFD software and methodologies such as a turbulence modelling, free-surface tracking method, wave absorption, solvers and so on in model scale to produce the best solution for the two-body interactions.

8.2 System Modelling

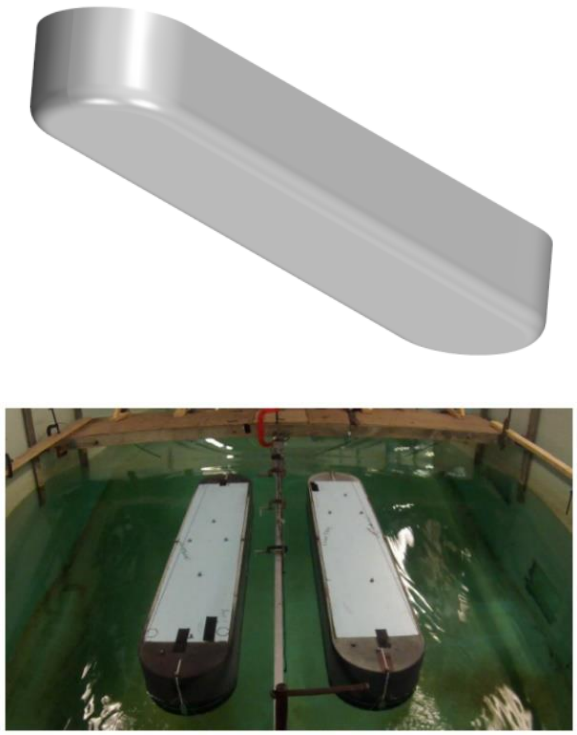

Figure 246: Ship modelling

8.1.1 Target model

- Two identical box-like models, as shown in Figure 246, are considered. Their main dimensions are given in Table 1.
- The model scale is 1:60.

Table 8 Main dimensions of ship models

	Ship 1		Ship 2	
	Full scale	Model	Full scale	Model
Length(m)	120.0	1.997	120.0	1.998
Breadth(m)	24.0	0.397	24.0	0.397
Depth (m)	18.0	0.301	18.0	0.301
Draft (m)	6.0	0.103	6.0	0.104
Δ (m)	1.64×10^7	76.6	1.64×10^7	76.6
KG (m)	7.68	0.128	7.56	0.126
R_{xx} *(m)*	7.02	0.117	7.08	0.118
R_{yy} *(m)*	28.02	0.467	28.92	0.482
GM_T *(m)*	3.24	0.054	3.18	0.053

8.2.2 Test basin

Three different basins: the towing tank of the Memorial University (MUN) - Canada, the wave basin of Ecole Centrale de Nantes (ECN) - France and the ocean basin of LabOceano – Brazil were considered to investigate the wall effect. The principal dimensions of basins are summarized in Table 2.

Table 9 Principal dimensions of test basins

	Towing tank (MUN)	***Wave basin (ECN)***	***Ocean basin (LabOceano)***
Length (m)	*58.0*	*50.0*	*40.0*
Width (m)	*4.5*	*30.0*	*30.0*
Depth (m)	*1.8*	*5.0*	*15.0*

8.2.3 Mooring system

- The two models are positioned near the middle of the test basin and each model is restraint by four soft mooring lines, as shown in Figure 247 and Figure 248.
- The stiffness of each spring is 3.4 N/m, which was determined to meet the equation below.

$$\sqrt{\frac{K'}{M+M'}} \leq \frac{\omega_{min}}{10}$$

where,

K = stiffness of each spring;

K' = effective stiffness ($=4K$);

M = mass of the model;

M' = added mass of the model;

ω_{min} = minimum value between the lowest wave frequency and model's natural frequency.

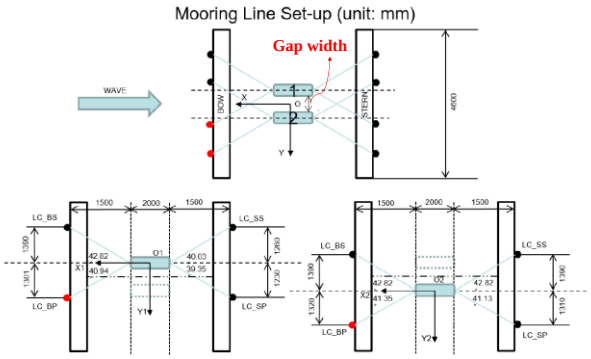

Figure 247: Set-up of the mooring system (at towing tank)

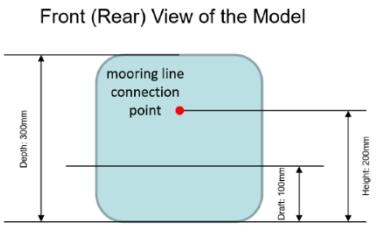

Figure 248: Mooring line connection point on a model

8.3 Test Case

8.3.1 Gap width

- The test cases are presented in Table 3.
- There is a little difference in 'Case 3' condition between MUN and ECN due to the installation constrains.

Table 10 Gap Width

Test case	Test basin	Full scale (m)	Model (m)
Case1	MUN	24.0	0.40
Case2	MUN	27.0	0.45
Case3	MUN	33.0	0.55
	ECN	31.2	0.52

8.3.2 Incident wave condition

- The test cases are presented in Table 4.
- The eighteen (18) wave period is considered with three different gap widths.
- The wave steepness is kept as 1/30.
- The tests are carried out in head seas (wave heading: 180°) only.

Table 11 Incident wave conditions

No.	ω(rad/s)	λ/L	No.	ω(rad/s)	λ/L
Case*-1	3.90	2.03	Case*-10	6.09	0.83
Case*-2	4.27	1.69	Case*-11	6.22	0.80
Case*-3	4.65	1.43	Case*-12	6.41	0.75
Case*-4	4.96	1.25	Case*-13	6.53	0.72
Case*-5	5.09	1.19	Case*-14	6.66	0.69
Case*-6	5.34	1.08	Case*-15	6.79	0.67
Case*-7	5.53	1.01	Case*-16	6.91	0.65
Case*-8	5.72	0.94	Case*-17	7.04	0.62
Case*-9	5.91	0.88	Case*-18	7.16	0.60

Case*: Test cases for gap width (1~3)

8.4 Calculation Item

Ship motions, wave elevation in the gap and mean drift forces are compared with the experimental results.

- 6-DOF (Surge, Sway, Heave, Roll, Pitch, Yaw) motions
- Wave elevation in the gap (WP 4,5,6)
- Mean drift forces (longitudinal and transverse)

Three wave probes (WP-4, 5 and 6) are positioned along the centre line of the gap, as shown in Figure 249. WP-5 is in line with the mid-ship sections of the two models. The spacing between these three wave probes is 0.5 m.

All items are calculated from average responses of at least ten (10) periods after truncating transient range and then nondimensionalized as shown below.

Translational motions: $X_j' = \frac{X_j}{\xi_0} \quad (j = 1,2,3)$

Rotational motions: $X_j' = \frac{X_j}{k\xi_0} \quad (j = 4,5,6)$

Wave elevation: $\xi' = \frac{\xi}{\xi_0}$

longitudinal drift force: $F_x' = \frac{F_x}{(1/4)\rho g \xi_0^2 L}$

Transverse drift force: $F_y' = \frac{F_y}{(1/4)\rho g \xi_0^2 L}$

Wave frequency: $\omega' = \omega \left(\frac{L}{g}\right)^{0.5}$

where,

X_j = 6-DOF body motion (j=1~6);

ξ_0 = amplitude of incident wave;

ξ_i = wave elevation at WP-i (i=4~6);

F_x = force in x-direction on model;

F_y = force in y-direction on model;

k = wave number;

L = model length;

ρ = fresh water density;

g = gravitational acceleration.

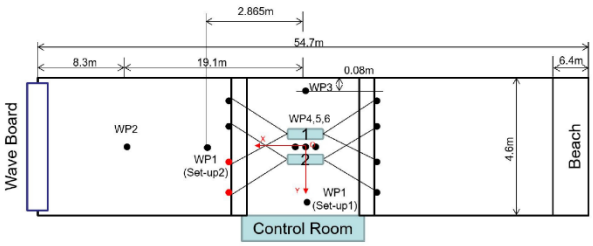

	X (from wave board)	Y
WP-4 (m)	26.9	0.0
WP-5 (m)	27.4	0.0
WP-6 (m)	27.9	0.0

Figure 249: Locations of wave probes

8.5 CFD methodologies

General information of CFD methodology such as grid system, numerical schemes, turbulence modelling and boundary conditions, should be specified in appendix.

8.6 Participated Research

Several facilities under KTTC (Korea Towing Tank Conference) have performed the cooperated study with their own CFD methodologies. Five (05) facilities below are carrying out the CFD benchmark study:

- SHI (Samsung Heavy Industries);
- KRISO (Korea Research Institute of Ships and Offshore Engineering);
- PNU (Pusan National University): 2 labs;
- KSOE (Korea Shipbuilding and Offshore Engineering);
- KMOU (Korea Maritime and Ocean University);

8.7 Potential Analysis

Before starting full CFD analysis, the potential computation was performed and compared to the experimental results.

SHI used the commercial tool HydroStar (BV) by using the 3D panel model denoted in Figure 250. The damping of 2% is applied at the gap between two bodies to prevent the spurious spiky response which is normally happened in potential calculation for two body located in proximity. The control surface is also modelled to obtain the mean drift force by middle field method. Total number of mesh is 3640. The results will be shown together with the CFD results in next section.

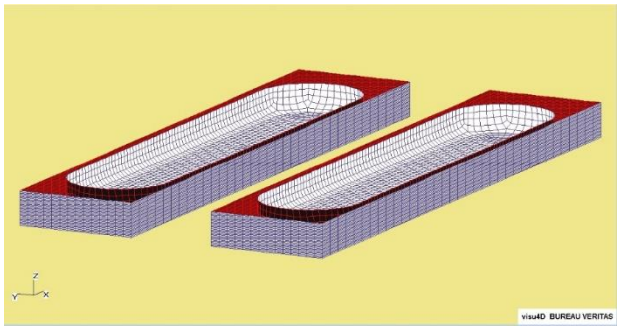

Figure 250: 3D Panel Model for Potential Calculation (HydroStar)

KRISO used the in-house code, AdFLOW, for the potential computation. The results will be shown in next section.

8.8 CFD Method Summary

The methodology used for CFD analysis is separately summarized in the appendix. It covers below:

- General Numerical Method (Software, Discretization scheme, Density definition, Pressure and velocity field, Treatment for unsteady characteristics)
- Grid System (Software, Coordinate, Dimension and type, Handling method for

body motion, Number of grids, Non-dimensional length of first grid size)
- Numerical Scheme (Convection term, Order of accuracy of convection term, Temporal term, Order of accuracy of temporal term, Conserved quantities, Linearization scheme, Iterative scheme, Pre-conditioning, or acceleration techniques)
- Boundary Condition (Boundary type, Wave generation, Wave absorption)
- Turbulence Modelling (Viscous Regime, Type of turbulence model, Transition treatment, Wall treatment)
- Free-surface treatment (Treat method)
- Computation (Computer performance in simulation, Computer system, Parallel computing, Computation time / finest grid)
- Etc.

For example, the CFD method used in SHI is summarized below.

- Software: STAR-CCM+
- Numerical modelling

Item	scheme
Governing equation	RANS (Reynolds-averaged Navier-Stokes equations)
Multiphase model	Implicit VOF (Volume of Fluid method)
Temporal discretization	2nd-order implicit unsteady
Turbulence model	k-Omega SST with all y+ wall treatment
Body-Environment coupling	Linear spring
Body motion	Overset mesh w/ 3-DOFs (surge, heave, pitch)

- Boundary conditions (Figure 251)

Type	Surface, Region
Velocity inlet	Inlet/Outlet/Side (far from the model)/Bottom boundary
Symmetry	Side boundary
Pressure outlet	Top boundary
Forcing zone (Relaxation zone)	Forward, Backward, Side region

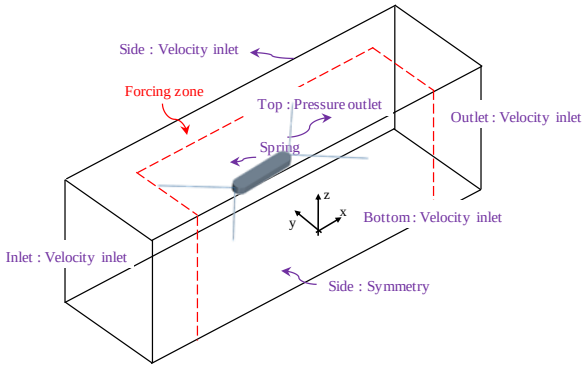

Figure 251: Boundary conditions for the numerical domain

- Computational Domain (Figure 252)
  - Total volume mesh: 1.5~2.5 million
  - Mesh refinement (x-dir: 70 or more per wavelength, z-dir: 15 or more per wave height)

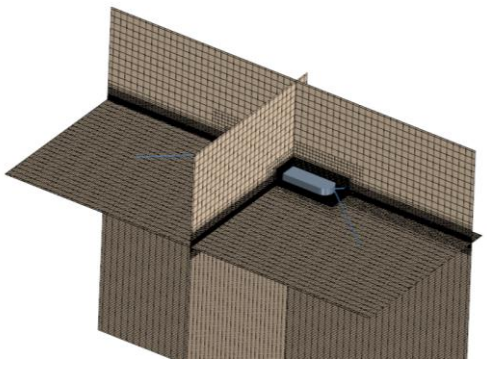

Figure 252: Mesh of the computational domain

8.9 CFD Results

8.9.1 SHI

The numerical wave test was performed without model in advance to the actual simulation. The result is depicted in Figure 253 with a wave period versus wave amplitude curve. The solid line means the theoretical target value.

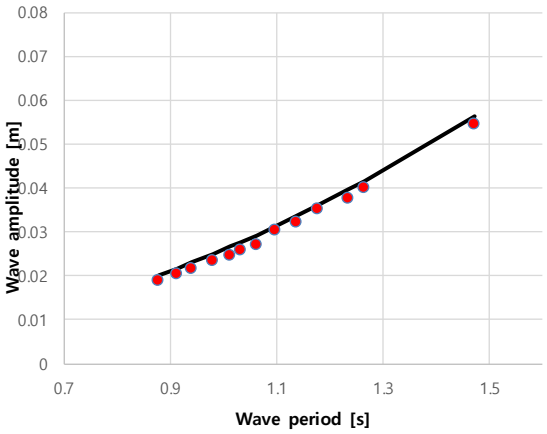

Figure 253: Numerical Wave Calibration Result by SHI

For simplicity, only the 3 DoF (Surge, heave, pitch) motion is considered in the simulation, the comparison of body motion for gap distance of 0.40 m is shown in Figure 254.

The potential and CFD calculation compare well with each other. The model test results show little bit larger value in low frequency range, but the accuracy of computation can be said quite good enough to simulate the model test. There is no effect from the viscosity on the motion at the gap distance of 0.4 m.

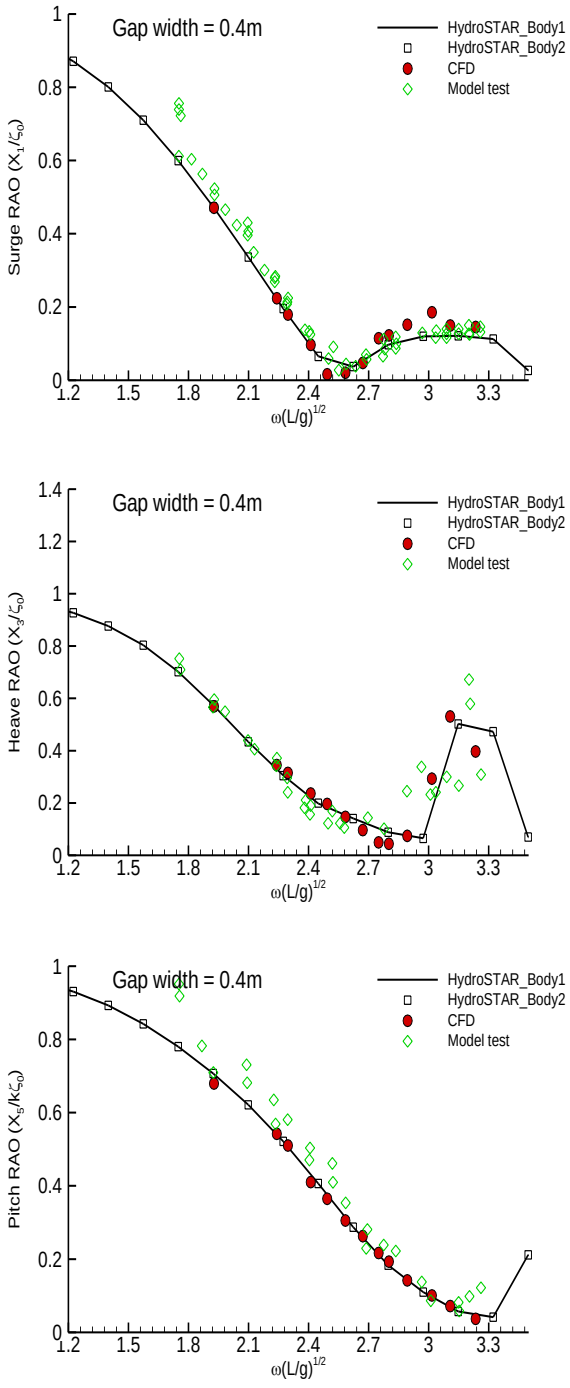

Figure 254: Motion Comparison of SHI (Gap=0.40 m)

The results of motion at the gap distance of 0.45 m are depicted in Figure 255.

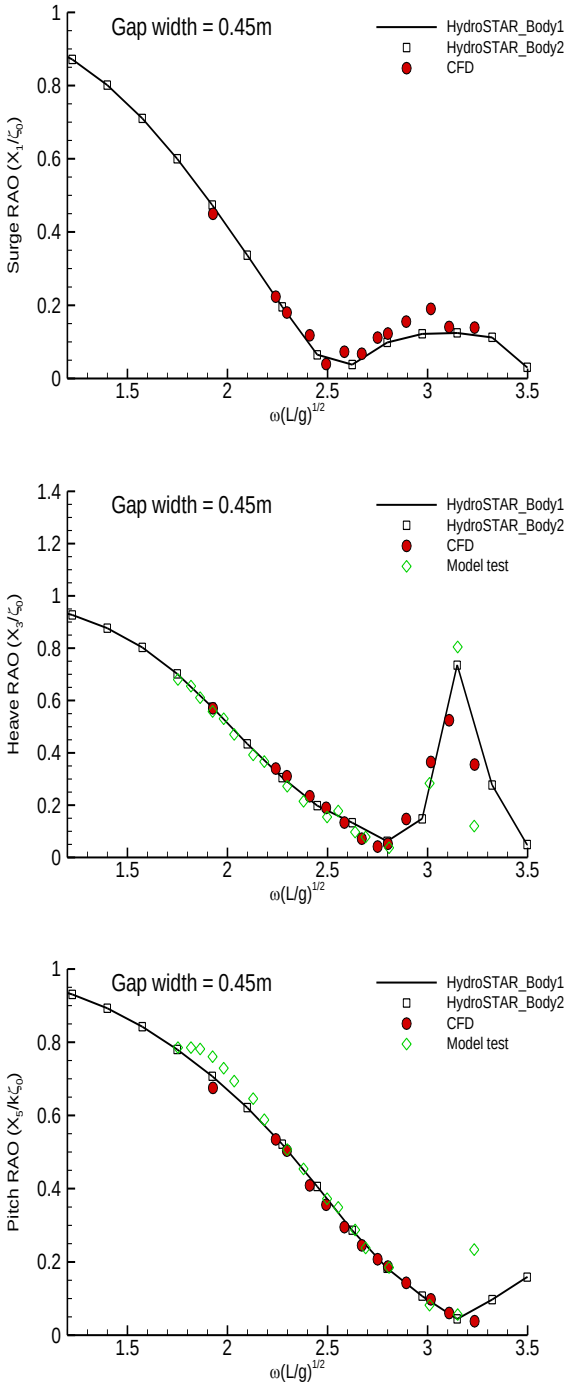

Figure 255: Motion Comparison of SHI (Gap=0.45 m)

The results among the potential, CFD calculation and the model test shows good correspondence. The 3 DoF motion calculation in CFD is comparable with that of 6 DoF in potential calculation and model test. It means that there is little effect from the gap between the bodies on the body motion under head sea condition at the gap distance of 0.45 m.

The motion comparison for the gap of 0.55 m is shown in Figure 9.

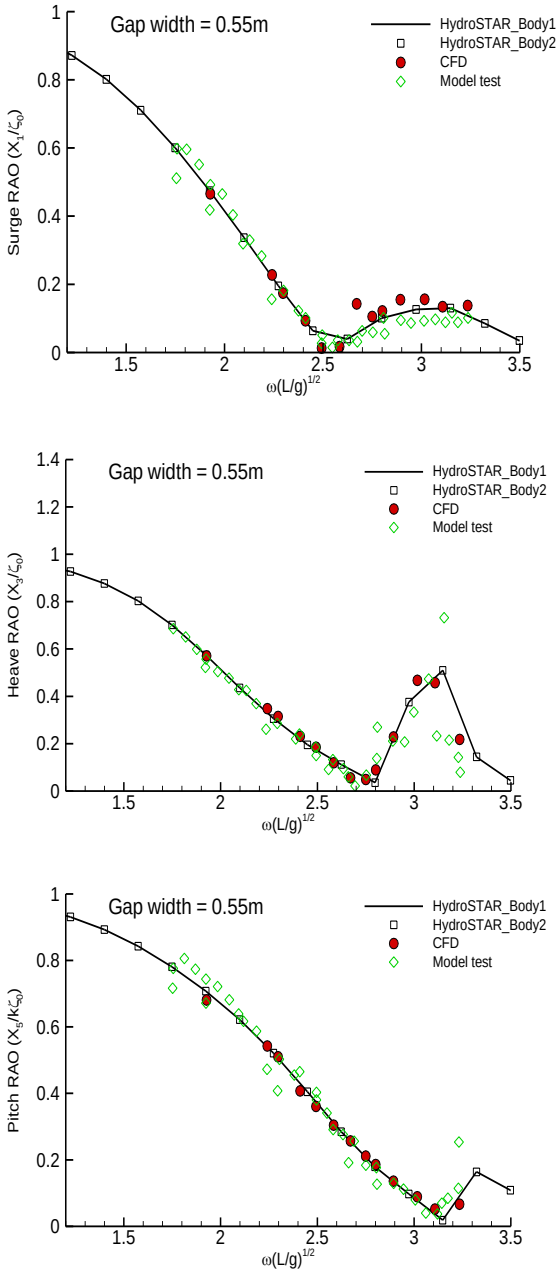

Figure 256: Motion Comparison of SHI (Gap=0.55 m)

The mean drift force is compared and depicted in Figure 10 for the gap of 0.40 m. The CFD (long) means longer the simulation duration (number of cyclic responses, i.e., short: 4~5 cycle, long: 15~20). For surge direction, the potential results correspond well with CFD calculation, but both shows little deviation in high frequency region. For sway direction, the CFD (long) results show good correspondence with the model test. The potential calculation shows the difference in very high frequency range. It is hard to quantify the viscous effect on the drift force, but the viscosity can make difference in the drift force on the models moored in side by side.

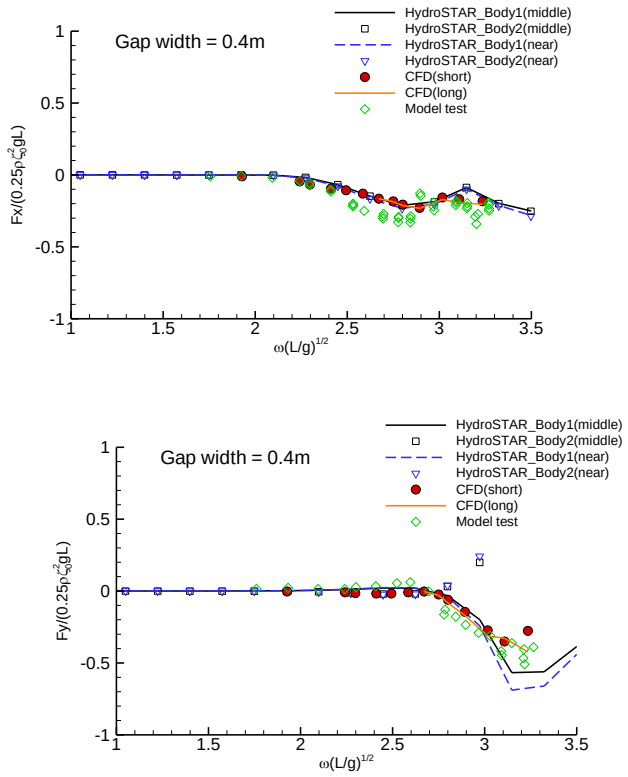

Figure 257: Mean Drift Force Comparison of SHI (Gap=0.40 m)

The mean drift force for the gap of 0.45 m is denoted in Figure 258. The potential results deviate more at the very high frequency region for the sway drift force.

The mean drift force for the gap of 0.55 m is also shown in Figure 259.

The wave elevation at the gap 0.40 m is compared in Figure 260. There is little deviation between CFD and model test, the trend of CFD results is closer to the model test than that of potential calculation. The potential calculation shows some deviation from the model test at a wide range of frequencies, and it means that viscosity affects the gap elevation.

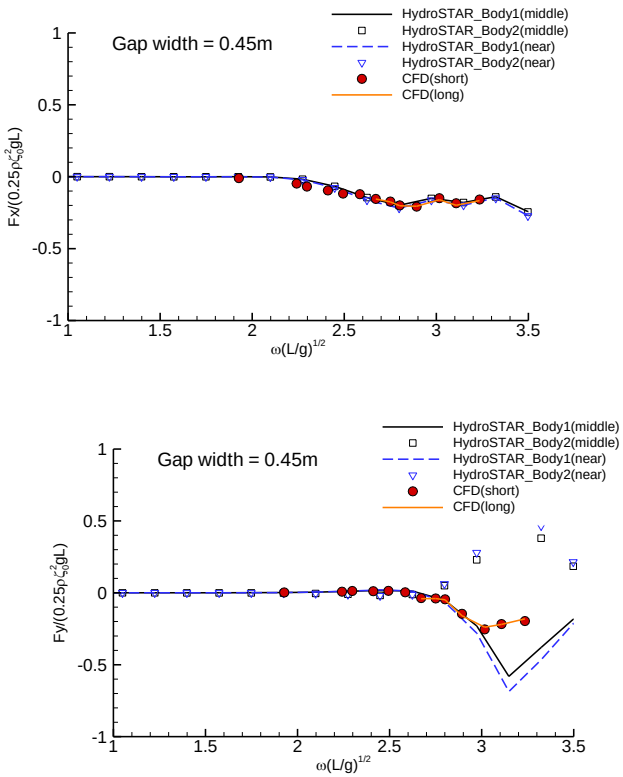

Figure 258: Mean Drift Force Comparison of SHI (Gap=0.45 m)

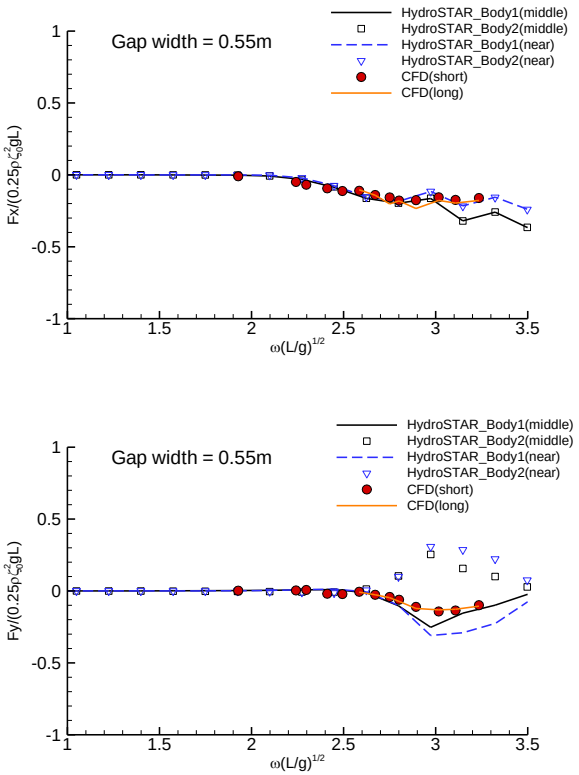

Figure 259: Mean Drift Force Comparison of SHI (Gap=0.55 m)

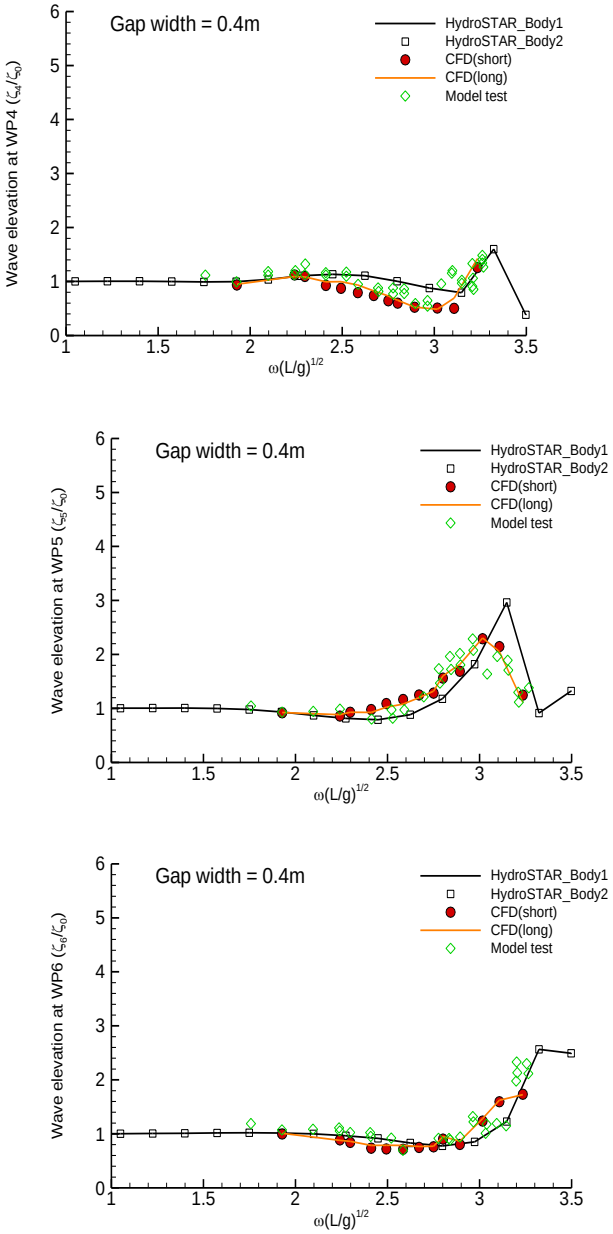

Figure 260: Gap Wave Elevation Comparison of SHI (Gap=0.40 m)

The comparison of gap wave elevation for the gap distance of 0.45 m is denoted in Figure 261. It shows the same trend compared to the case for the gap of 0.40 m. The CFD calculation shows different values compared to the potential calculation.

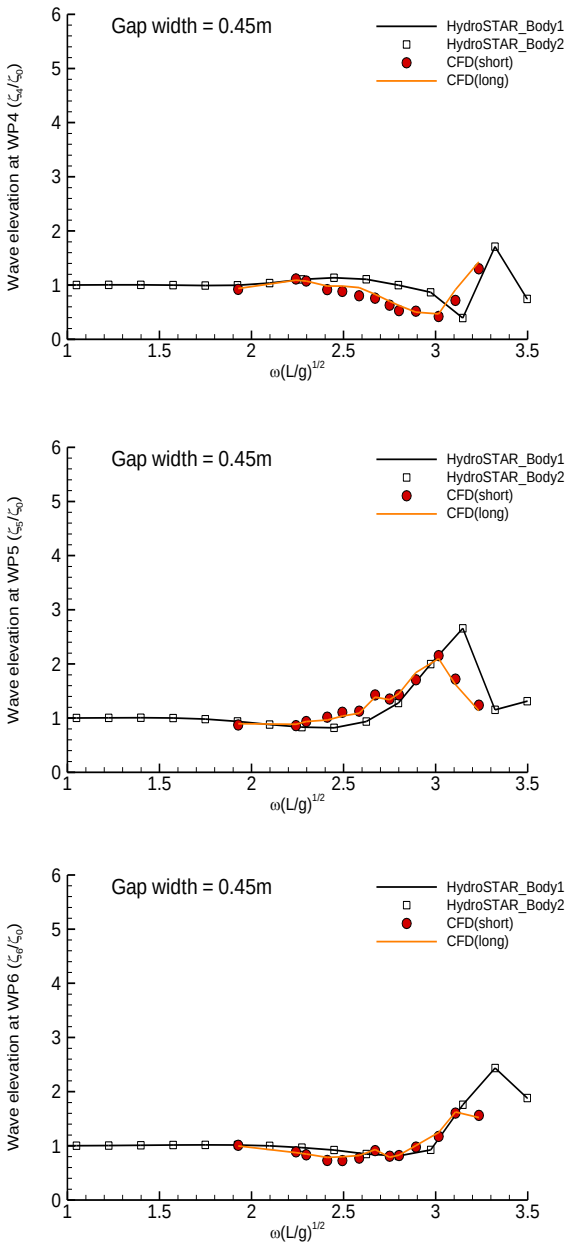

Figure 261: Gap Wave Elevation Comparison of SHI (Gap=0.45 m)

The gap wave elevation for the gap of 0.55 m is shown in Figure 262. The difference among the CFD, potential calculation and model test becomes smaller. It can be said that the viscous effect on the gap wave elevation is now negligible when the gap distance between the bodies is to be large enough.

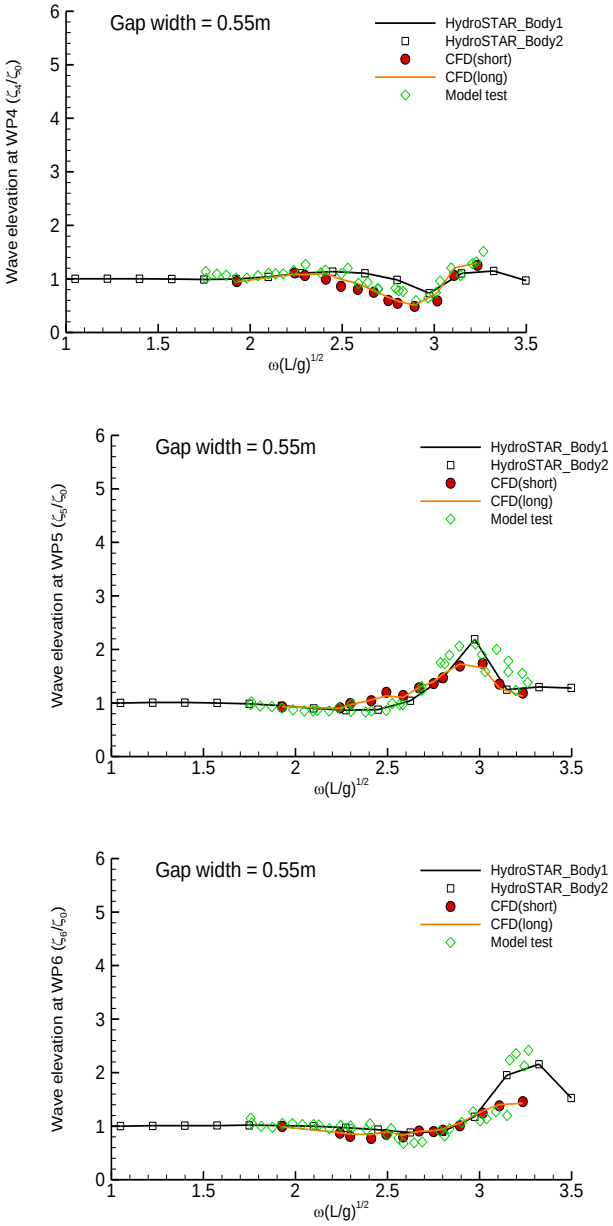

Figure 262: Gap Wave Elevation Comparison of SHI (Gap=0.55 m)

The raw time series of CFD results will be summarized and tabulated in a separated data sheet.

8.9.2 KRISO

The same calculation was performed by KRISO. In the analysis of KRISO, the 6 DoF motion is considered both the potential and CFD (Figure 263). KRISO used the StarCCM+ for

CFD analysis and the detail method is summarized in the appendix. The calculation (wave frequency) points for CFD analysis are not many for now and will be updated in the future.

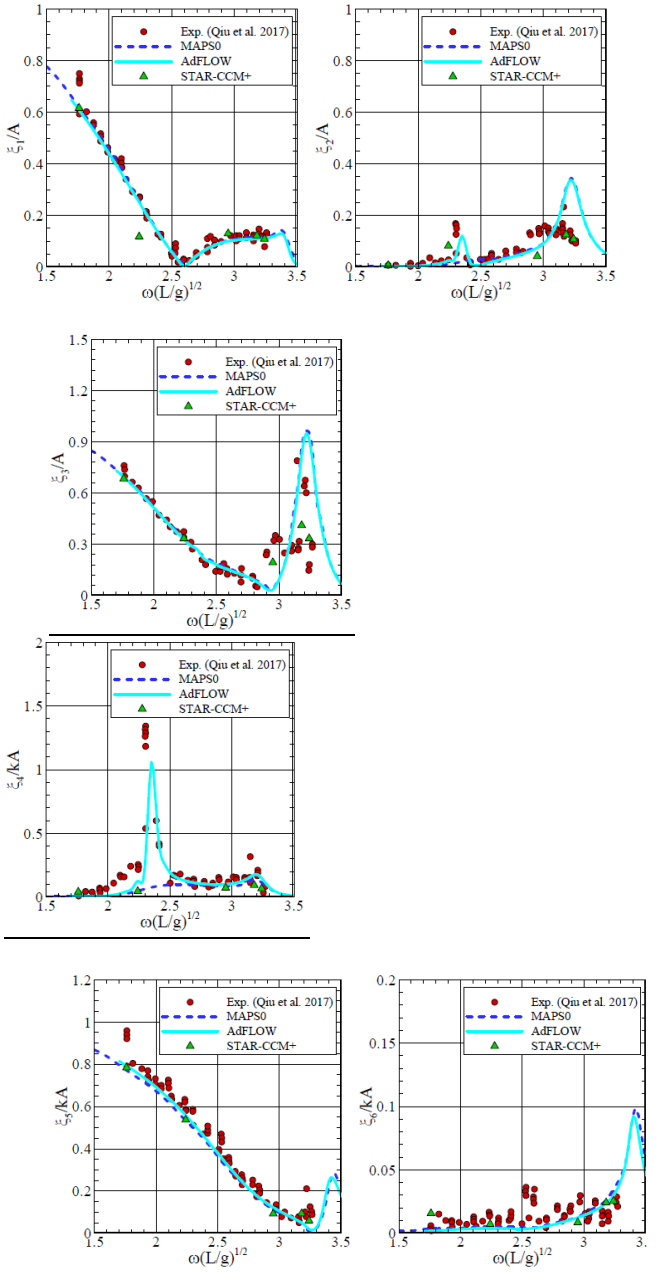

Figure 263: Motion Comparison of KRISO (Gap=0.40 m)

The potential calculation shows good correspondence with the model test in the motion. The sway and roll motion induced by two body interaction in head sea condition is well captured. The results of MAPS0 are also the potential calculation which was performed at the time of model test.

The mean drift force is compared and denoted in Figure 264. The potential calculation by AdFLOW shows the difference compared to the model test. There are five calculation points for CFD analysis. The sway drift force of CFD corresponds well with the model test. For the further discussion, more calculation will be needed in CFD analysis.

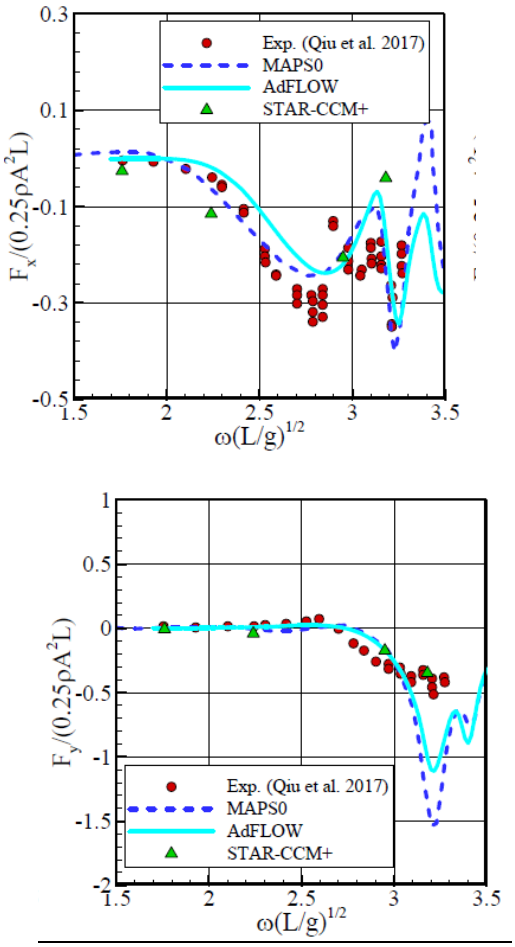

Figure 264: Mean Drift Force Comparison of KRISO (Gap=0.40 m)

For the gap wave elevation, the results are depicted in Figure 265. The CFD results at low frequency region show good correspondence with the model test, but those at high frequency

region deviate from the model test at some probe location. More calculation points are needed for further discussion.

8.9.3 PNU

The actual simulation for this benchmark study is not started yet. Some verification works are now performing for the numerical modelling, wave generation and system identification.

In the CFD calculation, the same tool of StarCCM+ is used. The detail method is also summarized in the appendix. The grid system and boundary condition were checked and the so called the numerical wave tank is established for this benchmark test.

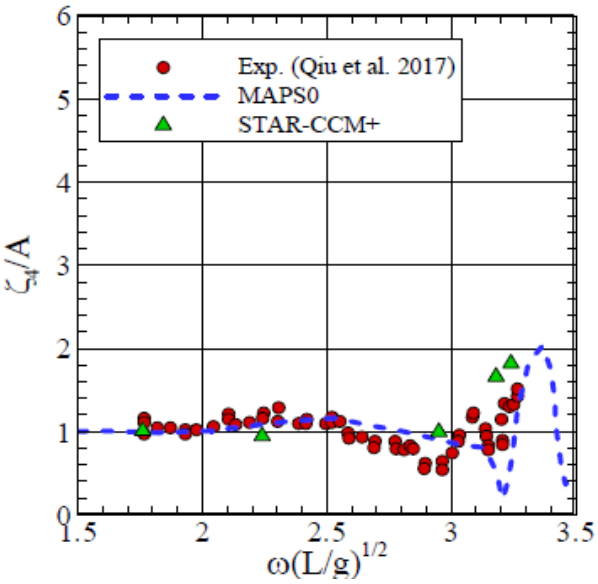

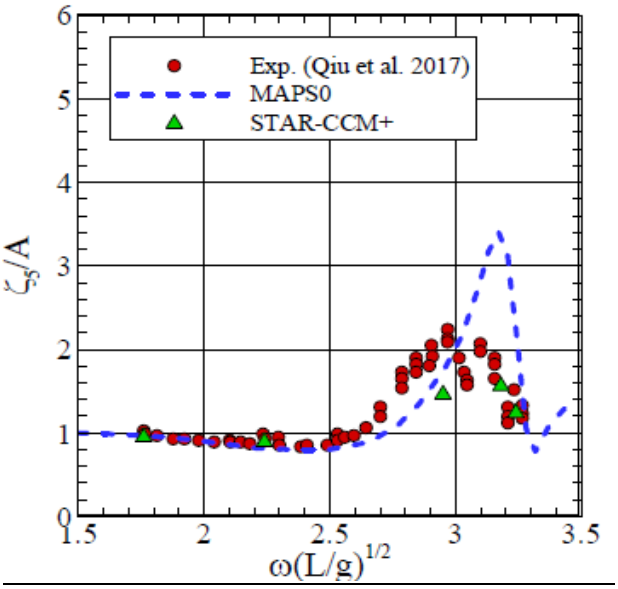

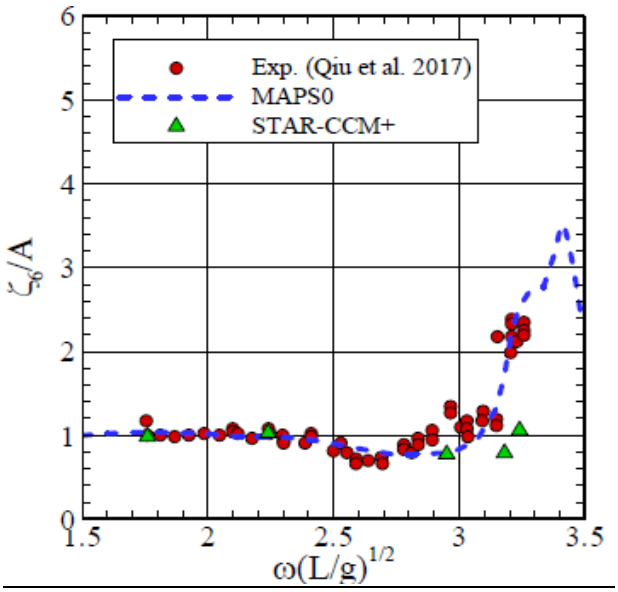

Figure 265: Gap wave elevation comparison of KRISO (Gap=0.40 m)

- Numerical Wave Calibration

	T(s) [Target wave period]	[CFD]	%D	H(m) [Target wave height]	[CFD]	%D
RW-01	1.611	1.600	0.687	0.135	0.132	2.380
RW-02	1.471	1.447	1.637	0.113	0.110	2.521
RW-03	1.351	1.355	-0.267	0.095	0.092	3.342
RW-04	1.267	1.280	-1.064	0.083	0.080	3.480
RW-05	1.234	1.235	-0.074	0.079	0.077	3.403
RW-06	1.177	1.183	-0.555	0.072	0.070	3.068
RW-07	1.136	1.115	1.881	0.067	0.065	3.570
RW-08	1.098	1.086	1.176	0.063	0.061	3.104
RW-09	1.063	1.044	1.775	0.059	0.057	2.978
RW-10	1.032	1.037	-0.472	0.055	0.053	3.926
RW-11	1.010	1.024	-1.377	0.053	0.051	4.291
RW-12	0.980	0.988	-0.809	0.050	0.048	3.724
RW-13	0.962	0.966	-0.414	0.048	0.046	3.823
RW-14	0.943	0.961	-1.822	0.046	0.044	3.346
RW-15	0.925	0.943	-1.853	0.045	0.043	3.285
RW-16	0.909	0.917	-0.803	0.043	0.041	4.611
RW-17	0.892	0.910	-1.952	0.041	0.039	4.747
RW-18	0.878	0.872	0.650	0.040	0.038	4.222

- Roll Free Decay
  - Grid and boundary condition (Overset body, No. of grid: 2.0M)
  - Convergence check for decay signal

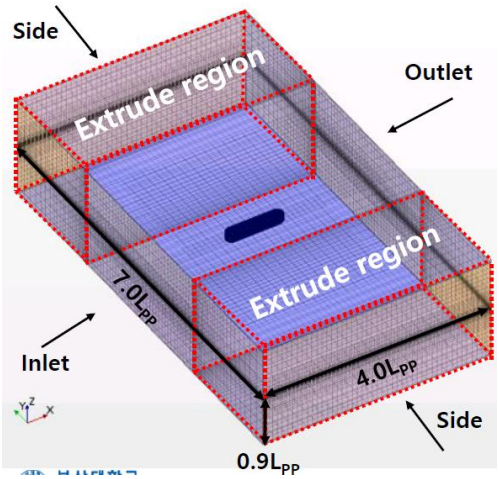

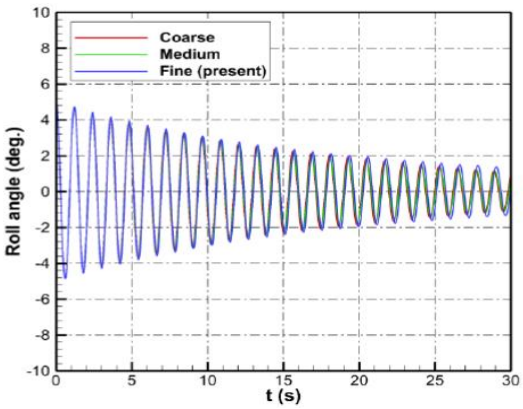

- Result of Roll Free Decay (single body)

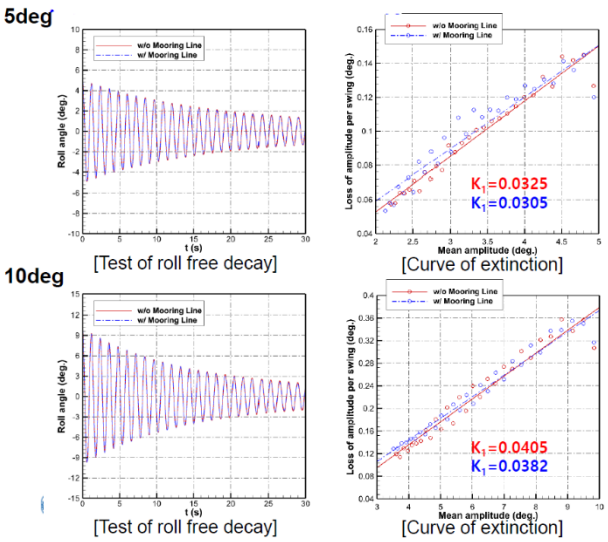

- Results of Roll Decay (two body)

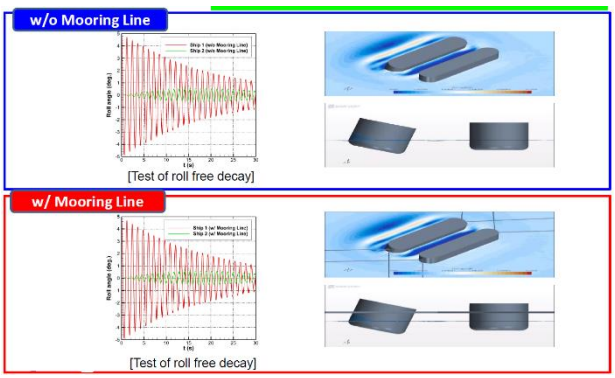

8.9.4 Other facilities

The results of CFD analyses for other facilities are not summarized yet. The CFD tool and method being tried by other facilities are summarized in the appendix and denoted in short as below.

- PNU (2): Tool (ReFRESCO by MARIN)
- KMOU: Tool (OpenFoam)

9. STATE-OF-THE-ART REVIEW IN LARGE DIAMETER FLEXIBLE RISERS FOR DEEP WATER MINING

9.1 Introduction

Deepwater mining has been proposed since the 1960s to meet the increasing demands of the natural resources. The most feasible concept of deep-water mining system is divided into three categories: a seafloor mining vehicle, a vertical transporting system and a surface supporting vessel. Two typical applications of vertical transporting systems are utilized: (1) a vertical rigid pipe connecting the support vessel and the free hanging buffer, and a flexible riser connecting the buffer and the mining vehicle (see Figure 266(a)); (2) a single flexible riser connecting the mining vehicle and the support vessel (see Figure 266(b)). The former has been adopted in projects such as Blue Mining, Blue Nodules and the coming commercial project Solwara 1; the latter has been proposed by scholars in India and Germany, and a sea test was conducted in 2004 (Deepak et al., 2001; Handschuh et al., 2001).

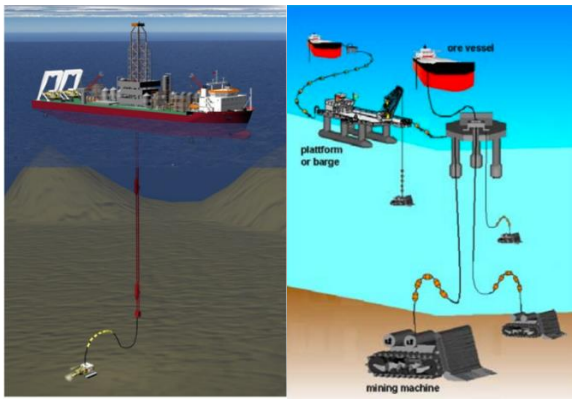

Figure 266: Typical vertical transporting systems: (a) Rigid pipe (Vercruijsse and Verichev, 2011); (b) Flexible riser (Deepak et al., 2007).

In vertical transporting systems, flexible risers/hoses are commonly used to cater the varying water depth, the seabed topography, and the movement of the mining vehicle. The material of flexible risers is usually composed of synthetic rubber, high strength-two stage cord, and synthetic rubber with enhanced tensile strength by using steel wires. The buoyant material is mounted to compensate for the weight of flexible risers and to make the shape of flexible risers to ensure the movement of a mining vehicle, as shown in Figure 267.

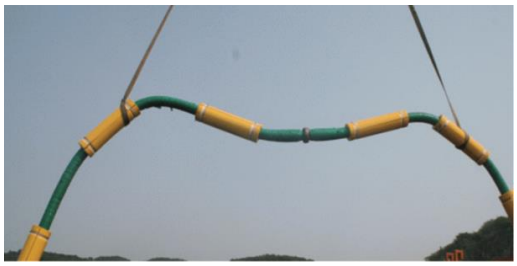

Figure 267: Flexible hoses with buoyancy materials (Yoon et al., 2011)

The studies on large diameter flexible risers for deep sea mining are mainly focused on three aspects: (1) pressure loss of the mixture; (2) dynamic responses and spatial configurations of the riser, and (3) flow assurance issues. Both full-scale and model tests have been carried out to provide guidance on the design of the flexible

riser. In addition, various numerical methods have been developed to address these issues.

9.2 Pressure drop inside the flexible riser

One of the critical parameters during the flexible riser transportation is the pressure drop of the mixture, which determines the pump head and energy consumption. Owing to large ore particles in the slurry, the pressure drop of the mixture is entirely different from that of seawater and is affected by many factors such as particle size, particle density, solid volume fraction, flow rate and spatial configuration of the flexible risers. Both experiments and numerical simulations have been conducted in recent years. The previous works in the literature are summarized as follows:

Yoon et al. (2002, 2001) analysed the flow characteristics of the solid-liquid two-phase mixture in a flexible hose by experiments and summarized the effects of volume fraction, hose shape and mixture velocity on the pressure drop. The experimental results show that the increase of discharged volume fraction and particle diameter causes the increase of the minimum velocity for transporting the solid particles. The pressure drop increases as the solid volume fraction increases irrespective of the shape of the flexible hose (also described in Yoon et al. (2006) and Yoon et al. (2009)). As for the mixture velocity and hose shape, the pressure drop increases when the superficial mixture velocity is more than a critical velocity (1.5 m/s in the experiments) and decreases as the more the pipe is curved in the case of low velocity below the critical velocity. Experiments conducted by Yoon et al. (2006) and Yoon et al. (2009) showed that the frictional hydraulic gradient becomes close to the hydraulic gradient of water as the mixture velocity increases. As the mixture velocity increases, the solid particles move at the centre of the pipe rather than at the wall side, and therefore the influence of the friction decreases.

The differences in flow characteristics between real and artificial manganese nodules-water mixture and synthetic nodules-water were experimentally studied by Yoon et al. (2009). The results show that the hydraulic gradients of the mixtures are almost identical in the case of both the real and synthetic nodules. However, when the solid volume fraction is high, the hydraulic gradient of the flow containing the real manganese nodules is a little lower than that of the artificial ones, because the drag effect is not so apparent.

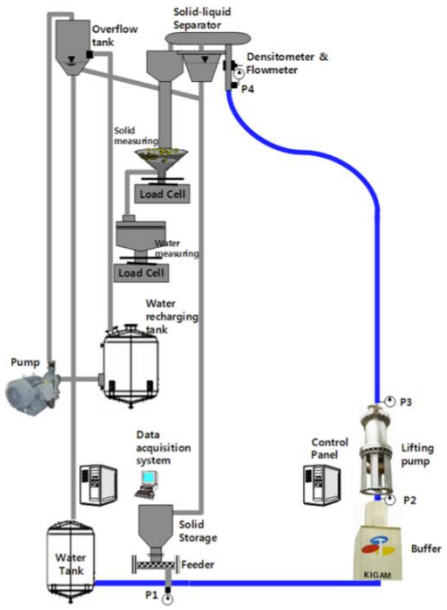

Figure 268: Flow experiment system for flexible riser by (Yoon et al., 2009).

Yu et al. (2010) developed a numerical method for computing the hydraulic power and pressure loss for the “S” shape jumper (flexible hose) in deep sea mining application based on Computational Fluid Dynamics (CFD). The CFD results were then used for calibrating a simplified equation for estimating pressure loss. Using specific energy consumption (SEC) numbers, it was found that if the delivered volumetric concentration (Cvd) is above 8%, SEC is relatively insensitive to the Cvd for the example system for deep sea mining. One of the key elements to ensure a successful hydraulic

lifting design is to keep the ratio between the average slurry flow velocity and the largest particle settling velocity for the vertical riser section above 4 to 1. For the horizontal and jumper sections, a minimum ratio of 5 to 1 is needed based on CFD simulation and reference.

The methods of estimating the pressure drop and the solid-liquid two-phase flow regimes were reviewed by Parenteau (2010). The CFD method was then conducted for understanding transient behaviour and pressure and power prediction for the wave-shaped riser. Further, coupling of CFD and discrete element method (DEM) was proposed to improve the computational efficiency and accuracy of computational results.

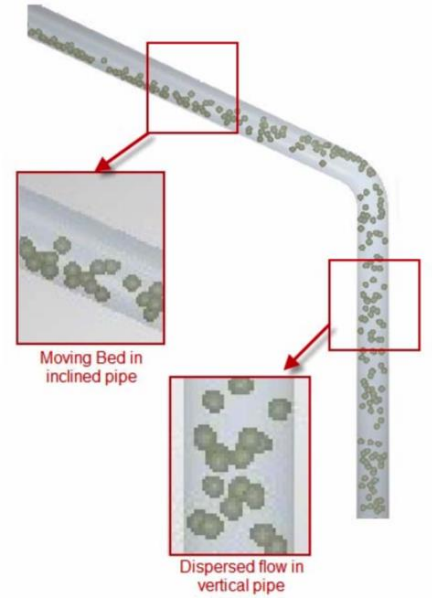

Figure 269: An example of CFD-DEM simulation of ore particles (Parenteau, 2010)

Parenteau and Lemaire (2011) summarized the flow tests made in a subsea mining experimental flow loop including horizontal and "S" shape sections. These tests allowed to identify the main flow characteristics of the slurry in subsea mining condition transporting large particles (5 mm to 20 mm) in reduced diameter "S" shape flexible riser (4"). Light glass beads and heavy alumina beads were demonstrated valid to represent the real solid flow and to simulate the impacts of the particle diameter and density on the pressure drop. "S" shape pipe has first shown higher pressure drop than the horizontal pipe in the tests. Pressure drop curves are influenced by two main slurry flow regimes: stratified below critical velocity, and homogeneous above critical velocity. The operating velocity should be well into developed homogeneous regime to avoid any potential solid deposit at the pipe bottom. Solid volume fraction clearly defined the level of pressure drop of the subsea mining system. The density has a significant impact on the pressure drop curves. The system needs to be designed for the maximum density observed on the field. Pressure drop follows the average density of the mixture. The particle size distribution also has a significant impact on the pressure drop. Increasing particle size reduces horizontal pressure drop but increases vertical pressure drop.

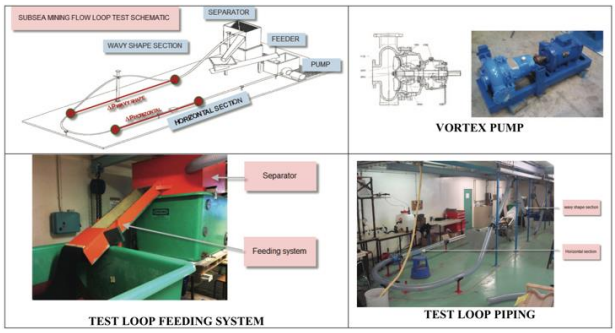

Figure 270: Subsea Mining small-scale flow loop test description (Parenteau and Lemaire, 2011)

Wang et al. (2012) investigated the resistance loss of transportation and the influences of buoyancy layout, solid volume fraction and elastic modulus of flexible hose using Finite Element Method (FEM). The numerical results show that the resistance loss increases with the increase of solid volume fraction and internal fluid velocity and decreases with the increase of elastic modulus of flexible hose. The buoyancy layout and the internal flow velocity have greater impacts on the resistance loss than the elastic modulus of flexible hose. To

reduce the resistance loss and improve the efficiency of deep-sea mining, solid volume fraction and flow velocity must be restricted in a suitable range (e.g., 10%~25% and 2.5 ~ 4 m/s, respectively). Effective buoyancy layout should be adopted, and the suitable material of moderate elastic modulus should be used for the flexible hose.

Ramesh et al. (2013) studied the pressure drop in flexible hoses of varied bend angles and various bend radii containing a pulsating flow. The studies were conducted for the most likely occurring bend angle of 70°, 20° and 60° with a bend radius of 5 times the hose diameter for various flow rates. The head losses in terms of differential pressure amplitude for clean water and slurry with solids of 10 mm size for various volume fraction were obtained experimentally. The authors concluded from the experimental results that the pressure drop of the mixture flow increased by 1.5 to 1.8 times for slurry flow when compared to the clear water.

Rhee et al. (2013) simulated the slurry behaviour in spooled hoses by using CFD (Figure 271). They described the phenomena that occur in elbows and in the spooled hoses at the entrance of the spool, the development of the slurry to a new stratification regime along the first part of the spooled hoses and the phenomena which occurred thereafter. The envelope of slurry conditions (concentration, particle size distribution, and velocity) has an impact on the dynamic pressure losses in the spooled hoses. When a stratified flow enters the spool, two vortices are identified, of which one is clearly stronger and dominates the other. For a stratified flow in the vertical spool, the pressure is approximately the same as that in a straight pipe. However, the pressure in a horizontal orientation of the spool is smaller than that in a straight pipe.

Figure 271: Spooled riser applied on a vessel (Rhee et al., 2013)

Beauchesne et al. (2015) developed a new transient flow assurance model named FASST: Flow Assurance Simulation for Slurry Transportation, to correctly assess the pressure drop in deep sea mining riser. The model was validated against both small-scale and large-scale tests. Theoretical results proved to agree with experimental results allowing a very good confidence in the FASST prediction of transient flow regimes.

Peng et al. (2015) analysed critical flow velocity of solid-liquid two-phase mixture and total pressure drop of flexible hose by existing formulas under conditions of different spatial configurations of hose, different particle sizes, and different solid volume fraction. The results show that the critical flow velocity and pressure drop regularly increase with the increase of particle size and volume fraction. Considering transmission efficiency and transportation safety, 10% to 15% is the optimal volume fraction, and critical flow velocity is about 2.8 m/s ~3.6 m/s. The results are close to those of Wang et al. (2012). To avoid clogging and reduce energy consumption, the critical flow velocity should be controlled according to the different relative distance between buffer and mining vehicle.

Nijun et al. (2017) investigated the flow characteristics in flexible hoses based on the experimental system shown in Figure 272. The hydraulic gradient of coarse particle slurry in flexible hoses increases with the increase of particle volume fraction and mixture velocity, and it decreases with the increase of particle size.

This change rule is similar to hydraulic transportation research results in inclined pipelines. In addition, with hose curvature increasing, the particle easily moves in turbulence, and the hydraulic gradient increases. Comparing hydraulic gradient in inclined pipelines and flexible hoses, the hydraulic gradient computational equations of coarse particles in flexible hoses were proposed.

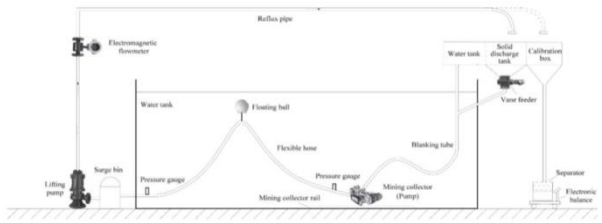

Figure 272: Experimental system of Nijun et al. (2017)

9.3 Dynamic responses and spatial configurations

During deep sea mining, one of the main tasks is to estimate the dynamic responses and spatial configurations of flexible risers under complicated sea states and operating conditions of the mining vehicle. Reliable experimental and numerical methods are required to predict the nonlinear geometric deformation and tension of the flexible risers. In recent years, both experiments and numerical simulations have been conducted. The main works are listed as follows.

Wang and Liu (2005) and Wang et al. (2007) established a 3D dynamic analysis model of 1000 m deep sea mining pipeline by FEM. The effect of concentrated buoyancy provided by buoyancy balls was analysed by simulating the configuration of a 400 m flexible hose. The results show that, to form the configuration of a saddle shape, the total concentrated suspension buoyancy of flexible hose should be 95% ~ 105% of the gravity of flexible hose in water, the first suspension point occupies 1/3 of the total buoyancy, and the second suspension point occupies 2/3 of the total buoyancy (Figure 273).

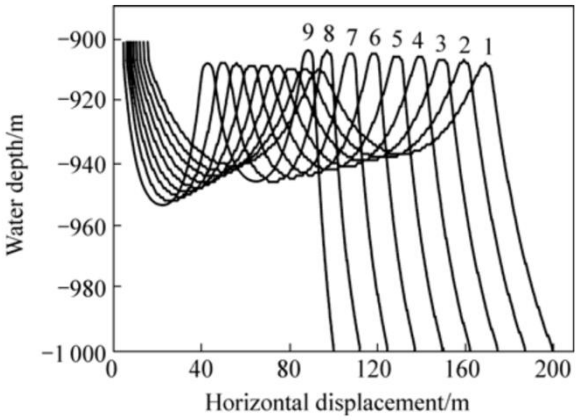

Figure 273: Shape of flexible hose due to movement of mining vehicle (Wang et al., 2007)

Wang and Liu (2005) and Li et al. (2007) analysed the deep sea mining pipe system using DEM. The results were validated and compared to the simulations based on FEM. The dynamic responses of the entire mining pipe system in different work conditions were discussed. Some suggestions were made for the actual operation of deep-sea mining systems.

Rao et al. (2009) studied the interaction of fluid-solid coupled flexible hose and mining vehicle in a 1000 m deep sea mining system based on nonlinear FEM with fluid-solid coupling model. Effects of the walking paths (e.g., line, circle, and square), walking velocities of the mining vehicle on the spatial configuration, support restrained force and maximum tensile stress of the flexible hose were investigated. Results show that the line walking of the mining vehicle is better for small lateral displacement, maximum tensile stress and support constrained force of the flexible hose than the circle and square walking. The walking velocities of the mining vehicle should be limited to an appropriate range (about 0.2 ~ 0.4 m/s when flow velocity in flexible hose is 4 m/s) for the safety and efficiency of the mining operation.

Wang et al. (2011) carried out a short 10 s simulation of the interactions between the dynamics of the mining vehicle on seabed and the flexible hose. The calculation results show that the hose has a relatively large vibration in the vertical direction and the maximum amplitude reached 1.5 m which may result in low efficiency of inner fluid transportation or poor safety and stability of the flexible hose.

Chen et al. (2014) developed a quasi-static analysis method that succeeded in finding equilibrium configurations of flexible marine hoses dragged by mining vehicles based on FEM. In addition, an experiment of the flexible hose has been conducted to validate the proposed numerical method. The numerical method was used in modelling a typical mining procedure in which the mining vehicle was moving counter clockwise in a circle. Simulation results show variations of configurations of the pipe and constraint forces/torques.

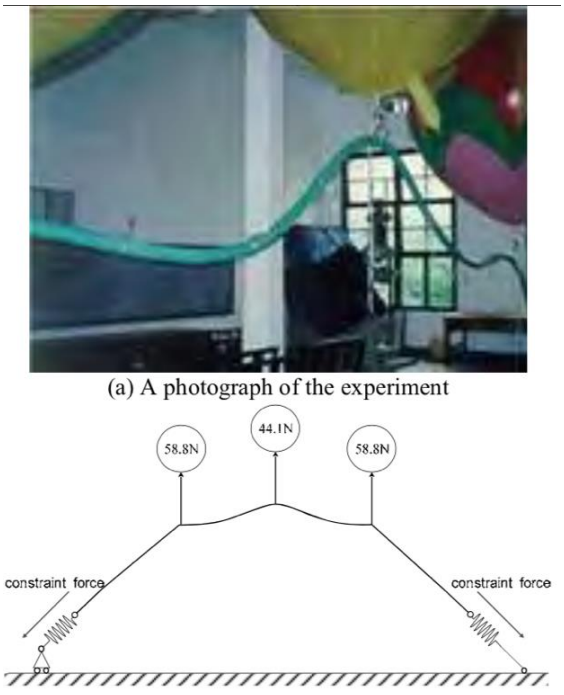

Figure 274: Photograph and schematic diagram of the experiment by Chen et al. (2014)

9.4 Flow assurance issues

Flow assurance issues of flexible risers, such as erosion and clogging, are of great importance in deep sea mining applications. The investigations on these issues have been conducted by means of full-scale experiments, model tests and numerical simulations recently.

Parenteau (2012) conducted the large-scale experiments for flow correlation validation and abrasion test to have an in-depth understanding of the flow assurance issues in deep-sea mining. This large-scale test used an innovative method to allow the reproduction of realistic erosion rate in the pipe by preventing the solid particle to be eroded when looping through the pump. The author assessed pressure drop and erosion rate close to real flow conditions and summarized the findings and results from this large-scale experimental set-up, testing concentration from 10% to 45%, velocities from 2.5 m/s to 5.5 m/s in an 8" flexible pipe with equivalent rocks particles.

Rongau and Viale (2017) built a large-scale bench test to reproduce realistic flow in a piping system and compare wear on different materials. A complete analysis of the wear patterns was conducted with the expertise of a laboratory. A statistical comparison between materials was presented. The response to wear, depending on material, geometry, and position, was better known. One of the materials showed much better wear resistance than the others and was selected for further development.

Figure 275: Large-scale rig test overview (Rongau and Viale, 2017)

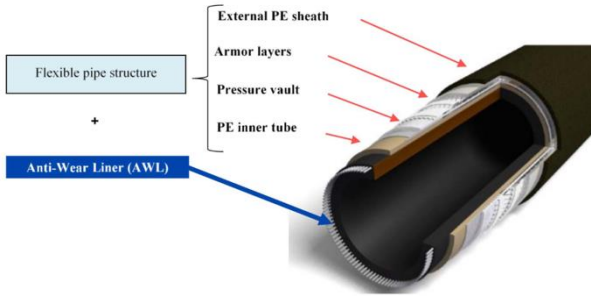

Figure 276: Design for flexible cross-section containing anti-abrasion layer (Rongau and Viale, 2017)

Neale et al. (2017) conducted a long-term abrasion test on 10" hoses and compared the results to those of abrasion calculations based on flow simulations. Three different lining materials were applied in the full-scale test. The abrasion rate increases in the following order: armoured liner, rubber, and plastic, although the plastic has better Schopper abrasion than rubber. The results indicate the superiority of rubber liner over plastic liner in high impact wear regime. Parameterized erosion model and a discrete phase model (DPM) combined in a CFD simulation proved to be an effective tool to predict erosion rate. The simulation proved to be very sensitive to the dependence of the impact angle on the abrasion rate, particularly at low impact angles. Breakdown of the abrading particles has a high influence on the results. Natural material, granite with wide size distribution (32 ~ 60 mm) was used in the full-scale abrasion test. In addition, there was significant batch to batch variation in the granite properties.

Figure 277: Rotating full-scale abrasion tester (Neale et al., 2017)

Takano et al. (2015) conducted a small-scale test for a fundamental understanding of pipe wear under hydraulic transportation of deep-sea mining. The small-scale test apparatus was set up using the pipes of about 80 mm in diameter and the rocks of which maximum particle diameters were about 20 mm. In the test, the pipe materials and the pipe inclination were changed to evaluate the differential of the amount of pipe material loss. Furthermore, the amount of the pipe material loss in full scale was estimated based on the small-scale test results. From the research on the wear of the riser with different inclinations, the authors concluded that the configuration of the flexible hose to connect the seafloor mining vehicle and the buffer should be considered carefully in designing of the mining system and preparing the operating procedure.

A novel framework for coupled analysis of risers with internal flow utilized to study the VIV of a mining riser was presented in Thorsen et al. (2019). Focus was on the effect of time-varying internal slurry flows, and the associated density waves traveling along the riser. Simulated VIV response and fatigue damage were reported in detail, to illuminate the effect of the period/wavelength of the internal flow. It was found that the internal flow produces

significant changes to the VIV fatigue damage, if the wavelength of the internal density wave is close to $\lambda_{cr} = L/n$, where L is the riser length, and n is the dominating VIV mode. The results suggest that careful analysis is necessary when designing a mining riser where internal density waves are expected to occur with a wavelength near or above the critical value. In such cases, the presented numerical method may be a useful tool.

10. PROCEDURE/GUIDELINE FOR MODEL CONSTRUCTION

The 28th Ocean Engineering Committee developed a preliminary procedure for model construction of floating offshore platforms; however, its Advisory Committee (AC) made a series of comments/recommendations and suggested to develop a guideline instead of a procedure. As indicated by the 28th AC, a procedure should provide specific details and criteria.

Since the nature of tests and models covered by the Ocean Engineering Committee is quite diverse and specific at the same time, to develop generic standards/procedures/criteria to attend all the possible scenarios is not feasible. So, after consulting the present AC, a new guideline was developed: 7.5-02-07-03.15 Model Construction of Offshore Systems.

The new guideline is based on the version submitted to the 28th Conference and incorporated the 28th AC's comments and suggestions. Focus on model construction issues regarding materials, tolerances, production methods, quality control, acceptance testing, etc. were also included as required by the current Terms of Reference.

The design, manufacture, and pre-tests in water of offshore systems models have been addressed. An offshore system can be composed of bottom-founded or stationary floating structures, mooring lines/risers and umbilicals, dynamic positioning systems, and/or any other auxiliary structure or equipment involved in offshore operations. Those structures may be subjected to environmental loads such as wind, water waves and current (excluding ice). The guideline may also be applied to subsea and coastal structures such as floating breakwaters and fish farms.

The purpose of this guideline is to ensure the correct design and manufacture of the model of the offshore system for its testing in towing tanks, wave/current basins, and/or wind tunnels (excluding field tests). In typical tests of offshore systems, hull platform models are assumed to be rigid bodies, so the focus of this guideline is on this type of structure. Additional considerations should be done when the elasticity of the platform must be modelled.

11. CONCLUSIONS & RECOMMENDATIONS

11.1 State-of-the-art reviews in offshore structures

In the present ITTC period (2017-2021), the review has allowed to identify some issues associated to bottom founded and stationary floating structures. For bottom-founded structures, life extension of existing fixed platforms has attracted attention. Fatigue and vessel impact loads are of concern. For (fixed) offshore wind turbines, besides waves, wind and current loads, earthquake loads have become an item of concern. Model and full-scale tests are needed for validation studies.

In the case of FPSO and/or FLNGs, several experimental and numerical studies have been devoted to green water and water impacts associated to extreme waves. Hydrodynamic behaviour associated to side-by-side configurations and viscous damping are also issues that have attracted much attention in the recent years. In the case of TLPs and

semisubmersibles, several works have been devoted to applications related to the investigation of the occurrence and mitigation of VIM as well as applications for floating offshore wind turbines. Operations under ice conditions have also attracted attention and deserve further experimental and numerical research.

11.2 Review of the Existing Procedures

The Committee has reviewed and updated nine (09) procedures and guidelines. In general, minor revisions have been made. The detailed comments from the Advisory Committee have been also incorporated.

Concerning the existing procedures and guidelines, the Ocean Engineering Committee would like to make the following recommendations to the 29th ITTC:

- Adopt the updated procedure: 7.5-02-07-03.1 Floating Offshore Platform Experiments;
- Adopt the updated procedure: 7.5-02-07-03.2 Analysis Procedure for Model Tests in Regular Waves;
- Adopt the updated procedure: 7.5-02-07-03.4 Active Hybrid Model Tests of Floating Offshore Structures with Mooring Lines;
- Adopt the updated procedure: 7.5-02-07-03.5 Passive Hybrid Model Tests of Floating Offshore Structures with Mooring Lines;
- Adopt the updated procedure: 7.5-02-07-03.6 Dynamic Positioning System Model Test Experiments;
- Adopt the updated guideline: 7.5-02-07-03.10 Guideline for VIV Testing;
- Adopt the updated guideline: 7.5-02-07-03.11 Model Tests of Multibodies in Close Proximity;
- Adopt the updated guideline: 7.5-02-07-03.13 Guideline for VIM Testing;
- Adopt the updated procedure: 7.5-02-07-03.14 Analysis Procedure of Model Tests in Irregular Waves.

Since, in the period 2017-2021, several works and developments on side-by-side configuration and VIM tests have been reported, it is recommended that Procedure 7.5-02-07-03.11 Model Tests of Multibodies in Close Proximity and Guideline 7.5-02-07-03.13 Guideline for VIM Testing should be continuously reviewed and updated accordingly, by the next committees.

11.3 State-of-the-art review in offshore aquaculture systems

Offshore aquaculture systems continue to attract attention, with particular focus on larger floating structures. Close containment tank systems have been proposed to avoid the effects of sea lice on fish. Hydrodynamic interaction among the main floating structure, mooring system, and the fishing nets continues to be a concern, especially under harsh environmental conditions.

According to Xu and Qin (2020), still several issues need to be addressed. More physical model tests and numerical simulations are required to study the fast-swimming behaviour and swimming efficiency of fish to select appropriate farming sites and improve the designs of offshore aquaculture cage systems. Fluid-ice-aquaculture structure interactions must be studied for aquaculture cages deployed in North Atlantic where drift ice could damage the cage structures. Some new elements have been introduced together with aquaculture

technology such as the integration of aquaculture farming and ocean renewable energy system. A vast array of applications is ready for the evolution of aquaculture engineering and technology.

11.4 State-of-the-art review in cable/pipe dynamics close to sea-surface

Although the number of applications of cable/pipes close to the sea surface is growing, there are still few experimental studies on this topic. Most of these works are concerned with fluid transfer lines (FTL) such as risers or offloading hoses. However, for other applications such as power cables for wave energy converters, cable net barriers or towing cables, only numerical studies have been found. Thus, it is suggested that model tests should be performed for the latter applications to validate the numerical results and gain more insight on the observed phenomena.

11.5 State-of-the-art review in Software-in-the-Loop (SiL) tests

A software in the loop (SIL) system for the use in experimental tests has been reviewed in this report. The SiL approach offers several advantages over conventional full-coupled modelling utilizing a working rotor in a wind field, including the ability to deploy in a wide range of facilities, reduced cost, greater flexibility of scale, and ability to simulate the impact of some features such as control systems and blade elasticity which may prove challenging with a working rotor. At present, the system is still under development and there are some issues regarding repeatability and experiment methodology which require further refinement.

11.6 Experimental benchmark on wave run-up on cylinders

As an extension of the benchmark studies of wave run-ups on single and four truncated circular cylinders conducted in 2013 during the 27th ITTC, the present benchmark tests were conducted to measure the wave run-ups and global wave loads on fixed four squared cylinders under regular and irregular waves. A set of benchmark data and results were provided for validating related numerical simulations. Owing to the complicated wave-column interactions, more experimental and CFD studies are recommended in consideration of four-column cases with different configurations and more extreme waves such as focused waves. In addition, local wave impact loads on the columns are also critical and deserve further in-depth studies.

11.7 CFD benchmark on two-body interactions

The CFD benchmark study for two-body interaction is now on going and the interim conclusion can be summarized as below:

- The model test and CFD results show the viscous effect on the motion and drift force on bodies and the gap wave elevation when comparing the potential calculation;
- The viscous effect on body motion is the smallest and it shows larger influence on the gap wave elevation;
- The viscous effect is more pronounced at the higher wave frequency region;
- The smallest gap distance of 0.40 m shows the largest viscous effect and the distance of 0.55 m shows negligible viscous effect on the body motion, drift force and gap wave elevation.

Further CFD studies are needed by the various participants to establish the CFD procedure for 2 body interaction problem and

resultantly to update the procedure for 2 body model test based on this CFD benchmark study. The conclusion will be made when the CFD study proposed as the cooperative work in this task is completed. It would be good if the model test and CFD study between the smaller gap are carried out. list.

11.8 State-of-the-art review in large diameter flexible risers for deep water mining

In general, many experimental and numerical investigations on flexible risers used in deep sea mining applications have been conducted. However, the technologies for the design of flexible risers are not firmly established yet. It is difficult to arrive to general conclusions or formulae to measure the parameters such as the pressure drop of the mixture, the spatial configurations of the risers and the erosion rate.

Owing to the complicated interaction of the flexible riser, the inner flow and the environmental loads, the coupled analysis of the inner flow regime and the external loads are rare. Additionally, the aggregation and clogging of the ores in the flexible riser should be investigated in detail due to the complex flow regimes and particle motion when the mixture flow is passing the crest and trough of the curved risers.

As the vertical ore transporting system consists of the rigid pipe, the pumps, the buffer and the flexible hoses, the integrated system should be experimental and numerical investigated to predict the dynamic responses of all the components, the continuous flow regimes and to address the flow assurance issues of the whole transporting system in the next step.

11.9 New Guideline for Model Construction

The Ocean Engineering Committee would like to make the following recommendation to the 29th ITTC:

- Adopt the new guideline: 7.5-02-07-03.15 Model Construction of Offshore Systems

12. REFERENCES

Abdussamie, N., Drobyshevski, Y., Ojeda, R., Thomas, G., Amin, W., 2017. "Experimental investigation of wave-in-deck impact events on a TLP model". Ocean Eng. 142, 541–562. https://doi.org/https://doi.org/10.1016/j.oceaneng.2017.07.037

An, S., Chen, D., Bai, Y., 2019. "Dynamic Positioning Observer Design Using Exogenous Kalman Filter". https://doi.org/10.1115/OMAE2019-96490

Asgari, P., Fernandes, A.C., Low, Y.M., 2020. "Most often instantaneous rotation center (MOIRC) for roll damping assessment in the free decay test of a FPSO". Appl. Ocean Res. 95, 102014. https://doi.org/https://doi.org/10.1016/j.apor.2019.102014

Avalos, G.O.G., Wanderley, J.B. V, 2018. "Numerical study of forced roll oscillation of FPSO with bilge keel". Ocean Eng. 147, 304–317. https://doi.org/https://doi.org/10.1016/j.oceaneng.2017.10.034

Azcona, J., Bouchotrouch, F., González, M., Garciandía, J., Munduate, X., Kelberlau, F., Nygaard, T.A., 2014. "Aerodynamic thrust modelling in wave tank tests of offshore floating wind turbines using a ducted fan", in: Journal of Physics: Conference Series.

IOP Publishing, p. 12089.

Bachynski, E.E., Thys, M., Sauder, T., Chabaud, V., Sæther, L.O., 2016. "Real-Time Hybrid Model Testing of a Braceless Semi-Submersible Wind Turbine: Part II — Experimental Results". https://doi.org/10.1115/OMAE2016-54437

Banik, A.K., Roy, S., Saha, K., Dey, S., 2019. "Effect of wave spreading including multi-directional wave interaction on the responses of a spar platform". Mar. Syst. Ocean Technol. 14, 153–165.

Batalla Toro, L.F., Reid, S.L., Tudela, A.S., Graham, D., 2018. "Integrated Decommissioning of a Pentagon Shaped Production Semisubmersible in the UK: A Unique Challenge". https://doi.org/10.1115/OMAE2018-77831

Bayati, I., Belloli, M., Ferrari, D., Fossati, F., Giberti, H., 2014. "Design of a 6-DoF Robotic Platform for Wind Tunnel Tests of Floating Wind Turbines". Energy Procedia 53, 313–323. https://doi.org/https://doi.org/10.1016/j.egypro.2014.07.240

Beauchesne, C., Parenteau, T., Septseault, C., Béal, P.-A., 2015. "Development & Large Scale Validation of a Transient Flow Assurance Model for the Design & Monitoring of Large Particles Transportation in Two Phase (Liquid-Solid) Riser Systems ". https://doi.org/10.4043/25892-MS

Beveridge, M.C.M., 2008. Cage aquaculture. John Wiley & Sons.

Bjerke, K.S., 1990. "Offshore fish-fanning platforms-development, design, construction and operation: the SEACON and SULAN concepts", in: Engineering for Offshore Fish Farming. Thomas Telford Publishing, pp. 153–169.

Bjørnø, J., Heyn, H.-M., Skjetne, R., Dahl, A.R., Frederich, P., 2017. "Modeling, Parameter Identification and Thruster-Assisted Position Mooring of C/S Inocean Cat I Drillship". https://doi.org/10.1115/OMAE2017-61896

Bugrov, L., 2006. "The" Sadco" underwater fish-farming system". Underw. Technol. Ocean World" Sci. Tech. J. about World Ocean Resour. Dev. 1, 34–45.

Cahay, M., Roberts, B.A., Sadouni, S., Béal, P.-A., Septseault, C., Mravak, Z., Benoit, C., 2017. "Ice Load Calculation on Semi-Submersible Platform". https://doi.org/10.1115/OMAE2017-61903

Carmo, B.S., Assi, G.R.S., Meneghini, J.R., 2013. "Computational simulation of the flow-induced vibration of a circular cylinder subjected to wake interference". J. Fluids Struct. 41, 99–108. https://doi.org/https://doi.org/10.1016/j.jfluidstructs.2013.02.010

Chadwick, E.M.P., Parsons, G.J., Sayavong, B., 2010. Evaluation of closed-containment technologies for saltwater salmon aquaculture. NRC Research Press.

Chang, S.-H.M., Isherwood, M., 2003. "Vortex-Induced Vibrations of Steel Catenary Risers and Steel Offloading Lines due to Platform Heave Motions ". https://doi.org/10.4043/15106-MS

Chen, H., 2017. "Safety of Marine Operations Involving Dynamically Positioned Vessels". https://doi.org/10.1115/OMAE2017-62708

Chen, L., Taylor, P.H., Draper, S., Wolgamot, H., Milne, I.A., Whelan, J.R., 2019. "Response based design metocean conditions for a permanently moored FPSO during tropical cyclones: Estimation of greenwater risk". Appl. Ocean Res. 89, 115–127. https://doi.org/https://doi.org/10.1016/j.apor.2019.05.003

Chen, Y., Fu, S., Xu, Y., Fan, D., 2013. "High order force components of a near-wall circular cylinder oscillating in transverse direction in a steady current". Ocean Eng. 74, 37–47. https://doi.org/https://doi.org/10.1016/j.oceaneng.2013.09.009

Chen, Y., Yang, N., Jin, X., 2014. "Nonlinear Finite-Element Analysis of Flexible Marine Pipes for Deep-Sea Mining ".

Cheng, J., Cao, P., Ren, H., Zhang, M., Fu, S., 2018. "Experimental Study of the Pipe With Buoyancy Modules ".

Cheng, N., Gaudin, C., Cassidy, M.J., 2019. "Physical and numerical study of the combined bearing capacity of hybrid foundation systems". Ocean Eng. 179, 104–115. https://doi.org/10.1016/j.oceaneng.2019.03.002

Choi, Y.-M., Nam, B.W., Hong, S.Y., Jung, D.W., Kim, H.J., 2018. "Coupled motion analysis of a tension leg platform with a tender semi-submersible system". Ocean Eng. 156, 224–239. https://doi.org/https://doi.org/10.1016/j.oceaneng.2018.01.031

Chong, S.H., 2017. "Numerical simulation of offshore foundations subjected to repetitive loads". Ocean Eng. 142, 470–477. https://doi.org/10.1016/j.oceaneng.2017.07.031

Chow, J.H., Ng, E.Y.K., Srikanth, N., 2019. "Numerical study of the dynamic response of a wind turbine on a tension leg platform with a coupled partitioned six degree-of-freedom rigid body motion solver". Ocean Eng. 172, 575–582. https://doi.org/https://doi.org/10.1016/j.oceaneng.2018.12.040

Chu, Y.I., Wang, C.M., Park, J.C., Lader, P.F., 2020. "Review of cage and containment tank designs for offshore fish farming". Aquaculture 519, 734928. https://doi.org/https://doi.org/10.1016/j.aquaculture.2020.734928

Cozijn, H., Choi, J.W., You, Y.-J., 2017. "Thruster-Wave Interaction During DP Stationkeeping: Model Tests in Open Water and Under a Ship Hull". https://doi.org/10.1115/OMAE2017-62168

da Silva Gomes, S., Pinheiro Gomes, S.C., 2021. "A new dynamic model of towing cables". Ocean Eng. 220, 107653. https://doi.org/https://doi.org/10.1016/j.oceaneng.2020.107653

Day, A.H., Clelland, D., Oguz, E., Dai, S., Azcona Armendáriz, J., Bouchotrouch, F., Lopez, J.A., Sánchez, G., González Almeria, G., 2017. "Realistic simulation of aerodynamic loading for model testing of floating wind turbines".

Deepak, C.R., Ramji, S., Ramesh, N.R., Babu, S.M., Abraham, R., Shajahan, M.A., Atmanand, M.A., 2007. "Development And Testing of Underwater Mining Systems For Long Term Operations Using Flexible Riser Concept ".

Deepak, C.R., Shajahan, M.A., Atmanand, M.A., Annamalai, K., Jeyamani, R., Ravindran, M., Schulte, E., Handschuh, R., Panthel, J., Grebe, H., Schwarz, W., 2001.

"Developmental Tests On the Underwater Mining System Using Flexible Riser Concept ".

Dehghani, A., Aslani, F., 2019. "A review on defects in steel offshore structures and developed strengthening techniques". Structures 20, 635–657. https://doi.org/10.1016/j.istruc.2019.06.002

Detlefsen, O., Theilen, L., Abdel-Maksoud, M., 2017. "Static and Dynamic Analysis Methods of Position-Keeping Capability for Offshore Supply Vessels With Voith-Schneider Propellers". https://doi.org/10.1115/OMAE2017-61893

DNV, 2010. Recommended Practice Global Performance Analysis of Deepwater Floating Structures.

Dong, Q., Lu, H., Yang, J., Guo, X., 2019. "Dynamic gangway responses between TLP and semi-submersible platform during tender-assisted drilling". Mar. Struct. 67, 102645. https://doi.org/https://doi.org/10.1016/j.marstruc.2019.102645

Fang, S.M., Niedzwecki, J.M., Fu, S., Li, R., Yang, J., 2014. "VIV response of a flexible cylinder with varied coverage by buoyancy elements and helical strakes". Mar. Struct. 39, 70–89. https://doi.org/https://doi.org/10.1016/j.marstruc.2014.06.004

Feng, X., Bai, W., Chen, X.B., Qian, L., Ma, Z.H., 2017. "Numerical investigation of viscous effects on the gap resonance between side-by-side barges". Ocean Eng. 145, 44–58. https://doi.org/https://doi.org/10.1016/j.oceaneng.2017.08.060

Fernandes, A.C., Asgari, P., Sales Junior, J.S., 2018. "Linear and non-linear roll damping of a FPSO via system identification of a third order equation with sway-roll coupled damping effects". Ocean Eng. 166, 191–207. https://doi.org/https://doi.org/10.1016/j.oceaneng.2018.08.006

Fernandez, C., Bhushan Kumar, S., Lok Woo, W., Norman, R., Kr. Dev, A., 2020. "Real-Time Prediction of Reliability of Dynamic Positioning Sub-Systems for Computation of Dynamic Positioning Reliability Index (DP-RI) Using Long Short Term Memory (LSTM)". https://doi.org/10.1115/OMAE2020-18844

Fernandez, C., Dev, A.K., Norman, R., Woo, W.L., Kumar, S.B., 2019. "Dynamic Positioning System: Systematic Weight Assignment for DP Sub-Systems Using Multi-Criteria Evaluation Technique Analytic Hierarchy Process and Validation Using DP-RI Tool With Deep Learning Algorithm". https://doi.org/10.1115/OMAE2019-95485

Fernandez, C., Kumar, S.B., Lok Woo, W., Norman, R., Kr. Dev, A., 2018. "Dynamic Positioning Reliability Index (DP-RI) and Offline Forecasting of DP-RI During Complex Marine Operations". https://doi.org/10.1115/OMAE2018-77267

Fonseca, N., Stansberg, C.T., 2017. "Wave Drift Forces and Low Frequency Damping on the Exwave FPSO", in: Proceedings of the ASME 2017 36th International Conference on Ocean, Offshore and Arctic Engineering. Volume 1: Offshore Technology. Trondheim. https://doi.org/10.1115/OMAE2017-62540

Føre, H.M., Dahle, S.W., Gaarder, R.H., 2018. "Tensile Strength of Nylon Netting Subjected to Various Concentrations of Disinfecting Chemicals". J. Offshore Mech. Arct. Eng. 141. https://doi.org/10.1115/1.4040562

Fredriksen, A.G., Bonnemaire, B., Nilsen, Ø., Aspelund, L., Ommundsen, A., 2018. "Irregular Wave and Current Loads on a Fish Farm System". https://doi.org/10.1115/OMAE2018-77482

Fu, Z., Li, W., Sun, H., Yuan, M., Li, X., Cai, L., Wang, A., Guo, X., Wei, H., Tian, X., 2020. "Experiment-Scale Multi-Vessel Dynamic Positioning System for the Twin-Lift Decommissioning Operation". https://doi.org/10.1115/OMAE2020-18631

Gang, C., Huan, Z., Yuhan, W., Chao, W., Wei, Z., Yan, Y., 2018. "Float-Over Installation Analysis of Semisubmersible Production Platform Topside". https://doi.org/10.1115/OMAE2018-77347

Gansel, L.C., Endresen, P.C., Steinhovden, K.B., Dahle, S.W., Svendsen, E., Forbord, S., Jensen, Ø., 2017. "Drag on Nets Fouled With Blue Mussel (Mytilus Edulis) and Sugar Kelp (Saccharina Latissima) and Parameterization of Fouling". https://doi.org/10.1115/OMAE2017-62030

Gao, J., He, Z., Huang, X., Liu, Q., Zang, J., Wang, G., 2021. "Effects of free heave motion on wave resonance inside a narrow gap between two boxes under wave actions". Ocean Eng. 224, 108753. https://doi.org/https://doi.org/10.1016/j.oceaneng.2021.108753

Gao, W., Zhu, W., Dong, L., Qi, X., 2016. "A Study of Spar-FPSO VIM Phenomenon and Its Influence to Mooring System ".

Gao, Z., Efthymiou, M., Zhao, W., Cheng, L., Zhou, T., 2020. "Experimental Study of Hydrodynamic Damping for Water Intake Risers". https://doi.org/10.1115/OMAE2020-18119

Ghassempour, M., Failla, G., Arena, F., 2019. "Vibration mitigation in offshore wind turbines via tuned mass damper". Eng. Struct. 183, 610–636. https://doi.org/10.1016/j.engstruct.2018.12.092

Gonçalves, R.T., Suzuki, H., Marques, M.A., Silva, L.S.P., Tian, C., Hirabayashi, S., 2020. "Experimental Study of the Effect of the Pontoon Dimensions on the Flow-Induced Motions (FIM) of a Semi-Submersible Platform With Four Square Columns". https://doi.org/10.1115/OMAE2020-18009

Gundersen, G., Stuberg, P., Kendon, T.E., Reinholdtsen, S.-A., 2018. "Improved FPSO Offloading Strategy Based on Analysis Including DP System". https://doi.org/10.1115/OMAE2018-78465

Ha, Y.-J., Kim, K.-H., Nam, B.W., Hong, S.Y., Kim, H., 2021. "Experimental study for characteristics of slamming loads on bow of a ship-type FPSO under breaking and irregular wave conditions". Ocean Eng. 224, 108738. https://doi.org/https://doi.org/10.1016/j.oceaneng.2021.108738

Handschuh, R., Grebe, H., Panthel, J., Schulte, E., Wenzlawski, B., Schwarz, W., Atmanand, M.A., Jeyamani, R., Shajahan, M.A., Deepak, C.R., Ravindran, M., 2001.

"Innovative Deep Ocean Mining Concept Based On Flexible Riser And Self-propelled Mining Machines ".

Harmsen, E., van Dijk, R., Stuberg, P., 2018. "DP-Stability During Heavy Lift Operations Using a Modified Kalman Filter". https://doi.org/10.1115/OMAE2018-77901

He, J., Wan, D., Hu, Z., 2018. "CFD Simulations of Helical Strakes Reducing Vortex Induced Motion of a Semi-Submersible". https://doi.org/10.1115/OMAE2018-78372

Hegseth, J.M., Bachynski, E.E., Karimirad, M., 2018. "Comparison and Validation of Hydrodynamic Load Models for a Semi-Submersible Floating Wind Turbine". https://doi.org/10.1115/OMAE2018-77676

Hill, H., 2018. "Future Proofing Fish Farming". Mar. Rep. 125.

Horn, J.T., Leira, B.J., 2019. "Fatigue reliability assessment of offshore wind turbines with stochastic availability". Reliab. Eng. Syst. Saf. 191, 106550. https://doi.org/10.1016/j.ress.2019.106550

Hu, X., Zhang, X., You, Y., 2017. "Numerical Studies on Vortex-Induced Motions of a Semi-Submersible With Four Columns Based on IDDES Model", in: Proceedings of the ASME 2017 36th International Conference on Ocean, Offshore and Arctic Engineering. Volume 1: Offshore Technology. ASME, Trondheim. https://doi.org/10.1115/OMAE2017-62164

Hu, Z.-Q., Wang, S.-Y., Chen, G., Chai, S.-H., Jin, Y.-T., 2017. "The effects of LNG-tank sloshing on the global motions of FLNG system". Int. J. Nav. Archit. Ocean Eng. 9, 114–125.

Hu, Z.Z., Mai, T., Greaves, D., Raby, A., 2017. "Investigations of offshore breaking wave impacts on a large offshore structure". J. Fluids Struct. 75, 99–116. https://doi.org/10.1016/j.jfluidstructs.2017.08.005

Hu, Z.Z., Yan, S., Greaves, D., Mai, T., Raby, A., Ma, Q., 2020. "Investigation of interaction between extreme waves and a moored FPSO using FNPT and CFD solvers". Ocean Eng. 206, 107353. https://doi.org/https://doi.org/10.1016/j.oceaneng.2020.107353

Huang, A.S., Tannuri, E.A., Queiroz Filho, A.N., Ianagui, A.S.S., Yuba, D.G.T., Nogueira, S., Abdalla, T.C., 2017. "The Influence of Hold-Back Vessels on the Operation of a DP Drilling Rig: Control System and Stability Analysis". https://doi.org/10.1115/OMAE2017-61153

Huang, X.-H., Liu, H.-Y., Hu, Y., Yuan, T.-P., Tao, Q.-Y., Wang, S.-M., Liu, Z.-X., 2020. "Hydrodynamic performance of a semi-submersible offshore fish farm with a single point mooring system in pure waves and current". Aquac. Eng. 90, 102075. https://doi.org/https://doi.org/10.1016/j.aquaeng.2020.102075

Ji, X., Li, Y., Tang, Y., Tong, B., 2019. "Viscous damping effect and vortex shedding performance of the novel anti-motion structures on a cylindrical FPSO". Ocean Eng. 190, 106430. https://doi.org/https://doi.org/10.1016/j.oceaneng.2019.106430

Jiang, S.-C., Liu, H., Sun, T.-Z., Gu, Q., 2020. "Numerical simulation for hydrodynamic behavior of box-systems with and without narrow gaps". Ocean Eng. 214, 107698.

https://doi.org/https://doi.org/10.1016/j.oceaneng.2020.107698

Jin, R., Xiong, Y., Wang, Y., 2018. "Motion response analysis of Truss spar platform with small-scale cylinders under bichromatic waves", in: The 28th International Ocean and Polar Engineering Conference. International Society of Offshore and Polar Engineers.

Jin, X., Wang, A.M., Li, H., Yu, W., He, M., Wang, A., 2018. "Floatover Installation Technology With a DP2 Class Dynamic-Positioning Semisubmersible Vessel ".

Jin, Y., Chai, S., Duffy, J., Chin, C., Bose, N., 2019. "Hydrodynamics of a conceptual FLNG system in side-by-side offloading operation". Ships Offshore Struct. 14, 104–124. https://doi.org/10.1080/17445302.2018.1482041

Jin, Y., Chai, S., Duffy, J., Chin, C., Bose, N., 2018. "URANS predictions on the hydrodynamic interaction of a conceptual FLNG-LNG offloading system in regular waves". Ocean Eng. 153, 363–386. https://doi.org/https://doi.org/10.1016/j.oceaneng.2018.01.102

Ju, S.H., Huang, Y.C., 2019. "Analyses of offshore wind turbine structures with soil-structure interaction under earthquakes". Ocean Eng. 187, 106190. https://doi.org/10.1016/j.oceaneng.2019.106190

Kang, Z., Zhang, C., Sun, L., 2017. "Research on truncation method of FPSO and offloading system in model test". Appl. Ocean Res. 67, 94–108. https://doi.org/https://doi.org/10.1016/j.apor.2017.06.007

Karimirad, M., Bachynski, E.E., 2017. "Sensitivity Analysis of Limited Actuation for Real-time Hybrid Model Testing of 5MW Bottom-fixed Offshore Wind Turbine", in: Energy Procedia. Elsevier, pp. 14–25. https://doi.org/10.1016/j.egypro.2017.10.331

Karimirad, M., Bachynski, E.E., Berthelsen, P.A., Ormberg, H., 2017. "Comparison of Real-Time Hybrid Model Testing of a Braceless Semi-Submersible Wind Turbine and Numerical Simulations". https://doi.org/10.1115/OMAE2017-61121

Kato, T., Kawamura, Y., Tahara, J., Baba, S., Sanada, Y., 2020. "Development of Side Thruster System for ASV ".

Kawahashi, T., Arai, M., Wang, X., Cheng, L.-Y., Nishimoto, K., Nakashima, A., 2019. "A study on the coupling effect between sloshing and motion of FLNG with partially filled tanks". J. Mar. Sci. Technol. 24, 917–929. https://doi.org/10.1007/s00773-018-0596-5

Kaynia, A.M., 2019. "Seismic considerations in design of offshore wind turbines". Soil Dyn. Earthq. Eng. 124, 399–407. https://doi.org/10.1016/j.soildyn.2018.04.038

Kerkeni, S., Liferov, P., Serré, N., Bridges, R., Jorgensen, F., 2018. "Station-Keeping Trials in Ice: Dynamic Positioning in Ice — Results and Learnings". https://doi.org/10.1115/OMAE2018-78556

Kiamini, S., Jalilvand, A., Mobayen, S., 2018. "LMI-based robust control of floating tension-leg platforms with uncertainties and time-delays in offshore wind turbines via T-S fuzzy approach". Ocean Eng. 154, 367–374.

https://doi.org/https://doi.org/10.1016/j.oceaneng.2018.02.027

Kim, J.-S., Yoo, S.O., Kim, H.J., Lee, J.H., Han, S.L., Lee, D.Y., 2019. "Experimental and Numerical Study of Horizontal Wave Impact Loads for a Semi-Submersible Drilling Unit". https://doi.org/10.1115/OMAE2019-96236

Kim, M., Jung, K.H., Park, S.B., Lee, G.N., Duong, T.T., Suh, S.-B., Park, I.-R., 2020. "Experimental and numerical estimation on roll damping and pressure on a 2-D rectangular structure in free roll decay test". Ocean Eng. 196, 106801. https://doi.org/https://doi.org/10.1016/j.oceaneng.2019.106801

Kitazawa, D., Mizukami, Y., Kanehira, M., Takeuchi, Y., Ito, S., 2017. "Water Tank and Field Tests on the Performance of a Submergible Fish Cage for Farming Silver Salmon". https://doi.org/10.1115/OMAE2017-61631

Koop, A., 2020. "Using CFD to determine scale effects on current loads of offshore vessels in side-by-side configuration". Ocean Eng. 195, 106707. https://doi.org/https://doi.org/10.1016/j.oceaneng.2019.106707

Koop, A., Cozijn, H., Schrijvers, P., Vaz, G., 2017. "Determining Thruster-Hull Interaction for a Drill-Ship Using CFD". https://doi.org/10.1115/OMAE2017-61485

Krishnan, R., Seeninaidu, N., 2017. "Hydrodynamic Response of Three Column Semi-Submersible Floater Supporting Vertical Axis Wind Turbine". https://doi.org/10.1115/OMAE2017-62452

Kristiansen, D., Aksnes, V., Su, B., Lader, P., Bjelland, H. V, 2017. "Environmental Description in the Design of Fish Farms at Exposed Locations". https://doi.org/10.1115/OMAE2017-61531

Kristiansen, D., Lader, P., Endresen, P.C., Aksnes, V., 2018. "Numerical and Experimental Study on the Seakeeping Behavior of Floating Closed Rigid Fish Cages". https://doi.org/10.1115/OMAE2018-77254

Kumar, N., Kumar Varma Kolahalam, V., Kantharaj, M., Manda, S., 2018. "Suppression of vortex-induced vibrations using flexible shrouding—An experimental study". J. Fluids Struct. 81, 479–491. https://doi.org/https://doi.org/10.1016/j.jfluidstructs.2018.04.018

Kvittem, M.I., Berthelsen, P.A., Eliassen, L., Thys, M., 2018. "Calibration of Hydrodynamic Coefficients for a Semi-Submersible 10 MW Wind Turbine". https://doi.org/10.1115/OMAE2018-77826

Lader, P., Kristiansen, D., Alver, M., Bjelland, H. V, Myrhaug, D., 2017. "Classification of Aquaculture Locations in Norway With Respect to Wind Wave Exposure". https://doi.org/10.1115/OMAE2017-61659

Larsen, K., Vigesdal, T., Bjørkli, R., Dalane, O., 2018. "Mooring of Semi Submersibles in Extreme Sea States: Simplified Models for Wave Drift Forces and Low Frequency Damping". https://doi.org/10.1115/OMAE2018-77178

Laugesen, R., Hansen, A.M., 2015.

"Experimental study of the dynamic response of the DTU 10 MW wind turbine on a tension leg platform", in: DTU Wind Energy. Phys Conf Ser. p. 92007.

Lee, D., Lee, S.-J., 2019. "Adaptive PD for Dynamic Positioning System Based on DDPG ".

Lee, J., Choi, S.-M., Lee, S.J., Jung, K.H., 2019. "Tension Based Heading Control Strategy of the Arctic FPSO With DP Assisted Mooring System". https://doi.org/10.1115/OMAE2019-96557

Li, B., 2020. "Multi-body hydrodynamic resonance and shielding effect of vessels parallel and nonparallel side-by-side". Ocean Eng. 218, 108188. https://doi.org/https://doi.org/10.1016/j.oceaneng.2020.108188

Li, B., Wang, L., Wang, X., Xu, S., Li, X., 2018. "Estimation of Thruster-Thruster/Current Interaction in a Dynamic Positioning System Through Supervised Learning With Neural Networks ".

Li, D.-J., Fu, Q., Du, Z.-F., Xiao, Y., Han, R.-G., Sun, H.-H., 2018. "Structural Configuration Selection and Optimization of 7th Generation Semi-Submersible Drilling Unit". https://doi.org/10.1115/OMAE2018-78688

Li, L., Jiang, Z., Ong, M.C., 2017. "A Preliminary Study of a Vessel-Shaped Offshore Fish Farm Concept". https://doi.org/10.1115/OMAE2017-61665

Li, L., Jiang, Z., Ong, M.C., Hu, W., 2019a. "Design optimization of mooring system: An application to a vessel-shaped offshore fish farm". Eng. Struct. 197, 109363. https://doi.org/https://doi.org/10.1016/j.engstruct.2019.109363

Li, L., Jiang, Z., Vangdal Høiland, A., Chen Ong, M., 2018a. "Numerical Analysis of a Vessel-Shaped Offshore Fish Farm". J. Offshore Mech. Arct. Eng. 140. https://doi.org/10.1115/1.4039131

Li, L., Jiang, Z., Wang, J., Ong, M.C., 2019b. "Numerical Study on the Heading Misalignment and Current Velocity Reduction of a Vessel-Shaped Offshore Fish Farm". J. Offshore Mech. Arct. Eng. 141. https://doi.org/10.1115/1.4042266

Li, L., Jiang, Z., Wang, J., Ong, M.C., 2018b. "Predicting the Heading Misalignment of a Vessel-Shaped Offshore Fish Farm Under Waves and Currents". https://doi.org/10.1115/OMAE2018-77476

Li, Q., Wang, J., Yan, S., Gong, J., Ma, Q., 2018. "A zonal hybrid approach coupling FNPT with OpenFOAM for modelling wave-structure interactions with action of current". Ocean Syst. Eng. 8, 381–407. https://doi.org/10.12989/ose.2018.8.4.381

Li, W., Tang, Y., Wang, B., Li, Y., 2018. "Internal Resonances for the Heave Roll and Pitch Modes of a Spar Platform Considering Wave and Vortex Exciting Loads in Heave Main Resonance". J. Mar. Sci. Appl. 17, 265–272. https://doi.org/10.1007/s11804-018-0023-7

Li, Y., Liu, S.-J., Li, L., 2007. "Dynamic analysis of deep-ocean mining pipe system by discrete element method". China Ocean Eng. 21, 175–186.

Li, Z.X., Wu, K., Shi, Y., Ning, L., Yang, D., 2019. "Experimental study on the interaction between water and cylindrical structure under earthquake action". Ocean Eng. 188, 106330.

https://doi.org/10.1016/j.oceaneng.2019.106330

Liang, Y., Tao, L., 2018. "Hydrodynamics Around a Deep-Draft Semi-Submersible With Various Corner Shapes". https://doi.org/10.1115/OMAE2018-77135

Liang, Y., Tao, L., Xiao, L., Liu, M., 2017. "Experimental and numerical study on vortex-induced motions of a deep-draft semi-submersible". Appl. Ocean Res. 67, 169–187. https://doi.org/https://doi.org/10.1016/j.apor.2017.07.008

Liao, K., Duan, W., Ma, Q., Ma, S., Zhao, B., Hu, C., 2017. "Numerical Analysis of Wave Impact Loads on Semi-Submersible Platform". https://doi.org/10.1115/OMAE2017-62464

Lim, D.-H., Kim, Y., 2019. "Probabilistic analysis of air gap of tension-leg platforms by a nonlinear stochastic approach". Ocean Eng. 177, 49–59. https://doi.org/https://doi.org/10.1016/j.oceaneng.2019.02.054

Liu, M., Xiao, L., Kou, Y., Lu, H., 2017a. "Numerical Study on Vortex-Induced Motions of Semi-Submersibles With Various Types of Columns". https://doi.org/10.1115/OMAE2017-62355

Liu, M., Xiao, L., Liang, Y., Tao, L., 2017b. "Experimental and numerical studies of the pontoon effect on vortex-induced motions of deep-draft semi-submersibles". J. Fluids Struct. 72, 59–79. https://doi.org/https://doi.org/10.1016/j.jfluidstructs.2017.04.007

Liu, M., Xiao, L., Yang, J., Tian, X., 2017c. "Parametric study on the vortex-induced motions of semi-submersibles: Effect of rounded ratios of the column and pontoon". Phys. Fluids 29, 55101. https://doi.org/10.1063/1.4983347

Liu, W., Wang, J., Huang, J., Liu, Y., Li, Y., 2017. "Spar Platform Oil Storage and Offloading System Design ".

Luo-Theilen, X., Rung, T., 2019. "Numerical analysis of the installation procedures of offshore structures". Ocean Eng. 179, 116–127. https://doi.org/10.1016/j.oceaneng.2019.03.004

Lyu, B., Wu, W., Yao, W., Wang, Y., Zhang, Y., Tang, D., Yue, Q., 2019. "Multibody dynamical modeling of the FPSO soft yoke mooring system and prototype validation". Appl. Ocean Res. 84, 179–191. https://doi.org/https://doi.org/10.1016/j.apor.2019.01.011

Lyu, N., Ding, J., 2020. "Numerical Research on Thrust Deduction of Submerged Waterjet Propelled Transport Vessels on Inland Rivers ".

Manikandan, R., Saha, N., 2019. "Dynamic modelling and non-linear control of TLP supported offshore wind turbine under environmental loads". Mar. Struct. 64, 263–294. https://doi.org/https://doi.org/10.1016/j.marstruc.2018.10.014

Martin, T., Kamath, A., Bihs, H., 2020. "A Lagrangian approach for the coupled simulation of fixed net structures in a Eulerian fluid model". J. Fluids Struct. 94, 102962. https://doi.org/https://doi.org/10.1016/j.jfluidstructs.2020.102962

Matoug, C., Augier, B., Paillard, B., Maurice, G., Sicot, C., Barre, S., 2020. "An hybrid approach for the comparison of VAWT and

HAWT performances for floating offshore wind turbines", in: Journal of Physics: Conference Series. IOP Publishing, p. 32026.

Meng, L., Sun, C., Zhang, M., Han, H., Li, Y., 2021. "Dynamic mesh simulation on the effect of sloshing on concurrent two-phase flow fields for two-dimensionally packed columns simulations". Cryogenics (Guildf). 113, 103231. https://doi.org/https://doi.org/10.1016/j.cryogenics.2020.103231

Molin, B., Remy, F., Kimmoun, O., Stassen, Y., 2002. "Experimental study of the wave propagation and decay in a channel through a rigid ice-sheet". Appl. Ocean Res. 24, 247–260. https://doi.org/https://doi.org/10.1016/S0141-1187(03)00005-1

Montasir, O.A., Yenduri, A., Kurian, V.J., 2019. "Mooring System Optimisation and Effect of Different Line Design Variables on Motions of Truss Spar Platforms in Intact and Damaged Conditions". China Ocean Eng. 33, 385–397. https://doi.org/10.1007/s13344-019-0037-1

Moreno, F.M., Amendola, J., Tannuri, E.A., Ferreira, M.D., 2019. "Development of a Control Strategy for Underway Tandem-Like Oil Transfer Operation Between a Conventional and a DP Tanker". https://doi.org/10.1115/OMAE2019-96335

Moulas, D., Shafiee, M., Mehmanparast, A., 2017. "Damage analysis of ship collisions with offshore wind turbine foundations". Ocean Eng. 143, 149–162. https://doi.org/10.1016/j.oceaneng.2017.04.050

Müller, K., Sandner, F., Bredmose, H., Azcona, J., Manjock, A., Pereira, R., 2014. "Improved tank test procedures for scaled floating offshore wind turbines".

Murai, M., Takahashi, K., 2017. "The Influence of an Arrangement of an Array of Semi-Submersible Type FOWTs to Their Hydrodynamic Responses". https://doi.org/10.1115/OMAE2017-61614

Neale, P., Nagy, T., Grepaly, I., Tóth, P., Kristóf, G., Csobán, A., 2017. "Long-Term Abrasion Test for Seabed Mining Hose Liners ". https://doi.org/10.4043/27707-MS

Niewiarowski, A., Adriaenssens, S., Pauletti, R.M., Addi, K., Deike, L., 2018. "Modeling underwater cable structures subject to breaking waves". Ocean Eng. 164, 199–211. https://doi.org/https://doi.org/10.1016/j.oceaneng.2018.06.013

Nijun, Y., Bin, C., Jianxin, X., 2017. "Presssure Loss of Flexible Hose in Deep-Sea Mining System", in: 18th International Conference on Transport and Sedimentation of Solid Particles. Prague, Czech Republic, pp. 393–400.

O'Connell, K., Thiebaut, F., Kelly, G., Cashman, A., 2018. "Development of a free heaving OWC model with non-linear PTO interaction". Renew. Energy 117, 108–115. https://doi.org/https://doi.org/10.1016/j.renene.2017.10.027

O'Leary, K., Pakrashi, V., Kelliher, D., 2019. "Optimization of composite material tower for offshore wind turbine structures". Renew. Energy 140, 928–942. https://doi.org/10.1016/j.renene.2019.03.101

Oguz, E., Clelland, D., Day, A.H., Incecik, A., López, J.A., Sánchez, G., Almeria, G.G.,

2018. "Experimental and numerical analysis of a TLP floating offshore wind turbine". Ocean Eng. 147, 591–605. https://doi.org/https://doi.org/10.1016/j.oceaneng.2017.10.052

Parenteau, T., 2012. "Flow Assurance for Deep Ocean Mining: Large-Scale Experiment for Flow Correlation Validation and Abrasion Testing ". https://doi.org/10.4043/23250-MS

Parenteau, T., 2010. "Flow Assurance for Deepwater Mining". https://doi.org/10.1115/OMAE2010-20185

Parenteau, T., Lemaire, A., 2011. "Flow Assurance for Deep Ocean Mining - Pressure Requirement Through S-Shape Riser and Jumper ". https://doi.org/10.4043/21237-MS

Park, S.H., Lee, S.J., Lee, S., 2021. "Experimental investigation of towing- and course-stability of a FPSO towed by a tug-boat with lateral motion". Int. J. Nav. Archit. Ocean Eng. 13, 12–23. https://doi.org/https://doi.org/10.1016/j.ijnaoe.2020.11.003

Peng, Y., Xia, J.X., Cao, B., Ren, H.T., Wu, Y., 2015. "Spatial Configurations and Particle Transportation Parameters of Flexible Hose in Deep-sea Mining System ".

Pessoa, J., Stansberg, C.T., Fonseca, N., Laranjinha, M., 2018. "Experimental and Numerical Study of the Free Surface Elevation Over the Pontoons of a Semisubmersible Platform in Waves". https://doi.org/10.1115/OMAE2018-78009

Pires, O., Azcona, J., Vittori, F., Bayati, I., Gueydon, S., Fontanella, A., Liu, Y., De Ridder, E.J., Belloli, M., Van Wingerden, J.W., 2020. "Inclusion of rotor moments in scaled wave tank test of a floating wind turbine using SiL hybrid method", in: Journal of Physics: Conference Series. IOP Publishing, p. 32048.

Pivano, L., Nguyen, D., Smøgeli, Ø., 2017. "Full-Scale Validation of a Vessel's Station-Keeping Capability With DynCap". https://doi.org/10.1115/OMAE2017-62666

Qin, H., Xu, Z., Li, P., Yu, S., 2020. "A physical model approach to nonlinear vertical accelerations and mooring loads of an offshore aquaculture cage induced by wave-structure interactions". Ocean Eng. 197, 106904. https://doi.org/https://doi.org/10.1016/j.oceaneng.2019.106904

Ramesh, N.R., Thirumurugan, K., Rajesh, S., Deepak, C.R., Atmanand, M.A., 2013. "Experimental and Computational Investigation of Turbulent Pulsatile Flow through a Flexible Hose ".

Rao, Q., Wang, Z., Liu, S., Fang, M., 2009. "Interaction of fluid-solid coupled flexible hose and mining machine in deep-ocean mining system", in: Eighth ISOPE Ocean Mining Symposium. International Society of Offshore and Polar Engineers.

Ren, H., Xu, Y., Cheng, J., Cao, P., Zhang, M., Fu, S., Zhu, Z., 2019a. "Vortex-induced vibration of flexible pipe fitted with helical strakes in oscillatory flow". Ocean Eng. 189, 106274. https://doi.org/https://doi.org/10.1016/j.oceaneng.2019.106274

Ren, H., Xu, Y., Zhang, M., Deng, S., Li, S., Fu, S., Sun, H., 2019b. "Hydrodynamic forces on a partially submerged cylinder at high Reynolds number in a steady flow". Appl. Ocean Res. 88, 160–169. https://doi.org/https://doi.org/10.1016/j.ap

or.2019.04.025

Ren, N., Ma, Z., Fan, T., Zhai, G., Ou, J., 2018. "Experimental and numerical study of hydrodynamic responses of a new combined monopile wind turbine and a heave-type wave energy converter under typical operational conditions". Ocean Eng. 159, 1–8. https://doi.org/https://doi.org/10.1016/j.oceaneng.2018.03.090

Rhee, C. van, Munts, E., Bosch, J. van den, Lotman, R., Heeren, J., 2013. "New Developments in the Simulation of Slurry Behaviour in Spooled Hoses for Offshore Mining Applications ". https://doi.org/10.4043/24082-MS

Rindarøy, M., Selvik, Ø., Ross, A., 2020. "Hybrid DP Simulations". https://doi.org/10.1115/OMAE2020-18309

Robertson, A.N., Bachynski, E.E., Gueydon, S., Wendt, F., Schünemann, P., Jonkman, J., 2018. "Assessment of Experimental Uncertainty for a Floating Wind Semisubmersible Under Hydrodynamic Loading". https://doi.org/10.1115/OMAE2018-77703

Rodríguez, C.A., Ramos, I.S., Esperança, P.T.T., Oliveira, M.C., 2020. "Realistic estimation of roll damping coefficients in waves based on model tests and numerical simulations". Ocean Eng. 213, 107664. https://doi.org/https://doi.org/10.1016/j.oceaneng.2020.107664

Rongau, J., Viale, S., 2017. "Development of a Flexible Pipe for Deep Sea Mining ". https://doi.org/10.4043/27658-MS

Rosetti, G.F., Pinto, M.L., de Mello, P.C., Sampaio, C.M.P., Simos, A.N., Silva, D.F.C., 2019. "CFD and experimental assessment of green water events on an FPSO hull section in beam waves". Mar. Struct. 65, 154–180. https://doi.org/https://doi.org/10.1016/j.marstruc.2018.12.004

Samadi, M., Ghodsi Hassanabad, M., 2017. "Hydrodynamic response simulation of Catenary mooring in the spar truss floating platform under Caspian Sea conditions". Ocean Eng. 137, 241–246. https://doi.org/https://doi.org/10.1016/j.oceaneng.2017.03.004

Sanchez-Mondragon, J., Vázquez-Hernández, A.O., Cho, S.K., Sung, H.G., 2018. "Yaw motion analysis of a FPSO turret mooring system under wave drift forces". Appl. Ocean Res. 74, 170–187. https://doi.org/https://doi.org/10.1016/j.apor.2018.02.013

Sanchez-Mondragon, J., Vázquez-Hernández, A.O., Cho, S.K., Sung, H.G., 2017. "Motion behavior in a turret-moored FPSO caused by piston mode effects in moonpool". Ocean Eng. 140, 222–232. https://doi.org/https://doi.org/10.1016/j.oceaneng.2017.05.025

Sauder, T., Chabaud, V., Thys, M., Bachynski, E.E., Sæther, L.O., 2016. "Real-Time Hybrid Model Testing of a Braceless Semi-Submersible Wind Turbine: Part I — The Hybrid Approach". https://doi.org/10.1115/OMAE2016-54435

Sauder, T., Tahchiev, G., 2020. "From Soft Mooring System to Active Positioning in Laboratory Experiments". https://doi.org/10.1115/OMAE2020-19103

Sayed, M., Islam, S., Watson, D., Kubat, I., Gash, R., Wright, B., 2017. "DP Drillship Stationkeeping in Ice - Comparison

Between Numerical Simulations and Ice Basin Tests ".

Scott, D.C.B., Muir, J.F., 2000. "Offshore cage systems: A practical overview". Option Mediterr. Cent. Adv. Mediterr. Agron. Stud. 79–89.

Seo, M.-G., Ha, Y.-J., Kim, N.-W., Nam, B.W., Lee, K.-S., 2019. "Experimental Evaluation of Wave Impact Loads on Semi-Submersible Structure According to Trim Angle". https://doi.org/10.1115/OMAE2019-95406

Silva, D.F.C., Coutinho, A.L.G.A., Esperança, P.T.T., 2017a. "Green water loads on FPSOs exposed to beam and quartering seas, part I: Experimental tests". Ocean Eng. 140, 419–433. https://doi.org/https://doi.org/10.1016/j.oceaneng.2017.05.005

Silva, D.F.C., Esperança, P.T.T., Coutinho, A.L.G.A., 2017b. "Green water loads on FPSOs exposed to beam and quartering seas, Part II: CFD simulations". Ocean Eng. 140, 434–452. https://doi.org/10.1016/j.oceaneng.2016.11.008

Skjong, S., Pedersen, E., 2017. "Co-Simulation of a Marine Offshore Vessel in DP-Operations Including Hardware-In-the-Loop (HIL)". https://doi.org/10.1115/OMAE2017-61164

Soeb, M.R., Islam, A.B.M.S., Jumaat, M.Z., Huda, N., Arzu, F., 2017. "Response of nonlinear offshore spar platform under wave and current". Ocean Eng. 144, 296–304. https://doi.org/https://doi.org/10.1016/j.oceaneng.2017.07.042

Song, H. Do, Kim, Y.-S., Suh, J.-C., 2019. "A Research of the DP Thruster Analysis with Various Duct Shapes for the Model Test ".

Subbulakshmi, A., Sundaravadivelu, R., 2021. "Effects of damping plate position on heave and pitch responses of spar platform with single and double damping plates under regular waves". Ocean Eng. 224, 108719. https://doi.org/https://doi.org/10.1016/j.oceaneng.2021.108719

Sun, L., Ding, Y.F., Zheng, J.T., Zong, Z., Liu, C.F., 2018. "Numerical Study of Vortex Induced Motions of Spar and Semi-Submersible Platforms at High Reynolds Numbers".

Takano, S., Ono, M., Masanobu, S., 2015. "Evaluation of Wearing Pipe for Subsea Mining With Large Particles in Slurry Transportation". https://doi.org/10.1115/OMAE2015-41217

Tan, J.H.C., Teng, Y.J., Kiprawi, F., 2017. "Vortex Induced Motion of a Dry Tree Semisubmersible". https://doi.org/10.1115/OMAE2017-61653

Tang, Z., Wang, L., Yi, F., He, H., 2020. "An Optimized Thrust Allocation Algorithm for Dynamic Positioning System Based on RBF Neural Network". https://doi.org/10.1115/OMAE2020-18267

Thorsen, M.J., Challabotla, N.R., Sævik, S., Nydal, O.J., 2019. "A numerical study on vortex-induced vibrations and the effect of slurry density variations on fatigue of ocean mining risers". Ocean Eng. 174, 1–13. https://doi.org/https://doi.org/10.1016/j.oceaneng.2019.01.041

Thys, M., Chabaud, V., Sauder, T., Eliassen, L.,

Sæther, L.O., Magnussen, Ø.B., 2018. "Real-Time Hybrid Model Testing of a Semi-Submersible 10MW Floating Wind Turbine and Advances in the Test Method". https://doi.org/10.1115/IOWTC2018-1081

Thys, M., Fontanella, A., Taruffi, F., Belloli, M., Berthelsen, P.A., 2019. "Hybrid Model Tests for Floating Offshore Wind Turbines". https://doi.org/10.1115/IOWTC2019-7575

Tian, X., Wang, Q., Liu, G., Liu, Y., Xie, Y., Deng, W., 2019. "Topology optimization design for offshore platform jacket structure". Appl. Ocean Res. 84, 38–50. https://doi.org/10.1016/j.apor.2019.01.003

Tidwell, J.H., 2012. Aquaculture production systems. Wiley Online Library.

Tsukada, Y., Ueno, M., Miyazaki, H., Takimoto, T., 2013. "An Auxiliary Thruster for Free-Running Model Ship Test". https://doi.org/10.1115/OMAE2013-10569

Tumen Ozdil, N.F., Akilli, H., 2019. "Flow comparison around horizontal single and tandem cylinders at different immersion elevations". Ocean Eng. 189, 106352. https://doi.org/https://doi.org/10.1016/j.oceaneng.2019.106352

Turner, A.A., Steinke, D.M., Nicoll, R.S., 2017. "Application of Wake Shielding Effects With a Finite Element Net Model in Determining Hydrodynamic Loading on Aquaculture Net Pens". https://doi.org/10.1115/OMAE2017-61330

Turner, A.A., Steinke, D.M., Nicoll, R.S., Stenmark, P., 2018. "Comparison of Taut and Catenary Mooring Systems for Finfish Aquaculture". https://doi.org/10.1115/OMAE2018-78261

Turner, R., 2000. "Offshore mariculture: Site evaluation". Mediterr. offshore Maric. 141–157.

Uzunoglu, E., Guedes Soares, C., 2019. "A system for the hydrodynamic design of tension leg platforms of floating wind turbines". Ocean Eng. 171, 78–92. https://doi.org/https://doi.org/10.1016/j.oceaneng.2018.10.052

Vercruijsse, P.M., Verichev, S., 2011. "Vertical Hydraulic Transport for Deep Sea Mining Applications", in: Proceedings of 40th Underwater Mining Institute Conference. pp. 14–18.

Vieira, D.P., de Mello, P.C., Dotta, R., Nishimoto, K., 2018. "Experimental investigation on the influence of the liquid inside the tanks in the wave behavior of FLNG vessels in side-by-side offloading operations". Appl. Ocean Res. 74, 28–39. https://doi.org/https://doi.org/10.1016/j.apor.2018.02.019

Vittori, F., Bouchotrouch, F., Lemmer, F., Azcona, J., 2018. "Hybrid Scaled Testing of a 5MW Floating Wind Turbine Using the SiL Method Compared With Numerical Models". https://doi.org/10.1115/OMAE2018-77853

Wang, A.-D., Bi, C.-W., Dong, G.-H., Guo, S.-A., 2020. "Numerical Study on the Dynamic Characteristics of a Fixed Horizontal Cylindrical Fish Cage under Earthquake Load ".

Wang, A.M., Chen, R., He, M., Zhu, X., Xu, J., van't Padje, W., 2019. "Virtual Reality Simulations for Dynamic Positioning Floatover Installation ".

Wang, C.M., Chu, Y.I., Park, J.C., 2019. "Moving offshore for fish farming". J Aquac Mar Biol 8, 38–39.

Wang, G., Liu, S., 2005. "Three-Dimensional DEM Model For Deep-Ocean Mining Pipe System ".

Wang, G., Liu, S., Li, L., 2007. "FEM modeling for 3D dynamic analysis of deep-ocean mining pipeline and its experimental verification". J. Cent. South Univ. Technol. 14, 808–813. https://doi.org/10.1007/s11771-007-0154-5

Wang, S., Wang, X., Woo, W.L., 2019. "Effects of the asymmetric riser and bilge keel arrangements on FPSO green water assessment". Appl. Ocean Res. 86, 166–176. https://doi.org/https://doi.org/10.1016/j.apor.2019.02.013

Wang, S., Wang, X., Woo, W.L., Seow, T.H., 2017. "Study on green water prediction for FPSOs by a practical numerical approach". Ocean Eng. 143, 88–96. https://doi.org/https://doi.org/10.1016/j.oceaneng.2017.07.052

Wang, X., Zhou, J.-F., 2020. "Numerical and experimental study on the scale effect of internal solitary wave loads on spar platforms". Int. J. Nav. Archit. Ocean Eng. 12, 569–577. https://doi.org/https://doi.org/10.1016/j.ijnaoe.2020.06.001

Wang, Z., Rao, Q., Liu, S., 2012. "Fluid-solid interaction of resistance loss of flexible hose in deep ocean mining". J. Cent. South Univ. 19, 3188–3193. https://doi.org/10.1007/s11771-012-1394-6

Wang, Z., Rao, Q., Liu, S., 2011. "Dynamic Analysis of Seabed-Mining Machine-Flexible Hose Coupling In Deep Sea Mining ".

Weiss, C.V.C., Castellanos, O., Ondiviela, B., Juanes, J.A., Guanche Garcia, R., 2018. "Development of a Tool to Identify Potential Zones for Offshore Aquaculture: A Global Case Study for Greater Amberjack". https://doi.org/10.1115/OMAE2018-77870

Wu, X., Ge, F., Hong, Y., 2012. "A review of recent studies on vortex-induced vibrations of long slender cylinders". J. Fluids Struct. 28, 292–308. https://doi.org/https://doi.org/10.1016/j.jfluidstructs.2011.11.010

Wu, X., Hu, Y., Li, Y., Yang, J., Duan, L., Wang, T., Adcock, T., Jiang, Z., Gao, Z., Lin, Z., Borthwick, A., Liao, S., 2019. "Foundations of offshore wind turbines: A review". Renew. Sustain. Energy Rev. 104, 379–393. https://doi.org/10.1016/j.rser.2019.01.012

Xu, N., Qin, L., Wang, Y., 2018. "Application of Dynamic Positioning Float-Over Technology to HZ25-8 DPP Topside Installation ".

Xu, S., Wang, X., Wang, L., Li, X., Yang, L., Li, B., 2017. "Investigation of the Positioning Performances for DP Vessels with Thruster Failure Modes by a Novel Synthesized Criterion ".

Xu, Z., Qin, H., 2020. "Fluid-structure interactions of cage based aquaculture: From structures to organisms". Ocean Eng. 217, 107961. https://doi.org/https://doi.org/10.1016/j.oceaneng.2020.107961

Yan, B., Luo, M., Bai, W., 2019. "An experimental and numerical study of plunging wave impact on a box-shape structure". Mar. Struct. 66, 272–287. https://doi.org/https://doi.org/10.1016/j.marstruc.2019.05.003

Yang, C.K., Kim, M., 2018. "Numerical assessment of the global performance of spar and FPSO connected by horizontal pipeline bundle". Ocean Eng. 159, 150–164. https://doi.org/https://doi.org/10.1016/j.oceaneng.2018.03.075

Yang, H., Xu, P., 2018. "Parametric Resonance Analyses for Spar Platform in Irregular Waves". China Ocean Eng. 32, 236–244. https://doi.org/10.1007/s13344-018-0025-x

Yang, L., Nestegård, A., Falkenberg, E., 2018. "Analysis of Semi-Submersible Under Combined High Waves and Current Conditions Compared With Model Tests". https://doi.org/10.1115/OMAE2018-78595

Yang, S.-H., Ringsberg, J.W., Johnson, E., 2018. "Parametric study of the dynamic motions and mechanical characteristics of power cables for wave energy converters". J. Mar. Sci. Technol. 23, 10–29. https://doi.org/10.1007/s00773-017-0451-0

Yang, S.-H., Ringsberg, J.W., Johnson, E., Hu, Z., 2017. "Biofouling on mooring lines and power cables used in wave energy converter systems—Analysis of fatigue life and energy performance". Appl. Ocean Res. 65, 166–177. https://doi.org/https://doi.org/10.1016/j.apor.2017.04.002

Yenduri, A., Magee, A.R., Liu, J., Xu, W., Choudhary, A., Hussain, A.A., 2019. "Realistic Adaptive DP Controller for Flotel Operating in Side-by-Side Configuration With FPSO". https://doi.org/10.1115/OMAE2019-96577

Yoon, C.-H., Lee, D.-K., Park, Y.-C., Kim, Y.-J., Kwon, S., 2006. "Flow Analysis of Lifting Pump And Flexible Hose For Sea-Test ".

Yoon, C.-H., Park, Y.-C., Park, J., Kim, Y.-J., Kang, J.-S., Kwon, S.-K., 2009. "Solid-Liquid Flow Experiment With Real And Artificial Manganese Nodules In Flexible Hoses". Int. J. Offshore Polar Eng. 19.

Yoon, C.H., Kwon, K.S., Kwon, S.K., Lee, D.K., Park, Y.C., Kwon, O.K., Sung, W.M., 2001. "An Experimental Study On the Flow Characteristics of Solid-liquid Two-phase Mixture In a Flexible Hose ".

Yoon, C.H., Lee, D.K., Kwon, K.S., Kwon, S.K., Kim, I.K., Park, Y.C., Kwon, O.K., 2002. "Experimental and Numerical Analysis on the Flow Characteristics of Solid-Liquid Two-Phase Mixtures in a Curvature Pipe", in: The Twelfth International Offshore and Polar Engineering Conference. International Society of Offshore and Polar Engineers.

Yoon, C.H., Park, J.-M., Kang, J.S., Kim, Y., Park, Y.C., Park, S.G., Kim, C., Kang, S.S., Kim, S.B., Kim, W.T., Kwon, S.K., Ahn, B.S., Ha, M.-K., 2011. "Shallow Lifting Test For the Development of Deep Ocean Mineral Resources In Korea ".

Yu, A., Cheng, Y., Eason, R., 2010. "Slurry Flow Simulation for Deepwater Mining Application", in: ASME 2010 29th International Conference on Ocean, Offshore and Arctic Engineering.

Yu, J., Hao, S., Yu, Y., Chen, B., Cheng, S., Wu, J., 2019. "Mooring analysis for a whole TLP with TTRs under tendon one-time failure and progressive failure". Ocean Eng. 182, 360–385. https://doi.org/https://doi.org/10.1016/j.oceaneng.2019.04.049

Yu, S., Yoshida, T., Han, J., Mizukami, Y.,

Kitazawa, D., Liu, L., 2018. "Model Experiment of a Controllable Depth Cage and its Mooring System". https://doi.org/10.1115/OMAE2018-77757

Yu, T., Zhang, Y., Zhang, S., Shi, Z., Chen, X., Xu, Y., Tang, Y., 2019. "Experimental study on scour around a composite bucket foundation due to waves and current". Ocean Eng. 189, 106302. https://doi.org/10.1016/j.oceaneng.2019.106302

Yu, Y., Feng, G., Ren, H., 2017. "Ultimate Strength Assessment of Semi-Submersible Platform Under Different Load Conditions". https://doi.org/10.1115/OMAE2017-61696

Zamora-Rodriguez, R., Gomez-Alonso, P., Amate-Lopez, J., De-Diego-Martin, V., Dinoi, P., Simos, A.N., Souto-Iglesias, A., 2014. "Model Scale Analysis of a TLP Floating Offshore Wind Turbine". https://doi.org/10.1115/OMAE2014-24089

Zanganeh, R., Thiagarajan, K., 2018. "Prediction of the mean heading of a turret moored FPSO in bi-modal and bi-directional sea states". Appl. Ocean Res. 78, 156–166. https://doi.org/https://doi.org/10.1016/j.apor.2018.04.006

Zangeneh, R., Thiagarajan, K.P., Cameron, M., 2017. "Effect of Wind Loads and Damping on Heading Stability of FPSOs". https://doi.org/10.1115/OMAE2017-62134

Zhang, Q., Ma, P., Liu, J., Kumar Jaiman, R., 2017. "Numerical Simulation of Single Thruster in Open Water". https://doi.org/10.1115/OMAE2017-61635

Zhang, X., Song, X., Qiu, W., Yuan, Z., You, Y., Deng, N., 2018. "Multi-objective optimization of Tension Leg Platform using evolutionary algorithm based on surrogate model". Ocean Eng. 148, 612–631. https://doi.org/https://doi.org/10.1016/j.oceaneng.2017.11.038

Zhao, D., Hu, Z., Chen, G., 2017. "Experimental investigation on dynamic responses of FLNG connection system during side-by-side offloading operation". Ocean Eng. 136, 283–293. https://doi.org/https://doi.org/10.1016/j.oceaneng.2017.03.034

Zhao, D., Hu, Z., Chen, G., Chen, X., Feng, X., 2018. "Coupling analysis between vessel motion and internal nonlinear sloshing for FLNG applications". J. Fluids Struct. 76, 431–453. https://doi.org/https://doi.org/10.1016/j.jfluidstructs.2017.10.008

Zhao, L., Tan, Z., Hou, Y., Yin, Y., Meng, W., 2018. "Experimental Research on Vortex-Induced Vibration of Flexible Catenary Riser Model". https://doi.org/10.1115/OMAE2018-78363

Zhao, L., Xu, S., Wang, X., Ding, A., 2020. "A Novel Saturation Protocol on the Thrust Allocation Strategy for Dynamic Positioning of Marine Vessels Operating in Extreme Wave Conditions ".

Zhao, W., Wan, D., 2018. "CFD Parametric Study of Geometrical Variations on the Vortex-Induced Motions of Deep-Draft Semi-Submersibles". https://doi.org/10.1115/OMAE2018-78377

Zhao, Y., Guan, C., Bi, C., Liu, H., Cui, Y., 2019.

"Experimental Investigations on Hydrodynamic Responses of a Semi-Submersible Offshore Fish Farm in

Waves". J. Mar. Sci. Eng. 7, 238. https://doi.org/10.3390/jmse7070238

Zhao, Z., Wang, W., Han, D., Shi, W., Si, Y., Li, X., 2020. "Structural Control of an Ultra-Large Semi-Submersible Floating Offshore Wind Turbine". J. Offshore Mech. Arct. Eng. 143. https://doi.org/10.1115/1.4048880

Zheng, H., Zheng, X.Y., Lei, Y., 2020. "A Novel Floating Wind-Solar-Aquaculture Concept: Fully Coupled Analysis and Technical Feasibility Study ".

Zhou, X., Mizukami, Y., Yoshida, T., Kitazawa, D., 2018. "Motion Analysis of Flexible Hose Based on Water Tank Experiment". https://doi.org/10.1115/OMAE2018-77597

Zhu, S., 2018. "Optimization of Heave Motions for a Four Column Semi-Submersible Based on Genetic Algorithm". https://doi.org/10.1115/OMAE2018-77289

Zhu, S., Rentsch, H.C., Lefranc, M., Haaheim, H., 2018. "Investigation of Fatigue Damage for Stiffened Plates in Splash Zone for a Semi-Submersible". https://doi.org/10.1115/OMAE2018-77294

The Seakeeping Committee
Final Report and Recommendations to the 29th ITTC

1. GENERAL

1.1 Membership and meetings

The Committee appointed by the 29th ITTC consisted of the following members:

- Pepijn de Jong (Chairman), Maritime Research Institute Netherlands (MARIN), Wageningen, The Netherlands;
- Christopher Kent (Secretary), Naval Surface Ship Warfare Centre Carderock Division (NSSWC-CD), West Bethesda, USA;
- Benjamin Bouscasse, École Centrale de Nantes (ECN), Nantes, France;
- Frederick Gerhardt, SSPA, Göteborg, Sweden;
- Ole Andreas Hermundstad, SINTEF Ocean, Trondheim, Norway;
- Toru Katayama, Osaka Prefecture University, Osaka, Japan;
- Munehiko Minoura, Osaka University, Osaka, Japan;
- Bo-Woo Nam, Seoul National University, Korea;
- Yin Lu (Julie) Young, University of Michigan, USA.

Three committee meetings were held at:

- Osaka University, Osaka, Japan, December 2018
- Maritime Research Institute Netherlands (MARIN), Wageningen, Netherlands, January 2019
- University of Michigan, Ann Arbor, USA, June 2019

Following the onset of the COVID-19 Pandemic no further in-person meetings were held. A series of regular video teleconferences were held to continue the work of the committee. These covered the time period of February 2020 to June 2021. The video conferences were found to be an effective way of replacing the face-to-face meetings, and by keeping a regular pace, helped the committee to continue its work.

1.2 Terms of Reference given by the 27th ITTC

The Seakeeping Committee is primarily concerned with the behaviour of ships underway in waves. The Ocean Engineering Committee covers moored and dynamically positioned ships. For the 29th ITTC, the modelling and simulation of waves, wind and current is the primary responsibility of the Specialist Committee on Modelling of Environmental Conditions, with the cooperation of the Ocean Engineering, the Seakeeping and the Stability in Waves Committees.

1. Update the state-of-the-art for predicting the behaviour of ships in waves, emphasizing developments since the 2017 ITTC Conference. The committee report should include sections on:
    1. the potential impact of new technological developments on the ITTC;
    2. new experiment techniques and extrapolation methods;
    3. new benchmark data;
    4. the practical applications of numerical simulation to seakeeping predictions and correlation to full scale;
    5. the need for R&D for improving methods of model experiments, numerical modelling and full-scale measurements.

2. Review ITTC Recommended Procedures relevant to seakeeping, including CFD procedures, and:
    1. identify any requirements for changes in the light of current practice, and, if approved by the Advisory Council, update them;
    2. identify the need for new procedures and outline the purpose and contents of these.

3. Update ITTC Recommended Procedure 7.5-02-07-02.5, Verification and Validation of Linear and Weakly Non-linear Seakeeping Computer Codes to include the verification and validation of ship hydroelasticity codes in response to any comments from the ISSC Loads and Response Committee.

4. Update 7.5-02-07-02.1 Seakeeping Experiments. The procedure should be extended to include the measurement of added resistance in waves with emphasis placed on the uncertainty in the measurement. Review procedures 7.5-02-07-02.2 and the new procedure on the calculation of the weather factor fw in the EEDI formula to ensure that they are consistent with the proposed update.

5. Update Recommended Procedure 7.5-02-07-02.8 “Calculation of the weather factor fw for decrease of ship speed in waves” to bring it in line with the terminology in the EEDI guidelines and submit to MEPC 72 (Spring, 2018). The submission should state that the procedure is applicable mainly for large ships and that additional work is required for smaller ships, and state the limit between large and smaller ships.

6. Expand Recommended Procedure 7.5-02-07-02.8 “Calculation of the weather factor fw for decrease of ship speed in waves” to include the uncertainty associated with each method.

7. Update 7.5-02-07-02.2 Prediction of Power Increase in Irregular Waves from Model Tests should be modified to make it more comprehensible for the wider community outside of the ITTC.

8. Update ITTC Recommended Procedure 7.5-02-07-02.3 Experiments on Rarely Occurring Events to include the measurement and analysis of impulsive loads, peaks in pressures and maximum accelerations.

9. Liaise with SIW Committee on the updates to the guideline 7.5-02-07-04.3 for the prediction of the occurrence and magnitude of parametric rolling.

10. Develop a procedure for undertaking inclining tests at full scale include estimates of the measurement uncertainty. Liaise with the Stability in Waves Committee, as required.

11. Develop a procedure for conditioning a model for seakeeping tests, e.g. CG position, GM, moments of inertia. Include in the procedure estimates for measurement uncertainty.

12. Survey and/or collect benchmark data for ship structural hydroelasticity in waves and for added resistance in waves tests.

13. Continue the collaboration with ISSC committees, including Loads and Responses and Environment Committees.

14. Undertake a complete review of the procedures related high speed marine vehicles (HSMV) and update according to recent advances in testing techniques, in particular,
    1. Update the seakeeping related HSMV procedures:
        - 7.5-02-05-04 Seakeeping tests;
        - 7.5-02-05-06 Structural loads;
        - 7.5-02-05-07 Dynamic instability.
    2. Develop a new procedure for motion control of HSMV during seakeeping tests.
    3. Use as a basis the reports of the various committees to undertake a review the state-of–the-art in seakeeping of HSMV.

2. STATE OF ART REVIEW

2.1 New Experimental Facilities

A worldwide survey identified a handful of new experimental seakeeping facilities that have been built or commissioned during the last three years.

2.1.1 Flanders Maritime Laboratory

In May 2019 Flanders Maritime Laboratory (FML) was officially opened in Ostend/Belgium. The laboratory is operated by Flanders Hydraulics Research, Ghent University, and KU Leuven University. It consists of two facilities, a Coastal & Ocean Basin (COB, Figure 278) and a Towing Tank for Manoeuvres in Shallow Water. It is planned that both become fully operational during 2020-2021. The COB is a midsize wave basin (30 x 30 m²) with a maximal water depth of 1.4 m (adjustable between 0.4 and 1.4 m), and a deeper (4.0 m), central pit. Its principal aim is to study the influence of waves, winds and currents on coastal defences and blue energy applications. The towing tank will mainly focus on ship behaviour in shallow water, see Delefortrie et al. (2019).

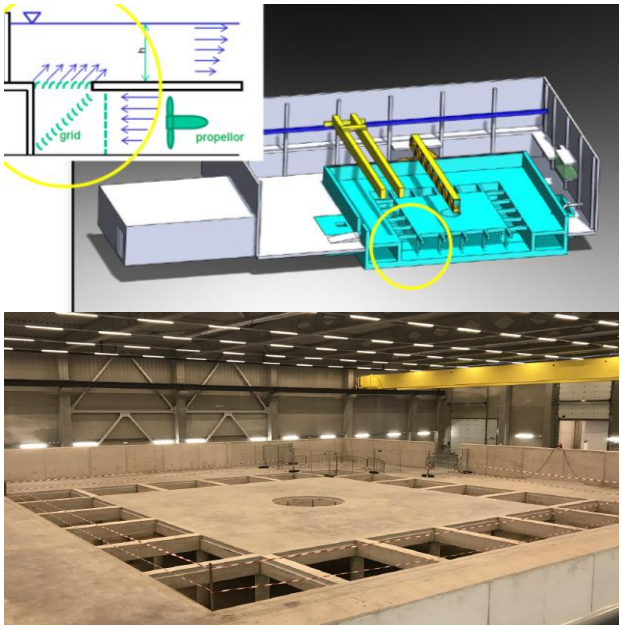

Figure 278: Coastal & Ocean Basin in Ostend. http://cob.ugent.be

2.1.2 Deep Ocean Engineering Basin at KRISO

The world biggest deep-water offshore basin was built at the Korea Research Institute of Ships and Ocean Engineering (KRISO), Sung et al. (2016). It has a floor area of 100 m x 50 m with a water depth of 15 m (50 m in the 12 m diameter pit), as shown in Figure 279. The basin was successfully commissioned during 2020 and is now operational. It has generation systems for wind, waves, and currents.

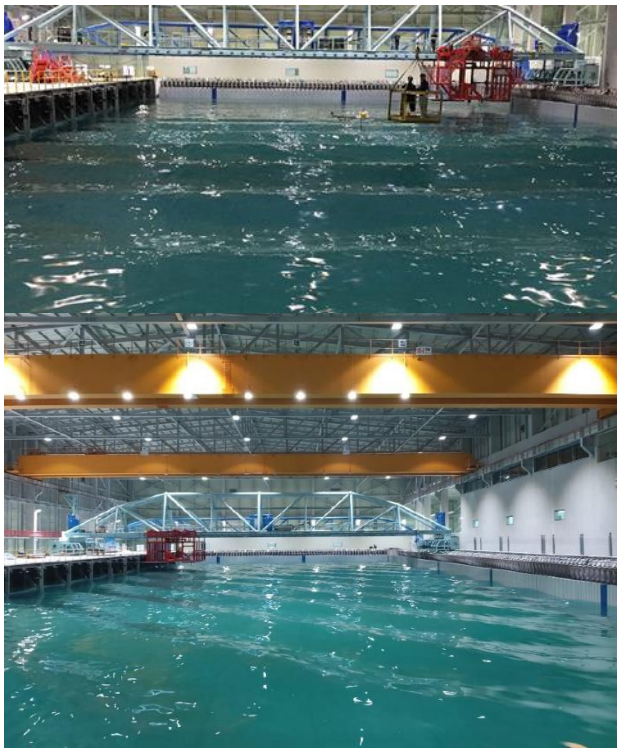

Figure 279: KRISO Deep Ocean Engineering Basin (DOEB). kriso.re.kr

2.1.3 Technology Centre for Offshore and Marine Singapore (TCOMS)

Another large deep-water basin with a 50 m deep centre pit is under construction in Singapore. The facility is slated to be operational by 2021.

2.1.4 University of Southampton Towing Tank

The recently constructed 138 m x 6 m towing tank at the University of Southampton's Boldrewood Innovation Campus is equipped with a 12-element wavemaker on one end. Straight and oblique waves of up to 0.7 m height can be produced. Malas et al. (2019) report on early sports engineering investigations in the facility (Figure 280). The tank (including carriage) became fully operational in late 2020, see Malas (2020) for more details.

Figure 280: Sports engineering in the Boldrewood tank. www.southampton.ac.uk/engineering/research/facilities/towing-tank-news

2.2 Experimental Techniques

2.2.1 Measurement of added resistance

The accurate measurement of "added resistance in waves" continues to be a hot topic. Added resistance is obtained by measuring the small difference between two large quantities (calm water resistance and mean resistance in waves) consequently demands on the quality of the experiments are high.

Park et al. (2019) show that the uncertainty of added resistance measurements is particularly high in short waves.

Kjellberg and Gerhardt (2019) discuss an improved evaluation method for free-sailing

model tests. The method is quasi-steady in nature and can take the small unwanted model accelerations into account that almost always occur during "real life" testing. They also explore the idea of towing a model in waves using a modified "soft-mooring" setup that consists of long lines and soft springs. Compared to the "free-sailing" technique such an approach reduces the number of tests that need to be re-run because the target speed was not achieved.

2.2.2 Instrumentation and measurement technology

Tukker et al. (2019) discuss the measurement quality of electrical resistance-type wave gauges. They point out, that especially thin wire gauges can show a non-linear behaviour. The common assumption of linearity will therefore result in systematic measurement errors. The authors present a way of quantifying the resulting errors and show that the size of the non-linear errors can easily be reduced by about 40% if stainless steel wires are replaced with titanium wires.

Zeraatgar et al. (2019) analysed the effect of sampling rate on slamming pressure measurements. A range of prismatic wedges with deadrise angles of 5°–35° were dropped into a small tank and impact pressures recorded at different sampling rates. Based on the results minimum sampling rates are recommended. For wedges with deadrise angles of 25° and higher, a sampling rate of 25 kHz is sufficient while, for deadrise angles smaller than 20°, higher sampling rates are required. For very small deadrise angles of 5° an acceptable sampling rate is 600 kHz at a water entry velocity of 3.13 m/s.

Mutsuda et al. (2019) used a combination of particle image velocimetry (PIV), high speed video cameras and pressure measurements to investigate the characteristics of stern slamming. Water entry tests with a prismatic wedge model and a 3D ship stern model were performed to examine nonlinear interactions between a body and the free surface with splashing and droplets. Especially the PIV results provide an interesting insight into the detailed flow field some distance away from the body. Tests with a complete ship model in following seas where also performed.

Fukushima et al. (2019) used "optical strain gauges" of the "Fiber Bragg Grating" (FBG) type to simultaneously measure the pressure at 146 points on the hull surface of the KVLCC2 tanker.

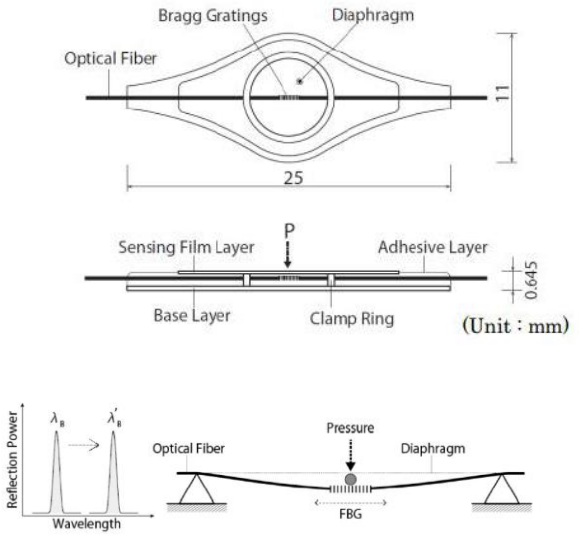

Figure 281: Schematic of the FBG sensors used by Fukushima et al. (2019)

Several of the 0.6mm thick glue-on sensors (Figure 281) were connected in series and arranged along different water lines (Figure 282). Measured pressures from the FBG-sensors compare well to more traditional tube-sensor arrangements and LES-CFD simulations. The advantages of the new sensors are a) low cost and b) short installation time (compared to traditional pressure tabs and tubes). The authors point out that the thickness of the sensor is sufficiently thinner than the boundary layer thickness over the hull. However, the thickness of the viscous sublayer is about the same as the sensor thickness. Results and a comparison to

the pressure-tap and LES results however indicate that this does not seem to affect the measurements. So far the system seems to have been used to study ship behaviour in calm water only. However, using the sensors to measure pressures during seakeeping tests appears to be a possibility.

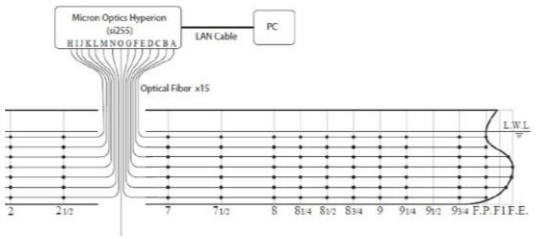

Figure 282: Arrangement of FBG sensors on KVLCC2 hull from Fukushima et al. (2019)

The use of cameras and optical systems to record ship motion in waves continues to increase across the industry, see e.g. Malas et al. (2019) or Mathew et al. (2018).

Mathew et al. (2018) describe an investigation into Replenishment at Sea (RAS) operations. They experimentally studied the influence of lateral and longitudinal separation on the wave induced motions of two vessels operating in close proximity to each other. While the actual testing technique is similar to single ship testing the simultaneous measurement of the motions of two models adds an additional level of complexity. Results show, that there can be significant interaction between the two vessels and that even in head seas substantial rolling can occur.

Silva et al. (2017) used a large number of wave probes and load cells to study green water impact on a Floating Production Storage and Offloading unit (FPSO). Considering the large number of monitored green water events, identification of critical regions near the deck edge and the water on deck propagation are characterized, including the influence of a riser balcony along the side hull.

Tsukada et al. (2017) describe the development of a “Wind Load Simulator” for free-sailing seakeeping model tests. The device consists of three pairs of ducted fans that are mounted on the ship model, one pair parallel to the centreline, the other two athwartships. The fan units are mounted on load cells and can be individually controlled to simulate the effect of wind on the above water part of a ship. During a seakeeping test ship motions due to waves are recorded and used in combination with wind-load coefficients to predict longitudinal and lateral wind forces and yawing moment in real time. The fans are then controlled to produce these target forces and moments. Feedback control from the load cells under the fans ensures that the target values are achieved.

2.2.3 Hydroelastic ship models

Studying the effects of hydroelasticity on global loads and fatigue of ships continues to be of interest to researchers. At the 8th International Conference on Hydroelasticity in Marine Technology (2018), a number of papers specifically addressed experimental techniques and focused on the design and construction of for hydroelastic models for seakeeping tests.

Houtani et al. (2018) describe the construction of a flexible container ship model where the vertical bending and torsional vibration modes of the full-scale ship are replicated. To achieve similarity in torsion the height of the shear centre of the model needs to be located below the keel. This is because the real ship has large deck openings. The resulting ship model is of similar construction and manufactured from urethane foam, without backbone and non-segmented, Figure 283.

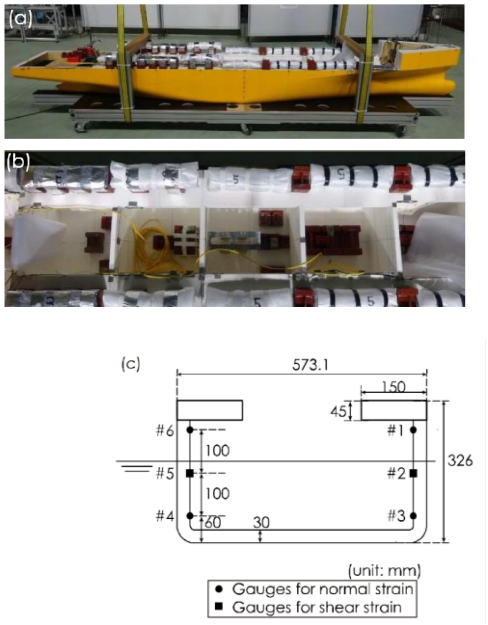

Figure 283: Continuous i.e. non-segmented hydro elastic container ship model designed by Houtani et al. (2018).

Grammatikopoulos et al. (2018) report on the design and manufacture of a barge-like hydroelastic model using 3D-printing techniques. The model design was inspired by the S175 container ship combined with the cross-sectional geometry of a realistic container ship. In contrast to most other ship models the inner details of the full-scale construction were also replicated. The study focused on structural and manufacturing issues and was aimed at demonstrating the possibilities and challenges of "additive manufacturing" when building hydroelastic models.

2.2.4 Seakeeping testing of wind assisted ships

The development of experimental techniques to study the seakeeping and manoeuvring behaviour of wind propelled/assisted ships is of significant current interest. Several alternative methods are currently investigated. These include:

a) Construction of a simple "wind tunnel" under the carriage of a seakeeping basin and equipping the model with scaled-down sails, Eggers and Kisjes (2019);
b) Simulation of sail forces by towing via a rope attached to a short mast (see Gauvain 2019 for examples);
c) A "hybrid approach" where the sail forces are simulated by rpm and azimuth-controlled fans/airscrews. See Gauvain (2019) and Gerhardt and Santén (2021).

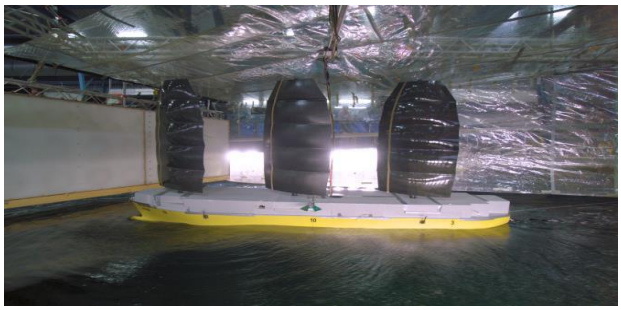

Figure 284: "Wind tunnel" in MARIN's seakeeping basin, from Eggers and Kisjes (2019)

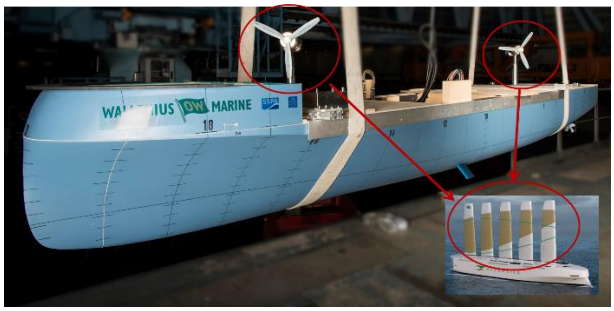

Figure 285: Simulation of sail forces via rpm azimuth-controlled fans, from Gerhardt and Santén (2021)

Due to this increased interest, there seems a clear need, and therefore an opportunity for ITTC, to develop guidance for performing model tests for wind assisted vessels.

2.3 Numerical Methods

2.3.1 General

This section gives an overview of recent developments within potential theory methods for ship motions predictions. The related topic of added resistance assessment is covered in Section 2.7. Moreover, developments within combined seakeeping and manoeuvring are covered by the Specialist Committee on Manoeuvring in Waves, while papers on stability in waves are dealt with by the Stability in Waves Committee.

2.3.2 2D and 3D methods

Despite the massive developments within methods solving the Navier-Stokes equations, the CFD methods are still not practical for routine seakeeping calculations. Hence, potential theory methods, with simplified models to account for viscous forces in e.g. roll motions, are the workhorses when it comes to ship seakeeping assessment. Even classical linear 2D strip theory methods are still widely used in practical applications. They are easy to use, robust and computationally very efficient; and for conventional seakeeping analyses they have shown to give sufficiently accurate results in most cases.

For higher forward speeds, non-slender structures, or for cases where the flow field and pressure distribution near the ship ends is of concern, 3D potential theory methods are used. Linear 3D methods for stationary floating structures are standard tools today. For ships at low and moderate speeds, "speed-correction" methods, where the forward speed is treated in the same manner as in classical strip theory, are efficient methods. More computationally demanding are the methods where the effect of forward speed is included in a more consistent manner, and the methods where nonlinearities are handled. Most of the recent developments in potential theory methods focus on 3D methods.

2.3.3 Boundary methods and field methods

The boundary methods, which require discretization of the domain boundaries only, are by far the most common in seakeeping analyses based on potential theory. When discretization of the whole computational field is avoided, the number of unknowns will normally be significantly reduced.

As an alternative to the popular boundary methods, some interesting developments with field methods using a high-order finite difference technique have been presented by Amini-Afshar and Bingham (2017, 2018) and Amini-Afshar et al. (2019). They are motivated by the fact that the finite difference method leads to a very sparse system of equations, as opposed to the boundary methods, which produce dense matrices. This allows for an optimum scaling of the computational effort with increasing resolution. This, combined with the high-order accuracy of the discrete operators, makes the approach competitive with boundary methods, especially for nonlinear problems. The method can be well suited for calculation of the second-order wave drift forces from the computed first-order results. The forward speed radiation problem is dealt with in Amini-Afshar and Bingham (2017), while Amini-Afshar and Bingham (2018) focus on the forward speed diffraction problem. A stability analysis of the solution scheme and application to the steady wave resistance problem is presented in Amini-Afshar et al. (2019). Comparison with results from experiments and other numerical methods show good agreement for spheres and ship-like structures.

2.3.4 Boundary element methods

The main advantage with the Green function method (GFM) is that the source function satisfies the free surface boundary conditions, and only the wet surface of the floating body needs to be discretized. One problem with the GFM is the presence of cavity resonance, or irregular frequencies, that correspond to eigenfrequencies of a fictitious inner problem,

and cause the solution of the outer problem to break down at these frequencies. For the zero-speed problem there are efficient ways of removing the irregular frequencies, e.g. by the lid method, while this is much more challenging with the forward speed Green function. Moreover, the forward speed Green function (translating-pulsating source) is substantially more complex to evaluate than the zero speed Green function, and it displays a highly oscillatory behaviour for field points near the free surface.

Assuming that the encounter frequency is high and the speed moderate, the forward speed only occurs in the body boundary condition, and the solution can be separated into a zero-speed solution and a correction due to forward speed; just like in the classical strip theory. With this approach, the robust and efficient zero-speed Green function can be used.

Due to the complexity of the forward speed Green function, the Rankine Panel Method (RPM) has become more popular for the forward speed seakeeping problem. The RPM, using the simple Rankine source, is generally easier to implement and more robust. It avoids the problem with irregular frequencies, and implementation of nonlinear free surface boundary conditions is easier. Disadvantages are that the free surface must be discretized, and special care must be taken to ensure that waves are not reflected at the outer boundary of the surface mesh. The discretized surface may need to be large and with high resolution, due to the different wavelengths involved in the wave systems generated by the ship. A time domain RPM is presented by Chen et al. (2018a) and applied to four different ship types. Yao et al. (2017) present a frequency-domain RPM for finite water depth. The method is used to study the influence of water depth on the hydrodynamic characteristics of two ship types at forward speed in water depths down to about twice the ship's draft.

As a logical consequence of the drawbacks and merits of the GFM and RPM, the hybrid, or multi-domain methods have evolved. In these methods the RPM is used in an inner domain, including the ship and a limited surface area surrounding it, while the GFM is used in the outer domain. The solutions for the two domains are matched at their common boundary.

A 3D multi-domain BEM is presented by Chen et al. (2018b). The boundary value problem is solved directly in time-domain with a RPM in the inner domain and a transient GFM in the outer domain, as shown in Figure 286.

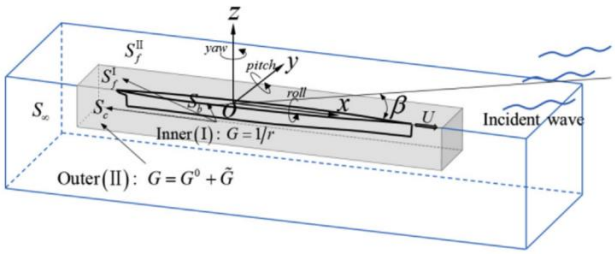

Figure 286: Principle sketch of the multi-domain BEM method (Chen et al. 2018b).

A new 3D multi-domain method for the linear and second order mean wave drift loads on floating bodies was presented by Liang and Chen (2017). The control surface, separating the inner and outer domains, is mesh-free and the quantities on it are expressed analytically. The method has been generalized to the ship motion problem with forward speed by Chen et al. (2018c). Frequency and time-domain formulations are presented, and comparisons are made with results from experiments and from the Hydrostar code.

Nwogu and Beck (2017) extend the FFT-accelerated method of Nwogu and Beck (2010) to simulate the 6 DOF motions of vessels moving in multidirectional waves. This is a variant of the mixed spectral-panel method, in which the kernels of the free surface boundary integrals are expanded in a wave steepness parameter and evaluated with FFT. A velocity-based boundary integral method is used to solve

the Laplace equation at every time-step for the fluid kinematics. Comparisons with semi-analytical results for a floating oscillating hemisphere show good agreement. Good agreement with experimental results is also demonstrated for a self-propelled ship in oblique waves.

2.3.5 Acceleration techniques and higher order methods

Several techniques have been applied to speed up the computations required to solve the dense matrix of equations that results from the boundary element methods. Two examples are the sparsification techniques based on the multipole expansion method and the pre-corrected FFT method. Desingularization is another popular acceleration technique. The sources are then distributed slightly above the calm water surface rather than on the surface itself. The source distribution over each panel can then be replaced by an isolated source, which greatly reduces the computational complexity of the influence matrix. The technique is recently used by e.g. Yao et al. (2017) in their RPM for finite water-depth.

The FFT-accelerated boundary integral method of Nwogu and Beck (2017) reduces the cost of evaluating the free-surface convolution integrals from $O(N^2)$ to O(NlogN), where N is the number of grid points on the free surface. They report that the method is an order of magnitude faster than non-accelerated boundary integral methods.

Shan et al. (2019) present algorithms for more efficient evaluation of the zero-speed Green function (pulsating source) in the frequency-domain. Both infinite and finite depth are studied. Parallelization of the serial code with the OpenMP library is also discussed.

Zangle et al. (2020) present three new techniques to improve boundary element methods. Triangular B-splines are introduced as an alternative to four-sided NURBS, which cause problems when modelling three-sided surfaces at e.g. bulbous bows and waterline cuts (Figure 287). They also present a mixed-order BEM, which allows body patches to be represented as meshes of low-order bilinear panels, while the free surface is represented as high-order NURBS. This simplifies the calculation of influence coefficients over the body patches and increases the efficiency of the method. Finally, a near field influence approximation with flat panel influence calculations is introduced to reduce the number of recursive calculations of the high-order near-field influence coefficients.

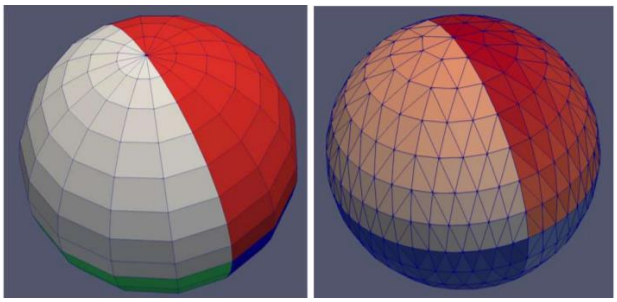

Figure 287: Quadrilateral NURBS (left). The degeneracy at the pole is removed when using triangular B-splines (right) (Zangle et al. 2020).

2.3.6 Forward speed effects

It is well known that the forward speed, *U*, and the steady flow field around the hull influences the seakeeping behaviour of a ship, and this must be accounted for in seakeeping prediction methods. One may distinguish three levels of refinement in representing the steady flow field:

- The Neumann-Kelvin approximation, where the steady flow is approximated by a uniform flow with velocity *U*;
- The double-body approximation, where the steady flow is approximated by that obtained by using a mirror condition on the calm water surface;
- The complete method, where the “exact” steady flow and wave elevation is used.

For ships at moderate speeds, the Neumann-Kelvin approximation is commonly used. With this simple approach one avoids the calculation of spatial derivatives of the steady potential. The double-body approximation is also only accurate for low speeds.

A recent study on the effect of the different flow representations was presented by Chen et al. (2018a). A time-domain RPM with higher order panels is used, so that second derivatives of the velocity potential and m_j-terms can be evaluated directly. They compared hydro-dynamic coefficients and motions obtained with the three formulations and with model tests for four different ship types: Series 60, Wigley-1, S-175 and a full-form tanker at various speeds. The conclusion was that the Neumann-Kelvin approximation gives less accurate results compared to the two more refined methods, and that for ships with complex and full-form hulls, the complete method gives the most accurate motion predictions.

Yao et al. (2017) use a frequency-domain RPM to compare excitation forces and heave and pitch motions, obtained with the Neumann-Kelvin and the double-body approximations, of two modern hull forms at Froude numbers between 0.13 and 0.27. Results were compared with model tests. For these cases, the double-body approximation did not show any significant improvement over the simpler Neuman-Kelvin approximation.

2.3.7 Nonlinear Froude-Krylov and hydro-static forces

In evaluation of seakeeping performance and hull girder load effects, nonlinear Froude-Krylov and hydrostatic forces are usually the first non-viscous nonlinearities to be considered. In the so-called weakly nonlinear (or body-nonlinear) methods, this is done by considering the instantaneous position of the ship hull relative to the incident (undisturbed) wave surface. Simulations are performed in time-domain, and a common approach is to obtain linear motion time-series by inverse Fourier transform of frequency-domain results. Then the nonlinear modifications of the Froude-Krylov and hydrostatic forces can be calculated, either by section-wise 2D calculations or by using a 3D mesh on the hull.

Rodrigues and Guedes Soares (2017) use the above approach to consider motions of the US Navy Destroyer Hull DTMB-5415 at zero speed. They use a newly developed adaptive panel mesh on the hull surface, where the Froude-Krylov forces are calculated analytically. Chen et al. (2018a) use B-spline interpolation to obtain a mesh on the instantaneous hull. Weems et al. (2018) express the Froude-Krylov and hydro-static forces in terms of the instantaneous submerged volume of each ship section, by assuming that the waves are longer than 2-3 times the section beam. The forces are then found in a section-wise manner without having to evaluate the pressure under the incident wave for a large number of wave components.

Sugimoto et al. (2019) apply an existing 3D body-nonlinear method and compare motions and hull girder loads with experimental results for a ship with pronounced bow flare. The results confirm that nonlinear Froude-Krylov and hydrostatic forces contribute significantly to the hull girder load effects, while their influence on heave and pitch motions is relatively small.

Another 3D body-nonlinear method is used by Park et al. (2017) and compared with experimental results for a tumblehome vessel, where the width of each section decreases from the waterline and up. Comparisons are also made with existing experimental results for the S175 containership. Whereas the heave and pitch RAO's for the conventional S175 ship decrease with increasing wave steepness, the opposite was the case for the tumblehome hull. The body-nonlinear method captured these trends with quite good accuracy.

Pollalis et al. (2018) applied a 3D body-nonlinear method to study heave and pitch of the KVLCC2 tanker. No significant influence of the nonlinearities was observed for the investigated cases.

Two levels of nonlinear methods were used by Van Walree et al. (2020) to study the motions of an appended version of the DTMB-5415 destroyer hull at high forward speed in extreme stern quartering seas. Comparisons were made with results from free-running model tests and CFD simulations. The first method is body-nonlinear. The second is body-exact, meaning that also the radiation and diffraction forces are found for the instantaneous position of the hull beneath the incident wave surface. Maneuvering, resistance and propulsion forces are included in the simulations. Viscous forces are added for roll damping and cross flow drag. Both methods gave fairly good predictions for heave, roll and pitch motions as well as forward speed variations. Sway velocity, yaw motions and deck edge immersion heights were more difficult to predict accurately with these methods. For a validation case involving large resonant roll motions, the simpler body-nonlinear method performed slightly better than the more time-consuming body-exact method. For another case the situation was the opposite. The CFD (URANS) results compared very well with the experiments, but the required computational efforts prohibit simulation of long time-series.

Rajendran et al. (2016) also present results from a body-nonlinear and body-exact method. Their simulations are based on precalculated 2D hydrodynamic coefficients. In the body-exact method, interpolation between coefficients for different drafts is used. Results were compared with experimental data for heave, pitch, relative motions and the vertical bending moment of a container ship at forward speed in extreme head seas. The agreement was generally good, and it was found that the body-exact method gave significantly better predictions for the peak sagging bending moment. These peaks were largely overpredicted by the simpler body-nonlinear method.

Gkikas and van Walree (2017) apply a body-nonlinear/body-exact time-domain forward-speed GFM to simulate drifting of a cruise ship in large waves. The second order forces are evaluated in the mean wetted body surface, while the Froude-Krylov and hydrostatic forces are evaluated on the exact wetted surface. In conventional seakeeping analyses, the forward speed is input to the BEM, but in this case it is a priori unknown. The problem is solved iteratively, by estimating the initial drifting velocity. Results were compared with model tests. Cross flow drag forces and a constant wind force were also included in the simulations. Since the drifting speed was dominated by the constant wind force, which was the same in model tests and simulations, it seems difficult to conclude on the method's ability to predict drift forces and speeds.

In the recent years there seems to have been less focus on the high-fidelity potential theory codes, where “fully” nonlinear formulations are pursued. The developments within RANSE-solvers may be one possible reason for this trend. Instead, activities within potential theory seakeeping seem to have shifted towards combined seakeeping and maneuvering codes. There has also been an increased interest in assessment of added resistance.

2.4 Rarely Occurring Events

Rarely occurring events for ships can usually be categorised into three aspects: (1) slamming, with the hull (bow, bottom or stern) of the vessel impacting onto the wave surface, (2) green water events, where a mass of water flows onto the deck, possibly impacting on the superstructure or cargo and (3) emergence events of propellers or other equipment, sometimes associated with ventilation. Other rarely occurring events, related to dynamic

stability are the topic of the Stability in Waves Committee and not included here.

2.4.1 Water entry

Water impact problems of wedge type shapes are often considered as a basic model for bow and stern slamming or flat plates for bottom slamming or green water impact problems. Studies can be experimental, looking into two- or three-dimensional impacts at model scale, or numerical, with methods ranging from semi-empirical and analytical, incompressible (potential flow and Euler methods) to fully compressible and two-phase CFD approaches.

2.4.1.1 Experimental.

Guo et al. (2017) performed wedge drop tests and compared the results against CFD simulations and the simplified analytic Wagner solution. They discussed the design of the drop test device (Figure 288), the measurement of the impact loads, the test procedure and data analysis. They highlighted that measuring space averaged forces during impact may be more relevant from a structural perspective than measuring local pressures, while local pressures can be very sensitive to randomness due to entrapped air. They designed a force panel to measure the impact force and used a Frequency Response Function to overcome the effect of the load cell's own dynamic response on the measured loads.

Hasheminasab et al. (2020) presented an experimental study on the water entry of a catamaran section. Their section consisted of identical asymmetric twin wedges connected with a wet deck structure. The wedges were vertical on the inboard side and non-vertical on the outboard side. They performed drop tests of a set of twin wedges with deadrise angles of 7, 15 and 20 degrees. They studied the effect of tank depth, three-dimensional effects, sampling rate and repeatability. The results showed that the demi-hull spacing did not have a considerable effect on the peak pressure on the bottom of the wedges. They found air entrapment on the vertical side of the twin wedges and below the wet deck.

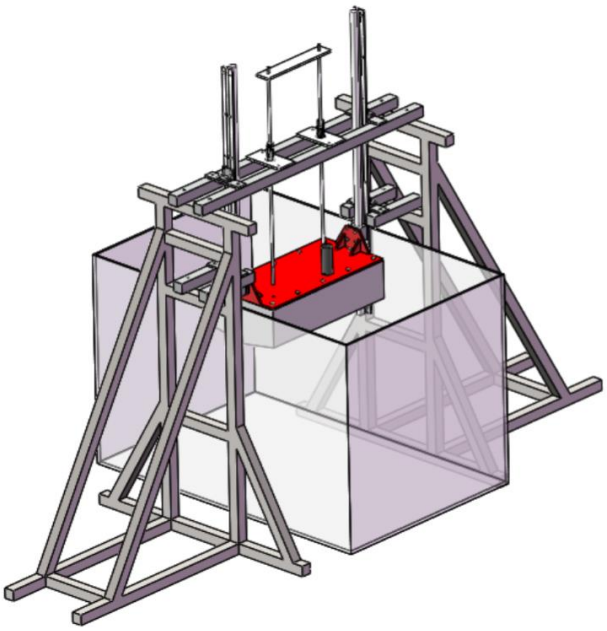

Figure 288: Drop test setup (Guo et al., 2017)

Kim et al. (2017a) studied the characteristics of various pressure sensors for measurement of wave impact loads. They used drop tests with a free-falling wedge to study peak pressures, rise times and pressure impulses measured by the different types of pressure sensors. On the basis of these results, the characteristics and reliability of the pressure sensor for the measurement of the water impact load were discussed.

Zeraatgar et al. (2019) discussed the effect of the sampling rate on the impact pressure of wedge water entry tests. Also they used drop tests, and showed that although 25 kHz sampling rates were appropriate for deadrise angles of 25 degrees and higher, for lower deadrise angles higher sample rates should be used, of up to 600 kHz for a deadrise angle of 5 degrees.

2.4.1.2 Numerical.

Where a decade ago analytical or empirical Von Karman or Wagner based approaches and two-dimensional potential flow solutions were still commonplace for water impact problems, over recent years a shift has taken place towards more advanced CFD methods and meshless methods such as the Smoothed Particle Hydrodynamics (SPH). Many studies focus on the effect of compressibility.

Bašić et al. (2017) presented a meshless Langrangian method for the hydromechanic loads during water entry of a rigid body. They based an unsteady incompressible solution on the Pressure Poisson Equation reformulation of the Navier-Stokes equations. They applied a novel meshless discrete Laplacian avoiding the need for a volumetric mesh. Validation against wedge section water-entry results from literature (Figure 289) showed that pressure and velocity fields during the water entry were well-reproduced. Numerical damping near walls and the free surface still needs further improvement.

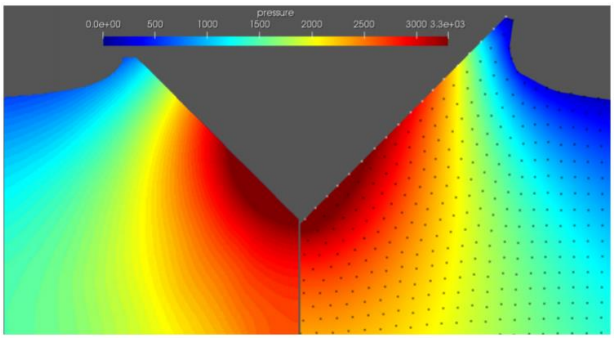

Figure 289: Comparison of numerical results (right) with PIV pressure contours (Bašić et al., 2017)

Falahaty et al. (2018) proposed a fully-Langrangian computational method for the simulation of incompressible fluid-nonlinear structure interactions, based on an enhanced Incompressible Smoothed Particle Hydro-dynamics (ISPH) solver combined with a SPH-based Hamiltonian structure model (HSPH). Validation included a dam break problem with an elastic gate as well as elastic wedge impact (Figure 290) and hydroelastic marine plate slamming.

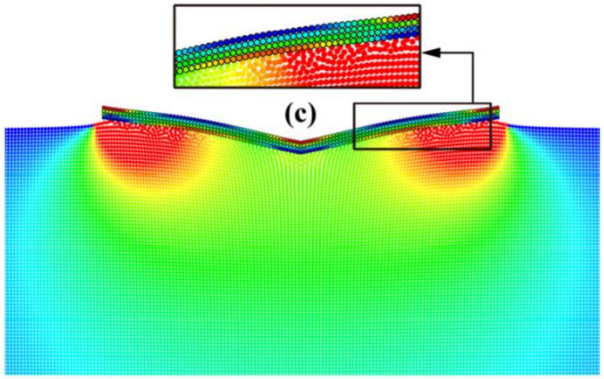

Figure 290: Hydro-elastic wedge impact with ISHP-HSPH method (Falahaty et al., 2018)

Sun at al. (2019) used a mixed mode function-modified MPS (Moving Particle Semi-implicit) method to simulate slamming on the cross deck of a trimaran with rigid and flexible arches. The water was considered as an incompressible inviscid fluid and the "conceptual particle" model was used to enhance the stability of the intense free surface interaction during the "filling-up" process under the cross deck. The results for rigid arches obtained with the use of an improved free surface condition show good improvement, in comparison to the experiment data. From the study of flexible arch cases with different flexibilities, it was found that the flexible structure can reduce the local pressures and slamming loads. In another study Sun et al. (2020) applied an incompressible CFD approach to study the pressures and load characteristics of a very similar trimaran section. They investigated three different motions: free fall, constant vertical velocity and harmonic vertical velocity, with all three motions having the same entry velocity of 1.7 m/s. The constant velocity case produced a significantly larger pressure compared to the other motions.

Jiang et al. (2018) also applied a RANS-based CFD method to the problem of water entry of a rigid body with a low deadrise. Both

water and air were included in the computations, allowing to study air-cushioning effects. They found that the average impact force coefficient was constant as function of entry depth and that the oscillation period of the impact force decreased after the air-cushion was formed.

2.4.1.2 Comparative study

A comparative study of a water-entry problem was conducted as a focused session of ISOPE-2016 in Rhodes by the International Hydrodynamic Committee (IHC) of ISOPE (Hong at al., 2017). Thirteen institutions participated, and twenty different numerical results were investigated and compared with one another and with model test data. Some promising results were obtained even though arriving at general conclusions is still a long way away.

The experimental results consisted of two-dimensional triangular wedge drop with a 30 degree deadrise angle and a ship section drop. The test results were provided by the WILS JIP-III. The wedge results included a symmetric impact case and a 20 degree inclined asymmetric case (Figure 291). Instrumentation included two pressure sensors, two impact force transducers and a high speed camera.

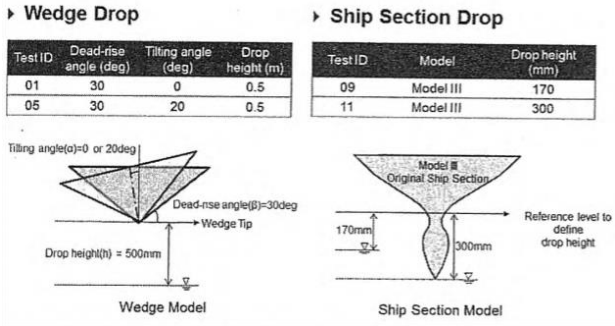

Figure 291: Wedge and ship section used for the IHC comparative study (Hong at al., 2017)

The numerical methods included potential flow Boundary Element Methods (BEM(based on Generalized Wagner Method and the Modified Logvinovitch Method, CFD methods based on the Finite Volume, Finite Element and Finite Difference Methods (FVM, FEM and FDM) and particle based methods (Langrangian methods such as SPH and MPS). In some cases compressibility was considered.

With the limited number of cases and participants it was not possible to arrive at general conclusions, but some important observations were made. CFD results were found to be very promising for symmetric impact, but there remained quite some uncertainty for the asymmetric impact case. The ship section drop case showed a larger spread in the results than the wedge drop, especially for the potential flow results. This is most likely related to the formation of air pockets for the ship section drop case. Peak pressures showed a better agreement than rise and decay times. The results were found to be very sensitive to grid generation and prone to human error, emphasizing the need for grid convergence studies. The use of filtering to remove oscillations in the time traces should be carefully considered and explained.

Yang et al. (2017b) applied an incompressible Immersed Boundary Method (IBM) to both the wedge and the ship section. Besides the incompressible IBM, they also performed numerical simulations with OpenFOAM that included compressibility and compared against experimental results. They found that the IBM performed reasonably well considering that compressibility was ignored and the results were sensitive to mesh and grid sizes.

Kim et al. (2017b) present the results of potential-based methods and computational fluid dynamics (CFD) for the water-entry impact of the wedge and ship-like section (Figure 292). In the potential-based computation, a Generalized Wagner Model (GWM) and a Modified Logvinovich Model (MLM) were used. In the CFD computations, a constrained interpolation profile (CIP)-based method and

commercial software were used for the prediction of fully nonlinear slamming phenomena. The grid convergence index for the peak pressure was analyzed for both CFD computations. Accuracy was investigated in terms of the peak pressure, pressure distribution, local hydrodynamic force, and free-surface shape.

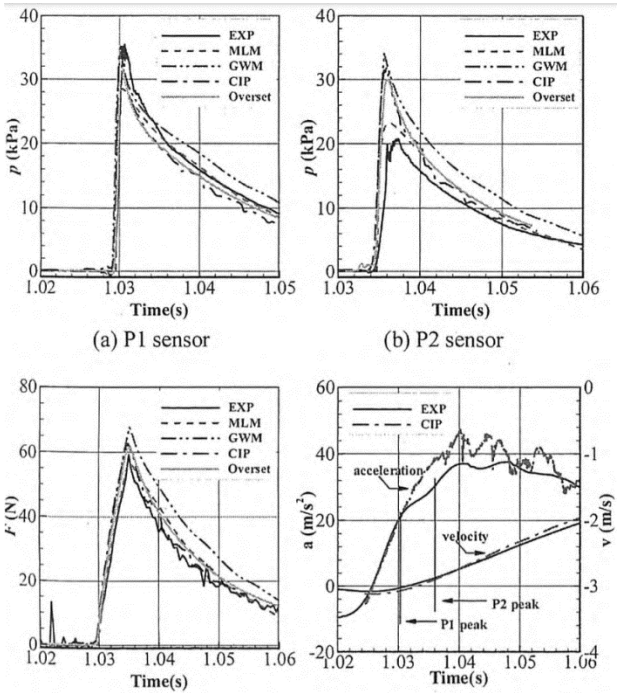

Figure 292: Comparison of experimental and computational results for wedge drop (Kim et al., 2017b)

Ma and Liu (2017) used a two-phase Smoothed Particle Hydrodynamics (SPH) method. From a comparison of the numerical results and the measured data, it was found that good agreement can be achieved. The later stage of the cavity evolution for the wedge water entry and the formation of the entrapped air cavity for the ship-section water entry were simulated well by the two-phase SPH method.

Monroy et al. (2017) compared two different classes of methods to the experimental cases: potential theory based on a Wagner model and computational fluid dynamics (CFD) based on a finite volume method with a volume-of-fluid (VOF) interface. They stressed the importance of finding a compromise among the wide range of available methods for slamming impacts related to CPU time, setup time (i.e. engineering time) and accuracy.

2.4.2 Slamming

1.1.1 SLAMMING

Slamming assessments are focused on quantifying the occurrence rates of bow slamming and stern slamming, as well as quantifying the magnitude of the impact loads. In recent years there is an increased focus on oblique wave impact, with multiple sources reporting larger impact loads than in head seas in particular cases. This highlights the need for carefully considering the influence of wave heading on slamming.

Most computational approaches employ a combination of calculation methods of different levels of fidelity. Lower fidelity methods such as 2D or 3D potential flow methods are used to quantify the overall motions, slam occurrence rates and relative impact velocities. Individual impacts are then investigated in further detail by using dedicated computational approaches. These approaches vary from considering water entry of two-dimensional ship sections, as described in section 0 to considering a three-dimensional impact of larger sections of the vessel.

Various methods are applied to obtain the structural response, from simple beam models to 3D FEM methods. In many cases hydroelastic coupling is considered. This section focuses on the quantification of occurrence and magnitude of slamming. Hydro-elasticity is treated in more detail in section 2.6.

2.4.2.1 Bow Slamming

Ge et al. (2018) performed CFD computations to predict slamming loads for a moving ship (Figure 293) in head waves and in oblique waves. They used an in-house code based on OpenFOAM. The CFD results for the head-sea case showed excellent agreement with the corresponding model experimental data (see for instance Figure 294). For oblique seas, the CFD results showed good comparisons with the model test data for the heaving, pitching motions, the hull pressure patterns, and the vertical forces on the ship segments. Higher discrepancies were evident in the comparison of rolling motions and transverse forces on ship segments as well as the peak values of the pressures, highlighting the need for further improvements for oblique sea cases.

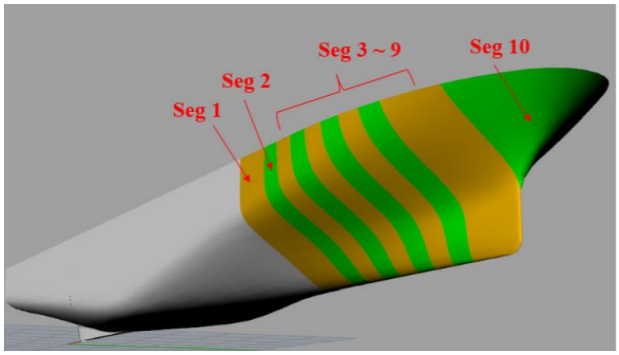

Figure 293: Forebody of the model split into 10 segments (Ge et al., 2018)

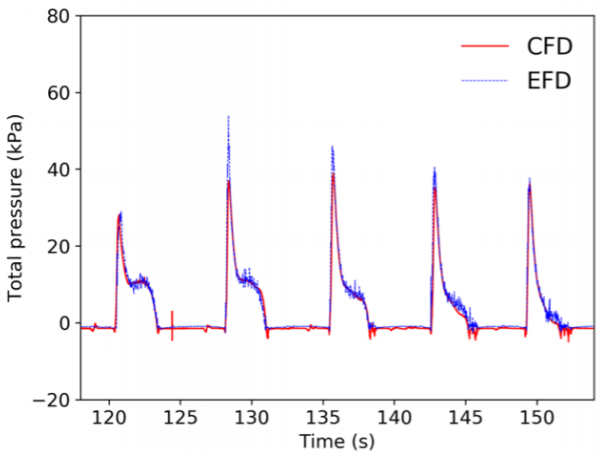

Figure 294: Pressures time histories for CFD vs EFD in head seas (Ge et al., 2018)

Kim et al. (2019a) conducted an experimental study on the spatial distribution of bow flare slamming loads of ultra-large container ships. They used a 1/60 six segmented scale model of a 10,000 TEU container ship, with 15 force transducers on the bow flare surface to measure impact loads. They found that in regular waves the slamming pressures were higher for oblique directions compared to head waves. In an irregular wave test, extremely large slamming loads were measured at the centre line at the bow, influenced by the horizontal relative velocity such as the ship speed and surge. They noted that in an analysis of the slamming load of the ship, the direction of the wave and forward speed of the ship should be carefully considered, which is difficult to achieve with two-dimensional analysis.

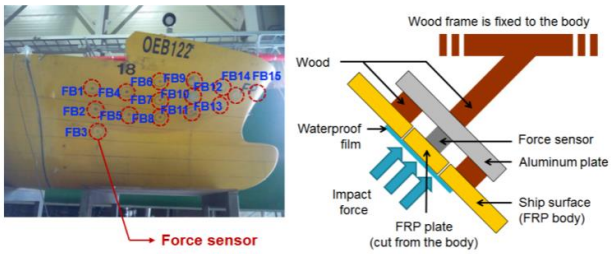

Figure 295: Setup for force sensors for measurement of impact loads (Kim et al., 2019)

Lin et al. (2018) proposed an approximate prediction method for slamming loads in parametric rolling conditions for large container vessels. They combined a weakly nonlinear time domain model for prediction of the ship motions with a Wagner model for asymmetric impact. They validated the approach with model tests with a segmented model of a 10,000 TEU container vessel. Their results indicate that while the bow flare slamming pressure is smaller than for bottom slamming, the pulse duration is longer and the occurrence of bow flare slamming is associated with the cycles of parametric rolling motions.

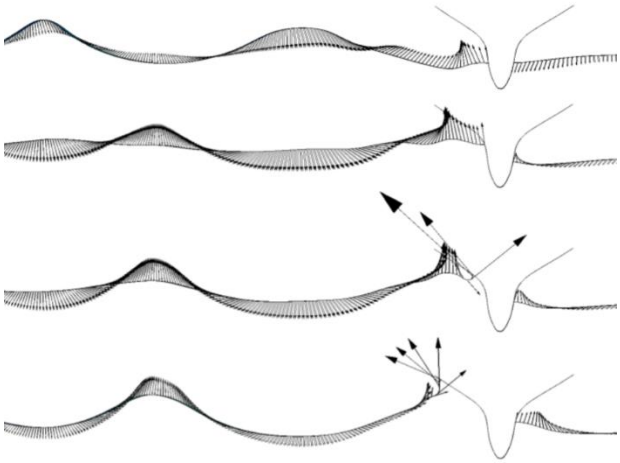

Figure 296: Free surface profiles and surface velocities of short waves (Sun and Helmers, 2020)

Sun and Helmers (2020) studied the influence of short wave components on the bow slamming loads. They developed a nonlinear numerical wave tank based on a Boundary Element Method and carried out simulations for a bow-flare section in short beam waves modelled with a nonlinear Higher Order Spectral Method (Figure 296). Their results imply that the nonlinear characteristics of the incident short wave components can lead to higher peak pressures.

Wang et al. (2018) investigated the bottom slamming at the bow and stern of a chemical tanker and an LNG carrier advancing in irregular waves numerically and experimentally. They applied a simplified method to include the effects of body nonlinearity by evaluating radiation and diffraction forces in the time domain as function of the instantaneous wetted surface. They determined the relation between relative wave height, impact velocity and peak slamming pressure at the stern and at the bow for both vessels from the experiments and combined this with the slamming probability obtained from the numerical simulations.

Xie et al. (2018) also systematically studied the bow-flare slamming loads of an ULCS in oblique waves. They combined a frequency domain Boundary Element Method to predict the relative motions at the bow and CFD on the oblique water entry of two bow sections to predict the slamming loads. Their results showed that transverse and roll motion cannot be ignored in oblique waves. Pressure characteristics in different wave directions were discussed and also their results showed that slamming loads in some oblique wave cases were larger than that in head seas.

Yang et al. (2017a) considered the dynamic response of the bow structure of a large container ship subjected to slamming pressures. They derived a simplified slamming pressure pulse characterized by its amplitude, duration, shape, spatial distribution and travel duration over the hull. Using this they studied the dynamic response of the bow structure as function of the pressure pulse characteristics. They found that for symmetric load shapes (i.e. the pulse rise time equals the duration of load decrease) led to lower stress responses compared to more realistic asymmetrical load shapes (i.e. the rise time is smaller than the duration of load decrease). The position of the maximum slamming pressure was found to be an important parameter for the dynamic response of bow structure under slamming pressures.

2.4.2.2 Stern Slamming

Mutsuda et al. (2018) investigated the characteristics of stern slamming pressures, such as occurrence mechanism, space-time distribution and influence of the local deadrise angle and relative vertical velocity by performing water entry tests of a wedge model and a stern section (Figure 297). Besides water entry tests they also performed model tests in irregular seas and numerical computations based on the Smoothed Particle Hydrodynamics method. They presented an extensive comparison of the results.

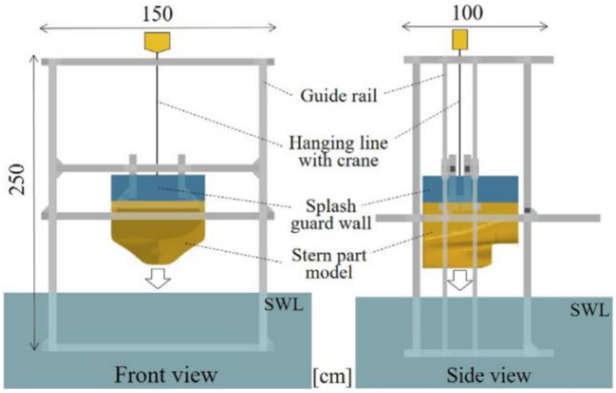

Figure 297: Experimental setup for the water entry tests of a stern model (Mutsuda et al., 2018)

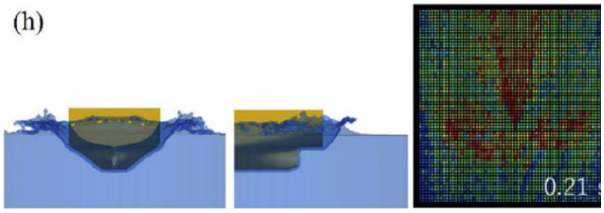

Figure 298: Numerical results of stern impact using SPH (Mutsuda et al., 2018)

Wang and Soares (2016) applied an Arbitrary Lagrangian Eulerian (ALE) algorithm implemented in LS-DYNA and a Modified Logvinovich Model (MLM) to predict the stern slamming loads of a chemical tanker. They used a nonlinear time domain strip theory program to compute the ship motions for a range of irregular sea states and used the relative vertical velocity in the ALE and MLM methods to simulate the water entry of 2D stern sections. A comparison of the results of both methods was made with results from model tests.

2.4.3 Slamming on high speed craft

For high speed craft operating at sea slamming becomes an event that occurs almost every single wave encounter – hardly a 'rarely occurring event'. For this reason slamming of high speed craft is an integral part of the assessment of its seakeeping performance with respect to structural integrity as well as human safety. This topic is included in section 2.9 on High Speed Marine Vehicles (HSMV).

2.4.4 Green water

Green water and impact due to green water on the deck is associated with very complex three-dimensional water flow. Enclosed air pockets can have a large effect on the magnitude of the impact loads. Similar to slamming, in many cases multiple fidelity levels are combined to make a full prediction of green water loading, with more standard and efficient potential flow methods employed to compute the overall motions and high fidelity multi-phase CFD computations for the green water problem itself. The well-known dam break problem is still an important validation case for these high fidelity tools.

2.4.4.1 Numerical

Van der Eijk and Wellens (2019) extended a volume of fluid method for simulations of extreme wave interaction with maritime structures with a Continuum Surface Force (CFS) model for surface tension to improve gas-water interaction after free surface wave impacts. The method was applied to a dam-break simulation in which the impact on a wall leads to an entrapped air pocket. Surface tension was found not to have an influence on entrapped air pocket dynamics of air pockets with a radius larger than 0.08 metres. For wave impacts it was found that the effect of compression waves in the air pocket dominates the dynamics and leads to pressure oscillations that are of the same order of magnitude as the pressure caused by the initial impact on the base of the wall.

He et al. (2017) performed time-domain simulations on green water of a Wigley hull sailing in regular head waves, using multiphase-flow CFD (Figure 299). They developed a solid-liquid-gas three-phase flow coupling model by adopting the BRICS compressible discrete scheme to reduce numerical diffusion near the free surface. By using this numerical model, impact loads on deck and hull, ship motions and

hydrodynamic characteristics during the green water process were investigated.

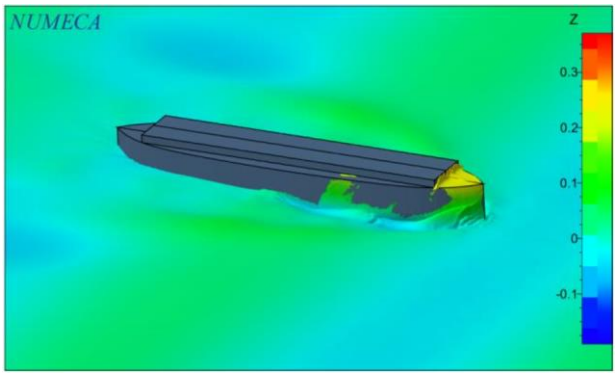

Figure 299: Green water on a Wigley hull (He et al., 2017)

Hernandez-Fontes et al. (2017) studied an alternative approach for isolated green water events by using a wet dam-break to generate the incoming flow. Tests were carried out in a rectangular tank with a fixed structure. Different freeboard conditions were tested for one aspect ratio of the wet dam-break (h0/h1=0.6). High speed cameras were used to investigate the initial phases of green water. The results demonstrated the ability of this approach to represent different types of green water events.

Kudupudi and Datta (2017) modelled green water loading on an oscillating body using CFD. The vessel motion was calculated a priory using time domain panel method code, before computing green water impact based on the pre-calculated motion. A Finite Volume Method was used to capture the green water impact combined with a Volume of Fluid Method to capture the free surface. They demonstrated that impact loading phenomena are significantly affected by the ship motions compared with results obtained from fixed vessel cases.

Kudupudi et al. (2019) used a similar approach combined with a Finite Element Method to study the effect of green water loading on the global structural response. They applied the approach to a large container vessel with and without forward speed in waves. They concluded that the proposed three-step (time domain simulation for motions, green water loading with CFD and FEM for the structural response) model is a useful practical tool to predict green water loading.

Liao et al. (2017) presented a 3D hybrid Eulerian-Lagrangian method for simulating green water on a ship. They considered three benchmark cases: dam-breaking, wave impact on fixed structure and green water on ship, showing reasonable comparison between experimental data and numerical results.

2.4.5 Emergence and Ventilation

Emergence is usually studied by obtaining the relative wave height at locations of interest. These locations can include propellers, rudders, stabilizer fins as well as sonar apparatus. Experimentally usually relative wave probes of various types are applied at such locations and counts where the relative wave height exceeds a threshold are used to identify emergence events. Numerically, usually a direct computation of the relative wave height at locations of interest can be made. Depending on the fidelity of the numerical approach, the disturbance of the local wave profile can be included with various degrees of accuracy.

Experimental measurements of the variation of the lift, drag, and moment coefficients on a rigid and a flexible surface-piercing hydrofoil at different submergence levels, angles of attacks, and speeds across a range of flow conditions ranging from fully wetted, partially cavitating, partially ventilated, and fully ventilated can be found in Harwood et al. (2016, 2019). The results show that the lift and moment coefficients reduce rapidly with reduce submerged aspect ratio (e.g. as the rudder or propeller emerges) because of increased 3-D effects and pressure relief at the free surface. In theory, the 2-D lift coefficient reduces by 75% in fully ventilated (FV) flow compared to fully wetted flow (FW). For 3-D bodies, the lift

coefficient generally reduces by ~50%, but the moment coefficient can reduce by 70% or more because of reduction in lift compounded with move of the center of pressure to near the midchord. The change in hydrodynamic load coefficients due to transition from FW to FV flow can occur gradually or very rapidly (in less than a second) depending on the ventilation mechanism.

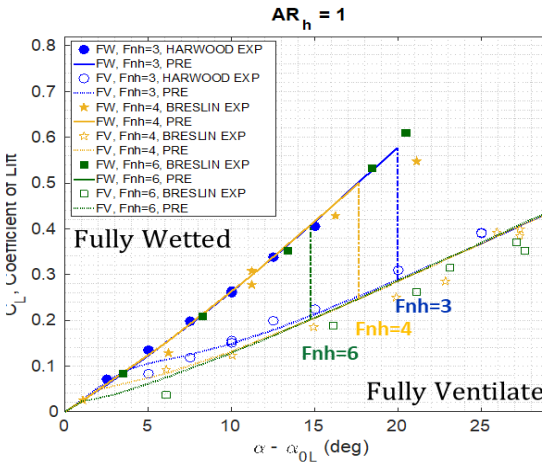

Figure 300: Hysteresis response of the lift coefficient as function of incidence angle and chord Froude number (symbols: experiments, lines: predicted, Damley-Strnad et al., 2019)

The hydrodynamic response is also highly hysteretic, as illustrated in Figure 300. The sudden and drastic load changes and hysteretic response can significantly challenge design of controllers and auto-pilots. To facilitate design and control of lifting devices subject to ventilation, semi-empirical equations of the hydrodynamic performance can be found in Damley-Strnad et al. (2019), which showed good comparison with experimental measurements, as demonstrated in Figure 300.

A series of experimental studies of ventilation of marine propellers can be found in Kozlowska et al. (2017, 2020), along with empirical equations to predict the steady and dynamic propeller performance in different flow regimes. Similar to a hydrofoil or strut, ventilation can lead to significant reduction in thrust and torque (as demonstrated in Figure 301), which will lead to rapid increases in propeller rpm to maintain thrust, or reduction in vessel speed. Scaling of the hydrodynamic performance of marine propellers in ventilated flows, and discussion of the hysteretic response can be found in Kozlowska et al. (2017, 2020). A recent review of the physics of ventilation can be found in Young et al. (2017).

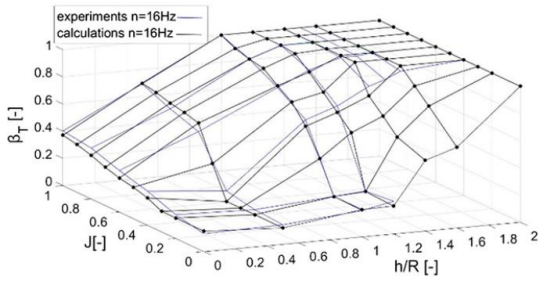

Figure 301: Comparison between calculation and experimental values of thrust loss ($\boldsymbol{\beta_T}$) due to ventilation and out of the water effects for shaft submerged depth to propeller radius ratio, h/R, and advance coefficient, J. (Kozlowska et al., 2017)

Recent reviews of the hydroelastic response of propellers and hydrofoils can be found in Young et al. (2016, 2017) and Young (2019). The topics discussed include the effects of emergence, cavitation, ventilation, hydroelastic performance and instability mechanisms. In general, for a hydrodynamic lifting device made of solid and homogeneous material with the center of pressure upstream of the elastic axis, elastic deformations will lead to bending towards the suction side and nose-up twist, which will act to increase the lift and moment, and accelerate cavitation, ventilation, stall, and may lead to static divergence instability. However, these effects can be countered by taking advantaged of material anisotropy and geometric bend-twist coupling provided by sweep (Liao et al., 2019).

The influence of changing submergence (such as caused by emergence) and ventilation on the hydroelastic response of a surface-piercing strut/hydrofoil was studied

experimentally in Harwood et al. (2019,2020) and Young et al. (2020). Examples of the measured variation of the measured modal fully wetted (FW) and fully ventilated (FV) modal frequencies as a function of the submerged aspect ratio (AR_h) are shown in Figure 302. They found that, in general, as submergence decreases (body emerges), the system modal frequency increases because of reduction in added mass. The modal frequencies also tend to be higher in FV flow compared to FW flow because the replacement of dense water to light air on the suction side of the body. In addition, since added mass depends on the direction of motion and/or deformation, mode switching and modal coalescence can occur (such as shown for the surface-piercing strut at $AR_h = 2$ shown in Figure 302). The measurements also showed significant dynamic load amplifications caused by modal coalescence (Young et al., 2020; Young, 2019).

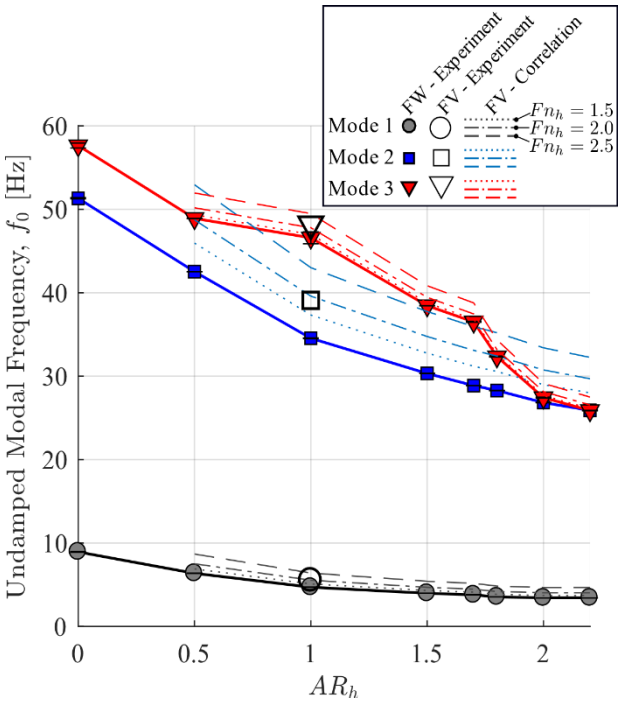

Figure 302: Measured variation of the fully wetted (FW) and fully ventilated (FV) modal frequencies as a function of the submerged aspect ratio ($\boldsymbol{AR_h}$). From Harwood et al. (2020) and Young et al. (2020).

2.5 Sloshing

Assessment of sloshing loads for LNG tanks has been an issue of significant interest by the shipbuilding industry owing to the recent renewed interest into the transportation of LNG. Until now, it has been believed that only experiments can provide reliable data to evaluate the impact load for the sloshing problem. Malenica et al. (2017) reviewed recent approaches to assess sloshing loads describing the industrial experiments as well as numerical simulations. The study concluded that performing model experiments has been the most frequently used and relatively reliable approach.

Ahn et al. (2019a) described details of sloshing experiments in an industrial site and investigated the possibility to adopt a machine learning scheme. They developed an artificial neural network (ANN) to predict the sloshing load severity. They showed the ANN model has an acceptable performance considering the highly nonlinear and complex nature of the sloshing problem, by comparing against experiments that have not been part of the training process (Figure 303).

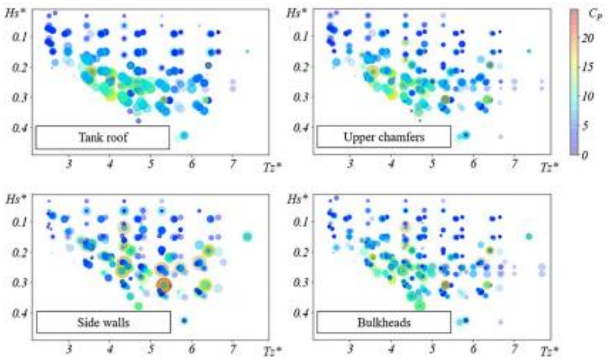

Figure 303: Scatter diagram of sloshing impact pressure coefficient with respect to environmental conditions (Ahn et al., 2019a)

Fluid-structure interaction (FSI) is an important topic for the sloshing tank. Taian et al. (2019) showed a numerical study on the influence of elastic baffles on the sloshing loads.

Zhang et al., 2018 performed numerical simulations of the sloshing flows inside an elastic wall tank (Figure 331). An analytic model was developed to assess the effectiveness of a porous elastic baffle on liquid sloshing by Cho (2021). He applied the matched eigenfunction expansion method (MEEM) with the Green function for the liquid sloshing interaction with the porous elastic baffle.

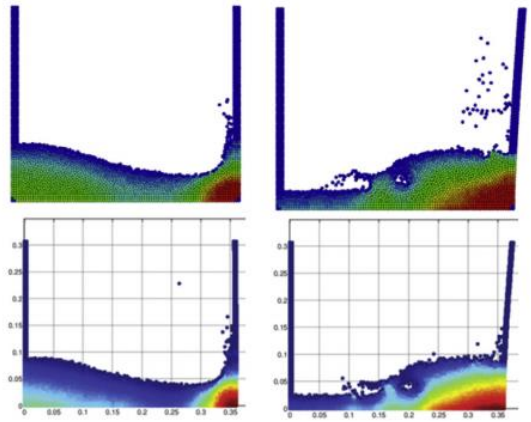

Figure 304: Numerical simulation for sloshing flows in an elastic tank (Zhang et al., 2018)

The most profound issues in violent sloshing flows are related to the effects of density ratio and bubbles on the sloshing impact. Ahn et al. (2019b) carried out a sloshing model tests considering gas-liquid density ratio. They proposed an experimental procedure for handling an alternative gas mixture to match the density ratio. Through a series of experiments, they showed that the density ratio clearly affected the sloshing impact pressure. It appears that the sloshing impact pressure decreases with the increase of density ratio, which means the conventional sloshing test using air-water may give more significant sloshing impact pressures compared to the model test based on the density ratio of an actual LNG cargo hold.

Kim et al. (2017c) observed the effects of the phase transition and bubbles on the impact pressure through a small scale drop test. On the basis of this experiment, it was confirmed that the existence of bubbles decreases both the peak pressure and the impact duration. In addition, it was found that the amount of vapour trapped in the gas pocket was important to generate the phase transition effect which is related to the damping effect.

Sloshing is induced by the ship motion but in return, the ship motion is also affected by the sloshing-induced load. There have been various research efforts on the coupled dynamics between the ship motions and sloshing problem. (Huang et al., 2018, Bulian et al., 2018, Saripilli and Sen., 2018, Lyu et al., 2019). Figure 305 shows snapshots of a coupled numerical simulation of an LNG carrier in waves with sloshing LNG tanks. In addition, Seo et al. (2017) studied the effect of internal sloshing on added resistance of ship applying numerical approaches. They showed the sloshing flows inside the inner tanks may significantly influence not only the ship motion, but also the added resistance, especially near the resonance frequency of the sloshing flow.

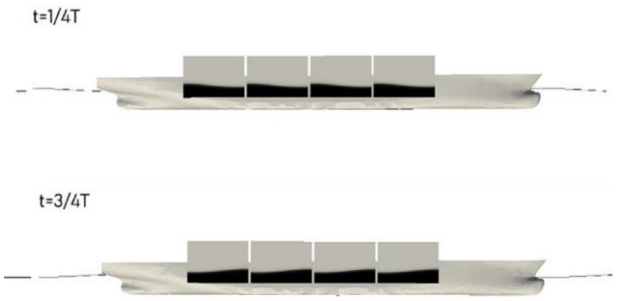

Figure 305: Numerical simulation of coupled ship motion and tank sloshing of an LNG carrier in head wave (Lyu et al., 2019)

Kwon et al. (2018) investigated the sloshing load for a single-row arrangement system into a midscale floating production unit of liquefied natural gas platform. Through the sloshing experiments, they evaluated the significant wave height limit for the offloading operation. Also, a sloshing severity index was calculated

and compared with the sloshing model test results.

2.6 Hydroelasticity

There has been much progress over the last five years on the experimental and numerical modelling of the hydroelastic response of marine vessels at sea. A brief summary of representative literature concerning experimental modelling is presented first, followed by theoretical and numerical modelling.

2.6.1 Experimental

2.6.1.1 Full scale studies

Full-scale measurements of slamming loads and structural responses of a 9.6 m high-speed planning craft in different sea conditions and at different speeds and headings can be found in Camilleri and Temarel (2018). They found that the ISO standard and DNV rules predicted pressures that are significantly lower than the measured values, while the LR rules predicted pressures that are higher than the measured data for high forward speeds and lower for moderate speeds.

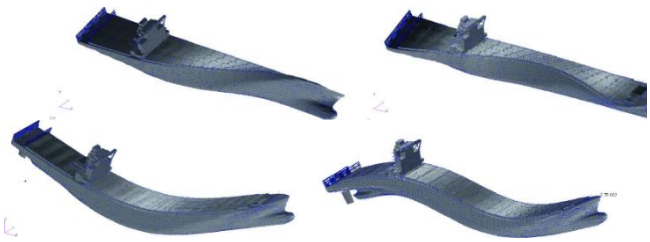

Figure 306: Predicted torsional and vertical bending modes of an 8,600 TEU container ship (Miyashita et al., 2020).

Miyashita et al. (2020) presented full-scale measurements of an 8,600 TEU container ship taken over four years and two months. The focus was on the influence of sea states and navigational conditions on the whipping response of hull girder. Vibration analysis, including the added mass on the hull surface, was used to derive the vibration modes related to vertical bending and torsion, such as shown in **Erreur ! Source du renvoi introuvable.**. They found that the vertical bending stress is dominant and accounts for 81% of the total stress. Whipping response on the vertical bending stress was significant in head seas, while it was not observed in beam seas or following seas. They also found that higher ship speed will lead to a higher whipping factor in head seas.

2.6.1.2 Operational Modal Analysis

Multiple full-scale studies were conducted to investigate the modal characteristics of marine vessels via operational modal analysis (OMA). One of the early works of OMA for marine vessels was conducted by Kim et al. (2016), who used OMA to extract the modal parameters (vertical and torsional mode shapes and damping ratios) to characterize the hydroelastic response of a 1/60-model scale segmented container carrier subject to head waves and oblique waves. They later extended the method to determine the modal characteristics of a full-scale 9400 TEU container ship by POD analysis of acceleration signals in Kim et al. (2018). They found that the natural frequencies and damping ratios vary with loading conditions, where the 2-node vertical bending varied from 0.45-0.6 Hz, and the damping ratio varied between 1-3%. They also noted that fatigue damage increased by ~70-85% due to vibrations.

Hageman and Drummen (2019) presented a time-domain Auto Regression Moving Average (ARMA) method for Operational Modal Analysis based on Stochastic Subspace Identification (SSI). The method was found to be able to determine the frequencies, mode shapes, and damping characteristics of the system based on acceleration and strain measurements. Hageman and Drummen (2020) later extended the method for in-service measurements of the operational mode and damping characteristics of a frigate type vessel.

They found that the added mass changed with operations in confined waters, heading, and speed, with variation in natural frequency as high as 10%. Moreover, they found that damping depended on speed and wave height, with values ranged from 0.6 to 2.5%.

Shakibfar et al. (2020) presented full-scale measurements of the damping characteristics of an 8400 TEU container ship obtained using operational modal analysis. They found that the natural frequencies of all the modes, except for 2-node vertical bending, decrease with increasing speed, and the damping factors to increase with increasing speed for both the vertical bending and the torsion mode.

Operational modal analysis was also used in Harwood et al. (2020) to determine the change in modal frequencies and damping coefficients of a cantilevered surface-piercing strut with operating conditions. They found that the modal frequencies reduced with increasing immersion, and increased with increasing cavitation and/or ventilation, due to changes in the fluid added mass. The damping ratios generally increased with increasing immersion and with forward speed, and is a nonlinear function of the reduced resonance frequency. A later work by Young et al. (2020) also showed that changes in modal characteristics with immersion can lead to frequency coalescence, which resulted in significant dynamic load amplification.

2.6.1.3 Scaling of vibrational Response

A new design procedure for model-scale testing of flexible containership was proposed in Houtani et al. (2018) to ensure similarity of the vertical-bending and torsional vibration response between the model and the prototype. They noted that the height of the shear center of the model must be located below the hull bottom, like that of an actual container ship with a large open deck, to achieve similarity in the torsional vibration mode. They met the design conditions by using urethane foam to build the hull and without a backbone, and demonstrated the ability of the method in measuring the dynamic elastic response in waves.

2.6.1.4 Slamming and Whipping

Wang et al. (2020) presented experimental data on the calm water slamming impact of a series of three aluminium plates with different thicknesses. The results showed that the peak force and moment increased, the time of the peak force increased, and spray height increased, with reduction in the plate thickness.

Javaherian et al. (2020) presented experimental study of calm water entry of flexible bottom panels, and towing tank test of a rigid composite planning hull. Compared to a rigid aluminium panel, the measured peak pressure of the flexible aluminium and composite panels dropped by 4% and 10%, respectively.

Spinosa and Iafrati (2021) presented experimental studies of the fluid-structure interaction of the high-speed water impact of varying thickness aluminium plates. They found that plate deformation lead to reduction in the pressure peak, a subsequent pressure rise, and a change in the direction and shape of the spray root. The structural deformation lead to an increase in the total loading by up to 50%. They also discussed the challenges with scaling the fluid-structure interaction response.

Full-scale measurements, as well as model-scale measurements and numerical simulations of a segmented model of wetdeck slamming on a wave-piercing catamaran can be found in Lavroff et al. (2017). The 2.5 m segmented model was designed to match the scaled first longitudinal modal (whipping) frequency and damping ratio measured for the 112 m full-scale INCAT vessel. Good general agreement is observed between the model-scale experiment

and predictions using CFD and FEA analysis, but there were some deviations in the peak slamming load and location. Full-scale measurements were complicated by uncertainty of the sea state, but the full-scale slam impulses were generally less than those measured at the model-scale. The authors suggested that the differences are probably due to a difference in the identification of the slam duration.

Slamming induced whipping computations were conducted for a large database of 17 post-Panamax container ship models in Lauzon et al. (2020). The calculations include 1-way and fully-coupled hydroelastic computations for long term wave vertical bending moments in full irregular sea states, with and without whipping, to get the global whipping factor for each ship. The results are summarized in Figure 307. They showed that 1-way coupling method always gave a large overestimation of the whipping factor for both hogging and sagging. The reason for the overestimation is because the slamming loads do not influence the rigid-body motions in the 1-way coupled simulations, which lead to over-prediction of the pitch motions, and hence higher slamming loads. The results also showed that using a low-pass filter of the measured response to extract the rigid-body moment, lead to negligible difference in the hogging, but a large overestimation of the whipping factor for bending due to under-estimation of the nonlinear rigid-body moment in sagging. The results also showed that both regular and irregular equivalent design waves (EDW) give acceptable precision in sagging, but there was a large scatter in hogging for regular design waves.

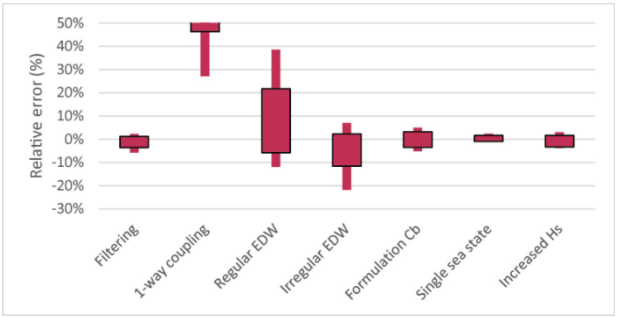

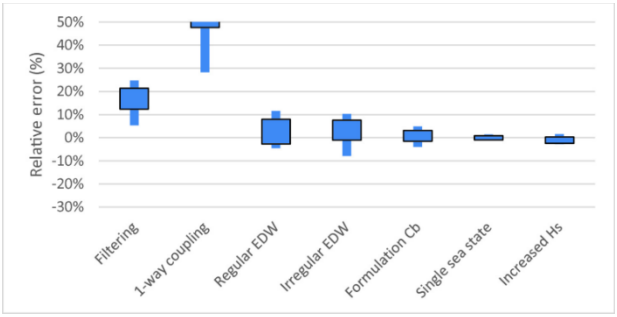

Figure 307: Relative error in the evaluation of the whipping coefficient in hogging (top) and sagging (bottom) (Lauzon et al., 2020).

2.6.1.5 Wave statistics of hydroelastic response

The short-term statistics of hydroelastic loads of an ultra large containership in head and oblique seas was investigated using combined numerical and experimental techniques in Rahendran and Soares (2018). A 2D body nonlinear time domain method was used for the numerical model, which showed good agreement with experiments of a container ship at low Froude numbers. The results show that the ship encountered the largest hogging and sagging peaks in oblique waves instead of head seas because the larger high frequency waves with shorter period was in proximity to the first natural period, i.e. dynamic load amplification due to near resonant condition.

The statistics of extreme hydroelastic response of large ships was examined using the ACER (Average Conditional Exceedance Rate) method in Gaidai et al. (2018). The results showed that the method can capture extreme tail statistics for sagging and hogging. The method also accounted for the effect of data clustering, which played an important role in whipping.

2.6.2 Analytical / Numerical

2.6.2.1 Analytical models

Sun et al. (2021) presented a semi-analytical model for hydroelastic slamming predictions. The method is based on analytical Modified Logvinovich Model of the hydrodynamic loads coupled with modal description of the elastic deflections. The analytical predictions were compared with experimental measurements of the forces and deflections for wedge water entry and cylindrical shell drop problems. The method provided efficient predictions at the initial slamming stage, but not the deep penetration stage with large flow deformation.

Yu et al. (2019) performed a hydroelastic analysis on water entry of a constant velocity three-dimensional wedge with stiffened panels, assuming incompressible flow while applying potential flow theory. Based on the Wagner theory, they developed a semi-analytical hydrodynamic impact theory for the analysis of elastic wedges. They coupled two-dimensional impact in the cross sectional fluid domain to modal analysis of the three-dimensional structure, making the model suitable for complex three-dimensional shapes. The new method incorporates the effect of flow separation on the responses and follows more detailed CFD results better than more traditional Wagner based approaches. Through the comparison between coupled and decoupled results of a 3D wedge, it is shown that the effect of fluid-structure interaction and the oscillatory response after flow separation are important for predicting the structural responses.

2.6.2.2 BEM-beam models

Riesner et al. (2018a) presented a linear frequency-domain hydroelasticity method to predict the wave-induced global hydroelastic ship response. They used a coupled 3-D boundary element method with a Timoshenko beam element model, and the method was designed to be suitable for both short and long period waves.

Heo and Kashiwagi (2019) used a time-domain higher-order boundary element method coupled with a generalized mode expansion model for the structure to predict the springing response of an elastic body. They used the method to demonstrate the importance of second-order velocity potential on wave-induced vibrations for different flexural rigidity and forward speed.

Bakti et al. (2021) coupled a discrete-module-beam structural model with a potential flow model based on slender body theory and low forward speed approximation. The predictions compared well with experimental and other computational results of a Wigley hull with and without forward speed. The results showed significant difference between dry and wet natural frequencies, and change in the first bending mode shape with forward speed.

Zhang et al. (2017) presented a 3-D nonlinear time-domain hydroelasticity method that combines a 3-D dynamic Timoshenko model with a 3-D nonlinear hydrodynamics model based on Green's function. Good comparisons of the predictions were observed with experimental measurements of the nonlinear effects on the vertical motions and loads on a container vessel advancing in irregular waves. The method was later extended in Jiao et al. (2019, 2020) to predict the motions and loads of a large bow-flared ship advancing in irregular seas. The effects of nonlinear Froude-Krylov force, radiation force, and slamming loads were considered. Good comparisons were observed with experimental measurements of the frequency spectra and statistics of the ship motions, deformations, and loads in regular and irregular waves of a 1:50 segmented model with large flare-bow.

2.6.2.3 BEM-FEA models

Im et al. (2017) used a fully coupled 3-D FEM-3-D BEM method to compare the hydroelastic performance of two design

concepts for a 19,000 TEU large container ship. The new design with higher loading capacity achieved via a mobile deckhouse structure on a special railing system lead to slightly lower natural frequencies compared to the conventional ship design. Although the extreme structural responses of both designs are safe, the conventional design performed slightly better with respect to fatigue because of higher torsional frequencies, which lead to lower local stress concentrations.

Chen et al. (2019) presented a 3-D nonlinear time-domain method to study the hydroelastic responses of high-speed trimaran in oblique irregular waves. The method is based on Green's function for the hydrodynamics and the commercial FEM solver MSC.Patran for the structural dynamics, together with a Proportional, Integral and Derivative (PID) autopilot model. The predictions compared well with experimental measurements from segmented model tests of a high-speed trimaran in oblique waves.

2.6.2.4 RANS-FEA models

Moctar et al. (2017) used RANS simulations (COMET and interDyMFoam) together with rigid body ship motion and Timoshenko beam model to determine the wave-induced structural loads for three containerships in regular and irregular waves. Good agreements were observed between predictions and measurements.

Takami et al. (2018) used a one-way coupled model with RANS CFD (STAR-CCM+) and dynamic FEA (LS-DYNA) to simulate hydroelastic response of a model-scale POST PANAMAX size container ship under severe wave conditions. Good comparisons of vertical bending moment were reported with experimental measurements and with weakly nonlinear method predictions. Some difference in natural frequencies were observed, which the authors attributed to the neglection of added mass effects.

Pellegrini et al. (2020) presented single and two-phase simulations of the hydroelastic response of vertical and oblique flexible plate slamming. The simulations used 1-way and 2-way coupling between CFDShip-Iowa and ANSYS finite element method, and the results were compared with experimental measurements presented in Wang et al. (2020a). Good agreements were observed for the forces and moments, but large errors for the strains and deformations, where the later was attributed to differences in assumed versus actual boundary conditions and material properties.

Takami and Iijima (2020) presented coupled CFD-FEA methods utilizing STAR-CCM+ and LS-DYNA to predict the global vertical bending moment and the local double-bottom bending moment of a 6600 TEU containership. The predictions were compared with towing tank test of a segmented model. Predictions with strong coupling compared better with measurements than one-way coupling, but discrepancies associated with hydroelastic vibrations were observed.

Lakshmynarayanana and Temarel (2020) presented two-way coupled RANS-FEM simulations using STARCCM+ and ABAQUS to predict the wave-induced loads of a self-propelled model-scale flexible containership. The predictions were compared with towing tank studies at CSSRC. The method was able to capture the nonlinearities in the wave-induced bending moments, and resulting hogging and sagging response.

2.6.2.5 Particle models

Khayyer et al. (2018) compared several full-Lagrangian fluid-structure interaction solvers for the simulation of hydroelasticity problems,

including slamming impact of an elastic beam and tank sloshing. The methods considered included projection-based MPS (Moving Particle Semi-implicit), and ISPH (Incompressible Smoothed Particle Hydrodynamics) fluid models coupled with Newtonian SPH/MPS or Hamiltonian MPS/SPH structural models. They found that Hamiltonian methods have the advantage of preserving conservation laws, but Newtonian structural models provide more stable pressure/stress fields. The Enhanced Multi-resolution MPS-based FSI solver was found to yield relatively accurate results in terms of deflections.

Andrun et al. (2020) presented a coupled Lagrangian meshless Finite Difference Method (Rhoxyz) and Finite Element Method (CalculiX) for prediction of hydroelastic slamming during water entries of a deformable symmetric wedge with low dead rise angle. Validations were shown for rigid body slamming and dam break with a flexible wall, and numerical results were presented for hydroelastic slamming.

2.7 Added Resistance in Waves and Power Requirements

2.7.1 Development of Numerical Methods to Predict Added Resistance in Head Waves

The mainstream numerical methods in head waves are the Reynolds-averaged Navier-Stokes (RANS) solver for CFD and the Rankin panel method (PRM) for potential flow. Several papers have shown that after checking the convergence CFD calculations provide results that shown that ship motions and added resistance in regular head waves are in good agreement with the experimental results. Lyu and el Moctar (2017), Sigmund et al. (2018), Zhang et al. (2019) systematically performed numerical calculations of both CFD and RPM and experiments with each method and publishes a series of results. After confirming the reliability of the regular head wave calculation, Yoo et al. (2020) verified the added resistance by the spectral method and the direct calculation method, and showed that the spectral method underestimated the added resistance. In addition, Crepier et al. (2020) showed with CFD that the quadratic assumption of wave height to the added resistance is not always satisfied depending on the wave steepness. The details are summarized in the following paragraphs.

Sigmund et al. (2018) systematically conducted CFD calculations and tank experiments for four different ship types, such as a post-Panamax containership (DTC), a KVLCC2, a medium-size cruise ship, and a Wigley hull, in regular head waves to investigate in detail the influence for added resistance due to ship speed, viscosity, interaction between the radiation and diffraction problem in a nonlinear regime, wave quadratic correlation in higher wave steepness. The friction added resistance in waves is shown to increases for short waves, but it was concluded to be less pronounced at full-scale ships (Figure 308).

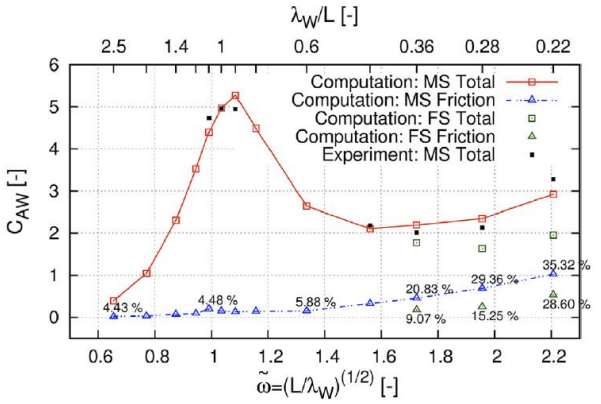

Figure 308: Computed and measured coefficients of total and frictional added resistance at model scale, Re=6.1x10^6, and full scale, Re=2.9x10^9, of the containership at Fn=0.14 in regular head waves.

Liu et al. (2018) discussed the motion and resistance of DTC ship at Fn=0.058 and 0.138 in short and long head waves using by in-house CFD code naoe-FOAM-SJTU. Predicted added resistance is underestimated by 6% compared with experimental data at Fn= 0.138, while the error can be up to 30% at lower speed. The second harmonic resistance and pressure distribution obtained by the Fourier analysis increases as ship speed increases and varies nonlinearly with wave amplitude. It is concluded that the bow region is critical to the seakeeping performance of DTC ship in moderate speed.

Yao et al. (2020) have predicted the motions and added resistance for KVLCC2 models in head regular waves by using the expanded RANS solver on OpenFOAM platform. The computed added resistance is decomposed into that due to pure hydrodynamic effect and the mean inertia forces due to the surge acceleration and the coupled motion of heave and pitch. The influences of ship speed, wave height, scale ratio, and spring stiffness on the components of added resistance and motions are analysed. When comparing CFD with experiments, it is suggested to be important to consider the effect of inertia forces.

Cakici et al. (2017) applied CFD to predict the motions and added resistance of DTMB5512 models at Fn=0.41 in head regular waves. The pitch and heave response calculated by CFD are in excellent agreement with those of experiments in the entire frequency range. CFD is confirmed to be effective for vertical motions.

Kim et al. (2019b) presented the numerical simulations for the prediction of added resistance in waves for KVLCC2 at three ship speeds which are the design speed (Vs = 15.5 knots), operating speed (Vs = 12 knots) and zero speed (Vs = 0 knots). These are calculated using RANS CFD and 3-D potential methods, both in regular head seas, and compared with those of experiments. It is concluded that vessels in stationary condition should be carefully operated in heavy weather conditions because the transient drift forces at zero speed may be larger than the transient drift forces of a vessel advancing in waves.

Hizir et al. (2019) performed numerical simulations for the prediction of added resistance for KVLCC2 with varying wave steepness using a CFD (STAR-CCM+) approached by RANS method and a 3-D linear potential method (PRECAL) developed by MARIN, and then investigated the non-linearities of added resistance and ship motions in regular short and long waves. It is concluded that CFD results have a reasonable agreement with the experimental data and estimate the non-linearity in the prediction of the added resistance and the ship motions with the increasing wave steepness in short and long waves. It is emphasised that the non-linearity of the added resistance and ship motions around the resonance period is larger than in short waves.

Seo et al. (2017) predicted the added resistance with the motions of KCS in head waves using OpenFOAM and compared with those of model experiments. Unstructured grid using a hanging-node and cut-cell method was used to generate fine grid around a free-surface

and ship. When the wavelength was similar to the ship length, the ship moved against the waves, and thus the added resistance was greater compared with other wavelengths. Large vortices structures were shown to be occurred under the transom and ship bottom due to the large ship motions (Figure 309).

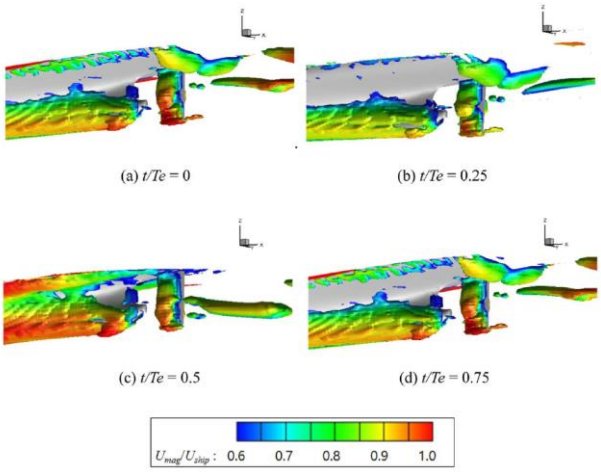

Figure 309: Vortices structures around stern for one encounter period (λ/L_{PP}=1.15) (Seo et al, 2020).

Yoo et al. (2020) investigated the added resistance in an irregular head sea using CFD. The reliability of results was confirmed by with those from model tests conducted in Samsung Ship Model Basin. The added resistance obtained by the spectral approach was reported to be underestimated by 20-40% over the direct estimate, suggesting that the direct estimation is required.

Crepier et al. (2020) compared the added resistances and pressure distribution on hull in head waves obtained by CFD, RPM and experiments conducted by MARIN. A very important result of this work is that it demonstrates that the traditionally assumed quadratic relationship between the wave amplitude and the added resistance is only partly valid. CFD results as well as the results of experiments show a clear relative decrease in higher waves. The effect of the temporary high steepness of individual waves in an irregular wave train may play a significant role.

In waves, CFD simulation can cover several effects such as viscosity, full nonlinearity, interactions of propeller-hull-rudder motions including some devices, however, still less time efficient compared to a potential flow method. Hence, a potential flow method is still indispensable in covering many operational conditions required for a complete assessment of the operational performance. Since there is almost no ship motion in the relatively short wavelength region, the component caused by diffraction is dominant, but in RPM, the discrepancy with the experiment is assumed by the fluid viscosity, and an empirical viscous drag equation is added. As a result, there are examples of improving the calculation accuracy, where developments of RPM in head waves are summarized below.

Riesner et al. (2018b) presented a partially nonlinear time-domain Rankine source method (nonlinear TDIR) to calculate the wave induced added resistance of ships advancing at constant forward speed in regular head waves according to Cummins approach. This nonlinearity comes from nonlinear Froude-Krylov and hydrostatic forces induced by wet area changing by undisturbed incident waves. In addition, the viscous component of wave added resistance was added empirically. Compared with CFD and EFD, the nonlinear TDIR with viscous effect (Figure 310) is concluded to provide more accurate predictions in waves of almost every wave length than frequency domain approach. In particular, this is remarkable in short wave length. Quadratic assumption of wave height and wave steepness are also discussed in detail.

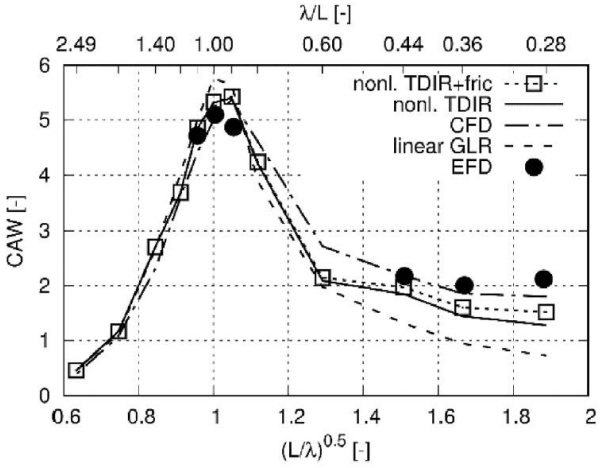

Figure 310: Wave added resistance coefficient including viscous effects for the DTC containership (*Fn*=0.139), EFD denotes experiments (Riesner et al., 2018b).

Zhang et al. (2019) developed a time domain Rankine panel method based on the double-body linearization with empirical viscous effect and a flow field described by the quadratic B-spline basis function. Through comparing with the motion and added resistance by experiment and CFD simulation for a Wigley hull, the S-175 container ship, and the KVLCC2 tanker, the effectiveness of the developed code is reported. The importance of the interaction between radiation force and diffraction force is shown.

2.7.2 Steady Force and Moment for Oblique Waves

Reliable prediction of second order forces and moments acting on ships in oblique waves is useful to assess the actual operational aspects, such as drifting angle, minimum power requirements, manoeuvring capabilities, and towing forces. However, the mean forces and moments is less studied so far in oblique waves than in head waves. This has resulted in only limited data on oblique sea conditions. Currently there is a trend to collect such data by numerical simulations and tank(basin) experiments. Through these studies, it is pointed out in several papers that ship motions appear to be significant even in short wavelengths and the radiation problem comes to be important. Research on oblique waves are summarized below.

Lyu et al. (2017) presented computational methods to reliably predict second order forces and moments acting on ships in waves using a Rankine source method and an extended RANS solver. Comparative results from model experiments by a DTC, a KVLCC2 and a medium-size cruise ship validated these methods to reliably and predict first and second order wave-induced ship response in different headings and wave lengths. Investigations systematically dealt with the influence of ship speed, hull shape, and encounter wave angle on second order forces and moments.

Park et al. (2019) experimentally and numerically estimated the added resistance of a large tanker in oblique waves by the self-propulsion test for seven wave directions between 0 and 180 degrees. The added resistance was estimated from the difference between the thrust of the propeller in calm water and waves. Experiments were performed in the SSPA seakeeping basin and compared with two numerical simulations: the strip method and the 3D Rankine panel method. Calculated results by the Rankine panel method agreed well with the experimental results, where viscous roll damping was accounted for by taking 3% of the critical roll damping (estimated from roll decay tests). The maximum added resistance is observed at wave headings between 180 deg and 150 deg. In the oblique sea conditions, the peak frequency of the motion response moves and the radiation-related component of added resistance can increase even in short waves. This means that it is equally important to predict the radiation related component as well as the diffraction component. The literature data of added resistance experiments were also summarized and trends were investigated (Figure 311 and Figure 312).

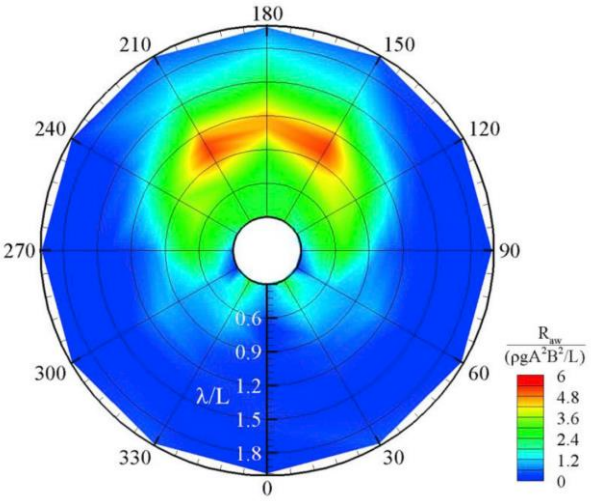

Figure 311: Polar diagram of added resistance, experiment, S-VLCC, Fn=0.137 (Park et al. 2019)

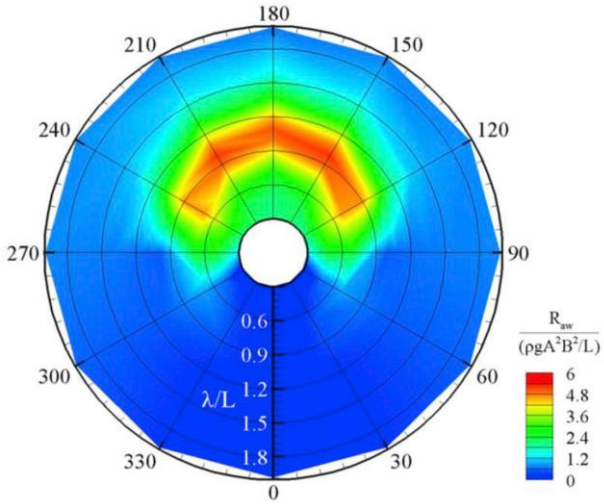

Figure 312: Polar diagram of added resistance, RPM, S-VLCC, Fn=0.137 (Park et al. 2019)

Wicaksono et al. (2018) simulated the mean forces and moments acting on an advancing ship in oblique waves based on the new strip method (NSM) and the enhanced unified theory (EUT) and compared them with published experiments. This experiment was carried out with a JASNAOE-BC084 tanker model for four different forward speeds and four wave directions. An equivalent damping coefficient was based on the component analysis method as formulated by Himeno. It was concluded from the comparison that for short waves such as wavelengths longer than λ/L=1.0, the contribution of the radiation Kochin function becomes important and the radiation Kochin function was rather sensitive to the ship's forward speed. EUT was shown to be able to predict steady force and moment better than NSM.

Zhang et al. (2020) conducted numerical prediction of wave-induced motions and steady drift forces for ships in oblique waves using a time domain Rankine panel method and validated the proposed method using published experiments of KVLCC2 of zero advance speed for six wave directions and S-175 of Fn=0.15 for head and beam waves. The roll damping coefficients were determined by the ITTC's Numerical Estimation of Roll Damping Procedure (ITTC, 2011). It was pointed out that numerical results explain the trend of experiments, but there was room for improvement.

2.7.3 Numerical and Experimental Investigation for Self-propulsion Factor & Power Increase

Added power involves propeller-hull-rudder interactions in addition to the increase in hull resistance in waves including added resistance in waves. These interactions generally add loading to the propeller and impact the wake fraction, advance coefficient, and the thrust deduction factor. As a result, the operating point shifts, requiring higher power, and possibly reducing the efficiency. Papers concerning these issues including benchmarking results are summarized below.

Sanada et al. (2020) benchmarked and assessed the capability of model experiments and CFD for the added power in head and oblique waves using experiments from three facilities and CFD from five facilities including one potential flow code. In experiments three different model sizes of KCS were used, depending on the tank size. The biases of scale

and facility are separated and validation data and uncertainties for CFD validation, including capability of predicting the scale effects were provided. It is emphasized to be important and necessary to understand hull-propeller (-rudder) interactions and scale effects, especially for single propeller/rudder ships.

Choi et al. (2020) proposed the modified thrust and revolution method to predict speed-power-rpm relationship along with resistance and propulsion characteristics in regular head waves with varying wave lengths and steepness ratios using the 'calm-water' and 'wave tests'.

Knight at el. (2018) presented a body force propeller model for unsteady conditions in order to train a semi-empirical algorithm, that with proper training data accurately predicts the thrust and torque of the propeller. This algorithm is based on analytical relations with coefficients that are determined from CFD calculations with steady motion and with harmonic surge.

Woeste et al. (2020) presented an efficient means of predicting the added resistance and added power in regular head waves, and investigated the change in added resistance and added power with different wave conditions and model sizes using the KCS model. A RANS solver was used to derive the self-propulsive factor according to RTIM and a potential flow code was used for the added resistance in waves. The added power coefficients were concluded to increase with decreasing model length scale ratio due to a reduction in advance coefficient and an increase in torque coefficient caused by a higher relative contribution of viscous effects. This added power coefficients are not simply proportional to the square of the wave amplitude.

Feng et al. (2020) studied the propulsion performance of a cruise ship with podded propulsion in waves based on model experiment. For podded propulsion, TNM was concluded to be most recommended. It is explained that the modified TNM proposed can avoid unnecessary assumptions on the wake fraction.

Hsin et al. (2018) presented numerical self-propulsion tests in waves by three different approaches of computing the ship resistance and propeller effects. A viscous flow RANS method, a potential flow boundary element method (BEM) and the strip theory were combined for computing. An unsteady body force method was developed for the propeller effect.

Tsujimoto et al. (2018) proposed the practical method to predict self-propulsion factors in waves based on the tank test. It was shown that the wake coefficient generally increases due to ship motion induced by waves, as a result the propulsion efficiency is changed.

Otzen et al. (2018) performed measurements including uncertainty with KCS during self-propulsion in calm water and head seas and experimentally assessed the added powering, and compared EFD and CFD(RANS) results to learn the performance of RANS for this application.

Sanada et al. (2018) conducted free-running tests of KCS to know more detail of added powering and propeller load fluctuations in regular waves during free-manoeuvring by CFD and EFD. The data shown in this paper is to be used as CFD validation data for several workshops.

Sigmund et al. (2017) numerically and experimentally investigated the influence of regular head waves on propulsion characteristics of a twin screw cruise ship and the single screw containership DTC using a RANS based flow solver. Experiment were used for the validation of CFD based on the RANS solver. It was concluded that for the twin screw ship the decrease of propulsion efficiency in waves was mainly caused by the propeller's efficiency and those for the containership was

caused by not only the propeller's efficiency but also the ship's hull efficiency.

2.7.4 Impact of Added Resistance in Seaway

Accurately knowing the proportion of the added resistance induced by waves in the total resistance is the basis for designing the optimum hull form based on the added resistance in waves. In addition, when combined with the problem of power estimation, a voyage simulation can be developed that can evaluate the service performance, and the role of the added resistance induced by waves in fuel efficiency performance can be visualised.

Taskar et al. (2020) discussed the impact on energy consumption by added resistance in waves. Voyage simulations were carried out using added resistance RAOs computed using different methods, CFD and potential flow, for four routes and four wave headings for the KVLCC2 and KCS at full load condition. It was concluded that the scatter in voyage energy consumption caused by different approaches and wave headings to added resistance in waves was sizable.

Skejic et al. (2020) calculated the total resistance in a seaway by combing empirical and theoretical formulae, and numerical calculations. The obtained calculation results were compared with published experimental and theoretical results and found to be in good agreement. It was pointed out that surge motion is important for the added resistance in waves.

2.7.5 Semi-empirical Formula of Added Resistance in Waves

To design a vessel that is well suited for the intended operational environment it is important to consider the effect of the main characteristics on the vessel's performance in the early deisgn stage, including added resistance in waves and its effect on EEDI and EEOI. Although resulting in reliable and accurate results, numerical calculations with CFD or Rankine Panel Methods require detailed knowledge on the ships design not yet available in the early design stage and often prohibitively high computation time, cost and effort. Semi-empirical formulae for fast estimation of added resistance in head waves have been improved based recent numerical calculations and experiments, and are much more suited for quick design iterations. Nevertheless, it must be noted that these formulae are not applicable for the design of innovative ships and hull shapes, as they are attuned to existing ships.

Lang et al. (2020) introduced a semi-empirical head wave added resistance calculation formula by combining the further tuned NMRI formula and Jinkine and Ferdinande's method. The results indicate that the proposed formula has achieved reasonable accuracy with fast calculation. Uncertainty and prediction capacity are discussed. This achievement can be expected to help evaluate the voyage optimization system requiring iteratively on millions of grid waypoints.

Lee et al. (2018) proposed a nonlinear approximation function to predict added resistance in waves using genetic programming (GP). In this paper, four Froude numbers and three types of ships (total 12 cases) were used as training data to generate a nonlinear approximation function. Accuracy was better than strip theory when comparing with experiments. It is suggested it is possible to apply GP as an alternative prediction method of added resistance in the early design process due to sufficiently accuracy in less time and at a low cost.

Cepowski (2020) proposed a nonlinear approximation function to predict added resistance in waves using an artificial neural network with basic design parameters of ship. The derived function was showed to provide good correlation with measured data. It could

have practical application in ship resistance analysis at the preliminary design stage.

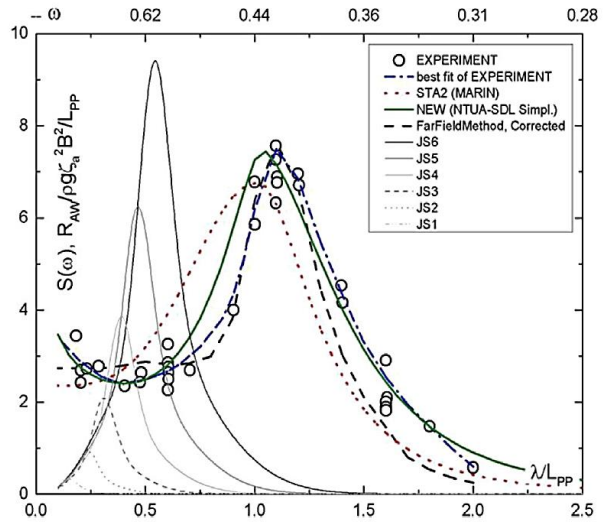

Figure 313: Prediction of added resistance of KVLCC2 ship, in irregular sea ways, Fn=0.142. NEW is proposed formula (Liu et al. 2016).

Liu et al. (2016) developed simple semi-empirical formulations for fast and satisfactory estimation of the added resistance of ships in head waves. New formulations were obtained by extending the approximate formula derived in the past to cover more types (tanker, bulk carrier, containership and cruise ship) of ships, a wider speed range (Fn = 0.0 - 0.3), and the whole range of wave lengths of interest. In short head waves the formulations were originally derived by Faltinsen et al. (1980) and in longer head waves these were proposed by Jinkine and Ferdinande (1974). Extensive validation of the proposed formula for various ship hulls in both regular and irregular waves were carried out and compared to other comparable methods and more complicated approaches to the determination of the added resistance in head waves (Figure 313**Erreur ! Source du renvoi introuvable.**).

2.8 CFD Applications

Over the period covered by the report, Computational Fluid Dynamics (CFD) popularity has kept increasing amongst researchers and naval architects interested in seakeeping. Where the previous seakeeping committee report reviewed also the basic approaches of CFD, this report section proposes a non-exhaustive review focusing on the applicative part. The significant number of published computations over the last years generally were set up for conditions where other faster methods show limitations. Most common CFD models are built on the Navier-Stokes equations with a turbulence model and discretized with Finite Volume Method, as this what is implemented in the most widely used open source and commercial fluid dynamics solvers.

As CFD allows flexibility in imposing initial and boundary conditions, therefore the topic of CFD studies is often at a crossover of traditional seakeeping applications. CFD is a high-fidelity expensive method from setting up methodology to performing computations, and some studies evaluate its accuracy and added value with respect to alternative traditional solutions.

2.8.1 Added resistance and forces on semi captive models

Wave loads on ship and specifically added resistance has been the subject of several CFD studies.

The influence of trim on the added resistance of the KRISO Container Ship (KCS) is investigated in Shivachev et al. (2020). They showed CFD is reliable enough to optimize the trim angle for added resistance on a set of regular waves. Figure 314 shows a comparison of the added resistance computed by CFD and Potential Flow compared to experiments.

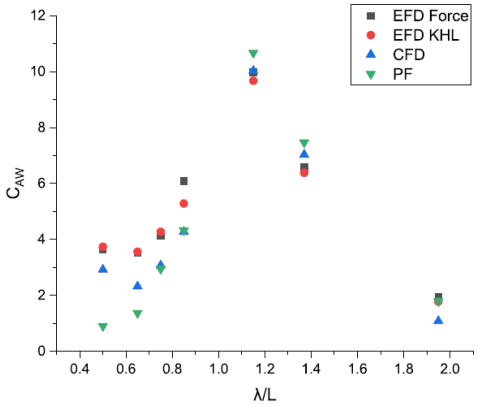

Figure 314: Comparison of CFD to Experiments and potential flow (Shivachev et al, 2020).

Added resistance in an oblique sea is investigated in Gong et al (2020) for a trimaran with forward speed up to Fr=0.47. The paper investigates the effect of wave steepness and Froude number on added resistance and discusses the influence of the numerical setup.

Wave induced forces and motions are compared with a semi captive experiment of ONR Tumblehome in irregular quartering seas in Hashimoto et al. (2019).

2.8.2 Role of shape and appendages in performance

Li et al. (2020) investigated the influence of T-foil appendages on the motions of a fast trimaran in head regular waves with three values for the wave steepness (Figure 315). The loads on the foil and their influence on the ship motions are presented. Liu et al. (2018) presented a similar simulation, investigating the role of the stern flap of a catamaran in regular and irregular sea.

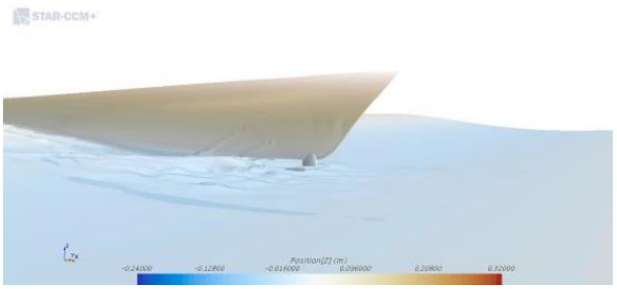

Figure 315: Snapshot of the instant where the T-foil enters the water (Li et al, 2020).

Bhushan et al. (2017) performed URANS simulations with a Surface Effect Ship (SES) in calm water and in head waves using an air cushion model. Niklas et al. (2019) performed advanced CFD full scale simulations to investigate the effect of a X-bow and a V-shaped bulbous bow form on the seakeeping performance.

2.8.3 Self-propulsion and manoeuvring in waves

In Toxopeus et al. (2018) a comparison of RANS, Potential Flow and system-based solvers performance is conducted on the free running self-propelled DTMB 5415 with and without waves. High-fidelity CFD methods are shown to be overall the best prediction tool, though the computational effort is much larger.

A set of simulations of a self-propelled free running KCS under course keeping control in head waves are performed and compared with experimental results in Choudoury et al (2020). Computations of turning circle in waves with a self-propelled Duisburg Test Case ship model are also presented in Liu et al. (2020).

2.8.4 Green water and extreme motions

The demonstration of the capability of CFD to compute loads and wave elevation occurring during a green water event is presented in Rosetti et al. (2019) with a comparison to a dedicated experiment.

The green water event is also investigated on a simplified FPSO shape with comparison to experiments in Gatin et al. (2018). A similar model but with a compressible air-phase is then used with Regular Conditioned Waves and Regular Equivalent Design wave approaches comparing the two in Gatin et al. (2019).

Impact loads exerted by focusing waves on FPSO are computed in Hong et al (2019), where motions and wave elevation and motion are compared with experiments (Figure 316).

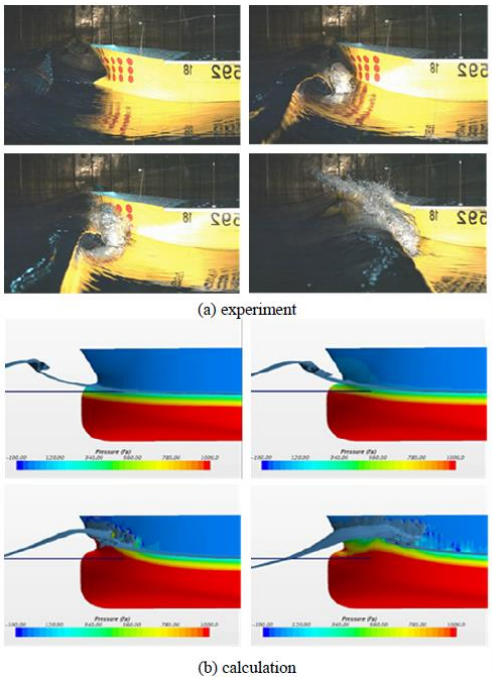

Figure 316: Comparison between experimental and numerical flow field (Hong et al, 2019)

Another simulation of a rogue wave packet impacting onto a containership is performed in O'Shea et al. (2018). The authors in this case use a procedure that incorporates a Higher Order Spectral (HOS) model and the Numerical Flow Analysis (NFA) code.

Zhuang et al. (2020) proposed the coupling of a HOS wave model to generate extreme wave conditions with finite volume CFD to simulate the response of a ship. Deterministic validation using experimental data is proposed in an irregular sea.

Similarly on the topic of design in extreme conditions, Knight et al. (2020) performed a study of a self-propelled ship using the Design-Loads Generator (DLG) approach to construct a desired seaway over a short time window around an extreme response.

2.8.5 Hydrodynamic coefficients and roll damping

CFD is also used as an intermediate step in a hydrodynamic (seakeeping) assessment. Several works were dedicated to the computation of hydrodynamic coefficients. This is done for the heave and sway motions of several ship hull sections in Gadelho et al. (2018). The roll motion is also investigated, because of the importance of viscosity in this motion and its poor handling by the potential flow model. A detailed study about the role of bilge keel is presented in Irkal et al. (2019) and roll damping is investigated Kianejad et al. (2018) and added mass inertia in Kianejad et al. (2019).

2.8.6 Fluid Structure interaction

In Takami et al. (2018), a one-way coupling between high-fidelity CFD code for the fluid and Finite Element Analysis for the structure is performed to evaluate global and local loads. The results are compared with experiments and with strip methods and panel methods, showing that the gain of accuracy of the fully coupled model is not large for this case (a container ship).

In Lakshmynarayanana et al. (2019) two-way coupling is performed between commercial FEA and CFD solvers to predict dynamic behaviour of a flexible barge.

El Moctar et al. (2017) develop a two-way coupling with a finite element Timoshenko beam method and applied it to three different hulls, showing that the methodology is

satisfactory for assessing slamming-induced hull whipping.

2.9 Seakeeping of High Speed Marine Vehicles

Sailing with high speed craft in calm water and in waves is associated with very dynamic behaviour related to dynamic stability and impacts. High speed craft in waves are subjected to significant and frequent impacts with large effects not only on the structural integrity but also on human performance and human safety.

Research is not only focused on model tests and predictions by means of computations, but also full scale recordings play an important role. There is more and more interest in using ride control systems to not only improve passenger comfort, but also in actively reducing slamming itself.

Over the past five years the most investigated types of high speed marine vehicles are monohulls, followed by wave piercing catamarans and trimarans. There seems to be a growing interest in hydrofoiling craft and foil assisted craft, possibly related to the introduction of hydrofoils in high profile sailing matches such as the America's Cup.

2.9.1 Experimental

Camilleri et al. (2017) performed full-scale rough water trials and drop tests with a 9.6 metre high speed planing craft, measuring rigid body motions, accelerations, pressures and strains. They compared the full scale drop test results to CFD computations and predictions of classification society rules and standards to assess their accuracy. In addition they performed preliminary comparisons between the rough water trails and the drop tests, highlighting the need to further investigate how to relate both.

Davis et al. (2017), Shahraki et al. (2017) Shabani et al. (2018), and Shabani et al. (2019) describe model tests with a 2.5 metre hydroelastic model of a 112 metre fast wave-piercing catamaran fitted with a centre bow (Figure 317) in regular and irregular head waves. They measured loads and pressures on the centre bow and on the hull. Variations of centre bow length showed that for increasing centre bow length the slamming loads increased significantly while the maximum peak pressures varied to a lesser extent. Increasing the height of the centre bow archways (and thus wet deck height) led to a decrease of the slam loads and the vertical bending moment at the cost of larger heave and pitch motions while the peak pressures were less affected. It was also found that wave encounter frequency has a strong effect on the location of maximum pressure along the centre bow.

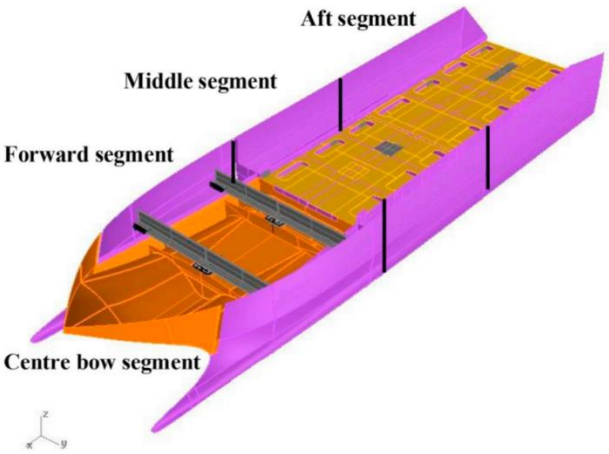

Figure 317: Hydroelastic segmented wavepiercing catamaran model with a centre bow (Shabani et al., 2018)

Katayama et al. (2018) noted the underprediction of roll damping in Ikeda's method for small planing craft due to the absence of lift damping. They investigated roll damping by means of model tests with a model of a small planing vessel forced in roll (Figure 318). They proposed an estimation method for the lift component of roll damping based on

previous work by Payne and showed a good comparison with their experimental results.

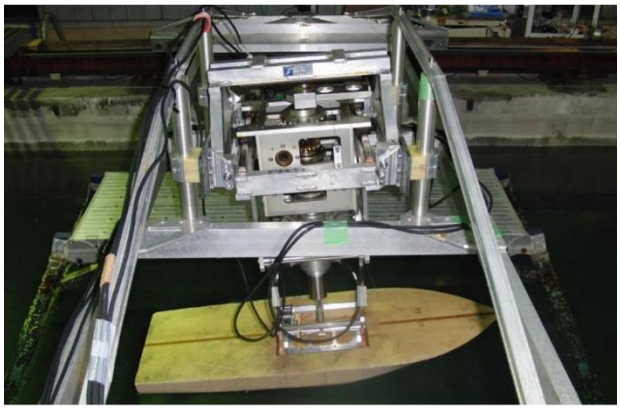

Figure 318: Forced roll test setup (Katayama et al., 2018)

Durante et al. (2020) performed an experimental study of a catamaran in head seas, including uncertainty quantification. The aim of the study was to obtain a statistically-converged experimental benchmark dataset of a catamaran in irregular waves, along with a regular-wave Uncertainty Quantification (UQ) model used to approximate the relevant statistical estimator.

Judge (2020) measured bottom pressures on a model of a high speed planing monohull in regular waves. She applied a pressure reconstruction method to obtain an estimate of the spatial pressure distribution based on point measurements and compared this against empirical formulations.

2.9.2 Numerical

Numerical methods applied for the seakeeping of high speed craft need to cope with highly nonlinear behaviour due to the large variations in wetted surface and impacts. This results in the adoption of nonlinear time domain methods. Besides the more traditional nonlinear 2D+t potential flow methods, nonlinear 3D panel methods have gained significant popularity in recent years. Also CFD methods are slowly gaining terrain. Nevertheless, the highly nonlinear nature of the problem and the importance of obtaining sufficient statistics (and hence requiring significant time durations of simulations) are still difficult to overcome with CFD.

2.9.2.1 Nonlinear 2D+T methods

Ghadimi et al. (2016) proposed a mathematical model based on the 2D+T potential theory and implemented pressure distributions over length of hull in order to compute forces for performance prediction of hard-chine boats which can be used in both semi-planing and planing regimes. Tavakoli et al. (2017a), (2017b) and (2018) extended the 2D+T potential theory to include the prediction of hydrodynamic coefficients of a heeled planing hull in the vertical plane. The accuracy of the method is evaluated by comparing its results against previous empirical methods. The same method is also validated for longitudinal motions without heel in waves for a wide speed and frequency range by Pennino et al. (2018). Allaka and Groper (2020) validated the approach using full scale results.

Consolo et al. (2020) attempted to improve a 2D+T strip theory method for seakeeping of high speed craft to enable the inclusion of roll motions. They treated asymmetric wedge impact by separately considering portside and starboard side wedge parts. Roll damping was estimated based on various methods and successfully validated against captive model tests. Results in waves still showed under prediction of the roll motions.

Garme (2020) studied the modelling implications of various three dimensional geometric variations such as bottom warp in a 2D+T method by comparing simulations with the results of model tests. He concluded that warp can indeed be modelled with the 2D+T method and stressed the importance of combining numerical and experimental methods in research and design.

2.9.2.2 Potential flow methods

Van Walree and Thomas (2017) and Van Walree et al. (2019) and Bird et al. (2017) developed a nonlinear time domain 3D panel code and validated it with both model scale and full scale test results for a Rigid Hull Inflatable Boat (Figure 319). Van Walree et al. (2018) also applied their nonlinear panel code for predicting the seakeeping behaviour of and hydrodynamic loads on high speed craft operating in a seaway.

Figure 319: Fully free running RHIB model during seakeeping model tests (Van Walree and Thomas, 2017)

Bonci et al. (2017a), (2017b) and (2020) modified the same time domain 3D panel code to include the heel-sway and heel-yaw coupled effects empirically and applied the modified approach to the manoeuvring in following waves of a rescue vessel of the Royal Netherlands Sea Rescue Institution (KNRM) shown in Figure 320. Finally, impulsive loads on the bow door of and water ingress into a landing craft shown in Figure 321 has been investigated by applying the same time domain 3D panel code (Van Walree and Sgarioto, 2019).

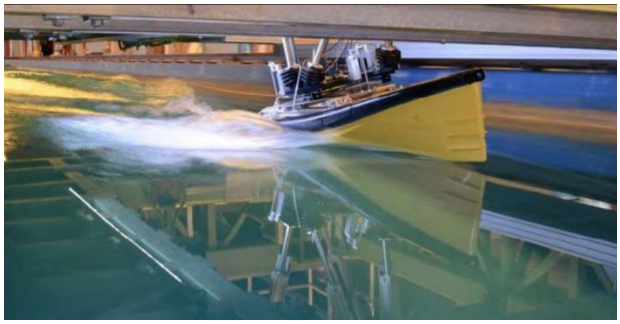

Figure 320: Captive model tests with a SAR boat of the Royal Netherlands Sea Rescue Institution (Bonci et al., 2017b)

Figure 321: Model of a fast landing craft used for impact and water ingress model tests (Van Walree and Sgarioto, 2019)

O'Reilly et al. (2017) and (2018) developed a new set of formulations for potential-flow methods that retains the important nonlinear features while maintaining computational efficiency. These formulations include steady and quasi-nonlinear approaches where memory effects are weak. Their initial results are encouraging, with better results in more extreme waves, but still over-predicting for more modest waves.

Kihara et al. (2019) investigated the strength of the cross deck of a trimaran sailing in regular beam and oblique seas by combining pressures obtained from 2D potential flow theory with a Finite Element Method for the whole vessel. They compared the predicted motions with the results of model experiments with reasonable results.

2.9.2.3 Computational Fluid Dynamics

The field of Computational Fluid Dynamics (CFD) continues to advance with several new accomplishments also in the field of high speed craft design. Ahmad et al. (2017) performed a literature review of the application of advanced CFD simulations over the time period 2007 to 2015 in terms of software tools available and the application to hull form optimization, resistance, and seakeeping analysis and propulsion systems.

Wei et al. (2017) attempted to predict hull hydrodynamics of a semi-planing wave-piercing craft shown in Figure 322 both in calm water and waves by numerical simulations based on CFD. They used a RANS based method and studied various mesh adaptation techniques. Although their calm water results compared reasonably against experimental data, their results for motions showed not a favourable match yet. Yuan and Wang (2018) used commercial CFD software (RANS) to simulate porpoising of a trimaran planing boat shown in Figure 323. They investigated the influence of speed and the centre of gravity location on the vessel motions, resistance, pressures and streamlines during porpoising. They noted the effect of aerodynamic lift on porpoising.

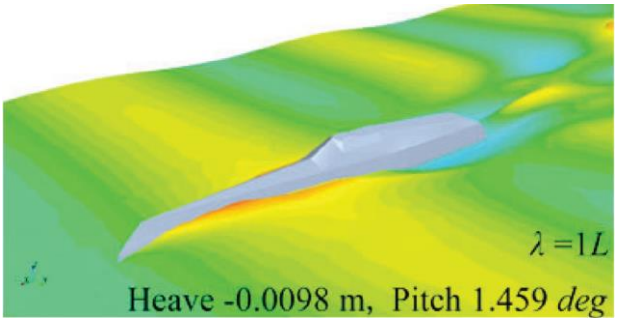

Figure 322: Snapshot of a semi-planing wave-piercing boat in waves using CFD (Wei et al., 2017)

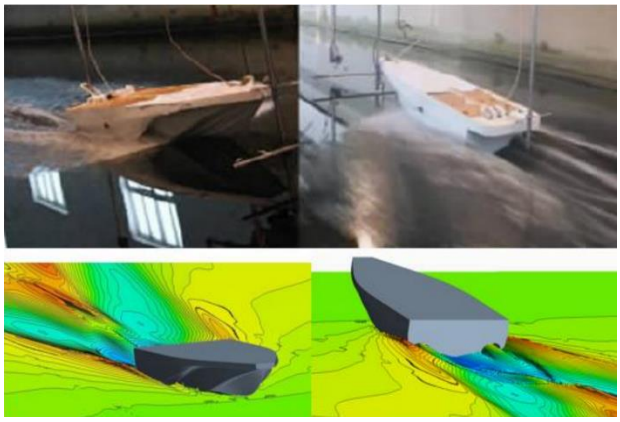

Figure 323: Bow and stern wave characteristics of a trimaran planing craft, CFD versus experiment (Yuan and Wang, 2018)

Yildiz et al. (2017) compared experimental data obtained from forced roll experiments (by Katayama et al., 2018) with CFD results obtained with commercial software, showing good agreement provided that the grid was sufficiently refined.

Ghadimi et al. (2019), through a two-stage approach, simulate the seakeeping and slamming phenomenon of a wave-piercing trimaran vessel by Flow-3D software. In the first stage, the seakeeping of the vessel was investigated in the presence of irregular waves. In the second stage, a water entry problem was simulated for bow section to calculate the slamming pressure for the worst sailing condition based on the relative vertical velocity obtained from the first step.

Diez et al. (2020) performed fluid structure interaction computations for 1-way and 2-way coupled computational fluid and structural dynamics for a bottom panel grillage of a high speed vessel in regular waves. They used an incompressible RANS/DES solver designed for ship hydrodynamics to compute the hydrodynamic loads (Figure 324). Only small differences between 1-way and 2-way coupling were observed in the pressure signals. They showed a good comparison of computational and experimental data, indicating that the accuracy of CFD, rigid-body motions, structural dynamics, and fluid-structure interaction was overall satisfactory.

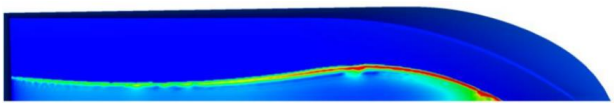

Figure 324: Evaluation of hydrodynamic loads by CFD (Diez et al., 2020)

Judge et al. (2020) presented the results of numerical simulations and model tests for a high speed deep-V planing hull operating in head waves. Both simulation and experimental pressure measurements showed re-entering and emerging peaks (Figure 325). Emerging slams

occur as the next wave peak arrives and pushes the boat to go airborne again. They evaluated the effectiveness of the most probably regular wave representation to predict hull performance in irregular waves with mixed results for emerging and re-entering slams and slam duration. The irregular wave comparisons between experiment and simulation indicated that longer run times are required to achieve statistical convergence for the slamming variables. The experimental mount and wave quality, especially for irregular waves, were factors for validation of resistance and slamming.

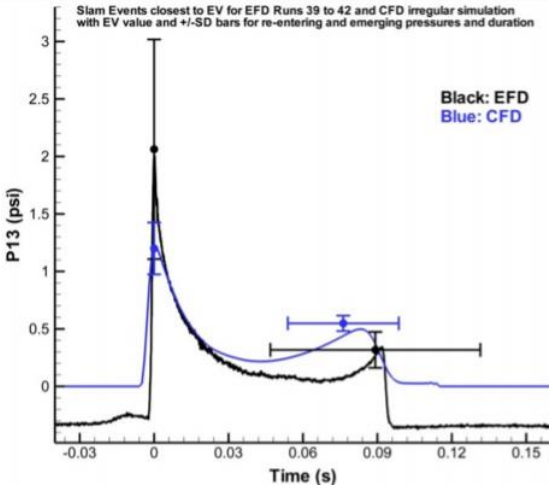

Figure 325: Computed and experimental slamming with emerging and re-entering pressure peaks (Judge et al., 2020)

2.9.3 Statistical analysis

Alwis et al. (2017) investigated the association between working conditions aboard HSC (High-Speed Craft) and its outcomes in terms of acceleration exposure and crew health and systems performance respectively. They collected data through questionnaires tailored to personnel operating high speed craft and by monitoring craft accelerations over longer periods of time. Their results show a promising correlation between the self-reported subjective exposure and the measured objective acceleration. Data indicates a comparatively higher prevalence of musculoskeletal pain in the study population than that of the general population.

Magoga et al. (2017) investigated various methods for identifying slamming impacts in full-scale time records for structural response analysis for an aluminium high speed patrol boat. They discussed an approach to analyse full-scale time records of hull girder stresses, decomposition of the wave-induced and impact components of stress, and definition and detection of slam events. Such knowledge supports informed decision-making in regards to the sustainability and maintainability of the vessel.

For safe operation, it is important to estimate statistical short-term or long-term prediction of occurrence of undesirable large vertical accelerations and avoid its occurrence. Begovic et al. (2016), Katayama and Amano (2016) and Rosen et al. (2018) investigated the statistical characteristics of vertical accelerations and probability distribution of individual acceleration maxima. Begovic et al. (2016) concluded that the Weibull distribution provides the best balance between accuracy and practical use for statistical analysis of vertical acceleration maxima. Rosen et al. (2018) scrutinized the various semi-empirical methods in use by classification societies for the assessment of vertical accelerations. They raise important questions about usage of these semi-empirical methods in high speed craft design and the assessment of safety levels. Figure 299 illustrates how various aspects limit the attainable speed in waves.

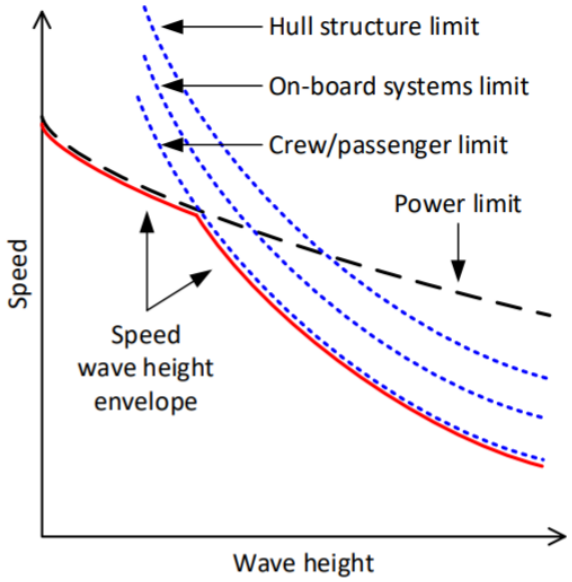

Figure 326: Different aspects limiting the speed in waves and definition of the speed-wave height envelope (Rosen et al., 2018)

2.9.4 Ride control systems

Terada et al. (2017) investigated a time series model for model predictive control to develop a control method for automatic dangerous situations avoidance using an on-board monitoring system of the vertical acceleration. A radial basis function-based state-dependent autoregressive (RBF-AR) model is selected, since it is confirmed that the model is effective to predict nonlinear phenomena. De Castro-Feliciano et al. (2018) applied an ACS (Active Control Systems) to improve seakeeping and propulsive performance.

AlaviMehr et al. (2019) investigated the optimisation of a Ride Control System to reduce the motion, global loads and slamming responses of the same 112 metre catamaran by means of model tests. The ride control system comprised two transom stern tabs and a T-foil beneath the bow (Figure 327). Various control modes were investigated. It was found that the pitch control mode was most effective, reducing the water entry impulse by 40% and the total strain energy by 90% when compared to a bare hull with no control surfaces fitted.

Figure 327: Wavepiercing catamaran model fitted with RCS (AlaviMehr et al., 2019)

2.9.5 Novel and complex concepts

The application of foils to high speed craft is undergoing a revival in recent years. A development that is possibly driven by the adoption of foiling craft in high profile sailing races such as the America's Cup and the Volvo Ocean Race. Also the advances in material science and the increased adoption of carbon reinforced plastics could play a role in this: making it easier to manufacture light and strong complex structures.

2.9.5.1 Foiling and Foil Assisted Craft

Labat (2017) developed a simplified 2D heave-pitch model of a 45 feet foiling catamaran to study control strategies for the vertical plane dynamic stability. study about evolution of equilibrium of a fast Morace and Ruggiero (2018) performed comparative model tests in calm water and in waves for two surface piercing hydrofoil configurations of a new fast ferry (Figure 328). They touch upon fundamental points such as the wing profile optimization and the structural design and manufacture process to improve both resistance characteristics as ride comfort.

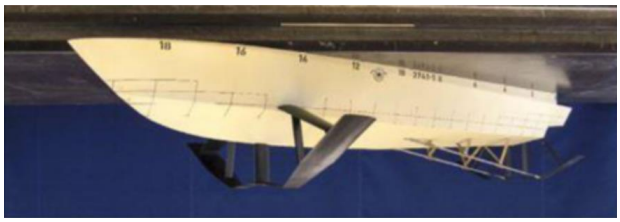

Figure 328: Model of hydrofoil ferry (Morace and Ruggiero, 2018)

Wang et al. (2019) investigated the motions of an unmanned catamaran with fixed horizontal tandem foils to drive the catamaran using a RANS CFD method and a BEM method. Wang et al. (2016a) investigated the vertical plane motion control in rough waves of an S-SWATH (S-type Small Waterplane Area Twin Hull) vehicle equipped with a flapping foil stabiliser. They modelled the fin forces with CFD and the hull forces with strip theory and derived a numerical model and a controller. The concluded that the flapping fins outperformed a conventional fin due to higher lift coefficients and lower drag coefficients.

2.9.5.1 Other Complex Craft

Liu et al. (2019) presented an experimental study of the motions of an ACV (Air Cushion Vehicle) in regular waves. They used customized fans with characteristic curves similar to the ones installed in the ACV to satisfy the laws of similarity. They explored different bag-to-cushion pressure ratios, which usually have a significant influence on the motion. The experiment was carried out with a variety of wave parameters in order to investigate the motions in waves.

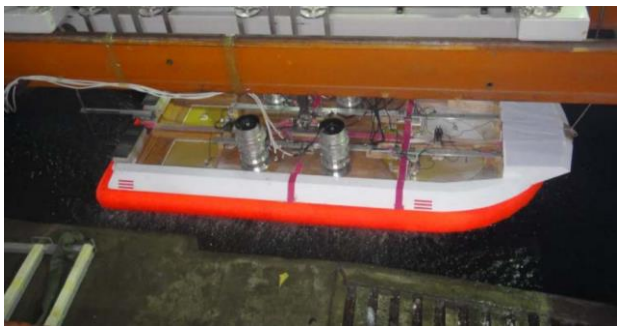

Figure 329: Model of ACV (Liu et al., 2019)

Suspension systems. Han et al. (2018) give an overview of an evolution of cabin suspended ships, called Wave Harmonizer (WHzer). An example is shown in Figure 330. The main focus of this concept is motion reduction and wave energy extraction. The configuration studied were catamaran or trimaran ships with the hulls attached to the cabin by means of suspension systems (passive or active spring-dampers) to isolate the motions of the hulls from the cabin. They developed various passive and active control systems. Model tests in waves were performed to determine motion characteristics and energy production.

Figure 330: WHzer Type 7 (Han et al., 2018)

Li et al. (2018) performed numerical simulation of a trimaran with a deformable (elastic) connection between main and side hulls at design speed in head waves. Their results indicated that the elastic connection helps to reduce heave motions of the main hull and the added resistance in regular waves.

Wielgosz et al. (2020) explored the prospects of using scaled model experiments for capturing the influence of a novel spray deflection concept on planing craft performance in calm water and in waves. Their results give a first indication of the potential for both reduction of the resistance and the accelerations on waves.

3. DISCUSSION OF SPECIFIC TOPICS

3.1 Benchmarks

A review of available benchmark data related to seakeeping issues was performed in relation to Task 12 of the Terms of Reference of the Seakeeping Committee. A discussion of the analysis can be found in Appendix A. A table to the identified benchmarks can be found in Appendix B.

3.2 Uncertainty in Added Resistance

The 'weather factor' f_w for decrease of ship speed in wind and waves is one of the terms in the Energy Efficiency Design Index, EEDI, (IMO, 2014). A key component to determine f_w is the added resistance of a vessel in waves. At this point the relevant ITTC, ISO and IMO procedures leave open many options to determine the added resistance in waves, by model experiments or by various levels of computations. In this section various sources of uncertainties that arise for the various approaches for added resistance in waves are outlined. The details regarding the determination of f_w are outlined in ITTC Recommended Procedure 7.5-02-07-02.8 (ITTC, 2018).

3.2.1 Model Experiments

Experimental methods to determine added resistance in waves rely on the measurement of the total resistance obtained from model tests in either regular or irregular waves R_W and subtracting the total calm water resistance R_T obtained from model tests in calm water.

$$\Delta R_{wave} = R_W - R_T \tag{1}$$

Both total resistance components are relatively large in magnitude compared to their difference: the added resistance in waves. This makes added resistance based on model tests in waves inherently vulnerable to uncertainty. The effect is discussed by Park et al (2019), see also Figure 331 below.

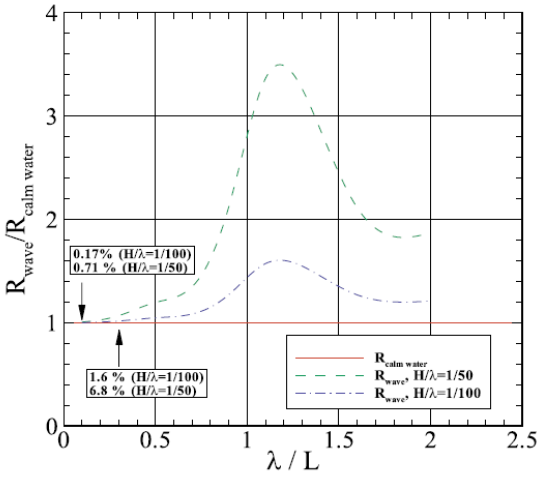

Fig. 2. Approximate ratio of added resistance to calm water resistance, KVLCC2 model (1/100 scale), $Fn = 0.142$.

Figure 331: Approximate ratio of added resistance to calm water resistance KVLCC2 model. (Park et al. 2019)

There are not many papers available that systematically investigate the uncertainty associated with added resistance model tests. One of the more complete attempts is described Park et al. (2015). They performed an uncertainty assessment in accordance with the

ITTC Procedures and Guidelines for an added resistance test with the KVLCC2 in regular head waves. They summarized the sources of uncertainty and propagated these to obtain the uncertainty of the heave and pitch motions and the added resistance.

The results of Park et al. (2015) indicate that the uncertainty for added resistance in regular waves is dominated by the measurement accuracy of the resistance in calm water and in waves and the wave amplitude (Figure 332). The uncertainty levels they obtained for short waves, at the RAO peak, and for long waves are indicated in Figure 333. A more detailed assessment showed that this mainly related to the Type B uncertainty of these components, i.e. calibration and measurement uncertainty of these three quantities.

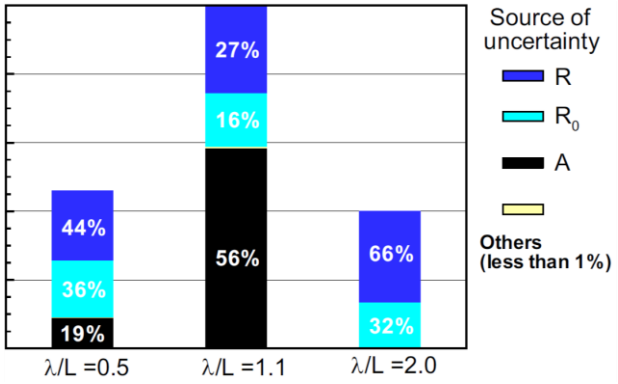

Figure 332: Sources of uncertainty in added resistance (R – resistance in waves, R_0 – resistance in calm water, A – wave amplitude) (Park et al., 2015)

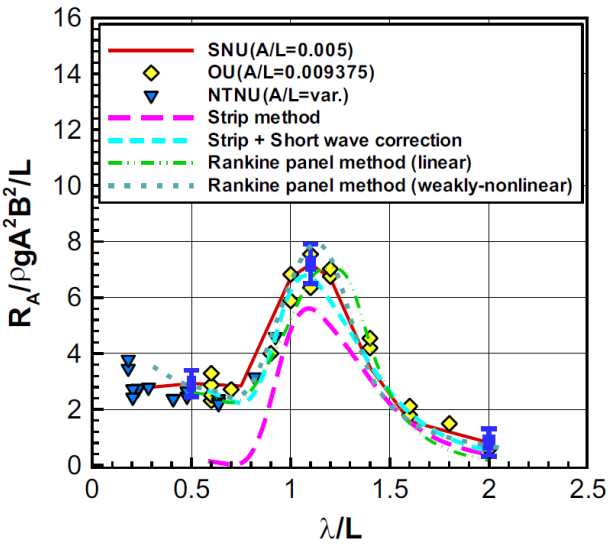

Figure 333: Added resistance with uncertainty bands (at 95% confidence level) of added resistance tests (Park et al., 2015)

These results highlight the need for a focus on accurate measurement of the resistance force and wave elevation. This will be further elaborated below by focusing on the test setup for added resistance tests and the incident waves.

A number of choices are available for the experimental setup of added resistance tests, each with their own advantages and disadvantages. These choices include:

1. Whether to perform tests in regular versus irregular waves,

2. Whether and how to constrain the forward speed,

3. Using self-propelled (and auto pilot controlled) versus unpowered models,

Testing in regular waves is the only way that allows to obtain the Quadratic Transfer Function (QTF) of the added resistance with respect to the incident waves directly. Tests in irregular waves are interesting, as they provide more realistic results, including all possible nonlinearities. When performing tests in irregular waves it is important to allow speed variations of the model

to temporarily slow down when sailing in a higher wave group to have realistic motions.

For added resistance tests in general the model needs to, at least, be free to heave and pitch, as these motions are strongly linked to the generation of added resistance in waves. For oblique conditions also the roll and possibly sway and yaw degrees of freedom need to be free. The surge motion can be fully restrained (captive), partly restrained (for instance soft-moored, or using a sub-carriage) or fully free. It is advised to use the same model (with the same loading condition) and test setup for both the calm water tests and the tests in waves to reduce uncertainty e.g. with respect to model building inaccuracies and scaling effects.

Captive setups are easy to implement and allow direct measurement of the surge force at a constant speed. A main disadvantage is the relatively high loading of the force transducers: a relatively high capacity force transducer is needed to cope with large forces during the model acceleration and deceleration phases and with the oscillation of the instantaneous (first order) forces. This reduces the accuracy of the mean force measurement that is required for determination of the added resistance (Park et al., 2015). An advantage of the constant speed is that the interpolation error when obtaining the calm water resistance can be very low, by simply performing the calm water tests at the exact same model speed.

Soft-moored test setups or setups that allow the first order surge motions by using lightweight actively controlled or spring-mounted sub-carriages have the advantage that the transducer loads are reduced by avoiding the first order surge forces. These tests are also referred to as surge free or ‘constant thrust’ tests (Park et al., 2015), although the latter is only strictly true when using an actively controlled towing device.

Surge free test setups allow the use of more sensitive force transducers and therefore can offer better accuracy. The soft-moored test setup needs to be carefully designed to not affect the magnitude of the first order surge motions and the added resistance by using an appropriately selected spring stiffness. Sadat-Hosseini et al. (2013) describe a test setup using a soft-moored test setup with an external force to avoid too much stretch in the soft springs. Gerhardt et al. (2020) used a similar test setup with soft springs to let the model free to surge, but do not introduce external forces.

Multiple sources indicate that the differences in added resistance due to waves measured with surge free or surge fixed is negligible. Sadat-Hosseini (2013), Park et al. (2018), and Kjellberg and Gerhardt (2019) confirmed this in both experimental and numerical results (for instance in Figure 334 and Figure 335). Surge free setups are necessary when performing tests in irregular waves.

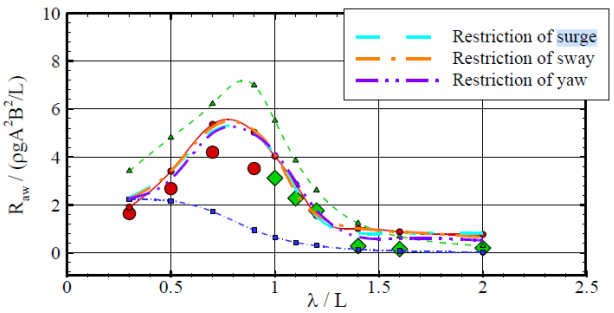

Figure 334: Effect of motion restriction on added resistance in oblique waves (Park et al., 2018)

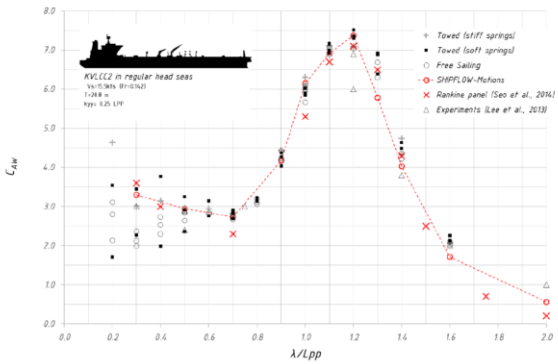

Figure 335: Effect of test setup on added resistance (Kjellberg and Gerhardt , 2019)

An alternative is to perform self-propulsion tests in waves using a fully free-running test setup with a self-propelled model, see for instance Lee et al. (2020). Then the thrust is measured directly on the model propeller and the added resistance is determined by taking the difference between the thrust in waves and the thrust in calm water and using the thrust deduction factor *t*:

$$R_{AW} = \left(T_{wave} - T_{calm}\right)\left(1-t\right) \tag{2}$$

The advantage is that model is allowed to perform completely realistic motions for all possible headings, while avoiding a complex semi-captive test setup. Nevertheless, the added resistance is derived from the thrust under the assumption that the thrust deduction factor remains unchanged in waves. There does not seem to be very much systematic research available to verify this.

Rather than determining the added resistance, self-propulsion tests in calm water and in waves can also be used to determine the added thrust or added power in waves directly. Added power is different than added resistance, as it also involves complex propeller-hull-rudder interactions on top of the hull resistance in waves (Woeste, 2020). To maintain speed in waves the increased propeller loading must be compensated by increased propeller revolutions, torque and power. In experiments care needs to be taken to compensate Reynolds scale effects on the viscous resistance. Tsukada et al. (2013) developed an auxiliary thruster for free running model tests to obtain a correct propeller loading at model scale on a free running model. Otzen et al. (2018) provide a complete uncertainty assessment of captive added powering tests in waves.

A further complication of a surge-free test setup can be that the ship speed now varies over time and the average speed is not exactly controlled. The mean speed is therefore probably slightly different in the test in calm water and in the corresponding test in waves. This may introduce interpolation errors when subtracting the calm water resistance.

Hybrid solutions also exist that combine a captive or soft-moored test setup with a self-propelled model or an additional external force allowing more sensitive and accurate force transducers. Examples can be found in the work of for instance Son et al. (2010), Sadat-Hosseini et al. (2013) and Crepier at al. (2019). The added resistance is then determined by combining the towing force with the additional forces. Again, when using a propeller, the assumption is made that the thrust deduction factor is constant in waves. In some cases clamps are used to temporarily restrain the model during acceleration and deceleration, to allow more sensitive force transducers, similar setups are sometimes used for soft-moored and fully free running tests.

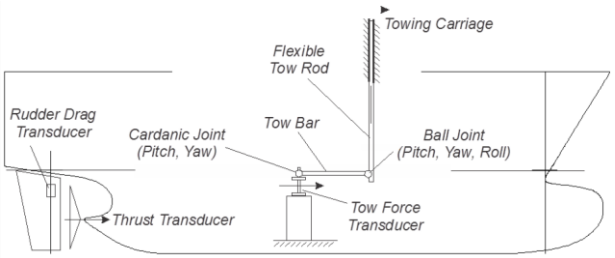

Figure 336: Hybrid test setup for added resistance tests (Crepier et al., 2018)

Regarding the incident waves, these are subject to variability. If the input conditions are accurately repeated (same wave generator flap motions, same location of the wave probe and model, perfectly still starting conditions) then two types of variability can be considered. First, the 'seed variability' (Scharnke et al., 2012) related to the finite duration of wave generation, where different random phase distributions of the wave components in the wave spectrum realisation lead to different statistical

characteristic values (i.e. standard deviation, significant value) of the wave elevation realisation. Increasing the test duration will reduce this variability; ITTC Procedure 7.5-02-07-02.2 (ITTC, 2014) recommends 1 to 1.5 hours real time equivalent for irregular waves. This is especially important for 2nd order forces such as added resistance forces.

The second variability can be termed 'basin generation variability'. This variability is related to the repeatability of waves generated in a test basin. This type of variability was studied by Van Essen (2019) and Van Essen et al. (2020), including the effect on the responses of a vessel moving at forward speed in waves. They demonstrated that this variability increased with increased propagation distance from the wave generator, even though the wave generator flap motions and the model location in the basin were very well repeatable. Likely causes are the basin memory effects such as small residual currents after repeated wave generation that die out only very slowly as indicated by Van Essen and Lafeber (2017) and the poorly repeating influence of wave breaking for steeper wave conditions. Variability in ship responses is strongly related to the variability of the incident waves.

Residual basin flows can also have an effect on the calm water resistance. Repetition of calm water tests between tests in waves can be used to obtain the evolution of the calm water resistance of time and monitor or even correct their effect in the added resistance. Residual basin flows and overall turbulence levels in the basin can have a significant effect on the added resistance, especially for low valued added resistance associated with low forward speed and small wave amplitudes. This is again related to the subtraction of two large total resistance values to obtain the added resistance, especially for low wave amplitude conditions, resulting in a very large uncertainty of the added resistance. Crepier at al. (2019) demonstrated the effect of the uncertainty of the calm water resistance as function of wave amplitude on the quadratic transfer function of the KCS (Figure 337).

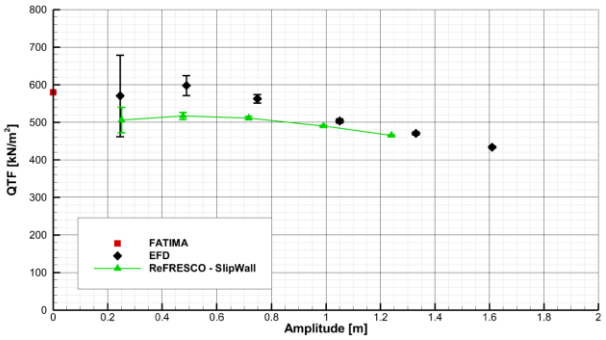

Figure 337: Effect of uncertainty of the calm water resistance on added resistance of the KCS from model tests (EFD), potential flow (FATIMA) and CFD (ReFRESCO) (Crepier et al., 2019)

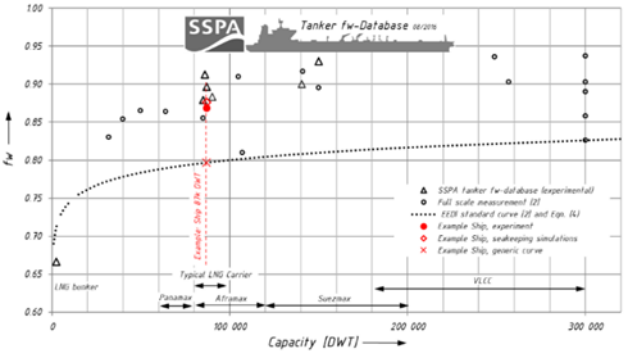

Figure 338: Weather Factor f_w as function of DWT from Gerhardt and Kjellberg (2017)

3.2.2 Numerical Methods

As outlined in ITTC Recommended Procedure 7.5-02-07-02.8 (ITTC, 2018) on the calculation of f_w there exist four categories of prediction methods, with ever increasing fidelity:

1. Empirical prediction methods,
2. Slender body theory (two-dimensional strip theory) frequency domain methods,
3. Three-dimensional panel methods, frequency or time domain,

4. CFD methods, based on the Euler Equations or on the Navier-Stokes equations.

Whereas most of the current numerical methods give very reasonable results for the added resistance for the longer wave length to ship length ratios, the accurate prediction of added resistance for shorter waves is still challenging for many approaches. Liu and Papanikolaou (2016a) give a good overview of the challenges of various numerical methods to capture added resistance in particular in short waves.

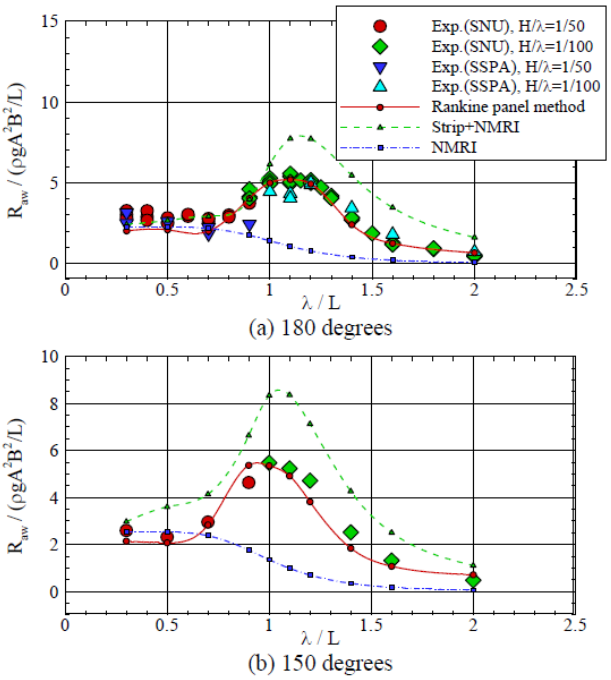

Figure 339: Added resistance of a VLCC by various experiments, empirical correction methods and potential flow methods (Park et al., 2018)

Slender body (or strip) theory does not sufficiently capture abrupt hull form changes in the bow region that drive the generation of added resistance in short waves. This may be to some extent corrected by extensions to slender body theory such as the EUT method (Kashiwagi, 1992). Oblique headings often are even more challenging to predict by slender body theory as illustrated by Figure 339. Three-dimensional panel methods are better at capturing hull form effects, but often underestimate the added resistance.

Forward speed effects are often ignored in both two and three dimensional potential flow methods. Proper wave propagation at forward speed of the radiated and diffracted waves can significantly. Modern advanced panel methods such as Rankine Panel Methods and Green function methods with exact forward speed effects or similar that resolve the potential flow interactions at forward speed show significantly improved results compared to linear zero speed free surface Green function methods (Park et al., 2016, 2018, Bunnik, 1999, Bunnik et al. 2010, Woeste et al., 2020). Often very small fine grids are required on the bow and the free surface around the bow to correctly resolve the flow (Seo et al., 2014).

However, wave-breaking and viscous effects are not captured by potential flow methods. In short steep waves waterline variations due to the changing submerged geometry of the bow and wave-breaking can cause the relation between added resistance and incident wave height to deviate significantly from being quadratic as demonstrated by for instance Crepier et al. (2019) for a wave length to ship length ratio of 1. They showed that the majority of the added resistance is generated in a small region around the waterline at the bow and fore shoulder.

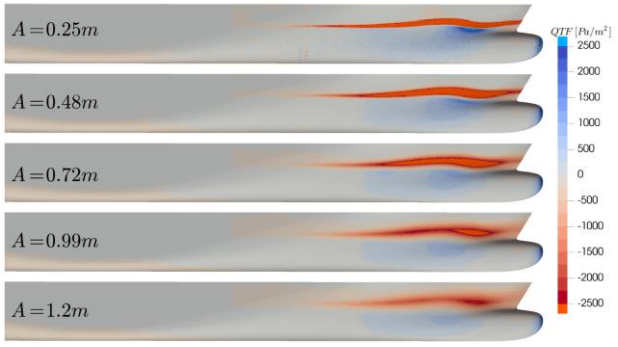

Figure 340: Spatial QTF distributions of pressure over wave amplitude squared for the KCS for various wave amplitudes A, λ/L = 1 (Crepier et al.,2019)

The dynamic waterline variations as function of the ship motions cannot be captured by linear and weakly nonlinear panel methods, breaking the quadratic relation between added resistance and incident wave height. This is illustrated in Figure 337 by Crepier et al. (2019), showing a reduction in QTF as function of wave amplitude. The plot illustrates that CFD results predict a similar trend as the experiments for increasing wave amplitude, and converge to the linear potential flow result for decreasing wave amplitude.

CFD can offer improved predictions of the added resistance that account for these nonlinear effects, viscous effects and wave breaking. This is illustrated by a large number of verification and validation studies, such as Sadat-Hosseini et al. (2013) and Seo et al. (2014) amongst many others. Nevertheless, although nowadays CFD methods can be very useful to validate the added resistance for a few specific conditions, they are still too expensive to compute a full matrix of speed, heading, and wave frequency conditions. Also, it should be noted that currently most CFD work focussed into the wave added resistance, and not the wave added power which is significantly more expensive to simulate. The quality of the outcomes of advanced CFD methods still highly depend on the experience of the user. To obtain satisfactory results requires significant attention to grid generation, grid density and modelling details.

Many semi-empirical methods are proposed to compute or correct the added resistance in short waves, these include the NMRI method (Kuroda et al., 2008), StaWAV I and II methods (ITTC, 2014), Faltinsen's method (Faltinsen et al., 1980). The NMRI method seems to be most widely used. Combined with relatively simple potential flow methods relatively complete and in many cases reasonable estimations of the added resistance can be obtained. Nevertheless, there are also many examples, especially in oblique conditions (Park et al., 2018), where these methods offer less than reasonable agreement with experiments. Also, like strip theory methods, these methods have a larger uncertainty compared to panel methods, CFD and experiments, and have limited capability to distinguish the effect of small design changes (see for instance Park et al., 2016).

At this moment, for modest sea states where nonlinear effects do not play an important role modern panel methods that account for the steady flow interactions seem to offer a reasonable balance between modelling effort and calculation time and accuracy of the results. For these cases the quadratic relation between wave height and added resistance holds. For very short and steep waves and breaking waves, model experiments and/or complex CFD computations currently still seem to be the best options to obtain accurate predictions of the added resistance. Achieving sufficiently accurate predictions of added resistance requires careful attention to the details of the computations or experiments, as well as significant computational resources for CFD.

3.3 Control of High Speed Marine Vehicles in Model Tests

Model tests with High Speed Marine Vehicles are a very common choice for studying their hydrodynamic performance. Phenomena of importance for their operation and safety such as large relative motions, impacts in waves and dynamic stability are highly nonlinear and still difficult to fully and accurately capture in numerical simulations.

Nevertheless, performing model tests with high speed craft comes with its own set of challenges related to scaling of time and model size and weight. To evaluate the hydrodynamic performance the experimental conditions for the model tests are determined according to Froude's similarity law. For a model scale α where the length of the model is $1/\alpha$ of its full value, the weight of the model is a factor $1/\alpha^3$ of its full scale weight, while the time and speed at

model scale are $1/\sqrt{\alpha}$ times of the full scale values.

3.3.1 Issues with model size and weight

To keep the model speed and to a lesser extend the wave height within the practical limits of the test basin requires a sufficiently large model scale factor α. A too large model speed leads either to impractically short run duration or a speed beyond the capabilities of towing apparatus. Nevertheless, a larger scale factor α can lead to impractically light models with too little weight margin to setup the correct loading condition and allow installation of drive and measurement equipment.

The high speeds and test conditions of interest can result in violent motions and impacts. Despite their small size and lightweight construction, this poses high demands on structural integrity and water tightness of the models used.

Fortunately, advances in model making techniques using lightweight materials and drive systems, high quality battery packs and miniature computers for data acquisition have made fully free running model tests with remote (auto-pilot) controlled models much more feasible, both in test basins and in outside bodies of water such as lakes. A number of examples of such tests are given in the following paragraphs. Most of the models used are constructed from lightweight material such as Carbon fibre Reinforced Plastics, and a combination of hobby equipment, miniature controllers and computers, wireless technology and custom made parts. The complexities of the instrumentation of these models are illustrated by Figure 341 and Figure 343.

Katayama et al. (2014) developed a free running model test system to safely and easily investigate the occurrence of instabilities as an alternative to full scale trials. They used a 1 metre radio-controlled scale model of a planing hull that included on board measurement devices and its own propulsion and steering system. It was made of thin Fibre Glass Reinforced Plastics and equipped with miniaturized measurement equipment to allow speeds of up to 12 m/s.

Figure 341: Instrumentation of free running HSMV model (Katayama et al., 2014)

Van Walree and Struijk (2021) carried out model tests and full scale trials for the FRISC-type RHIB of the Royal Netherlands Navy. Due to the high speed and large motions in the horizontal plane of the model the carriage could not always follow the model (Figure 342). The model therefore needed to be fully free running with an on-board position measurement system, autopilot computer, power supply, measurement instrumentation and data storage. The optical motion tracking system functioned when the model was in the measurement window of the carriage, sending position information to the on-board autopilot. When not in the measurement window an on-board inertial (IMU-based) navigation system took over.

Their trial data was obtained with the full scale FRISC under more realistic conditions, with a human in the control loop, with inherently much larger uncertainties on wave conditions. The effect of human course keeping was found to be significant, not only on yaw but also on the other modes of motion: it removes much of the dependency of motions and accelerations on the wave direction.

Figure 342: Fully free running model of the FRISC RHIB (Van Walree and Struijk, 2021)

Wang et al. (2020b) outline a preliminary design and testing plan for a free running (self-propelled, autonomously controlled model) of a high speed craft. The considered the design of the hull, the propulsion system to reach the desired speed and a steering system utilizing IMUs (Inertial Measurement Units) and a proportional derivative (PID) control. Methods for monitoring the outdoor environment using floating wave buoys and/or ultrasonic sensors mounted to the model were explored and specific instrument options were presented. Furthermore, sensor implementation to record necessary performance data was explored and the requirements for eventual testing locations where the model will be used wee detailed.

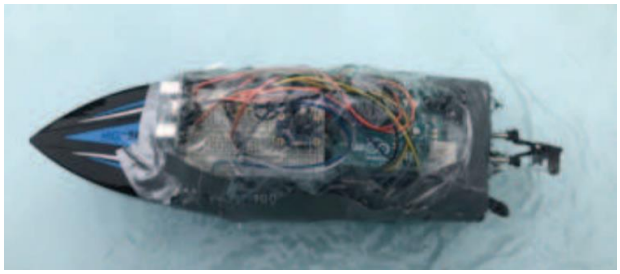

Figure 343: Instrumentation of free running HSMV model (Wang et al., 2020)

3.3.2 Issues with model scale time and control

Another issue is related to model scale time and control. Due to the small scales also model scale time becomes relatively small (due to aforementioned the laws of similarity). This may result in problems in control systems, as inherent time delays in control systems that may not pose problems for model testing at larger model scales now may introduce unacceptably large time and phase shifts in controller actions. This means that a controller at model scale can act unexpectedly different than intended. This may affect control algorithms and hardware, steering servos, data communication systems, etcetera. Unfortunately, in open literature no previous work could be found on the effects of these phase shifts on HSMV testing.

3.3.2 Scale effects of hydrodynamic forces on hull and control surfaces

Although not exclusively for HSMV model tests, the (Reynolds) viscous scale effects on the hydrodynamic forces have to be considered. As described in the above, due to other scale limitations, models of high speed craft and appendages, tend to be relatively small. Boundary layer effects, such as laminar to turbulent flow transition, flow separation and boundary layer thickness, on hull and appendage forces need to be considered.

The relatively higher resistance at model scale can affect the steering behaviour and therefore the course keeping and broaching, as the steering forces are proportional to the thrust (Van Walree et al., 2004). Applying compensating pulling forces is either impractical due to unintended inertial effects of such setups in unsteady tests or impossible for free running models. Katayama et al. (2012) (in Japanese) try to compensate the viscous effects on running attitude of a free running model by using an air fan on the deck of model to generate compensating forces. Not only friction forces are affected by scale effects, also lift generation can be significantly affected. Katayama et al. (2011) indicated the effect of viscosity on the

running attitude of a high speed craft model in calm water.

With respect to controllability the scale effect on lift of control surfaces is of significant importance. Van Walree and Luth (2000) reviewed the scale effects on foils and fins in steady and unsteady flow. The stressed the need of careful turbulence stimulation, and considering the local Reynolds number of each lifting surface. They indicate that for turbulence stimulation to be effective, lifting type control surfaces should not be too small and recommend a Reynolds number of the foil of at least 5 to $7.5 \cdot 10^5$, depending on the foil section type.

Despite using turbulence stimulation, still the lift may be lower at model scale than at full scale. To correct for this Van Walree et al. (2004) suggest the option of using adapted control surfaces at model scale, in size or in foil section. Cavitation is not a limitation at model scale, permitting the usage of higher lift sections at model scale. A priori viscous flow calculations are necessary to assess the lift and drag at low Reynolds numbers to ensure a correct adaptation is done to the model scale appendages.

Still, some results indicate a difference of the lift generated by foils and fins in steady versus unsteady flows. Early results indicate that the lift-curve slope seems to be less affected by scale effects and therefore most of the scale effect on lift may be avoided by choosing an appropriate offset in angle of attack of a lifting surface. More research is needed to further investigate this.

Additional, often secondary, scale effects can be expected due to the surface tension (Van Walree et al., 2004). Spray formation at model scale is different than at full scale. At full scale spray tends to consists of droplets, whereas at model scale more often coherent spray sheets are observed that generally cause a larger spray wetted area.

Combined with the (relatively) too high atmospheric pressure at model scale the incorrectly scaled surface tension may affect ventillation. This can cause thrust breakdown of the propulsor and reduction of controllability due to ventilation of control surfaces. Due to the complexity of the physics involved, no scaling rules or empirical corrections are available to correct for scale effects in spray and ventilation. Young et al. (2017) presented an overview of scaling effects associated with ventilation of lifting bodies. Besides scaling the fluid flow correctly, they also focused on Fluid Structure Interaction and correctly scaling the deformation of lifting surfaces to achieve dynamic similitude in the dynamic hydroelastic response.

4. COLLABORATION

Within the ITTC, the Seakeeping Committee (SKC) has collaborated mainly with the Stability in Waves Committee (SIW). On suggestion of the Seakeeping Committee and after discussion with the AC/EC and the Stability in Waves Committee it was decided to transfer the task (Task 10 of the SKC Terms of Reference) for developing guidelines on the inclination experiment from the SKC to the SIW. The SKC has provided support to the SIW on this task and has provided a review on the draft version of the new procedure on inclining experiments. Various topics have been discussed between the two committees, including various techniques for assessing roll damping from model tests, details of inclination tests, including uncertainty and self-repetition in computationally generated long duration wave elevation time traces.

In response to Task 9 of the SKC Terms of Reference and upon request by the SIW the SKC has provided an extensive review of the Recommended Guideline 7.5-02-07-04.3 on the prediction of the occurrence and magnitude of parametric rolling.

In Task 13 of the Terms of Reference the Seakeeping Committee was requested to continue the collaboration with the ISSC Loads and Responses and Environment Committees. Two members of the SKC were also part of either the ISSC Loads Committee or the Joint ISSC/ITTC Committee. The main result of this collaboration is the 5th Joint ISSC/ITTC International Workshop on Uncertainty Modelling in Wave Description and Wave Induced Responses to organized near the 29th ITTC Full Conference. Three contributions by SKC members on wave modelling, the effect of variability of wave generation in test basins on seakeeping responses such as impact loads and added resistance in waves, and propeller-hull-rudder interaction effects and scaling effects on the added power in waves are to be presented at this workshop. Unfortunately, related to the COVID pandemic, the workshop comes too late to include its results in the 29th ITTC Final Report.

5. ITTC RECOMMENDED PROCEDURES

5.1 ITTC Procedure 7.5-02-07.02.1 Seakeeping Experiments

For the 29th ITTC the Seakeeping Committee was requested to extend this procedure to include the measurement of added resistance in waves, including attention to the uncertainty of added resistance. To maintain consistency between this procedure, procedure 7.5-02-07.02.2 on the prediction of power increase in waves and procedure 7.5-02-07-02.8 on determining the weather factor f_w, details on performing added resistance were transferred from procedure 7.5-02-07.02.2 to this procedure. In this way all experimental test execution is covered in a single procedure on seakeeping experiments, avoiding redundancy between multiple procedures. Procedure 7.5-02-07.02.2 then provides details on how to extract power increase in irregular waves and refers to this procedure for details on test execution of model tests in waves. Procedure 7.5-02-07-02.8 also refers to the aforementioned procedures for details on test execution and data processing and has been checked on using consistent symbols and terminology.

Recommendations for the conditioning of a model for seakeeping tests in terms of required model completeness, model mass properties and the model ballasting procedure were introduced, as requested in the Terms of Reference. Additionally, guidelines on using pre-simulations for the selection of relevant test conditions were added.

The section on measurement of wave loads was brought in line with procedure 7.5-02-07.02.6 on the prediction of global wave loads, by making a distinction between rigid body segmented model tests and elastic (segmented) models and referring to procedure 7.5-02-07.02.6 for more details. Additional remarks on wave generation and the effects of wave steepness on non-linearity, wave breaking and statistical stationarity have been included. The formulation of wave energy spectra have been updated for consistency.

With the above substantial updates were made to procedure 7.5-02-07.02.1. In consultation with the Advisory Council and the Executive Committee it has been decided to include a discussion on uncertainty in added resistance in waves from model tests in this Final Report of the Seakeeping Committee (refer to Section 3.1), in preparation of adaptation of the uncertainty assessment in Appendix A with added resistance in waves by a future committee.

5.2 ITTC Procedure 7.5-02-07-02.2, Predicting Power Increase in Irregular Waves from Model Tests

Recommended Procedure 7.5-02-07-02.2 was updated in conjunction with the previous

procedure 7.5-02-07-02.1, by moving the section on execution of model tests for added resistance in waves from this procedure to 7.5-02-07-02.1. A reference was added in this procedure to the new section in 7.5-02-07-02.1.

Furthermore, updates were made to the text of this procedure to enhance readability for a wider audience, as requested in the Terms of Reference. In addition, the formulations and symbols used to describe directional wave energy density spectra were brought in line between this procedure and the previous one, while maintaining consistency with the ITTC Symbols list.

Besides a number of additional editorial corrections, an error was fixed in the formula to compute the power in irregular waves, that incorrectly used a factor associated with Horsepower instead of Watt.

5.3 ITTC Procedure 7.5-02-07-02.3, Experiments on Rarely Occurring Events

The Seakeeping Committee was requested to update this procedure to include the measurement and analysis of impulsive loads, peaks in pressures and maximum accelerations. To address this a number of details on the measurement and recording of extreme impact and green water events were added, with references to useful and more detailed background literature.

Suggestions were added to correctly and completely document the means used to record impact pressures such as sensor type, calibration, sensor arrangement, sampling rate and results of hammer tests to obtain model and sensor eigenfrequencies. Corrections were made to inconsistent suggestions for run durations and outdated usage of expressing wetting event frequencies of occurrence as ‘wets per ship model length’. A statement was included on the effect of air-pocket on the impact loads when applying Froude scaling.

5.4 ITTC Procedure 7.5-02-07-02.5, Verification and Validation of Linear and Weakly Non-Linear Seakeeping Computer

This procedure was revised substantially to minimize redundancies and to use consistent terminology. Improvements were made to the language used to improve clarity and readability. It was made clear that the current procedure is focused on the verification and validation of linear and weakly nonlinear seakeeping computer codes based on potential flow theory. In the future a new procedure may be developed for CFD based methods.

The sections on weakly nonlinear and on hydroelastic seakeeping codes were considerably improved. A note was added to check the natural frequencies and damping coefficients for dynamic simulations and quantification of uncertainties. Remarks on appropriate verification and validation procedures such as definition of model assumptions, checks on numerical convergence as well as quantification of modelling uncertainties were introduced in the procedure.

5.5 ITTC Procedure 7.5-02-07-02.6, Prediction of Global Wave Loads

Besides a number of minor editorial revisions to improve readability more details were added on the usage of elastic segmented models. This includes a discussion on the advantages of using internal rigid structures with instrumented elastic joints that allow better tuning to a specific natural frequency for the two-node bending mode regarding slamming-induced-whipping responses.

5.6 ITTC Procedure 7.5-02-07-02.7, Sloshing Model Tests

During the 29th ITTC only minor changes were introduced into this procedure, that was first introduced during the 28th ITTC. These changes include an update to the data measurement sections with a comment on thermal shock issues of pressure transducers, updated and corrected references, language revisions and an updated figure to improve readability.

5.7 ITTC Procedure 7.5-02-07-02.8, Calculation of the weather factor fw for decrease of ship speed in wind and waves

The Seakeeping Committee was requested to update this procedure in two steps. The first step was to update the procedure very early in the 29th ITTC term to bring it in line with the terminology in the EEDI guidelines and to enable the ITTC to submit it to MEPC 72 (in the spring of 2018). Based on the discussion during the Full Conference of the 28th ITTC the procedure was updated with a statement that the procedure is applicable mainly for large ships and that additional work is required for smaller ships, and state the limit between large and smaller ships. Besides this substantial improvements to the terminology and symbols were made to improve readability for more general audience and to be consistent with existing EEDI guidelines. References to recent and relevant benchmark data were added.

In the second round of improvements, as part of the regular round of revisions a few minor additional revisions were made. These were aimed at improvement of consistency between this procedure and the related procedures 7.5-02-07-02.1 and 7.5-02-07-02.2 as noted in the above, mainly in the symbols for spectral wave period symbols. A discussion on the uncertainty of various prediction methods was included as a discussion in Section 3.1 of this Final Report, as agreed upon with the Advisory Council and the Executive Committee.

5.8 ITTC Procedures on Tests with High Speed Marine Vehicles

Similar to the 28th ITTC, the Seakeeping Committee was requested to review the procedures on High Speed Marine Vehicles (HSMV). These include Procedure 7.5-02-05-04 HSMV Seakeeping Tests, procedure 7.5-02-05-07 HSMV Structural Loads, and procedure 7.5-02-05-07 HSMV Dynamic Instability Tests. A specific request was made to add guidelines on motion control for high speed craft.

The procedure on HSMV Seakeeping Tests was found to be the most mature of the three procedures. Besides minor editorial changes, more substantial revisions include a modernisation of the section on model construction, materials used and manufacturing tolerances, removal of outdated or incorrect sections on run duration (based on linear statistics) and side-by-side comparison testing and a removal of superfluous discussion of very specific details of wave and motion measurement systems. As the derivation of linear Response Amplitude Operators (RAOs) is generally not advised for nonlinear motions such as those of high speed marine vehicles recommendations on the use of RAOs are removed.

In addition to reviewing the procedure on HSMV Seakeeping Tests the Seakeeping Committee was requested to develop a new procedure for motion control of HSMV during seakeeping tests. Due to the high workload of the committee, the Seakeeping Committee proposed in consultation with the Advisory Council and the Executive Committee to defer this activity to a future committee, possibly a specialist committee of HSMV. In preparation for this new procedure, the 29th Seakeeping Committee prepared a comprehensive

discussion on HSMV control during seakeeping tests in Section 3.3 of this Final Report.

Procedure 7.5-02-05-07 on HSMV Structural Loads was found to be at a significant lower level of maturity. The description of the purpose of the procedure was considerably updated to provide more context to this procedure and to explain the link to related procedures, most notably the general seakeeping procedure on global loads, 7.5-02-07-02.6. The unrealistically high recommended sampling rate of 100kHz for impacts was reduced to 10-20kHz and the section on the parameters to be taken into account was expanded. Finally, the language was improved and references were updated.

Lastly, procedure 7.5-02-05-07 on HSMV Dynamic Instability Tests was reviewed and found to be inadequate. The introduction and stated purpose were found to be not appropriate, dynamic instability behaviour types should be more adequately defined and consistently treated. In its current state the procedure is not clear on whether it treats with instability in calm water or in waves, or both. The descriptions on the experiments to be performed were found to be inconsistent and to only cover planing mono hulls. Due to the workload the Seakeeping Committee has requested to defer the activity of the complete revision of this procedure to a future specialist committee on high speed marine vehicles and in the meantime strongly recommends to withdraw this procedure from the ITTC Recommended Procedures.

6. CONCLUSIONS

6.1 General Technical Conclusions

6.1.1 New Experimental Facilities

Only a limited number of new experimental facilities have opened since 2017 or are about to become operational. These include two large offshore basins, a facility for studying the influence of waves, winds and currents on coastal defences and blue energy applications, and a towing tank with wave making capabilities.

6.1.2 Experimental Techniques

The accurate experimental determination of “added resistance in waves” continues to be a challenging topic. Added resistance is obtained by measuring the small difference between two large quantities (calm water resistance and mean resistance in waves). This makes determining added resistance in short waves particularly difficult and places high demands on the quality of such experiments. There remains a need to gain a better understanding of the uncertainties associated with seakeeping tests in general and added resistance experiments in particular. Although some pioneering work has been done in this area, including uncertainty analysis in added resistance evaluations is still rare. Only a handful of papers deal with the different sources of uncertainty and their relative importance in seakeeping.

An emerging trend is the prediction of the seakeeping performance of sail assisted vessels, where various approaches to include the effect of sail aerodynamics on the seakeeping performance are proposed. There seems to be a clear need to develop guidance on how to perform such model tests.

6.1.3 Numerical Methods

Despite the significant developments within Navier-Stokes solvers (CFD), potential theory-based boundary element methods are still the workhorses in practical seakeeping analyses.

Whereas efficient strip theory methods are still widely used, most recent developments focus on 3D methods. For ships at forward speed, multi-domain (hybrid) methods seem to gain more popularity, since they utilize the relative merits of the Rankine panel method and

the Green function method in an inner and outer domain, respectively. The two methods are matched at their common boundary, and there have been some recent developments in matching techniques. There are also activities aiming at making the boundary element methods more computationally efficient.

Regarding forward speed effects, comparisons with experiments indicate that the simple Neumann-Kelvin approximation for the steady flow may sometimes give acceptable accuracy, compared to the more complex methods based on the double-body potential or the complete solution of the steady flow.

In time-domain simulations, it is common to include nonlinear Froude-Krylov and hydrostatic forces, by considering the instantaneous position of the hull beneath the incident wave profile. The so-called fully nonlinear methods, where the nonlinear boundary value problem is solved at every time-step, seem to receive less attention. The reason could be that the Navier-Stokes solvers are gradually filling this niche of high-fidelity hydrodynamic simulations. Instead, research on time-domain methods based on potential theory seem to be more focused on practical ways of addressing the combined seakeeping and manoeuvring problem.

6.1.4 Rarely Occurring Events

In many experimental studies considering impact and slamming there is an increased focus on oblique wave impact, with multiple sources reporting larger impact loads than in head seas in particular cases. This highlights the need for carefully considering the influence of wave heading on slamming both in model tests and in numerical calculations.

Most computational approaches for rarely occurring events related to slamming, green water, and impact, employ multiple fidelity levels, with more standard and efficient 2D or 3D potential flow methods to compute the overall motions and occurrence rates and higher fidelity dedicated methods for individual impacts and green water events. For the later, a shift is taking place away from analytical or empirical Von Karman or Wagner based approaches towards advanced CFD methods and meshless methods such as Smoothed Particle Hydrodynamics (SPH), often including the effects of compressibility and air-pockets on the impact load. In many cases hydrodynamic impact loading is combined with the partly or fully hydro-elastic coupled structural assessment.

Due to the usage of complex CFD there is an increased focus on validation. A comparative study of a water-entry problem was conducted by the International Hydrodynamic Committee. Thirteen institutions participated, and twenty different numerical results from a variety of computational approaches were investigated and compared with one another and with model test data. CFD results were found to be very promising for symmetric impact of simple section shapes, but there remained quite some uncertainty for the asymmetric impact case, possibly related to the formation of air-pockets.

Research on emergence of propellers and other appendages is more focused on the effects of ventilation on the performance of propellers and lifting surfaces. Detailed experiments and CFD computations are conducted to predict the steady and dynamic propeller/foil performance in different flow regimes. Similar to a hydrofoil or strut, ventilation of a propeller can lead to significant reduction in thrust and torque. This in turn can lead to rapid propeller rpm variations to maintain thrust or involuntary loss of speed and heading, with significant consequences for vessel control in a seaway and hydro-elastic propeller loading and deformation.

6.1.5 Sloshing

Assessment of sloshing loads for LNG tanks has been an important issue in the design of LNG carriers or LNG FPSOs (FLNG). For practical purposes, the experimental approach based on sloshing model tests has been the most frequently used. Many studies were focused on the evaluation of the impact load for the sloshing problem. Sophisticated phenomena that have been considered in model tests include the effects of gas-liquid density ratio and bubbles on the sloshing impact.

A large number of numerical investigations have been carried out to study the fluid-structure interaction inside the sloshing tank and the coupling effects of sloshing and ship motions. In an attempt to capture the highly nonlinear and complex nature of the sloshing problem, new techniques based on a machine learning scheme have been introduced to predict the sloshing load severity.

6.1.6 Hydroelasticity

Several advances have been made in the last decade with respect to (full-scale and model-scale) experimental, numerical and analytical modelling of the hydroelastic response of ship structures in waves. Experimental and numerical results both point to the importance of accounting for flow-induced vibrations on the dynamic loads and stresses. In particular, significant dynamic load amplification can occur near resonant conditions, which can drastically increase the vibrations and accelerate fatigue. The added mass, modal frequencies and damping coefficients change with operating conditions (confined water, speed, wave heading, submergence/draft, etc), which must be considered to avoid dynamic load amplification.

In some cases, the operational dependence of modal characteristics can lead to mode switching and modal coalescence, which can drastically increase the vibrations and dynamic load fluctuations. Such mode changes would also challenge the validity of modelling methods based on superposition of modal responses, which typically assume the mode shapes and mode order to be the same in dry and wet conditions. Recent studies of a large database of 17 post-Panamax container ship models by Lauzon et al. (2020) showed that 2-way coupled fluid-structure interaction models are needed to correctly capture the slamming loads and motions.

Even with recent advances in computing, performing fully coupled CFD-FEM calculations of a vessel oscillating and vibrating in waves is still not yet practical. However, such simulations are needed to advance our understanding of hydroelastic effects, as model-scale experiments are challenged by scaling effects, and full-scale measurements are challenged by the ability to control the loads and motions. Since much more work is still needed to improve the accuracy and efficiency of numerical fluid-structure interaction models, more experiments are also needed to validate the numerical solutions.

6.1.7 Added Resistance in Waves and Power Requirements

Predictions of ship motions and added resistance in head waves by CFD have become reliable, whereas potential flow codes often provide underestimation in the short wavelength region and overestimation at the resonance point with encounter waves. It has also been confirmed by CFD that the quadratic linear assumption for the wave height of added resistance in head waves is not satisfied in the higher wave steepness region in for short waves. This is caused by viscosity and the non-linear interaction between the fluid and the hull shape. CFD is not suitable for a practical calculation at present because of its high calculation cost, but visualization of these phenomena can deepen the understanding of hydrodynamic phenomena.

By mathematically modelling these phenomena and combining with potential flow

codes, a more practical and highly accurate calculation method can be created. On the other hand, there are a number of proposals for estimating added resistance by semi-empirical formulae that do not require high-performance computation were also made. Compared to the past, the range of ship types and wave lengths that can be modelled by these methods has become much wider. This makes these semi-approaches useful for considering a wide range of design variations that meet EEDI requirements in the preliminary design phase.

There were many numerical studies and experiments that systematically investigated variations and trends of self-propulsion factors and added power in waves. In particular, experimental data obtained from various basins and numerical results from various CFD codes have been accumulated in benchmark studies, which is expected to form a good basis for further validation studies in the future.

The focus has conventionally been on ship motions and added resistance in head waves and so far there have been few theoretical studies and experimental examples for oblique waves. This is partly caused to the limited number of seakeeping basins where experiments can be conducted in oblique waves with sufficient accuracy. However, in a few of last years, such experimental data has been accumulated. Early results hint at cases where the added resistance in waves is higher in oblique seas compared to head seas, making it important to also assess added resistance in oblique conditions. In oblique waves, the effect of viscosity of the fluid appears to be stronger, making CFD the better suited to tool to complement basin experiments. In oblique waves, improving accuracy in the short wave length region is more important than in heading waves.

6.1.8 CFD Applications

The use of CFD for seakeeping has continued increasing over the past few years. It has been applied over a large variety of topics essentially thanks to two intrinsic advantages of the method: the flexibility in imposing boundary conditions; and its natural treatment of nonlinear problems. This flexibility however comes with the computational cost, which is had not become any more efficient over the years as the software used are mostly based on the same consolidated and robust methodology (implicit or semi-implicit finite-volume solvers). To overcome this issue, progress is being made on the design methodology with CFD, by reducing the number and the physical time needed in the simulations to achieve the goals.

6.1.9 Seakeeping of High Speed Marine Vehicles

Sailing with high speed craft in calm water and in waves is associated with very dynamic behaviour related to dynamic stability and slamming impacts. High speed craft in waves are subjected to significant and frequent impacts with large effects not only on the structural integrity but also on human performance and human safety. Research has not only focused on model tests and predictions by means of computations, but also full scale recordings play an important role as well as the statistics of extremes of the vertical accelerations.

Over the past five years, the most investigated types of high speed marine vehicles are monohulls, followed by wave piercing catamarans and trimarans. There seems to be a growing interest in hydrofoiling craft and foil assisted craft, possibly related to the introduction of hydrofoils in high profile sailing matches such as the America’s Cup. There is more and more interest in using ride control systems to not only improve passenger comfort, but also in actively reducing slamming itself.

The nonlinear nature of the responses of high speed vessels has resulted in the adoption of nonlinear time domain methods. Besides the more traditional nonlinear 2D+t potential flow

methods, nonlinear 3D panel methods have gained significant popularity in recent years. Also CFD methods are slowly gaining ground, but still suffer from the computational burden needed to obtain sufficient time duration of simulations.

The various semi-empirical methods in use by classification societies for the assessment of vertical accelerations were scrutinized by a number of authors and important questions were raised about the actual safety levels that are achieved when applying these semi-empirical methods.

6.1.10 Uncertainty in Added Resistance

The 'weather factor' f_w for decrease of ship speed in wind and waves is one of the terms in the Energy Efficiency Design Index (IMO, 2014). A key component to determine f_w is the added resistance of a vessel in waves. At this point the relevant ITTC, ISO and IMO procedures leave open many options to determine the added resistance in waves, by model experiments or by various levels of computations.

There are various ways of conducting measurements to obtain the added resistance in waves, mainly differing in the way a model is restrained, whether the model is powered or not and whether tests are performed in regular or irregular waves. A balance is sought between realism in the representation of the vessel behaviour and its propulsor and minimization of uncertainty that is inherently caused by determining the added resistance by subtraction of the relatively large values of total resistance in calm water and that in waves. This report describes in detail the various advantages and disadvantages of the choices that can be made when performing added resistance tests. Besides the test setup, a key factor in controlling uncertainty in added resistance is the understanding and management of the variability of the incident waves in the test basin. This is related to statistical variability due to the finite time duration of wave generation and to the repeatability of waves generated in a test basin.

Various numerical methods to obtain added resistance in waves are described, including their advantages and disadvantages, ranging from empirical (correction) methods, strip theory to panel methods and CFD. At this moment, for modest sea states where nonlinear effects do not play an important role modern panel methods that account for the steady flow interactions seem to offer a reasonable balance between modelling effort and calculation time and accuracy of the results. For these cases the quadratic relation between wave height and added resistance holds. For very short and steep waves and breaking waves, model experiments and/or complex CFD computations currently still seem to be the best options to obtain accurate predictions of the added resistance. Achieving sufficiently accurate predictions of added resistance requires careful attention to the details of the computations or experiments, as well as significant computational resources for CFD.

6.1.11 Control of High Speed Marine Vehicles in Model Tests

Model tests with High Speed Marine Vehicles are a very common choice for studying their hydrodynamic performance. Phenomena of importance for their operation and safety such as large relative motions, impacts in waves and dynamic stability are highly nonlinear and still difficult to fully and accurately capture in numerical simulations.

Nevertheless, performing model tests with high speed craft comes with its own set of challenges related to scaling of time, model size and weight and model control. To evaluate the hydrodynamic performance the experimental conditions for the model tests are determined according to Froude's similarity law. For high

speed craft this typically leads to very small and light models that can be very challenging to build while accurately representing the loading condition.

Especially when model control is important this typically lead to small scale fully self-propelled and self-steered free running models. This is made possible by recent advances in miniaturized computing devices and battery technology. The small scale may also result in problems in control systems, as inherent time delays in control systems that may not pose problems for model testing at larger model scales now may introduce unacceptably large time and phase shifts in controller actions.

Reynolds scale effects on lift and drag by control surfaces, again exacerbated by the typical small scale models used, need to be carefully considered and mitigated. In addition, scale effects related to surface tension, spray formation and ventilation may need to be considered. Fluid-structure interactions of lifting surface may require also dynamic similitude in the hydroelastic response.

6.2 Recommendations To The Full Conference

Adopt the updated procedure No. 7.5-02-07-02.1 Seakeeping Experiments.

Adopt the updated procedure No. 7.5-02-07-02.2 Prediction of Power Increase in Irregular Waves from Model Tests.

Adopt the updated procedure No. 7.5-02-07-02.3 Experiments on Rarely Occurring Events.

Adopt the updated procedure No. 7.5-02-07-02.5 Verification and Validation of Linear and Weakly Non-linear Seakeeping Computer Codes.

Adopt the updated procedure No. 7.5-02-07-02.6 Global Loads Seakeeping Procedure.

Adopt the updated procedure No. 7.5-02-07-02.7 Sloshing Model Tests.

Adopt the updated procedure No. 7.5-02-07-02.8 Calculation of the Weather Factor fw for Decrease of Ship Speed in Wind and Waves

Adopt the updated procedure for high speed marine vehicles No. 7.5-02-05-04 HSMV Seakeeping Tests.

Adopt the updated procedure for high speed marine vehicles No. 7.5-02-05-06 HSMV Structural Loads.

Withdraw the existing procedure for high speed vehicles No. 7.5-02-05-07 HSMV Dynamic Instability Tests; due to this procedure not being up to standard for ITTC. The extensive work needed to revise this procedure is recommended as future work for a special committee.

6.3 Proposals For Future Work

6.3.1 Verification and Validation for CFD Seakeeping Applications

The Seakeeping Committee notes that the application of CFD methods such as RANS and LES, as well as particle methods, is becoming more and more common-place to seakeeping problems. Of these methods, the Finite Volume Method with Volume of Fluid interface description is the most wide-spread at this moment for practical applications. To ensure the correct applicability of these methods, there is clear need for guidance on verification and validation of these methods. The Seakeeping Committee is of the opinion that this should lead to a new procedure, next to the already existing procedure No. 7.5-02-07-02.5 Verification and Validation of Linear and Weakly Non-linear Seakeeping Computer Codes. This work is proposed as future work for the Seakeeping Committee in close collaboration with the

Specialist Committee on Combined CFD/EFD Methods.

6.3.2 Weather factor for small ships

In the current procedure No. 7.5-02-07-02.8 on the calculation of the weather factor f_w it is noted that the selected 'representative sea conditions' as specified by IMO (2012) may not be suitable for ships smaller than about 150 m in length. These wave conditions may result in 'voluntary' speed reduction by the ship's master to avoid excessive motions and loads on these small-sized vessels. Figure 338 from Gerhardt and Kjellberg (2017) for instance shows that f_w for small ships is predicted to drop significantly for small vessels. More work is needed to understand and quantify this issue further. A possible outcome of this work can be the development of alternative approaches for determining weather factors for smaller vessels, e.g. reduced wave heights/milder environmental conditions like in the IMO guideline on "minimum power requirements". More experimental studies are also needed for validation of the various prediction methods.

6.3.3 Minimum Power Requirements

The Seakeeping Committee recommends the development of an ITTC Guideline to determine the minimum power requirement as laid out in MEPC.1/Circ.850/Rev.2 based on the outcomes of the Specialist Committee on Manoeuvring in Waves. Determination of this minimum power requirement is mandatory under the current EEDI rules. Nevertheless, the Seakeeping Committee feels that the existing IMO Circular 850 is not well defined and open for interpretation, leading to uncertainty with ship operators and test facilities. To clarify this issue fits with the role of ITTC defining standards for model testing and as a technical advisor to IMO.

6.3.4 Wind Resistance

Accurate and consistent determination of both f_w and minimum power require realistic determination of the wind resistance, with an accuracy that matches the accuracy of all other resistance components. Current procedures do not seem to cover this in sufficient detail, leaving open a large room for interpretation by the evaluator of both f_w and minimum power requirements. The Seakeeping Committee sees a need for developing a better defined guideline on determining wind resistance. This need seems to be widely spread over multiple committees, not only related to EEDI issues, but also for more generic problems such as the effect of wind loads on manoeuvres and dynamic stability, calm water resistance and wind loads on offshore structures, thereby affecting almost all Technical Committees. It seems that the Specialist Committee on Modelling of Environmental Conditions as well as the Specialist Committee on Operation of Ships at Sea could have an important role in defining guidelines for wind resistance. There may be the need to setup a new Specialist Committee just for this task.

6.3.5 High-Speed Marine Vehicles

It is recommended to install a Specialist Committee on High Speed Marine Vehicles (HSMV) for the 30th ITTC term. After re-viewing the procedures for High Speed Marine Vehicles it was found that especially the HSMV procedure on Dynamic Instability lacked the desired quality to be included in the ITTC Quality Systems Manual. This Special Committee should perform a comprehensive review and revision of all related procedures for HSMV and draft a procedure for motion control of HSMV during model tests. The SC should therefore also consist of experts of all related fields, including but not limited to seakeeping, manoeuvring, dynamic stability, and powering.

6.3.5 Seakeeping Benchmark Campaign

A new benchmark experimental campaign is highly recommend with a focus on the characterization of the uncertainty in the measurement of added resistance. Candidates for this study would be the KCS or the KVLCC2. Typical models for this are available at the different institutes that could be circulated as was done in previous ITTC benchmark studies. Very careful attention should be spent on accurately defining wave and test conditions, control settings, model roughness and turbulence stimulation and the mass properties of the model. Such benchmark would be a key element in the discussion on measurement uncertainty in the determination of f_w and minimum power requirements. During next term, the test requirements should be defined first, before circulating a suitable model over the different facilities. Besides getting a better overview of the uncertainty of added resistance measurement, this campaign could also be used in the validation of computational methods.

6.3.6 Real-Time On-Board Data Processing

Identify the need for ITTC recommendations for the acquisition and analysis in real-time of data, for instance obtained on board of autonomous systems.

6.3.7 Seakeeping Assessment of Wind Assisted Ships

It is recommended to consider to develop guidelines for model tests with wind assisted ships, as this particular application has gained significant attention and there still seems a wide variety in approaches by various institutes. It would be valuable to bring together these experiences in a single comprehensive guideline.

7. ACKNOWLEDGEMENTS

The 29th Seakeeping Committee wishes to particularly recognize member Benjamin Boucasse for his considerable efforts to author the appendix “Note on Benchmarking”.

8. REFERENCES

Ahmad, H.A. and Ayob, A.F., 2017, “State of the Art Review of the Application of Computational Fluid Dynamics for High Speed Craft”, Journal of Ocean, Mechanical and Aerospace, 39:7-17.

Ahn, Y., Kim, Y., Kim, S.Y., 2019a, “Database of Model-Scale Sloshing Experiment for LNG Tank and Application of Artificial Neural Network for Sloshing Load Prediction”, Marine Structures, Vol. 66, pp 66 – 82.

Ahn, Y., Kim, Y., Kim, S.Y., 2019b, “Experimental Study and Method of Sloshing Model Test Considering Gas-Liquid Density Ratio”, International Journal of Offshore and Polar Engineering, Vol. 29, No. 3, pp 257 – 268.

AlaviMehr, J., Lavroff, J., Davis, M.R., Holloway, D.S. and Thomas, G.A., 2019, “An experimental investigation on slamming kinematics, impulse and energy transfer for high-speed catamarans equipped with Ride Control Systems”, Ocean Engineering, 178:410-422.

Allaka, H. and Groper, M., 2020, “Validation and verification of a planing craft motion prediction model based on experiments conducted on full-size crafts operating in real sea”, Journal of Marine Science and Technology, 25:1199-1216.

Alwis, M.P. de, Garme, K., Lo Martire, R. Kåsin, J.I. and Äng, B.O., 2017, “Crew acceleration exposure, health and performance in high-speed operations at sea”, Proceedings of the

11th International Conference on High Speed Marine Vehicles (HSMV), Naples, Italy.

Amini-Afshar M. and Bingham H.B., 2017, "Solving the linearized forward-speed radiation problem using a high-order finite difference method on overlapping grids", Applied Ocean Research, 69:220-244.

Amini-Afshar M. and Bingham H.B., 2018, "Pseudo-impulsive solutions of the forward-speed diffraction problem using a high-order finite-difference method", Applied Ocean Research, 80:197-219.

Amini-Afshar M., Bingham H.B. and Henshaw, W.D., 2019, "Stability analysis of high-order finite-difference discretizations of the linearized forward-speed seakeeping problem", Applied Ocean Research, 92.

Andrun, M., Basic, J., Blagojevic, B., and Klarin, B. 2020. "Simulating hydroelastic slamming by coupled Lagrangian-FDM and FEM," HSMV 2020, IOS Press, 2020.

Bakti, F.P., Jin, C., and Kim, M.H. 2021. "Practical approach of linear hydro-elasticity effect on vessel with forward speed in the frequency domain," Journal of Fluids and Structures, Vol. 101, 103204.

Bašić, J., Degiuli, N. and Ban, D., 2017, "Renormalised Lagrangian method for water entry impact simulation", Proceedings of the 11th Symposium on High Speed Marine Vehicles (HSMV), Naples, Italy.

Begovic, E., Bertorello, C., Pennino, S., Piscopo, V., and Scamardella, A., 2016, "Statistical analysis of planing hull motions and accelerations in irregular head sea", Ocean Engineering, 112:253-264.

Bhushan, S., Mousaviraad, M., and Stern, F. 2017. "Assessment of URANS surface effect ship models for calm water and head waves". Applied Ocean Research, 67, 248-262.

Bird, C., Walree, F. van, Sgarioto, D., Thomas, L. and Turner, T., 2017, "Validation of a time domain panel code for predicting the seakeeping behaviour of a rigid hull inflatable boat", Proceedings of the 15th International Conference on Fast Sea Transportation (FAST), Nantes, France, pp. 334-342.

Bonci, M., Jong, P. de, Walree, F. van, Renilson, M., Keuning, J.A. and Huijsmans, R.H.M., 2017a, "Experimental and numerical investigation on the heel and drift induced hydrodynamic loads of a high speed craft", Proceedings of the 15th International Conference on Fast Sea Transportation (FAST), Nantes, France, pp. 196-205.

Bonci, M., Jong, P. de, Walree, F. van, Renilson, M., Keuning, J.A. and Veer, R. van 't, 2020, "The heel-induced sway force and yaw moment of a high-speed craft", Journal of Marine Science and Technology, 25: 312-325.

Bonci, M., Renilson, M., Jong, P. de, Walree, F. van, Keuning, J.A. and Huijsmans, R.H.M., 2017b, "Heel-sway-yaw coupling hydrodynamic loads on a high speed vessel", Proceedings of the 11th International Conference on High Speed Marine Vehicles (HSMV), Naples, Italy.

Bulian, G., Cercos-Pita, J.L., 2018, "Co-simulation of Ship Motions an dSloshing in Tanks", Ocean Engineering, Vol. 152, pp 353 – 376.

Bunnik, T., 1999, "Seakeeping Calculations For Ships, Taking Into Account the Non-linear Steady Waves", Ph.D. thesis, Delft University of Technology, Delft, The Netherlands.

Bunnik, T., van Daalen, E., Kapsenberg, G., Shin, Y., Huijsmans, R., Deng, G., Delhommeau, G., Kashiwagi, M., Beck, B., 2010, "A comparative study on state-of-the-art prediction tools for seakeeping", Proceedings of the 28th Symposiumon on Naval Hydrodynamics, Pasadena, CA, USA.

Cakici, F, Kahramanoglu, E, Alkan, A. D., 2017, "Numerical Prediction of Vertical Ship Motions and Added Resistance", International Journal of Maritime Engineering, Vol. 159, Part A4, pp. 393-402.

Camilleri, J., Temarel, P., Taunton, D. and Saunders, C., 2017, "A study of slamming loads on high-speed craft and related responses through full-scale measurements and numerical simulation", Proceedings of the 15th International Conference on Fast Sea Transportation (FAST), Nantes, France, pp. 164-172.

Camilleri, J., Taunton, D.J., and Tamarel, P. 2018. "Full-scale measurements of slamming loads and responses on high-speed planing craft in waves," Journal of Fluids and Structures, Vol. 81, pp. 201-229.

Castro-Feliciano, E.L., Sun, J., Troesch, A.W., 2018, "Exploration of seakeeping and drag performance of planing craft with active control systems", Ocean Engineering, 151:57-70.

Cepowski, T., 2020, "The Prediction of Ship Added Resistance at the Preliminary Design Stage by the Use of an Artificial Neural Network", Ocean Engineering, 195, 106657.

Chen, X., Zhu, R. C., Zhao, J., Zhou, W. J. and Fan, J., 2018a, "Study on weakly nonlinear motions of ship advancing in waves and influences of steady ship wave", Ocean Engineering, 150:243-257.

Chen, X., Zhu, R. C., Zhou, W. J. and Zhao, J., 2018b, "A 3D multi-domain high order boundary element method to evaluate time domain motions and added resistance of ship in waves", Ocean Engineering, 159:112-128.

Chen, Xi. Liang, H., Li, R., and Feng, X. 2018c, "Ship seakeeping hydrodynamics by multi-domain method", Proceedings of the 32th Symposium on Naval Hydrodynamics, Hamburg, Germany.

Chen, Z., Gui, H., Dong, P., Yu, C. 2019, "Numerical and experimental analysis of hydroelastic responses of a high-speed trimaran in oblique irregular waves", International Journal of Naval Architecture and Ocean Engineering, Vol. 11, pp 409-421.

Cho, I.H., 2021, "Liquid sloshing in a swaying/rolling rectangular tank with a flexible porous elastic baffle", Marine Structures, Vol. 75, 102865.

Choi, J. E., Lee, C. M., Seo, J. H., Yu1, J. W., Lee, I., 2020, "Propulsive Characteristics and Comparative Study on the Prediction Methods of Power Increase in Regular Head Waves of KVLCC2 Using Model Tests", 33rd Symposium on Naval Hydrodynamics, Osaka, Japan.

Choudoury, R., Kawamoto, K., Wu, P., Sanada, Y., and Toda, Y., 2020, "Course-Keeping of KRISO Container Ship in Calm Water and Head Waves", 33rd Symposium on Naval Hydrodynamics

Consolo, O., Hillige, L. and Bonci, M., 2020, "The Roll Damping of High-Speed Craft in Waves", Proceedings of the 12th International Conference on High Speed Marine Vehicles (HSMV), pp. 143-151.

Crepier, P., Rapuc, S., Dallinga, R. P., 2020, "CFD Investigation into the Wave Added Resistance of Two Ships", 14th Practical Design of Ships and Other Floating

Structures (PRADS2019), Yokohama, Japan, pp. 95-114.

Damley-Strnad, A., Harwood, C. and Young, Y.L., 2019. "Hydrodynamic performance and hysteresis response of hydrofoils in ventilated flows," Sixth International Symposium on Marine Propulsors (SMP'19), Rome, Italy.

Davis, M.R., French, B.J., and Thomas, G.A. , 2017, "Wave slam on wave piercing catamarans in random head seas", Ocean Engineering, 135:84-97.

De Lauzon, J., Derbanne, Q., and Malenica, S. 2020, "Slamming Induced Whipping Computations on a Large Database of Container Ships," PRADS 2019: Practical Design of Ships and Other Floating Structures, pp. 857-877.

Delefortrie, G., Geerts, S., Lataire, E., Troch, P., Monbaliu, J., 2019, "Coastal & Ocean Basin and towing tank for manoeuvres in shallow water at Flanders Maritime Laboratory", 6th International Conference on Advanced Model Measurement Technology for the Maritime Industry (AMT), Rome.

Diez, M., Lee, E.J., Powers, A.M., Fullerton, A.M., Lewis, R.R. and Stern, F., 2020, "FSI and MDO for Weight Reduction of a Grillage Panel of a Fast Deep-V Planing Hull Subject to Slamming in Waves", Proceedings of the 33th Symposium on Naval Hydrodynamics, Osaka, Japan.

Durante, D., Broglia, R., Diez, M., Olivieri A., Campana, E.F. and Stern, F., 2020, "Accurate experimental benchmark study of a catamaran in regular and irregular head waves including uncertainty quantification", Ocean Engineering, 195:106685.

Eggers, R., Kisjes, A.,2019, "Seakeeping and Manoeuvring for Wind Assisted Ships", RINA Wind Propulsion Conference 2019, London.

Eijk, M. van der and Wellens, P.R., 2019, "A compressible two-phase flow model for pressure oscillations in air entrapments following green water impact events on ships", International Shipbuilding Progress, 66(4):315-342.

El Moctar, O., Ley, J., Oberhagemann, J., and Schellin, T., 2017. "Nonlinear computational methods for hydroelastic effects of ships in extreme seas". Ocean Engineering, 130, 659-673.

Essen, S. M. van and Lafeber, W., 2017, "Wave-induced current in a seakeeping basin", Proceedings of the 36th International Conference on Ocean, Offshore and Arctic Engineering (OMAE), Trondheim, Norway. OMAE2017-62203.

Essen, S. M. van, 2019, "Variability in encountered waves during deterministically repeated seakeeping tests at forward speed", Proceedings of the 38th International Conference on Ocean, Offshore and Arctic Engineering (OMAE), Glasgow, Scotland, UK. OMAE2019-95065.

Essen, S.M. van, Bandringa, H., Helder, J. and Buchner, B., 2020. "Non-linear wave run-up along the side of sailing ships causing green water on deck: experiments and deterministic calculations", Proceedings of the 39th International Conference on Ocean, Offshore and Arctic Engineering (OMAE), Fort Lauderdale, USA. OMAE2020-18130.

Falahaty, H., Khayyer, A. and Gotoh, H., 2018, "A Coupled Incompressible SPH-Hamiltonian SPH for Fluid-Structure Interactions", Proceedings of the 28th International Ocean and Polar Engineering Conference (ISOPE), Sapporo, Japan, pp. 581-588.

Faltinsen, O. M., Minsaas, K. J., Liapis, N., Skjordal, S. O., 1980, "Prediction of Resistance and Propulsion of a Ship in a Seaway", 13th Symposium on Naval Hydrodynamics, Tokyo, Japan.

Feng, P., Wu, Y., Feng, Y, Fan, S., Wang, J., 2020, "Study on the Power Increase in Waves of a Cruise Ship with Podded Propulsion", 14th Practical Design of Ships and Other Floating Structures (PRADS2019), Yokohama, Japan, pp. 150-162.

Fukushima, H., Wakahara, M., Kanai, T., 2019, "Hull Surface Pressure Measurement of the Affix-type Multipoint Pressure Sensor using Fiber Bragg Gratings", 14th International Symposium on Practical Design of Ships and Other Floating Structures (PRADS2019), Yokohama.

Gadelho, J. F. M., Rodrigues, J. M., Lavrov, A., and Soares, C. G., 2018, " Heave and sway hydrodynamic coefficients of ship hull sections in deep and shallow water using Navier-Stokes equations" Ocean Engineering 154: 262-276.

Gaidai, O., Storhaug, G., and Naess, A. 2018. "Statistics of extreme hydroelastic response for large ships," Marine Structures, Vol. 61, pp. 142-154.

Garme, K., 2020, "Warp Effects Studied by a Time-Domain Strip Model and Compared to Model Experiments", Proceedings of the 12th International Conference on High Speed Marine Vehicles (HSMV), pp. 152-159.

Gatin, I, Vukcevic, V., Jasak, H., Seo, J., and Rhee, S. H., 2018, "CFD verification and validation of green sea loads." Ocean Engineering 148 (2018): 500-515.

Gatin, I., Vladimir, N., Malenica, S., and Jasak, H., 2019, "Green sea loads in irregular waves with Finite Volume method." Ocean Engineering 171 554-564.

Gauvain, E., 2019, "The un-restrained sailing yacht model tests – A new approach and technology appropriate to modern sailing yacht seakeeping," SNAME 23rd Chesapeake Sailing Yacht Symposium, CSYS 2019, Annapolis.

Ge, Z., Shen, Z., Yan, D., and Chien, H.P., 2018, "CFD-Predicted Slamming Loads on a Ship in Head and Oblique Seas", Proceedings of the 32th Symposium on Naval Hydrodynamics, Hamburg, Germany.

Gerhardt F.G. and Kjellberg, M., 2017, "Determining the EEDI 'Weather Factor' fw" Royal Institute of Naval Architects, Influence of EEDI on Ship Design and Operation, London, UK.

Gerhardt, F.C., Kjellberg, M., Korkmaz, K., Ljungqvist, K. and Shiri, A., 2020, "Determining the EEDI "Minimum Propulsion Power", Proceedings of the RINA Conference on Influence of EEDI on Ship Design & Operation, London, UK.

Gerhardt, F., Santén, V., 2021, "Seakeeping model testing for a wind powered vessel", RINA Wind Propulsion Forum 2021, online event 17th February 2021.

Ghadimi, N., Sheikholeslami, M., 2019, "Numerical simulation of the slamming phenomenon of a wave-piercing trimaran in the presence of irregular waves under various seagoing modes", Journal of Engineering for the Maritime Environment, 233(4):1198-1211.

Ghadimi, P., Tavakoli, S. and Dashtimanesh, A., 2016, "Calm Water Performance of Hard-Chine Vessels in Semi-Planing and Planing Regimes", Polish Maritime Research, 23:23-45.

Gkikas, G.D. and Walree, F. van, 2017, "A Computationally Efficient Implementation of Nonzero-Speed Transient Green Functions for Zero-Speed Nonlinear Seakeeping Problems", J. Offshore Mech. Arct. Eng. 139.

Gong, J., Yan, S., Ma, Q., and Li, Y., 2020. "Added resistance and seakeeping performance of trimarans in oblique waves". Ocean Engineering, 216, 107721.

Grammatikopoulos, A., Banks, J., Temarel, P., 2018, "Experimental hydroelastic response of an elastic container ship-inspired barge model produced using additive manufacturing", 8th International Conference on Hydroelasticity in Marine Technology, Seoul.

Guo, Y., Xiao, L., Kou, Y. and Zhao, G., 2017, "A Method to Measure Wave Impact Force and Its Validation", Proceedings of the 27th International Ocean and Polar Engineering Conference (ISOPE), San Francisco, USA, pp. 280-288.

Hageman, R.B., Drummen, I. 2019, "Modal analysis for the global flexural response of ships," Marine Structures, Vol. 63, pp. 318-332.

Hageman, R.B., Drummen, I. 2020, "Calculation of Structural Damping of the Global Hull Structure from In-Service Measurements," PRADS 2019: Practical Design of Ships and Other Floating Structures, pp. 345-364.

Han, J., Kitazawa, D., Maeda, T. and Itakura, H., 2018, "Overview of the Development of a Series of Cabin-suspended Ships Governed by Different Motion Control Algorithms", Proceedings of the 13th International Conference on the Stability of Ships and Ocean Vehicles (STAB), pp. 462-477.

Harwood, C.M., Young, Y.L., and Ceccio, S.L., 2016, "Ventilated cavities on a surface-piercing hydrofoil at moderate Froude numbers: cavity formation, elimination, and stability,' Journal of Fluid Mechanics, 800: 5-56.

Harwood, C.M., Felli, M., Falchi, M., Ceccio, S.L., and Young, Y.L., 2019, "The Hydroelastic Response of a Surface-Piercing Hydrofoil in Multi-phase Flows: Part I – Passive Hydroelasticity," Journal of Fluid Mechanics, 801: 313-364.

Harwood, C.M., Felli, M., Falchi, M., Garg, N., Ceccio, S. L., and Young, Y.L., 2020. "The Hydroelastic Response of a Surface-Piercing Hydrofoil in Multi-phase Flows: Part II – Modal Parameters and Generalized Fluid Forces," Journal of Fluid Mechanics, 884:A3.

Hasheminasab, H., Zeraatgar, H., Moradi, H. and Sakaki, A., 2020, "Experimental study on water entry of twin wedges", Proceedings of the Institution of Mechanical Engineers, Part M: Journal of Engineering for the Maritime Environment, 234(2).

Hashimoto, H., Yoneda, S., Omura, T., Umeda, N., Matsuda, A., Stern, F., and Tahara, Y., 2019. "CFD prediction of wave-induced forces on ships running in irregular stern quartering seas." Ocean Engineering, 188, 106277.

He, G., Zhang, Z., Tian, N. and Wang, Z., 2017, "Nonlinear Analysis of Green Water Impact on Forward-speed Wigley Hull", Proceedings of the 27th International Ocean and Polar Engineering Conference (ISOPE), San Francisco, USA, pp. 313-319.

Heo, K., Kashiwagi, M. 2019, "A numerical study of second-order springing of an elastic body using higher order boundary element

method (HOBEM)," Applied Ocean Research, Vol. 93, 101903.

Hernandez-Fontes, J.V., Vitola, M.A., Silva, M.C.,Tarso T. Esperanca, P. de and Sphaier, S.H., 2017, "Use of Wet Dam-Break to Study Green Water Problem", Proceedings of the 36th International Conference on Offshore Mechanics and Arctic Engineering (OMAE), Trondheim, Norway.

Hizir, O., Kim, M., Turan, O., Day, A., Incecik, A., Lee, Y., 2019, Numerical Studies on Non-linearity of Added Resistance and Ship Motions of KVLCC2 in Short and Long Waves, International Journal of Naval Architecture and Ocean Engineering, 11, pp. 143-153.

Hong, S.Y., Kim, K.H. and Hwang, S.C., 2017, "Comparative Study of Water-Impact Problem for Ship Section and Wedge Drops", International Journal of Offshore and Polar Engineering, 27(2):123-134.

Hong, S. Y., Ha, Y. J., Nam, B. W., Kim, K. H., Hwang, S. C., Kim, H. J., Kim, J. W., and Huang, Z. J., 2019, "CFD Modeling Practice for Calculation of FPSO Bow Impact by Focusing Wave." The 29th International Ocean and Polar Engineering Conference. International Society of Offshore and Polar Engineers.

Houtani, H., Komoriyama, Y., Matsui, S., Oka, M., Tanaka, Y., and Tanizawa, K. 2018. "Designing a hydro-structural model ship to experimental measure its vertical bending and torisional vibrations," Proceedings of the 8th International Conference on HYDROELASTICITY IN MARINE TECHNOLOGY, Sept 10-12, 2018, Seoul, Korea.

Hsin, C., Lu, L., Huang, S., Mao, Y., Hsieh, Y., 2018, "Simulations of the Self-Propulsion Test in Seaway by Different Approaches", 32rd Symposium on Naval Hydrodynamics, Hamburg, Germany.

Huang, S., Duan, W., Han, X., Nicoll, R., You, Y., Sheng, S., 2018, "Nonlinear Analysis of Sloshing and Floating Body Coupled Motion in the Time-domain", Ocean Engineering, Vol. 164, pp 350–266.

Jiang, Z., Yang, J., Zong, M. and Xu, Y., 2018, "Air-cushion and Impact Force Coefficient with the Water Entry of a Flat Rigid Body", Proceedings of the 28th International Ocean and Polar Engineering Conference (ISOPE), Sapporo, Japan, pp. 89-93.

Im, H.I., Vladimir, N., Malenica, S., Cho, D.S. 2017, "Hydroelastic response of 19,000 TEU class ultra large container ship with novel mobile deckhouse for maximizing cargo capacity", International Journal of Naval Architecture and Ocean Engineering, Vol. 9, pp 339-349.

IMO, 2012, "Interim Guidelines for the Calculation of the Coefficient f_w for Decrease in Ship Speed in a Representative Sea Condition for Trial Use", IMO Circular MEPC.1/Circ.796.

IMO, 2014, "Guidelines on the Method of Calculation of the Attained Energy Efficiency Design Index (EEDI) for New Ships", IMO Resolution MEPC.245 (66).

IMO, 2017, "2013 Interim guidelines for determining Minimum Propulsion Power to maintain the manoeuvrability of ships in adverse conditions as amended" MEPC.1/Circ.850/Rev.2.

Irkal, Mohsin AR, S. Nallayarasu, and S. K. Bhattacharyya, 2019 "Numerical prediction of roll damping of ships with and without bilge keel." Ocean Engineering 179: 226-245.

ITTC, 2014, "Analysis of Speed/Power Trial Data", ITTC Recommended Procedures and Guidelines, 7.5-04-01-01.2.

ITTC, 2014, "Prediction of Power Increase in Irregular Waves from Model Test", ITTC Recommended Procedures and Guidelines, 7.5-02-07-02.2.

ITTC, 2018, "Calculation of the weather factor f_w for decrease of ship speed in wind and waves", ITTC Recommended Procedures and Guidelines, 7.5-02-07-02.8.

Javaherian, M.J., Ren, Z., Judge, C.Q., and Gilbert, C. 2020. "Structural Response due to the Slamming of High-Speed Craft by Water Entry and Towing Tank Experiments," 33rd Symposium on Naval Hydrodynamics, Osaka, Japan, May 31-June 5, 2020.

Jiao, J., Chen, Z., Chen, C., Ren, H., 2020, "Time-domain hydroelastic analysis of nonlinear motions and loads on a large bow-flare ship advancing in high irregular seas," Journal of Marine Science and Technology, Vol. 25, pp. 426-454.

Jiao, J., Yu, H., Chen, C. and Ren, H. 2019. "Time-domain numerical and segmented model experimental study on ship hydroelastic responses and whipping loads in harsh irregular seaways," Ocean Engineering, Vol. 185, pp. 59-81.

Jinkine, V., Ferdinande,V. ,1974, "A method for predicting the added resistance of fast cargo ships in head waves", International Shipbuilding Progress, 21(238), pp. 149-167.

Judge, C., 2020, "Pressure Distributions on the Bottom of a Planing Hull During Slamming", Proceedings of the 12th International Conference on High Speed Marine Vehicles (HSMV), pp. 170-178.

Judge, C., Mousaviraad, M., Stern, F., Lee, E., Fullerton, A, Geiser, J., Schleicher, C., Merrill, C., Weil, C., Morin, J., Jiang, M. and Ikeda, C., 2020, "Experiments and CFD of a high-speed deep-V planing hull – part II: Slamming in waves", Applied Ocean Research, 97:102059.

Kashiwagi M., 1992, "Added resistance, wave-induced steady swayforce and yaw moment on an advancing ship", Ship Technology Research (Schiffstechnik),.39(1):3-16.

Katayama, T. and Amano, R., 2016, "An Experimental Study on the Characteristics of vertical acceleration on small high speed passenger craft irregular head waves", Journal of the Society of Naval Architects and Ocean Engineers (JASNOE), 23:65-76

Katayama, T., Adachi, T. and Sawae, T., 2018, "Roll Damping Estimation for Small Planing Craft", Proceedings of the 13th International Conference on the Stability of Ships and Ocean Vehicles (STAB), pp. 369-377.

Katayama, T. and Hashimoto, T., 2012, "Development of Free Running Model Test System of Planing Craft using Small Model", Proceedings of the Japan Society of Naval Architects and Ocean Engineers (JASNOE), 15:187-190.

Katayama, T., Ohashi, S., 2014, "A Study on Spinout Phenomena of Planing Craft in High Speed Turning with Radio Control Small Model", Proceedings of 14th International Ship Stability Workshop (ISSW), Kuala Lumpur, Malaysia, pp. 249-253.

Katayama, T., Taniguchi, T. and Habara, K., 2011, "Tank Tests to Estimate the Onset of Dynamic Instabilities of High-Speed Planing Craft", Transactions of the Society of Naval Architects and Marine Engineers, pp. 106-118.

Khayyer, A., Gotoh, H., Falahaty, H., and Shimizu, Y. 2018. "Key aspects for development of reliable and efficient fully-

Lagrangian computational methods for hydroelastic fluid structure interactions," Proceedings of the 8th International Conference on HYDROELASTICITY IN MARINE TECHNOLOGY, Sept 10-12, 2018, Seoul, Korea.

Kjellberg, M. and Gerhardt, F. C., 2019, "Improved methods for the experimental determination of added resistance in waves", Proceedings of the 6th International Conference on Advanced Model Measurement Technology (AMT), Rome, Italy.

Kihara, H., Dobashi, J., Hibi, S., Uemura, M., 2019, "Fundamental studies on the influence of wave loads on a trimaran's cross-deck structure", Journal of Marine Science and Technology, 24(1):221-236.

Kim, Y., Park, S.G., Kim, B.H., and Ahn, I.G., 2016, "Operational modal analysis on the hydroelastic response of a segmented container carrier model under oblique waves," Ocean Engineering, Vol. 127, pp. 357-367.

Kim, K.H., Choi Y.M. and Hong, S.Y., 2017a, "Experimental Investigations of the Characteristics of Pressure Sensors for2D Wedge Drop", International Journal of Offshore and Polar Engineering, 27(2):144-151.

Kim, Y., Yang, K.K., Kim, J.H. and Zhu, Z., 2017b, "Study of Water-entry Impact of Wedge and Ship-like Section Using Potential Theories and CFD", International Journal of Offshore and Polar Engineering, 27(2):168-176.

Kim, Y., Lee, J., Kim, J., 2017c, "Experimental Observation of the Effects of Liquid Temperature and Bubbles on Impact Pressure Inside Gas Pocket", International Journal of Offshore and Polar Engineering, Vol. 27, No. 1, pp 1–10.

Kim, Y., Kim, B.H., Choi, B.K., Park, S.G., Malenica, S., 2018, "Analysis on the full scale measurement data of 9400TEU container Carrier with hydroelastic response", Marine Structures, Vol. 61, pp. 25-45.

Kim, K.H., Kim, B.W. and Hong, S.Y., 2019a, "Experimental investigations on extreme bow-flare slamming loads of 10,000-TEU containership, Ocean Engineering, 171:225-240.

Kim, M., Hizir, O., Turan, O., Incecik, A., 2019b, "Numerical Studies on Added Resistance and Motions of KVLCC2 in Head Seas for Various Ship Speeds", Ocean Engineering, 140, pp. 466-476.

Kianejad, S. S., Enshaei, H., Duffy, J., Ansarifard, N., and Ranmuthugala, D., 2018, "Ship Roll Damping Coefficient Prediction Using CFD", 32nd Symposium on Naval Hydrodynamics

Kianejad, S. S., Enshaei, H., Duffy, J. and Ansarifard, N., 2019 "Prediction of a ship roll added mass moment of inertia using numerical simulation." Ocean Engineering 173: 77-89.

Knight, B. G., Maki, K. J., 2018, "Body Force Propeller Model for Unsteady Surge Motion", 37th International Conference on Ocean, Offshore and Arctic Engineering (OMAE2018), Madrid, Spain.

Knight, B., Xu, W. and Maki, K., 2020, "Numerical prediction of Self-Propulsion in Extreme Head Seas", 33rd Symposium on Naval Hydrodynamics

Kozlowska, A.M., Savio, L., and Steen, S., 2017, "Predictng Thrust Loss of Ship Propellers

Due to Ventilation and Out-of-Water Effect," Journal of Ship Research, 61(4): 198-213.

Kudupudi, R.B. and Datta, R., 2017, "Numerical Investigation of the Effect due to Vessel Motion on Green Water Impact on Deck", Proceedings of the 36th International Conference on Offshore Mechanics and Arctic Engineering (OMAE), Trondheim, Norway.

Kudupudi, R.B., Pal, S.K. and Datta R., 2019, "A Three-Step Hybrid Method to Study the Influence of Green Water Impact on a Large Containership in Time Domain", Journal of Offshore Mechanics and Arctic Engineering, 141(5):051804

Kuroda, M., Tsujimoto, M., Fujiwara, T., Ohmatsu, S. and Takagi, K., 2008), "Investigation on components of added resistance in short waves", Journal of the Japan Society of Naval Architects and Ocean Engineers, 8:171-176.

Kwon, C.S., Kim, H.J., Park, J.J., Lee, D.Y., Kim, B., 2017, "Sloshing Load Assessment for a Midscale Single-Row FLNG", International Journal of Offshore and Polar Engineering, Vol. 28, No. 3, pp 232–239.

Labat, B., 2017, "Stability of coupled heave-pitch motions of a fast foiling boat", Proceedings of the 15th International Conference on Fast Sea Transportation (FAST), Nantes, France, pp. 273-282.

Lakshmynarayanana, P. A., and Temarel, P. (2019). "Application of CFD and FEA coupling to predict dynamic behaviour of a flexible barge in regular head waves". Marine Structures, 65, 308-325.

Lakshmynarayanana, P.A. and Temarel, P. 2020. "Application of a two-way partitioned method for predicting the wave induced loads of a flexible containership," Applied Ocean Engineering, Vol. 96, no. 102052.

Lang, X., Mao, W., 2020, "A Simplified Ship Wave Induced Added Resistance Calculation Method and Full-scale Measurements Validation in Head Sea", 30th International Ocean and Polar Engineering Conference (ISOPE2020), Sapporo, Japan, pp. 3394-3402.

Lavroff, J., Davis, M.R., Holloway, D.S., Thomas, G.A., and McVicar, J.J. 2017. "Wave impact loads on wave-piercing catamarans," Ocean Engineering, Vol. 131, pp. 263-271.

Lee, J., Kim, S., Lee, S., Kang, D.,Lee, J., 2018, "Prediction of Added Resistance using Genetic Programming", Ocean Engineering, 153, pp.104-11.

Lee, J.H., Kim, B.S., Kim, B.S., Lee, J. and Kim, Y., 2020, "Added Resistance of a Bulk Carrier in Regular Head and Oblique Waves", Proceedings of the 30th International Ocean and Polar Engineering Conference (ISOPE), Shanghai, China, pp. 3385-3392.

Li, A., and Li, Y., 2020. "Influence of Wave Amplitude on Seakeeping Performance of a High-speed Trimaran with T-foil in Head Seas." In The 30th International Ocean and Polar Engineering Conference. International Society of Offshore and Polar Engineers.

Li, Z., Gao, X. and Huo, C., 2018, "Numerical investigation of hydrodynamic behavior of a deformable trimaran in head waves", Proceedings of the 28th International Ocean and Polar Engineering Conference (ISOPE), Sapporo, Japan, pp. 316-323.

Liang, H. and Chen, X.B., 2017, "A new multi-domain method based on an analytical control surface for linear and second-order mean drift wave loads on floating bodies", Journal of Computational Physics, 347:506-532.

Liao, K., Duan, W., Ma, Q., Ma, S. and Yang, J., 2017, "Numerical Simulation of Green Water on Deck with a Hybrid Eulerian-Lagrangian Method", Proceedings of the 27th International Ocean and Polar Engineering Conference (ISOPE), San Francisco, USA.

Liao, Y., Martins, J.R.R.A. and Young, Y.L. 2019, "Sweep and Anisotropy Effects on the Viscous Hydroelastic Response of Composite Hydrofoils," Composite Structures, 230: 111471.

Lin, Y., Ma, N., Wang, D. and Gu, X., 2018, "Numerical Prediction and Experimental Validation of Slamming Load for Large Container Ship Undergoing Parametric Rolling Motion", Proceedings of the 37th International Conference on Offshore Mechanics and Arctic Engineering (OMAE), Madrid, Spain.

Liu, C., Chen, G., Wan, D., 2018, "CFD Study of Added Resistance and Motion of DTC in Short and Long Waves", 37th International Conference on Ocean, Offshore and Arctic Engineering (OMAE2018), Madrid, Spain.

Liu, C., Wang, J.H., and Wan, D.C., 2018, "CFD Simulations of Self-propulsion and Turning Circle Manoeuvre in Waves" 32nd Symposium on Naval Hydrodynamics

Liu, L., Wang, X., He, R., Zhang, Z. and Feng, D., 2020, "CFD prediction of stern flap effect on Catamaran seakeeping behavior in long crest head wave." Applied Ocean Research 104: 102367.

Liu, N., Zhuo, F., Zhou, X., Qiu, J., Li, C., and Ren, H., 2019, "Experimental Investigation of the Motion of a Fully Skirted Air Cushion Vehicle in Regular Waves", Proceedings of the 29th International Ocean and Polar Engineering Conference (ISOPE), Honolulu, USA, pp. 4447-4453.

Liu, S., Papanikolaou, A., 2016, "Fast Approach to the Estimation of the Added Resistance of Ships in Head Waves", Ocean Engineering, 112, pp. 111-225.

Liu, S. and Papanikolaou, G., 2016a, "Prediction of the Added Resistance of Ships in Oblique Seas", Proceedings of the 26th International Ocean and Polar Engineering Conference (ISOPE), Rhodes, Greece, pp. 495-502.

Lyu, W., el Moctar, O., 2017, "Numerical and Experimental Investigations of Wave-induced Second Order Hydrodynamic Loads", Ocean Engineering, 131, pp. 197-212.

Lyu, W., Riesner, M., Peters, A., Moctar, O., 2019, "A Hybrid Method for Ship Response Coupled with Sloshing in Partially Filled Tanks", Marine Structures, Vol. 67, 102643.

Ma, L. and Liu, H., 2017, "Numerical Study of 2-D Vertical Water-entry Problems Using Two-phase SPH Method", International Journal of Offshore and Polar Engineering, 27(2):160-167.

Magoga, T., Aksus, S., Cannon, S., Ojeda, R., and Thomas, G., 2017, "Identification of slam events experienced by a high-speed craft", Ocean Engineering, 140:309-321.

Malas, B., Banks, J., Cappelletto, J., Thornton, B., 2019, "Applications of motion capture technology in a towing tank", 6th International Conference on Advanced Model Measurement Technology for theMaritime Industry (AMT), Rome.

Malas, B., 2020, "The Boldrewood Towing Tank", The Naval Architect, Feb 2020, pp 30-34, RINA.

Malenica, S., Diebold, L., Kwon, S.H., Cho, D.S., 2017, "Sloshing Assessment of the LNG Floating Units with Membrane Type

Containment System Where We Are?", Marine Structures, Vol. 56, pp 99 – 116.

Mathew, J., Sgarioto, D., Duffy, J., Macfarlane, D., Denehy, S., Norman, J., Cameron, A., Eutick, N., van Walree, F., 2018, "An experimental study of ship motions during replentishment at sea operations between a supply vessel and a landing helicopter dock", Transactions of RINA, Vol. 160, Part A2, Intl J Maritime Eng. 2018.

Miyashita, T., Okada, T., Kawamura, Y., Seki, N., and Hanada, R. 2020, "Statistical Characteristics of Whipping Response of a Large Container Ship Under Various Sea States and Navigational Conditions Based on Full-Scale Measurements," PRADS 2019: Practical Design of Ships and Other Floating Structures, pp. 3-24.

Monroy, C., Seng, S., Diebold, L., Benhamou, A. and Malenica, Š, 2017, "A Comparative Study of the Generalized Wagner Model and a Free-Surface RANSSolver for Water Entry Problems", International Journal of Offshore and Polar Engineering (ISOPE), 27(2):135-143.

Morace, F. and Ruggiero, V., 2018, "Comparative Test in Design of Hydrofoils for a New Generation of Ships", Proceedings of the 19th International Conference on Ship & Maritime Research (NAV), Trieste, Italy, pp. 418-425.

Mutsuda, H., Kanehira, T., Kawawaki, K., Doi, Y. and Yasukawa, H. , 2018, "Occurrence of stern slamming pressure and its characteristics in following irregular waves. ", Ocean Engineering, 170:222-236.

Niklas, K., and Pruszko., H., 2019, "Full scale CFD seakeeping simulations for case study ship redesigned from V-shaped bulbous bow to X-bow hull form." Applied Ocean Research 89: 188-201.

Nwogu, O.G. and Beck, R.F., 2010, "Efficient computation of nonlinear wave interaction with surface-piercing bodies with an FFT-accelerated boundary integral method", Proceedings of the 28th Symposium on Naval Hydrodynamics, Pasadena, USA.

Nwogu, O.G. and Beck, R.F., 2017, "Fast computation of the transient motions of moving vessels in irregular ocean waves", Applied Ocean Research, 65:23-34.

O'Reilly, C., Murphy, M.J., Doyle, J. and Kring, D.C., 2017, "A quasi-nonlinear seakeeping model for planing hulls using a boundary element method", Proceedings of the 15th International Conference on Fast Sea Transportation (FAST), Nantes, France, pp. 257-265.

O'Reilly, C.M., Piro, D.J., Murphy, M.J., Miao, S., Liu, Y., and Kring, D.C., 2018, "A Quasi-Nonlinear Seakeeping Model for Planing Hulls using an Accelerated Boundary Element Method", Proceedings of the 32th Symposium on Naval Hydrodynamics, Hamburg, Germany.

O'Shea, T.T., Conroy, D.T., and Hall, R.E. 2018, "Nonlinear Simulation of a Rogue Wave and its Impact on a Ship", 32nd Symposium on Naval Hydrodynamics

Otzen, J. F., Esquivel, P., Simonsen, C. D., Stern, F., 2018, "CFD and EFD Prediction of Added Powering of KCS in Regular Head Waves", 32rd Symposium on Naval Hydrodynamics, Hamburg, Germany.

Park, D.M., Lee, J. and Kim, Y., 2015, "Uncertainty analysis for added resistance experiment of KVLCC2 ship", Ocean Engineering, 95:143-156.

Park, D.M., Kim, Y, Seo, M.G. and Lee, J., 2016, "Study on added resistance of a tanker in head waves at different drafts", Ocean Engineering, 111:569-581.

Park, D.-M., Lee, J. and Kim, Y., 2017, "Numerical and Experimental Study on Nonlinear Motion Response of Tumblehome Hull", Proceedings of the 15th International Conference on Fast Sea Transportation (FAST), Nantes, France, 71-77.

Park, D.M., Lee, J., Jung, Y.W., Lee, J. and Kim, Y., 2018 "Comparison of Added Resistance in Oblique Seas by Numerical Analysis and Experimental Measurement", Proceedings of the 28th International Ocean and Polar Engineering Conference (ISOPE), Sapporo, Japan, pp. 139-146.

Park, D.M., Lee, J., Jung, Y.W., Lee, J. and Kim, Y., and Gerhardt, F, 2018, "Experimental and numerical studies on added resistance of ship in oblique sea conditions", Ocean Engineering, 186, 106070.

Park, D.M., Lee, J., Jung Y., Lee, J., Kim, Y., Gerhardt, F., 2019, "Experimental and Numerical Studies on Added Resistance of Ship in Oblique Sea Conditions", Ocean Engineering, 186, 106070.

Pellegrini, R., Diez, M., Wang, Z., Stern, F., Wang, Z., Wong, Z., Yu, M., Kiger, K.T., and Duncan, J.H. 2020. "High-Fidelity FSI Simulations and V&V of Vertical and Oblique Flexible Plate Slamming," 33rd Symposium on Naval Hydrodynamics, Osaka, Japan, May 31-June 5, 2020.

Pennino, S., Begovic, E., Bertorello, C. and Scamardella, A., 2018, "Time Domain Assessment of Vertical Motions of Planing Hulls", Proceedings of the 19th International Conference on Ship & Maritime Research (NAV), Trieste, Italy, pp. 472-479.

Pollalis, C., Hizir, O., Boulougouris, E. and Turan, O., 2018, "Large Amplitude Time Domain Seakeeping Simulations of KVLCC2 in Head Seas Taking Into Account Forward Speed Effect", Proceedings of the 37th International Conference on Offshore Mechanics and Arctic Engineering (OMAE), Madrid, Spain.

Rajendran, S., Fonseca, N. and Soares, C. G., 2016, "Prediction of vertical responses of a container ship in abnormal waves", Ocean Engineering, 119:165-180.

Rajendran, S. and Soares, C.G. 2018. "Short term statistics of hydroelastic loads of a container ship in head and oblique seas," Proceedings of the ASME 2018 37th International Conference on Ocean, Offshore and Arctic Engineering (OMAE2018), June 17-22, 2018, Madrid, Spain.

Riesner, M., Ley, J., el Moctar, O. 2018a, "An Efficient Approach to Predict Wave-Induced Global Hydroelastic Ship Response", Proceedings of the 8th International Conference on Hydroelasticity in Marine Technology, South Korea, Sept. 10-12, 2018.

Riesner, M., el Moctar, O., 2018b, "A Time Domain Boundary Element Method for Wave Added Resistance of Ships Taking into Account Viscous Effects", Ocean Engineering, 162, pp. 290-303.

Rodrigues, J. M. and Soares, C. G., 2017, "Froude-Krylov forces from exact pressure integrations on adaptive panel meshes in a time domain partially nonlinear model for ship motions", Ocean Engineering, 139:161-183.

Rosen, A., Begovic, E., Razola, M. and Garme, K., 2017, "High-speed craft dynamics in waves: challenges and opportunities related to the current safety philosophy", Proceedings of the 17th International Ship Stability Workshop (ISSW), pp. 239-248.

Rosetti, G.F., Pinto, M.I., de Mello, P.C., Sampaio, C.M.P., Simos, A.N., and Silva, D.F.C, 2019, "CFD and experimental

assessment of green water events on an FPSO hull section in beam waves." Marine Structures 65: 154-180.

Sadat-Hosseini, H., Wu, P.C., Carrica, P.M., Kim, H., Toda, Y. and Stern, F., 2013, "CFD verification and validation of added resistance and motions of KVLCC2 with fixed and free surge in short and long head waves", Ocean Engineering, 59:240-273.

Sanada, Y., Kim, D., Sadat-Hosseini, H., Toda, Y., Simonsen, C., Stern, F., 2018, "Experiment and Numerical Simulation for KCS Added Powering in Regular Head/Oblique Waves", 32rd Symposium on Naval Hydrodynamics, Hamburg, Germany.

Sanada, Y., Kim, D., Sadat-Hosseini, H., Stern, F., Hossain, M. D., Wu, P., Toda, T., Otzen, J., Simonsen, C., Abdel-Maksoud, M., Scharf, M., Grigoropoulos, G., 2020, "Assessment of Experimental and CFD Capability for KCS Added Power in Head and Oblique Waves", 33rd Symposium on Naval Hydrodynamics, Osaka, Japan.

Saripilli, J.R., Sen, D., 2018, "Numerical studies on effects of slosh coupling on ship motions and derived slosh loads", Applied Ocean Research, Vol. 76, pp 71 – 87.

Scharnke, J., Berg, J. van den, Wilde, J. de, Vestbøstad, T. and Haver, S., 2012. "Seed variations of extreme sea states and repeatability of extreme crest events in a model test basin", Proceedings of the 31st International Conference on Ocean, Offshore and Arctic Engineering (OMAE), Rio de Janeiro, Brazil. OMAE2012-83303.

Seo, M.G., Yang, K.K., Park, D.M. and Kim, Y., 2014, "Numerical analysis of added resistance on ships in short waves", Ocean Engineering, 87:97-110.

Seo, S., Park, S., Koo, B., 2017, "Effect of Wave Periods on Added Resistance and Motions of A Ship in Head Sea Simulations", Ocean Engineering, 137, pp. 309-327.

Shabani, B, Lavroff, J., Davis, M.R., Holloway, D.S. and Thomas, G.A., 2019, "Slam loads and pressures acting on high-speed wave-piercing catamarans in regular waves", Marine Structures, 66:136-153.

Shabani, B., Lavroff, J., Holloway, D. S., Davis, M. R., and Thomas, G. A., 2018, "The effect of centre bow and wet-deck geometry on wet-deck slamming loads and vertical bending moments of wave-piercing catamarans", Ocean Engineering, 169():401-417.

Shahraki, J.R., Davis, M.R. and Thomas, G.A., 2017, "The Influence of Centre Bow Length on Slamming Loads and Motions of Large Wave-Piercing Catamarans", Transactions of the Royal Institution of Naval Architects Part A: International Journal of Maritime Engineering, 160:57-69.

Shakibfar, S., Anderson, I.M., and Brandt, A. 2020, "Vibration Damping of Large Containership in Operation," PRADS 2019: Practical Design of Ships and Other Floating Structures, pp. 321-329.

Shan, P., Zhu, R., Wang, F. and Wu, J., 2019, "Efficient approximation of free-surface Green function and OpenMP parallelization in frequency-domain wave–body inter-actions", Journal of Marine Science and Technology, 24(2):479-489.

Shivachev, E., Khorasanchi, M., Day, S., and Turan, O., 2020. "Impact of trim on added resistance of KRISO container ship (KCS) in head waves: An experimental and numerical study". Ocean Engineering, 211, 107594.

Sigmund, S., el Moctar, O., 2017, "Numerical and experimental investigation of propulsion in waves", Ocean Engineering, 144, pp. 35-49.

Sigmund, S., el Moctar, O., 2018, "Numerical and Experimental Investigation of Added Resistance of Different Ship Types in Short and Long Waves", Ocean Engineering, Vol. 147, pp 51-67.

Silva, D.F.C., Coutinho, A.L.G.A., Esperança, P.T.T., 2017, "Green water loads on FPSOs exposed to beam and quartering seas, part I: Experimental tests", Ocean Engineering, Volume 140, pp 419-433. https://doi.org/ 10.1016/j.oceaneng.2017.05.005.

Skejic, R., Steen, S., 2020, "On Total Resistance of Ships in a Seaway", 14th Practical Design of Ships and Other Floating Structures (PRADS2019), Yokohama, Japan, pp. 163-185.

Son, N.S., Kim, S.Y., Kim, Y.G., Oh, B.I. and Ha, W.H., 2010, "Development of Additional Towing Device with a Servo Motor for Free Model Tests", Proceedings of the 10th Asian Conference On Marine Simulator And Simulation Research, pp. 67-74.

Spinosa, E. and Iafrati, A. 2021. "Experimental investigation of the fluid-structure interaction during the water impact of thin aluminium plates at high horizontal speed," International Journal of Impact Engineering, Vol. 147, no. 103673.

Sugimoto, K., Fukumoto, Y., Kawabe, H., Ishibashi, K., Houtani, H., Oka, M., 2019, "Non-linear Effect on Wave-Induced Loads in Vehicles Carrier for Hull Design - Froude-Krylov Force", Proceedings of 14th International Symposium on Practical Design of Ships and Other Floating Structures, Yokohama, Japan.

Sun, H. and Helmers, J.B., 2020, "Influence of short-wave components on the slamming loads", Proceedings of the 30th International Ocean and Polar Engineering Conference (ISOPE), Shanghai, China, pp. 2155-2163.

Sun, Z., Deng, Y.Z., Zou, L. and Jiang, Y.C., 2020, "Investigation of trimaran slamming under different conditions", Applied Ocean Research, 104:102316.

Sun, Z., Jiang, Y., Zhang, G., Zong, Z., Xing, J.T. and Djidjeli, K., 2019, "Slamming load on trimaran cross section with rigid and flexible arches", Marine Structures, 66:227-241.

Sun, Z., Korobkin, A., Sui, X.P., and Zong, Z., 2021. "A semi-analytical model of hydroelastic slamming," Journal of Fluids and Structures, Vol. 101, 103200.

Sung, H.G., Hong S.W., Kim J.H., Yun, S.H., Cho, S.K., Nam, B.W., 2016, "Design Issues and Modeling [!] Perspectives of Offshore Basin", Offshore Technology Conference, Kuala Lumpur.

Taian, H., Shuangqiang, W., Guiyong, Z., Zhe, S., Bo, Z., 2019, "Numerical simulations of sloshing flows with an elastic baffle using a SPH-SPIM coupled method", Applied Ocean Research, Vol. 93, pp 71 – 87.

Takami, T., Matsui, S., Oka, M., and Iijima, K. 2018. "A numerical simulation method for predicting global and local hydroelastic response of a ship based on CFD and FEA coupling". Marine Structures, 59, 368-386.

Takami, T. and Iijima, K. 2020. "Numerical investigation into combined global and local hydroelastic response in a large container ship based on two-way coupled CFD and FEA," Journal of Marine Science and Technology, Vol. 25, pp. 346-362.

Taskar, B., Regener, P. B., Andersen, P., 2020, "The Impact of Variation in Added Resistance Computations on Voyage Performance Prediction", 14th Practical

Design of Ships and Other Floating Structures (PRADS2019), Yokohama, Japan, pp. 133-149.

Tavakoli, S., Dashtimanesh, A. and Mancini, S., 2017, "A theoretical method to explore influence of free roll motion on behavior of a high speed planing vessel through steady yawed motion", Proceedings of the 11th International Conference on High Speed Marine Vehicles (HSMV), Naples, Italy.

Tavakoli, S., Dashtimanesh, A. and Sahoo, P., 2017, "Theoretical model for roll dynamic response of a planing boat in oblique waves", Proceedings of the 15th International Conference on Fast Sea Transportation (FAST), Nantes, France, pp. 63-70.

Tavakoli, S., Dashtimanesh, A. and Sahoo, P., 2018, "Prediction of Hydrodynamic Coefficients of Coupled Heave and Pitch Motions of Heeled Planing Boats by Asymmetric 2D+T Theory", Proceedings of the 37th International Conference on Offshore Mechanics and Arctic Engineering (OMAE), Madrid, Spain.

Terada, D., Amano, R. and Katayama, T., 2017, "A motion estimation method of high speed craft in irregular sea by using onboard monitoring motion time series data for motion control", Proceedings of the 17th International Ship Stability Workshop (ISSW), pp. 233-238.

Toxopeus, S., Sadat-Hosseini, H., Visonneau, M., Guilmineau, E., Yen, T. G., Lin, W. M., and Stern, F., 2018. "CFD, potential flow and system-based simulations of fully appended free running 5415M in calm water and waves." International Shipbuilding Progress, 65(2), 227-256.

Tsujimoto, M., Sogihara, N., Kuroda, M., Kume, K., Ohba, H., 2018, "A Practical Prediction Method for Self Propulsion Factors in Actual Seas", 28th International Ocean and Polar Engineering Conference (ISOPE2018), Sapporo, Japan, pp. 863-870.

Tsukada, Y, Ueno, M, Tanizawa, K, Miyazaki, H, Takimoto, T and Kitagawa, Y, 2013, "Development of an Auxiliary Thruster for Free running Model Ship Tests", Journal of the Japan Society of Naval Architects and Ocean Engineers, 16:327-328.

Tsukada, Y., Suzuki, R., Ueno, M., 2017, "Wind Loads Simulator for Free-Running Model Ship Test", Proceedings of the ASME 36th International Conference on Ocean, Offshore and Arctic Engineering (OMAE), Trondheim, Norway.

Tukker, J., Bouvy, A., Bloemhof, F., 2019, "Measurement quality of electrical resistance wave gauges", 6th International Conference on Advanced Model Measurement Technology for theMaritime Industry (AMT), Rome.

Walree, F. van and Luth, H.R., 2000, "Scale Effects on Foils and Fins in Steady and Unsteady Flow", Hydrodynamics of High Speed Craft – Wake Wask and Motion Control, RINA, London.

Walree, F. van, Peters, A.J. and Kat, J.O. de, 2004, "Development of Model Testing and Numerical Simulation Techniques for Safety Assessment of High Speed Craft", Proceedings of the 2nd International Maritime Conference on Design for Safety, Sakai, Japan.

Walree, F. van and Thomas, W.L., 2017, "Validation of simulation tools for a RHIB operating in heavy seas", Proceedings of the 17th International Ship Stability Workshop (ISSW), pp. 249-258.

Walree, F. van and Sgarioto, D., 2019, "Impulsive loads on and water ingress in a landing craft: model tests and simulations",

Proceedings of the 17th International Ship Stability Workshop (ISSW), pp. 175-182.

Walree, F. van and Struijk, G.D., 2021, "Validation of a Time Domain Seakeeping Code by Model and Full Scale Experiments for a RHIB", Practical Design of Ships and Other Floating Structures (PRADS), pp. 843-856.

Walree, F. van, Serani, A., Dietz, M. and Stern, F., 2020, "Prediction of Heavy Weather Seakeeping of a Destroyer Hull Form by Means of Time Domain Panel and CFD Codes", Proceedings of the 33rd Symposium on Naval Hydro-dynamics, Osaka, Japan.

Wang, H. D., Qian, P., Liang, X. F. and Yi, H., 2016, "Vertical plane motion control of an S-SWATH vehicle with flapping foil stabilisers sailing in waves", Ocean Engineering, 121:184-195.

Wang, S. and Soares, C.G. , 2016, "Stern slamming of a chemical tanker in irregular head waves", Ocean Engineering, 122:322-332.

Wang, S., Rajendran, S. and Guedes Soares, C., 2018, "Investigation of Bottom Slamming on Ships in Irregular Waves", Proceedings of the 37th International Conference on Offshore Mechanics and Arctic Engineering (OMAE), Madrid, Spain.

Wang, D., Liu, K., Huo, P., Qiu, S., Ye, J. and Liang, F., 2019, "Motions of an unmanned catamaran ship with fixed tandem hydrofoils in regular head waves", Journal of Marine Science and Technology, 24(3):705–719.

Wang, X., Bonoli, J., Cohan, M. and Fürth, M., 2020b, "Design and Testing Outline for a Free Running Model of a High Speed Craft", Proceedings of the 12th International Conference on High Speed Marine Vehicles (HSMV), pp. 21-32.

Wang, A., Kim, H., Wong, K.P., Yu, M., Kiger, K.T., and Duncan, H.H. 2020a. "The Impact of a Flexible Plate on a Quiescent Water Surface," 33rd Symposium on Naval Hydrodynamics, Osaka, Japan, May 31-June 5, 2020.

Weems, K.M., Belenky, V., and Spyrou, K.J., 2018, "Numerical Simulations for Validating Models of Extreme Ship Motions in Irregular Waves", Proceedings of the 32th Symposium on Naval Hydrodynamics, Hamburg, Germany.

Wei, C., Mao, L., Li, Y. and Yi, H., 2017, "Hydrodynamics Prediction of a Semi-planning Wave-piercing Craft", Proceedings of the 27th International Ocean and Polar Engineering Conference (ISOPE), San Francisco, USA, pp. 977-983.

Wicaksono, A., Kashiwagi, M., 2018, "Wave-induced Steady Forces and Yaw Moment of a Ship Advancing in Oblique Waves", Journal of Marine Science and Technology, 23, pp. 767-781.

Wielgosz, C., Rosen, A., Datla, R., Chung, U. and Danielsson, J., 2020, "Experimental modelling of spray deflection influence on planing craft performance in calm water and waves", Journal on Engineering for the Maritime Environment, 234(2):399-408.

Woeste, J. T., Gouveia1, R. K., O'Reilly, C., Young, Y., 2020, "Added Resistance and Added Power of the KCS in Head Seas", SNAME Maritime Convention 2020 (SMC2020), Houston, USA.

Xie, H., Ren, H.,Li, H. and Tao, K., 2018, "Numerical Prediction of Bow-Flared Slamming on ULCS in Oblique Waves", Proceedings of the 37th International Conference on Offshore Mechanics and Arctic Engineering (OMAE), Madrid, Spain.

Yang, B. and Wang , D., 2017a, "The Dynamic Response of the Large Containership's Bow Structure under Slamming Pressures", Proceedings of the 27th International Ocean and Polar Engineering Conference (ISOPE), San Francisco, USA, pp. 273-279.

Yang, L., Yang H., Yan, S. and Ma, Q., 2017b, "Numerical Investigation of Water-Entry Problems Using IBM Method", International Journal of Offshore and Polar Engineering, 27(2):152-159.

Yao, C-B., Sun, X-S., Wang, W. and Ye, Q., 2017, "Numerical and experimental study on seakeeping performance of ship in finite water depth", Applied Ocean Research, 67:59-77.

Yao, J., Su, Y., Song, X., Liu, Z., Cheng, Z., Zhana, C., 2020, "RANS Analysis of the Motions and Added Resistance for KVLCC2 in Head Regular Waves", Applied Ocean Research, Vol. 105, 102398.

Yildiz, B., Kahramanoglu, E., Cakici, F. and Katayama, T., 2017, "Numerical and experimental prediction of roll damping for a high-speed planing hull", Proceedings of the 11th International Conference on High Speed Marine Vehicles (HSMV), Naples, Italy.

Yoo, O., Kim, T., Kim, H., 2020, "A Numerical Study to Predict Added Resistance of Ships in Irregular Waves", International Journal of Offshore and Polar Engineering, Vol. 30, No. 2, pp. 161-170.

Young, Y.L., Motley, M. R., Barber, R.B., Chae, E., and Garg, N., 2016, "Adaptive Composite Marine Propulsors and Turbines: Progress and Challenges," Applied Mechacnis Reviews, 68(6).

Young, Y.L., Harwood, C.M., Montero, F.M., Ward, J.C., and Ceccio, S. L., 2017, "Ventilation of lifting surfaces: review of the physics and scaling relations," Applied Mechacnis Reviews, 69(1).

Young, Y.L., 2019, "Hydroelastic Response of Lifting Bodies in Separated Flows," NATO-AVT-307: Symposium on Separated Flow: Prediction, Measurement and Assessment for Air and Sea Vehicles, Trondheim, Norway, Oct. 7-9, 2019.

Young, Y.L., Wright, T., Yoon, H. and Harwood, C.M., 2020, "Dynamic Hydroelastic Response of a Surface-Piercing Strut in Waves and Ventilated Flows," Journal of Fluids and Structures, 94:102899.

Yu, P., Li, H. and Ong, M.C., 2019, ""Hydroelastic analysis on water entry of a constant-velocity wedge with stiffened panels"", Marine Structures, 63:215-238.

Yuan, Y and Wang, C., 2018, "Study on the Porpoising Phenomenon of High-Speed Trimaran Planing Craft", Proceedings of the 37th International Conference on Offshore Mechanics and Arctic Engineering (OMAE), Madrid, Spain.

Zangle, T., Seekins, J., O'Reilly, C. and Kring, D., 2020, "An investigation of advanced boundary element methods", Proceedings of the 33rd Symposium on Naval Hydro-dynamics, Osaka, Japan.

Zeraatgar, H., Malekmohammadi, J., Javaherian, M.J. and Moradi, H., 2019, "Sampling rate effect on wedge pressure record in water entry by experiment", Ocean Engineering, 179:51-58.

Zhang, K., Ren, H., Li, H., Tong, X. 2017, "Nonlinear Wave Loads' Prediction Based on Three-Dimensional Hydroelasticity Theory in Irregular Waves," Proceedings of the Twenty-seventh (2017) International Ocean and Polar Engineering Conference, San Francisco, CA, USA, June 25-30, 2017.

Zhang, Y., Wan, D., 2018, "MPS-FEM coupled method for sloshing flows in an elastic tank", Ocean Engineering, Vol. 152, 101950.

Zhang, W., el Moctar, O., 2019, "Numerical Prediction of Wave Added Resistance using a Rankine Panel Method", Ocean Engineering, 178, pp. 66-79.

Zhang, W., el Moctar, O., Schellin, T. E., 2020, "Numerical Study on Wave-induced Motions and Steady Wave Drift Forces for Ships in Oblique Waves" Ocean Engineering, 196, pp. 106806.

Zhuang Y., Wan, D., Bouscasse, B., Ferrant, P., 2020, "A Combined Method of HOS and CFD for Simulating a Container Ship in Steep Waves", 33rd Symposium on Naval Hydrodynamics

Appendix A. : Note on Benchmarking

A.1. INTRODUCTION

Online definition of benchmark (Merriam-webster.com) is "a standardized problem or test that serves as a basis for evaluation or comparison". Benchmarks are key to monitor scientific progresses and evaluate uncertainty or precision of a model. Consequently they are of great interest to scientists, at least if the quality of the underlying data is sufficient for the scope of the benchmark. As numerical models and experimental techniques evolve, benchmarks can become obsolete but also they could also become relevant for a scope not previously identified.

This document lists the various benchmarks proposed successively in ITTC procedures in a more comprehensive form. Some comments are formulated on the quality or relevance of very old benchmark data, then some remarks are made about what could be done to improve ITTC benchmarks during future committees.

A.2. A BIT OF BACKGROUND

The ITTC seakeeping committee has been discussing benchmarks from its creation under the form of comparative tests between towing tanks. Some of those tests are reported in the seakeeping report of the 7th (1955), 11th (1966), 17th (1984) and 18th (1987) ITTC, and the word benchmark appears then in the final recommendation of the 19th ITTC (1990) "The committee should encourage well documented "benchmark" seakeeping experiments". This is also mentioned in the 21th ITTC (1996) "absolutely recommended to make available benchmarks (high precision experiments/computations) and make systematic use of them for (...) uncertainty analysis and (...) validation..".

Then in 25th ITTC (2008), the objectives about benchmarking are specified "determining the requirements for benchmark seakeeping tests in oblique waves", introducing criteria. The ITTC seakeeping committee also looked back to the previous benchmarks, suggesting that their quality and usability/availability should be reviewed. Then in the 26th ITTC (2011) the seakeeping committee specified the need of benchmarking for more specific topics like added resistance or slamming loads.

The ITTC-ISSC joint committee has also proposed benchmarks, though these are not systematically referenced in ITTC recommended procedures (Kim et al. (2016), Horel et al (2019)). Outside ITTC other benchmarks exist, particularly dedicated to CFD validation for seakeeping problems, see among others CFD workshops Larsson et al. (2010) and Larsson et al. (2018).

Generally for most ITTC committees the subject is still of great importance as testified by the ongoing development of the Benchmark repository section of the ITTC website.

A.3. DEFINITION AND CRITERIA

Definition and criteria for benchmark tests are retrieved from the 25th ITTC (2008) seakeeping committee report.

A.3.1. DEFINITIONS

Benchmark tests are those that generate experimental data, both model and full-scale, that are presented in a way that makes the results reproducible both numerically and experimentally, to be used for the validation of numerical methods and the verification of experimental procedures. These data should be fit for the intended purpose, should include some uncertainty analysis, and should be publicly available.

A.3.2. CRITERIA

Minimum information needed to be reported to accurately reproduce the experiment:

- *Ship/model condition* – Hull form (both above and underwater if necessary), model scale, appendage definitions, mass/displacement, draft/trim, hydrostatics, mass distribution, radii of gyration, centre of gravity, natural periods.
- *Sailing conditions* – Ship speed and heading.
- *Wave conditions* – Wave amplitude, frequency and wave slope; type of spectrum, significant wave height, modal period, and spreading.
- *Test Details* – Free running/towing arrangement, control laws, run duration/number of wave encounters, wave measurement (fixed or encountered), and facility parameters.
- *Presentation of Data* – Units/sign convention, reference system, definitions of presented data, tabular data preferred, and uncertainty analysis.

A.3.3. COMMENT

The definition and criteria proposed are still relevant. It might be important to further encourage the description of the setup keeping in mind the future use for validation of time domain CFD. CFD inherently produces much more detailed flow information than older panel and strip based seakeeping methods. More precise info of waves input could enhance the usability of the benchmarks.

A.4. LIST OF EXISTING BENCHMARKS

The list is provided in a table form given in Appendix B. It has been built by first listing the benchmarks provided in each recommended procedure and then gathering some additional candidate to be considered in next ITTC benchmarks selection. Litterature mentioned in Appendix B is detailed in the references of Appendix A. The table proposes also a first layout to compare the benchmark. This table would need to be further completed.

- 75-02-07-021 (Seak Exp - 4.2 Benchmark tests)
- 75-02-07-022 (Power Increase in IW - No benchmarks)
- 75-02-07-023 (Rarely Occuring Events - 4.2 Benchmark tests)
- 75-02-07-025 (Verification and Validation of Linear and Weakly Nonlinear Seakeeping Computer Codes - 5 Benchmark tests session is partially same as 21 procedure but not completely)

- 75-02-07-026 (Sloshing - 4.3 Benchmark Tests empty)
- 75-02-07-028 (fw factor - 7 Benchmark tests)

Each procedure does not correspond directly to a physical quantity to be assessed. A list of quantities relevant to seakeeping are discussed in the procedures.

Identified quantities that have to be benchmarked:

- Motions
- Loads
- Added resistance/ Added thrust
- Bending moment
- Green water
- Slamming

A.5. CONCLUSIONS AND RECOMMENDATIONS FOR FUTURE WORK

Benchmark criteria and definition from the 25th ITTC is still relevant but improvements might be needed to take into account the needs for benchmarking CFD methods that inherently generate much more detailed flow information than older seakeeping methods.

In procedure 7.5-02-07-02.8 the benchmarks are organized as a list of dataset references for each identified hull form. This might be a more efficient classification than experiment by experiment.

The proposed path forward is:

- Review criteria
- Review quantities
- Add missing relevant benchmarks
- Fill the table (checking scope and criteria)
- Decide whether existing benchmarks are obsolete or not
- Propose new distribution of benchmarks on procedures and websites

A.6. REFERENCES

7th , 11th , 17th , 18th , 19th , 20th , 21st , 25th ITTC . Report of the Seakeeping committee.

Bouscasse, B., Broglia, R., and Stern, F., 2013, "Experimental investigation of a fast catamaran in head waves" Ocean engineering, 72, 318-330.

Buchner, B., 2002, "Green water on ship-type offshore structures", Doctoral dissertation, Delft University of Technology.

Clauss, G. N. F., Klein, M., and Dudek, M., 2010, "Influence of the bow shape on loads in high and steep waves." In International Conference on Offshore Mechanics and Arctic Engineering (Vol. 49101, pp. 159-170).

Fonseca, N., and Guedes Soares, C., 2004, "Experimental investigation of the nonlinear aspects on the statistics of vertical motion and loads of a containership in irregular waves". Journal of Ship Research, 48(2):148{167}.

Gerhardt, F. C., Kjellberg, M., Korkmaz, B., Ljungqvist, K., and Shiri, A, 2020, "Determining the EEDI minimum propulsion power" Influence of EEDI on Ship Design & Operation. Online conference 27th May 2020,

UK: Royal Institution of Naval Architects, 1-15.

Gerritsma, J., and Beukelman, W., 1972. "Analysis of the resistance increase in waves of a fast cargo ship", International Shipbuilding Progress, Vol 19, No. 217, pp 285-293

Guo. B. and Steen. S., 2011, "Evaluation of added resistance of KVLCC2 in short waves", Journal of Hydrodynamics, Vol. 23, No. 6, pp 709-722.

Hamoudi H. and Varyami, K.S., 1998, "Significant Load and Green Water on Deck of Offshore Units/Vessels", Ocean Engineering, 25(8):715-731: S-175 Model Tests in Head Sea Waves for Deck Wetness Measurement

Horel, B., Bouscasse, B., Merrien, A., and de Hauteclocque, G., 2019, "Experimental assessment of vertical shear force and bending moment in severe sea conditions". In International Conference on Offshore Mechanics and Arctic Engineering, Vol. 58783, American Society of Mechanical Engineers.

Joncquez, S.A.G., 2011, "Comparison results from S-OMEGA and AEGIR", FORCE Technology report No. Force 107-24345.21.

Journee, J.M.J., 1992. "Experiments and calculations on four Wigley hull forms", Delft University of Technology Report 0909-DUT-92. Delft; Delft University. Kihara, H. Naito.

Kim, Y., and Kim, J.H., 2016, "Benchmark study on motions and loads of a 6750-TEU containership", Ocean Engineering

Larsson, L., Stern, F., and Visonneau, M., 2010, "A workshop on numerical ship hydrodynamics", Technical report, Chalmers University of Technology, Gothenburg.

Larsson, L., Stern, F., Visonneau, M., Hino, T. Hirata, H., and Kim, J., 2015: "A workshop on cfd in ship hydrodynamics." Workshop Proceedings, Tokyo, Dec, pages 2–4, 2018.

Lee, J.H., Park, D.M. and Kim, Y., 2017, "Experimental Investigation on the Added Resistance of Modified KVKCC2 Hull Forms with Different Bow Shapes" J.Engineering for the Maritime Environment, Vol. 231, pp. 395-410

Maury, C., Delhommeau, G., Ba, M., Boin, J. P., & Guilbaud, M. (2003). "Comparison between numerical computations and experiments for seakeeping on ship models with forward speed". Journal of ship research, 47(04), 347-364.

Park, D.M., Lee, J. and Kim, Y., 2015, "Uncertainty analysis for added resistance experimental of KVLCC2 ship", Ocean Engineering, Vol. 95, pp. 143-156.

Park, D. M., Lee, J. H., Jung, Y. W., Lee, J., Kim, Y., and Gerhardt, F., (2019). Experimental and numerical studies on added resistance of ship in oblique sea conditions. Ocean Engineering, 186, 106070.

Schellin, T. E., Beiersdorf, C., Chen, X. B., Fonseca, N., & Guedes Soares, C., 2003, "Numerical and experimental investigation to evaluate wave-induced global design loads for fast ships", Transactions-Society of Naval Architects and Marine Engineers, 111, 437-461.

Simonsen. C.D., Otzen, J.F., Nielsen, C. and Stern, F. 2014 "CFD prediction of added resistance of the KCS in regular head and oblique waves", Proc. of the 30th Symposium on Naval Hydrodynamics, November, Hobart, Tasmania.

Sprenger, F., Maron, A., Delefortrie, G., Van Zwijnsvoorde, T., Cura-Hochbaum, A., Lengwinat, A., & Papanikolaou, A. (2017). "Experimental studies on seakeeping and maneuverability of ships in adverse weather conditions". Journal of Ship Research, 61(03), 131-152.

Strom-Tejsen, J., Yeh, HYH and Moran, DD., 1976, "Added resistance in waves", Trans SNAME, Vol. 81, pp. 250-279

Van't Veer, R., 1998, "Experimental results of motions, hydrodynamic coefficients and wave loads of the 372 catamaran model", Delft University of Technology Report 1129, in coorperation with MARIN at Wageningen.

Appendix B. : Table of Benchmarks

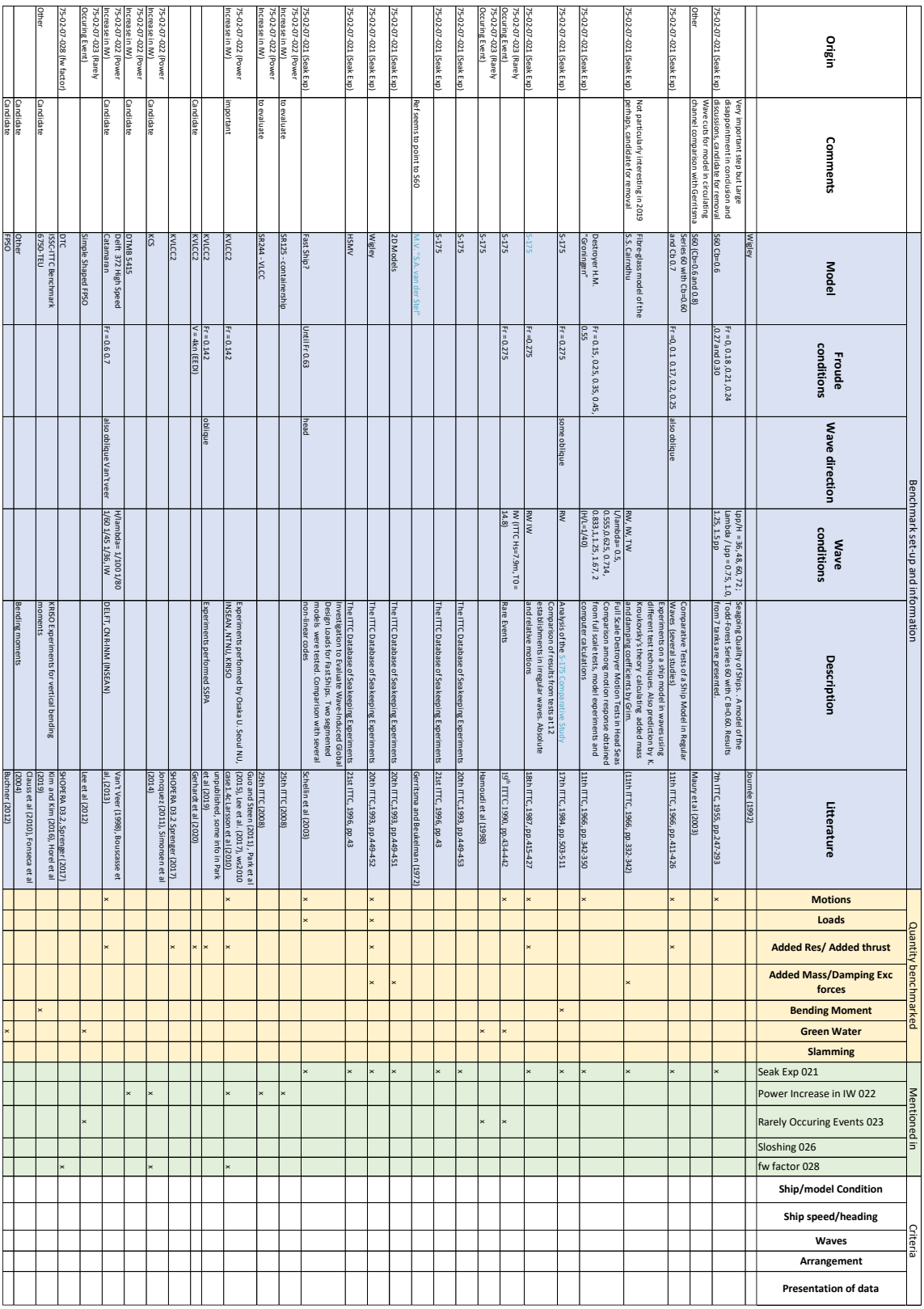

Origin	Comments	Model	Froude conditions	Wave direction	Wave conditions	Description	Litterature	Motions	Loads	Added Res/ Added thrust	Added Mass/Damping Exc forces	Bending Moment	Green Water	Slamming	Seak Exp 021	Power Increase in IW 022	Rarely Occuring Events 023	Sloshing 026	fw factor 028	Ship/model Condition	Ship speed/heading	Waves	Arrangement	Presentation of data
								Benchmark set-up and information							Quantity benchmarked					Mentioned in					Criteria					
		Wigley																						
75-02-07-021 (Seak Exp)	Very important step but Large disappointment in conclusion and discussions, candidate for removal	SSG Ch=0.6	Fr = 0, 0.18, 0.21, 0.24 ,0.27 and 0.30		Lpp/H =36; 48; 60; 72; Lambda / Lpp = 0.75; 1.0; 1.25; 1.5 pp	Seagoing Quality of Ships. A model of the Todd-Forest Series 60 with C B=0.60. Results from 7 tanks are presented.	7th ITTC, 1955, pp.247-293	x						x									
75-02-07-021 (Seak Exp)	Wave cuts for model in circulating channel comparison with Gerritsma	Series 60 (Cb=0.6 and 0.8) and Cb 0.7	Fr =0, 0.1, 0.17, 0.2, 0.25	also oblique		Comparative Tests of a Ship Model in Regular Waves (several studies).	11th ITTC, 1966, pp.411-426	x		x				x										
Other						Experiments on a ship model in waves using different test techniques. Also prediction by K. Kreukovsky's theory calculating added mass and damping coefficients by Girin.	Maury et al (2003)																	
75-02-07-021 (Seak Exp)	Not particularly interesting in 2019 perhaps, candidate for removal	Fibre-glass model of the S.S. Cairndhu				Full Scale Destroyer Motion Tests in Head Seas	(11th ITTC, 1966, pp.332-342)				x			x										
75-02-07-021 (Seak Exp)		Destroyer H.M. "Groningen"	Fr = 0.15, 0.25, 0.35, 0.45, 0.55		L/lambda= 0.5, 0.555,0.625, 0.714, 0.833,1,1.25, 1.67, 2 (H/L=1/40)	Comparison among motion response obtained from full scale tests, model experiments and computer calculations	11th ITTC, 1966, pp.342-350	x						x									
75-02-07-021 (Seak Exp)		S-175	Fr = 0.275	some oblique	RW	Analysis of the S-175 Comparative Study	17th ITTC, 1984, pp.503-511					x		x										
75-02-07-021 (Seak Exp)		S-175	Fr=0.275		RW IW	Comparison of results from tests at 12 establishments in irregular waves. Absolute and relative motions	18th ITTC, 1987, pp.415-427	x		x				x										
75-02-07-023 (Rarely Occuring Event)		S-175	Fr = 0.275		IW (ITTC Hs=7.9m, T0 = 14.8)	Rare Events	19th ITTC 1990, pp.434-442	x				x					x							
75-02-07-023 (Rarely Occuring Event)		S-175											Hamoudi et al (1998)					x					x			
75-02-07-021 (Seak Exp)		S-175				The ITTC Database of Seakeeping Experiments	20th ITTC,1993, pp.449-453																		
75-02-07-021 (Seak Exp)		S-175				The ITTC Database of Seakeeping Experiments	21st ITTC, 1996, pp.43																		
	Rel seems to point to S60	M.V. "S.A. van der Stel"					Gerritsma and Beukelman (1972)																		
75-02-07-021 (Seak Exp)		2D Models				The ITTC Database of Seakeeping Experiments	20th ITTC,1993, pp.449-451				x														
75-02-07-021 (Seak Exp)		Wigley				The ITTC Database of Seakeeping Experiments	20th ITTC,1993, pp.449-452	x	x	x	x														
75-02-07-021 (Seak Exp)		HSMV				The ITTC Database of Seakeeping Experiments Investigation to Evaluate Wave-Induced Global Design Loads for Fast Ships. Two segmented models were tested. Comparison with several non-linear codes	21st ITTC, 1996, pp.43								x										
75-02-07-021 (Seak Exp)		Fast Ship?	Unif Fr 0.63	head			Scheiffin et al (2003)	x	x					x										
75-02-07-022 (Power Increase in IW)		SR125 -containership					25th ITTC (2008)									x								
75-02-07-022 (Power Increase in IW)	to evaluate	SR244 - VLCC					25th ITTC (2008)									x								
75-02-07-022 (Power Increase in IW)	important	KVLCC2	Fr = 0.142			Experiments performed by Osaka U. Seoul NU, INSEAN, NTNU, KRISO	Guo and Steen (2011), Park et al (2015), Lee et al. (2017), ws2:00 case 1.4c, Larsson et al (2210)	x								x									
		KVLCC2	Fr=0.142	oblique			unpublished, some info in Park et al (2015)			x	x														
	Candidate	KVLCC2	V = 4kn (EEDI)			Experiments performed SSPA	Gerhardt et al (2020)			x	x														
75-02-07-022 (Power Increase in IW)	Candidate	KVLCC2					SHOPERA D3.2, Sprenger (2017)			x														
75-02-07-022 (Power Increase in IW)	Candidate	KCS					Jongsuwat (2011), Simonsen et al (2014)											x						
75-02-07-022 (Power Increase in IW)	Candidate	DTMB 5415																						
75-02-07-023 (Rarely Occuring Event)	Candidate	Delft 372 High Speed Catamaran	Fr = 0.6 0.7	also oblique Van't veer	H/lambda= 1/100 1/80 1/60 1/45 1/36 ,IW	DELFT, CNR-INM (INSEAN)	Van't Veer (1998), Bouscasse et al.,(2013)	x		x						x	x								
75-02-07-028 (fw factor)		DTC					SHOPERA D3.2, Sprenger (2017)												x					
Other	Candidate	ISSC-ITTC Benchmark 6750-TEU				KRISO Experiments for vertical bending moments	Kim and Kim (2016), Horel et al (2019).					x					x							
	Candidate					Bending moments	Clauss et al (2010), Fonseca et al (2004)																	
	Candidate	Other FPSO					Buchner (2012)						x											

The Stability in Waves Committee

Final Report and Recommendations to the 29th ITTC

1. INTRODUCTION

1.1 Membership and Meetings

Membership. The Committee appointed by the 28th ITTC consisted of the following members:

Dr. V. Belenky, (Chairman)
Carderock Division, Naval Surface Warfare Centre (NSWCCD), USA

J.-F. Leguen, (Secretary)
DGA Hydrodynamics, France

Dr. S. Cho
Korea Research Institute of Ships and Ocean Engineering (KRISO), South Korea

A. Matsuda
Japan Fisheries Research and Education Agency, Japan

Prof. J. Lu
China Ship Scientific Research Center (CSSRC), China

Dr. P. Feng
Marine Design & Research Institute of China (MARIC), China

Dr. Adriana Oliva-Remola (until May 2019)
Universitad Politécnica de Madrid, Escuela Técnica Superior de Ingenieros Navales (ETSIN), Spain

Prof. E. Boulougouris
University of Strathclyde, United Kingdom

Meetings. Four Committee meetings were held as follows:

University of Madrid, Spain, March 2018

Kobe, Japan, September 2018

DGA, Val de Reuil, France, June 2019

A fourth meeting was planned at NSWCCD, Washington D.C., U.S.A., in March 2020 but was replaced due to COVID-19 by a series of video meetings (every two weeks) from March 2020 to March 2021.

1.2 Tasks From The 28th ITTC

The Stability in Waves Committee covers the stability of intact and damaged ships in waves. For the 29th ITTC, the modelling and simulation of waves, wind and current is the primary responsibility of the Specialist Committee on Modelling of Environmental

Conditions, with the cooperation of the Ocean Engineering, the Seakeeping and the Stability in Waves Committees.

In the following, the Tasks received from the 28th ITTC are recalled for reference:

TOR 1: Update the state-of-the-art for evaluating the stability of ships in adverse weather conditions, emphasizing developments since the 2017 ITTC conference. The committee report should include sections on:

a) the potential impact of new technological developments on the ITTC,

b) new experimental techniques,

c) new benchmark data.

d) the practical applications of computational methods to prediction and scaling,

e) the need for R&D for improving methods of model experiments, numerical modelling,

f) include wind and current effects on stability assessments (intact and damaged ship, experimental and numerical methods),

g) review the effect of flooding on nonwatertight bulkheads due to fire fighting for example.

TOR 2:Review ITTC Recommended Procedures relevant to stability, including CFD procedures, and:

a) identify any requirements for changes in the light of current practice, and, if approved by the Advisory Council, update them,

b) identify the need for new procedures and outline the purpose and contents of these.

TOR 3: Review the IMO 2nd Generation Intact Stability Criteria and standards with a particular focus on the physics and background for each of the stability failure modes. It may be useful to develop a fault tree to better identify each of the stability failure modes.

TOR 4: Provide a recommendation on developing a procedure, or a set of procedures, for the direct assessment (computational methods) of the IMO 2nd Generation Intact Stability Criteria five modes of intact stability failure.

TOR 5: Review the state-of-the-art (both the experimental and the numerical studies) for free roll decay, forced rolling and excited rolling tests. Include methods of analysing time histories of data obtained from such tests and ways of deriving roll damping coefficients. Liaise with the Specialist Committee on Combined CFD/EFD Methods, as required.

TOR 6: Update Procedure 7.5-02-07-04.5 to “Numerical Estimation of Roll Damping”, giving detailed guidance on how to carry out real or numerical model tests (e.g. free roll decay, forced rolling and excited rolling tests).

TOR 7: Updating the guideline 7.5-02-07-04.3 for the prediction of the occurrence and magnitude of parametric rolling towards a procedure. Liaise with the Seakeeping Committee as required.

TOR 8: Update Procedure 7.5-02-07-04.4 Numerical Simulation of Capsize Behaviour of Damaged Ships in Irregular Beam Seas, to include the complete 6-DoF equations of motion for a damaged ship and numerical

methods for flooding based on more accurate hydraulic models (than estimated discharge coefficients).

TOR 9: Develop/suggest a method for estimating time to capsizing and/or sinking and include this in the report.

TOR 10: Continue the identification of benchmark data for validation of stability in waves predictions.

2. STATE-OF-THE-ART (TOR 1)

"Contemporary Ideas on Ship Stability - Risk of Capsizing" is a book recently edited (Belenky et al. 2019a). The book contains some of the most relevant papers from 2010 and 2012 presented at ISSW 2010-2011 and STAB 2012. The papers have been updated by their authors for the book. Most of those papers where referenced in previous ITTC reports in their original form. The up-to-date versions included in the book to be utilized from now on. The book is subdivided into four major parts: Mathematical Model of Ship Motions in Waves / Dynamics of Large Motions / Experimental Research / Requirements, Regulations, and Operations.

2.1 Potential impact of new technological developments on the ITTC (TOR 1 a)

During this period significant technological innovations have demonstrated the feasibility of active intervention in cases of flooding accidents on ships (beyond the counter-flooding of spaces). Although patents and concepts had proposed for several decades now, it is only recently that demonstrable systems have been developed. Special consideration should be given in the case of active buoyancy and stability recovery systems using inflatable devices (Chodankar, 2016; Zilakos and Toulios, 2018) and highly expandable foam (Vassalos et. al., 2016). Their underlying principle is to reduce significantly the permeability of the damaged space following an accident and regain partially the lost buoyancy. For such systems, it is crucial to capture accurately their impact on the floatability and the stability of the ship throughout the course of the event. This is equally important for their design and their actual deployment following the event. In this respect, they require accurate numerical simulation of the flooding process, considering as much as possible, all the contributing factors. Hence, numerical simulation codes that model correctly the timing and geometry of the inflation/expansion, the impact of the flood water pressure and air pressure build up due to potential blockage of the room vents, the impact of the position of the vessel (heel and trim) to the inflation/expansion process and any potential asymmetries resulting from them, are important integral parts to the design and operation of such systems. It should be noted, that although their impact on the survivability of the vessel can be significant, they are not covered under the existing SOLAS regulatory framework. Therefore, their developers are utilising the opportunity offered by the IMO's Circular, MSC.1/Circ.1455.

2.2 New experimental techniques (TOR 1 b)

Zhu et al. (2018) performed model grounding experiments in a water tank to study the coupling effects of both internal mechanics and external dynamics (see Figure 344). The influence of surrounding water on ship motions during grounding is taken into account. During their testing, varying rock penetrations are considered to study the grounding damage. Experimental results such as the horizontal grounding forces and damage extents are measured and analysed. The results show that the grounding damage depends on the rock penetration, and the surrounding water of the ship model has a big influence on the grounding damage assessment.

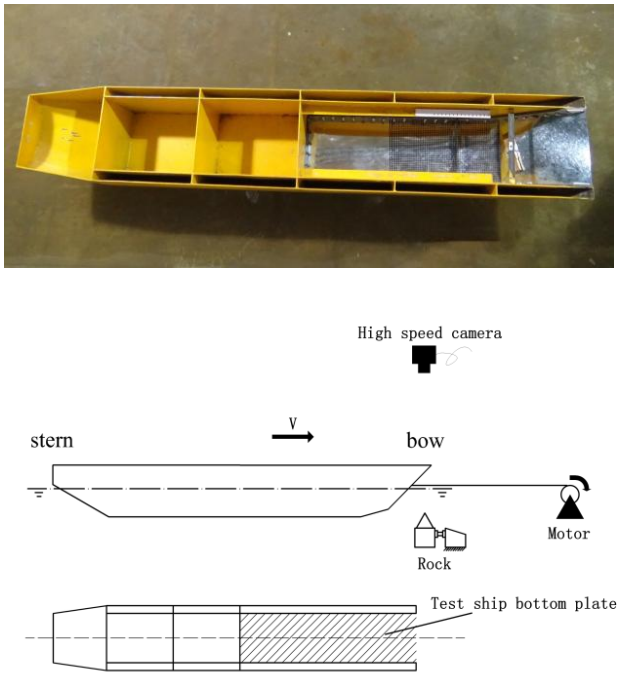

Figure 344: Experimental set-up for grounding from Zhu et al. (2018)

Hashimoto et al. (2019) designed and constructed a purpose-built device to obtain high-quality experimental data of roll decay motions for the quantitative validation of CFD methods. A certain initial heel angle was given to the ship model via the long square pipe as shown in Figs. 2 and 3. The square pipe can freely move in heave and pitch directions even when being held, thus, the change of ship attitude owing to the change of underwater ship volume and buoyancy balance is allowed. To start the roll decay test, the heel constraint is released momentarily by very swiftly open the aluminium frame through the strong tension of the connected rubber rope. As the rolling energy is consumed during the consecutive swings, the square long pipe will not reach the initial angle, thus will never hit the apparatus (see Figure 345 and Figure 346).

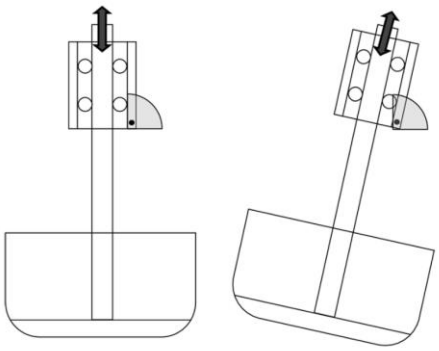

Figure 345: Schematic view of the apparatus

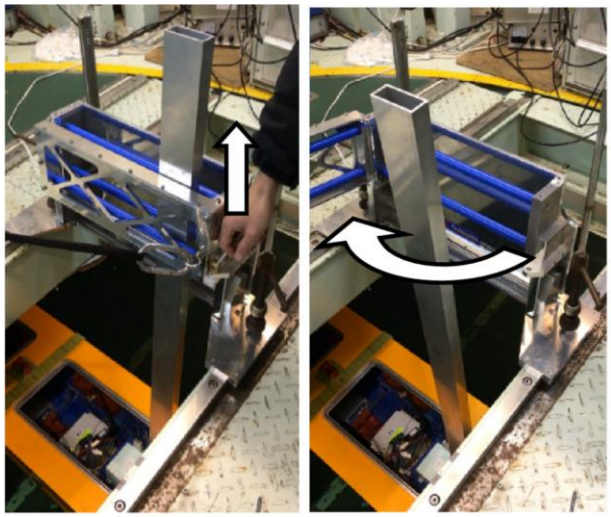

Figure 346. Opening mechanism of apparatus

Tsukada et al. (2017) and Ueno et al. (2019) have developed a wind loads simulator (WiLS) that enables us to carry out free-running model tests for investigating wind effects on ship performance (see Figure 347 and Figure 348). WiLS provides a free-running model ship with simulated wind loads taking into account the supposed true wind speed and direction, and instantaneous model ship speed, drift angle, and heading angle. It does not generate environmental wind but exerts forces and moment on a model ship using three pairs of duct fans. A control PC calculates time-varying longitudinal and lateral wind forces and yaw moment using wind loads coefficients estimated beforehand and ship motion data, and distribute them to the three pairs of duct fans. Feedback

control ensures the intended wind loads using data from load cells on which the duct fans are mounted and those from accelerometers for correcting inertia forces of the duct fans.

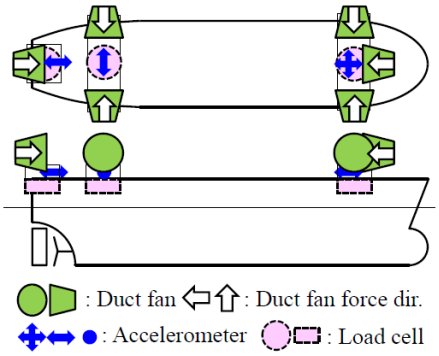

Figure 347: Configuration of onboard part of the wind loads simulator.

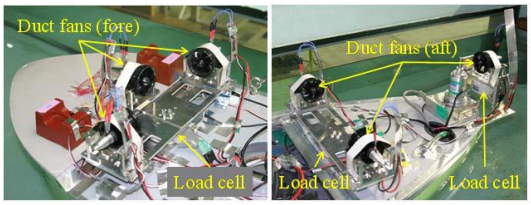

Figure 348: Wind loads simulator on a model ship

Asgari et al. (2020) investigated the Instantaneous Rotation Centres (IRC) and Most Often Instantaneous Rotation Centres (MOIRC) behaviour during the free roll decay tests of an FPSO by following the time series of the IRC. A static pure couple is applied to the hull to initiate the rolling. The motions during the test were tracked by an optical system using two Qualisys cameras, which measures the trajectory of the model, calculates the velocities, and transfer them into the non-inertial body-fixed coordinate system with the origin at the centre of gravity (see Figure 349). It is demonstrated through the experiment that IRC behaviour leads to distinct damping values. Two categories of IRC locus were devised according to observations. Category-I corresponds to a tangent type IRC locus. Category-II corresponds to a double parabolic IRC locus. The effect of the MOIRC on roll damping explains why the damping is different from the clockwise to the counter clockwise oscillation

.

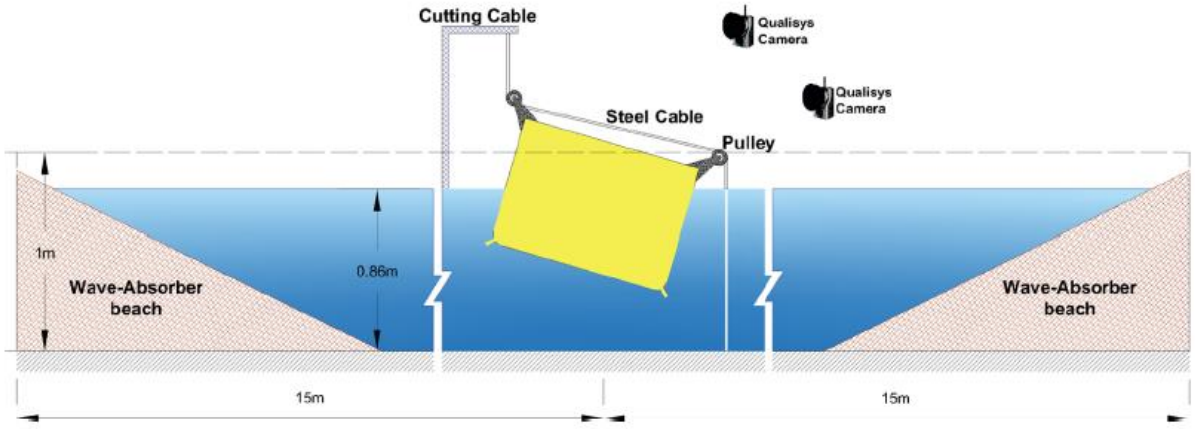

Figure 349: Motions track optical system, from Asgari et al. (2020)

2.3 Benchmark Data (TOR 1 c)

Only very few new benchmark data was identified. Three references of the numerical benchmark were added to the list, one from NSWCCD, Telste and Belknap (2008), about wave induces forces and moment, the second about roll damping, Irkal et al. (2019), and the last about CFD prediction of wave-induced forces on ONR-tumblehome hull form running in irregular stern quartering seas to study surf-riding/broaching, Hashimoto et al. (2018).

2.4 Practical applications of computational methods to the prediction of stability in waves (TOR 1 d)

Mizumoto et al. (2018) apply the system identification technique using a limited number of time histories from CFD in waves for broaching prediction. By applying system identification to wave forces from CFD, the broaching phenomenon observed during experiments was well predicted, and the broaching probability estimation in stationary irregular waves is also improved.

Htet et al. (2018) investigate the effect of the above-waterline hull shape on broaching danger in irregular stern-quartering waves, showing that the tumblehome vessel has a larger broaching probability because of its small calm-water resistance and small calm-water damping coefficients in the sway and yaw directions. It is also demonstrated in the paper that rudder gain plays an important role in the occurrence of broaching.

Sakai et al. (2017) studied quadratic equation describing zeros of Melnikov function leading to deriving a formula for the RPS value, corresponding to the second threshold of speed where surfriding occurs at any combination of instantaneous velocity and position on the wave.

Silva and Aram (2017), Aram and Silva (2019) applied regression to extract hydrodynamic derivatives from a simple double-body RANS simulation of drift and rotating arm tests. Araki et al. (2019) used a system identification technique to extract these derivatives from the simulated free-running test.

Meister et al. (2021) present several predictive modelling techniques that were used to investigate if parametric roll leading indicators can possibly be identified in the early stage design to avoid parametric roll resonance. They utilize four predictive models trained by the parametric roll data created through the execution of a nonlinear non-homogenous damped Mathieu equation, facilitating the prediction of parametric roll in early-stage design.

Sakai et al. (2018) applied an averaging method for evaluation of amplitude (with the super-harmonic effect) and critical speed of parametric roll in oblique waves without fitting calm water-$\overline{GZ}$ curve.

Sakai et al. (2019) calculated the encounter wave period for the Grim effective wave (Grim, 1961) to be used is the assessment of the amplitude of parametric roll.

Bu and Gu (2020) describe a combined numerical model of parametric roll and water sloshing in tanks. A potential flow solver was used for parametric roll, while CFD was employed for sloshing. As could be expected, sloshing may prevent the parametric roll from development.

Ma et al. (2018) performed the experimental and numerical study of the ship parametric rolling in regular head waves under different incident wave steepness for the C11 containership under two different drafts. Both the potential flow based on the nonlinear strip theory and viscous flow CFD method is used. It is found that the numerical results obtained by the CFD method give better results at larger incident wave steepness, especially for 0.05-0.07. It is concluded that it is necessary to consider the contribution of the radiation/diffraction force on the hydrodynamic restoring moment at large wave steepness in the case of the potential flow model if better numerical accuracy is desired.

Li et al. (2018) explore the influence of speed and course on ship parametric roll by using numerical and experimental method. Their results show that parametric roll will occur in bow waves when the encounter frequency is about twice the natural roll frequency, and the amplitude is equivalent to those in longitudinal waves. With the increase of wave height, the range of speed in which parametric rolling occurs will also expand.

Lindroth et al. (2019) point out that the stability at intermediate flooding stages has previously been ignored for cargo ships, but if the ship is equipped with cross-flooding devices, intermediate filling phases should be evaluated. Time-domain flooding simulation is used for a realistic assessment of intermediate stages and the actual time-to-flood, which enables realistic assessment of flooding progression and damage stability during these intermediate stages, while design improvements can be focused on factors that affect damage stability, such as efficient cross-flooding arrangement.

Yu et al. (2019b) investigates the influence of GM on surf-riding and broaching of the ITTC A2 fishing vessel using a time-domain 6-DoF numerical model. Through numerical simulations in following and quartering seas with different GM values, it is found that GM value has a significant influence on the occurrence of broaching and capsizing.

Begovic et al. (2018) verify the surf-riding/broaching vulnerability criterion of semi-displacement hull form of Systematic Series D, where the influence of the diffraction component on the wave surging force has been analysed. It is found that the limit Froude number for the considered hull form series is increased by improving the accuracy of 2nd level calculation, taking into account only nonlinear wave celerity or diffraction component and linear wave celerity.

Wang et al. (2018) explore the effect of propeller thrust reduction on ship's surf-riding and broaching events using a 6-DoF weakly nonlinear unified seakeeping-manoeuvring model. The effect of wave orbital velocity and the propeller submergence depth are considered in the numerical model. It is shown that propeller submergence ratio decreases and propeller thrust drops dramatically when surf-riding happens.

Gu et al. (2018b) compare the experimental results, using a 1/51 scale model of the 5415 frigate hull in a damaged condition, with CFD calculations. They investigate the impact of ingress and egress of floodwater and the interaction between the ship behaviour and water surface effect have on the ship motions and loads acting on the ship.

Begovic et al. (2017) comment that the CFD methods can predict the roll damping coefficient of a damaged ship in roll decay tests, reasonably well but the period of oscillations differs from the one measured in the model experiments. This has been observed also by Gao et. al. (2011, 2013). Furthermore, they note the significant challenge posed by the high computational time, which renders such methods impractical for common design practice. Furthermore, they conclude that the accuracy of the prediction is highly depended on the quality rather than the quantity of the mesh. They find the hexahedral trimmed mesh better than the hybrid (polyhedral and trimmed) and they recommend a time step less than the 1/100 of the phenomenon period, suggested by ITTC procedure 7.5-03-02-03 (Practical Guidelines for Ship CFD Applications, 2011).

Ruth et al. (2019) present the opportunities and challenges of using CFD for simulating the damage stability of cruise ships in waves, based on the experience gained in the joint industry project eSAFE.

Gu et al. (2017) conducted a model experiment with a tumblehome vessel for surf-riding and broaching in following and stern-quartering waves. Four types of ship motions

with periodic motion, stable surf-riding, broaching and capsizing due to broaching were observed in the model experiment while broaching was observed three times in one wave case. The results between the vulnerability criteria calculation and the model experiment were compared to verify the feasibility of vulnerability criteria for the tumblehome vessel.

Gu et al. (2018a) studied the free roll decay motions of different scales under different initial roll amplitudes are simulated using one two-dimensional ship section, and the influence of scale effect is considered. It is found that the effects of different scales mainly due to the bilge keels, and scale ratio could affect the free roll decay motion and the roll damping coefficients, especially for large initial roll amplitude.

Gu et al. (2019) studied several crucial factors for CFD simulations, such as boundary condition, wall function, mesh quantity and quality. The influences of bilge keels on roll damping are also studied, several questions related to the CFD simulation of roll damping are discussed and the suggestions for the simulation are also proposed.

Gu et al. (2020) tried to parametric rolling in irregular oblique sea using a three-dimensional hybrid panel method. It was concluded that 3DOF model (heave-roll-pitch) produces more conservative results compare to 6-DOF model.

Lu et al. (2016) investigated the effect of parametric roll on added resistance in regular head seas. A formulae was developed based on Maruo theory that takes into account influence of parametric roll on added resistance.

Lu et al. (2017) carried out free-running experiments with partially restrained model in head seas. Tests were complemented by numerical simulations. It was found that the surge effect on parametric roll is generally small, the heave and pitch motions can have subharmonic components, and the radiation and diffraction effect on restoring variation can result in more conservative prediction.

Umeda et al. （2019) concluded that sway and yaw motions affected the capsizing of the actual ship in stern quartering waves due to pure loss of stability.

Lu et al. (2019) studied a surge-heave-pitch-roll coupled equation for predicting pure loss of stability in following seas. It considers a variable forward speed. Heave and pitch motions were computed by a strip method with an enhanced integrating method. This approach can appropriately estimate pure loss of stability in following seas as it was experimentally verified using the ONR tumblehome configuration.

Lu et al. (2020) studied a 6-DOF model for predicting parametric roll in stern quartering seas. Horizontal motions were modelled using MMG method (Yasukawa and Yoshimura, 2015). The study confirmed the hypothesis (Kubo et al. 2012; Umeda et al. 2019）that coupling with sway and yaw motion is an important factor for capsizing due to pure loss of stability.

Bu et al. (2019b, 2019c) conduct systematic researches on the effects of the radiation and diffraction forces on the roll restoring arm ($\overline{GZ}_{RD}$) under different heeling angles and wave amplitudes. The $\overline{GZ}_{RD}$ values are calculated by the integral of instantaneously average wetted surface and instantaneously wetted surface, separately. They find that the $\overline{GZ}$ consists of two important harmonic components in head waves and $\overline{GZ}_{RD}$ is the main contribution of the second harmonic component. Therefore, $\overline{GZ}_{RD}$ should not be ignored in head seas. Furthermore, they investigate the effects of $\overline{GZ}_{RD}$ on the prediction of the parametric roll. All the hydrodynamic forces are calculated by integrating wave pressure up to the wave surface based on the three-dimensional mixed source method. They find the body exact method can provide more

accurate calculation accuracy compared with the commonly used body linear method.

Bu and Gu (2020) propose a nonlinear time-domain unified viscous and potential prediction method for the prediction of the time domain damaged ship motion coupled with damaged ship flow, in which the nonlinear three-dimensional time-domain hybrid source method is used for the simulation of damaged ship motion and the fully viscous method is used for the simulation of damaged ship flow. Two boundary conditions and two-time scales are used for the match between potential theory and viscous theory. The research shows that the proposed unified prediction method can predict the damaged ship motion and describe the details of damaged ship floodwater very well, at the same time, the calculation time can be saved a lot compared with the full viscous method as the mesh quantity for viscous simulation is considerably reduced.

Hu et al. (2019) proposed the capsizing probability calculation method for the dead ship condition. It is based on 1-DoF equation and Monte-Carlo simulation, as well as time-domain potential theory. Among this, the nonlinear righting lever $\overline{GZ}$ curve solution is obtained by two methods, one is the real-time calculation, the other subjects the influence of damaged tanks on the hull shape down to the wind and wave, thus combining combines the flooding process in the time domain of damaged ships with the capsizing probability research.

The roll damping and nonlinear roll restoring moment are important factors for the accurate prediction of both the onset and the amplitude of parametric roll. Yu et al. (2019a) conducted the quantitative prediction of the parametric roll of a KCS containership using a 5-DoF model to investigate the influence of different methods for nonlinear restoring moment and roll damping. Through comparison with model experiments, it was found that the accurate estimation of pitch motion is vital for the quantitative prediction of the parametric roll. The model considering only the nonlinearity of restoring forces caused by the instantaneous position of the ship with the wetted surface extending up to the still water level is found to be the most suitable restoring model for the quantitative prediction of the parametric roll. For cases close to the onset threshold of the parametric roll, the influence of roll damping can be dramatic.

Yu et al. (2018) proposed a detection algorithm based on Incremental Real-time Hilbert–Huang Transform (IR-HHT) to conduct early detection and advance warning of parametric roll in regular and irregular seas. Then, it was validated through free running model experiments that the detection algorithm can successfully detect the occurrence of parametric roll under different cases when the roll amplitudes are still small. Moreover, it was confirmed that the rudder anti-roll action after the detection can successfully stabilize parametric roll in regular and irregular head waves especially when the ship's speed is high.

Zhou (2019) conducted a further validation study of a hybrid prediction method of the parametric roll, using experimental results of two container ships and one Ro-Ro ship. This hybrid prediction method uses direct CFD approach to estimate roll damping coefficients, as well as a weakly-nonlinear model to predict 3-DOF motion responses. The upper limit wave steepness and parametric roll amplitude which can obtain satisfactory simulation have been investigated. On the other hand, this hybrid method is also found not applicable for simulating cases with strong nonlinearity like slamming, shipping-water and rudder-emergence.

Wawrzynski (2018) used a 1-DoF mathematical model to study the bistability and accompanying phenomena of rolling. A novel expanded form of the roll spectrum is proposed where bistability areas and the bistability origin point are included. The presented approach to the bistability phenomenon and amplitude jumps as

to the bifurcation phenomenon can be used in the explanation of notable divergences between the results of numerical simulations for rolling with large amplitudes at resonance frequencies.

Kianejad et al. (2018b) adopted a CFD approach based on harmonic exciting roll motion (HERM) technique to compute the roll motion characteristics and damping coefficients in different conditions. The impact of appendages, Froude number and DoF on roll motion characteristics and damping coefficients are investigated for model-scale as well as full-scale to study the scale effects.

Kianejad et al. (2020) performed experimental and numerical simulations at beam sea condition to investigate the behaviour of roll restoring moment variations. The ship model is excited by regular waves at different heights and frequencies to measure the motion characteristics and the restoring moment in dynamic conditions. The results show that the restoring moments in the dynamic condition have significant differences compared to the static condition. The magnitude of restoring moment in the dynamic condition is measured based on the variation of heave motion of the model and the location of the wave's crest and trough with respect to the model. The proposed method can be applied to other types of vessels to calculate the restoring moment in regular and irregular waves and increase the accuracy of dynamic stability investigation.

Shigunov (2019) estimated stability failure rate from simulated ship motion records by direct counting, considered and validated the applicability of Poisson process for the description of time dependence.

Reed (2019a) examined the requirements for the total duration of numerical simulation. In the linear regime, the extremes can be characterized, using the standard deviation of ship motions. In the nonlinear regime, the duration should be sufficient to fit an appropriate model for the tail of the distribution.

Wandji (2019) reviewed several probabilistic methods and applied these methods for large samples of parametric roll response and linear response with the same spectrum. Histograms of estimates for upcrossing rate, time to the first exceedance and time between the exceedances were obtained. Distribution of amplitudes and block maxima were estimated. The results were compared to FORM.

Smith T.C. (2019) formulated approaches and procedures for validation of statistical extrapolation methods based on large-volume simulation. Weems et al. (2018) described fast qualitative numerical simulation approach for such large-volume validation. The numerical simulation is based on the calculation of instantons submerged volume.

Weems et al. (2019b) describe an application of Envelope Peaks over Threshold (EPOT) method that was used as a background of proposed ITTC procedure.

Gong et al. (2020) considered the effect of nonlinear wave on extreme ship motions using sequential sampling algorithm developed by Mohammad and Sapsis (2018).

2.5 The need for R&D on improving methods for model experiments and numerical modelling (TOR 1 e)

The study of the stability of ships in a stochastic sea state is usually carried out by Monte-Carlo simulations, so as to determine the safe operating envelope. This approach may, however, be very time consuming when the treatment of the 6-DoF seakeeping problem is necessary and in conditions where nonlinear coupling between the vessel responses lead to loss of stability (e.g. parametric rolling, broaching). Choi et al. (2017) adopt the First Order Reliability Method (FORM) to define possible combined critical wave and wind scenarios leading to capsize and achieve the calculation of capsizing probability at a much lesser computational effort. Jensen et al. (2017)

show that the FORM can be an efficient method for estimation of outcrossing rates and extreme value statistics for stationary stochastic processes, suitable for the bifurcation type of processes such as a parametric roll. Sclavounos et al. (2019) develop a new methodology for the modelling of the nonlinear responses and stability of ships in stochastic steep waves, where a state-space stochastic differential equation is derived for the states governing the vessel nonlinear responses and a linear Fokker–Planck partial differential equation is obtained for the joint probability density function of the vessel motions, allowing the direct evaluation of the joint probability density function of the responses via the solution of the Fokker–Planck equation.

Irregularity of waves may alter the physics of a stability-in-waves-related phenomenon. Results on the computation of celerity of irregular waves are reviewed in Spyrou et al. (2019). As the celerity of irregular wave is a stochastic process, the surf-riding state is not equilibrium – the point where the sum of all the forces is zero moves with acceleration. The domain of surf-riding in phase space is described by a Lagrangian coherent structure (Kontolefas and Spyrou, 2016). Kontolefas and Spyrou (2018) related the Lagrangian coherent structure with "high runs" (instantaneous speed above the normally expected fluctuations) and the estimated probability of surf-riding.

The ultimate objective of probabilistic methods is the estimation of the rate of exceedance of a large roll threshold. A long-duration numerical simulation represents a challenge due to computational cost; thus the estimate may need to be obtained without observing actual event being essentially a statistical extrapolation problem.

Consistent multi-fidelity modelling may provide accuracy close to a high-fidelity model with the computational cost of a low fidelity model. Besides the consistency between the models of different fidelity, quantification of uncertainty, which is the key issue, considered in Brown and Pipiras (2019).

Maki (2017) developed a method for estimation of the probability of instantaneous values of roll motions. First, the shape of the distribution is obtained by subjecting a dynamical system to white noise excitation; it is further scaled with variance estimate. Further study of the method, including application, comparison and experimental validation is described in Maki et al. (2018, 2019a, 2019b).

Macé et al. (2019) developed a method for estimation of capsizing probability by extrapolation of an estimate of roll exceedance rate.

Chai et al. (2018) compared path integration method (Kougioumtzoglou and Spanos 2014) with the averaging method (Dostal et al. 2012; Dostal and Kreuzer 2014) and formulated recommendations for application based on the advantages of both methods.

There are several probabilistic methods based on extreme value theory. The extreme value theory states that the largest value in a sample of independent identically distributed variables tends to Generalized Extreme Value (GEV) distribution (the first extreme value theorem also referred to as Fisher-Tippet-Gnedenko theorem). It also states that a distribution above some large threshold can be approximated with Generalized Pareto Distribution (GPD) - the second extreme value theorem, referred as Pickands-Balkema-de Haan theorem (see e.g. Coles, 2001).

Pipiras (2020) examined issues associated with using GPD for modelling extreme roll motions. While universal applicability of GPD follows from the second extreme value theorem, its practical use may be associated with significant statistical uncertainty including the appearance of the upper bound, related to the negative value of the estimate of the shape parameter. The appearance of upper bound may prevent the use

of GPD for extrapolation if the target value is larger than the upper bound. Anastopoulos and Spyrou (2019a) found that while GPD works for large roll angle, it is not applicable for a description of escapes (capsizings). The issues of GPD may be resolved with "physics-informed model" where physical information is included into a statistical model in order to decrease the uncertainty (Glotzer et al. 2017).

Belenky et al. (2019a) proved that the response of a dynamical system with softening nonlinearity has a heavy tail of the distribution using a piecewise linear approximation of the restoring term. Belenky et al. (2018a) described a new version of EPOT using Pareto distribution to model a heavy tail. Belenky et al. (2018a, 2018b) described a new version of the split-time method using an exponential distribution for capsizing metric. Estimation of probability of capsizing caused by broaching with the split-time method is described in Belenky et al. (2017) and Weems et al. (2020) using an approximation of the boundary of Lagrangian coherent structures describing surf-riding states in irregular waves (Kontolefas and Spyrou, 2016; 2018).

The other group of methods is based on the critical wave group approach, where the extreme roll is estimated from a response to groups of large waves. Anastopoulos and Spyrou (2017) described further development of a realistic wave group model with a variation of amplitudes and periods (Anastopoulos and Spyrou, 2016). Initial conditions of a dynamical system upon the encounter of the wave group are treated in Anastopoulos and Spyrou (2019b). It describes a significantly more complete solution in comparison with the previous version (Themelis and Spyrou 2008). All the cited papers use Markov chain to model a wave group, originally proposed by Kimura (1980) and applied for probabilistic assessment of dynamic stability in waves by Themelis and Spyrou (2007).

Mohammad and Sapsis (2018) used a combination of an envelope of wave elevations and Gaussian-shape functions (Cousins and Sapsis, 2016; Farazmand and Sapsis, 2017) for detecting the wave groups. Adaptive sequential sampling was applied; the central idea is to use Gaussian process regression (GPR) that enables an optimization algorithm to drive the selection of critical wave groups that define the tail of the response distribution. The method offers sufficient computational efficiency to be used with advanced panel code (Stevens, 2018; Rathore, 2019) and CFD (Mohammad and Sapsis 2018; Gong et al. 2020) to evaluate the extreme roll response.

While not using the concept of wave groups explicitly, the Design Load Generator (DLG) can be considered as a part of the wave group approach as it searches for a sequence of waves leading to an extreme response as a combination of random phases. Originally developed for the assessment of extreme wave-induced loads (e.g. Alford and Troesch, 2009), it was extended to extreme motions (Kim and Troesch, 2013; 2019). Xu and Maki (2018, 2019), Xu et al. (2020) integrated DLG with RANS solution, using FOAM.

2.6 Include wind and current effects on stability assessments (TOR 1 f)

Speed and direction of current are not parameters of stability, it is the relative transverse speed of the structure that is. When it is a fixed structure or when it is not in line with the ship, we can speak of drift or current. MSC.1/Circ.1200 explains the conditions of a test making it possible to determine the forces due to drift for a relative incidence of 90° which corresponds to the dead ship situation, a case where the current is a significant parameter. MSC.1/Circ.1227 gives an example of an application for a cruise ship. It is not indicated how to determine the speed of drift other than by searching by iteration for the value allowing to counter aerodynamic forces. Note that the indeterminacy of the equation system

necessitates taking additional hypotheses such as the symmetry of the float for determining the point of application of the forces useful for estimating the heeling lever arm, or else using the same reduction point than during wind tunnel tests, generally taken at the waterline. Generally, the point of application of the drift forces is taken at half a draft under the waterline although it is rarely checked (see tests of the MSC.1/Circ.1227). A particular case is a gyration at high speed on calm water which can cause capsizing (some rules take into account a criterion related to this situation) but it can be treated in a complete and independent way by the field of manoeuvrability.

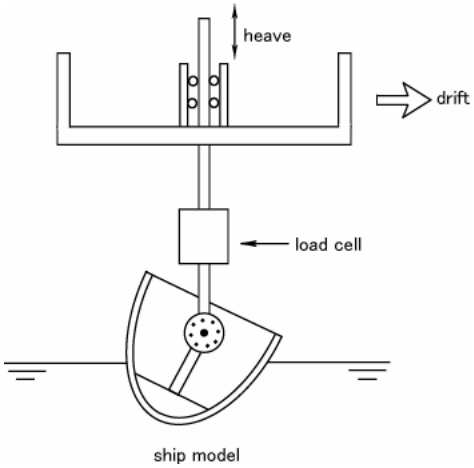

Figure 350: Set up proposed by IMO for hydrodynamic forces estimation due to current

Stability in waves committee recognizes the importance of wind. It is a strong parameter in the sense that different rules used a different way to take into account the wind (2008 IS code / NSC). Analysis of rules could be interesting to compare those rules. Stability in waves committee is interested to obtain the references for statistics of wind including nominal speed, vertical profile, speed spectrum and direction.

At this moment, stability in waves committee does not have an interest in data on currents and does not have plans to study current effects on the stability of either intact or damaged ships. Stability in wave committee is not specifically focusing on the stability of column-stabilized units beyond general state-of-the-art review. Potential interest in current is the similitude of current with the dead ship conditions when the ship is slowly drifting transversely by the action of wind (the drift speed and position of hydrodynamic forces are under questions in rules).

As it was pointed out by Francescutto (2015), so long as the wind was the propelling force for the ships, the master of a sailing ship was also aware at every moment of the approximate amount of the stability, because when sailing he constantly happened to perform some kind of inclining experiment with his vessel, even if it was primitive. It was therefore easy for the master to avoid imperilling the stability of his ship, and whenever he was tempted to load an excessive deck-cargo or otherwise reduce the stability, he probably did so well aware of the risk he was causing his vessel.

It is perhaps why obviously wind was pointed as a significant factor of risk of capsizing and then to stability checks. The first idea came by Pierrottet (1935), as mentioned by Francescutto (2015), and finally came out as the origin of the weather criterion. As explain by OMI in the explanatory notes to the international code on intact stability, 2008 (MSC.1/Circ.1281), the weather criterion firstly appeared in the IMO instruments as Attachment No.3 to the Final Act of Torremolinos International Convention for the Safety of Fishing Vessels, 1977 as an answer to a recommendation given in the conclusions of SOLAS'74. In the end, the Weather Criterion was adopted in 1985 as Res. A.562 even if it was already enforced in several countries including Japan, Russia and Australia. It is partly based on the Japanese stability standards for passenger ships as related by Tsuchiya (1975) and Watanabe (1956).

As mention by Francescutto (2015), weather criterion, however, in modern language is a (moderately) physical approach but it is not a risk-based approach. Results must be look in a

whole, from the definition of loading case to the final results which are, for a particular ship, the vertical position of the centre of gravity. Intermediate parameters have not to be used as a physical input. In particular, as clearly write in the explanatory notes to IMO 2008 IS Code, the wind speed is not linked to a real condition. Only ships characteristics can be modified as, for example, the default value as the drag coefficient can be modified accordingly IMO's Circular, MSC.1/Circ.1227, where an experimental solution to determine the heeling moment and the vertical position of aerodynamics forces is proposed (see Figure 351).

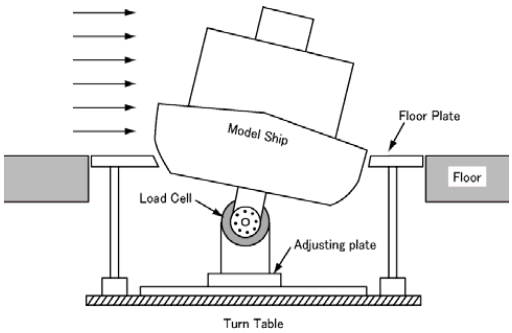

Figure 351: set up proposed by IMO for aerodynamic forces estimation

The methodology of weather criteria, in its entirety, only ensure that the initial populations (existing long before its adoption) used to establish it, is correctly separate in two-part, sure and more dangerous. The criteria were developed originally to guarantee the safety against capsizing for a ship losing all propulsive and steering power in severe wind and waves. It is a particular situation, one of the worst for a ship, and identified by OMI as one on the five failure modes, which is known now as a dead ship in the SGISC.

Even if the method must be considered as a whole, intermediate assumptions can be describe in order to be able to determine some possible improving.

As usually, the verification of the criteria must be done for all unfavourable loading cases, but, following the dead ship assumptions, only transverse relative wave heading at zero speed is taken into account. That means that it is assumed that the equilibrium of the ships is transverse to waves and that the wind is in the same direction. This strong assumption cannot be derogated easily.

The physics related to the wind is not taken into account with the same simplifications for all rules. Only some rules, even if it began to be generalised, consider the reduction of wind speed with the altitude from calm water, but no one's consider the shift in the direction against it. For some rules, as IMO one's, a gust factor is explicitly used to increase the wind speed. As explained before the wind speed, which is for a defined ship, the most important parameter cannot be related to the operational situation but because there is no physical relation with a real meteorological situation neither an estimation of a risk, it seems not be essential. For example for a ship, it is not allowed to determine the maximum speed by inversing the methodology (ship and characteristics fixed, varying wind speed to reach the criteria).

The variation of heeling moment with the heel angle is one of the most variable changes on various rules. Most of them are not justify then it is difficult to choose one even if some more physical solution is suggest nowadays on the base of experimental data in wind tunnel or by numerical calculations. Most of default values have physical sense and have be chosen in an objectives of simplification. For example the heeling moment is expected to be constant with heel angles for IMO standards rules but for most of naval rules a reduction is used. The true is certainly not one of the solutions but can be determined with appropriate experiments or simulations. Many propositions of modifications to improve some of the physical parameters where proposed as, for example by Brown and Deybach (1998). IMO Circ.1227 give the possibility to adjust the

aerodynamically force and the point of application of aerodynamic and hydrodynamic forces using experiments results.

When one wishes to compare regulations which take into account wind in one or more of their criteria it is necessary to consider the complete methodology. It is also necessary to compare the regulations on the same final objective which is, for a given ship, the vertical position of the centre of gravity. For the same ship at a given displacement, it is therefore necessary to consider not only the wind speed of each of the regulations, but also all the parameters influencing the final result including also the treatment of the $\overline{GZ}$ curve to obtain the criterion. The regulation using the strongest wind speed will not necessarily be the most conservative regulation in the end if other assumptions are less severe. A mix between the parameters is possible. We can thus create regulations, for educational purposes, very severe or very optimistic. Following an example of this type of comparison for the weather criteria (unpublished work following Luquet et al, 2015), red points are full rules, blue mix of them and black extreme fictive rules.

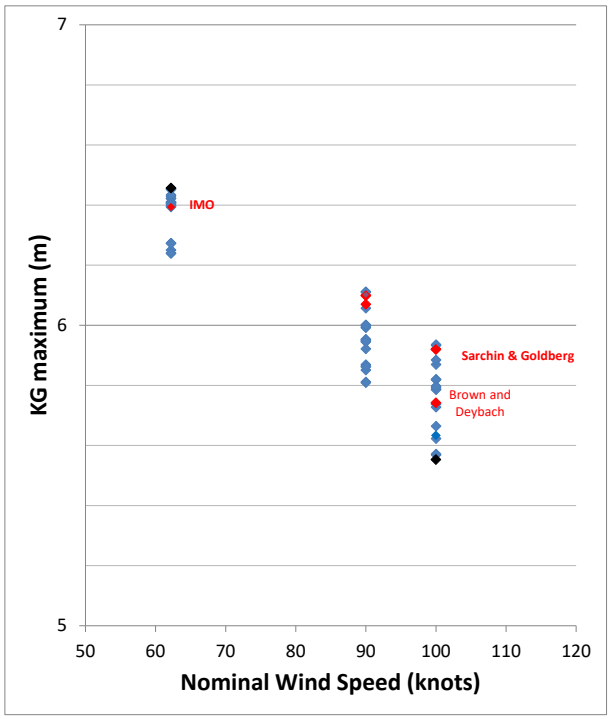

Figure 352: *KGmax* due to wind for a set of rules

2.7 Review the effect of flooding on non-watertight bulkheads due to firefighting (TOR 1 g)

Ruponen (2017) addresses this very important issue that may affect the intermediate stages of flooding and lead to asymmetries and potentially make the vessel more vulnerable to capsizals. It builds on the knowledge gained from a series of full-scale tests on leakage and collapse of various non-watertight structures carried out at CTO in Gdansk, Poland for the EU FP7 project FLOODSTAND (2009-2012) (Jalonen et.al., 2012). The test methodology and an analysis of the results on the leakage and collapse of non-watertight ship doors is presented in detail in Jalonen et al. (2017). A similar study on the leakage and collapse of non-watertight doors has been presented by Dankowski et al. (2014). They are all stem from the fact that modern passenger ships have complex transverse and vertical fire protection subdivisions. Many of them are not watertight. However, their presence may have a significant impact on the flooding process. This can be addressed by time-domain flooding simulation, combined with the latest research on the leakage and collapse of non-watertight structures. Ruponen (2017) has shown that the status of those non-watertight doors can have enormous effects on the progress of flooding, and particularly on the time-to-capsize (TTC). In contrast, the variation of the modelling parameters for the leakage and collapse of the closed doors had much smaller effects. Therefore, Ruponen (2017) proposes the following conservative approach for the door statuses in time-domain damage stability simulations: (a) the fire doors at the staircases and escape trunks that allow up and down-flooding, and all doors on the bulkhead deck could be considered as open; (b) the doors in the longitudinal bulkheads under the bulkhead deck should be considered as closed.

3. REVIEW ITTC RECOMMENDED PROCEDURES (TOR 2)

3.1 Introduction

In the following, some explanatory comments are given about the updating activity of the eight procedures reviewed and the six new procedures proposed.

3.2 Updated procedures (TOR 2 a)

Procedure 7.5-02-01-08 (Single Significant Amplitude and Confidence Intervals for Stochastic) is currently under responsibility of the Quality Systems Group. The procedure uses different algorithms for a large and small number of runs. Their unresolved issue of small-number of the run algorithm is the "cut-off" point for the autocorrelation estimate (equation 9 of the procedure 7.5-02-01-08) – it may be too large for a long record, containing a large number of points. Levine et al. (2017) proposed to identify the "cut-off" as a decorrelation time when the autocorrelation drops below 0.05. Pipiras et al. (2018), Weems et al. (2019a) considered the "cut-off" based on error minimization, using long-run variance (Lu and Park, 2019). The "cut-off" point issue is still pending. Upon its successful resolution, it will make sense to update the procedure 7.5-02-01-08. Unifying the algorithms for a small and large number of runs also may be considered. Quality Systems Group is expected to take a lead on such an update.

Procedure 7.5-02-05-07 (Dynamic Instability Tests from high-speed marine vehicles domain) was reviewed and no change is proposed by the committee.

Procedure 7.5-02-07-04.1 (Model Tests on Intact Stability) was reviewed and no change is proposed by the committee.

Procedure 7.5-02-07-04.2 (Model Tests on Damage Stability in Waves). The procedure was submitted by the previous Stability in Waves committee. No comments were received by previous and actual committee no improvement is requested by this committee.

Procedure 7.5-02-07-04.3 (Predicting the Occurrence and Magnitude of Parametric Rolling) was submitted. A three-level structure was adopted for the procedure, similar to the second-generation IMO intact stability (MSC.1/Circ.1627). Each level describes methods of prediction of different fidelity and thus complexity. The appropriate level is chosen by the user depending on the required prediction fidelity. The first-level predication is based on analytical and semi-analytical formulae. The second level prediction is a simplified numerical method. The third level prediction presumes using advanced numerical code. The procedure contains recommendations on specific issues, related to the assessment of parametric roll in irregular waves. The list of references has been updated.

Procedure 7.5-02-07-04.4 (Numerical Simulation of Capsize Behaviour of Damaged Ships in Irregular Beam Seas) was submitted. TOR 9 "Develop/suggest a method for estimating time to capsizing and/or sinking and include this in the report" will be answered in this procedure (see section 9). No other change is requested.

Procedure 7.5-02-07-04.5 (Numerical Estimation of Roll Damping) was reviewed and significantly updated by the committee; more detailed descriptions of the changes are summarized in section 7 of this report.

Procedure 7.5-03-02-03 (Practical Guidelines for ship CFD application) was reviewed and the committee proposes to modify Section 3.6. Time Step by adding the recommended time interval when an overset mesh is used, i.e., if an overset mesh is used, use at least 500-time steps per period.

3.3 News procedures (TOR 2 b)

Proposal for Guidance on Avoiding Self-Repetition Effect during Numerical Simulation of Ship Motions was submitted. Purpose of the Guidance is to formulate a process for verification of the absence of self-repetition effect and statistical validity of irregular waves in numerical simulation of ship motions. Currently used a mathematical model of irregular waves is based on work of St. Denis and Pearson (1953) and Longuet-Higgins (1962). Application of this model in time-domain numerical simulation requires discretization of the spectral density of wave elevations. An inappropriate choice of frequency discretization of the spectrum may lead to self-repetition effect, compromising statistical validity of the model. It may result in an incorrect assessment of statistical uncertainty of SSA and other estimates as required by procedure 7.5-02-01-08. The Interim Guidelines for the Second Generation IMO Intact Stability Criteria requires that modelling of irregular waves should be statistically and hydrodynamically valid and self-repetition effect should be avoided (Paragraph 3.3.2.1.2 of Annex of MSC.1/Circ.1627). To verify the absence of the self-repetition effect the auto-covariance function will be computed directly from the spectrum, using the chosen frequency discretization. The autocovariance of a statistically and hydrodynamically valid mathematical model of irregular waves should show no correlation beyond the initial decay. Theoretical background for the proposed Guidance is available in Belenky (2011).

Proposal for Computational Procedure for Predicting the Instantaneous $\overline{GZ}$ Curve during Time-Domain Numerical Simulation was submitted. Purpose of Procedure is to describe a process for computation of the instantaneous $\overline{GZ}$ curve in irregular waves to enhance the analysis of large roll angles. While the computation of stability curves in regular waves is wildly available from commercial software, similar capability for irregular waves is rare. At the same time knowing the form of the instantaneous $\overline{GZ}$ curve in irregular waves may help to explain large roll excursions, see Figure **353**. Calculation of the instantaneous $\overline{GZ}$ is fairly straightforward: for each time step of the calculation, the ship is heeled through a range of angles relative to its predicted position, the forces and moments on the ship are computed for the heeled position, the ship's heave position and pitch angle, expressed relative to a global coordinate system, are iteratively adjusted until the dynamic equilibrium in these modes is achieved, finally, the net roll moment defines the instantaneous $\overline{GZ}$ value. Theoretical and numerical background for the proposed procedure in available in Belenky and Weems (2008).

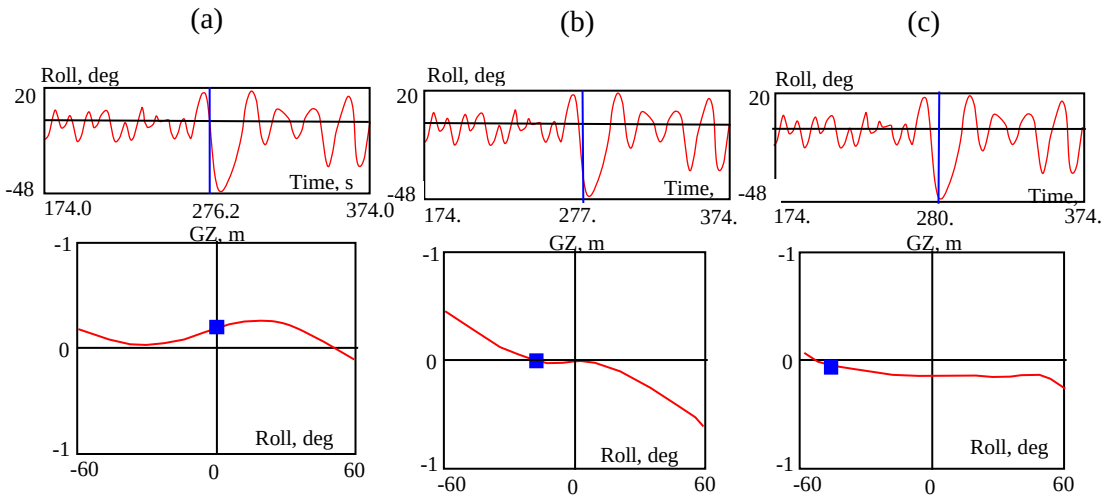

Figure 353: Time history and evolution of $\overline{GZ}$ curve in irregular waves a) zero roll angle; b) zero stiffness; c) Roll angle excursion

Proposal for Procedure Inclining test was submitted. The task done have started by an analysis of the many similar procedures written by the classification societies or standardisation offices. The most complete of those seem to be the ones from the American Standard taking into account several types of vessels. As requested, focus on uncertainty was performed, for example, suggesting a checklist in order to be sure that all precautions have been taken. It is also suggested to performed roll period measurement at the same time in order to be able to make an operational estimation of the *GM* as recommended by IMO.

4. IMO 2ND GENERATION INTACT STABILITY CRITERIA (TOR 3)

The task 3 of the TOR contains the statement "… it may be useful to develop a fault tree to better identify each of the stability failure modes".

Current international stability regulations are collected have been established from the International Code on Intact Stability 2008 (2008 IS Code). The Code was adopted by resolution MSC.267 (85) of the Maritime Safety Committee (MSC) of the International Maritime Organization (IMO) and came into force in July 2010.

Stability criteria intended for all types of ships can be found in two sections of the Code: requirements for $\overline{GZ}$ curve in section 2.2, and severe wind and rolling criterion (also known as the weather criterion) in section 2.3. The criteria from section 2.2 have originated from works by Rahola (1939), which is embodied in Res. A.167 (ES.IV). The work on the weather criterion that commenced in the 1950s (Kobylinski and Kastner, 2003) is embodied in Res. A.749 (18). The Code recognizes that the fleet is evolving and the Code "should not remain static" (paragraph 2 of the Preamble). The Code also notes the variety of types of ship and complexity of physical phenomena involved in the stability analysis and recognizes that "...problems of safety against accidents related to stability have generally not yet been solved" (paragraph 2 of the Preamble). Directions for further development are formulated in Chapter 1 of Part A of the Code. Priority is given to the development of performance-oriented criteria for:

- Righting arm variation, resulting in parametric roll resonance and pure loss of stability (paragraph 1.2.1);

- Resonant roll in dead ship conditions (paragraph 1.2.2);

- Broaching and other manoeuvring related phenomena (paragraph 1.2.3).

There are totally four distinct modes of stability failure. The fifth mode of failure, excessive accelerations, was added, following the German proposal (SLF 53/3/2).

The intact stability working group of IMO Subcommittee on Stability and Load Lines and on Fishing Vessels Safety (SLF) was assigned this task. The working group was re-established in 2002 with the dual purpose of finalizing the 2008 IS Code and further development.

Performance-oriented criterion is essentially a mathematical model of the physical phenomenon "responsible" for possible stability failure. A new framework was envisioned to confront the complexity of these physical phenomena and avoid unnecessary costs of analysis performed on irrelevant cases. The criteria is defined a multi-teared (or multi-leveled) structure, where the first tier defines if the case is relevant, and the second tier determines the loading conditions and environmental conditions that are likely to lead to stability failure. The most advanced

numerical techniques of analysis are to be used in the third tier. If a possibility of stability failure cannot be eliminated in a design stage, the information produced by the third tier analysis is applied to ship-specific operational guidance. This framework was formulated in a paper SLF 50/4/4, discussed on the 50th through 53rd sessions of SLF, taking the final form in Annex 1 of SLF 54/3/1.

During the intersessional period leading to SLF 55 and SLF 55th session, most of criteria were developed and agreed, in principle. The criteria for parametric roll and pure loss of stability were formulated as proposed amendments to part B of the 2008 IS Code (Annex 1 and 2 SLF 55/WP.3). Due to reorganization of some IMO sub-committees, the SLF Sub-Committee was amalgamated into the Sub-Committee on Ship Design and Construction (SDC) together with elements of the former DE Sub-Committee. During the intersessional period leading to SDC 1 explanatory notes for pure loss of stability and parametric roll was developed (Annexes 3 and 4 of SDC 1/INF.8). A text on draft amendments for surf-riding / broaching and dead ship condition was developed (Annexes 15 and 16 SDC 1/INF.8). The draft explanatory notes for dead ship condition (SDC 1/INF.6) and surf-riding broaching (SDC 1/5/4) is drafted and submitted. The first draft text of excessive acceleration was developed (Annex 33 of SDC 2/INF.10) during the intersessional period leading to SDC 2 and at the 2nd SDC session. The working group completed vulnerability criteria for pure loss, parametric roll and surf-riding, which were documented as Annexes 1 through 3 of SDC 2/WP.4

During the intersessional period leading to SDC 3 and 3rd SDC session, criteria for dead ship conditions and excessive accelerations were completed (Annexes 1 and 2 of SDC 3/WP.5 and SDC 3/INF.10). Explanatory notes for all failure modes documented and released as Annexes 3 through 7 of SDC 3/WP.5 and 16 through 20 of SDC 3/INF.10. Draft Guidelines on operational limitation were developed and documented in Annex 21 of SDC 3/INF.10. The intersessional period leading to SDC 4 and 4th SDC session focused on testing of the vulnerability criteria primarily with matrix calculations. Draft guidelines on direct stability assessment were documented (Annex 1 of SDC 4/WP.4).

The first draft complete of the complete Guidelines of the second generation intact stability was developed during the intersessional period leading to SDC 6 and 6th SDC session (SDC 6/WP.6). It was finalized during the intersessional period leading to SDC 7 and 7th SDC session (SDC 7/WP.6), approved and published by Maritime Safety Committee as MSC.1/Circ.1627. The completion of the explanatory notes is expected in early 2022 at the 8th Session of SDC.

Fault Tree Analysis (FTA) is a standard risk management tool, focusing on the safety-critical function of a complex engineering system. It models the development of a failure of the entire system based on different scenarios of failures of the elements of this system. A ship is considered as a system, including the ship itself, operator, and institutional policies. The system is subjected to various environments. A ship may have the following main scenarios for the end of her life: intact capsizing, capsizing due to damage (caused by collision or grounding, i.e. event not expected in the life of the ships…), structure collapse (due to environment or excessive loads), retirement from the service due to principle subsystem ageing and/or failure. As for a ship's end-of-life failure, the presentation in a format of a fault tree for some basic events may cause a failure to propagate through several brunches simultaneously. For example, collision damage could lead to damage stability failure and to further deterioration of structural integrity at the same time. Such interdependencies of branches usually are not considered within the FTA.

Most of these interdependencies are related to the environment. A loss of a ship is often a combination of many failures. Alman et al. (1999) refer to the letter by USN Admiral Chester W. Nimitz of 13 February 1945, summarizing the damage on the US fleet after crossing a typhoon (data that are the basis of the establishment of most of western navies rules, initiated by Sarchin and Goldberg in 1962). They mentioned, "*The most important is that in extreme seaway conditions, many things frequently go wrong at the same time or the worst possible times, leading up to a point where the crew are no longer take steps to save the ship. At this point the ship simply becomes a capsize 'waiting to happen*". As, a result, a conventional fault tree is not sufficient for a comprehensive presentation of the ship's failures.

The interdependences of the causes of failures are better presented with Venn diagram, the graph, shown in Figure 354, is a modification of one from Dahle and Nedrelid, (1982), see also Kobylinski and Kastner (2003). The Venn diagram in Figure 354 shows five modes of intact stability failure, covered by the second generation of IMO intact stability criteria (SGISC), corresponding to numbers 4, 6, 8 and 9.

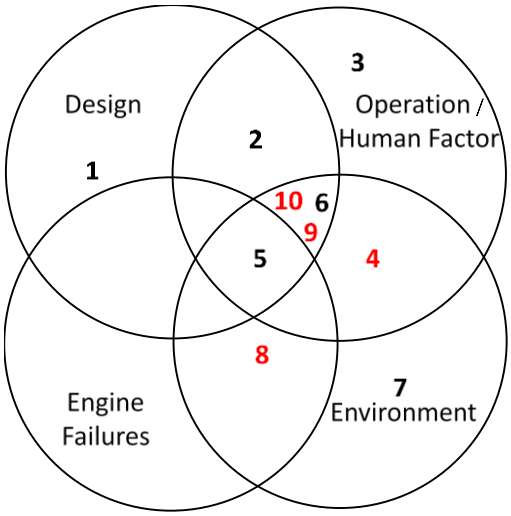

1. When launched due to faulty design
2. Turning at high speed
3. Overloading
4. High speed in following sea – broaching and pure loss of stability
5. Bad weather + lack of knowledge + low stability + subsystem failure
6. Excessive water on deck
7. Heavy icing combined with heavy sea preventing clearing off the ice
8. Dead Ship Condition
9. Parametric Roll
10. Excessive Acceleration

Figure 354: Venn diagram of ship's stability failure mode

The Venn diagram in Figure 354 provides a relatively simple presentation for "big picture" of stability failures and modes of stability failures, covered by SGISC. A further consideration is focused on these five modes. The development does not include any consideration of loads (height, shift of, liquefaction…), limited by design, environment, engine failure and human factors.

The interdependency of basic events cannot be completely not avoided for even only SGISC modes of failure. For example, high speed in following or stern quartering seas may lead by surf-riding, following by broaching-to or (if a variation of $\overline{GZ}$ curve in waves is significant) to pure loss of stability.

Also, each ship is functionally different to a certain extent and a fault tree is uniquely reflecting ship type, operational practice, and environment (Alman et al. 1999). It may be difficult to generalize following all possible consequences in a format of a single fault tree.

Thus, each mode of failure will be described by one fault tree.

What is a stability failure? The following capsizing definition is available in SLF 54/3/1: "capsizing is formally defined as a transition from a stable nearly upright equilibrium that is considered safe, or from oscillatory motions near such equilibrium, to another stable equilibrium that is intrinsically unsafe (or could be considered unacceptable from a practical point of view)". However, capsizing is not mentioned in the final version of SGISC in SDC 7/WP.6; the stability failure is defined as:

The roll angle exceeds prescribed limit (paragraph 1.1.2.2.2 of MSC.1/Circ. 1627).

Heel and list exceeds a certain limit (paragraph 1.1.2.2.1 of MSC.1/Circ. 1627). It may be generated cargo shift and then dynamic stability extreme events.

Lateral acceleration exceeds a certain limit (paragraph 1.1.2.2.3 of MSC.1/Circ. 1627) give limit value for.

The relation between these modes of failure is clearly strong but its description is out of the scope of the present task, as it is not addressed by SGISG. Many papers try to link the capsizing probability and failure as the probability to exceeds roll angle, as Maki et al. (2018) or Macé et al. (2018) but more work is needed.

Figure 355 shows a fault tree for the stability failure caused by broaching-to, preceded by surf-riding. The surf-riding occurs in following or stern-quartering seas, in high speed, when a long and steep wave is encountered. While such long and steep wave usually overtakes a ship, it creates significant surging force. The surging force may be sufficient to accelerate the ship to forward speed, corresponding to wave celerity. Then a ship may surf-ride. The surf-riding essentially is a dynamic equilibrium where surging wave force added to thrust equal to resistance at wave celerity.

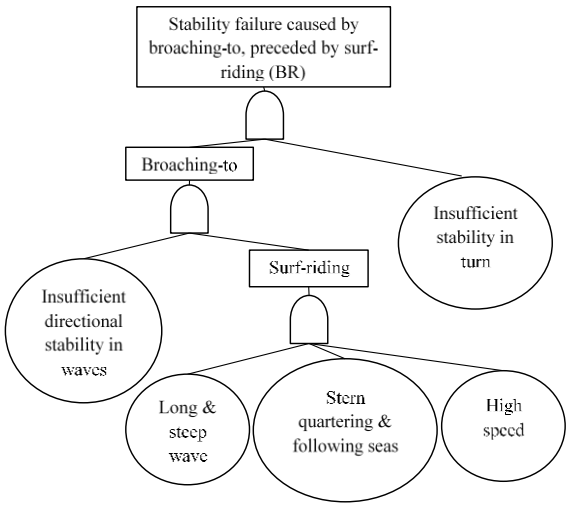

Figure 355: Fault tree for stability failure caused by broaching-to (BR)

A ship usually takes a position on the front slope of the wave, slightly pitching forward. The water flow around the hull and the rudder leads to decrease of directional stability of a ship. If the directional stability becomes insufficient, the ship makes a sharp uncontrollable turn.

If the stability of a ship is insufficient to withstand a moment of centrifugal force generated by the turn, a stability failure may develop.

Erreur ! Source du renvoi introuvable. shows a fault tree developed for the parametric roll. To occur, parametric roll requires encounter of several waves of similar length and height certain speed and heading. The frequency of encountering these waves should be about twice the natural frequency. This fulfils the frequency condition of the principle parametric resonance.

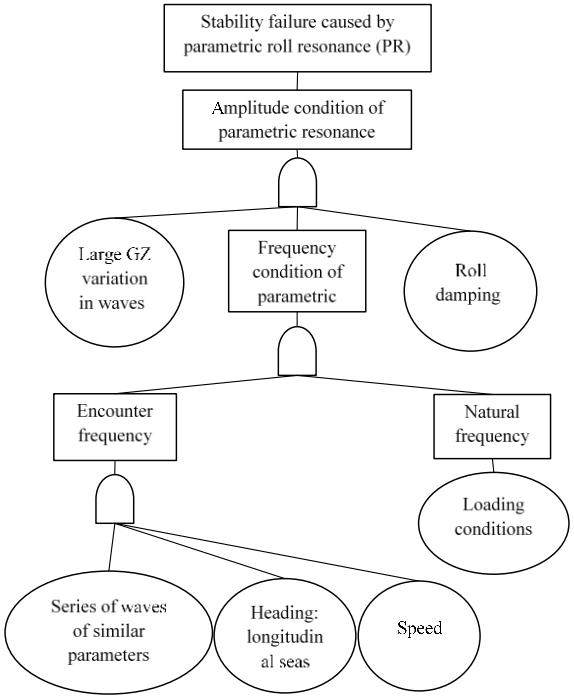

Figure 356: Fault tree for stability failure caused by parametric roll (PR)

If a ship has significant bow flares and a large stern overhang, $\overline{GZ}$ curve may experience significant variation if the sufficiently long and steep wave passes by. Decrease of stability while on the wave crest makes a ship 'sluggish' and makes her heeling more under an external heeling moment. When the mid-ship's sections pass the wave crest, stability improves and push–back from the inclined position is stronger. This combination of low and high- stability of "sluggish" heeling and strong push-back may lead to increasing magnitude of rolling if a ship does not have enough roll damping to disperse this additional energy. It is the essence of the amplitude condition of the parametric roll.

Figure 357 shows a fault tree for pure loss of stability. Similar to parametric roll, the pure loss of stability requires a significant variation of stability in waves, thus encounter with a wave of specific parameters is required.

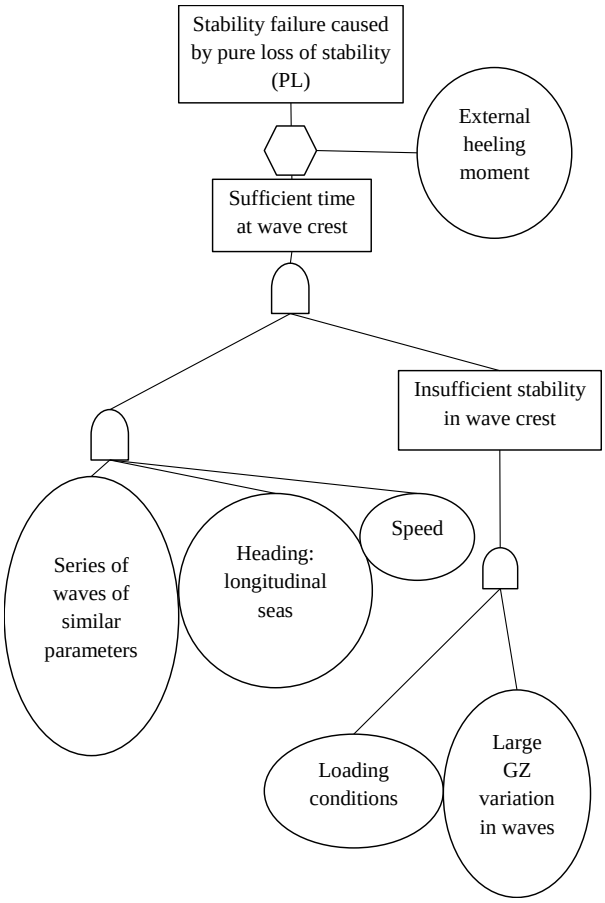

Figure 357: Fault tree for stability failure caused by pure loss of stability (PL)

Significant stability variation in a wave is necessary but not a sufficient condition. The

KG-value should be high enough to make the stability in wave crest insufficient to withstand an external heeling moment.

The decreased stability state should last long enough, for the external heeling moment to cause a roll angle, exceeding prescribed limit.

Figure 358 shows a fault tree for Dead Ship Condition. As it is clear from its term, the failure mode is initiated by loss of propulsion and steering. The conventional assumption is that the wind turns a ship into a beam or near beam seas position.

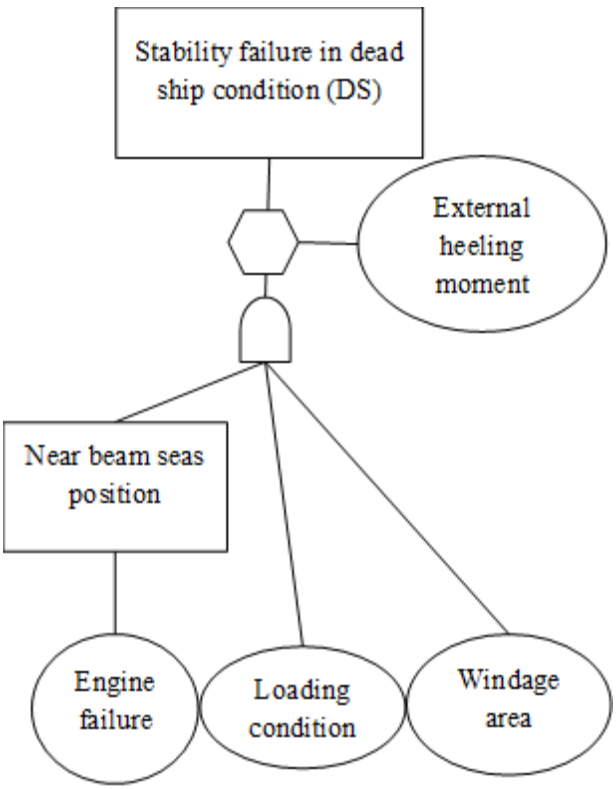

Figure 358: Fault tree for stability failure on dead ship condition (DS)

Lateral projection of the windage area plays a significant role in the development of stability failure in dead ship condition as the wind heeling moment is one of the principle environmental factors.

As expected loading state with high *KG* value is when a ship is the most vulnerable to stability failure in dead ship condition.

The external heeling moment is created by a wind gust, while a ship is assumed drift under the action of wind and waves. Hydrodynamic drag induced by the drift adds to the heeling actions of the wind.

Waves cause roll motions that may be significantly amplified by synchronous roll resonance when the natural roll frequency is close to the modal frequency of the wave spectrum.

A ship may be vulnerable to excessive acceleration stability failure mode in ballasting loading conditions when GM value is high.

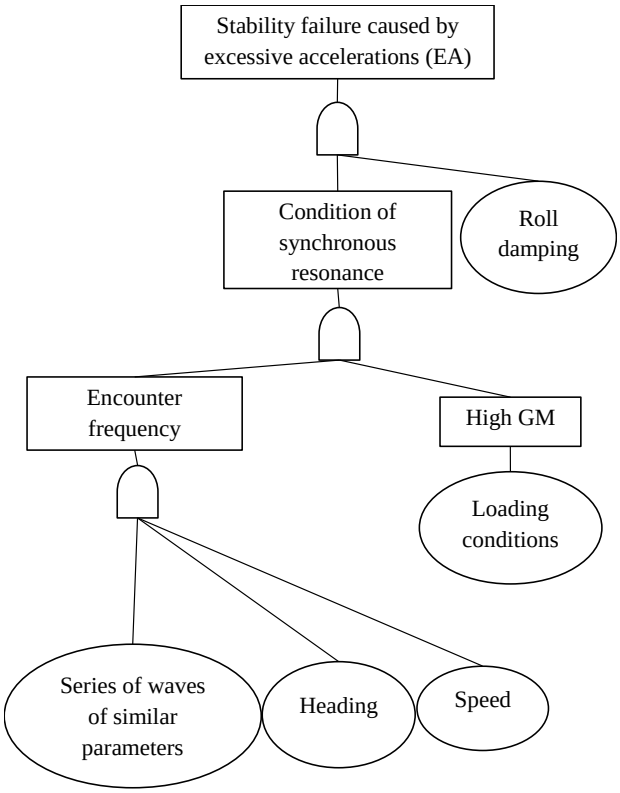

Figure 359: Fault tree for stability failure on excessive acceleration (EA)

The failure is initiated by an encounter of a series of waves with similar parameters. Speed and heading make the frequency of encounter close to the natural frequency of roll.

A similar value of encounter frequency and roll natural frequency creates a condition of synchronous resonance. If roll damping is not sufficient, the roll angles can increase together with lateral acceleration that is closely correlated with roll angle. The failure occurs when lateral acceleration at a high location (usually wheelhouse) exceeds a prescribed value.

Task 3 of the Terms of References calls for use of the fault tree for the identification of the failures. So, a stability failure (e.g. capsizing or high roll angle) from the full-scale record or numerical simulations can be associated with one of these fault trees. Indeed, more information is available; the more likely adequate fault tree is identified for the observed phenomenon. Many parameters can be useful for this evaluation. For the following consideration, all the parameters are assumed to be available; so, a particular fault tree can to be adapted to the specific case.

If a hull form is available, it can be useful to test the ship according to the level 1 and 2 of IMO SGISC for the four-roll angle-related stability failure modes (that can end in a capsize). Then the vulnerability of the ship will be pointed out for one or the other modes. For some failure modes, the IMO SGISC testing suggests estimating the probability of a large roll angle. Then it will give an indication of the most dangerous heading, speed and waves.

The first step could be related to the relative heading: What is the relative heading just before or during the capsize events?

If the answer is clear (the relative wave heading can be well determined) and can be identified as nearly transverse, head of following, then this first question is useful.

If relative wave heading approximately corresponds to beam seas dead ship condition is a good candidate for the failure mode. A factor, which increases this possibility, is high wind speed. As the stability failure is caused by excessive roll angle, it is expected to occur for the forced roll period to be close to the natural roll period (synchronous roll resonance condition) or for very high waves. The dead ship condition is defined as an event following by an engine failure, but it can be generalized to excessive roll motion caused by synchronous resonance, particularly without forward speed and beam waves.

If relative heading corresponds to approximately head or following waves, there may be several modes of failure. If the heading is head or oblique waves, the most probable mode of failure is parametric roll, which has to be confirmed by the second question.

The second step is related to the speed of the ship. The forward speed has to be compared to wave celerity (when it can be estimated and considered as a good characteristic of the real sea state) and critical speed for the parametric roll. The range of ship speeds characteristic of the parametric roll is given by Spyrou and cited in reference by IMO SGISC. A simple verification for parametric roll possibility is to check if encounter frequency is about twice the natural roll frequency with low roll damping. A development of parametric roll may be expected.

If wave speed is close to instantaneous wave celerity just before stability failure it means that surf-riding occurred. If so, the instantaneous ship speed must be closely analysed in order to determine if the average ship speed is abnormally increased due to the wave (high-run) which is a very good indicator. Looking for

high-runs as defined by Kontolefas and Spyrou (2018), as a significant time when the ship's speed is increasing, is useful. Figure 360 from the cited reference show an example of a high-run on a numerical simulation.

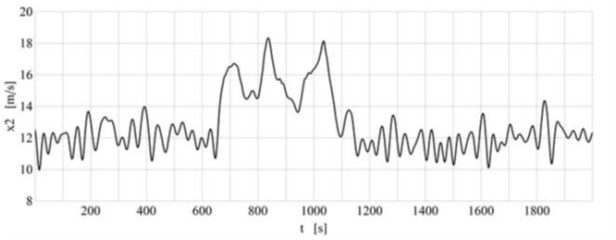

Figure 360: Time history of surge velocity with a high run

Surf-riding is usually not the mere reason for stability failure but very often it is a phenomenon which leads broaching. Broaching happens in following or stern quartering waves, after a surf-riding. Broaching can be identified by the activities of the rudder and the analyses of motions. Surf-riding occurs also for the low frequency of encounter, then the motions are ceased because the ships are "caught" by waves. In this situation, force in the vertical plane are quite important and have a strong effect on motions even at low frequency, then trim is the best indicator for this. Then a constant trim for a long time on high and steep waves is another good indicator of surf-riding.

As to broaching another point to look into is whether the ship loses yaw stability and has difficulties to keep constant her course including effect due to the characteristics of the autopilot. Then analysing yaw motion is a good idea because of the autopilot. Unexpected yaw motion can be observed (large amplitude and/or value). Rudder activity has also to be analysed. Rudder at its maximum value for a long time is a sign that the ship struggles to keep constant the direction, which means that broaching is about to occur. Then broaching occurs because the rudder cannot counteract the yawing moment induced by the wave and the vessel deviates rapidly from its initial heading (let us say 20° as given by Renilson and Tuite, 1998). It is often associated with an increasing roll angle partially due to the rudder heel moment, partially to the reduction of restoring moment and high centrifuge moment (see Figure 361). Surf-riding occurs only on high and steeped waves. The minimum value can be determined following IMO SGISC methodology.

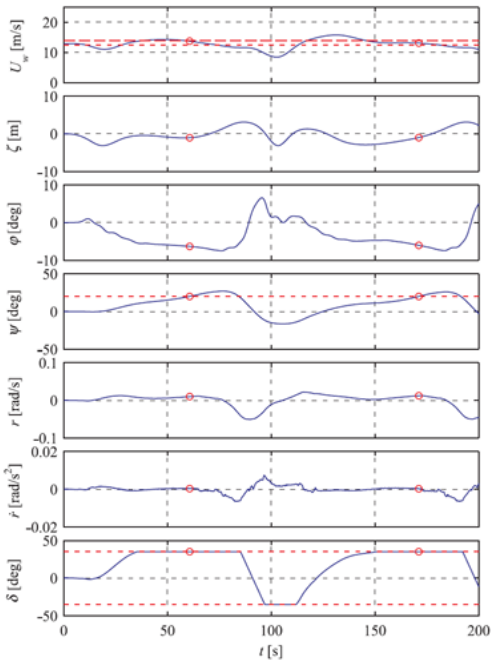

Figure 361: Time traces showing broaching (*Fr = 0.40, Ψ_w = 20°, H/λ = 1/20, λ /L = 1.04*) from P. de Jong (2025)

Some other checks can also help. If possible, if the natural roll period of the ship just before the failure can be determined and if it is close to twice of the wave encounter period it is a good indicator of Parametric Roll (depending on heading and waves) or a failure similar to Dead Ship Condition, as roll resonance.

Ship speed is also related to the time spent near the wave crest. If the time near the wave crest can be determined to be long enough for a ship to react on an external heeling moment then the

stability failure is likely to be pure loss of stability.

The review of the IMO Second Generation intact stability criteria and standards with a particular focus and background for each stability failure mode is prepared as a draft of IMO INF paper to be submitted by ITTC to 8th session of SDC.

The review starts with the probabilistic framework, which is common for all failure modes. Main probabilistic assumptions are discussed, leading to short- and long-term formulations. The short-term formulation assumes constant environmental (wave and wind spectra) and operational (forward speed and relative wave heading) leading to stationary ship response. The long-term formulation accounts for the variability of the environmental and operational condition during the service life of a ship.

Discussion of each failure mode (except for the dead ship condition) includes a short description of relevant stability accidents with references on official investigation reports. The accident description follows a discussion of physical mechanism and relevant mathematical models of stability failure, as well as a literature review.

Review of physics of the stability failure in dead ship condition starts from a discussion of forces acting on a ship in beam seas and the way these forces can be computed. The probabilistic formulation is based on upcrossing theory, so it is given a brief review. Further discussion is focused on equivalent failure angles (used in the level 2 vulnerability criteria) as a method to treat nonlinearity of roll motion in irregular waves, using energy/work balance.

Consideration of excessive acceleration failure mode includes a brief review of the kinematics of a point of a rigid body involved in arbitrary motion. Then the calculation of lateral acceleration is examined as well as specifics of the application of upcrossing theory.

Review of pure loss of stability includes basic dynamics rising form variation of stability in waves. Brief consideration is given to a repeller, a dynamical system with negative stiffness, modelling roll motion of a ship in the case of complete loss of stability on a wave crest. Then probabilistic properties of stability in waves are discussed and it is shown that changes of the $\overline{GZ}$ curve in a wave may be very complex. Grim (1961) effective wave is considered as a way to resolve this complexity.

Review of parametric roll mode of failure starts from the derivation of the Mathieu equation - most basic mathematical model of parametric resonance. Then the solution of Mathieu equation and its properties are considered and Ince-Strutt diagram (graphic depiction of instability zones of the solution) is introduced. The influences of damping and nonlinearity of stiffness are examined; finally, an account of the irregularity of realistic sea waves is addressed.

Discussion of surf-riding and broaching also starts form equation of surge motions as a transition to surf-riding from surging is a precursor of broaching-to. Mathematical modelling of surf-riding equilibrium and its stability is described, and phase plane presentation is introduced. The criterion is based on phase plane analysis and is expressed with the Melnikov function (Melnikov, 1963), which is given a brief review. Finally, mathematical modelling of broaching after surf-riding is discussed as well as probabilistic treatment of stability failure caused by broaching-to in irregular waves.

The document is concluded with a short summary and contains 129 references, covering most of the relevant literature. The document may be especially useful serving as the starting point for the future revisions of the second generation IMO intact stability criteria.

5. RECOMMEDATION ON DEVELOPEING A SET OF PROCEDURES FOR DIRECT ASSESSMENT OF THE SECOND GENERATION IMO INTACT STABILITY CRITERIA (TOR 4)

5.1 Introduction

Direct stability assessment is the top-tier of the second generation IMO intact stability criteria. It is an evaluation of dynamic stability of a ship in waves with the most up-to-date numerical simulation tools, model test or combination of thereof. Currently, direct stability assessment is described in Chapter 3 of the IMO Interim Guidelines on the second generation intact stability criteria, published in Circular 1627 of IMO Maritime Safety Committee (MSC.1/Circ.1627).

The Interim Guidelines formulates objective of the direct assessment (Section 3.1) and gives a definition of the stability failure event (Section 3.2). Requirements for predication of ship motion are formulated in Section 3.3. Requirements for model test are referred to ITTC Procedure 7.5-02-07-04.1 or as amended.

Requirements for numerical simulation tools include statistical validity of irregular wave model (subsection 3.3.2.1 of the Interim Guidelines). Self-repetition effect is one of the most important factors of the statistical validity, as it affects confidence interval of all ship motion estimates made with the model. Avoiding self-repetition effect is addressed in the proposal to develop an ITTC procedure, see Section 2 of this report.

The subsection 3.3.2.2 of the Interim Guidelines contains requirements for modelling of roll damping. Recently updated ITTC procedure 7.5-02-07-04.5 on Estimation of Roll Damping is relevant for these requirements (see Section 6 of this report). A new possible contribution may include an ITTC guidance or a procedure how to avoid duplication in modelling of roll damping. The duplication may be present when wave component of roll damping is included in model test data and internally computed by potential flow numerical simulation tool as a part of diffraction and radiation force and moment. No specific proposal has been developed yet.

The Interim Guidelines address validation of the numerical simulation tools in Section 3.4 of the Interim Guidelines. The validation is defined as “the process of determining the degree to which a numerical simulation is an accurate representation of the real physical world from the perspective of each intended use of the model or simulation”. Two phases of the validation process is distinguished: qualitative and quantitative. Developing a guidance or procedure for validation of numerical simulation tools is yet another potential area for ITTC contribution; however no specific proposal has been developed yet.

The Section 3.5 of the Interim Guidelines describes procedures for direct stability assessment. It recognizes the problem of rarity – “when the mean time to stability failure is very long in comparison with the natural roll period that serves as a main timescale for the roll motion process”. With the exception of the cases of extremely severe waves, application of sufficient-fidelity numerical simulation tool would be too computationally expletive to estimate of stability failure by direct observation. The solution for the moderate to high waves is statistical extrapolation based on a limited volume of ship motion sample, where stability failure may or may not be observed.

New ITTC procedure for statistical extrapolation has been developed and described in the subsection 5.4 of this report. Proposal for new ITTC procedure for estimation of failure rate by direct observation is placed in

subsection 5.2 of this report. A proposal for ne ITTC procedure for statistical validation of extrapolation procedures can be found in subsection 5.3 of this report.

The Interim Guidelines also offers alterative to the solution of the problem of rarity: assessment in design situation and assessment using deterministic criteria. Developing procedures for these methods of assessment is another potential contribution from ITTC; however no specific proposal has been developed yet.

Finally, a future ITTC procedure could address the issue of verification of failure modes, required by the subsection 3.5.2 of the Interim Guidelines. In general, ITTC can play an important role in developing and updating procedures for direct stability assessment as the ITTC members are likely performers of these services for the industry.

5.2 Proposal for Procedure of Estimation of Frequency of Random Events

Purpose of the procedure is to formulation a of estimating a rate of stability failures and its confidence interval based on observed random events in a record of ship motions produced by a model test or numerical simulation. The requirements for the estimation procedure are located in the section 3.5.4 of the Interim Guidelines.

The procedure should use all available data, presented as a set of records of different length. First the autocorrelation function is estimated as recommended by procedure ITTC procedure 7.5-02-01-08. Then the envelope of the autocorrelation function is computed by as a set of absolute values of its peaks. The decorrelation time is evaluated as an instant when autocorrelation function falls below 5% (if such instant cannot be found, the time of the first minimum of the envelope is taken as the decorrelation time).

The next step is counting the events for each record; if there is more than one event within the decorrelation time, only one is counted to preserve independence of the events. The rate of events is estimated as $\hat{\lambda} = n/\sum_i T_i$ where T_i is the duration of a simulation time history or model tank run and n is the total count for independent events. The confidence interval is computed using binomial distribution for the random variable n or its normal approximation.

The procedure will also address algorithms applicable to numerical simulation only as mentioned in paragraph 3.5.4.4 of the Interim Guidelines. Theoretical background for the proposed Procedure is available in (Leadbetter et al. 2019).

5.3 Proposal for Procedure "Statistical Validation of Extrapolation Methods for Time Domain Numerical Simulation of Ship Motions and Loads

The purpose of the procedure is to formulate a process for validation extrapolation methods for time domain numerical simulation of ship motions and loads. The purpose procedure if limited by the establishing the validity of the extrapolation procedure and does not address the validation of numerical simulation tool. Requirements for statistical validation of extrapolation methods are found in the section 3.5.6 of the Interim Guidelines.

The first step of the validation is production of a validation dataset of large volume where statistically sufficient number of failures can be observed. To produce a large sample in a practical time, a mathematical model of reduced complexity can be used. This reduced complexity, however should not compromise the qualitative validation of the

mathematical model. A volume-based numerical simulation is one example of mathematical model of reduced complexity (see e.g. Weems and Wundrow, 2013 or Weems et al., 2018). The validation dataset is produced for a number of ship speeds, relative wave headings and sea states.

Direct counting procedure (see section 5.2 of this report) is applied to the validation dataset. The rate of failures, estimated from the validation dataset serves as a “true value” for the statistical validation purposes.

Validation of the extrapolation procedure is performed for 50–100 statistically independent data sets, and evaluated for a number of ship speeds, relative wave headings and sea states. The extrapolation datasets are subsets of the validation dataset. Extrapolation procedure is carried out for each of the extrapolation dataset, see e.g. subsection 5.4 of this report.

A comparison is made between the extrapolation and the "true value" for each extrapolation dataset. The comparison should be considered successful if the extrapolation confidence interval and the confidence interval of "true value" overlap.

Validation should be considered successful if a specified number of individual dataset comparisons were successful (88% for 50 sets, 90% for 100 — may be decreased by an “approximation allowance”).

Theoretical background for the validation of the procedure is available from Smith (2019).

5.4 New Procedure “Extrapolation for Direct Stability Assessment in Waves”

New ITTC procedure was developed describing two extrapolation methods for direct stability assessment. Section 3.5.5 of the Interim Guidelines mentions envelope peak-over-threshold (EPOT) paragraph 3.5.5.4.1.1 and split-time method/motion perturbation method (MPM) paragraph 3.5.5.4.1.2 among others. The developed ITTC on extrapolation contains brief theoretical background and application process as well as an example and brief validation results for these two methods. This new ITTC procedure is mean to be updated on the future date by adding description for other extrapolation methods mentioned in the Section 3.5.5 of the Interim Guidelines.

Theoretical background of EPOT and MPM is the extreme value theory, describing probabilistic properties of the largest observation in a sample (e.g. Coles, 2001).

The first extreme value theorem (also referred as Fisher-Tippett-Gnedenko theorem) proves that a distribution of the largest values in a sample of independent observations has a limit in the form of a Generalized Extreme Value (GEV) distribution:

$$\mathrm{cdf}(y) = \begin{cases} \exp\left\{\left(1+\xi\dfrac{y-u}{\sigma}\right)^{-\left(1+\frac{1}{\xi}\right)}\right\} & \xi \neq 0 \\ \exp\left\{\exp\left(-\dfrac{y-u}{\sigma}\right)\right\} & \xi = 0 \end{cases}$$

where ξ is a shape parameter, σ is a scale parameter and u is a location parameter. The case $\xi = 0$ is known as Gumbel family of distributions. There are two more particular cases: Fréchet and Weibull families of distributions (when the location parameter has a bound).

Fitting GEV distribution to numerical simulation or model test data, in principle, allows extrapolation beyond the observed values. As required by the first extreme value theorem, the data points must be independent. It is achieved by application of “block maxima” technique. The time series data are separated into independent fragments, “blocks” (e.g. using decorrelation time) and the largest value in each

"block" is used to fit the GEV; see example in Wandji (2019).

First application of GEV in the form of Gumbel distribution for dynamic stability in waves was carried out by McTaggart (2000a, 2000b), McTaggart and de Kat (2000c).

The second extreme value theorem (also referred as Pickands-Balkema-de Haan theorem) states that the GEV distribution can be approximated by a Generalized Pareto Distribution (GPD) above a large-enough threshold. That means, a tail of ($y > u$) of any distribution can be approximated with a GPD:

$$\mathrm{pdf}(y) = \begin{cases} \frac{1}{\sigma}\left(1 + \xi\frac{y-u}{\sigma}\right)^{-\left(1+\frac{1}{\xi}\right)} & \xi \neq 0 \\ \frac{1}{\sigma}\exp\left(-\frac{y-u}{\sigma}\right) & \xi = 0 \end{cases}$$

$$\mathrm{cdf}(y) = \begin{cases} 1 - \left(1 + \xi\frac{y-u}{\sigma}\right)^{-1/\xi} & \xi \neq 0 \\ 1 - \exp\left(-\frac{y-u}{\sigma}\right) & \xi = 0 \end{cases}$$

where ξ is a shape parameter, σ is a scale parameter and u is a location parameter that here has a meaning of a threshold value for the tail of distribution of y.

The extrapolation for the rate of exceedance is expressed as:

$$\hat{\lambda}(c) = \hat{\lambda}(u)\left(1 - \widehat{\mathrm{cdf}(c)}\right)$$
$$= \hat{\lambda}(u)\mathrm{P}(Y > c|Y > u)$$

where $\hat{\lambda}(u)$ is the rate of upcrossing (or down crossing) of the threshold u, which can be estimated directly form the time series (see section 5.2 of this report).

The scale parameter σ is positive, while the shape parameter ξ can be either positive or negative. A negative shape parameter imposes a limitation on the expressions in parenthesis of the equations and formally introduces a right bound to the distribution:

$$\mathrm{pdf}(y) = 0 \; if \;\; y > u - \frac{\sigma}{\xi} \text{ and } \xi < 0,$$

The shape parameter defines the type of tail: heavy, exponential, or light, as shown in Figure 362.

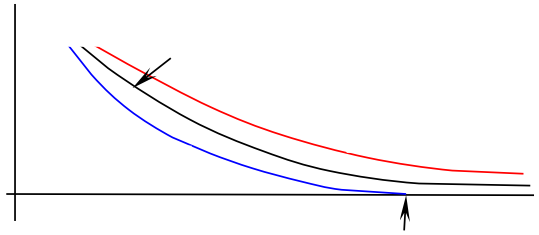

Figure 362: Types of tails per GPD approximation

The peak-over-threshold (POT) method is a generic extrapolation method based on GPD (Pickands, 1975). Similar to the GEV case, application of GPD also required independent data. Ship motion time series is dependent data, so independent data points have to be extracted – "de-clustered". A technique to extract independent data form the ship motion time series is to collect peaks of an envelope, shown in Figure 362, and referred as Envelope-peak-over-threshold (EPOT), see e.g. Campbell et al. (2016). The envelope approach is not applicable to parametric roll data, where decorrelation time can be used (Kim et al. 2014).

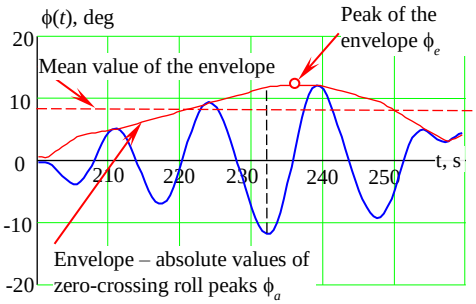

Figure 363: De-clustering using an envelope

Smith (2019) reported results on sample statistical validation of EPOT method for roll, pitch, POT/EPOT method with GPD is entirely data-driven; it is applicable to any ship motion process if sufficient data available. Otherwise,

statistical uncertainty may be too large for practical use. One of the manifestations of this large statistical uncertainty may be an inability to complete extrapolation because for $\hat{\xi} < 0$ when the target of extrapolation *c* lies beyond the GPD bound (Pipiras, 2020). While EPOT with GPD still can be used (see validation example reported by Smith, 2019), better solution with less uncertainty may be achieved with physics-informed extrapolation method.

The roll restoring arm ($\overline{GZ}$) curves of most ships have a limited range of stability, leading to the appearance of an unstable equilibria at the angle of vanishing stability. A peak value of roll angle is quite unlikely to exceed the angle of vanishing stability – ship is likely to capsize. Therefore, the tail of the distribution of roll peaks has a bound near the angle of vanishing stability. The term "peak value" stipulates that the roll angle will reach the peak and then returns back, i.e. no capsizing occur.

All positive ($\overline{GZ}$) curves have maxima. The value of roll resting decreases after the maximum of ($\overline{GZ}$) curve, thus the instantaneous *GM* value is negative after the maximum. There is no instantaneous natural roll frequency after the maximum of ($\overline{GZ}$) curve, so there is no resonance and roll forcing is decreased. Thus, the ship tends to roll slower and spend more time beyond the maximum of ($\overline{GZ}$) curve, leading to increased probability of observing ship in this position, i.e. to heavy tail.

The tail of roll peaks is expected to have a complex structure: a heavy tail right after the maximum of ($\overline{GZ}$) curve, turning into a light tail near the angle of vanishing stability. Figure 364**figure 364** illustrates this tail configuration. See Belenky et al. (2019a) for more formal argument and details.

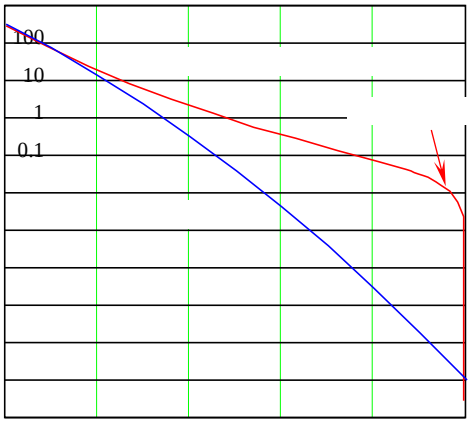

Figure 364: Types of tails per GPD approximation

As the target of extrapolation likely is located beyond the maximum of ($\overline{GZ}$) curve, but not too close to the angle of vanishing stability, the tail of the distribution of roll peaks is supposed to be heavy. When the shape parameter $\xi > 0$ and threshold value $u = \sigma/\xi$, the GPD is equivalent to Pareto distribution with scale $y_m = \sigma/\xi$ and shape $\alpha = 1/\xi$

$$\text{pdf}(y) = \frac{\alpha y_m^{\alpha}}{y^{\alpha+1}} = \frac{\alpha u^{\alpha}}{y^{\alpha+1}}$$

$$\text{cdf}(y) = 1 - \left(\frac{y_m}{y}\right)^{\alpha} = 1 - \left(\frac{u}{y}\right)^{\alpha}$$

To fit the Pareto tail, the parameter α has to be estimated and threshold *u* has to be found. The estimation of the parameter α is done from the data and it has to be treated as a random number. The threshold is found by minimizing of the fitting error. Fitting GPD is similar, but two parameters have to be estimated from the data. As a result, statistical uncertainty for fitting GPD is larger. The decrease of uncertainty is achieved by adding physics information to the statistical model – using heavy tail approximation, based on dynamical considerations. The physics-informed model is applicable within while these physical considerations are valid. i.e. while the target is sufficiently large so the tail can be assumed heavy, see Belenky et al. (2018a).

The heavy tail approximation also implies no significant change of physics. Split-time /motion perturbation method (MPM) complements EPOT with a capability to include changes of physics. The idea of MPM is to compute a metric of likelihood of a stability failure at an instant of crossing of an intermediate threshold and then extrapolate this metric for its critical value corresponding to the imminent failure.

For example to formulate the MPM metric for capsizing, the roll rate at each observed crossing is perturbed until capsizing is observed, see Figure 365. The metric is the difference between the observed roll rate at the crossing of an intermediate threshold and the roll rate that leads to capsizing.

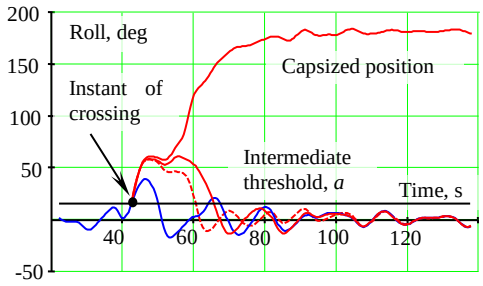

Figure 365: Motion perturbation for computing the capsizing metric

The capsizing metric is a random number showing how likely capsizing is at a given instant of time. It the tail of the MPM capsizing metric is described by exponential distribution:

$$\text{pdf}(y) = \frac{1}{\gamma}\exp\left(-\frac{y-u}{\gamma}\right)$$

$$\text{cdf}(y) = 1 - \exp\left(-\frac{y-u}{\gamma}\right)$$

where γ is the parameter of exponential distribution.

The reason why the tail of the MPM metric is described by exponential distribution is also physical. The MPM metric is the difference between two roll rates. The roll rate is related to a roll damping, which is weak nonlinearity, leading to normal distribution for the roll rate. The distribution of the roll rate at the instant of crossing is described by Rayleigh distribution see e.g. p. 201 of Leadbetter et al. (1983). The tail of Rayleigh distribution tends to exponential tail, see example 1.1.7 of de Haan and Ferreira (2007), while application details are available in Belenky et al. (2018a, 2019a).

The developed procedure covers the following aspects of the EPOT and split-time / MPM methods:

- Abridged version of the theoretical background given above;
- Data requirements for extrapolation
- Data preparation steps
- Fitting the distribution: estimating the parameters and finding the threshold
- Assessment of uncertainty and calculation of confidence interval

Application example is given in the Appendix. Available statistical validation data is reported in Belenky et al. (2018a).

6. FREE ROLL DECAY, FORCED ROLLING AND EXCITED ROLLING TESTS (TOR 5)

Existing ways for the estimation of roll damping include model testing, numerical simulations and the empirical formula approach. Considering the fact that roll damping is one of the most intriguing and difficult research topics in ship dynamics due to its nonlinear nature and the rather complicated viscous effects of the fluid, the experimental approaches are still so far the most reliable. Generally speaking, there are two main types of tests devoted to the determination of roll damping, i.e., roll decay tests and forced roll tests. The latter can be further categorized into the free running forced roll test where the roll moments are designated while the resulting roll motions are measured, and the (semi-) captive forced roll test where the roll motions are designated while the roll moment to generate the motions are measured.

Among them, the roll decay tests are the most widely adopted due to its relative simplicity. The state-of-the-art focus is to reduce human interventions during the testing, i.e, to conduct the roll decay test in a sophisticated manner in order to obtain high-quality data which can withstand the quantitative validation of CFD. One example was already described in Figure 345 and Figure 346 (Hashimoto et al. 2019). By using this kind of purpose-built device, it is possible to repeat the same roll decay test from a fixed angle/attitude and to reduce the uncertainty due to the scattering of initial conditions in roll decay tests.

Free running forced roll tests are based on exciting the ship to continue rolling through internal roll moment generators (RMGs) or external waves, with the ship free to move in all DoF. The requirements on the model and installation are similar to those of the roll decay test. The key difference lies in the instrumentation, especially when the roll moment generator is used. Several types of RMGs are widely used, e.g., the gyroscopic type, the contra-rotating masses type and the moving mass type. The moving mass type seems to be more popular in recent years and has been intensively studied reported by Oliva-Remola, (2018) and Park et al. (2018), see Figure 366.

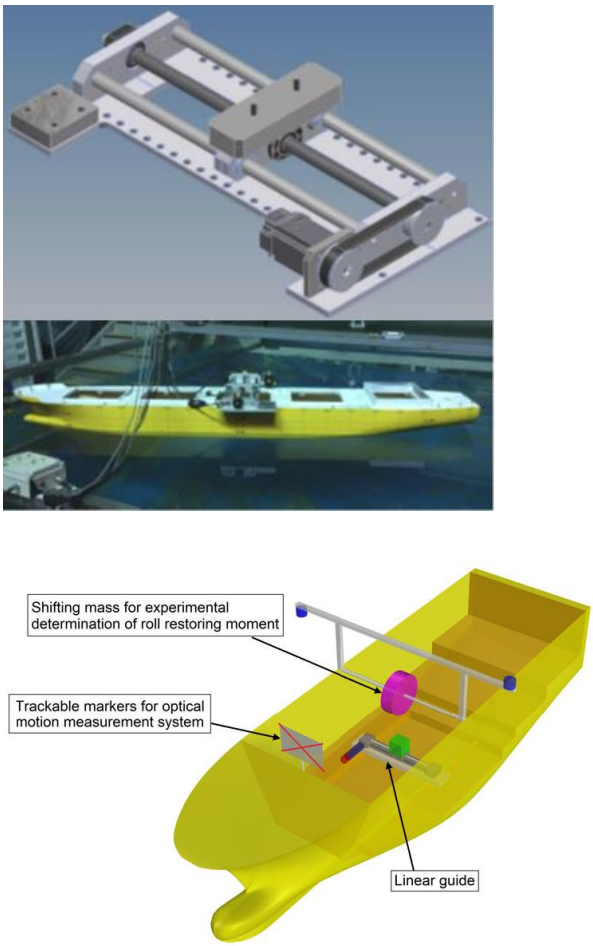

Figure 366: Moving mass type RMGs (Up: Park et al., 2018; Down: Oliva-Remola, 2018)

Captive or semi-captive forced roll tests refer to ships being excited to continuously roll through an externally applied roll moment from an external oscillator between the towing carriage and the model. In such tests, a fixed roll axis is typically being prescribed. Such setup is good for the comparison with numerical simulations, as it can guarantee a pure roll motion, hence reduces the analysis complexity.

Same as the free running forced roll tests, special instrumentation is required, which should be able to generate the designated roll motions about the prescribed axis and measure the roll moment simultaneously. These are the so-called forced roll mechanisms. One example of such instrumentation is shown in Figure 367. The mechanism is developed by the Marine Design and Research Institute of China (MARIC), where the forced roll is achieved by a motor while the roll moment is directly measured through a torque sensor

Figure 367: Forced roll mechanism developed by MARIC

Different methods to determine roll damping coefficients from roll decay tests exist. Most of them use the measured amplitude of the time history of rolling motion, as well as the instantaneous time where the amplitude occurs. Commonly used methods to analyse roll decay tests include the following.

Logarithmic decrement method: this method determines the equivalent linear roll damping coefficient by assuming the linear roll differential equation and determines the nonlinear roll damping coefficients by least-squares fitting. The benefits of this methodology are that it may consider nonlinearities in restoring and damping terms, it is simple and also allows to aggregate data from different decay tests prior to performing the least-square fitting, which is more reliable than analysing each decay tests separately and calculating the mean of the determined nonlinear damping coefficients. Further information on this method may be found in Wassermann (2016) and Oliveira et al. (2019).

Froude energy method: this method equates the energy lost to damping in each half-cycle to the work done by the restoring moment during the same period. Further information may be found in Wassermann (2016) and Oliveira et al (2019).

Roberts energy method: this method is based on energy conservation, where the roll decrement is treated as an energy loss function, which is related to the roll damping. Further information may be found in Roberts (1985) and Wassermann (2016).

Least-squares iterative method: this method constitutes a Parameter Identification Technique and is based on the fitting of the numerical solution of the nonlinear differential equation of roll to the time series of the decay test, performing an iterative fitting based on the least-squares method. Further information may be found in Oliveira (2018). It is possible to use a 1-DoF systems but in some cases it can be more efficient to use (Luthy et al. 2021) a complete 6-DoF simulator. This is particularly useful in the case where the damping estimated must be used by this same simulator for simulations in waves. In this case all questions about coupling with others motions, origin of moment and position of centre of rotation are automatically solved.

On the other hand, commonly used methods to analyse forced roll tests include:

The quasi-linear method or Blume's method: the equivalent linear roll damping coefficient is determined from the ratio of the quasi-static heel angle and the measured dynamic roll amplitude, assuming that, at resonance, the inertial part and the restoring part of the equation of motion (approximately) cancel out, directly relating the amplitude of the forcing term at the peak response frequency with the

damping term. Further information may be found in Oliveira et al. (2019).

Fourier transformation method: this method uses a Fourier analysis to determine linear and non-linear components of the roll moment which are in phase with the roll velocity (Handschel et al. 2014).

A general comparison of the fore-mentioned test methods for roll damping measurement is given in table 1.

Table 12: General comparison of the test methods for roll damping measurement

Item	Free Decay	Free Running Forced Roll	(Semi-) Captive Forced Roll
Steady roll ampl.	Impossible	Steady	Steadiest
Large roll ampl.	Temporarily	Depends on RMG	Easy to achieve
Forward speed effect	Possible	Possible but difficult	Possible and easy
Memory effect	Not fully included	Included	Included
CFD validation	Medium	Hard	Easy (1-DoF Case)
Roll axis	Real/Time-varying	Real/Time-varying	Prescribed/ Fixed
Time & cost	Cheap	Costly	Costly

Besides the experimental approaches, CFD simulations for roll damping estimation are getting more and more mature and have already become an effective way for roll damping estimation. The following combination of calculation parameters are recommended by Gu et al. (2018a) when simulating free roll decay motion: unsteady RANS equations combined with RNG k-ε / SST k-ω two-equation turbulent model to solve flow field, VOF method to capture free surface, sliding interface technique or dynamic overset mesh technique to compute bodies motions, enhanced wall function to treat near-wall boundary layer. Moreover, it is pointed by Hashimoto et al. (2019) that it is necessary to solve 3-DoF of sway-heave-roll motions or more DoFs for the CFD simulation of roll decay motions. As for the forced roll simulations, Kianejad et al. (2018a) proposed a CFD method based on the harmonic excited roll motion (HERM) technique to compute the roll motion and the roll damping moment of a containership model in different conditions. The influence of excitation frequency, forward speed and DoF at beam-sea and oblique-sea realizations are considered in estimating the roll damping coefficients. The results are validated against model tests, where a good agreement is found.

7. UPDATE PROCEDURE 7.5-02-07-04.5 ESTIMATION OF ROLL DAMPING (TOR 6)

Name of the procedure has been changed from “Numerical Estimation of Roll Damping” to “Estimation of Roll Damping” because the scope of the procedure has been extended from purely numerical estimation based on an empirical formula to include also the relevant experimental approaches (including some IMO methodologies) to obtain the roll damping. Section “2.1 Background equations” is added to

give a clearer introduction of the subject, and section "3. Procedure for estimating roll damping from experiments" is added, where sections "3.1 Roll decay tests in calm water", "3.2 Free running forced roll tests", "3.3 (Semi-) Captive forced roll tests" are discussed. A new section of "4.3 Simplified Ikeda's method" is added in the updated procedure. Section "3.3 Decay coefficients" in the original procedure is deleted and rewritten as section "3.1.7 Data reduction and analysis", where available methods are summarized into four categories: (1) Logarithmic decrement method; (2) Froude energy method; (3) Roberts energy method; (4) Least-squares iterative method. The updated new procedure is more comprehensive compared with the original version.

8. UPDATING THE GUIDELINE 7.5-02-07-04.3 FOR PARAMETRIC ROLL (TOR 7)

The Guidelines 7.5-02-07-04.3 (Predicting the Occurrence and Magnitude of Parametric Rolling) was updated towards Recommended Procedure. The updated procedure was structured in three levels, similar to the second generation IMO intact stability criteria. Each level corresponds to different fidelity and complexity of methods described. An extensive example has been added as an Appendix.

The purpose of the procedure is to provide a detailed guidance on assessment occurrence and magnitude of parametric roll using analytical, semi-analytical and numerical methods.

A review of other procedures and guidances produced by IMO and class societies has been added to the introduction along with appropriate references. Brief explanation of the new structure of the procedure has been included as well.

The level 1 section starts from the description of the simplest generic mathematical model of ship rolling that allows parametric resonance. A review of semi-analytical and continuation methods have been added. The semi-analytical methods are based on certain functional representation of the expected solution. The result is usually presented in a form of an algebraic equation that is to be solved numerically. A continuation method is completely numerical, based on the "predictor/corrector" scheme. The continuation methods are known for their efficiency. The main advantage of the semi-analytical and continuation methods is that they can find unstable solutions as well as stable once. While unstable solution cannot be realized in the time-domain or in the real world for any significant amount of time; they are very useful as they reveal the structure of phase space.

The level 2 method is essentially simplified method of time-domain simulation. This is a mostly new section of the Procedure. Three different mathematical models are considered: 1-DoF, 3-DoF and 6-DoF.

The single DoF model uses precomputed $\overline{GZ}$ curve in wave presented as a function of wave frequency and height as well as a position on the wave and roll angle. Roll damping can include quadratic and cubic terms or roll velocity. The solution of the roll equation is carried out numerically. Solution in irregular waves is not considered, as it can be done in a simpler way using the 3-DoF model.

Pre-calculation of the $\overline{GZ}$ curve in wave is not recommended for 3-DoF equations of motions, as the volume of data may be too large. Instead the restoring moment can be computed as a part of inseparable hydrostatic and Froude-Krylov force/moment. Calculation hydrostatic and Froude-Krylov force/moment is carried out by integration of hydrostatic and wave pressures over the instantaneous submerged part of the hull. As a fast alternative (that may be useful for irregular waves) the hydrostatic and Froude-Krylov force/moment can be computed through

the instantaneous submerged volume and coordinates of its centre (Weems et al. 2018). As it was already mentioned, usage of the 3-DoF model with pressure- or volume–based hydrostatic and Froude-Krylov force/moment is equally simple in regular or irregular waves.

Damping, diffraction and radiation are added in the 3-DoF model in a form of coefficients as it would be done with any other system of ordinary differential equations. The 3-DoF-system can be upgraded to the all 6-DoF model using manoeuvring coefficients. Influence of surging on parametric roll may be important.

The level 3 assessment is geared to use advanced hydrodynamic simulation tools. The updates give a specific description of recommended formulations used the simulation tools with known to work well for predication of parametric roll. These include body-nonlinear formulation for Froude-Krylov and hydrostatic forces/moments, body-nonlinear or body-linear formulation for diffraction and radiation, coefficient-based models for viscous-related forces/moment and use of 3- to 6-DoF dynamic solvers.

Combination of the internal calculation of radiation with coefficient-based models for viscous-related terms (roll damping and manoeuvring) may represent a challenge. If the viscous-related coefficients were obtained from a model test or CFD calculation with the free-surface, the wave effect will be included twice. The updates include recommendation how to correct these coefficients to avoid double counting.

The updated procedure covers choice of conditions for simulation in regular and irregular waves. Particular attention is paid to post-processing results of assessment of parametric roll in irregular waves. Caution is raised for long de-correlation time, typical for parametric roll that may affect assessment of SSA as recommended by the procedure 7.5-02-01-08. Capsizing observation are addressed separately.

The appendix includes example of prediction of occurrence and magnitude of parametric roll, using all three levels. C11-class containership, known for being vulnerable to parametric roll (France et al. 2003), is used as a sample ship. The appendix also addresses some practical calculation issues. In particular, the effect of inclusion of weathertight volume into stability-in-waves calculation is discussed. While weather-tight volumes are not included in the static stability calculation, there is a rational reason to consider them for dynamic stability. Time, while these volumes are submerged, is too short for them to be flooded due to dynamic nature of the phenomenon.

The results of calculation in regular waves are presented as a dependence of the magnitude of parametric roll on the circular frequency of wave for zero forward speed, see e.g. Figure 368. A plot like that shows both occurrence and magnitude of parametric roll.

For the level 1, the example includes a demonstration of the effect of cubic vs 5th-order polynomial fit of the calm-water stability curve on the occurrence and magnitude of parametric roll. While there is almost no effect of the polynomial order on the frequency interval of parametric roll occurrence, some effect was observed for the magnitude, see Figure 368.

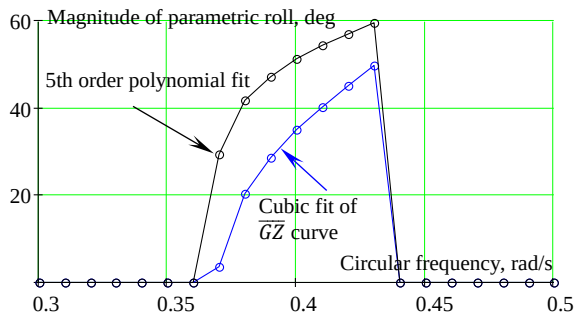

Figure 368: Magnitude of parametric roll as a function of the wave frequency

For the level 2, the example includes a demonstration of the effect of the inclusion of the weather-tight volume, using 1-DoF model. As it is shown in Figure 369, inclusion of the watertight volumes only may lead to conservative results in terms of the magnitude but has a little effect on occurrence.

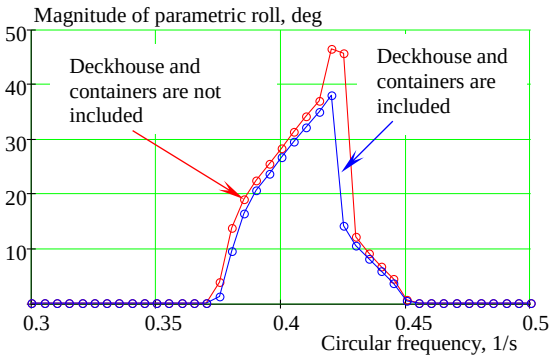

Figure 369: Magnitude of parametric roll by numerical integration of 1-DoF roll equation

The level 2 example also includes a demonstration of the influence of heave and pitch on magnitude and occurrence of parametric roll, shown in Figure 370. The 1-DoF solution seems to be non-conservative in the considered case.

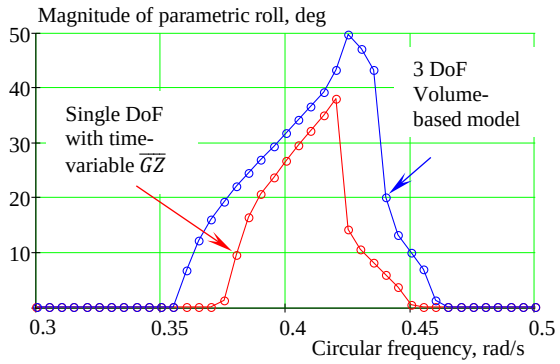

Figure 370: Magnitude of parametric roll. Weather-tight volume is included

For the level 3, the example includes results in regular and irregular waves. Similar to the level 2 cases, the regular wave calculations are presented as a magnitude vs. frequency, see Figure 371. Comparing all four magnitude curves presented in Figure 368 through Figure 370, one can see that the methods on all three levels agree on the frequency interval of occurrence of parametric roll. In general, prediction of magnitude seems to be more conservative from the level 1 methods and the least conservative from the level 3 methods. The consistency between the levels on magnitude seems to be reasonable in the considered example.

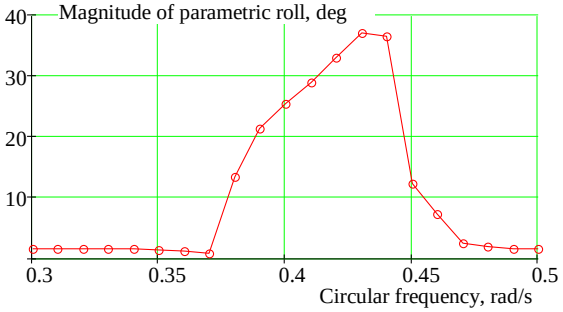

Figure 371: Magnitude of parametric roll computed with LAMP-2 (Shin et al. 2004)

To assess magnitude of parametric roll in irregular waves, the procedure 7.5-02-01-08 has been applied to estimate the SSA. Following the recommendation of Reed (2019b) 20 half-hour long records were generated with LAMP-2 (Shin et al. 2004). The SSA was estimated by direct counting as an average of 1/3 largest peaks, following recommendation of in the subsection 3.2.2 of the Procedure 7.5-02-01-08. The data acquisition process is illustrated in Figure 372: mean-crossing peaks are found (shown as circles), sorted and the 1/3rd largest values collected (shown as squares).

To compute confidence interval of estimated SSA, autocorrelation of 1/3rd largest peaks needs to be estimated. The estimate of autocorrelation function of 1/3rd largest peaks is computed as directed by the section 3.2.2 of the

Procedure 7.5-02-01-08 and is shown in

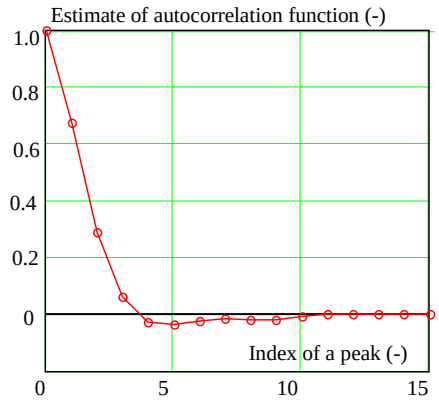

Figure 373. Note, that the estimate of autocorrelation function of the largest 1/3rd peaks is computed for a number or an index of a peak, rather than a time lag. The estimation of SSA yielded 22.5°±0.5° for the significant wave height 3.5 m and mean zero-crossing period of 14 seconds.

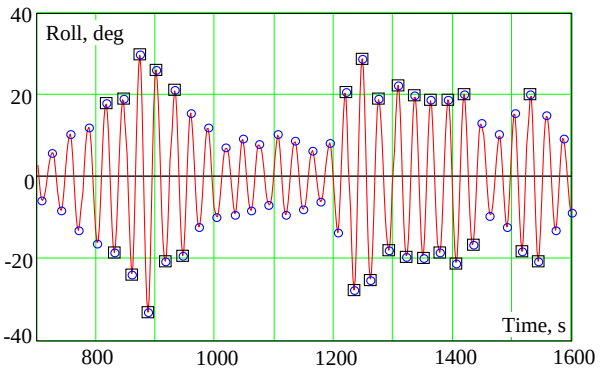

Figure 372: Data acquisition for SSD: mean-crossing peaks (circles), 1/3rd largest peaks (squares)

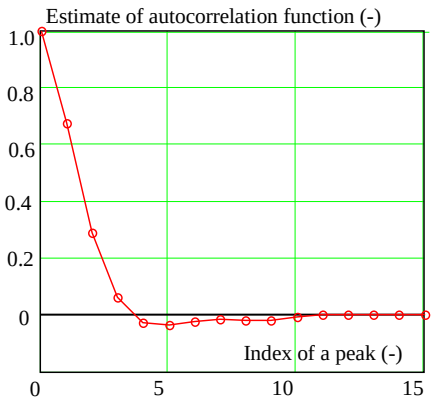

Figure 373 Estimate for the auto-correlation function for 1/3rd largest peaks of roll motion

The appendix contains an example of treating capsizing events as described in the updated procedure. The weather-tight volumes (containers and a deckhouse) were not included and significant wave height was increased up to 9 m, while mean zero-crossing period remained 14 s. SSA estimate was 40.1°, the upper boundary of confidence interval was 40.9° and the lower boundary of confidence interval 39.4°.

9. UPDATE PROCEDURE 7.5-02-07-04.4 NUMERICAL SIMULATION OF CAPSIZE BEHAVIOUR OF DAMAGED SHIPS IN IRREGULAR BEAM SEAS (TOR 8)

The update of the Guideline 7.5-02-07-04.4 on "Numerical Simulation of Capsize Behaviour of Damaged Ships in Irregular Beam Seas" included a number of corrections and addition of references to published original contributions. More specifically, the modelling methods for the free surface in tanks and flooding open spaces were added. A reference to technological innovations in the area of active buoyancy and stability recovery systems which may affect the permeability of a space over time is now included. Such systems may provide significant improvements to the survivability of a ship in

the future. Furthermore, the concepts of the capsize band, the capsize rate, the critical wave height and the time to capsize (TTC) were included as they are important attributes of the capsizal behaviour.

Ongoing research work (Boulougouris et.al. 2020), a coupling of the TTC with the time available to evacuate (TTE) and fusing real-time sensor information, will allow the development of real-time risk assessment during uncontrolled flooding incidents. Recent work and findings on the use of CFD methods on the prediction of the behaviour of the damaged ship in waves have shown the increasing interest for such applications. However, the challenges of high computational power and time are still present and the need for expertise and attention to the quality of the mesh is still evident. This suggests that these methods are not ready yet for general use in the prediction and analysis of stability issues. Nevertheless, they provide valuable input for hybrid or blended methods and their performance continues to improve, presenting future opportunities.

10. DEVELOP/SUGGEST A METHOD FOR ESTIMATING TIME TO CAPSIZING AND / OR SINKING (TOR 9)

The time interval between the start of the flooding of the vessel and its final capsizal determines the "time to capsize" (TTC). This is a significant output from the time domain simulations. Several researchers have proposed concepts such as "survival time" (Jasionowski, 1999) or "time to sink" (van Veer et al., 2002). Jasionowski et al. (2002) proposed the consideration of individual waves or groups as an integral element of the capsizing process. The capsize event is identified from the presence of the incidence of the critical groups. TTC is then calculated by the statistical analysis of the results.

Van Veer et al. (2002) referred to the time required to reach specific SOLAS static criteria such as a maximum roll of 30°, mean roll angle of 20° within 3 min and mean roll angle of 12°. Spanos et al. (2007) distinguish between TTC and the "time to ship loss" that corresponds to the loss of adequate floatability or stability. Valanto (2006) proposed alternatively the term "time to flood", representing the time from the initiation of the water ingress and the steady-state ensuing progressive flooding.

Atzampos (2019) underlines that TTC is fundamentally linked to the critical wave height (HScrit) concept since it forms an upper boundary of the area where it is likely to observe capsizes. That conceptually forms an asymptote of the TTC distribution (see Figure **364**). Generally, TTC will decrease with the increase of the encountered wave height. Therefore, the TTC is inversely proportional to the difference between HScrit and the actual sea state.

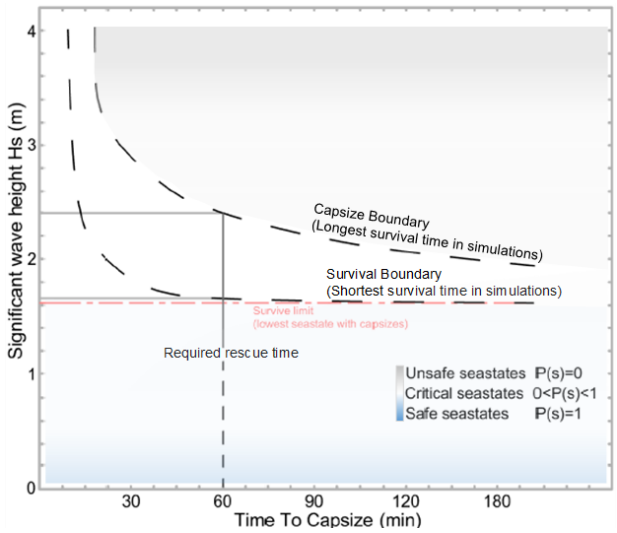

Figure 374: Capsize and survival boundary concept with indication of the safe and unsafe regions with respect to change of the Time to Capsize as a function of the significant wave height. (Atzampos, 2019)

Monte Carlo sampled numerical simulations are used to determine the relationship between the TTC and the survivability. Spanos and

Papanikolaou (2012) compared the TTC with the IMO stipulated time for the orderly abandonment. Atzampos (2019) used a direct approach based on time-domain simulations to estimate the expected probability of survival and the TTC for a given group of damages characterised by random damage locations, damage extent and sea-states. The direct approach derives from the non-zonal approach presented by Bulian et al. (2018) and Zaraphonitis et al. (2013). Instead of using the probabilistic survivability index (s-index), a numerical simulation is performed.

11. CONTINUE THE IDENTIFICATION OF BENCHMARK DATA FOR VALIDATION OF STABILITY IN WAVES PREDICTIONS (TOR 10)

The list started by the previous ITTC in China was updated. A new column was added in order to mention the ITTC Recommended Procedures in relation to each benchmark data. The list is available on request.

There is an ITTC guideline about benchmarking, 4.0-01, but the objectives were not to describe the data collection. There is no available description of a good benchmark in terms of minimum data needed or results given. In particular, it should be stated how numerical benchmark, without comparisons to experiments, could be considered or not.

12. RECOMMENDED PROCEDURES FOR INCLINING TESTS (TOR 11)

A new Term of Reference was added to the committee. Develop a procedure for undertaking inclining tests at full scale include estimates of the measurement uncertainty. Originally it was given to the Seakeeping committee (TOR 10) but finally it was assigned to Stability in Waves Committee to liaise with the Seakeeping Committee.

The need of an update procedure was made clear by the fact that the post processing was always the one used more than two centuries ago an could be improved by the modern numerical capabilities. Dunworth (2013, 2014, 2015), Wilezynski (1995), Smith et al. (2016) and Karolius and Vassalos (2018) present a new methodology to improve the accuracy of the estimation of the position of the centre of gravity which is recommended in the proposed procedure.

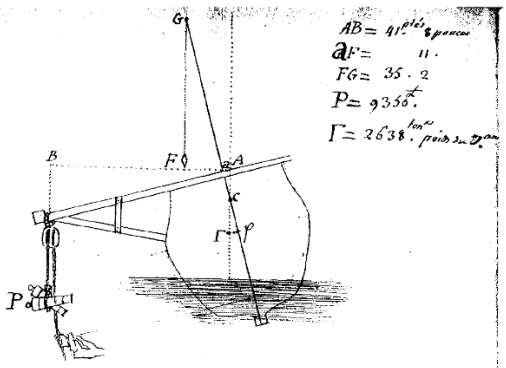

Figure 375: First referenced inclining experiment in 1748, according Nowacki and Ferreiro (2003)

This procedure established by the committee is the first step because it doesn't take into account the whole process of the determination of the vertical position of the centre of gravity of a real ship for all loads cases. In particular, the procedures is concentrated to the evaluation of the characteristics of the ship during the tests and then doesn't mentioned the inventory, usually performed before "official" inclining test by a classification society or the extrapolation to others loads case as full loads.

In the procedure, a chapter is dedicated to uncertainties. It is noted that the calculation of the final uncertainty on the *KG* can be carried out with simple methods, including a linear regression of the processing graph, but is a function of the building (presence and number of non-empty capacity), means of inclination

used (moving mass or ballasting) and of the instrumentation used (pendulum or inclinometer). A table provided a non-exhaustive list indicating the classic uncertainties usually taken into account for different parameters and means of measurement.

13. IMO LIAISON

The ITTC Stability in Waves Committee representatives attended SDC 6 and SDC 7.

At SDC 6, 4 to 8 February 2019, the ITTC Stability in Waves Committee representatives participated in the meeting of the Expert Group on Intact Stability. Much of the effort of the 2008 IS Code Expert Group focused on the finalizing of the Second Generation Intact Stability Criteria. One of the central issues for discussion was the level of maturity of the vulnerability criteria. Based on extensive sample calculations, it was concluded that vulnerability criteria for parametric roll and for surf-riding/broaching were ready for test application. Multiple inconsistency cases were observed for vulnerability criteria for the rest of failure modes: pure loss of stability, excessive acceleration and dead ship condition. Also it was not clear how the vulnerability criteria for dead ship condition that will have a recommendatory status in the near future will be used together with mandatory weather criterion, Paragraph 2.3 of Part A of the 2008 IS Code. The Expert Group recommended and subcommittee has agreed to go ahead and finalize the vulnerability criteria for all 5 modes of failure, but with understanding that the current level of maturity will be properly reflected in the final documents as well as the relationship between mandatory and recommendatory criteria.

The Expert group has considered in details and finalized drafts for three documents making the mainstay of the IMO Second Generation Intact Stability Criteria:

- Draft interim guidelines on the specification of direct stability assessment procedures, in annex 1 of SDC 6/WP.6
- Draft interim guidelines for the preparation of operational limitations and operational guidance in annex 2 of SDC 6/WP.6
- Draft interim guidelines on vulnerability criteria for the second generation intact stability criteria in annex 2 of SDC 6/WP.6

The expert group agreed that these documents contain all necessary technical information and require editorial work by the Intersessional Correspondence Group. The final editing (SDC 7/WP.1) was done by the Drafting Group at SDC 7 in 2020. Upon completion, and subcommittee has forwarded the draft to Maritime Safety Committee (MSC) for their approval and publication in a form of MSC Circulars for test application by the Maritime Industry

At SDC 7, 3 to 7 February 2020, the ITTC Stability in Waves Committee representatives participated in the meeting of the Drafting Group on Intact Stability. Much of the effort of the Drafting group focused on the finalizing of Interim Guideline on the Second Generation Intact Stability Criteria.

The central issues for discussion were finalizations of draft MSC circular and the Interim Guidelines on the Second Generation Intact Stability Criteria.

The Drafting group has considered in details and finalized two documents:

- Draft MSC circular, in annex of SDC 7/WP.6
- Interim guidelines on the Second Generation Intact Stability Criteria,

in annex of SDC 7/WP.6

The Maritime Safety Committee on its 102nd session (4 to 11-th November 2020) has approved the Interim Guidelines on the Second Generation Intact Stability Criteria. The Interim Guidelines was published as an Annex to MSC.1/Circ.1627.

The Drafting group recommended that the Intersessional Correspondence Group develop the draft Explanatory notes on the Second Generation Intact Stability Criteria coordinated by Dr. Umeda, Japan. The subcommittee agreed with this recommendation and created the Correspondence group. The final editing is expected to be done at SDC 8 in 2021. However, due to the COVID-19, SDC 8 has been postponed until 2022.

This IMO development is well aligned with a number of ITTC aims, making ITTC participation in this development very relevant. In particular, we start to try Interim Guideline on the Second Generation Intact Stability Criteria. The experience gained in implementing the Interim guidelines is very important for ITTC, so it will continue to stimulate improvement of methods for numerical modelling of extreme ship motions with model experiments. In pursue of this aim ITTC has a chance to have a positive impact on this international development that may improve ITTC's stance.

14. CONCLUSIONS AND RECOMMEN-DATIONS

14.1 Technical conclusions

(1) A survey of literature for new experimental techniques has been conducted. Several recent advancements have been identified. Among them is the new method of measurement of roll damping, where the motion is excited by moving weights. Updated publications describe the development, focused on decreasing cost of conducting an experimental assessment of stability in waves, by using regular wave or a fixed set of wave groups. Another aspect of experimental stability assessment in waves, reflected in the literature is using modelling of wind for stability assessment in dead ship condition.

Following the tendencies of the previous reporting period, CFD application continues to be of interest. High computation cost still prevents use CFD directly for capsizing simulation, however, use of CFD as a "numerical tank", to characterize vortexes and some other forces, seems to become more frequent. Reliable assessment of the uncertainty of CFD-included solution may be the next technical challenge.

(2) The central event of the reporting period is a formal completion of the development of the second generation of IMO stability criteria on the 7th session of the IMO Subcommittee on Ship Design and Construction (SDC 7). The second generation of IMO intact stability criteria covers 5 failure modes: dead ship condition, excessive accelerations, pure loss of stability, parametric roll and surf-riding / broaching-to. All these modes are directly relevant to stability in waves; excessive accelerations are also relevant to seakeeping while broaching is also relevant to manoeuvring in waves. To avoid unnecessary costs, the assessment can be done in three different levels of complexity. Increase of complexity (and cost) of application is meant to be related to decrease of conservatism (if a ship found not to be vulnerable to a particular mode of failure, using lower complexity criteria, there is no need for further assessment). The second generation intact stability criteria also include operational measures, as not all the stability-in-waves problems can be addressed during the design. The description of the second generation criteria

and operational measures are included in interim guidance for trial application, issued by the Circ. 1627 of the IMO Maritime Safety Committee.

(3) The most technically complex part of the second generation intact stability criteria is the direct stability assessment. The core of the direct stability assessment is a state-of-the-art numerical simulation of extreme ship motions in severe weather conditions. As direct stability assessment may require numerical simulation of ship motion in irregular waves in time domain, the resulted time histories should be of sufficient length to apply statistical processing. The speed of calculation becomes an important factor, thus emphasizing the use of potential flow and hybrid solvers. Correct statistical modelling of encounter waves is a key technology for correct statistical estimates. In particular, the self-repeating effect is a concern.

(4) Direct stability assessment requires estimation of the statistical frequency of stability failures. If a sufficient number of stability failures can be observed during numerical simulation, direct counting procedure can be applied. The key technologies are an assurance of independent of counted events and assessment of statistical uncertainty of the estimate.

(5) If a sufficient number of stability failures cannot be observed during numerical simulation, methods of statistical extrapolation are meant to be used. Four methods are mentioned in MSC.1/Circ.1627: extrapolation over wave heights, envelope peak over threshold (EPOT), split-time/ motion perturbation (MPM) and critical wave method. The committee has developed a new draft ITTC procedure that contains EPOT and split-time MPM methods with the view of further extension of the procedure, once more information becomes available. Another key technology is a validation of extrapolation methods. There are many other technical challenges associated with the deployment of the direct stability assessment as a regular service. Towing tanks are in a good position to develop and offer this service as an extension to the currently available model tests and numerical simulations. Establishing recommended procedures to support these new services should be made a priority of the work of the Stability in Waves Committee for the next ITTC period.

(6) The committee has updated the ITTC recommended procedure for roll damping 7.5-02-07-04.5, covering both numerical and experimental methods. Simplified Ikeda method was added to the procedure. The committee has also made substantial updates to the ITTC Recommended Guideline 7.5-02-07-04.3 “Predicting the Occurrence and Magnitude of Parametric Rolling” towards a Recommended Procedure. The procedure was given a tiered structure similar to IMO second generation intact stability criteria. The level 1 includes formulae for approximate assessment, while level 2 contains a description of numerical techniques that can be used without specialized software. Finally, level 3 is focused on the assessment of parametric roll with numerical simulations. Example of calculations for all three levels was included as an appendix.

(7) In the Guideline 7.5-02-07-04.4 “Numerical Simulation of Capsize Behaviour of Damaged Ships in Irregular Beam Seas” a number of corrections to has been implemented and additional references to published original contributions were added. The modelling methods for the free surface in tanks and flooding open spaces have been added. A reference to the use of active buoyancy and stability recovery systems which may affect the permeability of a space over time is now included. Such systems may provide significant improvements to the survivability of a ship in the future. Furthermore, the concepts of the capsize band, the capsize rate, the critical wave height and the time to capsize (TTC) were included as they are important attributes of the capsizal behaviour. Recent work and findings

on the use of CFD methods on the prediction of the behaviour of the damaged ship in waves have shown the increasing interest for such applications. However, the challenges of high computational power and time are still present and the need for expertise and attention to the quality of the mesh is still evident. This suggests that these methods are not ready yet for general use in the prediction and analysis of stability issues. Nevertheless, they provide valuable input for hybrid or blended methods and their performance continues to improve, presenting future opportunities

(8) The committee has developed a new draft ITTC recommended procedure on Inclining Tests. The procedure covers environmental and ship conditions, survey, displacement measurements, the actual tests, post-processing and uncertainty assessment.

(9) The committee confirmed the need of a list of good benchmark and a storage place for available data, at least for ITTC benchmarks. It is suggested that this effort should be done commonly by all committees for more beneficial result seed of task common to all groups, need of a unified format and a web site to depose data.

(10) The committee has,

- Reviewed ITTC Recommended Procedure 7.5-02-01-08, "Single Significant Amplitude and Confidence Intervals for Stochastic" and found that there is insufficient data to propose any changes at this moment;
- Reviewed ITTC Recommended Procedure 7.5-02-05-07, "Dynamic Instability Tests" from high speed marine vehicles domain and found no changes necessary at this moment;
- Reviewed ITTC Recommended Procedure 7.5-02-07-04.1, "Model Tests on Intact Stability" and found no changes necessary;
- Reviewed ITTC Recommended Procedure 7.5-02-07-04.2, Model Tests on Damage Stability in Waves and found no changes necessary;
- Reviewed ITTC Recommended Guideline 7.5-02-07-04.3, "Predicting the Occurrence and Magnitude of Parametric Rolling" towards a Recommended Procedure and submitted updated document;
- Reviewed ITTC Recommended Procedure 7.5-02-07-04.4, "Numerical Simulation of Capsize Behaviour of Damaged Ships in Irregular Beam Seas" and submitted updated document;
- Reviewed ITTC Recommended Procedure 7.5-02-07-04.5, "Numerical Estimation of Roll Damping" and submitted updated document;
- Reviewed ITTC Recommended Procedure 7.5-03-02-03, "Practical Guidelines for ship CFD application" and proposed changes;
- Submitted a new ITTC recommended procedure and two proposals for new ITTC recommended procedures in support of direct stability assessment within Second generation IMO intact stability criteria;
    - Developed and submitted a new ITTC Procedure "Extrapolation for direct stability assessments in waves, including split-time and POT/EPOT methods";
    - Submitted a proposal for a new ITTC Procedure "Estimation of Frequency of Random Events by Direct Counting";
    - Developed and submitted a proposal for a new ITTC Procedure "Statistical Validation of Extrapolation Methods for Time Domain Numerical Simulation of Ship Motions";
- Submitted a proposal for a new ITTC Procedure "Guidance on Avoiding self-repeating effect in time-domain numerical simulation of ship motions";
- Submitted a proposal for a new ITTC

Procedure "Computational procedure for instantaneous $\overline{GZ}$ curve during time-domain numerical simulation in irregular wave";
- Submitted a new ITTC Recommended Procedure "Inclining Tests";
- Developed draft of IMO INF paper on the review of SGISC submitted by ITTC to the 8th session of SDC.

14.2 Recommendations to the Conference

- Adopt the updated ITTC Procedure 7.5-02-07-04.5 "Estimation of Roll Damping";
- Adopt the updated ITTC Procedure 7.5-02-07-04.3 "Predicting the Occurrence and Magnitude of Parametric Rolling";
- Adopt the updated ITTC Recommended Procedure 7.5-02-07-04.4, "Numerical Simulation of Capsize Behaviour of Damaged Ships in Irregular Beam Seas";
- Adopt the updated ITTC Recommended Procedure 7.5-03-02-03, "Practical Guidelines for ship CFD application";
- Adopt the new ITTC Recommended Procedure, "Inclining Tests".
- Adopt the ITTC Recommended procedure "Extrapolation for direct assessment stability in waves";
- Develop new ITTC Recommended Procedure "Statistical Validation of Extrapolation Methods for Time Domain Numerical Simulation of Ship Motions and Loads";
- Develop new ITTC Recommended Procedure, "Guidance on Avoiding Self-Repetition Effect During Numerical Simulation of Ship Motions";
- Develop new ITTC Recommended Procedure " Estimation of Frequency of Random Events";
- Develop new ITTC Recommended Procedure "Predicting the Instantaneous $\overline{GZ}$ Curve during Time-Domain Numerical Simulation";
- Update ITTC Procedure 7.5-02-01-08 "Single Significant Amplitude and Confidence Intervals for Stochastic Processes" when new information becomes available;
- Submit IMO INF paper on the review of SGISC to 8th session of SDC.

15. REFERENCES AND NOMENCLATURE

15.1 References

Alford, L.K. and Troesch, A.W., (2009). Generating extreme ship responses using non-uniform phase distributions. *Ocean Engineering*, Vol. 36 No 9-10, pp. 641-649.

Alman, P.R., Minnick, P.V. and Thomas W.L., (1999). Dynamic Capsize Vulnerability: Reducing the Hidden Operational Risk. *SNAME Transactions*, Vol. 107, pp. 245-280.

Anastopoulos, P.A. and K.J. Spyrou, (2016). Ship Dynamic Stability Assessment Based on Realistic Wave Group Excitations. *Ocean Engineering*, Vol. 120, pp. 256-263.

Anastopoulos, P.A. and Spyrou, K.J., (2017). Evaluation of the critical wave groups method for calculating the probability of extreme ship responses in beam seas. *Proc. of the 16th Intl. Ship Stability Workshop*. Belgrade, Serbia, pp. 131-138.

Anastopoulos, P.A. and Spyrou, K.J., (2019a). Can the generalized Pareto Distribution be useful towards developing ship stability criteria. *Proc. of the 17th International Ship Stability Workshop*, Helsinki, Finland.

Anastopoulos, P.A. and Spyrou, K.J., (2019b). Evaluation of the critical wave groups method in calculating the probability of ship capsize in beam seas. *Ocean Engineering*, Volume 187, 106213.

Araki, M., Sadat-Hosseini, H., Sanada Y., Umeda, N., and Stern, F., (2019). Improved Maneuvering-Based Mathematical Model for Free-Running Ship Motions in Following Waves using High-Fidelity CFD Results and System-Identification Technique. Chapter 6 of *Contemporary Ideas on Ship Stability. Risk of Capsizing*, Belenky, V., Spyrou, K., Walree F. van, Neves, M.A.S., and N. Umeda, eds., Springer, ISBN 978-3-030-00514-6, 2019, pp. 91-115.

Aram, S. and Silva, K.M., (2019). Computational Fluid Dynamics Prediction of Hydrodynamic Derivatives for Maneuvering Models of a Fully-Appended *Ship. Proc. of the 17th Intl. Ship Stability Workshop*, Helsinki, Finland pp. 57-66.

Asgari, P., Fernandes A.C., Low Y.M., (2020). Most often instantaneous rotation centre (MOIRC) for roll damping assessment in the free decay test of a FPSO. *Applied Ocean Research*, 95 (2020) 102014.

Atzampos, G., (2019). Direct Survivability Assessment of Passenger Ships A Holistic Approach to Damage Survivability Assessment of Large Passenger Ships. Ph. D. Thesis, University of Strathclyde.

Begovic, E., Mancini, S., Day, A.H., Incecik, A., (2017). Applicability of CFD Methods for Roll Damping Determination of Intact and Damaged Ship: Results and Scientific Applications Derived from the Italian PON ReCaS Project. Chapter in book: *High Performance Scientific Computing Using Distributed Infrastructures*, World Scientific, ISBN 978-981-4759-71-70-0.

Begovic, E., Bertorello, C., Boccadamo G., Rinauro, B., (2018). Application of surf-riding and broaching criteria for the systematic series D models. *Ocean Engineering*, 170, 246–265.

Belenky, V., and Sevastianov, N., (2003). Stability and Safety of Ships. Vol. II: *Risk of Capsizing*. Elsevier, ISBN: 0 08 044354 0 (a 2nd edition was published by SNAME in 2007, ISBN 0-939773-61-9).

Belenky, V. and Weems, K.M., (2008). Probabilistic Qualities of Stability Change in Waves. *Proc. 10th Int. Ship Stability Workshop*, Daejon, Korea, pp. 95-108.

Belenky, V.L., (2011). On Self-Repeating Effect in Reconstruction of Irregular Waves. Chapter 33 of *Contemporary Ideas on Ship Stability*, Neves, M.A.S., Belenky, V., de Kat, J.O., Spyrou, K. and N. Umeda, eds., Springer, ISBN 978-94-007-1481-6, pp. 589-598.

Belenky, V., Weems, K., Spyrou, K., Pipiras, V. and Sapsis, T., (2017). Modelling Broaching-to and Capsizing with Extreme Value Theory. *Proc. of the 16th Intl. Ship Stability Workshop*, Belgrade, Serbia, pp. 125-130.

Belenky, V., Weems, K., Pipiras, V., Glotzer, D., and Sapsis, T., (2018a). Tail Structure of Roll and Metric of Capsizing in Irregular Waves. *Proc. of the 32nd Symp. on Naval Hydrodynamics*, Hamburg, Germany.

Belenky, V., Weems, K., Pipiras, V. and Glotzer, D., (2018b). Extreme-Value Properties of the Split-Time Metric. *Proc. 13th Intl. Conf. on Stability of Ships and Ocean Vehicles STAB 2018*, Kobe, Japan.

Belenky, V., Spyrou, K., Walree F. van, Neves, M. A. S., and Umeda, N., (2019a), *Contemporary Ideas on Ship Stability. Risk of Capsizing*, eds., Springer, ISBN 978-3-030-00514-6.

Belenky, V., Glotzer, D., Pipiras, V. and Sapsis, T., (2019b). Distribution tail structure and

extreme value analysis of constrained piecewise linear oscillators. *Probabilistic Engineering Mechanics,* Vol. 57, pp 1-13.

Boulougouris, E., Vassalos, D., Stefanidis, F., Karaseitanidis, G., Karagiannidis, L., Amditis, A., Ventikos, N., Kanakidis, D., Petrantonakis, D. and Liston, P., (2020). SafePASS-Transforming Marine Accident Response. *Transport Research Arena 2020*, Helsinki, Finland (Conference cancelled).

Brown, A.J. and Deybach, F., (1998). Towards a Rational Intact Stability Criteria for Naval Ships. *Naval Engineers Journal*, 110 (1), pp. 65-77.

Brown, B. and Pipiras, V., (2019). On extending multifidelity uncertainty quantification methods from non-rare to rare problems. *Proc. of the 17th International Ship Stability Workshop*, Helsinki, Finland, pp.151-157.

Bu, S.X., Gu, M., (2019a). Study on damaged ship motion coupled with damaged flow based on the unified viscous and potential model. *Proc. 17th ISSW*, Helsinki, Finland, 2019: 616-626.

Bu, S.X, Gu, M, Lu, J, Abdel-Maksoud, M. (2019b). Effects of radiation and diffraction forces on the prediction of parametric roll. *Ocean Engineering*, 175:262-272.

Bu, S.X., Gu, M, Abdel-Maksoud, M. (2019c). Study on roll restoring arm variation using a three-dimensional hybrid panel method. *Journal of Ship Research*, 63(2): 94-107.

Bu, S.B. and Gu, M. (2020). Unified Viscous and Potential Method for the Study of Parametric Roll with Sloshing. *Proc. of the 13th Intl. Ocean and Polar Engineering Conf.*, Shanghai, China, pp.3882-3889.

Bulian, G., Cardinale, M., Francescutto, A. and Zaraphonitis, G., (2018). Complementing SOLAS framework with a probabilistic description for the damage extent below water. *Proceedings of the 13th International Conference on the Stability of Ships and Ocean Vehicles*, Kobe, Japan.

Campbell, B., Belenky, V. and Pipiras, V., (2016). Application of the Envelope Peaks over Threshold (EPOT) Method for Probabilistic Assessment of Dynamic Stability. *Ocean Engineering*, Vol. 120, pp. 298-304.

Chodankar, D., (2016). Inflatable Airbag Systems to Improve Ship's Attained Subdivision Index. SNAME *Maritime Convention 2016*, Bellevue, Washington, USA.

Coles, S., (2001). *An Introduction to Statistical Modeling of Extreme Values*. Springer, London, ISBN 978-1-4471-3675-0.

Chai, W., Dostal, L., Naess, A. and Leira, J.B., (2018). A Comparative Study of the Stochastic Averaging Method and the Path Integration Method for Nonlinear Ship Roll Motion in Random Beam Seas. *Journal of Marine Science and Technology*, Vol.23, No.4, pp.854-865.

Choi, J.H., Jensen, J.J., Kristensen, H.O.H., Nielsen, U.D. and Erichsen, H., (2017). Intact stability analysis of dead ship conditions using FORM. *Journal of Ship Research*, 61(3), 167-176.

Coles S., (2001). *An Introduction to Statistical Modeling of Extreme Values*. Springer, London, ISBN 978-1-4471-3675-0.

Cousins, W. and Sapsis, T., (2016). Reduced order precursors of rare events in unidirectional nonlinear water waves. *J. Fluid Mech.*, 790:368–88

Dankowski, H, Russel, P., Krüger, S., (2014). New Insights into the Flooding Sequence of the Costa Concordia Accident. *Proc. OMAE2014*, San Francisco, California, USA.

Dahle, E. A. and Nedrelid, T. (1982). "Stability criteria for vessels operating in a seaway", Proc. of STAB'82: 2nd International Conference on Stability of Ships and Ocean Vehicles, Tokyo.

De Haan, L. and Ferreira, A., (2007). *Extreme Value Theory: An Introduction*. Springer Science & Business Media.

Dostal, L., Kreuzer, E. and Namachchivaya, N.S., (2012). Non-standard stochastic averaging of large-amplitude ship rolling in random seas. *Proc. R Soc A Math Phys Eng Sci*., Vol. 468 pp. 4146–4173.

Dostal, L. and Kreuzer, E., (2014). Assessment of extreme rolling of ships in random seas. *ASME 2014 33rd international conference on ocean, offshore and arctic engineering*, American Society of Mechanical Engineers, p V007T12A-VT12A.

Dunworth, R. J., (2013) "Up Against the Wall" in *International Maritime Conference, Pacific*, Sydney Australia.

Dunworth R. J., (2014) "Back Against the Wall", Transactions RINA, Vol 156, Part B2, *International Journal of Small Craft Technology*, pp 99-106.

Dunworth R. J., (2015) "Beyond the Wall", *Proceedings of the 12th International Conference on the Stability of Ships and Ocean Vehicles*, 14-19 June, Glasgow, UK

Farazmand, M, and Sapsis, T., (2017). Reduced-order prediction of rogue waves in two-dimensional deep-water waves. *J. Comput. Phys.*, 340:418–34.

France, W.M, Levadou, M., Treakle, T.W. Paulling, J.R., Michel, K. and Moore, C., (2003). An Investigation of Head-Sea Parametric Roll-ing and its Influence on Container Lashing Systems. *Marine Tech.*, Vol. 40, N° 1, pp. 1–19.

Francescutto, A., (2015). Intact Stability Criteria of Ships – Past, Present and Future. *STAB 2015*.

Gao, Z., Gao, Q., Vassalos, D., (2011). Numerical study of damaged ship motion in waves". *Proc. ISSW 2011*, pp. 257–261.

Gao Z., Gao Q., Vassalos, D., (2013). Numerical study of damaged ship flooding in beam seas. *Ocean Engineering*, 72: 77-87.

Glotzer, D., Pipiras, V., Belenky, V., Campbell, B., Smith, T.C., (2017). Confidence Interval for Exceedance Probabilities with Application to Extreme Ship Motions. *REVSTAT Statistical J.*, Vol. 15, No 4, pp.537-563.

Gong, X., Zang, Z. Maki, K. and Pan, Y., (2020). Full Resolution of Extreme Ship Response Statistics" *Proc. of 33rd of Symp. Naval Hydrodynamics*, Osaka, Japan

Grim, O., (1961). Beitrag zu dem Problem der Sicherheit des Schiffes im Seegang. *Schiff und Hafen*, 6:490–491.

Gu, M., Chu, J.L., Han, Y., Lu, J., (2017). Study on Vulnerability Criteria of Surf-riding / Broaching with a Model Experiment. *Proceedings of the 16th International Ship Stability Workshop*.

Gu, M., Bu, S. X., Wu, C. S., (2018a). Numerical Study on the Scale Effect of Ship RollDamping. *Proc. 13th Int'l. Conf. on the Stability of Ships and Ocean Vehicles*, Kobe, Japan, pp. 323–330.

Gu, Y., Day, A., Boulougouris, E., and Dai, S., (2018b). Experimental investigation on stability of intact and damaged combatant ship in a beam sea. *Ships and Offshore Structures*, 13.

Gu, M., Bu, S.X., Zeng, K., (2019). Analyse on several crucial factors for CFD simulation of roll damping". *Proc. 17th Int'l. Ship Stability Workshop*, Helsinki, Finland, pp. 297–302.

Gu, M., Bu, S.X. and Lu, J., (2020). Study of parametric roll in oblique waves using a three-dimensional hybrid panel method. *Journal of Hydrodynamics*, volume 32, 126–138.

Handschel, S., Abdel-Maksoud, M., (2014). Improvement of the harmonic excited roll motion technique for estimating roll damping. *Ship Technology Research*, 61(3), pp. 116-130.

Hashimoto, H., Yoneda, S., Omura, T., Umeda, N., Matsuda, A., Stern, F., Tahara, Y., (2018). CFD prediction of wave-induced forces on ships running in irregular stern quartering seas. International *Conference on the Stability of Ships and Ocean Vehicles 2018*, Kobe, Japan.

Hashimoto, H., Omura, T., Matsuda, A., Yoneda S., Stern, F., Tahara, Y., (2019). Several Remarks on EFD and CFD for Ship Roll Decay. *Ocean Engineering*. 186, 106082.

Htet T.Z., Umeda N., Matsuda A., Terada D., (2018). Effect of above-waterline hull shape on broaching-induced roll in irregular stern-quartering waves. *Journal of Marine Science and Technology*, 24(1), 166-173.

Hu, L., Zhang, K., Li, X., Chang, R., (2019). Capsizing Probability of Dead Ship Stability in Beam Wind and Wave for Damaged Ship. *China Ocean Engineering*. 33(2), 245–251.

Irkal, M.A. R., Nallayarasu, S., Bhattacharyya, S.K., (2019). Numerical prediction of roll damping of ships with and without bilge keel. *Ocean Engineering*, 179, 226–245.

Jalonen, R., Ruponen, P., Jasionowski, A., Maurier, P., Kajosaari, M., Papanikolaou, A., (2012). FLOODSTAND: overview of achievements. *Proc. STAB2012*, Athens, 23-28 September.

Jalonen, R., Ruponen, P., Weryk, M., Naar, H., Vaher, S., (2017). A study on leakage and collapse of non-watertight ship doors under floodwater pressure. *Marine Structures*, 51, 188-201.

Jasionowski, A., Dodworth, K. & Vassalos, D., (1999). Proposal of passenger survival-based criteria for ro-ro vessels". *International Shipbuilding Progress*, Vol. 46.

Jasionowski, A., Vassalos, D. and Guarin, L., (2002). Time-Based survival criteria for passenger ro-ro vessels". *Proceedings of the 6th International Ship Stability Workshop*, New York. Webb.

Jensen, J.J., Choi, J.H., Nielsen, U.D., (2017). Statistical prediction of parametric roll using FORM. *Ocean Engineering*, 144, 235–242.

Jong P. de, Renilson, M., Walree F. van, (2015). The effect of ship speed, heading angle and wave steepness on the likelihood of broaching-to in astern quartering seas. *Proceedings of the 12th International Conference on the Stability of Ships and Ocean Vehicles*, Glasgow, UK.

Karolius, K.B. and Vassalos, D., (2018). Weight and buoyancy is the foundation in design: Get it right. *Proceedings of 13th*

International Marine Design Conference, Espoo, Finland.

Kianejad, S., Lee, J., Liu, Y., Enshaei, H., (2018a). Numerical Assessment of Roll Motion Characteristics and Damping Coefficient of a Ship. *Journal of Marine Science and Engineering*,. 6, 101.

Kianejad, S., Enshaei, H., Duffy, J., Ansarifard, N., Ranmuthugala, D., (2018b). Investigation of Scale effects on Roll Damping through Numerical Simulations. *32nd Symposium on Naval Hydrodynamics*, Hamburg, Germany, 5-10 August 2018.

Kianejad, S., Enshaei, H., Duffy, J., Ansarifard, N., (2020). Ship roll restoring moment calculation in beam sea condition. *Journal of Marine Science and Technology*, published online.

Kim, D.H., and Troesch, A.W., (2013). Statistical Estimation of Extreme Roll Responses in Short Crested Irregular Head Seas. *Tr. SNAME*, Vol. 121.

Kim, D.H., Belenky, V., Campbell, B.L. and Troesch, A.W., (2014). Statistical Estimation of Extreme Roll in Head Seas. *Proc. of 33rd Intl. Conf. on Ocean, Offshore and Arctic Engineering OMAE 2014*, San-Francisco, USA.

Kim, D.H. and Troesch, A.W., (2019). Stochastic Wave Inputs for Extreme Roll in Near Head Seas. Chapter 23 of *Contemporary Ideas on Ship Stability. Risk of Capsizing*, Belenky, V., Spyrou, K., Walree F. van, Neves, M.A.S., and N. Umeda, eds., Springer, ISBN 978-3-030-00514-6, pp. 393-405.

Kimura, A., (1980). Statistical properties of random wave groups. *Proc. 17th Int. Conf. on Coastal Eng.*, Sydney, pp. 2955-2973. New York: Am. Soc. Civ. Engrs.

Kobylinski, L.K. and Kastner, S., (2003). *Stability and Safety of Ships, Volume 1: Regulation and Operation*, Elsevier Ocean Engineering Book Series, Vol. 9. Elsevier, Amsterdam.

Kontolefas, I., and Spyrou, K.J., (2016). Coherent structures in phase space, governing the nonlinear surge motions of ships in steep waves. *Ocean engineering*, Vol. 120, pp. 339-345.

Kontolefas, I. and Spyrou, K. J., (2018). Predicting the Probability of Ship High-Runs from Phase Space Data. *32nd Symposium on Naval Hydrodynamics*, Hamburg, Germany.

Kougioumtzoglou, I.A. and Spanos, P.D., (2014). Stochastic response analysis of the softening Duffing oscillator and ship capsizing probability determination via a numerical path integral approach. *Probabilistic Engineering Mechanics*, Vol. 35 pp. 67–74.

Kubo, H., Umeda, N., Yamane, K. and Matsuda, A., (2012), Pure Loss of Stability in Astern Seas -Is It Really Pure?. *Proceedings of the 6th Asia-Pacific Workshop on Marine Hydrodynamics*, pp. 307-312.

Leadbetter, M.R., Lindgren, G. and Rootzén, H., (1983). *Extremes and Related Properties of Random Sequences and Processes*, in: Springer Series in Statistics, Springer-Verlag, New York-Berlin, ISBN 978-1-4612-5449-2.

Leadbetter, M.R., Rychlik, I. and Stambaugh, K., (2019). Estimating Dynamic Stability Event Probabilities from Simulation and Wave Modeling Methods" Chapter 22 of *Contemporary Ideas on Ship Stability. Risk of Capsizing*, Belenky, V., Spyrou,

K., Walree F. van, Neves, M.A.S., and N. Umeda, eds., Springer, ISBN 978-3-030-00514-6, pp. 381-391.

Levine, M. D., Belenky, V., Weems, K. and Pipiras, V., (2017). Statistical Uncertainty Techniques for Analysis of Simulation and Model Test Data" *Proc. 30th American Towing Tank Conference*, West Bethesda, MD, USA.

Li, H., Zhu, B., Zhou, X., (2018). Variation in Ship Parametric Roll Amplitude with Forward Speed and Heading Angle. *International Conference on the Stability of Ships and Ocean Vehicles 2018*, Kobe, Japan.

Lindroth, D., Tompuri, M., Ruponen, P., Haruyama M., Always A., (2019). Advanced Damage Stability Analyses for Design of Cargo Ships. *PRADS'2019*, Yokohama, Japan.

Liu, L., Liu, Y., Xu, W., Li, Y., Tang, Y., (2018). A Semi-Analytical Method for the PDFs of a Ship Rolling in Random Oblique Waves. *China Ocean Engineering*, 32(1), 74-84.

Longuet-Higgins, M.S., (1962). The statistical analysis of a random, moving surface. *Phil. Trans. Royal Soc.* London, Series A, Mathematical and Physical Sciences, Vol. 249, No. 966, pp. 321–387.

Lu, J., Gu, M. and Umeda N., (2016). A study on the effect of parametric roll on added resistance in regular head seas. *Ocean Engineering*, Vol. 122, pp.288-292.

Lu, J., Gu, M. and Umeda N., (2017). Experimental and Numerical Study on Several Crucial Elements for Predicting Parametric Roll in Regular Head Seas. *Journal of Marine Science and Technology*, Vol. 22, pp. 25-37.

Lu, J., Gu, M. and Boulougouris, E., (2019). Model Experiments and Direct Stability Assessments on Pure Loss of Stability of the ONR Tumblehome in Following Seas. *Ocean Engineering*, Vol. 194, 106640.

Lu, J., Gu, M. and Boulougouris, E., (2020), Model Experiments and Direct Stability Assessments on Pure Loss of Stability of the ONR Tumblehome in Stern Quartering Waves. *Ocean Engineering*, Vol. 216, 108035.

Lu, Y. and Park, J.Y., (2019). Estimation of longrun variance of continuous time stochastic process using discrete sample, *Journal of Econometrics*, 210(2), pp. 236-267.

Luquet, R., Vonier, P., Prior, A., Leguen, J.-F., (2015). Aerodynamics Loads on a Heeled Ship, *International Conference on the Stability of Ships and Ocean Vehicles 2015*, Glasgow, UK.

Luthy, V., Grinnaert, F., Billard, J.-Y., Delhaye, T., Claudel, R., Leguen, J.-F., (2021). An iterative method to estimate damping coefficients from roll decay time series, submitted to STAB&S2021.

Ma, S., Ge, W.P., Ertekin, R.C., He, Q., Duan, W.Y., (2018). Experimental and numerical investigation of ship parametric rolling in regular head waves. *China Ocean Engineering*, Vol. 32, No. 4, 431-442.

Macé, R., Billard, J.-Y., Lannel, G. and Leguen, J.-F., (2019). Approximation of capsize probability using a Roll Exceedance (RE) probability with a threshold chosen in roll phase plane. *Ocean Engineering*, 187 106098.

Maki, A., (2017). Estimation method of the capsizing probability in irregular beam seas

using non-Gaussian probability density function". *Journal of Marine Science and Technology*, Vol. 22, No. 2, pp. 351–360.

Maki, A., Umeda, N., Matsuda, A. and Yoshizumi, H., (2018). Non-Gaussian PDF of ship roll motion in irregular beam sea and wind conditions-Comparison between theory and experiment, *STAB 2018*. Kobe, Japan.

Maki, A., Umeda, N., Matsuda, A. and Yoshizumi, H., (2019a). Non-Gaussian PDF of ship roll motion in irregular beam sea and wind conditions-Comparison between theory and experiment. *Ocean Engineering*, Vol. 188, 106278.

Maki, A., Maruyama, Y., Umeda, N. Miino, Y., Katayama T., Sakai M. and Ueta T., (2019b). A Perspective on Theoretical Estimation of Stochastic Nonlinear Rolling. *Proc. of the 17th International Ship Stability Workshop*, Helsinki, Finland.

McTaggart, K.A., (2000a). Ship Capsize Risk in a Seaway Using Fitted Distributions to Roll Maxima. *J. Offshore Mechanics and Arctic Engineering*, Vol. 122, No. 2, pp. 141-146.

McTaggart, K.A., (2000b). Ongoing Work Examining Capsize Risk of Intact Frigates Using Time Domain Simulation" in: *Contemporary Ideas of Ship Stability*, Vassalos, D., Hamamoto, M., Papanikolaou, A. and D. Moulyneux, eds., Elsevier Science, pp. 587–595, ISBN 9780080436524.

McTaggart, K.A. and de Kat, J.O., (2000c). Capsize Risk of Intact Frigates in Irregular Seas. *Trans. SNAME*, Vol. 108, pp. 147-177.

Meister S., Taylordean S., Singer D. (2021) Predicting Extreme Parametric Roll in Container Ships. In: Okada T., Suzuki K., Kawamura Y. (eds) *Practical Design of Ships and Other Floating Structures. PRADS 2019.* Lecture Notes in Civil Engineering, vol 63. Springer, Singapore.

Melnikov, V.K., (1963). On the stability of a center for time-periodic perturbations. *Trans. Moscow Math. Soc.*, 12:3–52 (in Russian).

Mizumoto, K., Araki, M., Stern, F., Hashimoto H., Umeda N., (2018). Improvement of Broaching Prediction Method by System Identification Using CFD. *STAB'2018*, Kobe, Japan.

Mohamad, M.A. and Sapsis, T., (2018). Sequential sampling strategy for extreme event statistics in nonlinear dynamical systems. *Proc. of the Natl. Acad. of Sciences of United States of America PNAS*, 115:11138–43.

Nowacki, H. and Ferreiro, L.D., (2003). Historical Roots of the Theory of Hydrostatic Stability of Ships. *Proceedings of 8th International Conference on the Stability of Ships and Ocean Vehicles*, Madrid, Spain.

Oliva-Remola, A., (2018). On Ship Roll Damping: Analysis and Contributions on Experimental Techniques. Ph.D. Thesis, Escuela Tecnica Superior de Ingenieros Navales (ETSIN) of Universidad Politecnica de Madrid, Spain.

Oliveira, M.C, Kassar, B.B.M, Coelho, L.C., Monteiro, F.V., Santis,R.T, Castillo, C.A.R., Neves, M.S.A., Polo, J.S.F, and Esperança, P.T.T. (2019) "Empirical and experimental roll damping estimates for an oil tanker in the context of the 2nd generation intact stability criteria", *Ocean Engineering*, Volume 189, 1 106291.

Park B., Jung D., Park, I., Cho, S., Sung, H., (2018). Study on the Estimation Methods of

Roll Damping Coefficients Using Designed Excitation Device for Harmonic Roll Motion. *Proceedings of the 28th International Ocean and Polar Engineering Conference (ISOPE18)*, Sapporo, Japan, pp. 330–337.

Pickands, J., (1975). Statistical Inference Using Extreme Order Statistics. *The Annals of Statistics*, Vol. 3, No. 1, pp. 119-131.

Pierrottet, E., (1935). Standards of Stability for Ships. *Transactions Institution of Naval Architects*, Vol. 77, pp. 208-222.

Pipiras, V., Glotzer, D., Belenky, V., Levine, M. and Weems, K., (2018). On Confidence Intervals of Mean and Variance Estimates of Ship Motions. *Proc. 13th Intl. Conf. on Stability of Ships and Ocean Vehicles STAB 2018*, Kobe, Japan.

Pipiras, V., (2020). Pitfalls of data-driven peaks-over-threshold analysis: Perspectives from extreme ship motions. *Probabilistic Engineering Mechanics*, Vol. 60, 103053.

Rahola, Y., (1939). The Judging of the Stability of Ships and the Determination of the Minimum Amount of Stability," Ph. D. Thesis, HelsinkiRathore, U. (2019) Quantification of Extreme Event Statistics, MSc. Thesis, MIT, 86 p.

Reed, A., (2019a). Interpretation of results of numerical simulation" *Proceedings of the 17th International Ship Stability Workshop*, Helsinki, Finland, 2019.

Reed, A.M., (2019b). 26th ITTC Parametric Roll Benchmark Study. Chapter 37 of *Contemporary Ideas on Ship Stability. Risk of Cap-sizing*, Belenky V., Spyrou K., Walree F. van, Neves M.A.S., and Umeda N., eds., Springer, ISBN 978-3-030-00514-6, pp. 619-636.

Renilson, M.R. and Tuite A.J., (1998). Broaching-to – A proposed definition and analysis method. *Proceedings of the 25th American Towing Tank Conference*, Iowa, USA.

Roberts, J., (1985). Estimation of Nonlinear Ship Roll Damping from Free-Decay Data. *Ship Research*, 29(2), pp. 127-138.

Ruponen, P., (2017). On the effects of non-watertight doors on progressive flooding in a damaged passenger ship. *Ocean Engineering*, Vol. 130:115-125.

Ruth E., Olufsen O. and Rognebakke O., (2019). CFD in damage stability. *Proc. 17th Int. Workshop on Ship Stability*, Helsinki, Finland.

Sakai, M., Maki, A., Murakami T. & Umeda N., (2017). Analytical Solution of Critical Speed for Surf-Riding in the light of Melnikov Analysis. *Proc. Conf. of the Japan Society of Naval Architects and Ocean Engineers*, Vol. 24 pp. 311–314.

Sakai, M., Umeda, N., Yano, T., Maki, A., Yamashita Y., Matsuda A. and Terada D., (2018). Averaging Methods For Estimating Parametric Roll in Longitudinal and Oblique Waves. *J. of Mar. Science and Tech.*, Vol. 23, pp. 413–424.

Sakai, M., Umeda., N. and Maki, A. (2019) "Encounter frequency effect on the simplified design criteria against parametric roll" *Ocean Engineering* 182, pp.21–27

Sarchin, T.H. and Goldberg, L.L. (1962) "Stability and Buoyancy Criteria for US Naval Surface Ships", *Transactions SNAME*

Sclavounos, P.D., Larson D.F.H., Ma E.Y., (2019). Ship Stability in a Seastate by the State-Space Fokker - Planck Method.

Journal of Ship Research, 63(1), 30-40.

Shigunov, V., (2019). Direct counting method and its validation. *Proc. 17-th Int. Ship Stability Workshop*, Helsinki, Finland, pp. 119-128.

Shin, Y.S, Belenky, V.L., Paulling, J.R., Weems, K.M. and Lin, W.M., (2004).Criteria for Parametric Roll of Large Container-ships in Longitudinal Seas. *SNAME Trans.,* Vol. 112, pp. 14-47.

Silva, K. M. and Aram, S., (2018). Generation of Hydrodynamic Derivatives for ONR Topside Series Using Computational Fluid Dynamics, *Proc. of the 13th Intl. Conf. on the Stability of Ships and Ocean Vehicles STAB2018*, Kobe, Japan, pp. 71-81.

Spanos, D. and Papanikolaou, A., (2007). On The Time to Capsize. *Proc. 9th Int. Workshop on Ship Stability*, Hamburg, Germany, 2007

Spanos, D. and Papanikolaou, A., (2012). Time-dependent survivability against flooding of passenger ships in collision damages". Proceedings of the 11th Int. *Conference on the Stability of Ships and Ocean Vehicles STAB2012*, Athens, Greece.

Smith, A.C., Dunworth R., J., Hel-More, P., J., (2016). "Towards the Implementation of a Generalised Inclining Method of the Determination of the Centre of Gravity", *The Australian Naval Architect*, Vol. 20 No 1.

Smith, T.C., (2019). Validation Approach for Statistical Extrapolation. Chapter 34 of *Contemporary Ideas on Ship Stability*, Belenky V., Neves M., Spyrou K., Umeda N., Walree F. van, eds. Springer, ISBN 978-3-030-00514-6, pp. 573-589.

Spyrou, K., Belenky, V., Themelis, N., and Weems, K. M., (2019). Definitions of Celerity for Investigating Surf-riding in An Irregular Seaway, Chapter 21 of *Contemporary Ideas on Ship Stability. Risk of Capsizing*, Belenky V., Spyrou K., Walree F. van, Neves M. A. S. and Umeda N., eds., Springer, ISBN 978-3-030-00514-6, pp. 359-377.

St. Denis, M. and Pierson, W.J., (1953). On the motion of ships in confused seas. *Trans. SNAME*, Vol. 61, pp. 280–354.

Stevens, K.W., (2018). Adaptive Sequential Sampling for Extreme Event Statistics in Ship Design. MSc. Thesis, MIT, 105 p.

Telste, J.G., Belknap, W. F., (2008). Potential Flow Forces and Moments from Selected Ship Flow Codes in a Set of Numerical Experiments. Naval Surface Warfare Center, report n° NSWCCD-50-TR–2008/040.

Themelis, N. and Spyrou, K.J., (2007) Probabilistic Assessment of Ship Stability, *Transactions SNAME*, Vol. 115, pp. 181-206.

Themelis, N. and Spyrou, K.J., (2008). Probabilistic assessment of ship stability based on the concept of critical wave groups. *Proceedings of the 10th Intl Ship Stability Workshop*, Daejeon, Korea, pp. 115–125.

Tsuchiya, T. (1975). An Approach for Treating the Stability of Fishing Boats. *Proceedings of International Conference on Stability of Ships and Ocean Vehicles*, University of Strathclyde, 5.3:1-9.

Tsukada, Y., Suzuki, R., and Ueno, M. (2017). Wind Loads Simulator for Free-running Model Ship Test. *Proceedings of the ASME 36th International Conference on Ocean, Offshore and Arctic Engineering (OMAE2017)*, OMAE2017-61158.

Ueno, M., Suzuki, R. and Tsukada, Y., (2019).

Full-scale ship propeller torque in wind and waves estimated by free-running model test. *Ocean Engineering*, 184, pp.332-343.

Umeda, N., Osugi, M., Ikenaga, Y. and Matsuda, A., (2019). Pure loss of stability in stern quartering waves: revisited with numerical simulations reproducing accidents.*17th International Ship Stability Workshop*, Helsinki, Finland.

Valanto, P., (2006). Time-Dependent Survival Probability of a Damaged Passenger Ship II – Evacuation in Seaway and Capsizing. HSVA Report No. 1661/2006. (IMO SLF 49 Inf. 5), London.

Vassalos, D., Boulougouris, E., Paterson, D., (2016). An alternative system for damage stability enhancement. *Proceedings of the 15th International Ship Stability Workshop*, Stockholm, Sweden.

Veer R. van, de Kat, J.O. and Cojeen P., (2002). Large passenger ship safety: time to sink". *Proceedings of the 6th International ship stability workshop*, Webb Institute, NYC.

Wang, T., Ma N., Gu, X., Feng, P. (2018). Effect of propeller thrust reduction on ship surf-riding/broaching prediction. *STAB 2018*, Kobe, Japan.

Wanji, C., (2019). Review of Probabilistic Methods for Dynamic Stability of Ships in Rough Seas. *Proc. of the 17th Intl, Ship Stability Workshop*, Helsinki, Finland.

Wassermann, S., Feder, D., Abdel-Maksoud, M., (2016a). Estimation of ship roll damping – A comparison of the decay and the harmonic excited roll motion technique for a post Panamax containership. *Ocean Engineering*, 120, pp. 371-382.

Watanabe, Y. et al., (1956). A Proposed Standard of Stability for Passenger Ships (Part III: Ocean-going and Coasting Ships). Journal of Society of Naval Architects of Japan, Vol. 99: 29-46.

Wawrzynski, W. (2018). Bistability and accompanying phenomena in the 1-DoF mathematical model of rolling. *Ocean Engineering*, 2018, 147: 565-579.

Weems, K., and Wundrow, D., (2013). Hybrid Models for Fast Time-Domain Simulation of Stability Failures in Irregular Waves with Volume-Based Calculations for Froude-Krylov and Hydrostatic Force. *Proc. 13th Intl. Ship Stability Workshop*, Brest, France.

Weems, K., Belenky, V. and Spyrou, K.J., (2018). Numerical Simulations for Validating Models of Extreme Ship Motions in Irregular Waves. *Proc. of the 32nd Symp. on Naval Hydrodynamics*, Hamburg, Germany.

Weems, K. M., Belenky, V., Levine, M.D., Pipiras, V., (2019a). Statistical Uncertainty of Measured and Simulated Ship Motions. *Proc. 8th Intl. Conf. Computational Stochastic Mechanics (CSM 8)*, Deodatis G. and Spanos P. D., eds., Research Publishing, Singapore, ISBN: 978-981-11-2723-6.

Weems, K., Belenky, V., Campbell, B., Pipiras, V. and Sapsis, T., (2019b). Envelope Peaks Over Threshold (EPOT) Application and Verification. *Proc. of the 17th Intl. Ship Stability Workshop*, Helsinki, Finland.

Weems, K.M. Belenky, V., Spyrou, K. Aram, K. and Silva, K., (2020). Towards Numerical Estimation of Probability of Capsizing Caused by Broaching-to. *Proc. 33rd Symposium on Naval Hydrodynamics (33 SNH)*, Osaka, Japan.

Wilezynski, V., Diehl, W. J., (1995). An Alternative Approach to Determine a Vessel's Center of Gravity: The Center of Buoyancy Method. *Ocean Engineering*.

Xu, W. and Maki, K.J., (2018). A Method for the Prediction of Extreme Roll Suitable for Nonlinear Time-Domain Realization. *Proc. 13th Intl. Conf. on Stability of Ships and Ocean Vehicles STAB 2018,* Kobe, Japan pp.554-564.

Xu, W. and Maki, K.J., (2019). Time domain realization of extreme responses of a bilinear oscillator. *Proceedings of the 17th International Ship Stability Workshop*, Helsinki, Finland.

Xu, W., Filip G. and Maki, K.J., (2020). A method for the prediction of extreme ship responses using design-event theory and computational fluid dynamics. *J. of Ship Research,* Vol. 64 Vol. 1, pp 48-60.

Yasukawa, H. and Yoshimura Y., (2015) Introduction of MMG standard method for ship manoeuvring prédictions *J Mar Sci Technol* 20:37–52 DOI 10.1007/s00773-014-0293-y

Yu, L., Taguchi K., Kenta, A., Ma, N., Hirakawa, Y., (2018). Model Experiments on the Early Detection and Rudder Stabilization of KCS Parametric Roll in Head Waves. *Journal of Marine Science and Technology*, Vol. 23(1), pp. 141–163.

Yu, L., Ma, N., Wang, S., (2019a). Parametric Roll Prediction of the KCS Containership in Head Waves with Emphasis on the Roll Damping and Nonlinear Restoring Moment. *Ocean Engineering*, Vol.188.

Yu, L., Ma, N., Wang, S., Wang, T., (2019b). Influence of GM on Surf-riding and Broaching of the Fishing Vessel. *PRADS'2019*, Yokohama, Japan.

Zaraphonitis, G., Bulian, G., Lindroth, D., Luhmann, H., Cardinale, M., Routi, A.-L., Bertin, R. and Harper, G., (2013), Evaluation of risk form ranking damages due to grounding. EMSA/OP/10/2013 report 2015-0168. DNV-GL.

Zhou, Y., (2019). Further validation study of hybrid prediction method of parametric roll. *Ocean Engineering*, 186(2019) 106103.

Zhu, L., Zhou Q., Chen, M., Chen, X., (2018), Grounding experiments of a ship model in water tank. *Proceedings of the 37th International Conference on Ocean, Offshore and Arctic Engineering OMAE'2018*, Madrid, Spain.

Zilakos, I. and Toulios, M., (2018). On Modeling and Simulation of Innovative Ship Rescue System. *Journal of Offshore Mechanics and Arctic Engineering*, 140(6).

IMO Res. A.167 (ES.IV) Recommendation on Intact Stability and Cargo Ships under 100 meters in Length. London, November 1968.

IMO Res. A.749 (18) Code on Intact Stability for all Types of Ships Covered by IMO Instruments, London, November 1993.

IMO International Code on Intact Stability, 2008, IMO, London, 2009.IMO MSC.1/Circ.1200 Interim Guidelines For Alternative Assessment Of The Weather Criterion; 24/05/2006.

IMO MSC.1/Circ.1227, Explanatory notes to the interim guidelines for alternative assessment of the weather criterion, 2007.

IMO MSC.1/Circ.1281, Explanatory notes to the international code on intact stability, 2008.

IMO MSC.1/Circ.1455, Guidelines for the

approval of Alternatives and Equivalents as provided for in various IMO Instruments, 2013.

IMO MSC.1/Circ.1627 Interim Guidelines on the Second Generation Intact Stability Criteria. London, 2020.

IMO SDC 1/5/4 Proposal of working version of explanatory notes on the vulnerability of ships to the broaching stability failure mode. Submitted by Japan, London, 2013.

IMO SDC 1/INF.6 Vulnerability assessment for dead ship stability failure mode. Submitted by Italy and Japan London, November, 2013.

IMO SDC1/INF.8 Development of Second Generation Intact Stability Criteria. Information collected by the intersessional correspondence group. Submitted by Japan London, 2013.

IMO SDC 2/INF.10 Development of Second Generation Intact Stability Criteria. Information collected by the intersessional correspondence group. Submitted by Japan London, 2014.

IMO SDC 2/WP.4 Development of the Second generation Intact Stability Criteria. Report of the Working Group (part 1). London, 2015.

IMO SDC 3/INF.10 Finalization of Second Generation Intact Stability Criteria. Information collected by the intersessional correspondence group. Submitted by Japan, London, 2015.

IMO SDC 4/WP.4 Finalization of the Second generation Intact Stability Criteria. Report of the Working Group (part 1). London, 2017

IMO SDC 6/WP.6 Finalization of the Second generation Intact Stability Criteria. Report of the Experts' Group on Intact Stability. London, 2019.

IMO SDC 7/WP.6 Finalization of the Second generation Intact Stability Criteria. Report of the Drafting Group on Intact Stability. London, 2020.

IMO SLF 50/4/4 Framework for the Development of New Generation Criteria for Intact Stability, submitted by Japan, the Netherlands and the United States, London, 2007

IMO SLF 53/3/2 Incorporation of excessive stability in the list of stability failure modes as a separate item. Submitted by Germany, London, 2010.

IMO SLF 54/3/1 Development of Second Generation Intact Stability Criteria. Report of the Working Group at SLF 53 (part 2), Submitted by the Chairman of the Working Group, London, 2011.

IMO SLF 55/WP.3 Development of the Second generation Intact Stability Criteria. Report of the Working Group (part 1). London, 2013.

15.2 Nomenclature

BR	Broaching-to
CFD	Computational Fluid Dynamics
CRNAV	Cooperativ Research NAVies
CTO	Centrum Techniki Okrętowei - Maritime Advance Research Centre
Circ.	IMO Circular
DoF	Degree of Freedom
EA	Excessive Acceleration
EPOT	Envelope Peaks over Threshold
EU	European Union
FORM	First Order Reliability Method
FTA	Fault Tree Analysis
FORM	First Order Reliability Method
GEV	Generalized Extreme Value
GPD	Generalized Pareto Distribution

HERM	Harmonic Exciting Roll Motion
IMO	Int'l. Maritime Organisation
2008 IS Code	Code on Intact Stability 2008
ISSW	Int'l Ship Stability Workshop
ITTC	Int'l Towing Tank Conference
MPM	split-time/ Motion Perturbation Method
MSC	Maritime Safety Committee of IMO
NSC	Naval Ship Code, published by NATO as ANEP-77
ONR	US Office of Naval Research
OMAE	Int'l Conference on Ocean
PL	Pure Loss of stability
POT	Peak-Over-Threshold method
PR	Parametric Roll
RANS	Reynolds Average Navier Stokes
RPS	Revolution per Second
RNG	Renormalisation Group (related to CFD)
SDC	Sub-Committee on Ship Design and Construction of IMO
SGISC	Second Generation of Intact Stability Criteria of IMO
SOLAS	International Convention for the Safety of Life at Sea
SSA	Single Significant Amplitude
SST	Share Stress Transport (related to CFD)
TOR	Terms of Reference
TTC	Time To Capsize
TTE	Time available To Evacuate
VCG	Vertical Centre of Gravity
VOF	Volume of Fluid method

Appendix 1
Committees members of the 29th ITTC

Executive Committee
ITTC Association Chairman: **Fabio di Felice**, CNR
Northern Europe representative: **Kourosh Koushan**, SINTEF Ocean
Central Europe representative: **Janou Hennig**, HSVA
Southern Europe representative: **Fabio di Felice**, CNR
Pacific Islands representative: **Shotaro Uto**, NMRI
East Asia representative: **Suak Ho Van**, KRISO, until 2018, **Yonghwan Kim**, SNU, from 2019 onwards
Americas representative: **Antonio Fernandes**, LabOceano.
Non-voting ex-officio members of the Executive Committee were:
Didier Fréchou, DGA Hydrodynamics, as Chairman of the 29th Conference
Gerhard Strasser, Vienna Model Basin, as Advisory Council Chairman,
Zhenping Weng, CSSRC, as past Chairman,
Aage Damsgaard, FORCE Technology, as ITTC Secretary.

Advisory Council Committee
Gerhard Strasser (Chairman), Schiffbautechnische Versuchsanstalt in Wien
Andy Peters, QinetiQ
Antonio Fernandes, LOC/COPPE/UFRJ
Bas Buchner, MARIN
Bettar Ould el Moctar, Development Centre for Ship Technology and Transport Systems
Bob Beck, University of Michigan
Booki Kim, Korea Research Institute of Ships and Ocean Engineering (KRISO)
Christian Masilge, Schiffbau Versuchsanstalt Potsdam GmbH
Claus Daniel Simonsen, FORCE Technology
Daisuke Kitazawa, University of Tokyo
Daisuke Matsumoto, Mitsubishi Heavy Industries, Ltd.
David Murrin, NRC-CNRC
Decheng Wan, Shanghai Jiao Tong University (SJTU)
Didier Fréchou, DGA Hydrodynamcs
Fabio di Felice,CNR-INM
Guoxiang Dong, Shanghai Ship and Shipping Research Institute (SSSRI)
Hideo Orihara, Japan Ministry of Defence
Hyun Joe Kim, Samsung Heavy Industries
Hyun-ho Lee, Hyundai Heavy Industries
Janou Hennig, Hamburgische Schiffbau-Versuchsanstalt GmbH (HSVA)
Kourosh Koushan, SINTEF Ocean (formerly MARINTEK)
Lars Gustafsson, SSPA Sweden AB
Leszek Wilczynski, Maritime Advanced Research Centre (CTO S.A.)

Marta Pedisic Buca, Brodarski Institute, Ship Hydrodynamics and Physical Modelling
Martin Donnelly, Naval Surface Warfare Center, Carderock Division
Moon Chan Kim, Pusan National University
Pengfei Liu, Newcastle University
Pierre Ferrant, Ecole Centrale - Nantes
Rumen Kishev, Bulgarian Ship Hydrodynamics Centre
Seppo Kivimaa, VTT
Sheming Fan, Marine Design and Research Institute of China (MARIC)
Shotaro Uto, National Maritime Research Institute (Japan)
Takashi Mikami, Akishima Laboratories (Mitsui Zosen) Inc.
Takuya Mori, Japan Marine United Corporation
Viacheslav Magarovskii, Krylov State Research Centre
Yonghwan Kim, Seoul National University
Zhenping Weng, China Ship Scientific Research Centre (CSSRC)

Resistance and Propulsion Committee
Richard Pattenden , Qinetiq (Chair)
João L. D. Dantas, IPT
Bryson Metcalf, NSWCCD
Wentao Wang, CSSRC
Yasuhiko Inukai, JMUC
Tokihiro Katsui, Kobe U.
Seok Cheon Go, HHI
Haeseong Ahn, KRISO
Patrick Queutey, ECN
Devrim Bulent Danisman, ITU
Yigit Demirel, Strathclyde U
Aleksey Yakovlev, Krylov (until Nov 2019)
Nikolaj Lemb Larsen, FORCE
Pavel A. Poltavets, Krylov (from Nov 2019)

Manoeuvring Committee
Guillaume Delefortrie, FHR (Chair)
Eduardo Tannuri, USP
Takashi Kishimoto, Akishima
Sang Hyun Kim, Inha U.
Xide Cheng,WUT
Salvatore Mauro, CNR-INSEAN (until dec 2018)
Zhiming Yuan, Strathclyde U
Janne F. Otzen, FORCE
Zhi Quan Leong, AMC (from jan 2019)

Seakeeping Committee
Pepijn de Jong, MARIN (Chair)
Yin Lu (Julie) Young, U. Michigan
Munehiko Minoura, Osaka U.
Toru Katayama, Osaka Pref. U.
Bo-Woo Nam, KRISO
Benjamin Bouscasse, ECN
Ole Andreas Hermundstad, SINTEF Ocean
Frederik Gerhardt, SSPA

Ocean Engineering Committee
Claudio Rodríguez, LabOceano (Chair)
Yasunori Nihei, Osaka Pref. U.
Longfei Xiao, SJTU
Rae Hyoung Yuck, SHI
Ayhan Mentes, ITU
Qing Xiao, Strathclyde U
Halvor Lie, SINTEF Ocean
Viacheslav Magarovskii, Krylov

Stability in Waves Committee
Vadim Belenky (NSWCCD) (Chair)
Akihiko Matsuda, NRIFE
Jiang Lu, CSSRC
Peiyuan Feng, MARIC
Seokkyu Cho, KRISO
Jean-Francois Leguen, DGA
Adriana Oliva Remola, ETSIN (until May 2019)
Evangelos Boulougouris, Strathclyde U

SC on Ships in Operation at Sea
Jinbao Wang, MARIC (Chair)
Hideo Orihara, JMUC
Koutaku Yamamoto, Mitsui
Masaru Tsujimoto, NMRI (until Nov. 2017)
Se-Myun Oh, SHI
Gongzheng Xin, CSSRC
Dominic Hudson, Southampton U.
Henk van den Boom, MARIN
Sebastian Bielicki, CTO

Florian Kluwe, HSVA
Kenichi Kume, NMRI (from Nov. 2017)

SC on Hydrodynamic Noise
Johan Bosschers, MARIN (Chair)
Kei Sato, MHI
Bryce Pearce, AMC
Yezhen Pang, CSSRC
Cheolsoo Park, KRISO
Michele Viviani, Genova U.
Claudio Testa, CNR-INSEAN
Romuald Boucheron, DGA
Ian Eames, UCL
Tuomas Sipilä, VTT

SC on Hydrodynamic Modelling of Marine Renewable Energy Devices
Petter Berthelsen, SINTEF Ocean (Chair)
Irene Penesis, AMC
Jonathan Pitt, Penn State (until July 2018)
Keyyong Hong, KRISO
Ye Li, SJTU
Hyunkyoung Shin, Ulsan U.
Giuseppina Colicchio, CNR-INSEAN
Sylvain Bourdier, ECN
William Batten, Qinetiq
Maurizio Collu, Cranfield U. (Strathclyde University from August 2018)
William Straka, Penn State (from July 2018)

SC on Ice
Topi Leiviskä, Aker Arctic (Chair)
Takatoshi Matsuzawa, NMRI
John Wang, NRC
Yinghui Wang, CSSRC
Yan Huang, Tianjin U.
Jinho Jang, KRISO
Nils Reimer, HSVA
Rüdiger von Boch und Pollach, TUHH
Mikko Suominen, Aalto U (until July 2018)
Dobrodeev Aleksei Alekseevich, Krylov
Pentti Kujala, Aalto U. (from July 2018)

SC on Energy Saving Methods
In Won Lee, PNU (Chair)
Munehiko Hinatsu, Osaka U.
Jianting Chen, SSSRI
Tie Li, SJTU
Ramon Quereda, CEHIPAR
James W. Gose, Michigan (from Oct 2017)

SC on Modelling of Environmental Conditions
Alessandro Iafrati, CNR-INSEAN (Chair)
Solomon Yim, Oregon State
Pedro C. Mello, Numerical Tank USP
Toshifumi Fujiwara, NMRI
Xinshu Zhang, SJTU
Hyun Joe Kim, SHI
Yuxiang Ma, Dalian U.
Jule Scharnke, MARIN
Marcin Drzewiecki, CTO

SC on Combined CFD/EFD Methods
Sofia Werner, SSPA (Chair)
Ayhan Akinturk, NRC
Kevin Maki, Michigan U.
Takanori Hino, Yokohama Nat. U.
Feng Zhao, CSSRC
Shin hyung Rhee, SNU
Hyung Taek Ahn, UoU
Peter Horn, HSVA
Tahsin Tezdogan, Strathclyde U
Joe Banks, Southampton U

SC on Manoeuvring in Waves
Hironori Yasukawa, Hiroshima U. (Chair)
Young-Jae Sung, HHI
Xiechong Gu, SJTU
Yeongyu Kim, KRISO
Wenyang Duan, HEU
Evgeni Milanov, BSHC
Marc Steinwand, SVA Potsdam (until Sept 2019)
Manasés TELLO RUIZ, University of Gent and Flanders

Quality Systems Group
Marco Ferrando, Genova U. (Chair)
Joel Park, NSWCCD
Joel Sales Sena Jr., LabOceano
Art Reed, NSWCCD
Daisuke Kitazawa

Weimin Chen, SSSRI
Lanfranco Benedetti, CNR-INSEAN
Jesus Valle (CEHIPAR)
Grigoropoulos Gregory (NTUA)
Derradji Aouat, Ahmed (NRC) (from aug 2019)

Appendix 2
Proposed Task and Structure of the 30th ITTC Technical Committees and Groups

1. STRUCTURE OF TECHNICAL COMMITTEES

The structure of the technical committees includes six General Committees, five Specialist Committees and one Group.

1.1 GENERAL COMMITTEES

- Resistance and Propulsion
- Manoeuvring
- Seakeeping
- Ocean Engineering
- Stability in Waves
- Full Scale Performance

1.2 SPECIALIST COMMITTEES

- Cavitation and Noise
- Ocean Renewable Energy
- Ice
- Wind Powered Ships
- Combined CFD/EFD Methods

1.3 GROUPS

- Quality Systems Group

2. TERMS OF REFERENCE FOR THE GENERAL AND SPECIALIST TECHNICAL COMMITTEES AND GROUPS

2.1 GENERAL COMMITTEES

Each General Committee will be responsible for a general subject area. It will review the state-of-the-art, identify the need for research and development, and carry out longer term studies with broad impact.

Each General Committee will submit a report on the results of its work to the Full Conference. The conclusions and the recommendations of the General Committee report should be structured as follows:

1. General technical conclusions
2. Recommendations to the Full Conference, which require actions such as, e.g., adopting ITTC procedures.

In addition, each General Committee shall submit proposals for future work of the General Committee and identification of tasks, which may be appropriate for Specialist Committees. These proposals shall be submitted to the Advisory Council which will compile the proposals and present them to the Full Conference.

2.2 SPECIALIST COMMITTEES

The ITTC Advisory Council will propose Specialist Committees. Each Specialist Committee will be responsible for studying a specific technical problem. The Specialist Committees will be appointed for a limited duration. It is expected that they will complete their tasks within maximum two ITTC periods (6 years). They shall interact closely with the appropriate General Committees.

Each Specialist Committee will present a final report on the results of its work to the Full Conference and interim reports on progress if the duration of the committee spans more than one Conference. The conclusions and the recommendations of the Specialist Committee report should be structured as follows:

1. General technical conclusions
2. Recommendations to the Full Conference, which require actions such as, e.g., adopting ITTC procedures.

In addition, each Specialist Committee shall submit proposals for future work and identification of tasks, which may be appropriate for Specialist Committees. These proposals shall be submitted to the Advisory Council which will compile the proposals and present them to the Full Conference.

2.3 GROUPS

Groups may be established from time to time by the Executive Committee to carry out specific tasks for the Conference, which are generally not technical issues.

Each Group will present a final report on the results of its work to the Full Conference. The conclusions and the recommendations of the Group report should be structured as follows:

1. General conclusions
2. Recommendations to the Full Conference, which require actions such as, e.g., adopting ITTC procedures.

In addition, each Group shall submit proposals for future work and identification of tasks, which may be appropriate for General and Specialist Committees. These proposals shall be submitted to the Advisory Council which will compile the proposals and present them to the Full Conference.

3. MECHANISM FOR IDENTIFYING NEW SPECIALIST TECHNICAL COMMITTEES

As part of their Terms of Reference, the General Committees shall consider the need for new tasks and include appropriate proposals in their technical reports. If the Advisory Council identifies a need for a new Specialist Committee when it reviews the draft recommendations of the General Committees, the Advisory Council will prepare and agree on a statement of the technical aims and objectives for the work of the Specialist Committee.

Independent of the proposals of the General Committees, the Advisory Council will keep the requirement for Specialist Committees under continuous review.

When the Advisory Council has agreed on the need for a new Specialist Committee, the draft statement of technical aims and objectives will be presented to the Executive Committee for endorsement. If the Executive Committee approves the formation of a new Specialist

Committee, it will present the proposal to the Full Conference for approval.

4. TASKS OF THE TECHNICAL COMMITTEES AND GROUPS OF THE 30TH ITTC

4.1 GENERAL TERMS OF REFERENCE

1. All committees shall observe the Terms of Reference and general obligations. The committees are expected to perform all the tasks defined in this document. However, should a committee be unable to do this, it shall consult the Advisory Council with regard to reduction of the work.
2. All committees shall identify areas of mutual interest with other committees and the concerned committees shall establish active co-operation/liaison in these areas
3. All committees shall endeavour to identify benchmark data and submit these to the ITTC Secretary for inclusion in the benchmark data repository on the ITTC website. Each committee shall appoint a member responsible for this.
4. In their work, the committees shall follow the guidelines given in ITTC Recommended Procedure 1.0-03, General Guideline for the Activities of Technical Committees, Liaison with the Executive Committee and Advisory Council.
5. All committees shall monitor and propose possible application of combined CFD/EFD methods and liaise with the SC on Combined CFD/EFD Methods.
6. Committee reports to the Conference should be structured in line with the terms of reference of the committee and in accordance with Recommended Procedure 4.2.3-01-02, Guidelines for Preparation of Committee and Group Reports.

4.2 REQUIREMENTS TO NEW AND REVISED RECOMMENDED PROCEDURES AND GUIDELINES

An important part of the work of the committees will be to establish Recommended Procedures and Guidelines to help the ITTC member organizations maintain their institutional credibility with regard to quality assurance of products and services such as predictions and evaluations, and quality assurance of designs. The committees will develop detailed plans in accordance with these Terms of Reference and their work should be directed towards the techniques and the understanding of physical and numerical modelling as a means of predicting full-scale behaviour. While maintaining an awareness of progress, fundamental theoretical studies and fundamental aspects of numerical fluid computation should be covered by other fora. Recommended Procedures and Guidelines shall contain only techniques which are applicable in commercial practice.

In the preparation of new or revision of existing Recommended Procedures and Guidelines, the committees shall observe the following:

1. Committees that have a task to review ITTC Recommended Procedures shall identify and report any proposed changes in their first annual report to the Advisory Council. The changes approved by the Advisory Council shall be implemented in the second year and the draft revised procedure submitted to the Advisory Council for comment.
2. Committees that have a task to write new procedures or guidelines shall submit an outline of these with their first annual report to the Advisory Council. The outline shall be reviewed by the Advisory Council and comments made to the committees. The draft new procedures or guidelines shall be prepared during the second year and

submitted to the Advisory Council for review.

3. New and revised draft procedures shall subsequently be updated, incorporating the comments made by the Advisory Council, and in February of the third year of the period be submitted to the Advisory Council for final review and approval. Following AC review, the committee will have three weeks to make the final adjustments to the procedure and resubmit them to the AC. After approval by the AC, the Quality Systems Group shall perform a formal check of the procedures.
4. Procedures and Guidelines must be in the format defined in the ITTC Recommended Procedure 4.2.3-01-03 "Work Instruction for Formatting ITTC Recommended Procedures", and they will be included in the ITTC Quality Manual. Symbols and terminology must be in accordance with those used in the current version of the ITTC Symbols and Terminology List. If necessary, new symbols, complying with ISO 80000-1, should be proposed in collaboration with the Quality Systems Group. Recommended Procedure 4.2.3-01-03 contains a template, which shall be used for all new procedures and guidelines.
5. When a committee is given the task to write a new procedure or guideline or revise an existing procedure or guideline, the committee shall ensure that symbols and terminology as well as the contents of this procedure or guideline is consistent with any other procedure or guideline, which may deal with a related matter.
6. If relevant, procedures and guidelines shall specifically describe the deliverable to the customer for the described test.
7. All new and revised procedures shall, as far as feasible, include a procedure for uncertainty analysis. All procedures for uncertainty analysis in experiments shall follow ITTC Procedure 7.5-02-01-01 "Guide to the Expression of Uncertainty in Experimental Hydrodynamics" and JCGM 100:2008 "Evaluation of measurement data – Guide to the expression of uncertainty in measurement", also known as the GUM. All existing procedures on uncertainty analysis, that for other reasons are going to be updated, shall also be updated to follow this standard. The Quality Systems Group will assist the committees with regard to uncertainty analysis.
8. All revisions to ITTC Procedures shall be updated referring to the ITTC Procedures from the latest ITTC Register. The latest ITTC procedures shall be included in the References of the revised procedure. Revisions for the 30th ITTC shall be updated with the ITTC Procedures from the Register for the 29th ITTC.

4.3 TERMS OF REFERENCE FOR THE GENERAL COMMITTEES

Resistance and Propulsion Committee

1. Update the state-of-the-art for predicting the performance of different ship concepts emphasizing developments since the 2021 ITTC Full Conference. The committee report should include sections on:

A) The potential impact of new technological developments on the ITTC, including, for example new types of hull and propeller coatings, propulsors, rudders.
B) New experimental techniques and extrapolation methods.
C) New benchmark data.
D) The practical applications of computational methods to performance predictions and scaling.
E) The need for R&D for improving methods of model experiments, numerical modelling and full-scale measurements.

2. Review ITTC Recommended Procedures relevant to resistance and propulsion, and

A) identify any requirements for changes in the light of current practice, and, if approved by the Advisory Council, update them,
B) identify the need for new procedures and outline the purpose and contents of these.

3. Rewrite procedure 7.5-02-03-01.2, Uncertainty Analysis, Example for Propulsion Test (old procedure deleted 2021), complying with current ITTC guidelines for uncertainty analysis. Include a worked example complying with current ITTC procedures for propulsion tests. Cooperate closely with the Quality Systems Group
4. Rewrite procedure 7.5-02-03-02.2, Uncertainty Analysis, Example for Open Water Test (old procedure deleted 2021), complying with current ITTC guidelines for uncertainty analysis. Include a worked example complying with current ITTC procedures for open water tests. Cooperate closely with the Quality Systems Group.
5. Update procedure 7.5-02-05-03.3, Uncertainty Analysis, Example for Water Jet Propulsion Test, complying with current ITTC guidelines for uncertainty analysis. Include a worked example complying with current ITTC procedures for water jet propulsion tests. Cooperate closely with the Quality Systems Group.
6. Conduct a benchmark study focusing on the effect of Re at model scale and scaling methods for full scale prediction. CFD calculations would be run at a range of Re at model scale and full scale, along with open-water model tests at a range of Re. The study could use two propellers that were provided for the previous benchmark study run by the 28th ITTC.
7. Investigate the issue of laminar effects in self-propulsion test of propeller with low blade area.

A) Conduct a survey how ITTC members tackle this issue, and which scaling method they use for low blade area propellers.
B) Investigate the sufficiency of conduction two open water tests at different Reynolds numbers for full scale extrapolation.
C) Review literature on the subject.
D) Suggest modification to recommended procedures.

8. Investigate the issue of extrapolation of model tests with ducted propellers to full scale according to different Re-numbers. Identify the need and change relevant procedures if necessary.
9. Update Load variation test method in 7.5–02-03–01.4 "1978 ITTC Performance Prediction Method"

A) Review of Load Variation Test method taking into consideration a wider range of resistance and develop a new method if necessary.
B) Review the effectiveness of shallow water effects in Load Variation Test method and develop of a new method if necessary.

10. Monitor the experience of ITTC members using CFD-based form factors and, if necessary, update the Recommended Procedures accordingly. This includes the correlation with sea trial data, numerical friction line, how to handle a submerged transom, the possibility to handle separation in model scale by deriving model and full scale form factors. Continue the comparative studies on CFD methods for form factor derivation.
11. Investigate the requirements for testing and numerical evaluation of high-speed marine vessels. Address the need of updating the relevant procedures.
12. Investigate the use of CFD methods in scaling of model test results for a more precise speed-power prediction. The issues with high priority are:

A) propeller open water scaling

B) difference in Reynolds number at self-propulsion and open water test, laminar effect in self-propulsion test
C) effective wake scaling
D) scaling of immersed transoms
E) energy saving devices

13. Investigate the measurement and prediction methods for breaking waves.
14. Investigate scaling of sinkage and trim in deep water, as well as their effect on the form factor.
15. Investigate the scale effects of ships advancing through shallow/restricted waters, in particular scaling of sinkage.
16. Monitor the developments in hull and propeller model manufacturing. Investigate the advances in additive manufacturing techniques and novel materials. Investigate the use of 3D scanning techniques to validate the model geometry in view of updating the procedures.
17. Develop guidelines for model testing of coatings; in particular, skin friction reducing and air lubrication systems, including scaling laws.
18. Review CFD methods for roughness effects and recommend best practice; in particular, in terms of wall resolved as well as wall function methods.
19. Identify the necessity of guidelines for CFD methods, model tests and scaling for energy saving devices.
20. Investigate the issue of powering and resistance for slower speed submerged vehicles due to the resurgence of UUV (Unmanned Underwater Vehicle) and AUV (Autonomous Underwater Vehicle). The UUV's and AUV's can be plagued by the added drag of appendages, sensors and add-ons. They can have much greater impact on performance (% wise) than typical submerged vehicles (torpedo/subs) since UUV's and AUV's typically operate at much slower speeds. The community would benefit with a better correction for Cf than the flat plate curve. Identify the need and, if necessary, update the procedures to better handle transition issues that would be present in these lower Re submerged vehicles.

Manoeuvring Committee

1. Update the state-of-the-art for predicting the manoeuvring behaviour of ships, emphasizing developments since the 2021 ITTC Conference. The committee report should include sections on:

A) the potential impact of new technological developments on the ITTC, such as unmanned ship and autonomous navigation
B) new experiment techniques and extrapolation methods
C) the practical applications of computational methods to manoeuvring predictions and scaling, including CFD methods
D) the need for R&D for improving methods of model experiments, numerical modelling and full-scale measurements

2. During the first year, review ITTC Recommended Procedures relevant to manoeuvring, and

A) identify any requirements for changes in the light of current practice and, if approved by the Advisory Council, update them,
B) identify the need for new procedures and outline the purpose and contents of these.

3. Update procedure 7.5-02-06-05 "Uncertainty Analysis for Free Running Model Tests" complying with current ITTC guidelines for uncertainty analysis. Cooperate closely with the Quality Systems Group.
4. Survey the state of the art of the development of autonomous navigation technology such as the application of artificial intelligence schemes, and investigate potential impact to ITTC, including the impact to autopilot of full-scale ships.
5. Update 7.5-02-06-02, Captive Model Test, particularly with specific attention to the

treatment of amplitudes, frequencies and inertial coefficients and to have a single integrated example for uncertainty analysis, based on the SIMMAN results.

6. Update 7.5-02-06-03 Validation of Manoeuvring Simulation Models, reflecting the outcome of SIMMAN and any other new developments.
7. Continue the work with underwater vehicles towards and complete the guidelines, extending to submarines and ROV's, if possible.
8. Update the guidelines proposed by Special Committee on Manoeuvring in Waves of the 29th term, collaborating with the Seakeeping Committee.
9. Support and collaborate with SIMMAN group for post processing and analysis of the submitted results and collect the benchmark data for the validation of numerical methods of ship manoeuvring, including the wave-induced forces and moments in waves.
10. For the minimum propulsion power to maintain the manoeuvrability of ships in adverse conditions, validate the Level 2 – Simplified Assessment Method of the 2013 Interim Guidelines (MEPC.1/Circ.850) by enhanced and comprehensive methods, and review the Level 3 – minimum power assessment of the Draft Amendments to Guidelines (MEPC.1/Circ.850).
11. Collect benchmark data for

A) underwater vehicles
B) inland navigation
C) model-scale vessels with a documented full-scale variant

12. Survey the captive test in waves and collect the data of the hydrodynamic forces acting on the ship in waves, which can be used for the validation and application of simulation tools, including

A) Oblique towing test data in waves
B) Circular motion test data in waves
C) PMM test data in waves
D) Rudder force data in waves when ship is moving straight ahead

13. Considering the effect of novel devices and clean fuel technology on available installed power, investigate its implications on manoeuvrability in wind and waves

Seakeeping Committee

Note: The Seakeeping Committee is primarily concerned with the behaviour of ships underway in waves. The Ocean Engineering Committee covers moored and dynamically positioned ships. For the 30th ITTC, the modelling and simulation of waves, wind and current is the primary responsibility of the Ocean Engineering Committee, with the cooperation of the Seakeeping and the Stability in Waves Committees.

1. Update the state-of-the-art for predicting the behaviour of ships in waves, emphasizing developments since the 2021 ITTC Conference. The committee report should include sections on:

A) the potential impact of new technological developments on the ITTC
B) new experiment techniques and extrapolation methods
C) new benchmark data
D) the practical applications of numerical simulation to seakeeping predictions and correlation to full scale
E) the need for R&D for improving methods of model experiments, numerical modelling and full-scale measurements.

2. Review ITTC Recommended Procedures relevant to seakeeping procedures, and

A) identify any requirements for changes in the light of current practice, and, if approved by the Advisory Council, update them,
B) identify the need for new procedures and outline the purpose and contents of these.

3. Create a new guideline on verification and validation of the CFD methods for seakeeping analysis. For example, finite-volume-based methods and particle methods which solve RANS and LES, for seakeeping procedures, collaborating with the Specialist Committee on Combined CFD/EFD Methods and taking existing procedures for verification and validation of CFD methods into account.
4. Considering Procedure 7.5-02-07-02.8, Calculation of the Weather Factor fw, investigate the functionality of the procedure when applied to ships smaller than 150m in length, and provide any method to improve the current procedure for small ships.
5. Investigate if there is any practical problem in the application of MEPC.1/Circ.850/ Rev.2 for minimum power requirement, and develop a new ITTC guideline, if needed.
6. Develop a guideline for wind loads for ships, collaborating with the committees related to this issue, particularly the Ocean Engineering Committee, the SC on Renewable Ocean Energy, Manoeuvring Committee and the Full-Scale Performance Committee.
7. Organize a benchmark experimental campaign, including the added resistance measurement in oblique seas and different loading conditions, and the characterization of the uncertainty in the measurement of added resistance.
8. Survey the state of the art for the acquisition and analysis in on-board and/or real-time seakeeping data, and investigate the need of ITTC activities, including future issues related to autonomous vessels.
9. Collaborate with Manoeuvring Committee for the development of guidelines related to manoeuvring in waves.

Ocean Engineering Committee

Note: The Ocean Engineering Committee covers moored and dynamically positioned ships and floating structures. For the 30th ITTC, the modelling and simulation of waves, wind and current is the primary responsibility of the Ocean Engineering Committee with the cooperation of the Seakeeping and the Stability in Waves Committees.

1. Update the state-of-the-art for predicting the behaviour of bottom founded or stationary floating structures, including moored and dynamically positioned ships, emphasizing developments since the 2021 ITTC Conference. The committee report should include sections on:

A) the potential impact of new technological developments on the ITTC
B) new experimental techniques and extrapolation methods
C) new benchmark data
D) the practical applications of computational methods for prediction and scaling
E) the need for R&D for improving methods of model experiments, numerical modelling and full-scale measurements.

2. Review ITTC Recommended Procedures relevant to ocean engineering, including CFD procedures, and

A) identify any requirements for changes in the light of current practice, and, if approved by the Advisory Council, update them,
B) identify the need for new procedures and outline the purpose and contents of these.

3. Review and identify areas of concern in modelling and simulation of waves, wind and currents. In particular:

A) report on methods to generate extreme wave packets for studying responses to extreme waves in a towing tank. Examine the effects of wave breaking and statistics of occurrence on the wave spectrum, its spectral shape, extreme wave generation, and the role of wind-wave interaction on wave breaking occurrence.

B) investigate the influence of the vertical wind profile on the aerodynamic loads experienced by platforms and other offshore objects. Develop a standard vertical wind profile for model testing purposes and methods for modeling it both numerically and experimentally.
C) Continue work on using a small controllable fan to mimic forces developed during a floating offshore wind turbine test due to the turbine itself. Expand the work on Software-in-the-Loop (SiL) systems for modeling wind turbine loads to be used as a general tool to model many types of wind loads. For example, wind loads on a ship during a maneuvering in waves test. Liaise with the SC on Ocean Renewable Energy and the Seakeeping Committee.
D) develop specifications for a benchmark test program for wind loads and their influence on the motions of floating structures. Compare wind loads developed using SiL to model the wind loads versus using fans to produce an actual model scale wind. Among other data, repeatability, and consistency between the methods and between different facilities should be reported. The benchmark study may also include CFD comparisons.
E) report on state-of-the-art for wave-current interactions. In particular, the role played in terms of the generation of extreme waves.

4. Review the state-of-the-art in offshore aquaculture systems since the 2021 report of the Ocean Engineering committee including large volume closed containment systems, extreme wave environments, and modelling of entire systems.
5. The benchmark tests with the square cylinders are complete. However, it is recommended that, owing to the complicated wave-column interactions, more experimental and CFD studies should be considered for four-column cases with different configurations and more extreme waves such as focused waves. In addition, local wave impact loads on the columns are also critical and deserve further in-depth studies.
6. The work on the CFD benchmark study of two-bodies in close proximity shall be continued. Smaller gaps need to be studied and the procedure for 2-body model tests shall be updated based on the CFD benchmark study.
7. Investigate extraction methods of nodules from the seabed. Develop a guideline for testing Nodule Mining Machines in a towing tank including their riser systems.
8. Investigate testing methods to characterise the influence of changing bottom bathymetry and coastline for tankers at offloading terminals.

Stability in Waves Committee

Note: The Stability in Waves Committee covers the stability of intact and damaged ships in waves. For the 30th ITTC, the modelling and simulation of waves, wind and current is the primary responsibility of the Ocean Engineering Committee with the cooperation of the Seakeeping and the Stability in Waves Committees.

1. Update the state-of-the-art for evaluating the stability of ships in adverse weather conditions, emphasizing developments since the 2021 ITTC conference. The committee report should include sections on:

A) the potential impact of new technological developments on the ITTC
B) new experimental techniques
C) new benchmark data
D) the practical applications of computational methods to prediction
E) the need for R&D for improving methods of model experiments, numerical modelling.

2. Review ITTC Recommended Procedures relevant to stability, including CFD procedures, and

A) identify any requirements for changes in the light of current practice, and, if approved by the Advisory Council, update them,
B) identify the need for new procedures and outline the purpose and contents of these.

3. Update ITTC Procedure 7.5-02-01-08, Single Significant Amplitude and Confidence Intervals for Stochastic Processes when new information becomes available.
4. Develop new ITTC recommended procedures in support of direct stability assessment within 2nd generation IMO intact stability criteria:
5. Avoiding self-repeating effect in time-domain numerical simulation of ship motions,
6. Procedure of Estimation of Frequency of Random Events by Direct Counting,
7. Statistical Validation of Extrapolation Methods for Time Domain Numerical Simulation of Ship Motions
8. Develop a new procedure, Computational procedure for instantaneous GZ curve during time-domain numerical simulation in irregular waves.
9. Investigate the current state of the art on flooding dynamics of damaged ship in waves, including EFD and CFD.
10. Continue the identification of benchmark data for validation of stability-in-waves predictions.

Full-Scale Ship Performance Committee

1. Update the state-of-the-art for investigation of full-scale ship performance, emphasizing developments since the 2021 ITTC Conference. The committee report should include sections on:

A) the potential impact of new technological developments on the ITTC
B) new measuring techniques
C) new benchmark data
D) the practical applications of numerical simulation to full-scale ship performance
E) the need for R&D for improving methods of full-scale measurements and numerical modelling.

2. Review ITTC Recommended Procedures relevant to full-scale performance, and

A) identify any requirements for changes in the light of current practice, and, if approved by the Advisory Council, update them,
B) identify the need for new procedures and outline the purpose and contents of these.

3. Address issues related to hull and propeller surface roughness such as:

A) Definition of roughness properties
B) Components of roughness
C) Measurement of roughness
D) Effects of roughness on in-service performance including filtering and analysis methods for evaluating hull and propeller performance separately
E) Roughness usage in performance prediction and cross effects with correlation

4. Provide technical support to ISO and IMO in further development of approaches to in-service performance monitoring (e.g. ISO19030)
5. Address the following aspects of the analysis of speed/power sea trial results:

A) Initiate and conduct speed trials on commercial ships on deep and shallow water to further validate Raven method.
B) More validation of wave-added resistance method, in particular SNNM, covering all wave encounter angles based on a set of significant ship parameters including the short-term estimation of wave-added resistance in irregular waves.
C) Investigate the influence of drift, rudder action, short wave and wave height on wave-added resistance.

D) Investigate the influence of water depth on the hull-propeller interaction (thrust deduction, relative rotative efficiency)
E) Explore and monitor new developments in instrumentation and measurement equipment relevant for sea trials and in-service performance assessment (e.g. wind, waves, thrust, speed through water)

6. Study accuracy of CFD for shallow water applications – cooperate with CFD/EFD Committee
7. Update the speed/power sea trial procedures 7.5-04-01-01.1 where appropriate, in particular:

A) complement it by a procedure for the correction of yawing (caused by wind) and rudder angle
B) wind averaging method to correctly reflect the wind effect in double run (true wind vector in each run).

8. Support ISO in updating ISO15016 in compliance with 7.5-04-01-01.1
9. Update guideline for determination of model-ship correlation factors, including shallow water and draft dependency (in cooperation with AC Working Group)
10. Update guideline on CFD-based wind coefficient; in particular, re-assess database of wind resistance coefficients and update it according to the new procedure for non-dimensionalising.
11. Continue to monitor the development of relevant techniques for ship energy saving and identify the needs to complement the present EEDI framework in response to the adoption of alternative fuels and the receptivity of innovative technologies. Consider, if necessary, a complementary metric to EEDI to represent power savings.
12. Collect full scale data obtained through relevant benchmark tests on the effect of energy saving methods (ESM). Use the full scale data for validating the effect of ESM. Develop a guideline to conduct in-service performance evaluation for ESM. Full-scale data showing the benefits of ALDR (Air Layer Drag Reduction) would be of particular interest.
13. Consider the hydrodynamic aspect of design for Smart Ship and Unmanned Surface Vehicles as the smart ship technology for cargo or passenger transportation is one of the emerging technologies in maritime industry. Explore the suitability of the traditional design spiral for the smart ship and USVs. Identify the need for new or modified procedures of experiment and simulation for performance evaluation in this particular field.

4.4 TERMS OF REFERENCE FOR SPECIALIST COMMITTEES

Specialist Committee on Ocean Renewable Energy

The following list of tasks is rather ambitious. Based on the expertise of the committee members, the specialist committee should review the TOR and decide what can be accomplished and is more relevant from a practical point of view in a three-year period.

1. An official type A liaison has been established with the International Electro Technical Commission (IEC), TC114 and TC 88 technical committees in order to:

A) Verify, integrate, and remove conflicts of actual ITTC procedures and guidelines for testing marine current turbines and wave energy devices with the IEC guidelines
B) Monitor and contribute to the discussion within the IEC for the definition of standards and protocols for testing ocean energy devices.

2. Review testing techniques for deployment (transportation, installation), operations, and maintenance of marine renewable energy devices.

3. Review testing techniques for multipurpose platforms (e.g. combinations of WEC/OWT/Current Turbines/Solar/Aquaculture)
4. Continue reporting on full scale installations

A) Type of device
B) Problems in installation
C) Success of energy extraction
D) Survivability
E) Investigate and report on the correlation between the model-scale predictions and full-scale results.

5. Wave Energy Converters (WEC)

A) Monitor and report on new concepts for WEC's
B) Review and report on the progress made on the modelling of arrays. Update and extend array section of the guideline for numerical modelling of WEC's.
C) Continue to monitor developments in PTO modelling both for physical and numerical prediction of power capture. Discuss different PTO control strategies for power optimisation and survivability modes.
D) Develop a guideline for numerical and experimental survival testing of WEC's
E) Assess level of support for a benchmark study of comparisons between numerical computations and physical testing of WEC's. If there is sufficient interest, develop specifications for the benchmark study.

6. Current Turbines

A) Obtain and analyze benchmark data for current turbines from IEC.
B) Continue to monitor developments in physical and numerical techniques for prediction of performance of current turbines.
C) Assess support and if sufficient interest, develop specifications for a benchmark study of a horizontal axis turbine (for instance the 3-blade DoE turbine).
D) Review and report the techniques used for CFD modelling of current turbines. This should include the use of combined EFD/CFD techniques for scaling and blockage corrections and methodologies for replicating environmental conditions.
E) Investigate effects and reproduction at model scale of inflow turbulence and unsteadiness to the turbine including the effects of waves.
F) Review and report on the progress made on the modelling of arrays, elaborating on wake interactions and impact on performance
G) Investigate and develop blockage corrections for testing current turbines in water channels.

7. Offshore Wind Turbines

A) Continue monitoring and report on the developments in full-scale installations of floating offshore wind turbines.
B) Report on possible full-scale measurement data availability and address how these data can be utilized for validation of simulation tools and evaluation of scaling effects from model scale tests.
C) Continue monitoring and report on the development in model testing methodology for offshore wind turbines.
D) Review and report on recent developments of physical wind field modelling in open space with application for wave tank testing of floating offshore wind turbines, including modelling of turbulence and the measuring and documentation of the wind field.
E) Investigate the influence of the vertical wind profile on the operation and efficiency of offshore wind turbines
F) Liaise with the Ocean Engineering Committee regarding their work on SiL and a small controllable fan to model the loads due to an operating wind turbine.
G) Review and report on the development of numerical offshore wind farm modelling.

H) Monitor and report on recent research related to model tests of bottom-fixed offshore wind turbines including modelling the influence of structural stiffness and soil stiffness.
I) Report on other existing regulations related to model tests of offshore wind turbines (e.g. IEC, classification societies, DoE) and update procedures/guidelines as appropriate.
J) Continue monitoring the developments in model testing methodology with respect to Froude/Reynolds scaling issues and incorporating control system strategies.

Specialist Committee on Cavitation and Noise

1. Review and update the current guidelines on model and full scale noise measurement and review and update the existing procedures on cavitation; provide recommendations for new guidelines / procedures, if any.
2. Review the state of the art on cavitation model testing (cavitation appearance, hull pressure fluctuation, thrust break down, cavitation erosion) with a focus on ways to reproduce the scaling effects on ship wakes. Conduct an Uncertainty Analysis on the full-scale prediction of all the cavitation parameters (cavitation appearance, hull pressure fluctuation, thrust break down, cavitation erosion).
3. Review the current CFD method for cavitation extent and hull pressure fluctuation prediction and especially on the use of a dummy model (defined by using CFD calculation) on propellers / pods / other types. Liaise with the Specialist Committee on CFD/EFD Combined methods. Provide recommendation for a new guideline on how to proceed for the dummy model definition.
4. Review the currently available CFD benchmark data, including the on-going projects, such as JORES, and investigate the feasibility to establish ITTC benchmark database.
5. Review new measurement techniques used for cavitation model testing and full-scale trials (optical measurement for blade cavity extent, fluctuating forces on blades…).
6. Organize the proposed round-robin test case as recommended in the 29th Noise committee.
7. Further monitor and investigate specific aspects of model-scale noise measurements including reverberation, tip vortex scaling, water quality and the effect on uncertainty.
8. Review any open literature dealing with the respective contributions of the hull vibrations and of the propeller in the ship radiated noise at full scale (frequency line and broad band spectrum) and investigate ways of assessing those contributions
9. Continue monitoring progress on shipping noise measurement procedures for shallow water and regulations as developed by ISO, classification societies and regulatory agencies.
10. Continue monitoring progress on ship noise prediction by computational methods with emphasis on the prediction of cavitation noise using CFD methods and methods such as data driven models and machine learning techniques, and noise propagation modelling, especially for shallow waters

Specialist Committee on Ice

1. Continue to maintain, review, and update existing accepted procedures and guidelines in accordance with current practice.
2. Continue work on uncertainty analysis including conducting benchmarking study among ice model basins. Focus on the largest error sources is recommended such as the uncertainty related to the ice properties. Based on conducted measurement and analyses, include a review of how the findings may reflect ice measurements.
3. Develop Guideline 7.5-02-04-02.5 – Experimental Uncertainty Analysis for Ship Resistance in Ice Tank Testing, including findings related to the uncertainty analysis.

4. Revise the procedure 7.5-04-03-01 Ship Trials in Ice. Pay special attention to ice conditions (such as flexural strength, thickness, snow coverage / density and ice types).
5. Continue to develop a Guideline for the Testing of Fixed Structures, including monopiles, based on prepared outline (Table of Content). Pay special attention to scaling issues for vertical structures where crushing strength is dominant.
6. Review State of the Art on numerical modelling.
7. Review and study current methods for testing waves in ice and based on this prepare outline for guidelines.

Specialist Committee on Performance of Wind Powered and Wind Assisted Ships

1. Review technologies for wind propulsion and wind assistance. Clarify the distinction between wind powered and wind assisted ships.
2. Review methods of ship model hydrodynamic tests, wind tunnel tests, CFD, ship dynamics simulations and routing relevant for predicting the performance and safety of wind powered and wind assisted ships at design stage with particular attention paid to higher side forces and drifting of the ship due to wind powering.
3. Review long-term statistics of winds and waves from the point of view of applicability for the evaluation of wind assisted ships at design stage.
4. Derive a guideline for predicting the fuel consumption of a wind propulsion ship on a route at design stage with the consideration of weather-routing effects.
5. Review safety and regulatory issues related to hydro/aero dynamic testing and evaluation and recommend measures to take at design stage.
6. Derive performance indicators for comparing the performance of wind propulsion at design stage.
7. Investigate the effect on propulsive factors due to reduced propeller load arising from the use of wind power. Identify the effects of wind propulsion on the propulsion system, e.g. pressure side cavitation occurrence. Liaise with Resistance and Propulsion Committee and SC on Cavitation and Noise.
8. Derive a modified procedure for full scale trial of wind propulsion ships. Liaise with Full Scale Performance Committee.
9. Cooperate with MEPC on the continuous development of the EEDI for wind propulsion ships. Liaise with Full Scale Ship Performance Committee.
10. Liaise with the Ocean Engineering Committee regarding their work on SiL and controllable fans to model wind loads.

Specialist Committee on Combined CFD and EFD Methods

For the 30th ITTC, the Specialist Committee on CFD and EFD Combined Methods has the responsibility for CFD/EFD combined methods including CFD issues on an overview level. This includes the procedures for uncertainty assessment and quality assurance of CFD, review and highlight good examples of combined methods, suggest, and initiate new applications of combined methods. Co-ordinate, advise and encourage each technical committee to perform the detail work related to CFD/EFD combined methods.

1. Coordinate and advise all other Technical Committees on CFD/EFD Combined Methods and encourage them to investigate and develop CFD/EFD combined methods within each specific area. Summarize common challenges, conclusions, and new applications.
2. Monitor and review the advances, accuracy and challenges within full-scale and model-scale CFD of maritime applications with special focus on speed/power predictions.
3. Review the outcome of ongoing CFD benchmark campaigns. Liaison with relevant

technical committees, discuss the impact on existing ITTC procedures and propose relevant updates. Liaison with organisers of future benchmark studies of ship and ocean hydrodynamics when applicable.

4. Encourage the establishment of open validation data for high Reynolds number flow cases for marine applications. Initiate, promote, suggest or in other way support more open data to be available.
5. Review and study the performance of turbulence models and wall treatments at full scale. Monitor the development of new turbulence modelling approaches when they become available. Evaluate their performance for marine applications.
6. Monitor advances in the application of detailed flow measurements in the ITTC community and assess the need for detailed evaluation and implementation of best-practice, uncertainty analysis, and benchmark guidelines.
7. Develop a standard process of performing a CFD benchmark study within ITTC. Assist other Technical Committees to plan and analyse benchmark studies.
8. Monitor how Verification and Validation is applied and reported in research publications and commercial work. Monitor new approaches and existing procedures for Verification and Validation.
9. Continue to maintain and improve the existing Recommended Procedure 7.5-03-01-01, "Uncertainty Analysis in CFD, Verification and Validation Methodology and Procedures". Consider narrowing down the different options.
10. Monitor the use of the new Recommended Procedures 7.5-03-01-02 "Quality Assurance in CFD Ship Applications" and update it if needed. This includes the way to present the statistics of the comparison error in the demonstration process.
11. Produce information material (articles, conferences, social media) directed towards stakeholders who receive and use the results hydrodynamic predictions, such as designers, yards, shipowners and authorities. Explain issues like uncertainty level, state-of-the-art capability, and challenges of CFD versus EFD and Combined methods. This should be done in cooperation with other technical committees.

Additional Remark:

The following procedures will be handled by this specialist committee:

- 7.5-03-01-01, "Uncertainty Analysis in CFD, Verification and Validation Methodology and Procedures"
- 7.5-03-01-02 "Quality Assurance in CFD Ship Applications" (replace previous procedure 7.5-03-01-02 "Uncertainty Analysis in CFD, Guidelines for RANS codes)"

4.5 TERMS OF REFERENCE FOR THE GROUPS

Quality Systems Group

1. During the first six months after the conference perform a detailed review of all ITTC Recommended Procedures and Guidelines for compliance with ITTC quality requirements with regard to format, references, symbols, terminology, uncertainty analysis and parameter lists, and either update the procedures in these aspects or cooperate with the relevant committee on these updates. Submit the updated procedures to the Advisory Council before 31.12.2021.
2. During the first six months after the conference perform a detailed review of all uncertainty analysis procedures for compliance with ITTC quality requirements about format, references, symbols, terminology and parameter lists. Check that all uncertainty analysis

procedures contain a worked example based on the current versions of model test procedures. Cooperate with the relevant technical committees on updating the procedures, including a worked example. Submit a status report on this task to the Advisory Council before 31.12.2021. Updating expected to be completed before 30.06.2022.

3. Review the titles and numbering of technical procedures and propose changes, if any, for approval by the Advisory Council before 31.12.2021.
4. Maintain the Register of ITTC Recommended Procedures and Guidelines.
5. Introduce New Uncertainty Analyses Guidelines to include data anomalies in Machine Learning Algorithms for Autonomous and Intelligent ships.
6. Observe the development or revision of ISO Standards regarding Quality Control.
7. Update the ITTC Symbols and Terminology List.
8. Update the Uncertainty Analysis section of the Symbols & Terminology List.
9. Update the ITTC Dictionary of Hydromechanics.
10. Expand the content of current ITTC dictionary version, considering CFD, MASS, etc.
11. Support the technical committees dealing with stochastic processes with guidance on development, revision, and update of procedures for the inclusion of confidence bands on their computational and experimental results.
12. Observe BIPM/JCGM standards for uncertainty analysis, in particular the uncertainty analysis terminology.
13. Review developments in metrology theory and uncertainty analysis and issue appropriate procedures.
14. Setup an effective way to collect benchmark data.
15. Upload all the collected and verified benchmark data into the ITTC benchmark data repository
16. Liaise with relevant technical committees to complete a questionnaire about the demand and use of benchmarks, not to be limited to model scale.
17. Cooperate with technical committees to establish the ITTC benchmarks, including definition, raw data, data format, etc.
18. Prepare a procedure on the internal calibration of steel rulers or a practical way to check length measurement devices in towing tanks.

Appendix 3
Revised Description and Rules of the ITTC

1. DESCRIPTION

The International Towing Tank Conference (ITTC) is a world-wide independent association of hydrodynamics research organizations that support the designers, builders and operators of ships and marine installations by giving advice and information regarding the performance, safety and environmental impact of ships and marine installations using the results of physical model tests, numerical modelling and full-scale measurements.

2. AIMS

The aims of the ITTC are:

C) To stimulate progress in solving the technical problems which are of importance to the member organisations;
D) To stimulate research in areas in which a better knowledge is required in order to improve methods of predicting the full-scale hydrodynamic performance of ships and marine installations;
E) To stimulate the improvement of methods of model experiments, numerical modelling and full-scale measurements;
F) To recommend procedures for carrying out physical model experiments, numerical modelling and full scale measurements of ships and marine installations;
G) To validate the accuracy of full-scale predictions for quality assurance;
H) To formulate collective policy on matters of common interest;
I) To provide an effective organization for the interchange of information.

3. ACTIVITIES

The aims of the ITTC shall be pursued by:

J) Stimulating research into specific topics;
K) Organising and encouraging meetings to review progress in this research;
L) Making such recommendations and decisions on joint action and policy as seem desirable to the members of the ITTC;
M) Establishing procedures and guidelines to help the member organizations to maintain their institutional credibility with regard to quality assurance of products and services, such as, performance prediction and evaluation of designs by either experimental or computational means;
N) Recording and publishing discussions taking place at ITTC meetings.

4. MEMBERSHIP

Membership of the ITTC shall be open to all organisations that carry out hydrodynamic work in support of the designers, builders and operators of ships and marine installations, and to other organisations that contribute to the aims of the ITTC.

Applications for membership shall be made to the Executive Committee through the ITTC Secretary. Each such organisation shall satisfy the Executive Committee that it is eligible for membership.

Each member organisation shall be represented by its director or other senior officer having the authority to bind the member organisation in matters relating to the ITTC (the designated representative).

A membership fee shall be payable by all member organisations. The Executive Committee shall propose the annual fee for the next three years for approval by the Full Conference. The fee shall be payable annually by October 1st . Member organisations may choose to pay annually or once for all three years. Members admitted during an ITTC period shall pay the full membership fee for the year they are admitted and for the following years.

A member organisation, which has not paid the fee by March 31st the following year shall no longer be a member organisation of ITTC and the name of the organisation shall be removed from the membership list. The Executive Committee may extend this deadline if unusual financial or administrative circumstances delay the payment of the fee.

5. FULL CONFERENCE

The Full Conference comprises the designated representatives of member organisations eligible to vote and present at general sessions that take place during the Conference.

5.1 ROLES AND RESPONSIBILITIES

The Full Conference shall:

O) Determine the policies of the ITTC;
P) Approve changes to the rules of the ITTC;
Q) Appoint the Chairman of the Executive Committee and the ITTC Secretary;
R) Appoint the Chairman and members of each technical committee or group;
S) Approve financial reports and plans and the ITTC membership fee;
T) Approve the host organisation for the next Conference;
U) Approve terms of reference for technical committees and groups;

Approve recommended procedures and guidelines.Only member organisations are eligible to vote. The vote shall be exercised by the designated representative of the organisation and no organisation shall be entitled to more than one vote. A designated representative who is unable to attend the meeting may choose to delegate the voting rights of the member organisation to another employee of the organisation. The designated representative must inform the Chairman of the Executive Committee of the name of the alternate before the start of the general session at which the vote will take place. Postal or email votes shall not be allowed.

Voting may be by secret ballot or a show of hands as determined by the Executive Committee. An affirmative vote of at least 2/3 of members present shall be required to carry a motion.

A record of the decisions of the Full Conference shall be published in the proceedings of the Conference.

5.2 DECISION MAKING BETWEEN FULL CONFERENCES

If for any reason a decision is required in the time gap between Full Conferences with regard

to the items listed in 5.1, the Executive Committee unanimously and supported by a majority of the Advisory Council is mandated to make such decision. If a unanimous decision cannot be made, a decision shall be made in accordance with a procedure approved by the Full Conference.

Any decisions made in accordance with 5.2 shall be reported to the Full Conference and recorded in the proceedings of the Conference.

6. EXECUTIVE COMMITTEE

6.1 ROLES AND RESPONSIBILITIES

The Executive committee shall:

V) Implement the decisions of the Full Conference;
W) Represent the ITTC between Conferences;
X) Replace members of technical committees or groups as necessary between Conferences;
Y) Accept new member organisations to the ITTC;
Z) Manage the income from the ITTC and Advisory Council membership fees.
AA) Approve the arrangements and associated costs and registration fees for the Conference;
BB) Prepare a report on its activities for presentation at a general session of the Conference.

The Executive Committee shall propose the following for approval by the Full Conference:

CC) The Executive Committee Chairman, ITTC Secretary and members and Chairmen of technical committees and groups;
DD) The terms of reference of technical committees and groups;
EE) Recommended procedures and guidelines
FF) The host organisation for the next Conference;
GG) A financial plan and the ITTC membership fee.

In order to pursue the aims of the ITTC the Executive Committee may initiate formal interactions or collaborations between the ITTC and other organisations (for example the IMO or ISSC). The Executive Committee may require technical committees to carry out specific tasks in support of such interactions.

Votes by the Executive Committee may be by a show of hands or secret ballot at the call of the Chairman. A simple majority shall carry a motion.

The Executive Committee shall meet at least three times between Conferences.

6.2 MEMBERSHIP

The Executive Committee shall normally consist of eight full-voting members including the Chairman.

HH) There shall be one representative from each of the seven geographic areas listed in Appendix A. (the area representative). Where at all possible, the area representative shall represent a member organisation of the Advisory Council. The Executive Committee may approve exceptions to the area representative being from a member organisation of the Advisory Council. Each area representative shall normally serve for two terms of three years each. The area representatives shall be appointed at least one-half year prior to the Conference by the member organisations of that area. Each region shall decide on its own procedure for selection (election) of its area representative.
II) The Chairman of the next Executive Committee shall be appointed by the Full Conference at the end of the Conference and act as Chairman until the end of the next Conference. The Chairman of the Executive Committee is usually the designated

representative of the member organisation that will host the next Conference, but the Executive Committee may propose as its Chairman the designated representative of any member organisation in the area where the next Conference will be held. The Vice Chairman of the Executive Committee shall be elected by the Executive Committee from its members.

The following shall be ex-officio non-voting members of the Executive Committee:

JJ) The Chairman of the Advisory Council
KK) The ITTC Secretary
LL) The past Chairman of the Executive Committee. If the past Chairman is the representative of a geographic area then that person shall be a full voting member of the Executive Committee.
MM) The Conference Organiser, if that person is not a member of the Executive Committee.

In the absence of the Chairman, meetings of the Executive Committee shall be conducted by the Vice Chairman.

7. ADVISORY COUNCIL

7.1 ROLES AND RESPONSIBILITIES

The Advisory Council proposes to the Executive Committee the topics that should be addressed by the ITTC, bearing in mind that the primary aim of the ITTC is to solve technical problems of importance to the member organisations. It proposes new technical committees and recommends terms of reference for all technical committees based on input from technical committees, ITTC members at large and the expertise and priorities of Advisory Council members.

The Advisory Council proposes recommended procedures and guidelines to the Executive Committee based on proposals by technical committees and groups.The Advisory Council may provide advice or recommendations to the Executive Committee on any other topics agreed by the Chairmen of the Executive Committee and Advisory Council.

The Advisory Council may set up mechanisms to support and monitor the work of Technical Committees. The Advisory Council may communicate with technical committees through the ITTC Secretary.

Votes on matters other than the appointment of the Chairman or Vice Chairman may be by a show of hands or secret ballot at the call of the Chairman. A simple majority shall carry a motion.

The Advisory Council shall meet at least three times between Conferences at times and places coordinated with meetings of the Executive Committee.

7.2 MEMBERSHIP

The Executive Committee appoints members to the Advisory Council. Applications for membership shall be made to the Executive Committee through the area representative. Each such organisation must satisfy the Executive Committee that:

NN) The purpose of the organisation is the prediction of performance of marine vehicles, marine structures and marine installations. The organisation provides information, on a fee-for-service basis, to clients who are the designers, builders, owners or operators of these assets. The work is directed and executed by full time professional staff. The organisation may also conduct research, technology development, and education activities, provided the funding for these is secondary to its client revenue.
OO) It has a long history of work in support of the ITTC as evidenced by membership of Committees and Groups, providing data in

support of committee and group work, or making written contributions to committees and groups;

PP) It operates at least two model test facilities and has the capability of performing a variety of experimental and numerical investigations within the scope of the ITTC.

No limit shall be put on the total number of members. However, the Executive Committee shall confirm the membership of each member of the Advisory Council once every six years. In order to remain a member of the Advisory Council members must demonstrate to the Executive Committee that they meet the criteria A), B) and C) and that in addition, they have had a record of regular attendance at meetings of the Advisory Council and the Full Conference and have made meaningful contributions to the Advisory Council. Half the Advisory Council member organisations shall be confirmed every three years. The Advisory Council shall recommend the process for confirmation to the Executive Committee.

Member organisations appointed to the Advisory Council shall be represented on the Advisory Council by their designated ITTC representative. In the event of the designated representative being unable to attend a meeting, the member organisation may send an alternate who shall be a senior technical member of the management of the member organisation, able to contribute to technical discussions on hydrodynamic testing, numerical modelling and full-scale measurement.

Each member of the Executive Committee shall be an ex-officio member of the Advisory Council if he/she is not already a member in his own right as a representative of a member organisation.

The Chairman and Vice Chairman of the Advisory Council shall be elected by its members between one year and one-half year prior to the next Conference. The election shall be by secret ballot, the candidate with the maximum number of votes shall be elected. The Chairman shall take office immediately following the end of this Conference. In the absence of the Chairman, the meetings of the Advisory Council shall be conducted by the Vice Chairman.

Secretarial support to the Advisory Council shall be provided by the ITTC Secretary.

7.3 ADVISORY COUNCIL FEE

Advisory Council members shall pay a fee to provide sufficient money to cover the cost of the additional workload on the ITTC Secretary of performing secretarial duties directly for the Advisory Council. The fee shall be approved by the Advisory Council and paid at the same time and under the same conditions as the ITTC membership fee. The Advisory Council shall be responsible for managing the income from the Advisory Council fee.

8. TECHNICAL COMMITTEES

8.1 ROLES AND RESPONSIBILITIES

The technical committees carry out the technical work of the ITTC defined in their terms of reference. The results shall be documented in reports published in the proceedings of the Conference.

Technical committees shall develop detailed plans in accordance with their terms of reference. The work of all technical committees shall be directed towards the techniques and understanding of physical and numerical modelling as a means of predicting full-scale behaviour. While maintaining an awareness of progress, fundamental theoretical studies and fundamental aspects of numerical fluid computation shall be covered by other forums, such as the ONR Symposium on Naval Hydrodynamics or Conference on Numerical Ship Hydrodynamics.

Technical committees may contact member organisations to request assistance (for example, by completing a questionnaire, participating in comparisons of the results of experiments or calculations or providing other information) or accept offers assistance from member organisations or individuals to help them carry out their work. Written contributions to the program of work of a technical committee may be submitted to its Chairman by any member organisation or individual. The technical committee may include a short abstract of any such contribution in its report, with an indication of the source from which the full document may be obtained. The conclusions and recommendations published in the committee report are the sole responsibility of the committee.

A technical committee may make informal contact with technical committees of other organisations which may be working in areas of interest to the ITTC committee.

The report of a technical committee shall reflect the opinion of the complete committee. If the committee is unable come to a consensus, the different opinions of committee members shall be published. The length, structure and format of the report shall be in accordance with guidelines set by the Executive Committee. The report shall include a general technical conclusion and recommendations for future work.

Technical committees may make proposals for future work in the subject area covered by the committee. Such proposals shall be communicated to the Advisory Council through the ITTC Secretary.

Reporting schedules for the technical committees shall be set by the Executive Committee and communicated by the ITTC Secretary.

Technical committees shall meet no more than four times in person between Conferences. Use of virtual meetings is encouraged.

8.2 MEMBERSHIP

Each technical committee shall normally consist of not more than eight members, including the Chairman. The Chairman and members shall in all cases be selected for their personal contributions to, interest in, and ability to contribute to the subject area of that technical committee. Formal qualifications and a balanced geographic representation shall also be considered in the selection process. The organisation sponsoring the candidate must have agreed to support the candidate financially in carrying out his/her committee work and travel to committee meetings.

The membership of each technical committee shall be reviewed by the Full Conference at intervals of not more than three years. A person shall not serve on technical committees for more than a total of four three-year terms, and shall not be a member on any one technical committee for more than three terms.

A member of a technical committee who is unable to continue in committee work shall be replaced by a qualified expert from a member organisation.

9. GROUPS

The Executive Committee may establish groups to carry out specific non-technical tasks for the ITTC. Examples of groups are the Symbols and Terminology Group and the Quality Systems Group. Groups may have fewer members than the technical committees. Membership on a group shall normally not exceed three consecutive terms of three years, but the Executive Committee may make exceptions. Groups shall be disbanded upon completion of their tasks. Groups shall meet no more than four times in person between Conferences. Use of virtual meetings is encouraged.

10. SERVING IN MORE THAN ONE CAPACITY

No person shall serve in more than one official capacity, or on more than one technical committee, at the same time. The official capacities are:

QQ) Membership of the Executive Committee;
RR) Chairman of the Advisory Council;
SS) Chairman of a technical committee or group.

A member of the Executive Committee or the Chairman of the Advisory Council shall not also be a member of a technical committee or group except for short periods of time at the expressed recommendation of the Executive Committee.

11. ITTC SECRETARY

11.1 ROLES AND RESPONSIBILITIES

The ITTC Secretary shall undertake all administrative and secretarial tasks in support of the operation of the ITTC.

The duties of the ITTC Secretary may include maintaining lists of ITTC memberships, publishing the ITTC Newsletter and maintaining the ITTC website. The ITTC Secretary provides secretarial support to the Executive Committee and the Advisory Council and is the primary point of contact for communications within the ITTC and between outside organisations and the ITTC.

The ITTC Secretary shall be responsible for the administration of ITTC funds. The ITTC Secretary shall:

TT) set up a bank account for ITTC funds;
UU) collect ITTC membership fees and Advisory Council fees;
VV) Perform accounting and arrange auditing of the accounts
WW) prepare proposed budgets and financial reports for ITTC and ITTC Association;
XX) make authorized withdrawals from the account.

11.2 SELECTION OF THE ITTC SECRETARY

The ITTC Secretary shall be employed by or in the case of a retiree, directly supported by a member organisation of the Advisory Council which undertakes to provide necessary services such as office space, internet, email etc. (The host organisation for the ITTC Secretary). The Secretary shall have experience as a representative on the Advisory Council or as a member of a technical committee.

The Advisory Council shall give the name of a qualified person willing to become ITTC Secretary for the next ITTC period to the Executive Committee between one year and one-half year prior to the next Conference. The name shall be chosen by secret ballot and the candidate with the maximum number of votes shall be passed on to the Executive Committee. The Executive Committee shall propose the ITTC Secretary to the Full Conference for appointment.

The ITTC Secretary shall normally serve for at least two terms.

The remuneration for the ITTC Secretary shall be decided by the Executive Committee.

12. MANAGEMENT OF ITTC FUNDS

The Executive Committee shall be responsible for the management of income from ITTC and Advisory Council membership fees. Income from membership fees shall be used to cover the costs of the ITTC organisation, including the remuneration of the ITTC Secretary, part of the cost of producing the proceedings of the Conference and other costs approved by the Executive Committee.

Once each year the Executive Committee shall review and approve the budget. The budget shall show actual income and expenditures to date, including any balance or deficit remaining from previous ITTC periods, and income and expenditures planned for the remainder of the current ITTC period.

The ITTC Secretary shall set up a separate bank account for ITTC funds. The ITTC membership fees and Advisory Council fees may be kept in the same bank account (the ITTC Account). Withdrawals from the account shall be made only by the ITTC Secretary with the written authority of the Chairman of the Executive Committee..

A financial report shall be included in the Executive Committee Report to the Conference. The Executive Committee shall also present an outline financial plan for the upcoming period including a proposal for the ITTC membership fee, for approval by the Full Conference. The financial reporting period for the ITTC is from October 1st to September 30th in the following year.

13. THE CONFERENCE

The Conference shall be held at three-year intervals.

Invitations from organisations to host the Conference of the next interval must be sent to the Executive Committee, through the area representative, at least one year before the Conference of the current interval.

The Executive Committee and the Full Conference shall ensure a balanced rotation of the Conference venue among the seven geographic areas. Each area shall decide on its own procedure for the rotation of venue among the countries in the area.

The host organisation for the Conference may be either an ITTC member organisation or an association whose mandate or aims are relevant to the aims of the ITTC, such as the American Towing Tank Conference, the Society of Naval Architects of Japan or the British Marine Hydrodynamics Panel.

The host organisation shall have overall responsibility for the organisation of the Conference.

When the host organisation is an ITTC member, the Conference organiser shall be the designated representative of the host organisation. When the host is a local association, the Conference organiser shall be the designated representative of an ITTC member organisation chosen by the association.

The Conference organiser shall be responsible for the detailed arrangements for the Conference including the preparation and publication of the Conference proceedings.

ITTC Association shall have the copyright to the Proceedings of the conference.

The arrangements, associated costs and registration fees for the Conference must be proposed by the host organisation for approval by the Executive Committee.

Participation in the Conference is by invitation only. The host organisation shall invite designated representatives of ITTC member organisations and members of technical committees and groups to the Conference. The host organisation may also invite observers and seniors to attend. The names of observers shall be proposed by their area representative. Seniors are persons now retired who have had a long association with the ITTC and whose attendance is proposed by their area representative and endorsed by the Executive Committee. The host organisation shall offer reduced registration fees to seniors.

13.1CONFERENCE ARRANGEMENTS

The Conference shall include general and technical sessions.

General Sessions shall include discussion of the report of the Executive Committee and presentations of proposals from the Executive Committee for decisions by a vote of the Full Conference. The agenda and decision record of the general sessions shall be published in the proceedings of the Conference. General Sessions shall be chaired by the Chairman of the Executive Committee.

Technical sessions shall discuss the reports and recommendations of the technical committees. No discussion shall be permitted that is not directly related to the report and recommendations under consideration. The Conference proceedings shall not be used as vehicles for disseminating technical papers. Technical sessions shall be chaired by members of the Executive Committee or Advisory Council.

The Conference may also include group discussions, to provide opportunity for discussion of topics of current interest to members. The Advisory Council shall propose topics for group discussions to the Executive Committee. The Executive Committee shall choose suitably qualified individuals to organise and Chair the group discussions. A summary of the discussion shall be published in the proceedings.

Designated representatives, members of technical committees and groups, observers and seniors may participate in discussions at technical sessions (including submitting written discussion) and in group discussions. Designated representatives may submit written discussion on behalf of colleagues from their organisation. Presentation of written discussion during the technical session shall be at the discretion of the session chairman. Only designated representatives of member organisations may participate in discussions at general sessions.

14. COMMUNICATIONS

The Executive Committee shall regularly communicate with member organisations on activities relating to the work of the Executive Committee, the Advisory Council and technical committees and groups and any other matters judged by the Executive Committee to be of concern to ITTC member organisations. The communications may be through the use of a web site, the publication of a newsletter or any other means chosen by the Executive Committee.

Member organisations may bring issues to the attention of the ITTC through their area representative. Members of the Advisory Council may do so at a meeting of the Advisory Council.

14.1 ITTC Website

There shall be only one ITTC web site. The ITTC Secretary shall maintain the site.

The ITTC website shall provide access to:

YY) Membership information, rules, procedures and guidelines, and the archive of Conference proceedings;
ZZ) Information relating to the upcoming Conference, including location, hotels, travel, technical and social programs, and committee reports, and other documentation for discussion at the Conference.

14.2 ITTC Newsletter

A newsletter may be used to communicate with member organisations. The newsletter shall be published twice a year. It shall be edited and produced by the ITTC Secretary. The newsletter may be published in paper or electronic form.

Appendix A.

Geographic areas

Area	Countries Included
Americas	Argentina, Brazil, Canada, Chile, Ecuador, Mexico, USA, Venezuela
Central Europe	Austria, Belgium, Germany, The Netherlands, United Kingdom Ireland
North and West Asia	China, Iran, Israel
Northern Europe	Denmark, Finland, Norway, Poland, Russia, Sweden Estonia
Pacific Islands	Australia, Indonesia, Japan,
Southern Europe	Bulgaria, Croatia, France, Greece, Italy, Portugal, Romania, Spain, Turkey
South and East Asia	Korea India Malaysia Vietnam Singapore

Countries not listed will be placed in an area to be decided by the Executive Committee

Appendix B.

B.1. NOTES ON THE ORGANISATION AND OPERATION OF THE ITTC

This Appendix provides information to help new members of ITTC or members joining committees for the first time, understand the workings of the ITTC organisation. It includes background information, explains some rules in more detail than is appropriate in the formal rules document and includes brief descriptions of current practice.

The Appendix is supplementary to the Rules, and does not take the place of the Rules. In case of a perceived conflict between this Appendix and the Rules, the Rules shall be followed.

B.2. DEFINITIONS

In previous versions of the Rules and colloquially, the words ‘International Towing

Tank Conference', its initials, ITTC, and shortened form, 'Conference' have been used to mean different things depending on the context. The present Rules attempt to avoid this confusion by using these words with specific meanings:

The four letters **ITTC** means the association of organisations which functions according to these rules.

The Conference means the tri-annual meeting of ITTC member organisations.

The Full Conference means the representatives of member organisations with authority to vote.

The name "**International Towing Tank Conference**" is not used in the Rules except as the title. In other documents it may be used to mean the organisation (ITTC) or the tri-annual meeting (the Conference), depending on the context.

In addition the following three words are used in the Rules:

Shall: Conveys commitment to doing something. Of these three words, shall is used in the Rules in paragraphs which describe the operation of the ITTC.

Must: The action is mandatory; there are no alternatives; gives emphasis; stronger than shall.

May: The action is optional; the choice is up to the person performing the action.

These definitions are also used in this Appendix.

B.3. BRIEF HISTORY OF THE ITTC

In 1933 23 representatives of tanks from 10 countries including the superintendents of 9 tanks met in The Hague, to "confer in an open and confidential manner on their own methods and also on the manner of publication of tank results." The program for the new Conference of Ship Tank Superintendents was focused on the everyday business of tanks. The conference appointed a committee to work out "in a more definite way the general conclusions." This was the forerunner of the technical committees we have today. All decisions were made by all those present at the "the conference".

This simple organisation continued until 1948, when a Standing Committee of six regional members was formed to give continuity from one Conference to another. it later became the Executive Committee. Up until 1948 individual Conference attendees made presentations, but from 1948 discussions at the Conference were based on reports of the technical committees. This continues to be the structure of the ITTC Conferences.

As the size and number of topics considered by the ITTC increased, there was concern that the ITTC should not evolve into a diffuse organisation loosely concerned with ship hydrodynamics. In addition, the member organisations whose primary business was model testing for clients were worried that they would be outnumbered by the tanks operated by educational and research institutions which did not share the same responsibilities to customers. There was a possibility that ITTC might adopt procedures and policies that would be harmful to the relationships between the more commercial facilities and their customers. The Advisory Council was formed at the 13th ITTC in 1972 in response to these concerns. The purpose of the Advisory Council was (and still is) to recommend the subjects to be considered "bearing in mind the primary aim of the conference is to solve technical problems of importance to tank superintendents." Organisations represented on the Advisory Council were selected from member organisations which met criteria chosen to show that their primary business was model testing for clients. In many ways the Advisory Council represents the community of Tank

Superintendents which first met over 80 years ago.

B.4. AIMS OF THE ITTC

The Aims of the ITTC written in the Rules have changed very little from the aims of the ITTC expressed in the first meetings over 80 years ago. Over the years they have been revised to keep them up to date by including numerical modelling and full-scale trials and work done by ITTC members on marine installations other than ships. The aims include stimulating relevant research in hydrodynamics, but the exchange of information concerning research in theoretical hydrodynamics and fundamental aspects of numerical fluid computations are not included. These are covered by other forums, such as the ONR Symposium on Naval Hydrodynamics or Conference on Numerical Ship Hydrodynamics. The ITTC establishes the need for research, encourages research and provides for coordination of research carried out by its members, but does not, as an organisation, fund or carry out research. The aims are written to ensure that the ITTC continues to focus on its unique role of meeting the needs of its members for giving advice and information on full-scale performance to the designers, builders and operators of ships and marine installations based on physical and numerical modelling.

B.5. THE ITTC ORGANISATION

MEMBERS

Members of the ITTC are organisations that satisfy the Executive Committee that they meet the criteria for membership stated in the Rules. (The ITTC does not have individual memberships; people participate in ITTC activities as representatives of member organisations).

DESIGNATED REPRESENTATIVES

Designated representatives are directors or senior officers of member organisations who have authority to bind the organisation in matters relating to ITTC. Each member organisation has one designated representative.

FULL CONFERENCE

Decision making authority for the ITTC rests with its member organisations. The Full Conference is the collective name of the designated representatives from member organisations present at general sessions held during the Conference. Votes taken during general sessions at the Conference are recorded as decisions of the Full Conference.

EXECUTIVE COMMITTEE

The Executive Committee is in effect, the ‘governing body’ of the ITTC. The Chairman is usually the organiser of the next Conference and members are representatives from each of seven geographic areas. The Executive Committee implements decisions of the Full Conference and may take actions between Conferences. The agenda of the Executive Committee includes applications for membership of the ITTC, membership of technical committees, arrangements for the next Conference, financial matters and relationships with other organisations.

CHAIRMAN OF THE EXECUTIVE COMMITTEE

The Chairman of the Executive Committee is the leader of the ITTC and Chairs general sessions at the Conference.

ADVISORY COUNCIL

The Advisory Council drives the technical agenda of the ITTC. It is comprised of about 30 of the larger member organisations whose primary business is model testing forclients and

have had a long history of involvement with the ITTC. The Advisory Council identifies topics of importance to the ITTC, drafts terms of reference for the technical committees and groups and provides ongoing support and monitoring of the technical committees as they carry out the work. It reviews proposed recommended procedures in detail, and ensures they are appropriate for practical application in work for clients. It reviews annual progress reports from technical committees.

ADVISORY COUNCIL WORKING GROUPS

To do its work effectively, the Advisory Council has set up four working groups. Each working group has responsibility for a technical area of importance to the ITTC. Members of the working groups are members of the Advisory Council who have an expertise or particular interest in the subjects covered by the group. The working groups take the lead in dealing with technical matters in their area of expertise and report at meetings of the Advisory Council.

TECHNICAL COMMITTEES

Technical committees carry out the technical work of the ITTC. Members of the technical committees are chosen for their ability to carry out the work. The Executive Committee chooses the Chairmen. The scope of work is defined in the terms of reference for the committee. All the technical committees have equivalent responsibilities. There is no hierarchy between technical committees. The reports of technical committees primarily contain reviews of research relevant to ITTC members and are not comparable in format or content with publications in technical journals or at other conferences.

GROUPS

Groups are similar to technical committees except that their work is primarily non-technical (for example symbols, quality control).

THE ITTC SECRETARY

The ITTC Secretary is a central point of contact for communications between ITTC members and to and from organisations outside the ITTC. The ITTC Secretary undertakes secretarial tasks in support of the operation of the ITTC. The duties of the Secretary include maintaining lists of memberships, the administration and collection of membership fees, accounting and arrangement of auditing of the accounts, publishing the ITTC newsletter, maintaining the ITTC website and preparing agenda and minutes of meetings of the Executive Committee and the Advisory Council.

THE CONFERENCE

The Conference is held once every three years, usually in September. The Conference agenda is based on the presentation and discussion of reports of technical committees, not presentations of papers by individuals. The plenary or general sessions are the opportunity for representatives of ITTC member organisations to discuss and for the Full Conference to vote on recommendations from the Executive Committee.

The Conference venue and host organisation are chosen to ensure a balanced rotation between geographic areas. The host organisation has overall responsibility for ensuring the Conference meets the requirements of the ITTC as described in the Rules and communicated by the Executive Committee. The detailed arrangements for the Conference are the responsibility of the Conference Organiser who is the designated representative of the host organisation. The Executive Committee must approve the arrangements and associated costs for the Conference. The Conference Organiser is usually Chairman of the Executive Committee. The rules are written to allow for the possibility that the Conference Organiser might have little experience of ITTC and that a different person might chair the Executive Committee.

Participation in the Conference is by invitation only. Invitations are sent to all designated representatives and members of technical committees and groups. In addition, area representatives may propose observers and seniors to attend. Employees of ITTC member organisations who are neither designated representatives nor members of technical committees or groups may attend the Conference as observers. Observers may also be persons with an interest in the work of the ITTC who are not affiliated with ITTC member organisations. Examples are representatives from ship designers and builders, classifications societies or other marine research organisations. Representatives of commercial companies with an interest in marketing to ITTC members may attend the Conference as observers, but no provision is made at most venues for the distribution of advertising material or product demonstrations.

MEETINGS

ITTC committees (including the Executive Committee and Advisory Council) meet three or four times between Conferences. The cost of attending these meetings is a significant cost to committee members' organisations and every effort is taken to minimize them. Meetings are often scheduled to coincide with major conferences likely to be attended by several committee members and the cost to the host is kept small by using in non-commercial facilities whenever possible. The high cost of long distance air travel is distributed among members by holding meetings in different geographic areas.

ITTC FEES

Member organisations pay a membership fee by which ITTC funds are raised. The ITTC funds are used to cover the cost of the ITTC organisation, including paying for the ITTC Secretary and a proportion of the cost of publishing the proceedings of the Conference. (Conference proceedings are distributed to all members, whether they attend the Conference or not). Registration fees paid by Conference attendees cover the cost of the Conference and the remainder of the cost of the Proceedings.

DECISION MAKING PROCESS

The Full Conference is the decision-making authority for the ITTC. Decisions by technical committees, the Advisory Council and Executive Committee (other than those concerning only the internal operation of these committees or otherwise mandated by these Rules) are made as recommendations for adoption to the next level on the organisation as follows:

1) Technical committees or groups
2) Advisory Council
3) Executive Committee
4) Vote by the Full Conference

Appendix 4
ITTC Member Organizations

Organisation	Country	Designated Representative
Australian Maritime College	Australia	Michael Woodward
Schiffbautechnische Versuchsanstalt in Wien	Austria	Prof. Gerhard Strasser
Towing Tank for Manoeuvres in Shallow Water	Belgium	Guillaume Delefortrie
University of Liege - ANAST	Belgium	Ass. Prof. HAGE André
Instituto de Pesquisas Tecnológicas do Estado de São Paulo - IPT	Brazil	Dr. Carlos Daher Padovezi, Director
LabOceano - Brazilian Ocean Technology Laboratory	Brazil	Prof. Antonio Carlos Fernandes
LOC/COPPE/UFRJ	Brazil	Joel Sena Sales Junior
Numerical Offshore Tank, University of São Paulo	Brazil	Eduardo Aoun Tannuri
Bulgarian Ship Hydrodynamics Centre	Bulgaria	Prof. Dr. Rumen Kishev
Memorial University of Newfoundland	Canada	Dr. Wei Qiu
National Research Council of Canada	Canada	David Murrin
Universidad Austral de Chile	Chile	Dr. Gonzalo Tampier
China Ship Scientific Research Centre (CSSRC)	China	Wentao Wang
Dalian University of Technology	China	Yuxiang Ma
Harbin Engineering University	China	Prof. Shan Ma
Huazhong University of Science and Technology	China	Prof. Jianglong Sun
Jiangsu University of Science and Technology	China	Prof. Renqing Zhu
Marine Design and Research Institute of China (MARIC)	China	Prof. Sheming Fan
Shanghai Jiao Tong University (SJTU)	China	Decheng Wan
Shanghai Ship and Shipping Research Institute (SSSRI)	China	Guoxiang Dong
Tianjin University	China	Prof. Yan Huang
Wuhan University of Technology	China	Prof. Zu-yuan Liu
Zhejiang Ocean University	China	Zhaode ZHANG
Brodarski Institute, Ship Hydrodynamics and Physical Modelling	Croatia	Ms. Marta Pedisic Buca
FORCE Technology	Denmark	Dr. Claus D. Simonsen

Organisation	Country	Designated Representative
Tallinn University of Technology	Estonia	Tarmo Sahk
Aalto University	Finland	Cheirdaris Spyridon
Aker Arctic Technology Inc.	Finland	Reko-Antti Suojanen
VTT	Finland	Dr. Seppo Kivimaa
DGA Hydrodynamics	France	Dr. Didier Fréchou
École Centrale de Nantes	France	Prof. Pierre Ferrant
Development Centre for Ship Technology and Transport Systems	Germany	Prof. Dr. Ing. Bettar Ould el Moctar
Hamburg University of Technology	Germany	R.U.Franz von Bock und Polach
Hamburgische Schiffbau-Versuchsanstalt GmbH (HSVA)	Germany	Dr. Janou Hennig
Schiffbau Versuchsanstalt Potsdam GmbH	Germany	Dr. Christian Masilge
Technische Universität Berlin	Germany	Prof. Dr.-Ing. Andres Cura Hochbaum
National Technical University of Athens	Greece	Gregory Grigoropoulos
Indian Institute of Technology Madras	India	Prof. V. Anantha Subramanian
Balai Teknologi Hidrodinamika, Laboratory for Hydrodynamics Technology	Indonesia	Fariz Maulana Noor
National Iranian Marine Laboratory (NIMALA)	Iran	AliAsghar Moghaddas Ahangari
Lir-NOTF, University College Cork	Ireland	Ian Power
CAMERI - Coastal and Marine Engineering Research Institute	Israel	Rotem Cohen
Centro Esperienze Idrodinamiche Marina Militare (CEIMM)	Italy	Lt Cdr Mario de Biase
Centro per gli Studi di Tecnica Navale (CETENA)	Italy	Dr. Giovanni Caprino
CNR-INM	Italy	Dr. Fabio di Felice
Università de Genova	Italy	Marco Ferrando
Università di Napoli	Italy	Prof. Carlo Bertorello
Università di Trieste	Italy	Prof. Mitja Morgut
Akishima Laboratories (Mitsui Zosen) Inc.	Japan	Takashi Mikami
Hiroshima University	Japan	Prof. Hironori Yasukawa
Japan Marine United Corporation	Japan	Hideo Orihara
Kawasaki Marine Engineering Co. Ltd., Akashi Ship Model Basin	Japan	Koji KATO
Kobe University	Japan	Prof. Shigeru Nishio
Kyushu University - NAMS	Japan	Prof. Jun Ando
Kyushu University - Research Institute for Applied Mechanics	Japan	Prof. Masahiko Nakamura
Meguro Model Basin	Japan	Takayuki Mori
Mitsubishi Heavy Industries, Ltd.	Japan	Mr. Daisuke Matsumoto
Nagasaki Institute of Applied Science	Japan	Shatoru Ishikawa
National Maritime Research Institute	Japan	Masaru Tsujimoto
National Research Institute of Fisheries Engineering	Japan	Mr. Akihiko Matsuda
Osaka Prefecture University	Japan	Prof. Toru Katayama

Organisation	Country	Designated Representative
Osaka University	Japan	Munehiko Minoura
Shipbuilding Research Centre of Japan	Japan	Masahiro Kishimoto
Sumitomo Heavy Industries	Japan	Mr. Kyoji Murakami
Tokyo University of Marine Science and Technology	Japan	Prof. Kiyokazu Minami
University of Tokyo	Japan	Daisuke Kitazawa
Yokohama National University	Japan	Takanori Hino
Changwon National University	Korea	Hyeon Kyu Yoon
Daewoo Shipbuilding & Marine Engineering Co	Korea	Hyun Se Yoon
Hyundai Heavy Industries Co. Ltd.	Korea	Hyun-ho Lee
Inha University	Korea	Prof. Young-Gill Lee
Korea Research Institute of Ships and Ocean Engineering (KRISO, formerly MOERI)	Korea	Booki Kim
Pusan National University	Korea	Moon Chan Kim
Samsung Heavy Industries	Korea	Hyun Joe Kim
Seoul National University	Korea	Prof. Yonghwan Kim

Appendix 5
ITTC Members and Observers invited to attend the 29th ITTC Conference

First Name	Last Name	Country	Organization
Haeseong	Ahn	South Korea	Korea Research Institute of Ships and Ocean Engineering (KRISO, formerly MOERI)
Ayhan	Akinturk	Canada	National Research Council of Canada
Batuhan	Aktas	United Kingdom	University of Strathclyde
Patrik	Almstrom	Sweden	Qualisys
Sverre Anders	Alterskjær	Norway	SINTEF Ocean (formerly MARINTEK)
Jun	Ando	Japan	Kyushu University - NAMS
Shawn	Aram	United States	Naval Surface Warfare Center, Carderock Division
mehmet	Atlar	United Kingdom	University of Strathclyde
Vivien	Aumelas	France	Australian Maritime College
Joseph	Banks	United Kingdom	University of Southampton
William	Batten	United Kingdom	QinetiQ
Robert	Beck	United States	University of Michigan
Vadim	Belenky	United States	Naval Surface Warfare Center, Carderock Division
Magnus	Berlander	Sweden	Kongsberg Maritime
Petter Andreas	Berthelsen	Norway	SINTEF Ocean (formerly MARINTEK)
Radomir	Beslać	Germany	Kongsberg Hydrodynamic Research Centre
Sebastian	Bielicki	Poland	Maritime Advanced Research Centre (CTO S.A.)
Félicien	Bonnefoy	France	École Centrale de Nantes
Johan	Bosschers	Netherlands	Maritime Research Instutute Netherlands (MARIN)
Romuald	Boucheron	France	DGA Hydrodynamics
Loic	Boudet	France	DGA Hydrodynamics
Evangelos	Boulougouris	United Kingdom	University of Strathclyde
Benjamin	Bouscasse	France	École Centrale de Nantes
Shuxia	Bu	China	China Ship Scientific Research Centre (CSSRC)
Bas	Buchner	Netherlands	Maritime Research Instutute Netherlands (MARIN)
Maxime	Canard	France	École Centrale de Nantes
Pedro	Cardozo de Mello	Brazil	University of São Paulo
Thierry	Chambenois	France	DGA Hydrodynamics
Weimin	Chen	China	Shanghai Ship and Shipping Research Institute (SSSRI)
Xide	Cheng	China	Wuhan University of Technology
Soonho	Choi	South Korea	Samsung Heavy Industries
Giuseppina	Colicchio	Italy	CNR-INM
Maurizio	Collu	United Kingdom	University of Strathclyde

First Name	Last Name	Country	Organization
Claus	D. Simonsen	Denmark	FORCE Technology
Aage	Damsgaard	Denmark	FORCE Technology
Pepijn	de Jong	Netherlands	Maritime Research Instutute Netherlands (MARIN)
Cédric	Degouet	Germany	Maritime Research Instutute Netherlands (MARIN)
Guillaume	Delefortrie	Belgium	Flanders Hydraulics Research (FHR), Belgium
Yigit Kemal	Demirel	United Kingdom	University of Strathclyde
Rui	Deng	China	Sun Yat-sen University, China
Ahmed	Derradji-aouat	Canada	National Research Council of Canada
Jean-baptiste	Deuff	France	DGA Hydrodynamics
Fabio	Di Felice	Italy	CNR-INM
Aleksei	Dobrodeev	Russian Federation	Krylov State Research Centre
Guoxiang	Dong	China	Shanghai Ship and Shipping Research Institute (SSSRI)
Martin	Donnelly	United States	Naval Surface Warfare Center, Carderock Division
Wenyang	Duan	China	Harbin Engineering University
Guillaume	Ducrozet	France	École Centrale de Nantes
Bettar Ould	el Moctar	Germany	Development Centre for Ship Technology and Transport Systems
Arash	Eslamdoost	Sweden	Chalmers University of Technology, Sweden
Janne	F. Otzen	Denmark	FORCE Technology
Sheming	Fan	China	Marine Design and Research Institute of China (MARIC)
Dariusz	Fathi	Norway	SINTEF Ocean (formerly MARINTEK)
Peiyuan	Feng	China	Marine Design and Research Institute of China (MARIC)
Antonio	Fernandes	Brazil	LOC/COPPE/UFRJ
Marco	Ferrando	Italy	Università de Genova
Pierre	Ferrant	France	École Centrale de Nantes
Andrea	Franceschi	Italy	Università de Genova
Didier	Frechou	France	DGA Hydrodynamics
Toshifumi	Fujiwara	Japan	National Maritime Research Institute (Japan)
Yoshitaka	Furukawa	Japan	Kyushu University - NAMS
Yuling	Gao	China	Shanghai Ship and Shipping Research Institute (SSSRI)
Lionel	Gentaz	France	École Centrale de Nantes
Frederik	Gerhardt	Sweden	SSPA Sweden AB
Hossein	Ghaemi	Poland	Gdansk University of Technology
Jean-Christophe	Gilloteaux	France	École Centrale de Nantes
Seok Cheon	Go	South Korea	Hyundai Heavy Industries Co. Ltd.

First Name	Last Name	Country	Organization
Grigorios	Grigoropoulos	Greece	National Technical University of Athens
Xiechong	Gu	China	Shanghai Jiao Tong University (SJTU)
Lars	Gustafsson	Sweden	SSPA Sweden AB
Guanghua	He	China	Harbin Institute of Technology, Weihai, China
Chunrong	He	China	China Ship Scientific Research Centre (CSSRC)
Janou	Hennig	Germany	Hamburgische Schiffbau-Versuchsanstalt GmbH (HSVA)
Jens	Hensse	Germany	LOC/COPPE/UFRJ
Ole Andreas	Hermundstad	Norway	SINTEF Ocean (formerly MARINTEK)
Munehiko	Hinatsu	Japan	Osaka University
Takanori	Hino	Japan	Yokohama National University
Spyros	Hirdaris	Finland	Aalto University
Peter	Horn	Germany	Hamburgische Schiffbau-Versuchsanstalt GmbH (HSVA)
Yan	Huang	China	Tianjin University
Dominic	Hudson	United Kingdom	University of Southampton
Hans	Huisman	Germany	Maritime Research Instutute Netherlands (MARIN)
Alessandro	Iafrati	Italy	CNR-INM
Yasuhiko	Inukai	Japan	Japan Marine United Corporation
Satoru	Ishikawa	Japan	Nagasaki Institute of Applied Science
Sandrine	Jamet	France	CNR-INM
Jinho	Jang	South Korea	Korea Research Institute of Ships and Ocean Engineering (KRISO, formerly MOERI)
Yichen	Jiang	China	Dalian University of Technology
Chen	Jianting	China	Shanghai Ship and Shipping Research Institute (SSSRI)
Marcus	Johansson	Sweden	LOC/COPPE/UFRJ
Takeshi	Kanai	Japan	Shipbuilding Research Centre of Japan
Henry Hooi-Siang	Kang	Malaysia	Universiti Teknologi Malaysia
Toru	Katayama	Japan	Osaka Prefecture University
Koji	Kato	Japan	Kawasaki Marine Engineering Co. Ltd., Akashi Ship Model Basin
Tokihiro	Katsui	Japan	Kobe University
Booki	Kim	South Korea	Korea Research Institute of Ships and Ocean Engineering (KRISO, formerly MOERI)
Kwang Soo	Kim	South Korea	Korea Research Institute of Ships and Ocean Engineering (KRISO, formerly MOERI)
Shinwoong	Kim	France	École Centrale de Nantes
Hyun Joe	Kim	South Korea	Samsung Heavy Industries

First Name	Last Name	Country	Organization
Sanghyun	Kim	South Korea	Inha University
Yonghwan	Kim	South Korea	Seoul National University
Rumen	Kishev	Bulgaria	Bulgarian Ship Hydrodynamics Centre
Takashi	Kishimoto	Japan	Akishima Laboratories (Mitsui Zosen) Inc.
Daisuke	Kitazawa	Japan	University of Tokyo
Seppo	Kivimaa	Finland	VTT
Florian	Kluwe	Germany	Hamburgische Schiffbau-Versuchsanstalt GmbH (HSVA)
Akihisa	Konno	Japan	Kogakuin University
Mihkel	Kõrgesaar	Estonia	Tallinn University of Technology
Kourosh	Koushan	Norway	SINTEF Ocean (formerly MARINTEK)
Kenichi	Kume	Japan	National Maritime Research Institute (Japan)
Benedetti	Lanfranco	Italy	CNR-INM
Nikolaj	Larsen	Denmark	FORCE Technology
Laurent	Le Saint	France	DGA Hydrodynamics
Inwon	Lee	South Korea	Pusan National University
Hyun-ho	Lee	South Korea	Hyundai Heavy Industries Co. Ltd.
Jean-francois	Leguen	France	DGA Hydrodynamics
Topi	Leiviskä	Finland	Aker Arctic Technology Inc.
Vincent	Leroy	France	École Centrale de Nantes
Liang	Li	United Kingdom	University of Strathclyde
Tie	Li	China	Shanghai Jiao Tong University (SJTU)
Ye	Li	China	Shanghai Jiao Tong University (SJTU)
Zhifu	Li	China	Jiangsu University of Science and Technology
Halvor	Lie	Norway	SINTEF Ocean (formerly MARINTEK)
Yi	Liu	China	Marine Design and Research Institute of China (MARIC)
Pengfei	Liu	United Kingdom	Newcastle University
Jiang	Lu	China	China Ship Scientific Research Centre (CSSRC)
Romain	Luquet	France	DGA Hydrodynamics
Shan	Ma	China	Harbin Engineering University
Gregor	Macfarlane	Australia	Australian Maritime College
Viacheslav	Magarovskii	Russian Federation	Krylov State Research Centre
Guillaume	Maj	France	Canal de Experiencias de Arquitectura Naval (CEAN)
Kevin	Maki	United States	University of Michigan
Bertrand	Malas	United Kingdom	University of Southampton
Xiaofei	Mao	China	Wuhan University of Technology
Blandine	Mariot	France	University of Southampton
Christian	Masilge	Germany	Schiffbau Versuchsanstalt Potsdam GmbH

First Name	Last Name	Country	Organization
Akihiko	Matsuda	Japan	National Research Institute of Fisheries Engineering
Daisuke	Matsumoto	Japan	Mitsubishi Heavy Industries, Ltd.
Takatoshi	Matsuzawa	Japan	National Maritime Research Institute (Japan)
Bryson	Metcalf	United States	Naval Surface Warfare Center, Carderock Division
Takashi	Mikami	Japan	Akishima Laboratories (Mitsui Zosen) Inc.
Evgeni	Milanov	Bulgaria	Bulgarian Ship Hydrodynamics Centre
Munehiko	Minoura	Japan	Osaka University
Morgut	Mitja	Italy	Università di Trieste
Takayuki	Mori	Japan	Meguro Model Basin
Ema	Muk-Pavic	United Kingdom	UCL Mechanical Engineering
Pol	Muller	France	Sun Yat-sen University, China
Motohiko	Murai	Japan	Yokohama National University
Kyoji	Murakami	Japan	Sumitomo Heavy Industries
Jean-roch	Nader	Australia	Australian Maritime College
Bo Woo	Nam	South Korea	Seoul National University
Yasunori	Nihei	Japan	Osaka Prefecture University
Janne	Niittymäki	Finland	Foreship Ltd.
Semyun	Oh	South Korea	Samsung Heavy Industries
Jeremy	Ohana	France	École Centrale de Nantes
Hideo	Orihara	Japan	Japan Marine United Corporation
Geir Åge	Øye	Norway	Kongsberg Maritime
Florin	Pacuraru	Romania	University of Galati
Kwang-Jun	Paik	South Korea	Inha University
Yezhen	Pang	China	China Ship Scientific Research Centre (CSSRC)
Cheolsoo	Park	South Korea	Korea Research Institute of Ships and Ocean Engineering (KRISO, formerly MOERI)
Joel	Park	United States	Naval Surface Warfare Center, Carderock Division
Bryce	Pearce	Australia	Australian Maritime College
Marta	Pedišić	Croatia	Brodarski Institute, Ship Hydrodynamics and Physical Modelling
Luis	Perez-Rojas	Spain	Escuela Técnica Superior de Ingenieros Navales (ETSIN)
Andrew	Peters	United Kingdom	QinetiQ
Wei	Qiu	Canada	Memorial University of Newfoundland
Patrick	Queutey	France	École Centrale de Nantes
Arthur	Reed	United States	Naval Surface Warfare Center, Carderock Division
Maciej	Reichel	Poland	Gdansk University of Technology

First Name	Last Name	Country	Organization
Nils	Reimer	Germany	Hamburgische Schiffbau-Versuchsanstalt GmbH (HSVA)
Shin Hyung	Rhee	South Korea	Seoul National University
Christopher	Richardsen	United Kingdom	QinetiQ
Claudio	Rodríguez	Brazil	LabOceano - Brazilian Ocean Technology Laboratory
Shaun	Ross	United Kingdom	Korea Research Institute of Ships and Ocean Engineering (KRISO, formerly MOERI)
Pierre	Roux De Reilhac	France	DGA Hydrodynamics
Tarmo	Sahk	Estonia	Tallinn University of Technology
Ilkka	Saisto	Finland	Aker Arctic Technology Inc.
JOEL SENA	Sales Jr.	Brazil	LOC/COPPE/UFRJ
Kei	Sato	Japan	Mitsubishi Heavy Industries, Ltd.
Jule	Scharnke	Netherlands	Maritime Research Instutute Netherlands (MARIN)
Michaela	Schläger	Germany	LaVision
Malte	Schümann	Germany	LaVision
Nobuyuki	Shimizu	Japan	Imabari Ship model Basin (ISMB)
Hyunkyoung	SHIN	South Korea	University of Ulsan
Shoji	Shingo	Japan	Shipbuilding Research Centre of Japan
Tuomas	Sipila	Finland	ABB
Magnus	Sjölin	Sweden	Qualisys
Harri	Soininen	Finland	Seniors members
SeokHo	Son	South Korea	Hyundai Heavy Industries Co. Ltd.
Roberto	Sosa	Argentina	Canal de Experiencias de Arquitectura Naval (CEAN)
Antonio	Souto-Iglesias	Spain	Escuela Técnica Superior de Ingenieros Navales (ETSIN)
Jean	Stefanini	France	TSI GmbH
William	Straka	United States	Applied Research Labratory
Clemens	Strasser	Austria	Schiffbautechnische Versuchsanstalt in Wien
Gerhard	Strasser	Austria	Schiffbautechnische Versuchsanstalt in Wien
Jianglong	Sun	China	Huazhong University of Science and Technology
Young Jae	Sung	South Korea	Hyundai Heavy Industries Co. Ltd.
Michio	Takai	Japan	Sumitomo Heavy Industries
Eduardo	Tannuri	Brazil	Numerical Offshore Tank, University of São Paulo
Claudio	Testa	Italy	CNR-INM
Tahsin	Tezdogan	United Kingdom	University of Strathclyde

First Name	Last Name	Country	Organization
Yukui	Tian	China	China Ship Scientific Research Centre (CSSRC)
Simon	Tiedeman	United Kingdom	HR Wallingford
Vincent	Tissot	France	SIREHNA
Masaru	Tsujimoto	Japan	National Maritime Research Institute (Japan)
Stephen	Turnock	United Kingdom	University of Southampton
Shotaro	Uto	Japan	National Maritime Research Institute (Japan)
Rodolphe	Veillard	France	DGA Hydrodynamics
Diego	Villa	Italy	Università de Genova
Michele	Viviani	Italy	Università de Genova
Franz	Von Bock Und Polach	Germany	Hamburg University of Technology
Decheng	Wan	China	Shanghai Jiao Tong University (SJTU)
Kai	Wang	China	Sun Yat-sen University, China
Jungyong	Wang	Canada	National Research Council of Canada
Yinghui	Wang	China	China Ship Scientific Research Centre (CSSRC)
Wentao	Wang	China	China Ship Scientific Research Centre (CSSRC)
Jinbao	Wang	China	Marine Design and Research Institute of China (MARIC)
Olle	Wennberg	Sweden	Kongsberg Hydrodynamic Research Centre
Sofia	Werner	Sweden	SSPA Sweden AB
Leszek	Wilczyński	Poland	Maritime Advanced Research Centre (CTO S.A.)
Michael	Woodward	Australia	Australian Maritime College
Jing Ping	Wu	China	Wuhan University of Technology
Chengsheng	Wu	China	China Ship Scientific Research Centre (CSSRC)
Gong	Xiang	China	Huazhong University of Science and Technology
QING	Xiao	United Kingdom	University of Strathclyde
Longfei	Xiao	China	Shanghai Jiao Tong University (SJTU)
Gongzheng	Xin	China	China Ship Scientific Research Centre (CSSRC)
Gang	XU	China	Jiangsu University of Science and Technology
Kotaku	Yamamoto	Japan	Akishima Laboratories (Mitsui Zosen) Inc.
Kai	Yan	China	China Ship Scientific Research Centre (CSSRC)
Hironori	Yasukawa	Japan	Hiroshima University

First Name	Last Name	Country	Organization
Hyunse	Yoon	South Korea	Daewoo Shipbuilding & Marine Engineering Co
Julie	Young	United States	University of Michigan
Zhiming	Yuan	United Kingdom	University of Strathclyde
Raehyoung	Yuck	South Korea	Samsung Heavy Industries
Xinshu	Zhang	China	Shanghai Jiao Tong University (SJTU)
Zhiguo	Zhang	China	Huazhong University of Science and Technology
Weiwen	Zhao	China	Shanghai Jiao Tong University (SJTU)
Feng	Zhao	China	China Ship Scientific Research Centre (CSSRC)
Lilan	Zhou	China	Wuhan University of Technology
Renqing	Zhu	China	Jiangsu University of Science and Technology
Renchuan	Zhu	China	Shanghai Jiao Tong University (SJTU)